PALACKÝ UNIVERSITY
Olomouc

Faculty of Science

Department of Organic Chemistry

Derivatives of Benzoimidazolylbenzoic Acid as the Axially Chiral Derivatizing Agent and Organocatalyst

Ph.D Thesis

Mgr. Michal Kriegelstein

Supervisor: Doc. RNDr. Petr Cankař, Ph.D.

2020/2021

Bibliographic entry

Author	Mgr. Michal Kriegelstein Faculty of Science, Palacky University Department of Organic Chemistry
Title	Derivatives of Benzoimidazolylbenzoic Acid as the Axially Chiral Derivatizing Agent and Organocatalyst
Degree program	Chemistry
Field of study	Organic Chemistry
Supervisor	Doc. DNDr. Petr Cankař, Ph.D.
Academic year	2020/2021
Number of pages	223
Keywords	Benzimidazole, axial chirality, atropisomerism, asymmetric synthesis, organocatalysis

Bibliografický záznam

Autor	Mgr. Michal Kriegelstein Přírodovědeká fakulta, Univerzita Palackého Katedra organické chemie
Název práce	Deriváty benzimidazolbenzoové kyseliny jako chirální derivatizačí činidla a organokatalyzátory
Studijní program	Chemie
Obor	Organická chemie
Vedoucí práce	Doc. RNDr. Petr Cankař, Ph.D.
Academický rok	2020/2021
Počet stránek	223
Klíčová slova	Benzimidazol, axiální chiralita, atropoisomerie, asymetrická syntéza, organokatalýza

I declare with my signature, that this is my original work. Further, I confirm that all used sources are refenced according to the department requirements.

Olomouc 24.5.2021

……..

Mgr. Michal Kriegelstein

Abstract

The thesis deals with the synthesis of axially chiral benzimidazoles and their potential applications in the assignment of absolute configuration and organocatalysis. The introduction part is divided into the three chapters. The first chapter introduces the reader into an area of axially chiral compounds with focus on atropoisomers, especially those containing C-N bond as the chiral axis. The remaining two chapters introduce the reader into the two projects.

The first, and major, project deals with the design and development of the novel axially chiral derivatization agent (CDA) for the NMR assignment of absolute configuration of chiral compounds. While there are multiple methods that allow the configuration assignment, the common availability of NMR instruments makes this method very interesting for the general use. Many different CDAs have been reported together with their limitations in the past. In this chapter, the general principles of the method are summarized and the most relevant CDAs are discussed to show their limitations.

The second, minor, project deals with the development of a novel organocatalytic system for an asymmetric reduction of prochiral imines. The current methods are presented with focus on those using $HSiCl_3$ as a reducing agent due to its high availability and low price.

The results and discussion part is divided into two chapters, each dedicated to one of the projects. In this part, the results of each project are discussed, including various dead ends and unsuccessful attempts. A comparison to relevant data from the literature is included as well.

The experimental part includes experimental procedures for the conducted experiments which are not included in the publications that arised from this thesis.

Abstrakt

Tato disertační práce se zabývá syntézou axiálně chirálních benzimidazolů a jejich potenciálními aplikacemi v oblasi analýzy a katalýzy. Úvodní část je rozdělena do tří capitol, které uvedou čtenáře do problematiky v oblasti chirálních sloučenin se zaměřením na atroposiomery. Zbývající dvě kapitoly poskytují úvod do problematiky dvou projektů, kterými se tato práce zabývá.

Prvni project se zabývá vývojem nového chirálního derivatizačního činidla (CDA) pro určení absolutní konfigurace chirálních sloučenin pomocí NMR spektroskopie. Ačkoliv existuje celá řada metod, které jsou vhodné k tomuto účelu, snadnost a vysoká dostupnost NMR spektrometrů v chemických laboratořích je nespornou výhodou této metody. Několik různých CDA bylo již v minulosti popsáno a využito nicméně jejich využití není bez omezení. V této kapitole jsou popsány obecné principy těchto metod a nejpoužívanější CDA jsou popsána spolu s jejich limitacemi.

Druhý project se zabývá vývojem nového ligandu pro organokatalytické redukce prochirálních iminů. V této kapitole jsou popsány aktuální systémy pro organokatalytické redukce prochirálních iminů se zaměřením na využití $HSiCl_3$ jako redukčního činidla a to zejména z důvodu snadné dostpupnosti a nízké ceny tohoto činidla.

Následuje část výsledky a diskuse, která je rozdělená na dvě podkapitoly, ke každému projektu jedna. V této kapitole jsou prezentovány a diskutovány výsledky každého z projektů, která jsou dale srovnány s literaturou.

Následuje experimentální část, která popisuje jednotlivé experimenty.

Acknowledgement

Writing this thesis was definitely much more difficult than I expected and it would not have been possible without the help and support of many people who were directly or indirectly involved in my work.

At first, I have to thank to my advisor Petr Cankař for the opportunity to work in his research group and for his supervision. He was able to cheer me up when it was needed and help me when I was struggling in the lab.

Second, huge thank goes to my family especially my dear and beloved wife Patricia who was cheering me up when stuff was not going well. I am gratefull for her presence in my life and I cannot imagine finishing this thesis without her support and love.

I would like to thank to David Profous, the first undergraduate student I was mentoring in the lab and at the same time, the "radio manager" of our lab. I had great time working with you and thank you for bailing me out during the last few months.

Next, I would like to thank to my labmates from 3.029: Lukáš, Monika, Ondra, Franta, and Dave. Thank you for all your advice and fun time in the lab.

The large part of my work consisted of measuring various NMR spectra and this would not have been possible without the help of Soňa and Ondra, our great NMR operators. I greatly enjoyed our NMR and chemistry related conversation with or without shisha. I am sorry that my carbons took so much time.

I would like to thank Tomáš Hudlický who allowed us to stay in his lab during our research internship. I learned a great deal of new stuff while being there and I greatly enjoyed working with his group.

Furthermore, I would like to thank to everyone who collaborated on my projects and is not mentioned elsewhere in this acknowledgement: Sandra Benická, Ondřej Kurka, Antonín Lyčka, Zdeněk Trávníček, and Adam Přibylka. Great thanks goes to Radka Navrátilová, our administrative assistant who provided excellent help with all the paperwork and her help was very valuable during the planning of our research internship.

Last, but not least, there are some friends I want to mention: Stanko, Maťo, David, Ivan, Jaro and Paša I really enjoyed our D&D sessions and Im going to miss our game. I would also like to thank various online friends I met on chemicalforums.org, r/ChemPros and chemistry discord channel. I had a great time discussing chemistry online and your technical experience proved crucial on multiple occasions.

I would like to thank the funding from IGA grants for funding (IGA_PrF_2019_027, IGA_PrF_2020_012, IGA_PrF_2018_029, and IGA_PrF_2017_009).

Organic chemistry is very specific. One spends a lot of time in the lab. Eighty percent of reactions have negative results. Few of us like this selftorture.

František Zálešák

Table of contents

List of abbreviations

CDA	chiral derivatization agent	**Napth**	napthyl
NMR	nuclear magnetic resonance	**Hex**	hexyl
Ent	enantiomer	**RT**	room temperature
BINOL	1,1´-bi-2-naphthol	**BINAM**	1,1´-bi-2-napthylamine
HPLC	high performance ligquid chromatography	**TBBA**	2-(2-(trifluoromethyl)-1*H*-benzo[*d*]imidazol-1-yl)benzoic acid
dba	dibenzylidene acetone	**TLC**	thin layer chromatography
Me	methyl	**TMEDA**	tetramethylethane-1,2-diamine
TBS	*tert*-Butyl dimethylsilyl	**DBU**	1,8-diazabicyclo[5.4.0]undec-7-ene
Bn	benzyl	**TFA**	trifluoroacetic acid
tBu	*tert*-butyl	**MS**	mass spectrometry
Ph	phenyl	**HPLC-MS**	high performance ligquid chromatography coupled with mass spectrometry
Tf	trifluoromethylsulfonate	**TFAA**	trifluoroacetic acid anhydride
Tol	tolyl, toluene	**PE-Mix**	
THF	tetrahydrofurane	**T3P**	2,4,6-tripropyl-1,3,5,2,4,6-trioxatriphosphorinane-2,4,6-trioxide
DMF	dimethylformamie	**CDI**	1,1′-carbonyldiimidazole
NaPHhePHOS	(1-(2-(diphenylphosphanyl)-6-methoxyphenyl)naphthalen-2-yl)diphenylphosphane	**EDCl**	*N*-Ethyl-*N*′-(3-dimethylaminopropyl)carbodiimide hydrochloride
BINAL	lithium dihydrido(binaphthoxy)aluminate)	**HOBt**	1-Hydroxybenzotriazole hydrate
CBS	Corey-Bakshi-Shibata catalyst	**TEA**	triethylamine
de	diastereomeric excess	**pTSA**	toluene-4-sulfonic acid monohydrate
ee	enantiomeric excess	**SFC**	supercritical fluid chromatography
CPA	chiral phosphonic acid	**SCDI**	1,1′-thiocarbonyldiimidazole
TRIP	(*S*)-3,3′-Bis(2,4,6-triisopropylphenyl)-1,1′-bi-2-naphthol cyclic monophosphate	**10-CSA**	10-camphorsulfonic acid
mCPBA	meta-chloroperbenzoic acid	**TBDPS**	*tert*-Butyldiphenylchlorosilane
NHC	*N*-heterocyclic carbine	**ACN**	acetonitrile
VCD	vibrational circular dichroism	**XPhosPdG2**	chloro(2-dicyclohexylphosphino-2′,4′,6′-triisopropyl-1,1′-biphenyl)[2-(2′-amino-1,1′-biphenyl)]palladium(II),
ORD	optical rotary dispersion	**TBBACl**	2-(2-(trifluoromethyl)-1*H*-benzo[*d*]imidazol-1-yl)benzoyl chloride
CSA	chiral solvating agent	**OSU**	*N*-hydroxysuccinimide
MTPA	3,3,3-trifluoro-2-methoxy-2-phenylpropanoic acid	**MMFF**	molecular mechanics force field
MTPA-Cl	3,3,3-trifluoro-2-methoxy-2-phenylpropanoyl chloride	**TFAOMe**	methyl trifluoroacetate

CIP	Cahn-Ingold-Prelog	**DIAD**	diisopropylazodicarboxylate
ap	antiperiplanar	**HOAc**	acetic acid
sp	synperiplanar	**DIEA**	diisopropylethylamine
MPA	2-methoxy-2-phenylacetic acid	**TMSOK**	potassium trimethylsilanolate
1-NMA	2-methoxy-2-(naphthalen-1-yl)acetic acid	**HATU**	1-[bis(dimethylamino)methylene]-1*H*-1,2,3-triazolo[4,5-*b*]pyridinium 3-oxid hexafluorophosphate
2-NMA	2-methoxy-2-(naphthalen-2-yl)acetic acid	**Py**	pyridine
9-AMAA	2-(anthracen-9-yl)-2-methoxyacetic acid	**PPA**	polyphosphoric acid
Boc	*tert*-butoxycabonyl	**Ac_2O**	acetic anhydride
Boc-PHG	2-((*tert*-butoxycarbonyl)amino)-2-phenylacetic acid	**LTA mix**	L-diabenzoyltartaric acid L-ditoluolyltartaric acid L-ditoluolyltartaric acid
DCM	dichloromethane	L-**DBT**	L-diabenzoyltartaric acid
DMSO	dimethylsulfoxide	L-**DTT**	L-ditoluolyltartaric acid
DMAP	4-dimethylaminopyridine	L-**DAT**	L-dianisoyltartaric acid
DCC	dicyclohexylcarbodiimide	**TES**	triethylsilane
HMPA	hexamethylphosphoramide	**NLE**	nonlinear effect
Ts	tosyl	**(-)-NLE**	negative nonlinear effect
Cp	cyclopentyl	**(+)-NLE**	positive nonlinear effect

Aims of this thesis

1) Development of a novel chiral derivatization agent for NMR spectroscopy

The synthesis and resolution of an axially chiral benzimidazole derivative as a chiral derivatization agent (CDA) and its study of capability to distinguish between the enantiomers of the analyte based on the ^{1}H, ^{13}C, or ^{19}F NMR spectra. The design of a conformational model for the assignment of absolute configuration deduced from the NMR data and in-silico modeling of model compounds.

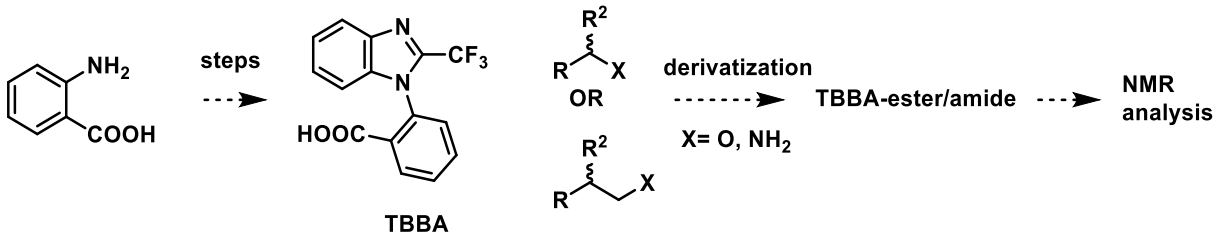

2) Design and development of an organocatalytic system for the asymmetric additions of organosilicon reagents to prochiral imines.

The synthesis and resolution of an axially chiral benzimidazole-pyridine ligand for the asymmetric reduction of prochiral imines by $HSiCl_3$ and the addition of allyl-$SiCl_3$. The optimization of the ligand for the highest enantiomeric purity of the product. The best ligand will be tested on a set of various model imines to further evaluate the applicability of the proposed catalytic system.

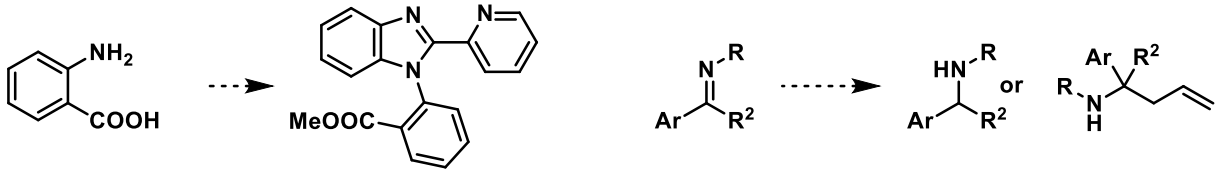

State of the art

Axial chirality

Axial chirality is a special case of chirality in which the molecule does not possess stereogenic center but a chiral axis. The chiral axis is an axis about which the set of substituents is held in a special arrangement that is not superimposable with its mirror image.[1] There are several types of axially chiral compounds: atropoisomeric compounds such as biphenyls **1** or isoquinoline alkaloids[2] **2**, allenes **3** or helical structures (such as helicenes or DNA) **4** (Figure 1). Because this work deals only with atropoisomeric compounds such as **1**, further discussion will focus only on those.

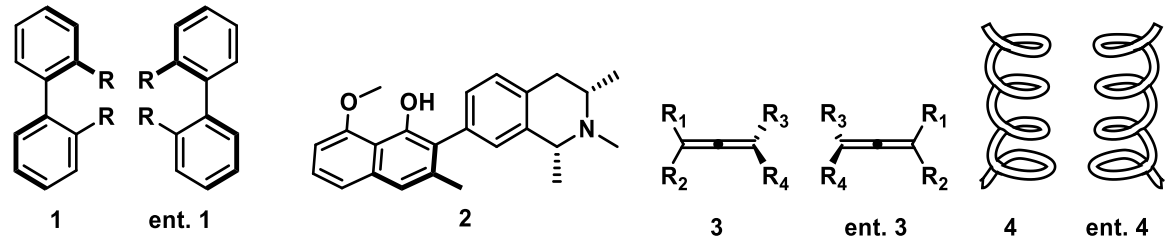

Figure 1 Examples of axially chiral compounds

Atropoisomers

Introduction

Atropoisomers are a subgroup of axially chiral compounds, where the chirality is caused by hindered rotation around a single bond in the molecule. Technically, those compounds are conformers with sufficiently high barrier of rotation which allows for isolation of individual conformers.[2]

The first experimental results from this area come from Christie and Kenner from 1922. They were able to separate axially chiral diphenic acid **5** via crystallization as a brucine salt (Figure 2).[3]

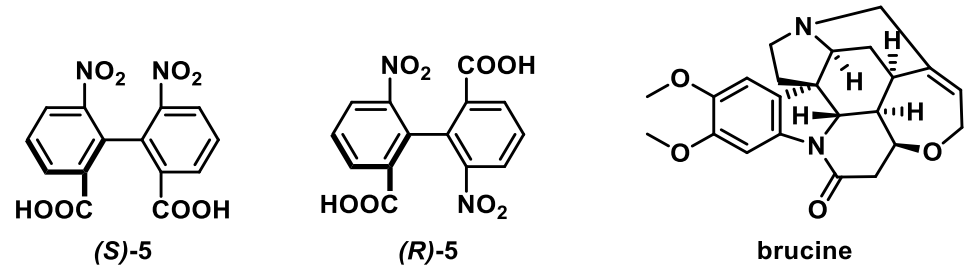

Figure 2 The first resolved atropoisomers

Later, Kuhn and Albrecht were able to resolve [1,1'-binaphthalene]-2,2'-dicarboxylic acid **6** using quinine as the resolving agent (Figure 3).[4]

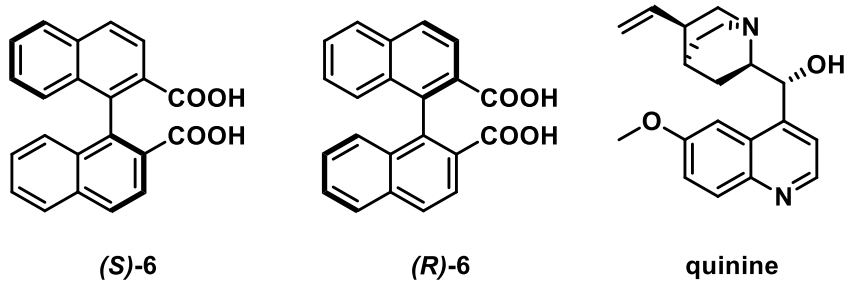

Figure 3 Resolution of 1,1′-binapthalene derivative

Another early example comes from W. M. Stanley who was able to resolve 8,8′-dicarboxy-1,1′-dinaphthyl **7** again as a quinine salt (Figure 4). Interestingly, 8,8′-diacid **7** is less stable compared to 2,2′-diacid **6:** it took 4.5 hours in a boiling aqueous solution of NaOH to completely racemize **6** while only 30 minutes for diacid **7**, which also racemized in aqueous ammonia within15 hours at room temperature. [5]

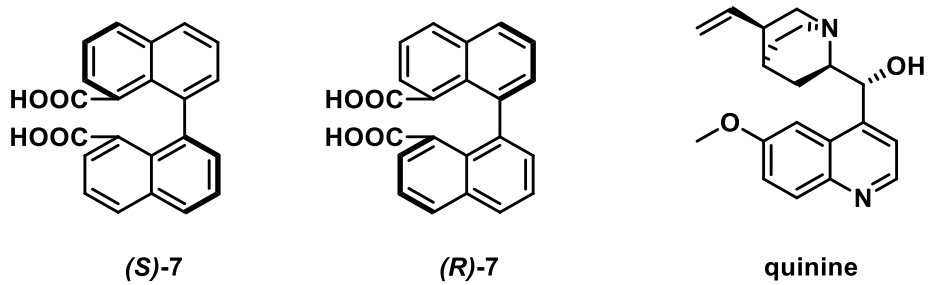

Figure 4 Resolution of 8,8′-binapthalene derivative

The first examples of 5-membered biaryl came from Adams in 1931 who prepared arylpyrrole **8** and carbazole **9** and was able to resolve it using brucine as a resolving agent.[6,7]

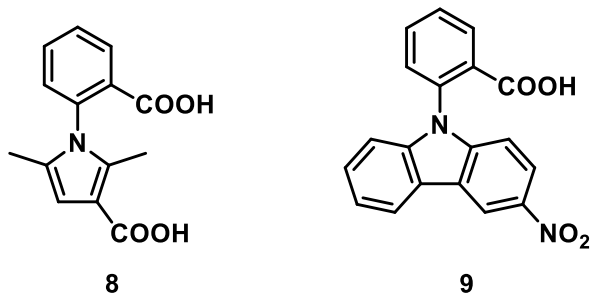

Figure 5 The first examples of 5-membered biaryls

Stability and racemization of atropisomers

Unlike point chirality, the atropisomeric compounds racemize via simple rotation around a single bond. The energy required for this rotation depends on a specific structure of a given compound, temperature, or solvent. Atropisomers are generally recognized when their half-life at given temperature is at least 1000 s (17 min). This half-life corresponds to energy barrier of 93 kJ/mol or 22 kcal/mol at 300K (27°C).[2,8] The conformational stability of a compound depends on the following factors[2]:

a) Combined steric demand of the substituents close to the chiral axis
b) Existence and structure of bridges
c) Presence of racemization mechanism different from simple rotation

Furthermore, the biaryls with two six membered rings such as **5**, **6**, or **7** are more stable than those with one six membered ring and one five membered such as **8** due to the increased distance between ortho substituents next to the axis which is responsible for the lowering of the rotational barrier.[9]

The effect of ortho substituents was studied by Bott[10] and, in general, the rotational barrier increases with the Van Der Vaals radius of those substituents: I > Br > Me > Cl > NO_2 > COOH > OMe > F > H and with the number of those substituents (Figure 6). The di-ortho substituted binapthalene **10** has fairly low rotational barrier of 101 kJ/Mol at 317K (44 °C)[11,12] while addition of one substituent in biaryl **11**[13,14] increased the rotational barrier to 125 kJ/Mol at 383 K (110 °C) and further addition of ortho-substituents in BINOL **12** increased the rotational barrier up to 158 kJ/Mol at 493 K (220 °C).[15] This also explains the results of Kuhn[4] and Stanley[5] and why the 2,2′-dinapthalene dicarboxylic acid **6** (di-ortho substituted) is more stable than 8,8′-diacid **7** (tetra-ortho substitued).

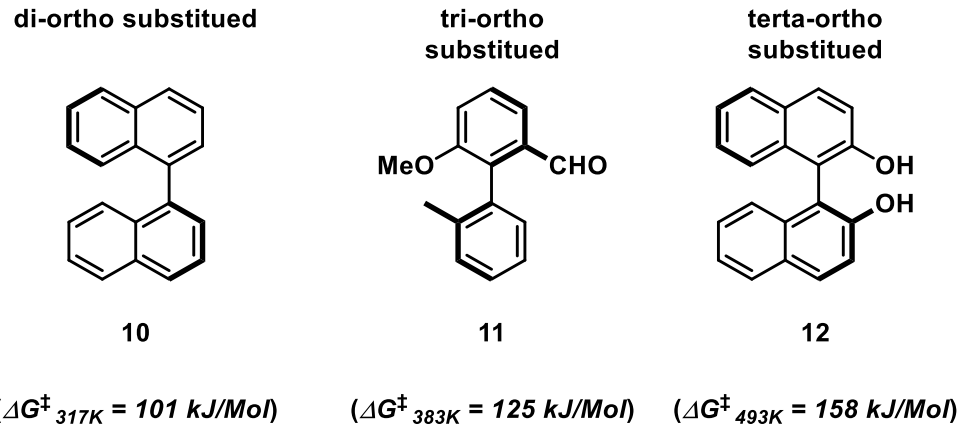

Figure 6 Influence of substituents on the rotational barrier

The presence of a bridge connecting the *ortho*-positions can have a strong influence on the rotational barrier of the biaryl atropoisomers. If the *ortho* positions are bridged by one atom bridge as in compound **13**, the rotation is usually not hindered at room temperature.[16]

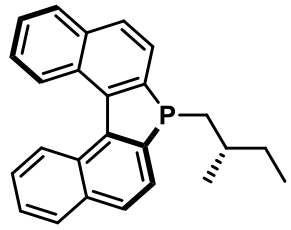

15

Figure 7 Example of an *ortho*-bridged atropoisomer

The rotational barrier for phosphole **15** was calculated to be 55 kJ/mol at room temperature. This significant instability compared to unbridged compounds such as **12** was explained by distortion of the binapthyl ring caused by the presence of the bridge which caused the protons at positions 8 and 8´ to be further apart from each other and thus facilitating the rotation.[16]

The presence of two-atom bridge partially hinders the rotation based on the specific structure of given compound (Figure 8).[17] It can be readily acknowledged, that the most important substituent in this case is the R substitutent in the *ortho* position to the chiral axis. Small substituents (**16a-c**, **f-h**) have practically zero impact on the rotational barrier and both atropoisomers readily interconvert between each other. The more dedmanding iPr group in **16E** increases the half-life from <1 minute to almost half an hour while t-butyl group further increases the stability to $T_{1/2}$ = 2.2 days.

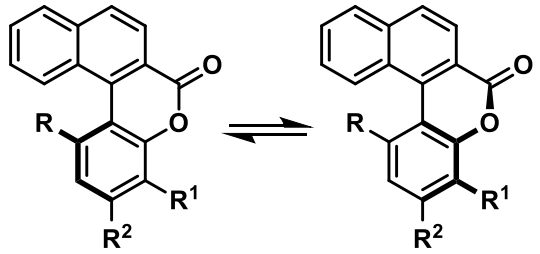

***(M)*-16** ***(P)*-16**

	16a	**16b**	**16c**	**16d**	**16e**	**16f**	**16g**	**16h**
R	H	OMe	Me	Et	iPr	H	Me	tBu
R^1	iPr	Et	iPr	iPr	Me	H	H	H
R^2	H	H	H	H	H	H	Me	tBu
$\Delta G^{\ddagger}_{298K}$ (kJ/Mol)	--	54.4	73.9	83.7	92.3	--	--	104.4
$T_{1/2}$	< ms	0.4 ms	1 s	52 s	28 min	--	--	2.2 d

Figure 8 The effect of substituents on racemization kinetics

Derivatives with a three atom bridge show similar stability to unbridged biaryls[18] and further enlarging the bridge have similar effects. Interestingly tripeptidic antibiotic biphenomycin A **17** (Figure 9) exists as a single diastereomer, even though there are no ortho-substituents next to the chiral axis.[19,20]

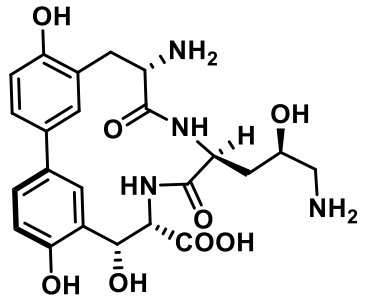

17

Figure 9 biphenomycin A

In some examples, the racemization occurs via a more complex mechanism than a simple rotation around the bond. The simplest example[21] is shown in Figure 10.

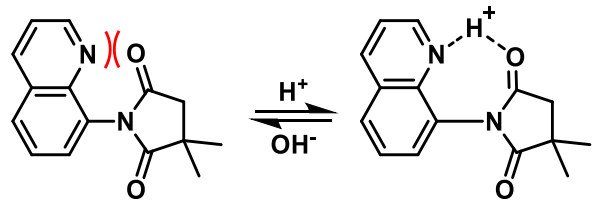

steric repulsion **hydrogen bond**

$\Delta G^{\ddagger}$ = 92.8 kJ/Mol **$\Delta G^{\ddagger}$ = 38.9 kJ/Mol**

18 **18b**

Figure 10 Lowering the roational barrier by protonation

The protonation of quinoline **18** caused a significant drop of the rotational barrier **18b** *via* the formation of a hydrogen bond. This process was reversible and an addition of the base stopped this rotation. Another example is acid catalyzed racemization of BINOL **12.** While BINOL itself is conformationally stable even at elevated temperatures (no racemization after heating under neutral conditions at 100°C for 24 hours), heating in an acidic media (1.2N HCl in dioxane/water) at 100°C for 24 hours caused complete racemization. The exact mechanism is not known but cationic species **19** was suggested as the intermediate (Figure 11). The presence of sp3-sp2 bond instead of original sp2-sp2 likely facilitates the transformation from **19a** towards **19b.**.[22]

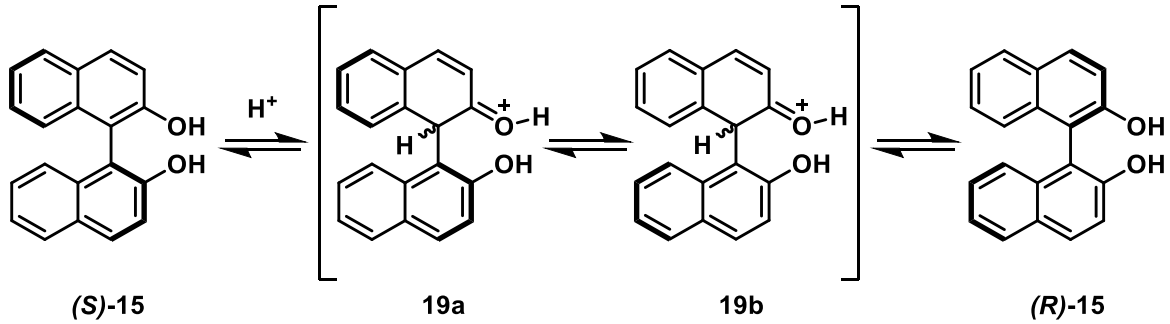

Figure 11 Acid catalyzed racemization of BINOL

In some cases the mere presence of suitable functional groups in the *ortho* position to the chiral axis can induce the racemization as was described for cynandione A **20** (Figure 12).[23] Cynandione A **20**, with a tetra-*ortho* substitued chiral axis, was only isolated as a racemic mixture.[23] The structurally similar hydoxyaldehyde **21** has the tetra-substituted chiral axis as well, the racemization barrier of **21** is also fairly low: $\Delta G^{\ddagger}_{296K}$ = 99 kJ/Mol. This is explained by formation of hemiacetal **21a** which quickly atropisomeries to enantiomer (***P*)-21**. Methyl-protected derivative **22** is configurationally stable.[24]

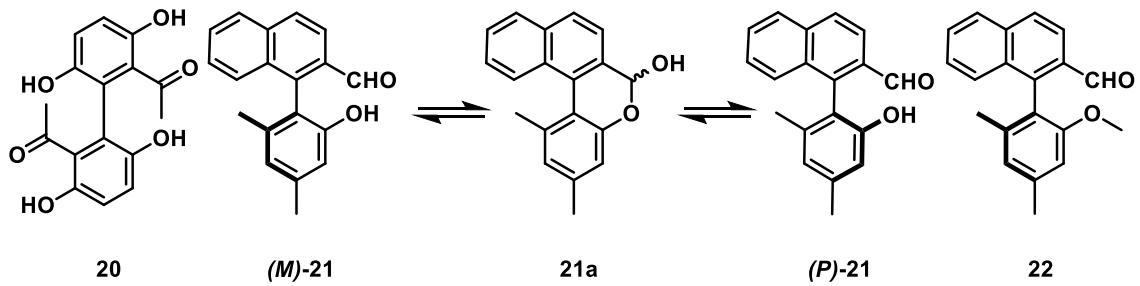

Figure 12 Racemization via formation of hemiacetal

Synthesis of biaryl atropisomers

The synthesis of biaryl atropisomers can be categorize into two main approaches: a) synthesis of racemate followed by resolution or b) atroposelective synthesis. The racemic synthesis uses common arylation reactions such as Suzuki coupling, Buchwald-Hartwig amination, Ullmann coupling, or Chan-Lam coupling. The cyclization reactions in case of the atropisomeric heterocycles are usually followed by resolution by common methods such as crystallization or chiral HPLC. The atroposelective synthesis is often complicated because it requires formation of a sterically hindered bond which might require harsher conditions (usually higher temperatures). These conditions might frequently result in a negative effect on stereoselectivity of the reaction.[2] Some of the developed methodologies (Figure 13) are briefly reviewed in this chapter.

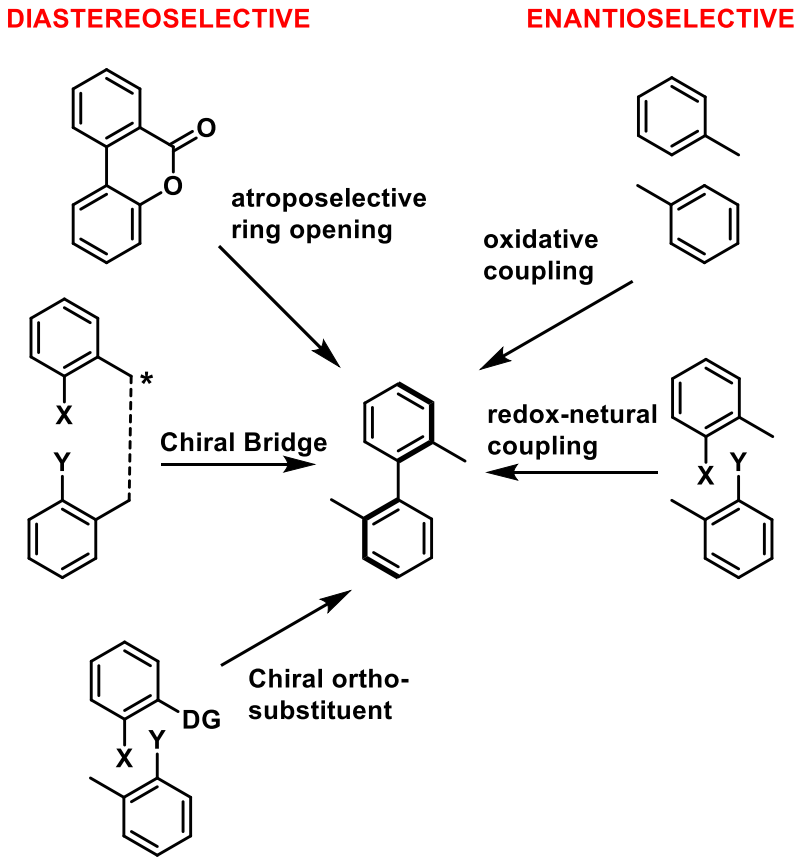

Figure 13 Synthetic strategies leading to atropisomeric biaryl compounds

Oxidative coupling

BINOL **12** can be prepared by oxidative coupling of naphthalen-2-ol using various metal oxidants , such as $FeCl_3$,[25] and subsequent resolution *via* cinchonine salt after conversion phosphoric acid ester **23** **(**Scheme 1). After $LiAlH_4$ reduction, (*R*)-BINOL was isolated in 41% yield and 96% ee while (*S*)-BINOL was isolated in 56% yield but only 90 %ee. [26] The procedure was further modified with 2-

aminobutanol in the resolution step to improve the optical purity to >99 %ee although the yield was reduced to 30% and 15%.[27]

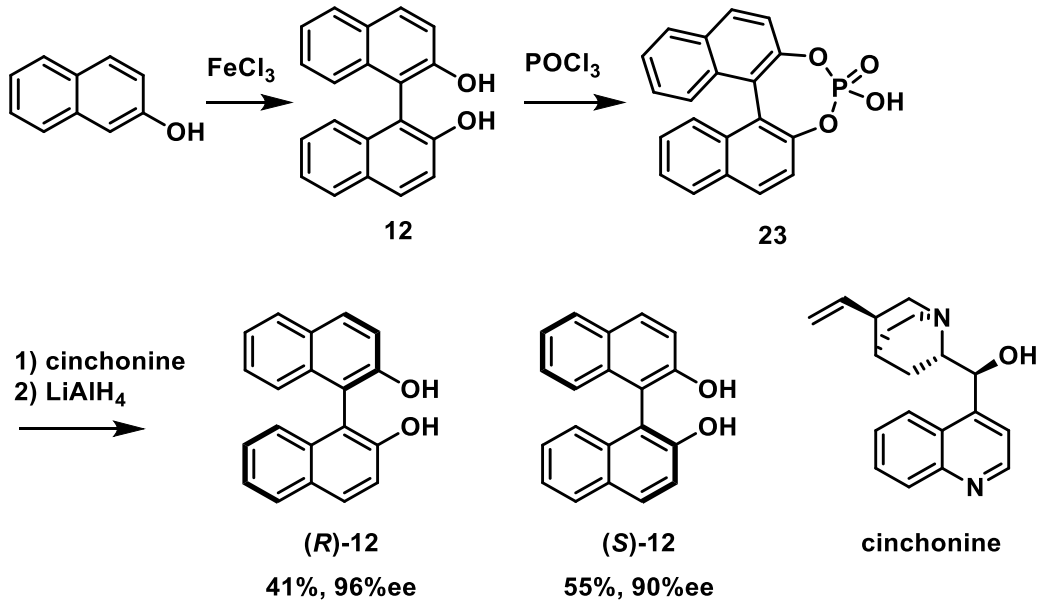

Scheme 1 Synthesis and resolution of BINOL

While the resolution methods allowed for synthesis of both enantiomers of BINOL, atroposelective oxidative coupling allows for easier and simpler synthesis because it does not require the enantioresolution step. The first synthesis, used $Cu(NO_3)_2$, as an oxidant together with (*S*)-phenetylamine as a chiral ligand to prepare BINOL in 63% yield and only 3% ee.[28] Further optimization of chiral ligand increased the enantioselectivity to 96% and the yield to 94%.[29] However, the large exess of a chiral salt (8 equivalents) was needed. This was solved by Smrčina and Kočovský, who developed a procedure using one equivalent of the Cu-sparteine complex. This method allowed atroposelective synthesis for unsymmetrical biaryls as well, nevertheless it was optimized for the synthesis of BINOL which was obtained in excellent enantioselectivity (>99 %ee) but only modest yield (36 %).[30] Further modification included enzymatic resolution or the use of different resolving agents, which were thoroughly reviewed by Brunel.[31]

Redox-neutral coupling

Unlike oxidative couplings, atroposelective redox-neutral couplings offer several advantages. The biggest are zero requirements for specific substitution patterns and option for regioselective coupling of two different aromatics. This allows simple synthesis of various biaryls which are lacking specific functional groups required for oxidative coupling. The first atroposelective example of redox-neutral coupling is from Hayashi from 1988 (Scheme 2).[32] The Grignard reagent **24** was coupled together with various aryl bromides **25a-b** under mild conditions using a chiral Ni catalyst. Products **26a-b** were

isolated in good yields and enantioselectivities. Various ligands for asymmetric Kumada coupling were screened, however, with low success.[33,34]

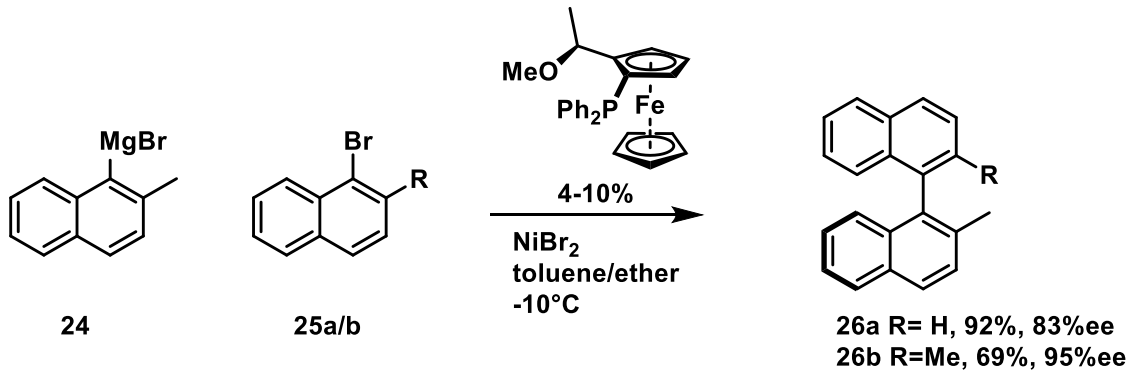

Scheme 2 Atroposelective Kumada coupling

The first example of atroposelective Suziki-Myarura coupling comes from groups of Crépy[35] and Buchwald.[36] Crépy obtained various biaryls with %ee between 5 and 85%. Interestingly, use of pinacolboronates gave opposite configuration of product compared to boronic acid or ethyleneglycol esters. Buchwald used phosphonate-substituted napthylhalides **27** as a coupling parthers, which proved beneficial and obtained products in high yields and %ee using axially chiral biaryl ligands (Scheme 3). The use of phosphonate ester in ortho position proved crucial for high enantioselectivity and they were further transformed by Grignard reaction followed by reduction into phosphine derivatives, which could be used as chiral ligands.

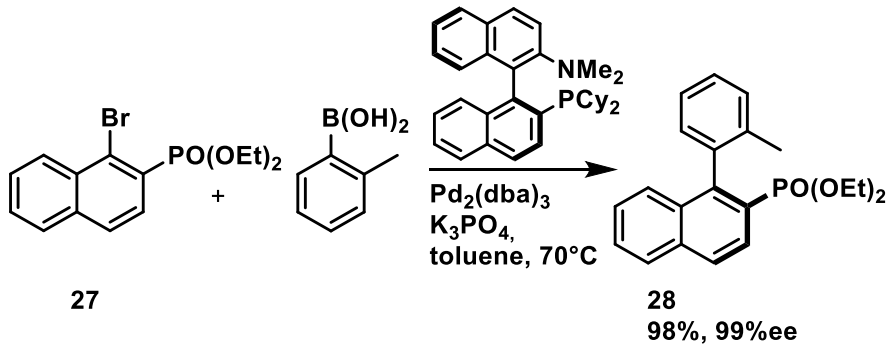

Scheme 3 Atroposelective Suzuki coupling

Use of chiral directing group

Use of a chiral directing group is another approach for the synthesis of axially chiral biaryls. Compared to oxidative and redox-neutral couplings it offers one distinctive advantage: the products are formed as a diastereomeric mixture, which subsequently allows for easier separation *via* crystallization

or column chromatography. In most cases, the chiral auxiliary group needs to be removed afterwards. This might lower the overall yield or even cause partial racemization.

The first example of a chiral directing group in *ortho*-position came from Miyano who coupled chiral esters of 1-bromo-2-napthoic acid esters **28a-d** under Ullman conditions (Scheme 4) to yield various binapthyls **29a-d**.[37] Yields were high, up to 93%, however, the enantioselectivity was poor.

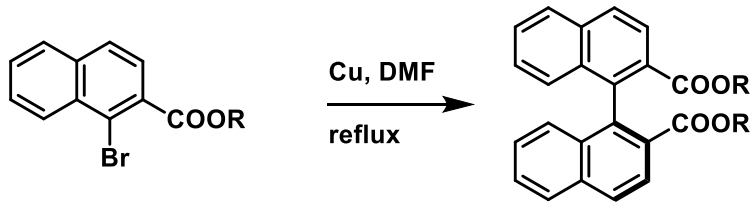

28a R= menthol,
28b R= cholesterol
28c R= (-)-1-phenyletanol,
28d R= (-)-2-octanol

29a R= menthol, 13%ee
29b R= cholesterol, 5.3%ee
29c R= (-)-1-phenyletanol, 5.0%ee
29d R= (-)-2-octanol, 7.5%ee

Scheme 4 Diastereoselective Ullman coupling

This methodology was further improved by Meyers, who used aryl grignards and methoxy-phenyl oxazolines in S_N2-Ar type reaction (Scheme 5).[38,39] The oxazolines are easily prepared from required benzoic acid and amino alcohols[40,41] by various methods. The stereoselectivity of reaction highly depends on the structure and coordination ability of the "R" group compared to the methoxy group (In case, where the R group is only weakly or not at all coordinating to magnesium **33**, (R= Me, OTBS), the methoxy group coordinates to magnesium and directs the orientation of the aryl ring (Scheme 5, **33**) and the product can be obtained in high %ee. In the other case, where the R group is coordinating strongly than the methoxy group (R= 1,3-dioxolan-2-yl), the proposed coordination **34** rotates the aryl ring in an opposite direction and the product with reversed configuration is obtained in high chiral purity. At the edge case, where the R group has similar coordinating properties as OMe group (R= OBn), the product with very low chiral purity is obtained, due to low preference for given transition state **33** or **34.**

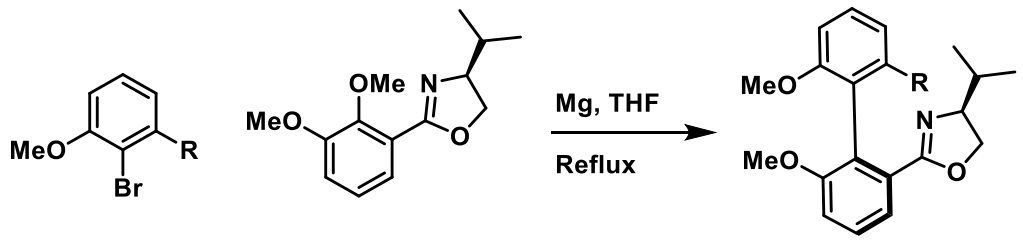

30 **31** **32**

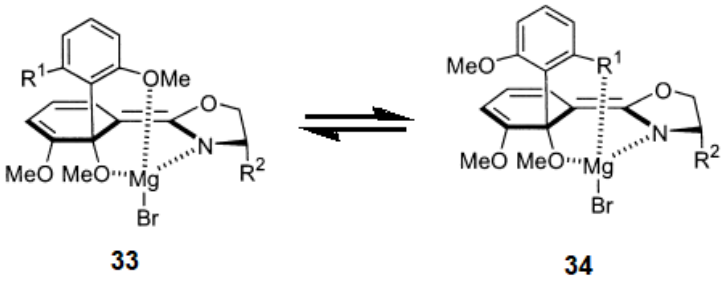

33 34

Scheme 5 Oxazoline-directed atroposelective arylation (taken from ref. [39])

While those methods are fairly robust and work well to prepare biphenyl or binapthyl type of atropoisomers, the synthesis of C-N biaryl atropoisomers is far less developed. This might be due to the Ullmann and Buchwald-Hartwig reactions, which, in general, require more forcing conditions compared to oxidative couplings or Grignard reactions. This was partially overcome by Colobert by use of chiral sulfinyl iodanes **35** and copper catalysis (Scheme 6) to prepare atropoisomeric *N*-aryl indolines **36** in high enantiomeric purity and yields.[42] While there are other reported atroposelective syntheses of C-N atropoisomers, either biaryls[43–46] or other types[47,48] this is the only example that features direct *N*-arylation to form the chiral axis in the same step we found in literature.

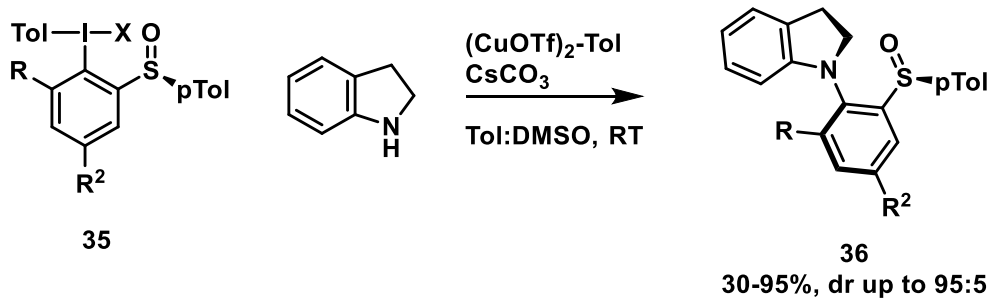

35 36

30-95%, dr up to 95:5

Scheme 6 Atroposelective synthesis of *N*-aryl indoline

Chiral bridge mediated synthesis

The use of a chiral bridge provides another synthetic tool leading to atropoisomers. This method is similar to use of a chiral directing group in the *ortho* position as described above. Unlike the previous method, the two coupling partners are joined together by a chiral bridge. This allows for high yields of intramolecular coupling and option to prepare both symmetrical and asymmetrical biaryls. This approach was firstly pioneered by Miyano (Scheme 7).[49,50] While forcing conditions were used (Ullman coupling, refluxing DMF), the chiral tether allowed for high chiral purity of products, compared to intermolecular Ullmann coupling (Scheme 4). The use of BINOL as a chiral tether proved to be critical to ensure high enantiomeric purity although the yields were lower in some cases (36-80%, mostly around 40%).

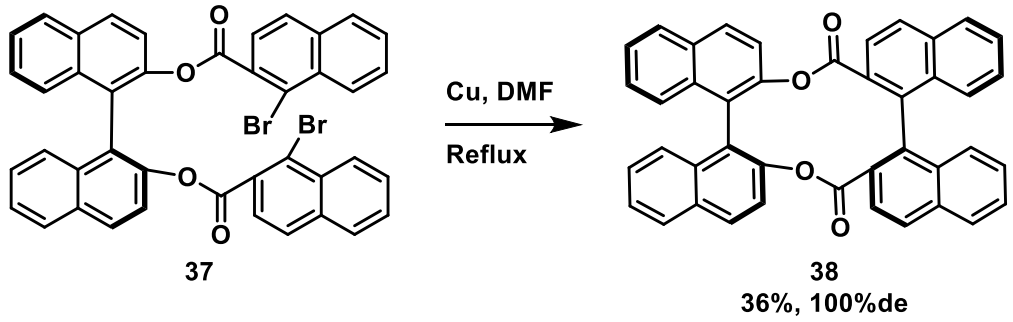

Scheme 7 Atroposelective synthesis of BINOL directed by chiral bridge

Further improvements were made by Lipchutz who used cyanocuprate coupling that allowed to use lower temparatures[51] and introduced diether tethers[52] which were used with high success in total synthesis of natural products such as (+)kotanin **38**[53] or synthesis of chiral biaryl ligand NAPhePHOS **39** (Scheme 8).[54]

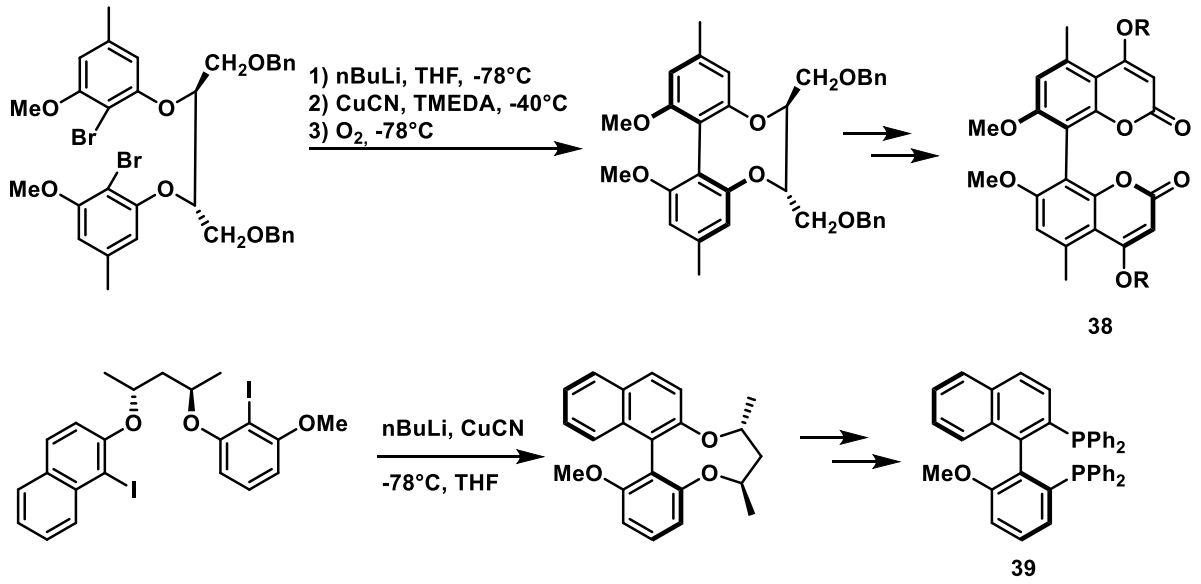

Scheme 8 Chiral bridge directed biaryl synthesis

Atroposelective ring opening

As was mentioned in a previous chapter, biaryls bridged with two atom bridge (Figure 8, Figure 12) are not conformationally stable and – depending on an exact structure – quickly convert between each other. This instability can be exploited, assuming one can open the lactone bridge with a suitable chiral nucleophile (Scheme 9) which leads to dynamic-kinetic resolution.

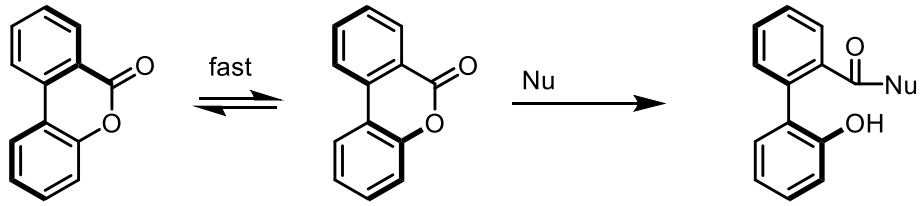

Scheme 9 Diastereoselective ring opening

Various nucleophiles ranging from sodium salts of menthol **41,** its derivatives,[55] or phenetylamine **42,**[56] to even hydride using BINAL-H,[57] or CBS-borane catalyst **43** [58,59] were used to stereoselectively open the lactone **40** (Scheme 10).

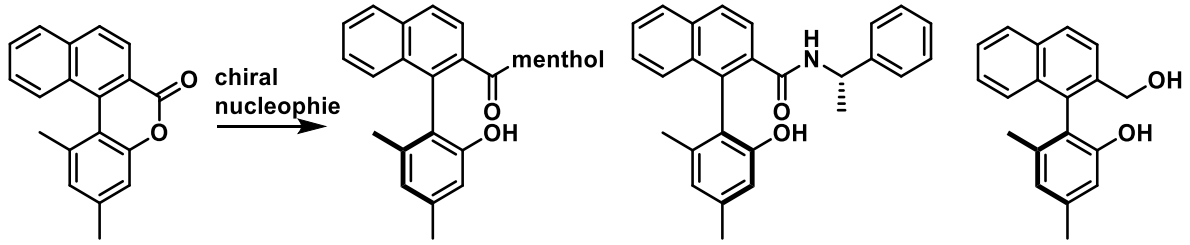

40

41
Nu= Menthol
76% de

42
Nu= (*S*)-2-Phenetylamine
90% de

43
Nu= H- (CBS-BH_3)
97% de

Scheme 10 Diastereoselective ring opening

Atroposelective ring closing reactions

Atroposelective ring closing reactions provide an alternative approach; however, they are limited towards synthesis of heterocyclic biaryls due to the ease of ring closing reactions. Recent example comes from the Miller group (Scheme 11).[45]

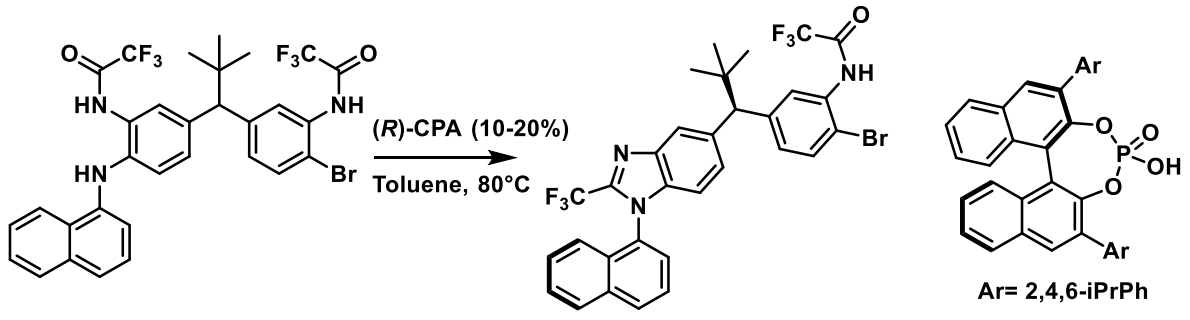

44

90%, 17:1 dr, >99:1 er
45

(*R*)-TRIP

Scheme 11 Atroposelective cyclodehydration

The use of chiral acid allowed to form trifluoromethylbenzimidazole **45** from precursor **44** in a high yield and diastereomeric excess as a single enantiomer. Various other BINOL-derived phosphonic acids were used as well and the scope was broadened in the follow-up study.[46] Variously substituted phenylenediamines **46** were subjected to cyclization with chiral acids to yield axially chiral benzimidazoles **47a-e** in high yields and enantiomeric excess based on the type and location of substituents (Scheme 12). Unfortunately, the methodology is limited to trifluoroacetamides and it is not clear if it would work with less electrophilic amides.

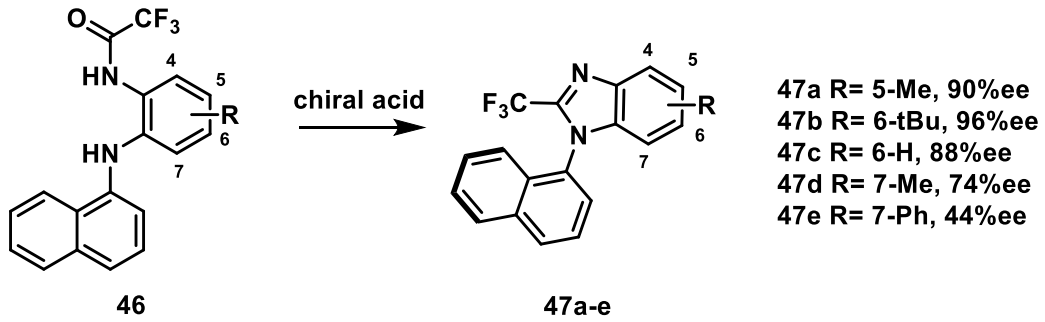

Scheme 12 Atroposelective cyclodehydration

Different cyclization was utilized by Pesch who used chiral 2-bromomenthone **48** as a starting material for synthesis of axially chiral thiazole **49** which was obtained as a single diastereomer after crystallization. Thiazole **49** was further oxidized by mCPBA in presence of $HClO_4$ to yield thiazolium salt **50** which was converted by treatment with triethylamine into atropoisomeric *N*-heterocyclic carbene **51** (Scheme 13) which was used as catalyst for asymmetric Strecker reaction and Benzoin condensations.[60] Unfortunately, while the thiazolium precursor **50** was atropoisomerically stable, the carbene **51** partially racemized during reaction and therefore proved unsuitable as a catalyst.

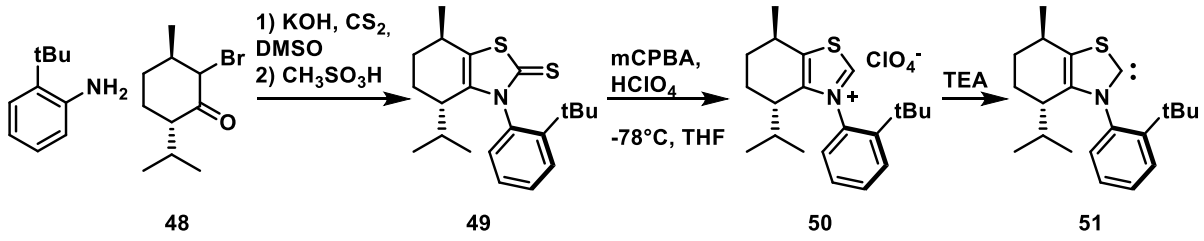

Scheme 13 Synthesis of axially chiral NHC

Assignment of absolute configuration by NMR

Introduction

The absolute configuration is one of the key characteristics of chiral compounds. There are several methods that allow the configuration assignment such as chiroptical methods[61] or X-ray crystallography,[62] however, the high availability of NMR instrumentation makes it competitive choice.

Chiroptical methods such as vibrational circular dichroism (VCD) or optical rotary dispersion (ORD) require significant time to perform required calculations and simulations of the spectra, which is then compared to experimentally obtained one. Those calculations become more difficult if the compound of interest is flexible. On the other hand, chiroptical methods are nondestructive and does not require chemical modifications and therefore allow analysis of compounds with no suitable functional groups.[61]

X-ray crystallography is robust method, however, the main limitation is requirement of high quality monocrystal which might take considerable time and effort to prepare even though there are numerous manuals[63,64] or significant improvement such as crystalline sponge.[65]or formation of guanidinium co-crystals.[62]

NMR spectroscopy can be used if several criteria are met. The most important is the requirement for suitable functional groups that allow for modification of the analyte with suitable chiral reagent. This modification can be either noncovalent using chiral solvating agents (CSA) or covalent using chiral derivatization agents (CDA). Since the experimental work described in this thesis deals with development of new CDA, this chapter will focus on the applications of various CDAs.

In theory, any chiral compound can be used as a CDA because covalent modification of given chiral analyte with chiral CDA will lead to diastereomeric compounds if we use different enantiomers of CDA. The diastereomers will differ in their NMR spectra unlike enantiomers but for compound to be used as a reliable CDA, the NMR difference in spectra of those diastereomers needs to be predictable which would lead to the assignment of the correct configuration of the analyte. This requirement disqualifies most of the chiral compounds. The "ideal" CDA should possess following structural features:[66]

a) A suitable functional group that allows covalent modification of the analyte – most often carboxylic acid but alcohols or amines could be used as well.
b) A suitable functional group that projects anisotropic effect on the analyte which causes the predictable change of NMR spectra ("shielding effect") - most often aromatic rings such as phenyl or anthryl.
c) A suitable polar group which "locks" the compound in preferred conformation which allows selective projection of the shielding effect on specific substituents of the analyte.

The structure of general CDA **52** is depicted on Figure 14. The X-group allows for modification of the analyte, Y-group projects the shielding effects towards the substituents R^3 **53** and R^4 **54** in the analyte which causes the selective change in the NMR spectra. R^1 and R^2 are other functional groups which play a role in maintaining the specific conformation of the diastereomers **53** and **54**.

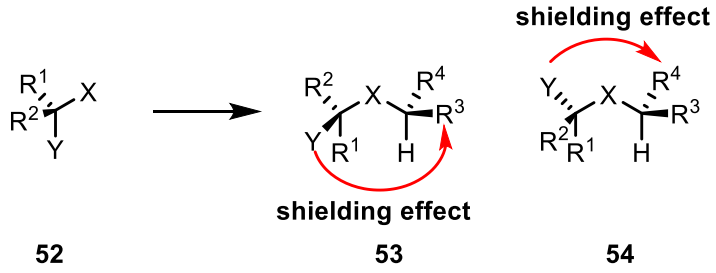

Figure 14 Schematic representation of the principle of the method

Most commonly, the analyte is modified separately with both enantiomers of the CDA and their NMR spectra are compared (Double derivatization method, Figure 15a). It is also possible to form only single diastereomer and compare two spectra measured at different temperature or after addition of an additive which cause conformational change (Single derivatization method, Figure 15b).[67] The last and most limited is comparing NMR spectra of CDA modified analyte with the spectra of unmodified analyte. In all those cases, two different NMR spectra are measured and compared (Single esterification method, Figure 15c).

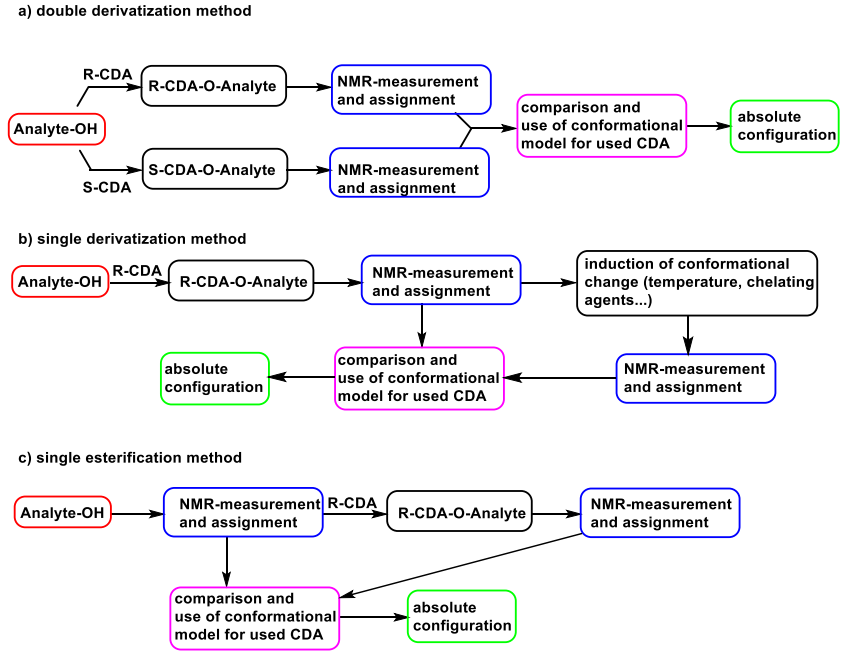

Figure 15 Approaches towards configuration assignment by NMR

The range of substrates includes α-chiral secondary alohols[68,69] and amines[70], β-chiral primary alchols[68,71], cyclic secondary amines,[72,73] tertiary alcohols,[74,75] thiols,[76] cyanohydrins[77–79] or polyfunctional aminoalcohols.[80,81] While the substrate scope is fairly broad, it is important to know, not every CDA is suitable for each of those analytes.

Analysis of chiral secondary alcohols

Mosher´s acid

Methoxytrifluoromethylphenylacetic acid (MTPA) or Mosher´s acid **55** (Figure 16) is the most commonly used acid since its description by Dale and Mosher in 1973.[82–84] Analytes can be acylated with MTPA and a suitable activator or directly with acid chloride MTPA-Cl **56.** Important note is that while the acid and chloride have the same spatial arrangement of substituents, the CIP priority is different therefore (*S*)-acid **(*S*)-55** provides (*R*)-chloride **(*R*)-56.**

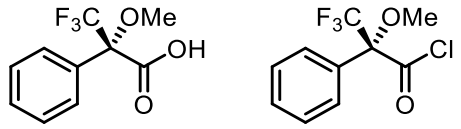

(*S*)-55 **(*R*)-56**

Figure 16 Structure of Mosher´s acid

At first, ^{19}F NMR was used by Mosher[83] with advantage due to simplified interpretation of ^{19}F spectra at that time. The proposed conformational model, which allows the assignment, is shown in Figure 17.

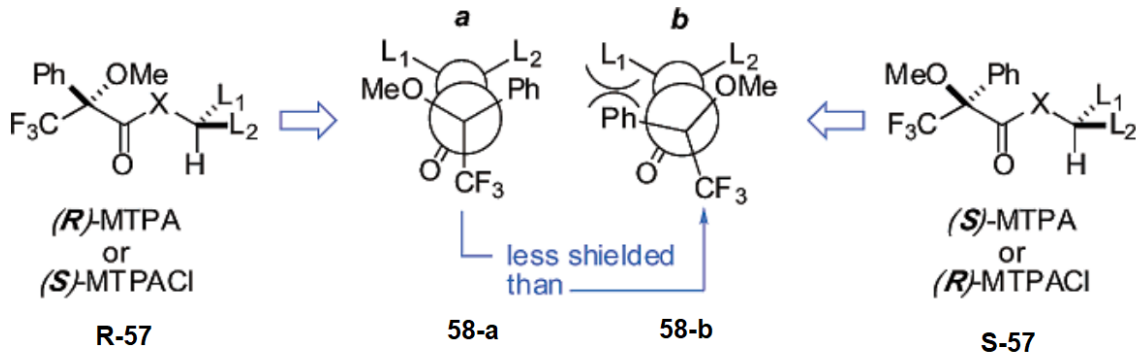

Figure 17 Conformational model used for configuration assignment on the basis of ^{19}F spectra (taken from [85])

Mosher assumed the preferred conformation being the one depicted in Figure 17 **(*R*)-57 or (*S*)-57.** The proton at the chiral carbon, carbonyl oxygen, and trifluoromethyl group are located in *syn*-periplanar

conformation. Assuming L^1 substituent is bulkier than L^2, when phenyl ring is on the same side as the bulkier substituent L^1, **58-b** the steric interaction causes the distortion of conformational equilibria and a slight rotation which moves the CF_3 group into the shielding zone of the carbonyl oxygen; therefore, lowering its chemical shift compared to **58-a**. This shielding can be expressed as a parameter $\Delta\delta^{SR}(^{19}F)CF_3$ which can be calculated by substracting the ^{19}F chemical shift of the (*R*)-MTPA ester from the (*S*)-MTPA ester: $\Delta\delta^{SR}(^{19}F)CF_3 = \delta CF_3(S) - \delta CF_3(R)$. In case of alcohol with configuration as depicted in Figure 17 (assuming L^1 is bulkier than L^2), the resulting calculation yields $\Delta\delta^{SR}(^{19}F)CF_3 < 0$. If the alcohol would have an opposite configuration, the resulting analysis would yield $\Delta\delta^{SR}(^{19}F)CF_3 > 0$. While the use of ^{19}F NMR allows straightforward assignment due to low number of signals in the spectra, the method was later rejected due to low reliability.[86]

The use of proton NMR is so far more common than use of ^{19}F. The greatest advantage of ^1H over fluorine NMR lies in the number of data points gathered. The ^{19}F NMR always gives one or the other configuration and because only one signal is obtained; there is no room for self-correction. On the other hand, most organic molecules have multiple protons, which can be analyzed and therefore any anomalous behavior can be revealed. The conformation model for use of proton spectra is different compared to ^{19}F and is shown in Figure 18.[85]

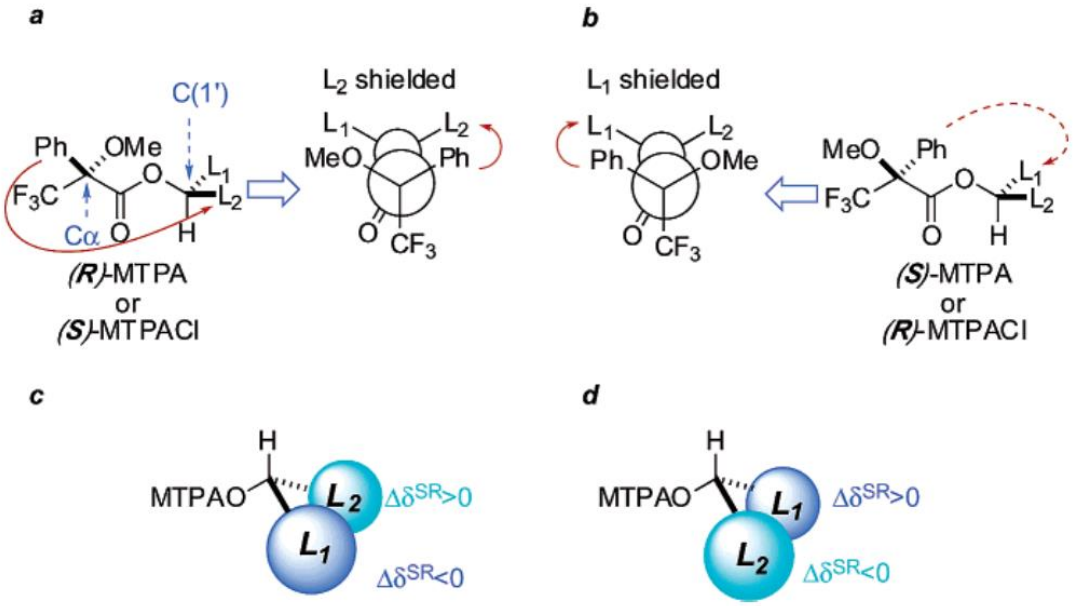

Figure 18 Conformational model for assignment of absolute configuration of chiral alcohols by Mosher´s acid (taken from [85])

The conformation is the same but the shielding effect is caused by the phenyl rings and is projected towards one of the substituents either L^1 or L^2. If (*R*)-MTPA is used, the shielding is projected towards the L^2 substituent (Figure 18a) and when opposite enantiomer, (*S*)-MTPA, is used, the shielding is projected towards the L^1 substituent (Figure 18b). This shielding is opposite if the alcohol has opposite

configuration. The shielding towards the substituents can be calculated in similar fashion as in the case of ^{19}F:

$\Delta\delta^{SR}(L^1) = \delta L^1(S) - \delta L^1(R)$

$\Delta\delta^{SR}(L^2) = \delta L^2(S) - \delta L^2(R)$

Due to the shielding depicted in this example

$\Delta\delta^{SR}(L^1) < 0$

$\Delta\delta^{SR}(L^2) > 0$

After the calculation is done, the spatial arrangement of substituents L^1 and L^2 can be decoded using simplified models shown in Figure 18c/d. Naturally, all protons located in L^1 or L^2 substituent should have the same sign of the $\Delta\delta^{SR}$ and is advised to calculate as many $\Delta\delta^{SR}$ parameters as many protons as possible because of higher reliability of such assignment. ^{13}C NMR analysis can be performed in the same manner as ^{1}H although it has several limitations[87].

Unfortunately, MTPA possess several limitations that complicate the structural assignment of MTPA esters or amides:

a) The $\Delta\delta^{SR}$ differences are often not high enough to be safely used
b) Anomalous values are often observed.

The selection of compounds, which do not follow the proposed model, is shown in Figure 19.

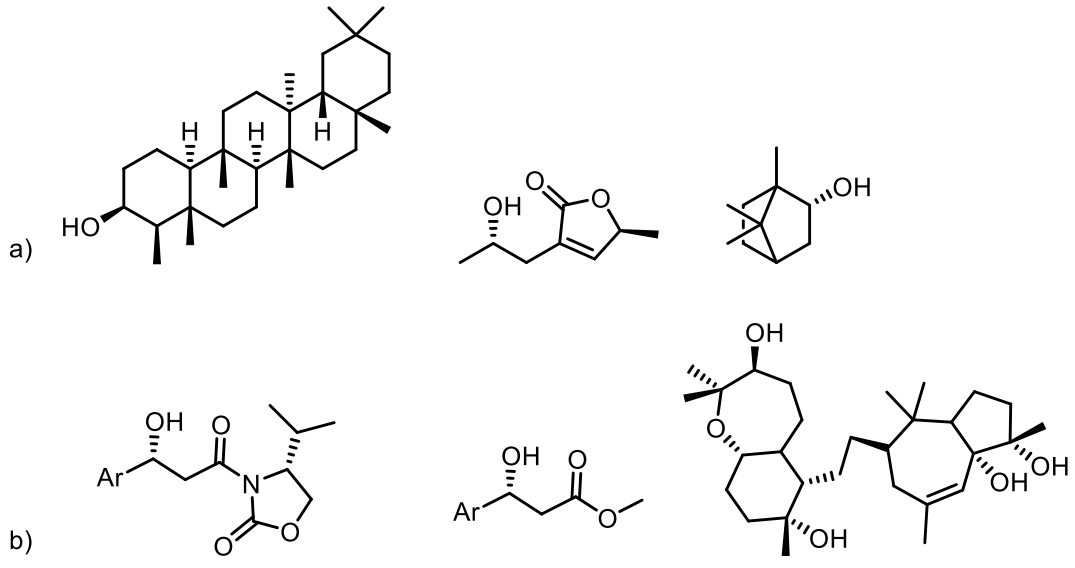

Figure 19 Examples of compounds that don't follow models developed for Mosher´s acid a) compounds that doesn't follow ^{19}F model b) Compounds that doesn't follow ^{1}H model

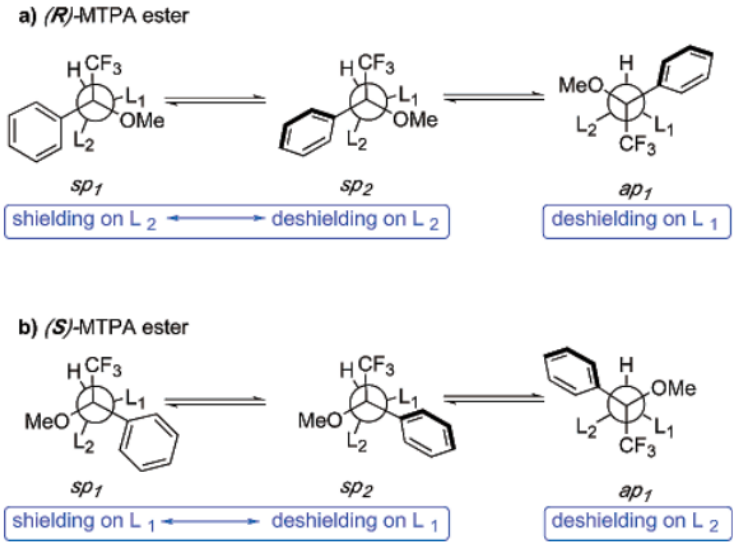

Figure 20 Major MTPA conformers and their shielding effects (taken from [85])

These anomalies in MTPA assignment were further reinvestigated using computational methods[68] and it was revealed that the conformational equilibrium is more complex than was assumed by Mosher. It was revealed, that MTPA exists in three conformers which produce different shielding and deshielding effects and are in a delicate balance with each other (Figure 20).

The sp_1 conformer of (*R*)-MTPA esters (Figure 20a) was assumed by Mosher and produces the shielding effect on substituent L^2 in accordance with the proposed model. The sp_2 conformer which is caused by simple rotation around C_{AR}-C bond produces deshielding effect on the same substituted therefore limiting the magnitude of observed $\Delta\delta^{SR}$. Further rotation around C-$C_{carbonyl}$ creates conformer ap_1 which produces deshielding effect on substituent L^1. Those major conformers are in balance which can be distorted by change of experimental conditions – such as concentration or temperature which therefore causes the irregularities in the observed $\Delta\delta^{SR}$ values.

Methoxyphenylacetic acid

Methoxyphenylacetic acid **58** (MPA, Figure 21) was also reported by Mosher,[84] however its application was limited due to observed racemization during the acylation step. This difficulties were later solved by Trost[88] by use of different acylation conditions.

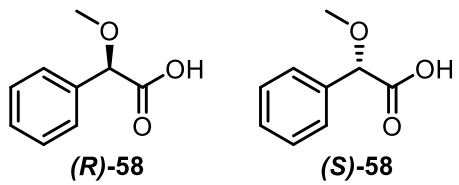

Figure 21 Methoxyphenylacetic acid (MPA)

The proposed conformational model[85] is depicted on Figure 22: The methoxy, carbonyl and C_1H groups are in *syn*-periplanar conformation which then allows the phenyl ring to produce shielding effect towards one of the substituents L^1 or L^2 (Figure 22a). The shielding parameter $\Delta\delta^{RS}$ is then calculated analogously as in the case of MTPA and based on the $\Delta\delta^{RS}$ values. The substituents are located in space (Figure 22b). It should be noted that MPA and other CDA except MTPA use opposite convention to describe the shielding effect which is $\Delta\delta^{RS}$ instead of $\Delta\delta^{SR}$ which is calculated using the similar procedure: $\Delta\delta^{RS}(L) = \delta L(R) - \delta L(S)$. It was noted that this convention is often overlooked and some publiations use the MPTA calulation method.

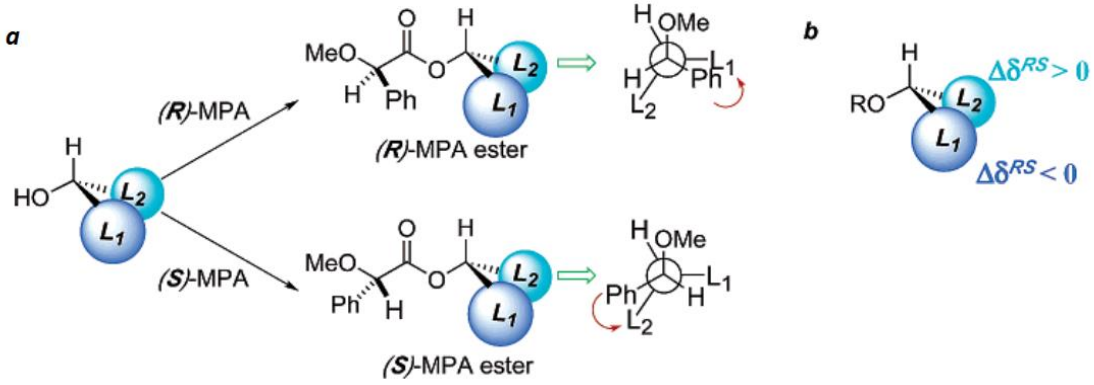

Figure 22 Conformational model for configuration assignment of alcohols using MPA (taken from ref. [85])

The conformation equilibria of MPA is significantly simpler compared to MTPA: only two major conformers were described[89] and are depicted on Figure 23.[85]

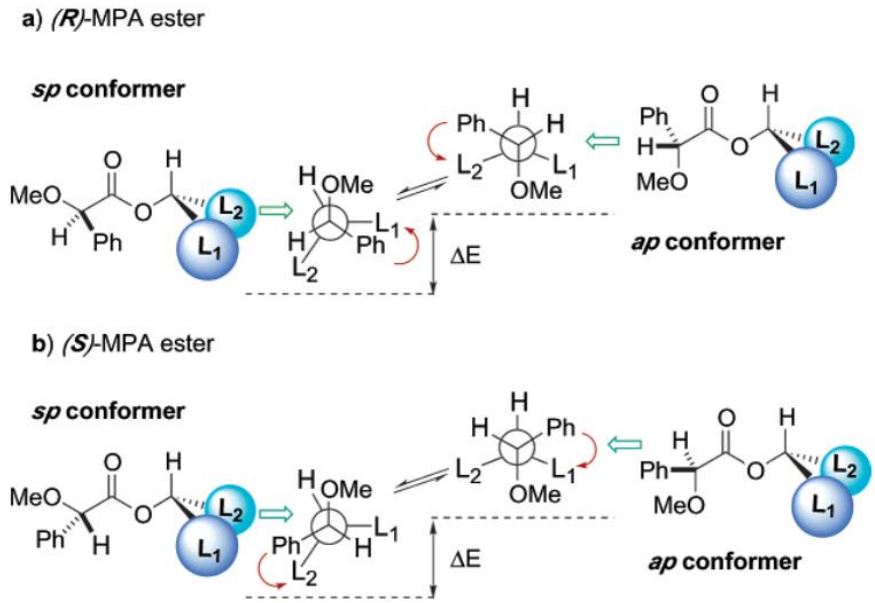

Figure 23 Major conformers of MPA esters (taken from ref. [85])

The major conformer, sp, has methoxy group, carbonyl, and proton H in the *syn*periplanar conformation which allows the phenyl ring to project the shielding effect towards L^1 (Figure 23a). The

minor conformer, ap, which is approx. 1 kcal/mol less stable, is formed by rotation of C-C bond between carbonyl carbon and carbon in position 2. In this case, phenyl ring projects the shielding effect towards substituent L^2. The shielding effect on L^2 is weaker because the phenyl ring and L^1 are not exactly aligned. The combination of higher stability of sp conformer and the weaker shielding on opposite substituent in the ap conformer, demonstrates itself in higher observed $\Delta\delta^{RS}$. Same conformational model can be used for analysis of thiols, however smaller $\Delta\delta^{RS}$ are observed.[76]

Other arylmethoxyacetic acids

Further modification of the structure of MPA were performed At first, a change of methoxy group to other alkyls or acyls was attempted.[90] This modification however did not provide significant improvement and in most cases, the $\Delta\delta^{RS}$ differences were smaller compared to MPA. The further modification was exchanging the phenyl ring for different aryls .[89,91] The structures of some of the arylmethoxyacetic acids are shown in Figure 24

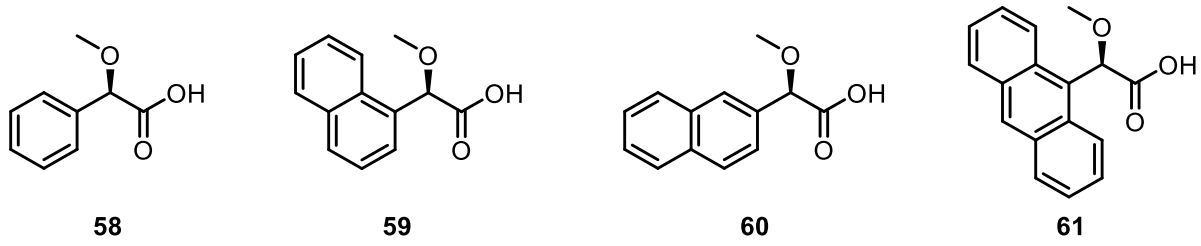

Figure 24 (*R*)-MPA **58**, (*R*)-1-NMA **59**, (*R*)-2-NMA **60** and 9-AMAA **61**

The most promising is 9-AMAA **61** which showed the most significant $\Delta\delta^{RS}$ differences as can be seen in Figure 25 on a model substrate: 3,3-dimethylbutan-2-ol **62,** 1-phenylethanol **63**, or menthol **64**.

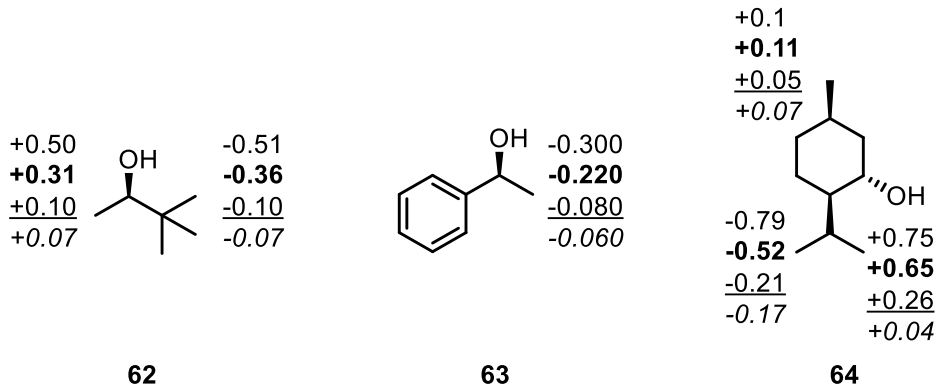

Figure 25 Comparison of $\Delta\delta^{RS}$ differences between 9-AMAA, **1-NMA,** MPA, and *MTPA*

There is a difference between MTPA and MPA in the magnitude of the $\Delta\delta^{RS}$ parameter as can be seen in **64**, however, the substitution of the phenyl ring for larger rings such as naphthyl in 1-NMA or anthryl in 9-AMAA shows significant improvement in the differentiation of signals of interest as can be

seen in **62**, **63**, **64**. The substitution of the aromatic moiety plays dual role: first, the larger aromatic ring is able to project the shielding effect towards larger area and second, the larger aromatic rings shift the conformational equilibrium towards more desirable sp conformer[89] (Figure 23).

Analysis of β-chiral primary alcohols

This improvement is especially significant in analysis of chiral primary alcohols. In this case, only 9-AMAA provided enough differentiation which allows reliable structural assignment of the absolute configuration.[69,71] The difference between 9-AMAA, MPA and MTPA is depicted in Figure 26.

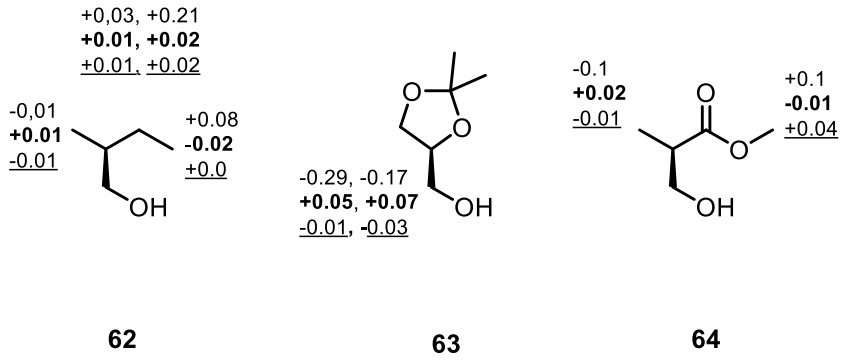

Figure 26 Comparison of $\Delta\delta^{RS}$ differences between 9-AMAA, **MPA,** MTPA esters

As can be seen the MPA the $\Delta\delta^{RS}$ values of 9-AMMA in derivatives **62**, **63**, and **64** are significantly larger than those obtained by MPA or MTPA. It was concluded that MTPA or MPA are not suitable for analysis of this type of alcohols and only 9-AMAA should be used. The conformation model is based on the previous models for MTPA and MPA and is shown in Figure 27.

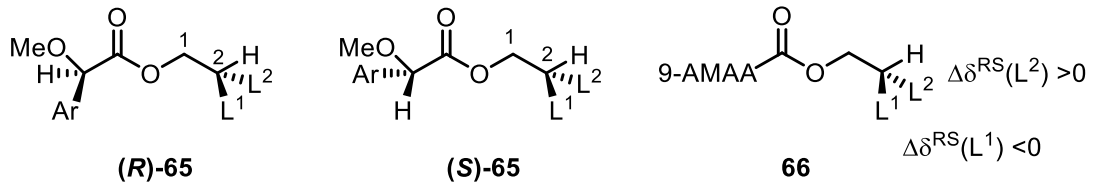

Figure 27 Conformational model for configuration assignment of primary alcohols

The methoxy and carbonyl groups and the proton located at the chiral center (C2) are in *syn*-periplanar conformation as is shown in (***R*)-65** and (***S*)-65.** The aromatic moiety can produce shielding effect towards one of the substituents either L^1 or L^2. The analysis is then conducted in a similar manner as with MTPA or MPA. The analysis of chiral primary alcohols and similar substrates is significantly more complex compared to analysis of chiral secondary alcohols:

a) The additional bond increases flexibility of the whole system and increase the ammount of possible conformers.

b) The chiral atom is located further apart from the functional group where the CDA is tethered.
c) The substituents L^1 and L^2 are also located further apart from the anisotropic group which causes the differences in the chemical shift

Those effects combined together cause the observed $\Delta\delta^{RS}$ values being significantly smaller compared to α-chiral secondary alcohols. The analysis can be further complicated by the presence of polar groups connected to a chiral center or by lack of observable signals in the substituents as can be exemplified with compounds **67**, **68**, and **69** (Figure 28). As can be seen, with the exception of **69,** those compounds possess substituents on a chiral center which does not have protons attached (with the exception of the proton itself, *vide infra*) therefore providing only one data point for analysis. This is not true for compound **69,** however the hydroxyl group protons are often exchanged with deuterium during the NMR experiments making them "invisible" in the experiment.

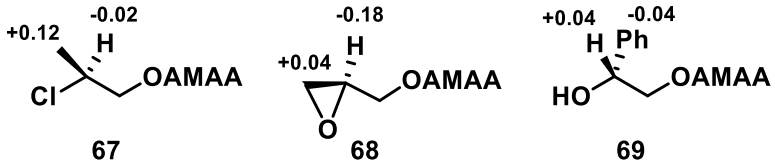

Figure 28 Examples of alcohols lacking protons at one of their substituents and their $\Delta\delta^{RS}$ values

This problem led to development of new conformational model for cases like this, which utilizes the proton bonded to the chiral atom (Figure 28, 29) which in the previous models is assumed to be coplanar (Figure 27) and therefore not showing any $\Delta\delta^{RS}$. This is often not true in real experiments, however the $\Delta\delta^{RS}$ is often smaller than those of substituents L^1 or L^2. Similar behavior can be observed in cases with significantly bulky group such as *Boc* being present in the molecule. (Figure 29).[92]

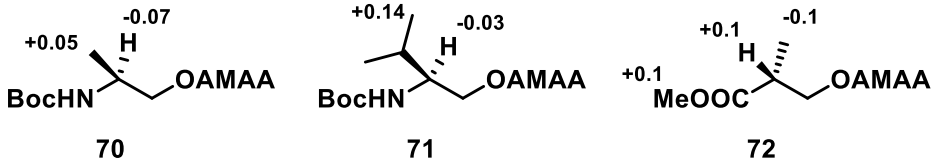

Figure 29 Major conformation of 9-AMAA esters with bulky substituents

As can be seen in Figures 28 and 29, the bulky group is located coplanar to the carbonyl group of 9-AMAA and the proton and other substituent assume the non-coplanar position which is then analyzed in a similar manner as described previously. The coplanarity of the bulky group is not exact and in some cases is slightly bent out of the plane. This non-planarity can be observed as $\Delta\delta^{RS}$ of the bulky group G and acts as another data point for the NMR analysis. The modified model is presented in Figure 30.

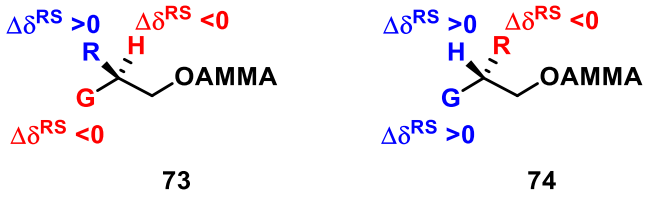

73 74

Figure 30 conformational model for assignment of configuration of 9-AMAA esters of alcohols without protons in their substituents

Analysis of cyanohydrins

MPA can be used to analyzed aldehyde[77] and ketone[78] cyanohydrins respectively. Although the cyanohydrin structure might structurally resemble structure of secondary and tertiary alcohols, the presence of highly polar cyanide group strongly affects the conformation. Both ^{1}H and ^{13}C spectra need to be analyzed, because the cyanide posses no observable hydrogen atoms. Since the aldehyde cyanohydrins are type of secondary alcohols, the conformation model described for compounds with no observable protons present (Figure 30) cannot be used. The modified MPA-model is shown in Figure 31.

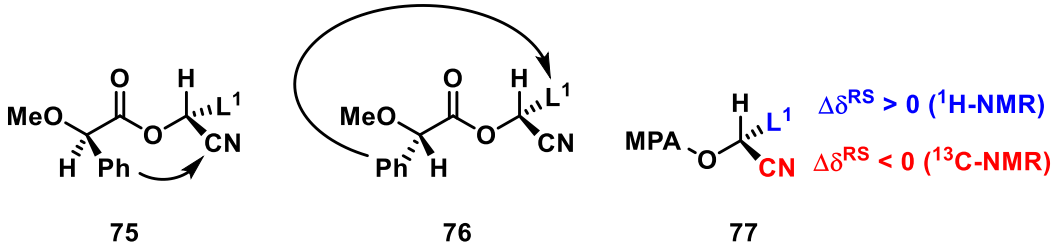

75 76 77

Figure 31 Conformational model for assignemtn of configuration of aldehyde cyanohydrins

The model (Figure 31) is based on MPA model for analysis of secondary alcohols (Figure 22, 23). Proton, carbonyl, and methoxy group are in *syn*-periplanar conformation which allows the phenyl ring to project the anisotropic shielding effect towards one of the substituents, either cyanide group in (*R*)-MPA ester **75** or L^1 in (*S*)-MPA ester **76**. The chemical shifts are compared and $\Delta\delta^{RS}$ calculated as usual. In this case, the ^{13}C spectrum is used as well to calculate $\Delta\delta^{RS}$(CN) to obtain the second data point for the analysis. If the configuration of the cyanohydrin is as shown in **77** in Figure 31, then the cyanide group has $\Delta\delta^{RS} < 0$ while the other substituent L^1 has $\Delta\delta^{RS} > 0$. Analogously, if the configuration is opposite, then the cyanide group has $\Delta\delta^{RS} > 0$ and the L^1 $\Delta\delta^{RS} < 0$.[77]

The analysis of ketone cyanohydrins[78] is more complicated since the esters are in dynamic equilibrium. Furthermore, the most stable conformer depends on the used enantiomer of MPA (Figure 32).

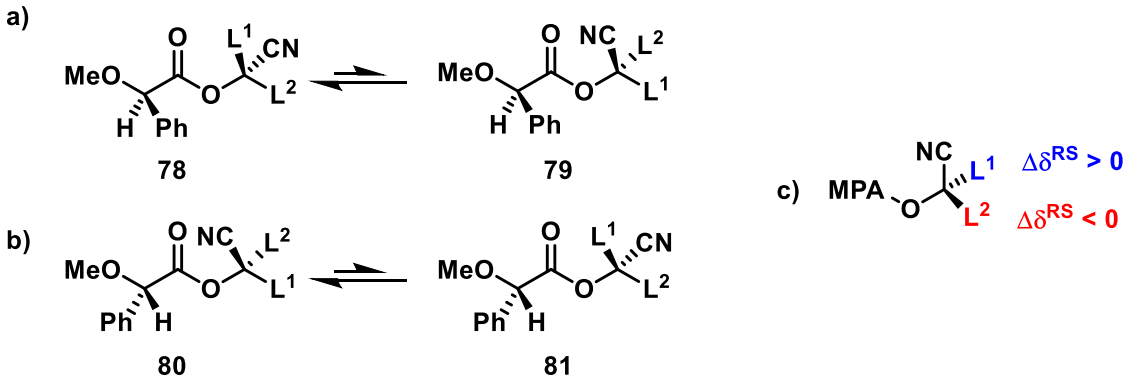

Figure 32 Conformational model for assignment of configuration of ketone cyanohydrins

a) Conformation of (*R*)-MPA esters b) Conformation of (*S*)-MPA esters c) simplification of the model

In the case of (*R*)-MPA esters (Figure 32a), conformer **78** is more stable than conformer **79** by 2.84 kcal/mol. In the case of (*S*)-MPA ester (Figure 32b), conformer **80** (similar in spatial orientation of substituents as **79**) is more stable than **81** by 0.94 kcal/mol.[78] In both cases, the more stable conformers **78** and **80** have the cyanide group opposite to phenyl in the MPA. This dynamic equilibrium can be simplified in the model depicted in Figure 32c with the cyanide group being syn-periplanar with carbonyl and methoxy groups which puts the L^1 and L^2 into the shielding zone of the phenyl ring.

Analysis of tertiary alcohols

Although the ketone cyanohydrins structurally resemble tertiary alcohols, the analysis of tertiary alcohols is significantly underdeveloped. The main limitation is the difficulty of esterification of such alcohols which still occurs with low yields eventhough new methods are emerging.[93] Furthermore, the substrate scope is limited to methyl substituted tertiary alcohols.[74,75,94]

MTPA **56** and MPA **58** can be used for this task but results in smaller $\Delta\delta^{RS}$ compared to 2-NMA **60** (Figure 33).[74,75] As can be seen for compounds **83**-**85**, the $\Delta\delta^{RS}$ is in the all cases smaller compared to secondary alcohols and comparable to MPA and MTPA esters of β-chiral primary alcohols. In all cases the carbon in α-position to the chiral center showed anomalous value therefore those are suggested to be not included in the analysis. Furthermore, the list of substrates tested was very limited and only includes those bearing methyl groups as the third substituent on the chiral center. This limitation is further increased because most of the tertiary aclohols tested were derived from geraniol. The likely cause is the lack of easily available enantiopure tertiary alcohols which could be used for the analysis.

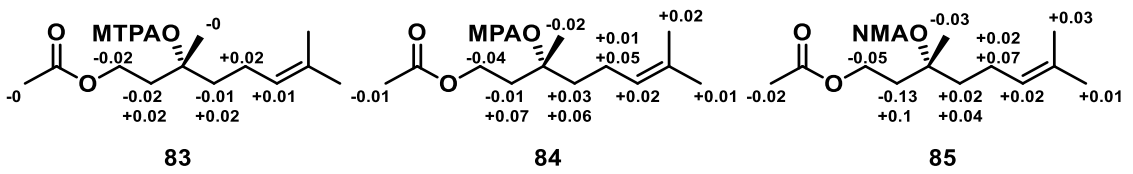

Figure 33 Examples of tertiary alcohols and $\Delta\delta^{RS}$ of their CDA esters

The conformational model is built upon the models previously developed for analysis of cyanohydrinds and secondary alcohols by MTPA or MPA. Similar to previous models, the methoxy group, carbonyl and methyl groups are in syn-periplanar configuration which leads to projection of the shielding effect towards L^1 in **86** or L^2 in **87** substituents. Due to the anomalous $\Delta\delta^{RS}$ detected in the α-position, proton and carbon signals associated with this position are omitted from the analysis as is shown in simplified model **88** (Figure 34).

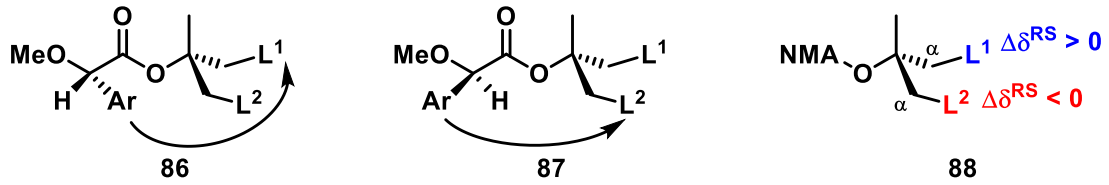

Figure 34 Conformation model for assignment of configuration of tertiary alcohols

Analysis of amines

Methoxyphenylacetic acid

The analysis of amines follows similar general procedures as analysis of hydroxy compounds. The most commonly used CDA is MPA. MTPA can be used as well and the use of different arylacetic acids has not shown significant improvement. The developed model for MPA is shown in Figure 35.[95] Interestingly, compared to MPA esters (Figure 22), the conformational equilibrium mainly consists of ap conformer which has the methoxy group *anti*-periplanar to carbonyl group and the proton bonded to chiral center (Figure 35a/b). It is important to mention this conformational preference, because using conformation model developed for MPA esters will lead to opposite configuration when used with MPA amides. This simplified model for MPA amides is shown in Figure 35c/d.

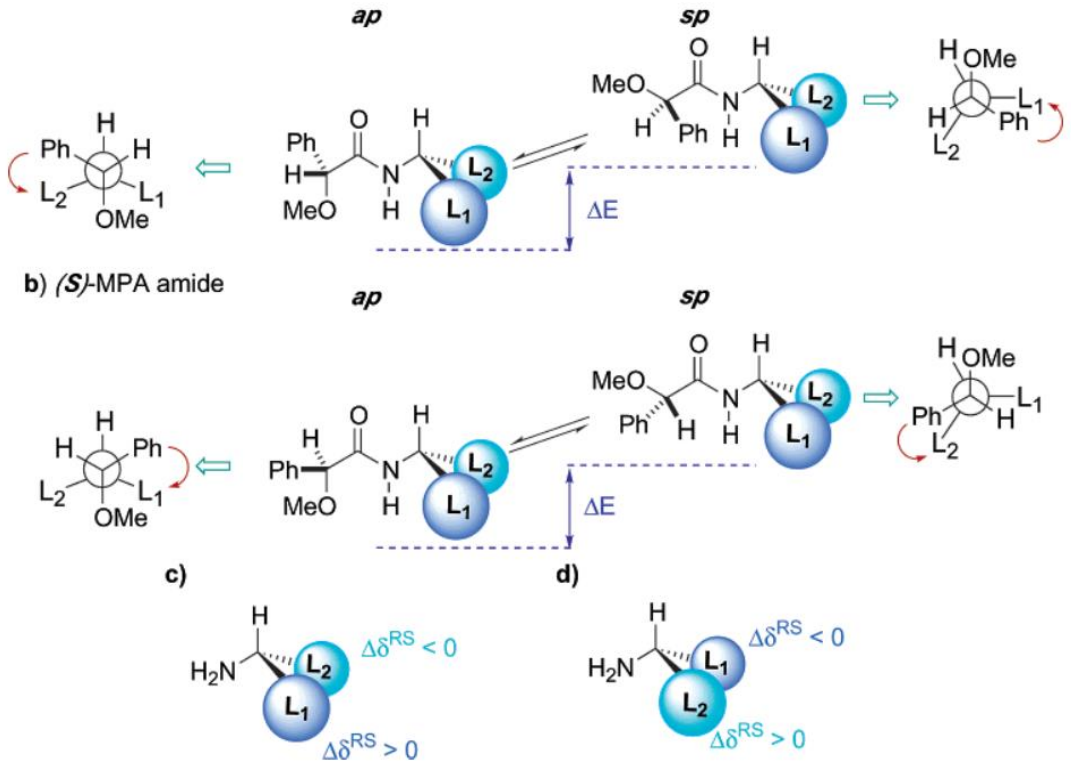

Figure 35 Major conformers of MPA amides (taken from [85])

Boc-phenylglycine

Boc-phenylglycine was tested as CDA for analysis of amines because unlike in case of esters, the structural modification of the CDA did not have significant effect. Compared to MPA or MTPA, boc-phenylglycine posess several advantages[70]:

a) Like MPA, the conformational equilibirium consists of only two conformers but the phenyl group is better positioned compared to MPA
b) Like MTPA the phenyl ring is in the better position but the effect of this ideal positioning in the case of MTPA is diluted by higher number of conformers.

The main NMR relevant conformer is shown in Figure 36. In the NMR-relevant ap conformer the proton on the phenylglycine part is in the *anti*-periplanar conformation with the carbonyl group and the proton on the chiral center. This configuration allows selective projections of the shielding effect towards the substituents. The calculations of $\Delta\delta^{RS}$ and configuration assignment are conducted analogously to the previously described MPA esters or amides.

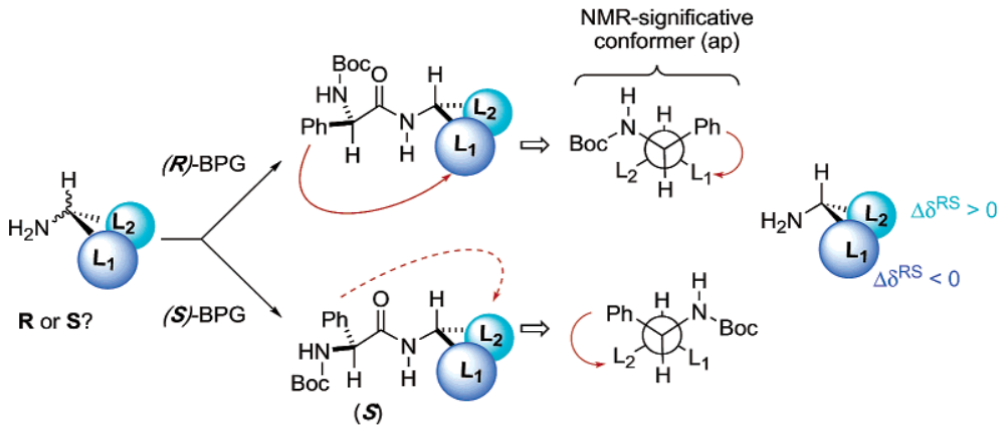

Figure 36 Conformational model for configuration assignment of chiral amines using Boc-PHG (taken from ref. [85])

Analysis of polyfunctional compounds

The analysis of polyfunctional compounds could be performed as well and was thoroughly reviewed by Seco.[96] It can be divided into two categories:

a) The case where the multiple bonded CDA does not interfere and therefore the analysis can be conducted in the same manner as described before.
b) The case where the multiple bonded CDAs interfere and therefore new models need to be described for the analysis of such compounds.

Examples of case a) are shown in Figure 37. In both *ent*-pimarane[97] **89** and foliasalacioside E1[98] **90** MTPA ester, the CDAs are bonded far apart from each other which shows no interference between them and therefore the previously described models can be easily used in the analysis of such compounds.

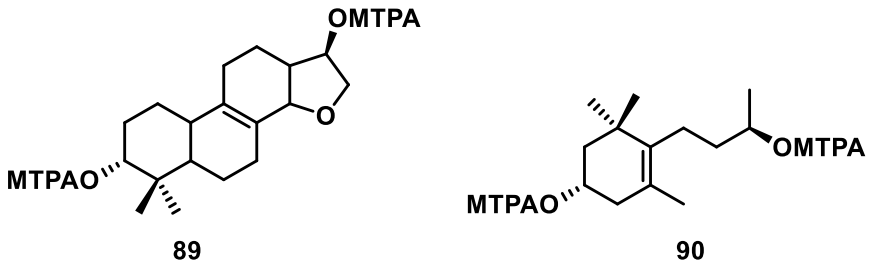

Figure 37 Configuration assignment of polyfunctional terpenes

In the cases where the CDAs are located closer together, interference of their influence towards the substituents in the molecule is complex and therefore new conformational models had to be developed. The models developed for 1,2, 1,3, 1,4-diols are shown in Figure 38. In those cases, the diols are

esterified with 2 equivalents of CDA to yield (*R*,*R*)-diester and (*S*,*S*)-diester and their NMR spectra are compared in similar manner as described previously.[96]

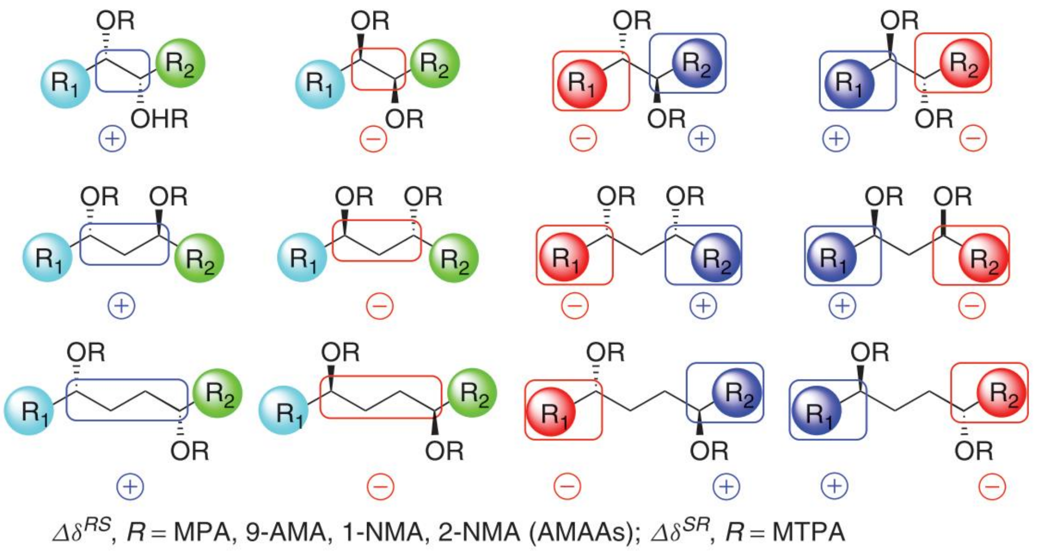

Figure 38 Observed differences of polyfunctional compounds with overlapping CDA effects (taken from ref. [99])

The analysis of 1,2-diamines proceeds similarly to 1,2-diols; however, they display different behavior than diols and require different conformational model (Figure 39).

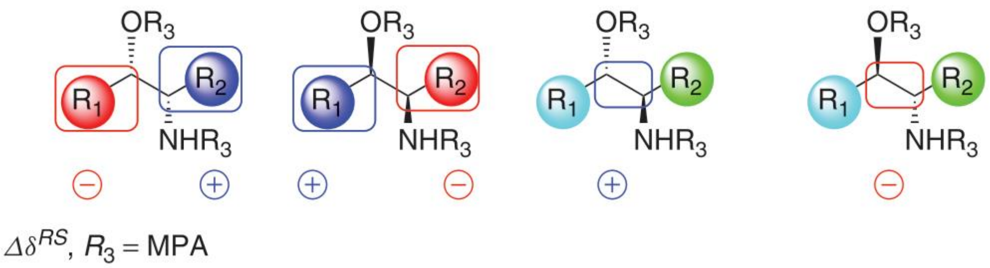

Figure 39 Observed differences of polyfunctional compounds with overlapping CDA effects (taken from ref.[99])

Interesting modification of previously described methods was recently reported by Orlov.[100] The modification consists of performing the derivatization in NMR tube without any purification. By using DCC+DMAP acylation in $CHCl_3$, the precipitated urea byproduct rises to the top of the solvent or falls down on the bottom of the NMR tube based on the used solvent (Figure 40)

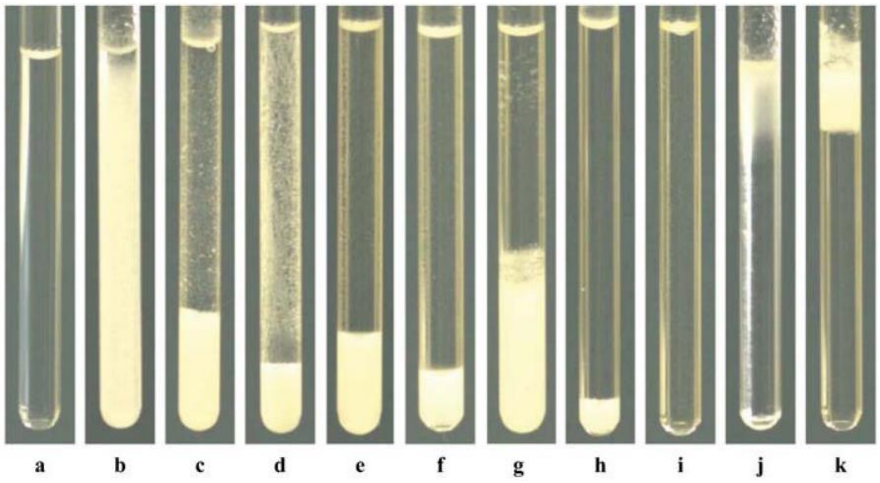

Figure 40 a) mixture of CDA and analyte, b) after addition of DCC, DMAP and shaking for 2 mins reactions after 1 hr in various deuterated solvents: c) ACN d) acetone e) toluene f) benzene g) THF h) DMF i) DMSO j) CS_2/DCM 4:1 k) $CDCl_3$ Picture taken from ref.[100]

This can be further exploited because the design of common NMR probe (Figure 41a) allows measurements of those samples because the measurement area is located approx. in the middle of the NMR sample as shown on Figure 41b/c.

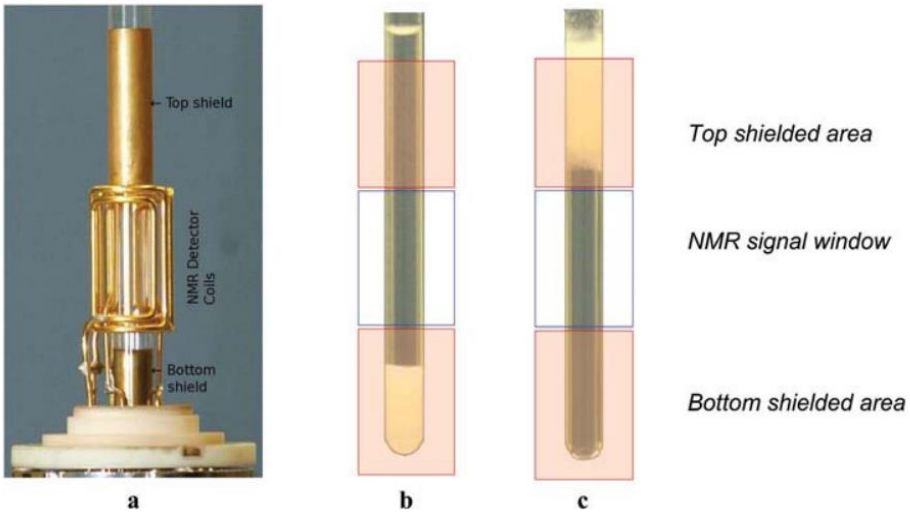

Figure 41 a) Common NMR probe b) schematics of NMR signal window and location of the residual resin. Taken from ref.[100]

This method allows for quick routine NMR configuration assignmnent or enantiomeric purity measurement of simpler structures since the presence of unreacted material might complicated more complex 2D NMR experiments.

Similar modification was already reported by Seco who used resin-bound MPA[101] for the analysis. Further addition of a scavenger resin traps any unreacted DMAP and MPA led only to the MPA ester in

solution. The procedure was further modified by use of mixed resin containing (*S*)- and (*R*)-MPA in 2:1 ratio. This allows for immediate configuration assignment because the mixture contains uneven ratio of diastereomers as can be seen in Figure 42. MTPA and Boc-phenylglycine resins were explored as well but they lost their floating properties which made them unsuitable for the task.

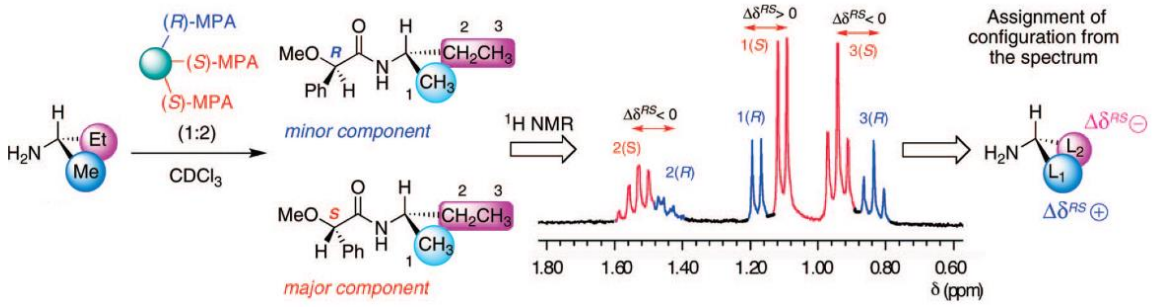

Figure 42 Assignment of configuration using resin bound CDA (taken from ref.[101])

Organocatalytic $HSiCl_3$ reduction of ketimines

The reduction of prochiral ketones or ketimines leading to chiral amines or alcohols is one the most important chemical transformations. There are various methods; some of them used in pharmaceutical industry were reviewed. [102,103] Those reaction often require use of metal catalysts which, although used in low % loadings, are not environmentally friendly.[104,105] The organocatalytic reductions provide interesting alternative because they do not require the use of transition metals. There are several approaches available: transfer hydrogenation using Hantzsch ester or other hydrogen sources and chiral acids, frustrated lewis pairs and hydrogen gas, borane reduction with CBS catalyst or trichlorosilane reduction using chiral catalysts.[106,107] Allylation raction using allyl-trichlorosilanes were reviewed by Denmark.[108] Due to the focus of the last project of this thesis on trichlorosilane reductions, only this area was reviewed.

One of the first examples of using trichlorosilane as a reducing agent comes from Benkesser (Scheme 14).[109]

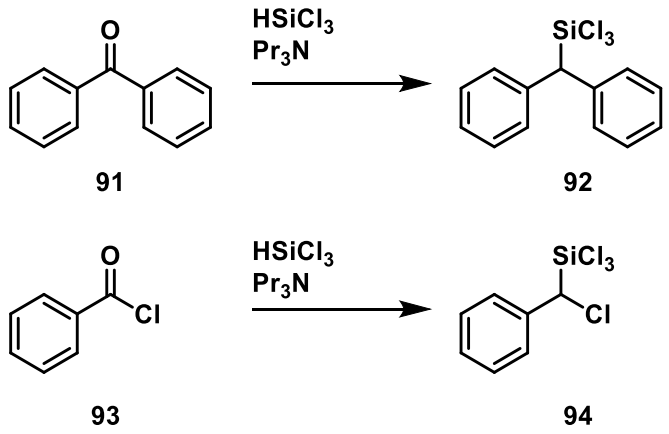

Scheme 14 First examples of reduction using $HSiCl_3$

Although organosilicon compounds were isolated instead of alcohols, it provides an interesting approach towards organosilicon compounds from carbonyls. The first real reduction of aldehydes and ketones was described in 1988 by Fujita who used fluoride source to activate the silane (Scheme 15).[110] The product **96** was obtained after hydrolysis of the resulting silyl-protected alcohols. Furthermore, the reaction proceeded with high *threo*-selectivity in the case of reduction of α-substitued-β-keto esters or amides **97**→**98**. Unfortunately, use of toxic HMPA as a solvent was required.

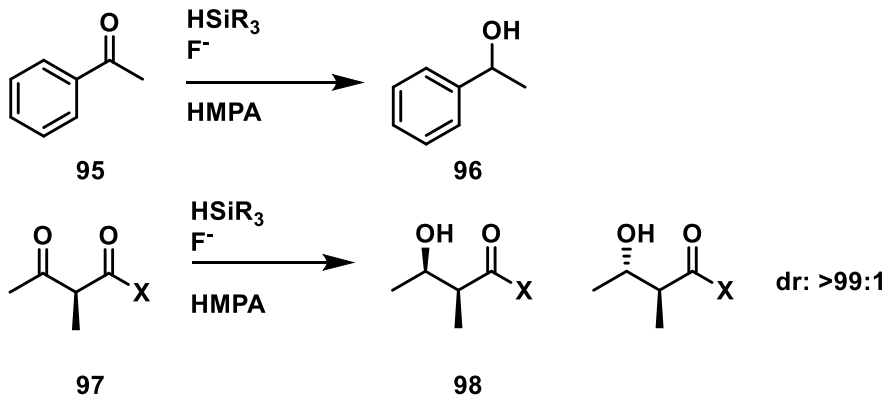

Scheme 15 Fluorine catalyzed reduction of ketones

Further modifications were performed by Kobayashi[111] who used DMF as a way to form active hypervalent silicon species which is the active reducing agent in the reaction. As could be seen in Scheme 16a the reaction proceeds with high yields using aldehydes as starting materials. Reduction of ketones proceeded slower with lower yields (Scheme 16b).

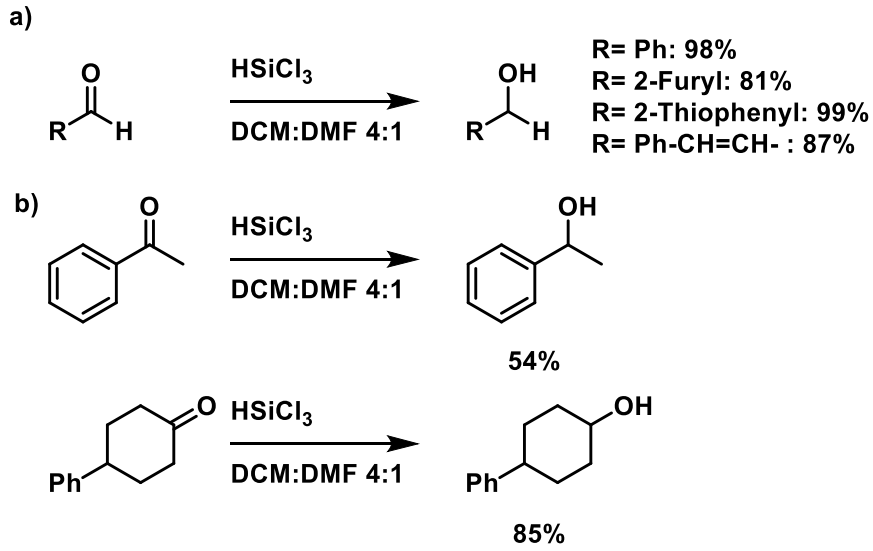

Scheme 16 DMF catalyzed reduction of ketones

High yields, although slightly lower compared to aldehydes, were also obtained using aldimines as starting materials (Scheme 17). Furthermore, in-situ reduction was also possible with yields ranging from 75-93%. This further expanded the scope to imines which are difficult to isolate.

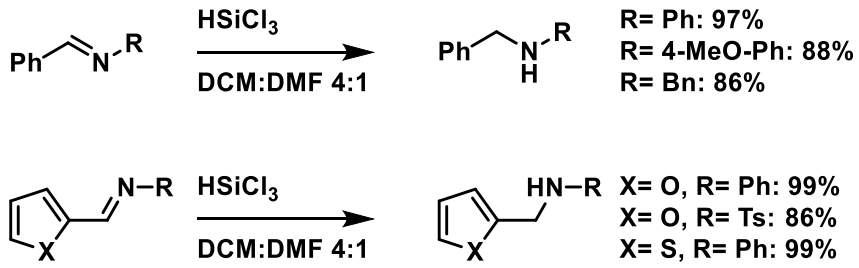

Scheme 17 DMF catalyzed reduction of imines

This methodology was further expanded to chiral DMF **99** (Figure 43) equivalent to promote organocatalytic asymmetric addition of allylsilanes (Scheme 18).[112]

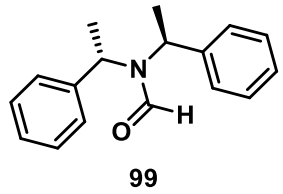

99

Figure 43 Chiral DMF analogue

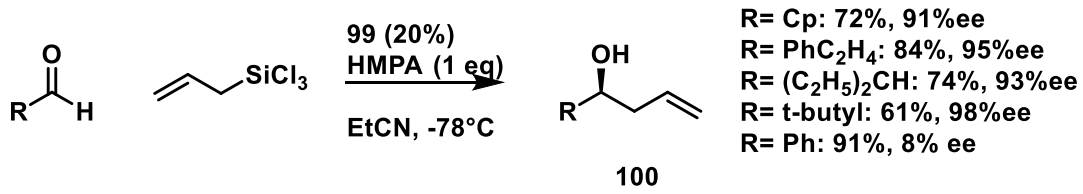

100

Scheme 18 Enantioselective allylaltion of aldehydes

Again, 1 equivalent of HMPA was used but various homoallylic alcohols were prepared in high yields (61-91%) and excellent enantioselectivity (91%-98%). Interestingly, in the case of benzaldehyde allylation only 8% enantiomeric excess was obtained. This methodology was further expanded on crotylation using (E)-crotylsilane **101** to obtain homoallylic alcohols **102** with high enantioselectivity and diastereoselectivity (Scheme 19).

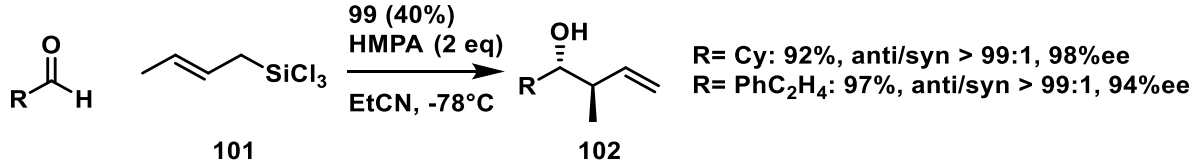

101 **102**

Scheme 19 enantioselective crotylation of aldehydes

Another reported ligands for asymmetric allylation come from group of Denmark who developed chiral phosphoramidites to obtain allylated products in high yields (67-95%) and moderate enantioselectivity (21-60%ee).[113]

There are examples using various silanes for asymmetric reduction they often used transitions metals as ligands.[114–116] The first organocatalytic asymmetric hydrosilylation of ketone imines comes from Iwasaki who developed chiral formamides based on proline.[117] Whole series of ligands **103-104** was prepared and tested.It was poved that the formamide moiety is the key for reactivity: reductions were attempted with DMAc as an activator but no product was obtained compared to reaction with DMF used as the activator.

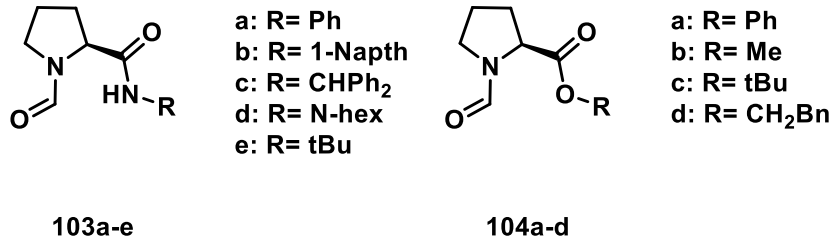

Figure 45 Proline-based formamide catalyst

The ligands were first tried to reduce acetophenone **105** (Scheme 20). The resulting phenylethanol **106** was obtained in high yields and moderate enantiomeric excess in the case of ligands **103.** The use of ligands **104** with ester functionality yielded products with lower yields and low enantiomeric excess.

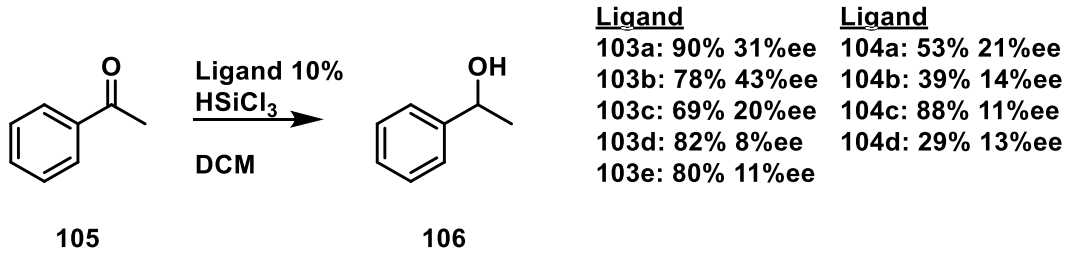

Scheme 20 Enantioselective reduction of ketones by proline-based catalyst

Five more ketones were reduced with ligands **103a** and **103b** and the alcohols were obtained in lower yields 21-87% and similar enantioselectivity (8-51%).

Ligands **103a** and **103b** were further used as ligands for asymmetric reduction of imines which were obtained in high yields (55-98%) and moderate enantioselectivity (49-66% ee).[118] Based on the (*R*)-configuration of the major enantiomer the transition state (Figure 46) was proposed. Trichlorsilane is activated by coordination of the ligand and the partially positively charged silicon atom is coordinated by imine nitrogen and the reduction is furnished by hydride transfer *via* the 4-membered cyclic state.

The orientation of the imine is preferably such that the aromatic ring of the "acetophenone part" of the imine is located on the opposite side than the aromatic ring of the catalyst (Figure 46a). The transition state leading to product with (*S*)-configuration is disfavored due to the steric interaction between aromatic rings (Figure 46b).

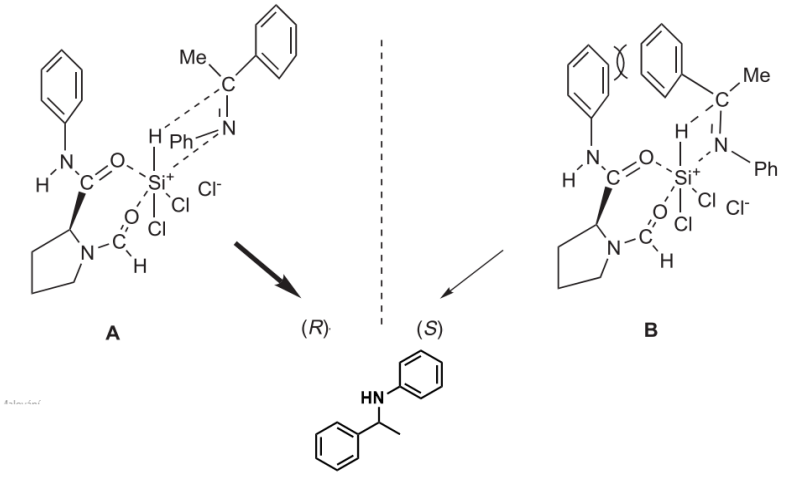

Figure 46 Transition state for reduction of imines by **103a**. Taken from ref.[118]

Kočovský further independently developed a similar valine based ligand **107.**[119] Multiple valine-based ligands were prepared with the optimal structure shown in Figure 47.

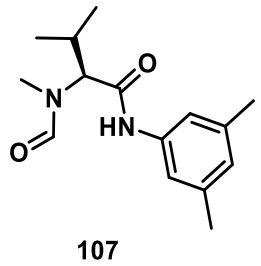

107

Figure 47 Valine-based ligand

The ligand was tested on variety of substituted imines (Figure 48) with products obtained in high yields (70-95%) and enantioselectivity (87-92% ee). Interestingly, the yields were slightly higher if the reaction was conducted at lower temperature -20°C (entries 1,4,6 vs entries 2,5,7) The effect of lower temperatuture on stereoselectivity was minor. The change of a solvent from $CHCl_3$ to toluene proved to be beneficial: the enantioselectivity of the reaction conducted in toluene at RT matched those attempts conducted in $CHCl_3$ at lower temperatures: entries 8,10,11 vs.2,5,7.

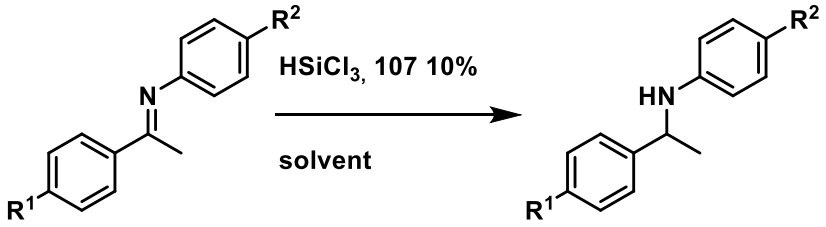

entry	R^1 / R^2	solvent	yield	%ee	temperature
1	Ph / Ph	$CHCl_3$	70	89	RT
2	Ph / Ph	$CHCl_3$	94	92	-20°C
3	4-MeOPh / Ph	$CHCl_3$	62	87	RT
4	4-CF_3Ph / Ph	$CHCl_3$	88	87	RT
5	4-CF_3Ph / Ph	$CHCl_3$	95	89	-20°C
6	Ph / 4-MeOPh	$CHCl_3$	79	86	RT
7	Ph / 4-MeOPh	$CHCl_3$	85	90	-20°C
8	Ph / Ph	Toluene	81	92	RT
9	4-MeOPh / Ph	Toluene	86	85	RT
10	4-CF_3Ph / Ph	Toluene	86	89	RT
11	Ph / 4-MeOPh	Toluene	85	91	RT
12	2-MePh / Ph	Toluene	90	92	RT

Figure 48 Reduction of prochiral imines catalyzed by **107**

Interestingly, although ligand **107** had the same configuration as previously reported proline ligands **103** products with the opposite configuration were obtained. The transition state was proposed according to the obtained configuration of the products (Figure 49).

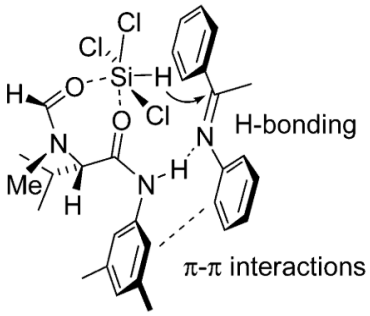

Figure 49 Transition state proposed for reduction catalyzed by ligand 107, taken from ref.[119]

Trichlorosilane is activated by coordination of formyl and amide carbonyl oxygens forming the active species. The imine is further activated by hydrogen bond from the amide nitrogen and the whole complex is held together by π – π interactions between the phenyl ring of the imine and the catalyst. Interestingly, this aryl-aryl interactions were reported to be the key for high enantioselectivity in spite of the previously reported transition state for proline-based ligands **103** (Figure 46). [117] This phenomena was investigated further[120] with series of modified ligands. Using ^{13}C NMR spectroscopy, the coordination of both formamide and amide oxygen atoms to $HSiCl_3$ was confirmed and further, the methyls in the amide moiety become non-equivalent suggesting hindered rotation around the C-N bond. Based on this investigation, the key features of the catalytic system were proposed (Figure 50).

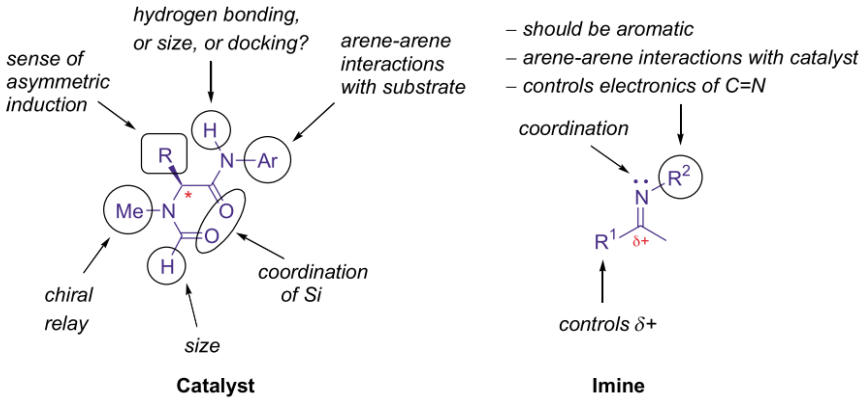

Figure 50 SAR of the aminoacid-based catalysts. Taken from ref[120]

The structure of the ligand was further modified by increasing the steric bulk of the structure[121] yielding ligand **108** (Figure 51,) which is commercially available. Ligand **108** was tested on more than 60 imines[122] with various structures including heteroaromatic and aliphathic imines. The yields were high: 20-99%, mostly 60-99% and enantioselectivities as well 6-95% mostly 75-95%. The low yields and enantioselectivities were encountered in the case of some heteroaromatic imines, especially pyridine-based which could coordinate to $HSiCl_3$ and induce the reaction *via* achiral transition state. This was confirmed by increase of the steric bulk around the pyridine nitrogen atom using 2,6-diisopropyl substitution which increased the enantioselectivity from 21 to 78 %ee compared to unsubstituted pyridine derivative. 2-chloroacetophenone derived imines were reduced as well which after treatment with a base yielded chiral aziridine derivatives with high enantiomeric purity.[121]

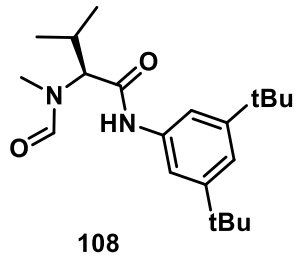

108

Figure 51 Optimized structure of valine-based catalyst

The structure was further modified and included fluorous tag[123] which simplified separation of the ligand or the ligand was immobilized on an insoluble polymer carrier[124] which allowed the catalyst to be reused at least five times without loss of the activity.

Structurally different oxazoline-pyridine ligands were also reported by Kočovský[125] (Figure 52)

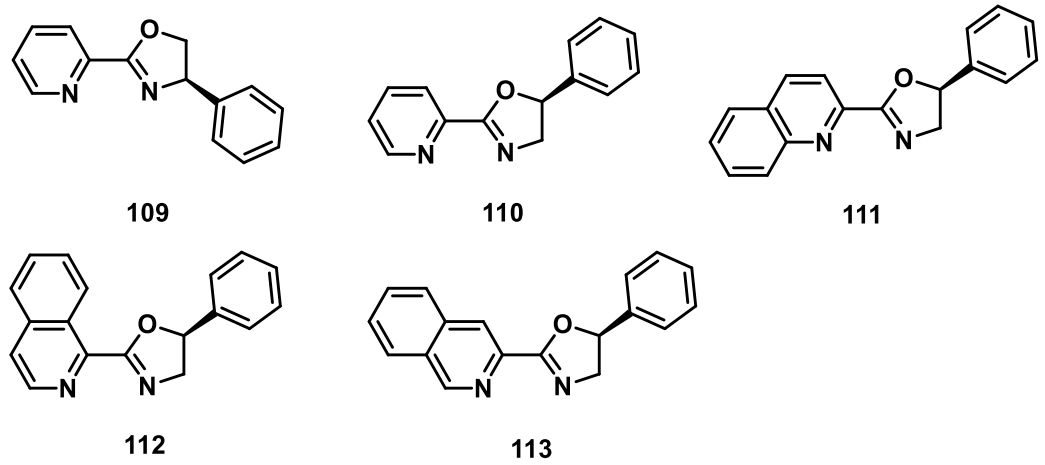

109 110 111

112 113

Figure 52 Oxazoline-based catalysts

At first acetophenone was used as model ketone. Ligand **109** derived from phenylglycinol yielded products in low 29% yield and 66 %ee which is significantly lower compared to previously described ligands. The isomeric ligand **110** derived from mandelic acid on the other hand provided enantioenriched alcohol in 85% yield and 78 %ee which is more comparable to previously reported ligands. Lower reactivity of ligand **109** is caused by close presence of the phenyl ring which is hindering the approach of the substrate as can be seen in intermediate **114**. This effect is not noticeable at assumed intermediate **115** derived from ligand **110** as can be seen in Figure 52. For this reason, further ligand optimization was conducted using the mandelate based structures **111-113.**[125]

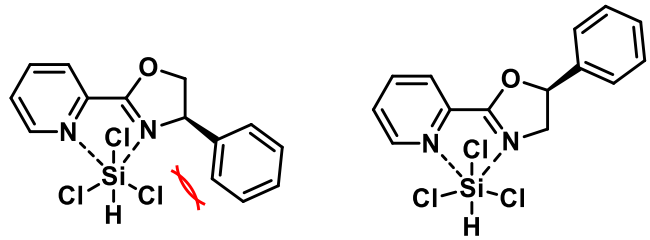

114 115

Figure 52 Proposed differences in transition states in reduction of imines with ligands **109** and **110**.

The best ligand showed to be **111** which provided reduced ketones in high yields 50-85% and enantioselectivities 70-95 %ee. Interestingly, in the case of ligand **110**, no products were obtained at all. Reduction of aliphatic ketone, cyclohexylmethylketone, provided product in 70% yield but as a racemate which suggests π – π interactions might play a role similar to ligand **107**. The proposed transition state is shown in Figure 53.[125]

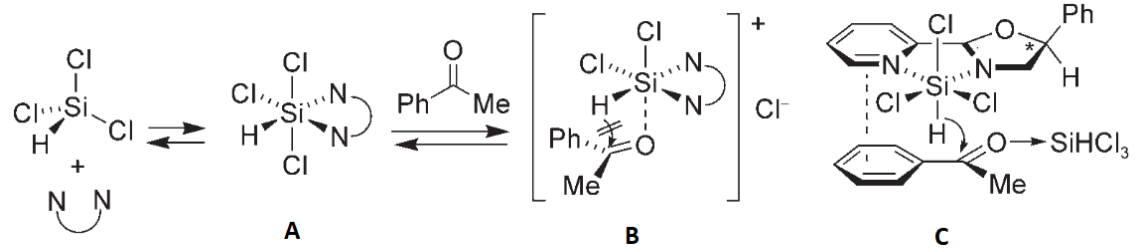

A B C

Figure 53 Proposed transition state for the $HSiCl_3$ reduction with ligand **107.** Taken from ref.[125]

At first the ligands coordinate to $HSiCl_3$ forming hexacoordinate silicone intermediate (Figure 53a). The intermediate can then react via 4-membered transition state (similar to one depicted on Figure 46) after the carbonyl oxygen coordinates to the silicon atom by displacing one of the chlorine ligands (Figure 53b). This transition state was deemed unlikely due to high strain in the 4-membered ring. Therefore the poposed transition state (Figure 53c) includes the activation of the ketone via coordination to another $HSiCl_3$ molecule while interacting with the ligand via aryl-aryl interaction.[125]

Different, pyridine-based ligands were developed by Zhang. The optimal structure **116** is shown in Figure 54.[126]

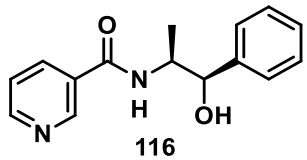

116

Figure 54 Zhang´s pyridine ligand

The use of ligand **116** catalyzed reduction of various imines in high yields (80-95%) and enantioselectivity 61-95%. This included amines **117** and **118** derived from aliphatic imine and benzylamine-derived imine which after deprotection yielded amine **119** (Scheme 21).

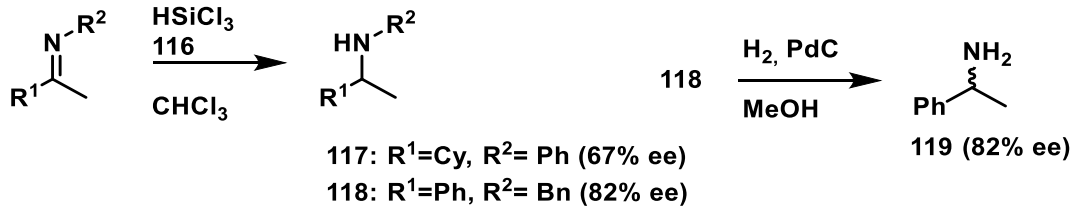

Scheme 21 Reduction of imines with ligand **116**

Different picolinic acid derived ligands were reported by Celentano[127,128] using binapthyl-2,2′-diamine including *N*-oxide **121** (Figure 55)**.** Ligand **120** provided amines in quantitative yields and moderate enantioselectivity (73-82%). The N-oxide derivative **121** yielded products in low yields 40-75% and inferior enantioselectivity (< 40% ee).

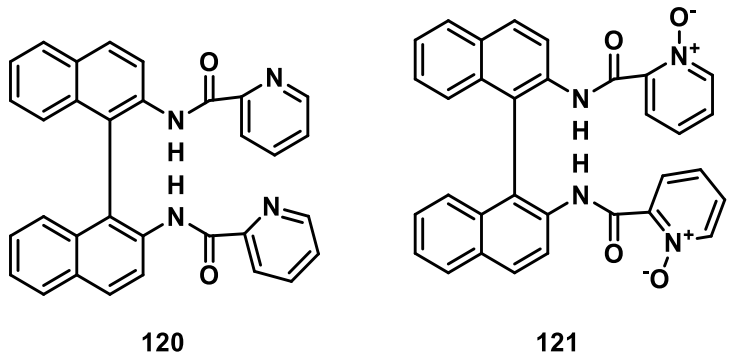

Figure 55 BINAM-derived ligands

Recently, chiral sulfinamide catalyst **122** (Figure 56) was reported[129] which yielded reduced amines in good yields (45-90%) and enantioselectivity (>90 %ee). (*P*)-chiral phosphineoxide ligand **123** and derivatives were presented by Jones[130]; however, only low enantioselectivity was observed (< 40 %ee, mostly around 20%).

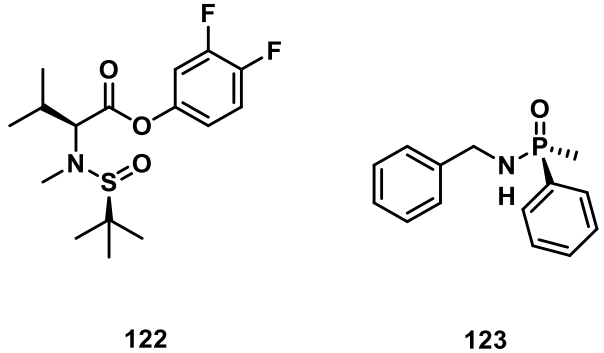

Figure 56 *S* and *P*-chiral ligands

Discussion and results: Project NMR

Synthesis of 2-(2-(trifluoromethyl)-1*H*-benzo[*d*]imidazol-1-yl)benzoic acid

Introduction

The structure of 2-(2-(trifluoromethyl)-1*H*-benzo[*d*]imidazol-1-yl)benzoic acid (TBBA) **1** is shown in Figure 1. The main features include the CF_3 group which should allow easy configuration assignment based on ^{19}F NMR. The carboxylic group functions as a tether to connect the analyte *via* an ester or amide bond. Last, the shielding effect is produced by the benzimidazole ring towards one of the substituents of the analyte. The main advantage over other CDAs was thought to be lower flexibility of the mostly aromatic system which possesses less flexible bonds compared to arylmethoxyacetic acids.

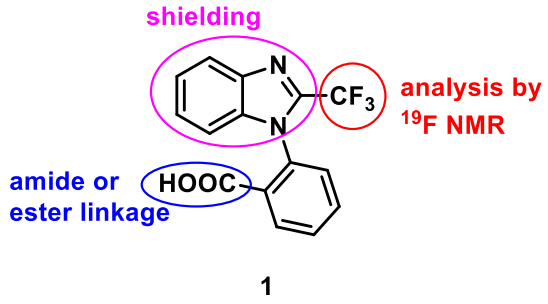

1

Figure 1 Structure of 2-(2-(trifluoromethyl)-1*H*-benzo[*d*]imidazol-1-yl)benzoic acid (TBBA) **1**

The proposed synthesis is depicted in Scheme 1. The key step is Chan-Lam arylation of benzimidazole **2** with 2-tolylboronic acid[131], followed by oxidation by $KMnO_4$ to yield **1** with subsequent chiral resolution of the racemate.

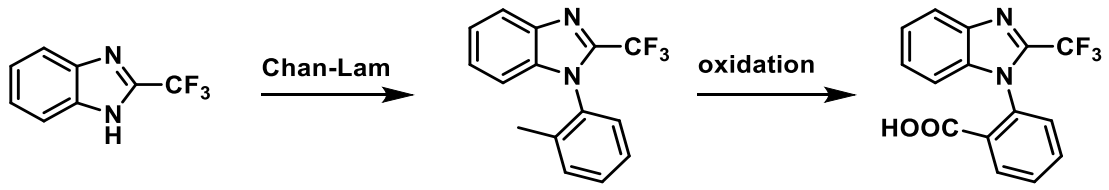

2 **3a** **1**

Scheme 1 Proposed Chan-Lam based synthesis of **1**

Chan-Lam approach

The starting benzimidazole **2** was prepared by refluxing *o*-phenylenediamine in trifluoroacetic acid according to the literature procedure in the high yield.[132] The reported arylation conditions were tried with *o*-tolylboronic acid (Table 1, entries 1and 2). No product was observed on TLC or HPLC analysis. To check the viability of reaction conditions, less sterically hindered *p*-tolylboronic acid was used as a

model substrate (entries 3, 4) and the catalyst loading was increased as well. Following those promising experiments with p-tolylboronic acids, further copper catalysts were screened with *o*-tolylboronic acid as a substrate (entries 5-11). Traces of product was observed in HPLC analysis; however, TLC showed starting materials and only faint new spots, which would make the isolation of product very difficult. The use of 2-boronobenzoic acid (entries 12,13) yielded no product at all. The low reactivity is likely due to the unfavorable structures of reagents: sterically hindered electron poor benzimidazole and sterically hindered boronic acid makes this coupling challenging. Because it was envisioned that the resolution of **1** by crystallization is going to require higher amounts of racemic material (grams) the coupling approach was abandoned.

Table 1 Chan-Lam coupling

entry	**Catalyst, %mol. equivalents**	**base**	**Boronic acid**	**Solvent**	**result**
1[131]	Cu_2S, 25%	TMEDA 1eq	o-tolylBA 1.5eq	DMF	No reaction
2[133]	$Cu(NO_3)_2$, 20%	TMEDA 10%	o-tolylBA, 2eq	MeOH	No reaction
3	Cu_2S, 50%	TMEDA 1eq	p-tolylBA 1 eq	DMF	70%*
4	$Cu(NO_3)_2$, 100%	TMEDA 2eq	p-tolylBA, 2 eq	MeOH	45%*
5	$Cu(OAc)_2.H_2O$, 100%	Pyridine 2eq	o-tolylBA, 2eq	DMF	Traces*
6	CuO, 100%	Pyridine 2eq	o-tolylBA, 2eq	DMF	No reaction
7	CuBr, 100%	Pyridine 2eq	o-tolylBA, 2eq	DMF	Traces*
8	CuI, 100%	Pyridine 2eq	o-tolylBA, 2eq	DMF	Traces*
9	$Cu(BF_4)_2$, 100%	Pyridine 2eq	o-tolylBA, 2eq	DMF	Traces*
10	$Cu(NO_3)_2$, 100%	Pyridine 2eq	o-tolylBA, 2eq	DMF	Traces*
11	Cu_2O, 100%	Pyridine 2eq	o-tolylBA, 2eq	DMF	No reaction
12	Cu_2S, 25%	TMEDA, 4eq	o-COOH-PhBA, 2eq	DMF	No reaction
13	$Cu(OAc)_2$, 100%	Pyridine 2eq	o-COOH-PhBA, 2eq	DMF	No reaction

* percentage of total area of peaks in HPLC at 260 nm

Cyclization approach

An alternative arylation-cyclization approach was further explored. At first, the 2-fluoronitrobenzene **4** was arylated with *o*-toluidine **5** followed by reduction of the nitrogroup and subsequent cyclization[132] to yield benzimidazole **3**.

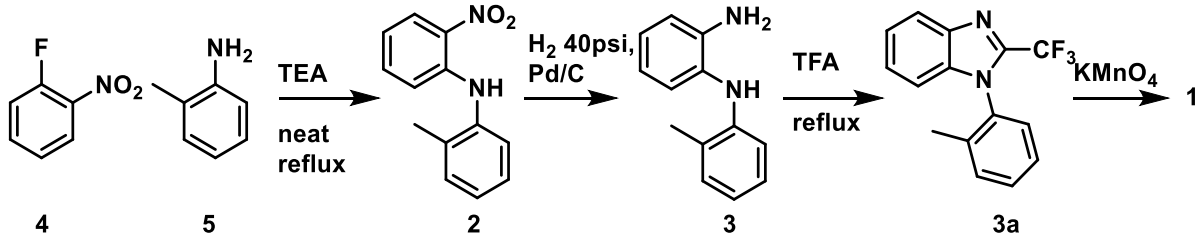

Scheme 2 Synthesis of **1** by oxidation of **3a**

Multiple arylation conditions were tried with a different success. The results are summarized in Table 2. Using NaH as a base the product was obtained in 70% yield while the use of triethylamine without any solvent provided product in 60% yield after simple dilution with water and filtration.

Table 2 *N*-arylation of 2-methylaniline **5** with 2-fluoronitrobenzene **4**

Entry	**Eq. 5**	**base**	**solvent**	**Temperature**	**yield**
1[134]	0.7	NaH	DMF	RT	70%
2	1	Et_3N	neat	150°C	60%
3[135]	1	--	water	100°C	No reaction
4[136]	1	DBU	neat	80→130°C	No reaction

The reduction of nitro group was performed by catalytic hydrogenation using palladium on carbon (Pd/C) as a catalyst at 40 PSI. Traces (<5% by HPLC) of starting material were still observed in the reaction mixture; therefore, purification by column chromatography was performed and the product was isolated in 75% yield. The arylated diamine **3** was then cyclized in boiling TFA and isolated after extraction to give 50% yield. Subsequently, oxidation was carried out with $KMnO_4$ in water. However, due to poor solubility of the starting material the reaction was sluggish and proceeded very slow (60% conversion after 48 hrs at reflux). The poor solubility was not the only problem. The product was isolated as an oil and, therefore, it adhered on the side of the reaction vessel, which further reduced the surface area available for the reaction. No product was isolated since an alternative approach was developed at the same time.

Further literature screening revealed another possible route which does not include the sluggish methyl oxidation step at the final stage of the synthesis. At first, 2-fluoronitrobenze **4** was arylated with anthranilic acid **6**, followed by reduction of nitro acid **7** and ring closure. This approach (scheme 3) not only removed the problematic oxidation step but also the arylation and reduction steps were reported on large scale.[137]

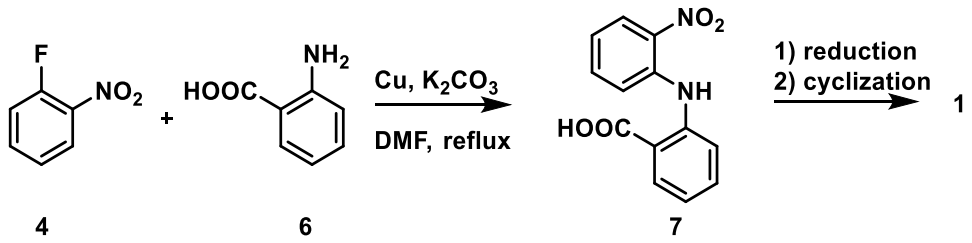

Scheme 3 Proposed synthesis of TBBA

The synthesis started with copper catalyzed Ullman arylation which after recrystallization from acetic acid yielded nitroacid **7** in 70%. The reaction worked on multiple scales ranging from 0.7 g to 33 g and was reproduced multiple times on the large scale with yields between 70-80%. The yields tend to increase with the reaction scale due to the slight difficulties in workup. The following reduction was slightly modified. Instead of Raney nickel and hydrogen at high pressures, Pd/C and a balloon filled

with hydrogen at atmospheric pressure was used. Using 5 mol% of palladium catalyst, the reaction was complete within two hours. The high speed of the reaction led us to reduce the amount of catalyst. In the end, 1 mol% of catalyst was used and the reaction was finished after 16 hours (overnight). Simple filtration through a short pad of silica or celite and evaporation provided the product in quantitative yields. The reaction was scaled up to 22 g of starting material. The higher scale up was not possible due to lack of suitable glassware: the solubility of nitroacid **7** in ethylacetate is relatively low; therefore, the reaction starts in a suspension. Furthermore, if the reaction flask was more than half filled with the reaction mixture, the rate of the reaction decreased. This was likely caused by the reduction of the surface contact between the reaction mixture and hydrogen gas in the flask.

The final cyclization was more complex than expected. Using the previously described conditions (refluxing TFA) yielded a complex mixture of products; however, desired benzimidazole **1** was detected in HPLC in aprox. 30%. Multiple other products were detected and their plausible structures deduced from the LCMS analyses are depicted in Figure 2.

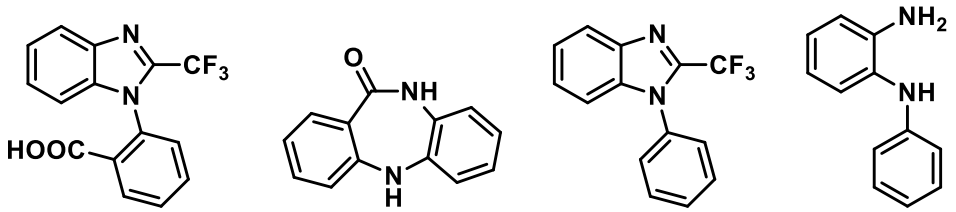

1 30% **8** 18% **9** 30% **10** 5%

Figure 2 Proposed structures of byproducts after cyclization to 1

Unsurprisingly, the 1,4-dibenzodiazepine was also detected. Interestingly, the decarboxylated compounds **9** and **10** were also detected in the HPLC-MS analyses as well. Although unexpected, examples of acid catalyzed decarboxylation can be found in the literature.[138,139] Optimization of the cyclization reaction is shown in Table 3.

Table 3 Cyclization to TBBA

entry	**reagent**	**solvent**	**temperature**	**result**
1	TFA	Neat	70°C	30%*, complex mixture
2	TFA	Neat	50°C	No reaction
3	TFA	Neat	RT	No reaction
4	TFA	DCM	RT	No reaction
5	TFAA	neat	RT	mixture
6	TFAA 10eq	THF	RT	mixture
7	TFAA 10eq	dioxane	RT	mixture
8	TFAA 10eq	acetone	RT	mixture
9	TFAA 10eq	$CHCl_3$	RT	mixture
10	**TFAA**	**neat**	**40°C**	**40-95% isolated yield**
11	TFAA 3eq	toluene	90°C	60% isolated yield

* percentage of total area of peaks in HPLC after integrating at 260 nm

At first, milder conditions were attempted; however, the decrease of the reaction temperature provided no reaction at all. Further dilution with DCM did not provide any improvements as well. The use of more reactive trifluoroaceticacid anhydride (TFAA) showed significant improvement. The use of various solvents (entries 6-9) gave a mixture of products. The cyclization in the boiling neat TFAA provided complete conversion to the product which was isolated in 40% yield after extractive workup. Further optimization of the workup improved the yields to 95% after simple precipitation in cold water. Slow addition into a large excess of cold water and vigorous stirring was found to be crucial. Higher rates of addition or slow stirring produced a gray-green oily material which was difficult to filter and contained residues of TFAA and TFA locked inside the solid material. Luckily, this material can be dissolved in a minimal amount of MeOH and re-precipitated again. Slow addition during vigorous stirring yielded light gray solid powder. The reaction was further scaled up to yield 15 g of **1** after precipitating in 2.7 litres of cold water under stirring with an overhead stirrer. Use of 3 equivalents of TFAA in toluene provided the product as well, however a byproduct identified as a mixed anhydride of the product and TFA was observed. This anhydride was attempted to hydrolyze with sodium hydroxide and after extractive workup the product was isolated in 60% yield. In the end of the optimization, the reaction in neat TFAA was used to produce racemic **1** on 15 g scale multiple times with high reproducibility.

Resolution of enantiomers

Crystallization

The resolution via crystallization was challenging. TBBA has good solubility in all tested organic solvents (EtOAc, THF, EtOH, acetonitrile, acetone, acetic acid and methanol) and usually precipitates by addition of water. The results are summarized in Table 4. Use of MeOH, isopropanol, acetonitrile, or THF as a solvent did not lead to precipitated product. The addition of the resolving agent in water instantly yielded oil with no enantioenrichment. The low solubility of the reasolving agent and TBBA was attempted to overcome by use of hydrochloride salt of the resolving agent and sodium salt of TBBA both being soluble in water. The mixing of their aquaeous solutions immediately produce an oily precipitate, which was not soluble in water even after heating; however, no enantioenrichment was observed.

Table 4: Resolution of TBBA by crystallization

Resolving agent	**equivalents**	**solvent**	**Additive**	**results**
(*R*)-1-phenylethan-1-amine	1	MeOH		No crystallization
(*R*)-1-phenylethan-1-amine	1	Water		oil
(*R*)-1-phenylethan-1-amine	1	Isopropanol		No crystallization
(*R*)-1-phenylethan-1-amine	1	Acetonitrile		No crystallization
(*R*)-1-phenylethan-1-amine	1	THF		No crystallization
(*R*)-1-phenylethan-1-amine.HCl	1	Water (0.15M)	KOH	No crystallization
(*R*)-1-phenylethan-1-amine.HCl	0.5	Water (0.15M)	KOH	No crystallization
(*R*)-1-phenylethan-1-amine.HCl	0.5	Water (0.1M)	KOH	No crystallization
(*R*)-1-phenylethan-1-amine.HCl	1	Water (0.3M)	KOH	oil
(*R*)-1-phenylethan-1-amine.HCl	0.5	toluene		No crystallization
PE-I-mix*[140]	1	MeOH		No crystallization
PE-I-mix*[140]	1	Acetonitrile		No crystallization
PE-I-mix*[140]	1	EtOAc		No crystallization
(*L*)-Proline	1	MeOH		No crystallization
Quinine	1	MeOH		No crystallization
(*S*)-Phenylglycinol	1	MeOH		No crystallization

* PE-I-mix: equimolar mixture of (*R*)-1-(*p*-chlorophenyl)ethylamine, (*R*)-1-(*p*-bromophenyl)ethylamine, (*R*)-1-(p-methylphenyl)ethylamine.

The use of "Dutch resolution"[140–142] method was attempted based on the experience from chiral resolution in one of the other projects. In general, the "Dutch resolution" is a method which utilizes a mixture of resolving agents used at once. Not only it allows rapid screening of various resolving agents, but often the components of a resolving mixture do not yield resolved material when used by themselves instead of in a mixture. It was shown that the diastereomeric salt consists of unequal ratios of the resolving agent and the minor component play important role in the crystallization.[140,141] Nevertheless, even this modified method did not work. Further, a few more resolving agents were attempted with zero success.

Conversion to diastereomers

Since the resolution by crystallization did not work, we turned our attention towards other methods. Acid **1** was converted into diastereomeric amides using L-alanine-methylester as a model example to develop suitable acylation conditions.

Table 5 Acylation of L-alanine methylester with TBBA

entry	Reagent	Solvent	results
1	T3P+pyridine	EtOAc	No reaction
2	Ethylchloroformate	DCM	Complex mixture
3	CDI	THF	Complex mixture
4	$SOCl_2$	Toluene, reflux	70%
5	$(COCl)_2$, cat. DMF	Toluene	No reaction
6	EDCl, HOBt	DMF	65%

Acylation conditions are summarized in Table 5. Use of propylphosphonic anhydride / pyridine in EtOAc (entry 1) provided no reaction.[143] Formation of mixed anhydride via ethylchloroformate (entry 2) or CDI (carbonyldiimidazole) (entry 3) yielded complex mixtures of products. Following those reactions, we turned to two step process via the intermediate acyl chloride (entry 4, 5). Use of 5 eq. of $SOCl_2$ in toluene at reflux provided the acyl chloride in the quantitative yield while the use of oxalylchloride-DMF at room temperatures proved to be unsuitable. The use of carbodiimide activator was explored as well (entry 6) with 1-Ethyl-3-(3-dimethylaminopropyl)carbodiimide (EDCl) in combination with 3-hydroxybenzotriazole in DMF provided similar results to the use of thionyl chloride. Due to much faster reactivity, the acyl chloride method was preffered initially. The diastereomeric mixture was inseparable with common methods.

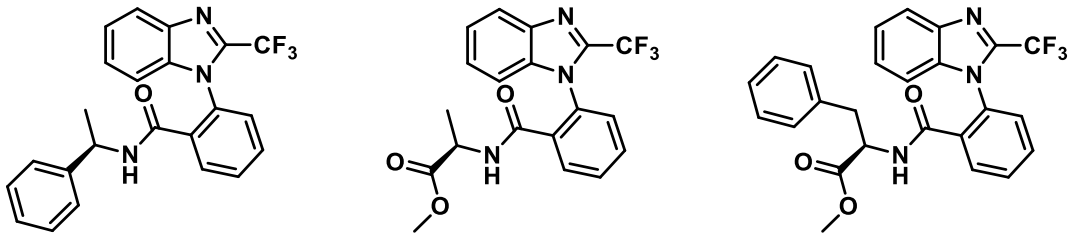

Figure 3 Amides prepared for separation of atropoisomers

Different amides were formed (Figure 3): (*R*)-1-phenylethan-1-amine **11,** L-alanine-methylester **12**, and L-phenylalanine-methylester **13.** Amide **11** provided 100:3 dr after three crystallizations from EtOAc:hexane mixture in low yield (10%). Although the resolution via formation of diastereomeric amides did not work, the analysis of NMR spectra of amide **11** revealed reasonable separation of the signals in NMR spectra (Figure 4), which would allow for the configuration assignment if a suitable conformation model was developed.

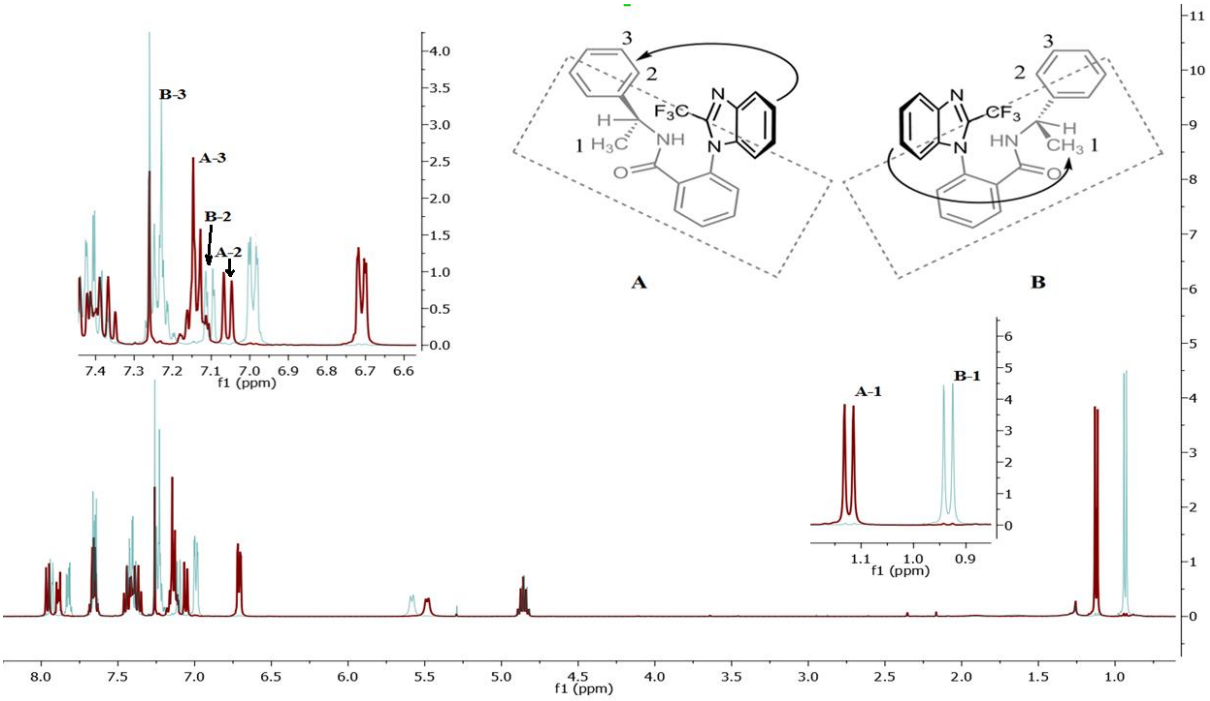

Figure 4 Overlaping NMR spectra of amide **11**

We assumed the high flexibility of the amide is the cause of difficult separation; therefore, more rigid oxazoline **15**was explored (Scheme 4). Multiple methods were investigated to form oxazolines.

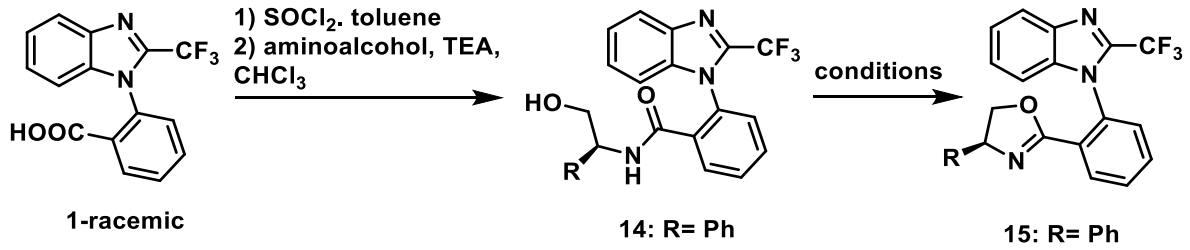

Scheme 4 Two step synthesis of oxazoline **15**

At first, a direct conversion of **1** into **15** was attempted by heating the acid in presence of the aminoalcohol in toluene; however, no product was observed. Second, the diasteremeric amides **14a** and **14b** were prepared using the previously described method, but they were not possible to separate by chromatography. Various cyclization conditions were then explored (Table 6).

Table 6 Synthesis of oxazolines **15**

entry	**conditions**	**results**
1[144]	Direct raction of **1** with aminoalcohol	No reaction
2[145]	BF_3.OEt	No reaction
3	T3P, TEA	Traces on TLC
4[146]	MsCl, TEA, DMAP	50% conversion
5[147]	pTSA,	No reaction
6[148]	$SOCl_2$ then NaOH	60-80% isolated

The cyclization with BF_3.OEt (entry 2) provided no product at all, while use of propylphosphonic anhydride (T3P) shown traces of new products on TLC and HPLC. Most importantly, those spots were separated enough to allow preparative separation (entry 3). The cyclization using MsCl and base provided aprox. 50% by HPLC while the acid catalyzed dehydration (entry 5) did not show any product. Two step reaction using $SOCl_2$ and then aq. NaOH provided full conversion to diasteremeric oxazolines **15a** and **15b** which were then separated using common column chromatography with 60 and 80% yields for each diastereomer. For the preparative separation, phenyl substituted oxazoline **15a** was used because the separation on TLC was slightly better compared to isopropyl derivative **15b**. Unfortunatelly, the separation could not be scaled up above aprox. 2g scale due to the poor separation of the diastereomers. This could be partially solved by separation of the mixed fractions by second column chromatography but further scale up was not attempted.

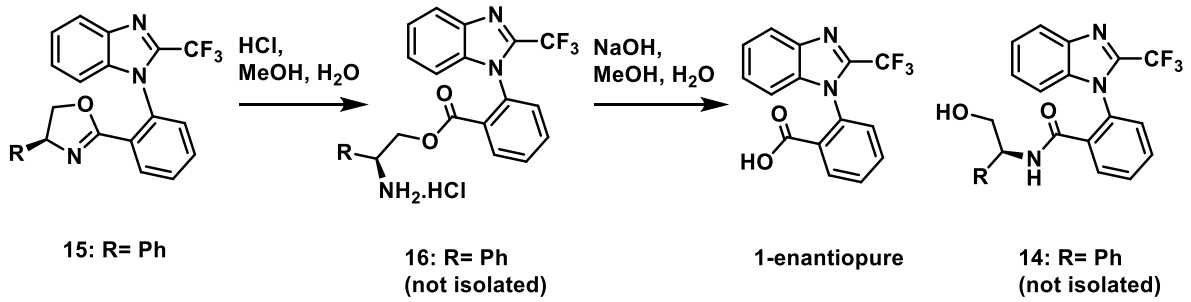

Scheme 5 Hydrolysis of oxazolines **15**

The oxazoline was then hydrolyzed using HCl promoted ring opening followed by NaOH hydrolysis of the resulting ester **16** (Scheme 5). One byproduct was observed during the hydrolysis with the same m/z ratio as the intermediate **16.** The proposed structure of the byproduct formed by the intramolecular amidation of **16** is shown in Scheme 5.[149] Fortunately, it was possible to remove this byproduct by simple exctraction and enantiopure acid **1** was isolated by precipitation from water in 60-70% yield. The enantiomeric purity was confirmed by chiral SFC analysis as shown in Figure 5.

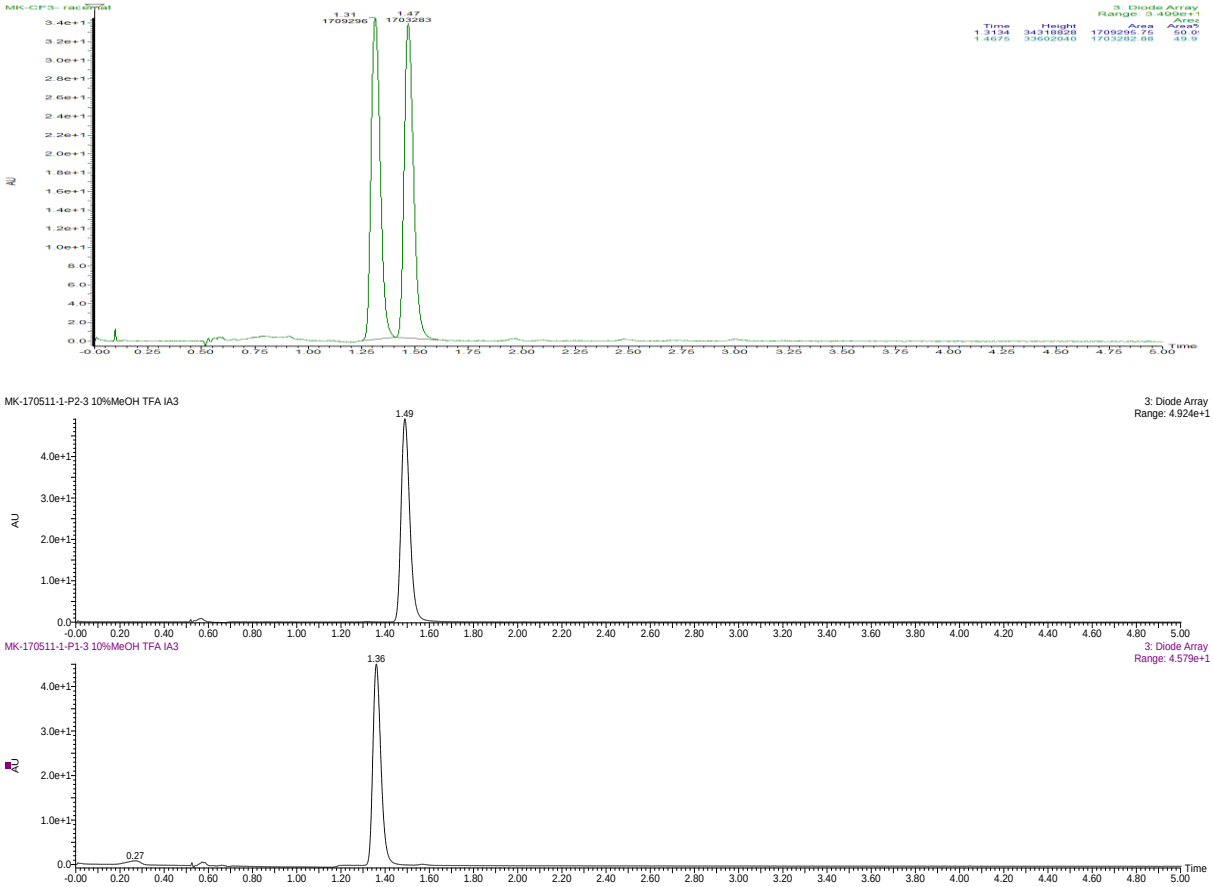

Figure 5 top: racemic mixture, middle: (*M*)-TBBA, bottom: (*P*)-TBBA

The absolute configuration of the chiral axis was determined by single crystal X-Ray crystallography of the derivative **11** prepared from enantiopure TBBA (Figure 6).

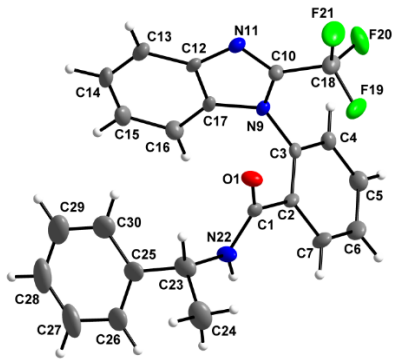

Figure 6 The molecular structure of (***R,P***)-**11** (CCDC 1871600) together with the atom labelling scheme. The thermal ellipsoids are drawn at the 50% probability level. Only one of the seven crystallographically independent molecules is depicted for clarity.

Atroposelective synthesis

Recently, atroposelective approach to 2-trifluoromethylbenzimidazoles was published by Miller group (Scheme 6a). The chiral acid catalyzed cyclization of the trifluoroacetamide **17** yielded the benzimidazole derivative **18** in high enantiomeric excess.[45,46] Similar approach towards the atroposelective synthesis was already attempted in our group by undergraduate student David Profous (Scheme 6b);[150] however, the results were disappointing since the cyclization of oxazoline **19** with various cyclization reagents yielded benzimidazoles. The diastereomeric ratio was poor and the best result was obtained in the ratio 1.3:1 dr for benzimidazole **20**.

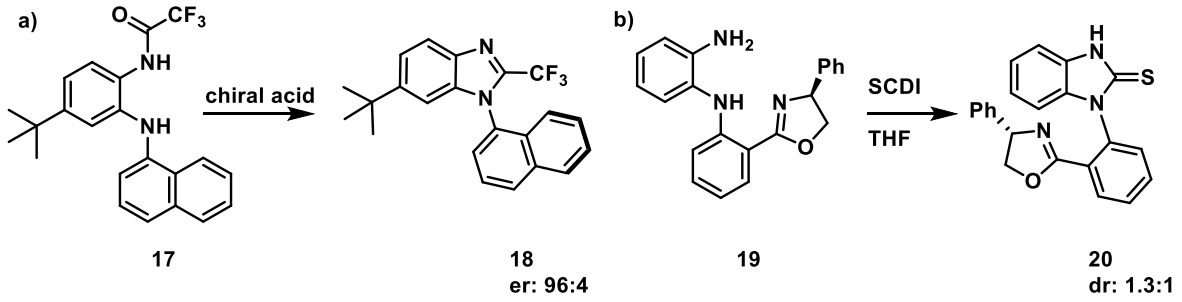

Scheme 6 a) atroposelective cyclization by Miller[45,46] b) atroposelective synthesis by David Profous[150]

This led us to investigate the possibility of the atroposelective routes towards **1**. At first the starting materials need to be prepared. The acylation of aminoacid **21** into trifluoroacetamide **22** seemed straightforward at fist and the product was isolated by simple filtration in 30% yield. The reaction proved to be hard to reproduce; however, enough material was isolated to attempt atroposelective cyclodehydration.

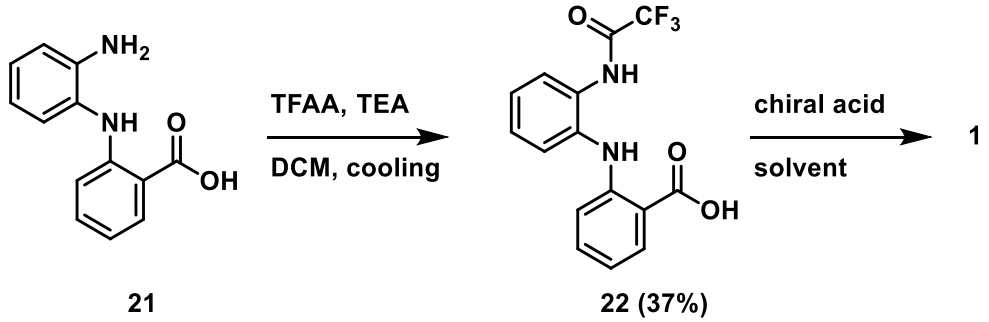

Scheme 7 Proposed synthesis of **1** by atroposelective cyclization

Various chiral acids were tested in the model reaction. The results are summarized in Table 7. Only trace conversion (<5%) was observed in entries 1-6. Nevertheless, the reaction mixtures were submitted to chiral SFC analysis and the enantiomeric ratio was determined. As can be seen in Table 7, moderate enantioselectivity was observed. At first, 10-camphorsulphonic acid (10-CSA) was tested (entry 1)

which provided the acid in 25/75 er. to prefer the (*M*)-isomer. Tartaric acid derivatives (entries 2-4) showed similar enantioselectivity as 10-CSA. In the case of entry 2, small crystals appeared in the flask after standing at room temperature. The quench of the reaction, which was analyzed as well, showed a racemic mixture. BINOL-derived phosphonic acid (*S*)-TRIP (entry 7) did not yield any product at all. Toluene was used as well in an attempt to increase the reaction rate at higher temperature. However, TLC analysis after 24 hours showed only faint shadows of the product, which was not possible to analyze *via* chiral SFC (only a starting material was detected).

Table 7 Chiral acid catalyzed cyclization of **22**

entry	**acid**	**Solvent**	**Er**
1	10-CSA	THF (65°C)	25 / 75
2	L-dibenzoyltartaric acid	THF (65°C)	26 / 74
			50 / 50 (precipitate)
3	L-dianisoyltartaric acid	THF (65°C)	26 / 74
4	L-ditoluolyltartaric acid	THF (65°C)	26 / 74
5	L-proline	THF (65°C)	40 / 60
6	(*R*)-Mandelic acid	THF (65°C)	28 / 72
7	(*S*)-TRIP	THF (65°C)	nd*
8	10-CSA	Toluene (80°C)	nd
9	L-dibenzoyltartaric acid	Toluene (80°C)	nd
10	L-dianisoyltartaric acid	Toluene (80°C)	nd
11	L-ditoluolyltartaric acid	Toluene (80°C)	nd
12	L-proline	Toluene (80°C)	nd
13	(*R*)-Mandelic acid	Toluene (80°C)	nd
14	TBBA	Toluene (80°C)	nd
15	(*S*)-TRIP	Toluene (80°C)	nd

* nd: not detected

Since the synthesis of starting material **22** provided irreproducible results, different approaches were explored. At first, we thought the carboxylic acid was responsible for the difficulties in preparation of the compound **21**; therefore, it was protected as a methylester.

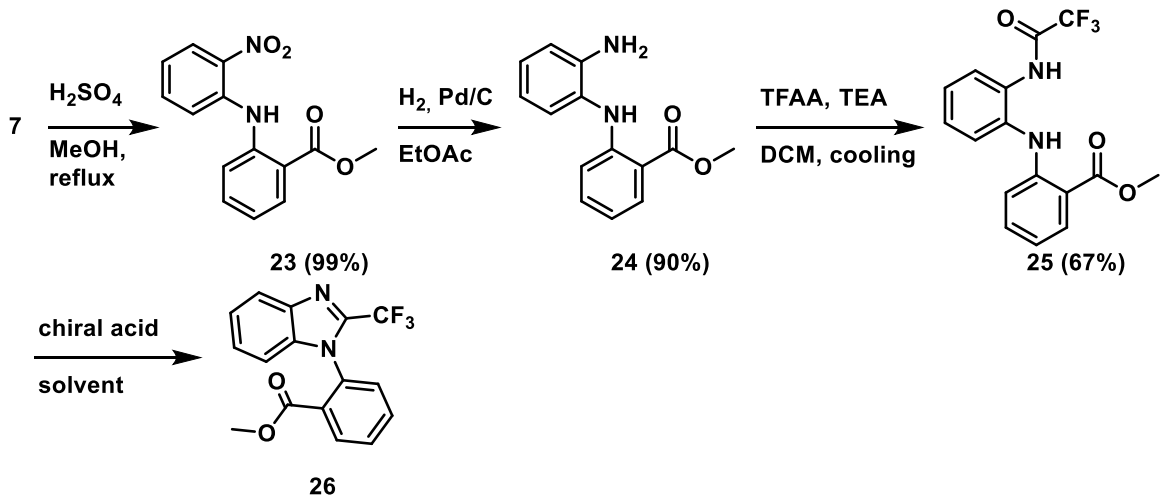

Scheme 8 Proposed synthesis of **26**

The nitro-acid **7** was refluxed in methanol in the presence of sulphuric acid. After simple filtration, methylester **23** was isolated in the 90% yield. The hydrogenation of the nitroester required slightly higher catalyst loading (5%); nevertheless, the reaction was finished overnight and after filtration the product was isolated in the quantitative yield. The synthesis of **24** was scaled up to 20 grams scale. The acylation with TFAA in the presence of TEA in DCM at low temperature yielded trifluoroacetamide **25** in 83-90% yield at 1 gram scale.

Table 9 Chiral acid mediated cyclization of **25**

entry	**acid**	**Solvent + temperature**	**results**
1	10-CSA	Toluene (80°C)	nd
2	L-dibenzoyltartaric acid	Toluene (80°C)	nd
3	L-dianisoyltartaric acid	Toluene (80°C)	nd
4	L-ditoluolyltartaric acid	Toluene (80°C)	nd
5	L-proline	Toluene (80°C)	nd
6	(*R*)-Mandelic acid	Toluene (80°C)	nd
7	TBBA	Toluene (80°C)	nd
8	(*S*)-TRIP	Toluene (80°C)	nd
9	10-CSA	Toluene (120°C)	nd
10	L-dibenzoyltartaric acid	Toluene (120°C)	nd
11	(*S*)-TRIP	Toluene (120°C)	nd

Trifluoroacetamide **25** was heated in toluene in a presence of catalytic amounts of chiral acids (Table 9). Traces of products were observed by TLC analysis, but the conversion was very low. Similarly, no product was detected by the chiral SFC analysis after cyclization of free carboxylic acid **22**.

Due to the low reactivity of organic acids, stronger lewis acids were tested. The cyclization catalyzed with lewis acids could then be conducted stereoselectively in a presence of suitable chiral ligands. 2 equivalents of lewis acid were used. The results are summarized in Table 10.

Table 10 Lewis acid mediated cyclization

entry	**Lewis acid**	**solvent**	**results**
1	$SnCl_4$, 2 eq.	DCM	Complex mixture
2	$TiCl_4$, 2 eq. (1M solution)	DCM	79%
3	$Ti(OiPr)_4$, 2 eq.	DCM	Complex mixture, low conversion

Tin tetrachloride (entry 1) and titanium isopropoxide (entry 3) yielded complex mixture of products and suffered from a low conversion of the starting material. Only the titanium tetrachloride provided full conversion of the starting material and the product **26** in 65% yield (entry 2). Further optimization focused on the amount of $TiCl_4$ in the reaction (Table 11).

Table 11 $TiCl_4$ mediated cyclization

entry	Eq. $TiCl_4$	solvent	result
1	0.2	DCM	Traces of product
2	0.5	DCM	Traces of product
3	1	DCM	65 % isolated
4	1 + 1eq. (*R*)-BINOL	DCM	10% conversion
5	2 + 2eq. (*R*)-BINOL	DCM	20% conversion, 50:50 er.

Reducing the amount of $TiCl_4$ provided marginal improvement. Sub-stochiometric amounts (Table 11, entries 1 and 2) yielded only traces of the product while the use of 1 equivalent provided the product in 65% yield. The lower yield compared to the use of 2 equivalents (Table 10, entry 2) was caused by incomplete conversion of the starting material. Use of chiral (*R*)-BINOL-$TICl_4$ catalyst for the cyclization severly slowed the reaction and after 24 hours only a trace conversion was observed (entry 4). Use of 2 eq. of $TiCl_4$ and (*R*)-BINOL provided 20% conversion of the starting material (entry 5). The product was analyzed by chiral SFC and only a racemic product was observed.

In view of the results provided by cyclization of acid **22** and ester **25**, further attempts were made to synthesize the benzimidazole core with high enantioselectivity. Based on the publications from Miller´s group[45,46], we thought the presence of the electronwithrdrawing group hampers the reaction by reduced nucleophility of the diarylamine nucleophile as is depicted in Scheme 9.

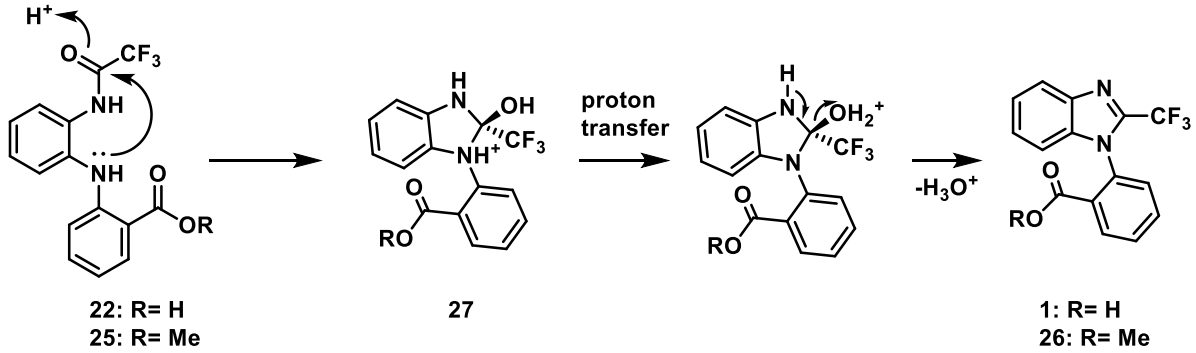

Scheme 9 Plausible mechanism of cyclization resulting in **1** or **26**

At first, the carbonyl group of the trifluoroacetamide is activated by the acid present in the reaction mixture and then attacked with the lone pair of the nitrogen forming intermediate **27.** This intermediate then undergoes proton transfer and further elimination of water to provide final benzimidazole **1** or **26**. The first step is likely to be the slowest one and is further slowed by the conjugation of the lone pair of the nitrogen into the aromatic ring which further lowers the reactivity. For this reason, we attempted to modify the synthesis to include electron donating groups to further improve the reactivity (scheme 10).

At first, *N*1-(*o*-tolyl)benzene-1,2-diamine **3** was acylated with TFAA in the presence of triethylamine at low temperature. The reaction proceeded smoothly to trifluoroacetamide **28**; however, while HPLC

analysis showed only one peak with correct m/z ratio. TLC analysis revealed a complex mixture of products. The reaction was then purified by column chromatography. Nevertheless, no pure product was obtained and the subsequent cyclization to **3a** was not attempted. Alternatively, aminoester **24** was reduced with $LiAlH_4$ to yield alcohol **29** in 67% yield. **29** was further acylated with TFAA to yield amide **30a** in 20% yield which was protected with tertbutyl-diphenylsilyl to yield amide **30b** in 50% yield. Further deprotection-oxidation sequence to yield the target acid **1** was not attempted due to lack of time before finishing this thesis.

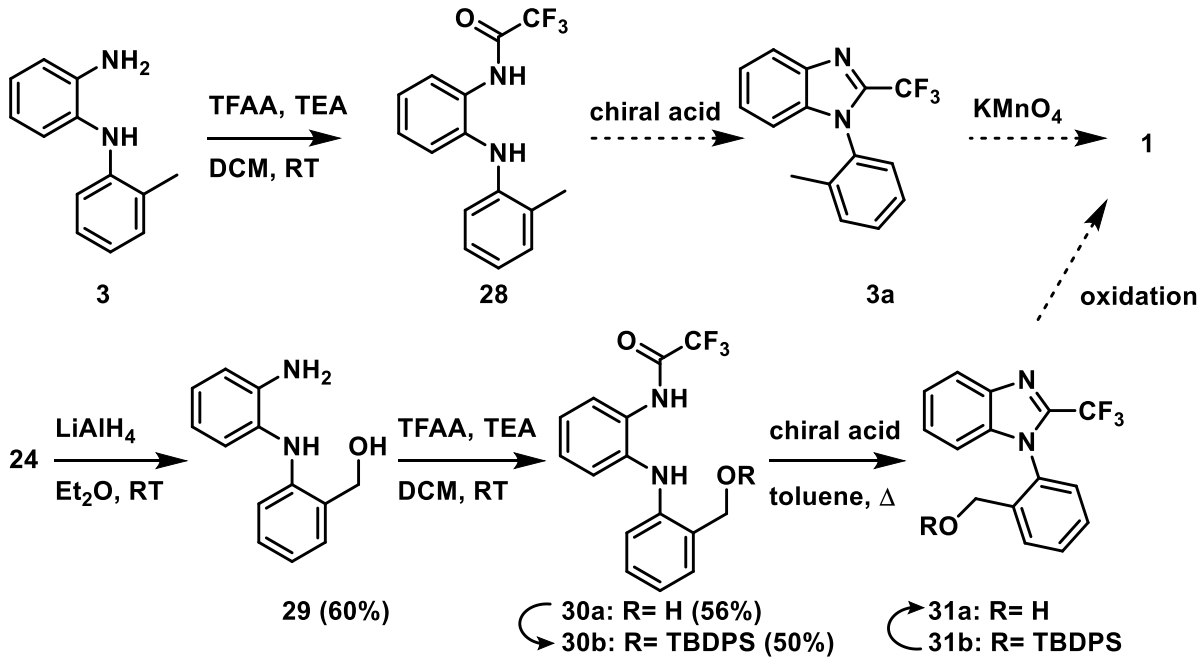

Scheme 10 Attempt to atroposelective synthesis of **1**

The cyclization of **30a** was attempted analogously to the previously described experiments: the starting material was dissolved in toluene and a catalytic amount of the acid was added. The reaction was heated to 65°C for 16 hours. The cyclization of compound **30a** did not provide any product when the tartaric acid derivatives were used (entries 1-3) while good conversion was obtained using stronger acids: 10-camphorsulphonic acid (entry 4) or BINOL-derived phosphonic acid (entry 5). SFC analysis showed encouraging atroposelectivity of the cyclization to compound **31a**. Using the 10-CSA as a catalyst yielded product in approximately 32/68 er. Unfortunately, impurity overlapping product peaks did not allow for exact integration.

Table 11 Atroposelective cyclization of compounds **30a/b**

Entry	Starting compound	acid	Solvent + temperature	results
1	30a	L-dibenzoyltartaric acid	Toluene 65°C	No reaction
2	30a	L-dianysoyltartaric acid	Toluene 65°C	No reaction
3	30a	L-ditoluolyltartaric acid	Toluene 65°C	No reaction
4	30a	(*S*)-TRIP	Toluene 65°C	Er. 73/27
5	30a	10-CSA	Toluene 65°C	Er. 32/68*
6	30b	(*S*)-TRIP	Toluene 65°C	decomposition

* overlapping integrals in SFC, the value is aproximate

Since the cyclization experiments were severly limited by the amount of starting materials **30a** or **30b** which could not be reliably prepared in reasonable amounts for the application, alternative pathways leading towards those compounds were explored. Firstly, different acylation coditions (TFA+T3P or TFA+DCC) were used; however, no product was formed. Following those failures, different approaches were explored (Scheme 11-12). Benzylalcohol **29** was protected with TBDPSCl to yield compound **32** using slight excess of TBDPSCl and imidazole as a base. Compound **32** was isolated in 75% yield after column chromatography. TBDPS protected aminoalcohol was then acylated with TFAA and the product was isolated in 50% yield after column chromatography. Unfortunately, the reactionwas not completed even after subsequent additions of more TFAA.

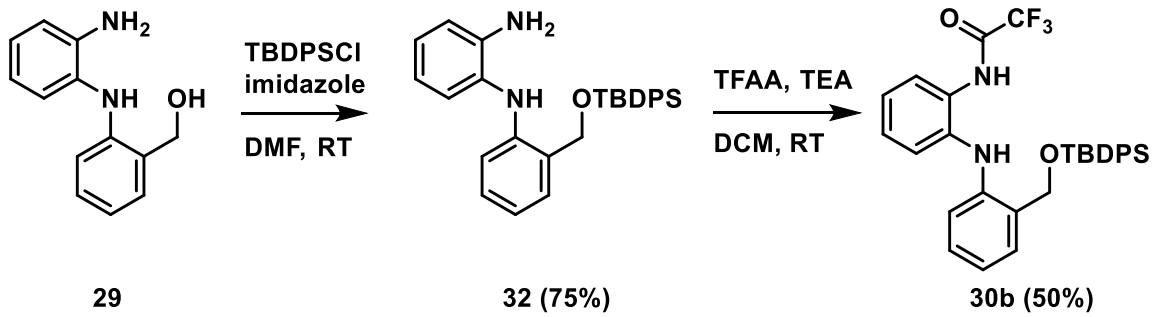

29 **32 (75%)** **30b (50%)**

Scheme 11 Alternative synthesis of compound **30b**

Alternatively, the benzylalcohol **33** was protected with TBDPS to yield **34** in 75% yield after chromatography. 2-Iodoaniline **36** was acylated with TFAA to yield **37** in various yields: previously performed acylation in DCM yielded product in 50% yield, but exchange of the solvent to THF improved the yield to 95%.[151]

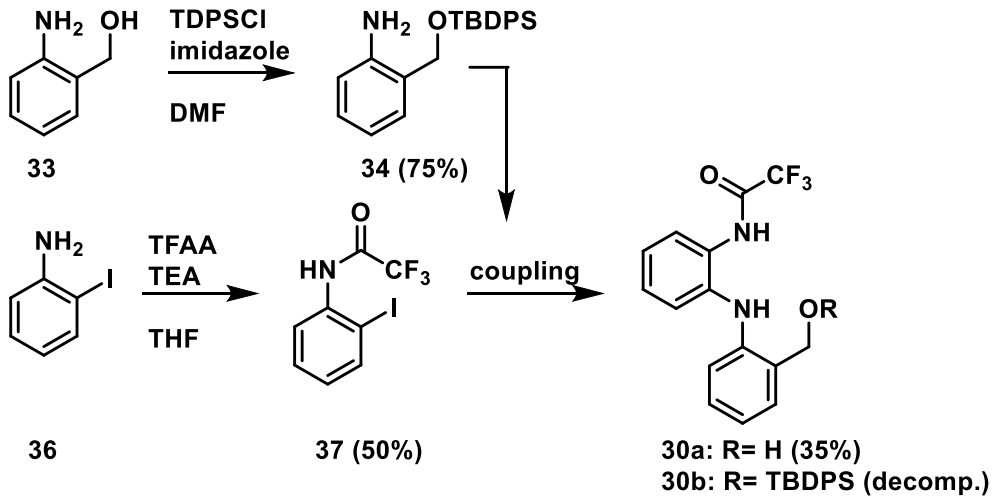

Scheme 12 Synthesis of **30a/b** by metal-catalyzed coupling reaction

Amines **33** and **34** were there coupled to the TFA-protected iodoaniline **37** under various conditions. Results are summarized in Table 12. Product **30a** was isolated in 25% yield using the previously reported conditions (entry 1).[45] The increase of the reaction scale from 0.2 mmol to 1 mmol (entry 2) slightly increased the yield but still not sufficient. The change from copper to palladium catalysis with XPhosPdG2 did not provide any improvements although the used catalyst was used with a great success in our research group.[152] Arylation of protected benzylalcohol **34** and copper catalyst (entry 4) did not work at all and a complete decomposition was observed.

Table 12 Synthesis of **30a/b** by metal catalyzed coupling reaction

entry	**amine**	**conditions**	**results**
1	33	CuI 10%, 2,2´-biphenol 10%, K_3PO_4, DMF, ACN, 60°C[45]	25%
2	33	CuI 10%, 2,2´-biphenol 10%, K_3PO_4, DMF, ACN, 60°C, 1 mmol scale	35%
3	33	XPhosPdG2 2%, K_3PO_4, dioxane	No reaction
4	34	CuI 10%, biphenol 10%, K_3PO_4, DMF, ACN, 60°C	decomposition

Since the coupling approach towards compound **30** was not very successful and the cyclization itself provided products only in a modest enantiomeric excess combined with the difficulties of the preparation of the starting materials, this approach was abandoned in favor of the synthesis of racemic TBBA and further resolution.

Conformational stability of TBBA

Since the most common mechanism of racemization of axially chiral compounds is a simple bond rotation, the stability of TBBA was tested. TBBA was heated at various temperatures in various solvents to determine the rate of racemization. The results are summarized in Table 13 and 14.

Table 13 Conformational stability of TBBA in alcohols

Entry	solvent	Temperature	Time (h)	%ee
1	MeOH	60°C	5	100
2	MeOH	60°C	8	100
3	MeOH	60°C	16	98
4	BuOH	80°C	5	96
5	BuOH	80°C	8	84
6	BuOH	80°C	16	82

At first, racemization was investigated in MeOH at 60 °C. Even after prolonged heating, no racemization was observed (entries 1-2) with a slight drop in enantiomeric purity after 16 hours (entry 3). Higher temperature at 80 °C increased the rate of racemization as expected and slight racemization was observed already after 5 hours (entry 4). The enantiomeric purity further decreased to 91:9 (entry 6). The temperature was further increased to accelerate racemization. A solvent was changed to higher boiling ethyleneglycol (Table 14).

Table 14 Racemization kinetics of TBBA in ethyleneglycol

Temperature	Time (min)	%ee	k_{rac}	$\Delta G^{\ddagger}_{rac}$ (kcal/kJ)	$t_{1/2}$ (min)
	10	99.42			
	20	98.90			
	30	98.24			
	60	96.04			
	90	93.82			
	120	91.54			
	180	87.12			
	240	82.78			
	300	78.86			
100°C	360	74.90	1.27×10^{-5}	30.37 / 127.05	906.1
	420	70.66			
	1620	24.48			
	1740	22.30			
	1860	19.94			
	2880	8.48			
	3000	7.68			
	3180	6.20			

At first, racemization was conducted at 100°C. Full racemization was observed after 3180 mins (53 hrs) with the half-life of the racemization 906 minutes (aprox. 15 hours). Then, the temperature was increased to 140°C and, as expected, the racemization was significantly faster and full racemization (%ee < 1%) was observed after 160 minutes. (Table 15) and the half-life being calculated to 25 minutes.

Table 15: Racemization kinetics of TBBA in ethyleneglycol

Temperature	Time (min)	%ee	k_{rac}	$\Delta G^{\ddagger}_{rac}$ (kcal/kJ)	$t_{1/2}$ (min)
	10	84.08			
	20	64.22			
	30	48.06			
	40	36.0			
	50	27.16			
	60	20.34			
	70	15.26			
	80	11.36			
	90	8.48			
	100	6.28			
	110	4.64			
140°C	120	3.54	4.56×10^{-4}	30.77 / 128.73	25.3
	130	2.44			
	140	1.64			
	150	1.24			
	160	0.94			
	170	0.42			
	180	0.38			
	190	0.18			
25°C	---	---	3.42×10^{-10}	30.37 / 127.05	64.2 years

From the data depicted in Tables 14 and 15, racemization kinetics were calculated using equations 1-3 (Figure 7).

Eq. 1 $$\ln\left(\frac{R_0}{R_0 - x}\right) = k_{rac} t$$

Eq. 2 $$\Delta G^{\ddagger}_{rac} = -RT \ln\left(\frac{h k_{rac}}{\kappa T k_B}\right)$$

Eq. 3 $$\tau_{1/2rac} = \frac{\ln 2}{k_{rac}}$$

R_0 = initial concentration of the enantiomer, x = concentration of the racemate at time t, h = Planck constant, k_b = Boltzman constant, κ = transmission coefficient (equals to 1), T = temperature, R = gas constant, k_{rac} = racemization rate constant, $\Delta G^{\ddagger}_{rac}$ = energy barrier for racemization, $\tau_{½rac}$ = half-life of racemization

Figure 7 equations used for calculation of racemization kinetics

At first, equation 1 was used to calculate racemization rate constant k_{rac} (average k_{rac} shown in Tables 14-15). This rate constant was then used to calculate energy barrier of rotation $\Delta G^{\ddagger}_{rac}$ (Equation 2) and half-life of racemization $t_{1/2}$ (Equation 3). The lower $\Delta G^{\ddagger}_{rac}$ (i.e. lower rotation barrier therefore lower stability) obtained from data at 100°C was used to calculate the half-life at room temperature. The

calculated half-life at room temperature was 64 years, which makes TBBA sufficiently stable to store at laboratory/room temperature.

NMR results

Analysis of α-chiral amines and alcohols

Based on the NMR spectra of amide **11** prepared from racemic TBBA and enantiopure amine, it was evident that TBBA can differentiate NMR signals between the enantiomers. For the configuration assignment, a conformational model had to be described based on the NMR spectra of tested derivatives. Furthermore, a mild acylation procedure had to be developed. At first, acylation of amines via acid chloride (TBBA-Cl) was performed using the already described procedure of heating enantiopure TBBA in toluene at 110°C in a presense of $SOCl_2$. The reaction is very fast and was complete within five minutes of heating. The time of heating was very important because longer heating times caused partial racemization as is evident from the racemization experiments (Table 14). Luckily, the reaction could be monitored visually: TBBA is not fully dissolved in the mixture of toluene and $SOCl_2$ at room temperature and slowly dissolves during heating. It was observed, that when the reaction mixture becomes clear solution, the formation of acyl chloride is complete.

The acylation of amines was then performed by slow addition of the solution of TBBA-Cl in $CHCl_3$ to the solution of the amine and trimethylamine in $CHCl_3$. Usually, the reaction was complete within one hour and, in most cases, a product was isolated by simple acidobasic extraction. Although the acyl chloride mehod worked well, alternative methods were explored to a) reduce the risk of racemization to absolute minimum and b) to possibly eliminate the need of additional work before the acylation (i.e. preparation of fresh TBBA-Cl before each reaction).

At first, the isolation of TBBA-Cl was attempted by precipitation in hexanes; nevertheless, the TBBA-Cl was always isolated as a brown oil, which complicated the weighing of the required amounts for the reaction. Second, TBBA-Cl was converted into OSU (N-hydroxysuccinimide) ester **31**[153] (Scheme 13), which could then act as an active acylation species in the reaction.

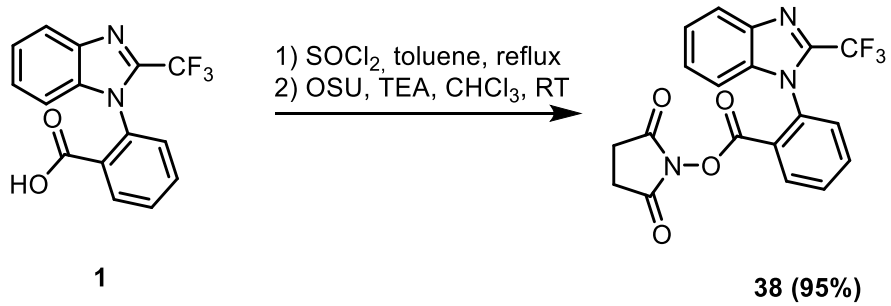

1 **38 (95%)**

Scheme 13 Synthesis of OSU ester **38**

The OSU ester was obtained in the high yield (96%) starting with racemic **1** after simple extraction on a gram scale and its utility as an acylation species was tested. The results are shown in Table 16. Simple stirring of the compound **38** with the amine in $CHCl_3$ at room temperature overnight yielded 80% conversion with the remaining 20% of reaction mixture was the unreacted starting material (entry 1). Simple addition of base caused full conversion to the product which was isolated in 90% yield after acidobasic extraction (entry 2).

Table 16 Acylation of amines with OSU ester **38**

Entry	**amine**	**conditions**	**results**
1	*(R)*-phenylethylamine	$CHCl_3$, no base, RT, 18 hrs	80% conversion
2	*(R)*-phenylethylamine	$CHCl_3$, triethylamine, RT, 18 hrs	90% yield

While the reaction worked well with racemic TBBA, the conversion of enantiopure TBBA to the OSU ester was more complicated. The preparation of TBBA-Cl on a small scale (<50 mg) and further conversion to **38** worked well. The scale-up of the reaction proved to be more complicated. This was mainly because the formation of the TBBA-Cl took longer time at higher temperature and, subsequently, aprox. 10% racemization was observed. Then, milder methods were investigated. The use of EDCl in DMF[154] did not yield the product at all. The direct acylation with TBBA in the presence of EDCl and hydroxybenzotriazole (HOBt) in DMF worked and produced the desired amides after simple acidobasic extraction without the need of the intermediate **38**, whichclearly simplified the procedure. At first, the set of amides was prepared (Figure 8) using EDCl+HOBt in DMF.[155,156] The amines were acylated with both enantiomers of TBBA.

^{1}H-NMR analysis

Compounds **39-50** were prepared in 50-98% yields after column chromatography. The shielding effects are displayed as $\Delta\delta^{PM}$. $\Delta\delta^{PM}$ is calculated by subtraction of the chemical shift of the given signal in *M*-diastereomer from the chemical shift of the same signal in *P*-diastereomer:

$$\Delta\delta^{PM} = \delta L1(P) - \delta L1(M)$$

If the $\Delta\delta^{PM} < 0$, the given proton is shielded in the *P*-diasteromer and analogously, if $\Delta\delta^{PM} > 0$ is deshielded in the *P*-diasteromer. This information then allows to locate the given substituents in space to deduce the correct configuration with the aid of conformational model (vide infra).

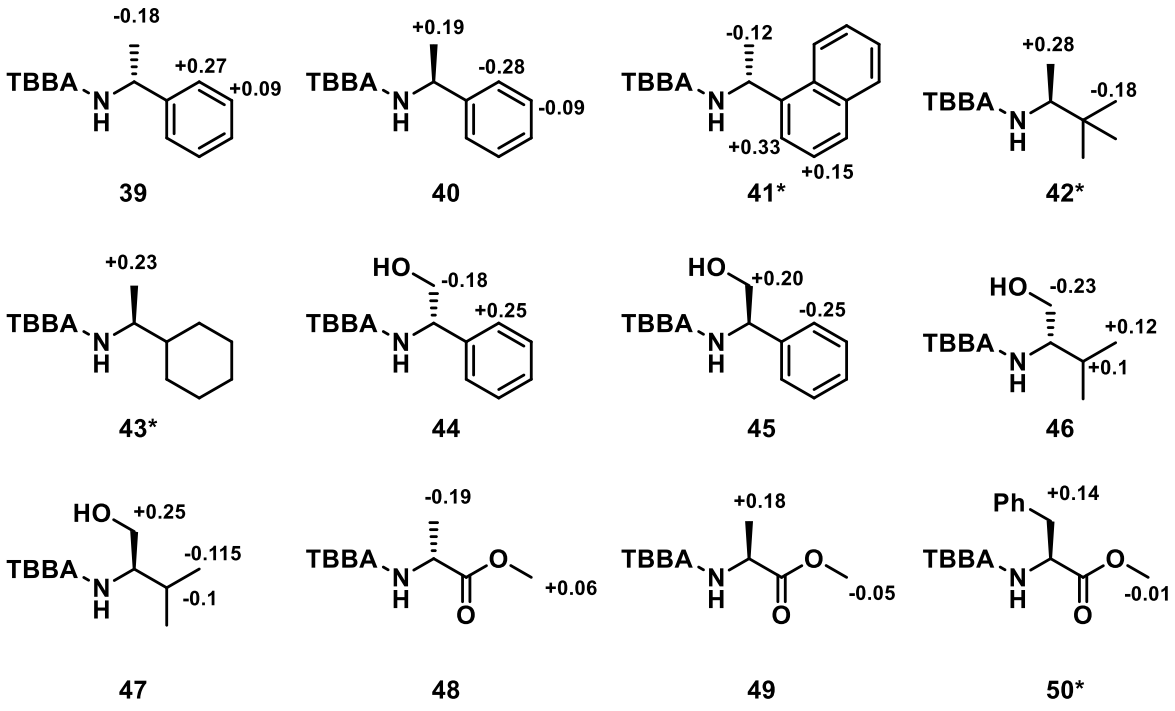

Figure 8 Observed $\Delta\delta^{PM}$ for compounds **39-50**

*Compound **50** was prepared by undergraduate student David Profous.

At first, phenetylamines were acylated with TBBA yielding compounds **39** and **40**. Both enantiomers of phenetylamine were separately analyzed to compare the differences between the enantiomers of the amine. As can be seen, the $\Delta\delta^{PM}$ of compounds **39** and **40** is identical in magnitude with the slight difference of 0.01 ppm which can be attributed to the limit of the method. As expected, the sign of the $\Delta\delta^{PM}$ were reversed due to the opposite configuration of tested amines. The most relevant signals of **39** (i.e. the closes to the chiral center) showed -0.18 ppm of the methyl group and +0.27 and +0.09 ppm for the aromatic *ortho* and *meta* protons. The analysis of compounds which possess aromatic rings close to the chiral center could be complicated and yield anomalous values;[157] nevertheless, none anomalous values were observed. Moreover, the magnitude of the $\Delta\delta^{PM}$ of the methyl group was significantly higher than in the case of MTPA (0.04), MPA (0.07), or MPA in the complex with $BaClO_4$ (0.09).[88,158,159]

Substitution of the phenyl ring for the larger napthyl ring in **41** had a slight effect on the $\Delta\delta^{PM}$. The $\Delta\delta^{PM}$ of the methyl group (-0.12) was slightly lower compared to **39** and **40** but higher compared to MPA (0.07)[159] and slightly smaller compared to Boc-phenylglycine (BPG) (0.17).[70] The aromatic protons showed slightly higher $\Delta\delta^{PM}$ compared to **39** and **40**. The nonaromatic amines **42** and **43** showed high $\Delta\delta^{PM}$ for the methyl group: +0.28 and +0.23 for **42** and **43** respectivelly.

Phenylglycinol was acylated under the same conditions without any detected *O*-acylation in the reaction mixture. Addition of the polar hydroxyl group in **44** and **45** did not have a significant effect on the observed $\Delta\delta^{PM}$ compared to non-hydroxylated derivatives **39** and **40**. The homobenzylic protons in **44** displayed -0.18 ppm, which was very similar to the homobenzylic protons at **39**. The protons in the *ortho* position showed +0.25 ppm difference, which was similar to the same protons at **39**. The same behavior was observed with the enantiomeric amnoalcohol **45**.

Substitution of the phenyl group for the more branched and sterically demanding isopropyl group at **46** and **47** slightly increased the $\Delta\delta^{PM}$ of the hydroxymethyl group compared to phenylglycinol derivatives. The isopropyl group showed significantly lower $\Delta\delta^{PM}$ (+0.12 and +0.1), but still sufficiently higher above the experimental limits of the method. Enantiomeric amide **47** displayed slightly higher (0.02 ppm) $\Delta\delta^{PM}$ compared to **46** while the $\Delta\delta^{PM}$ of the isopropyl group was pretty much same as expected.

The $\Delta\delta^{PM}$ of the methyl group in the alanine derivatives **48** and **49** showed -0.19 and +0.18 ppm, respectively, on a par with the phenethylamines **39** and **40** and phenylglycinols **44** and **45**, but slightly lower than the aliphatic amides **42**, **43**, **46**, and **47**. The $\Delta\delta^{PM}$ of the methylester was significantly smaller (+0.06 and -0.05), which was expected due to the group being located further away from the chiral center. The observed values were higher compared to MTPA (0.08 for the methyl and 0.03 for the methylester).[159] As expected, a comparison of enantiomers **48** and **49** shows no significant differences.

The phenylalanine derivative **50** showed lower $\Delta\delta^{PM}$ compared to alanine derivatives (+0.14 vs +0.18) and the methylester displayed only minimal 0.01 ppm difference. Compared to BPG[70] and MPA[88] the $\Delta\delta^{PM}$ of the benzylic proton was roughly the same (0.14 vs 0.18 and 0.08 respectively) while the $\Delta\delta^{PM}$ of the methylester was significantly lower (-0.01 vs 0.11 and 0.07 respectively).

Furthermore, esters **51**-**59** (Figure 9) were prepared in 50-86% yields. Different acylation conditions were used for synthesis of esters: dicyclohexylcarbodiimide (DCC) and dimethylaminopyridine (DMAP) in DCM. Although the dicyclohexylurea precipitated from the reaction mixture and was filtered away, column chromatography was necessary to use for all compounds.

Ester **51**, an analogue of **39**, displayed significantly higher $\Delta\delta^{PM}$ values. The difference at the methyl group showed -0.32 ppm which was almost a double value compared to **39** (-0.18). Analogously, the $\Delta\delta^{PM}$ of the proton at the *ortho*-position of the phenyl ring was significantly higher compared to **39** (+0.45 vs +0.27) and MPA and MTPA (0.06 and 0.08 respectively). Only 9-AMAA showed comparable differentiation (0.3 ppm).[91] The substitution of the phenyl ring for aliphatic ethyl at **52** showed a slight increase in the $\Delta\delta^{PM}$ of the methyl group (+0.49) while the ethyl group displayed high $\Delta\delta^{PM}$ difference on both the methyl and methylene protons. Further substitution of the ethyl for the more rigid ethynyl at **53** lowered the $\Delta\delta^{PM}$ on both the methyl group (+0.26 vs +0.49 at **52**) and the terminal alkyne (-0.28

vs -0.33 terminal methyl at **52**). Compared to MPA, the $\Delta\delta^{PM}$ at **53** were significantly higher (0.207 and 0.086).[100]

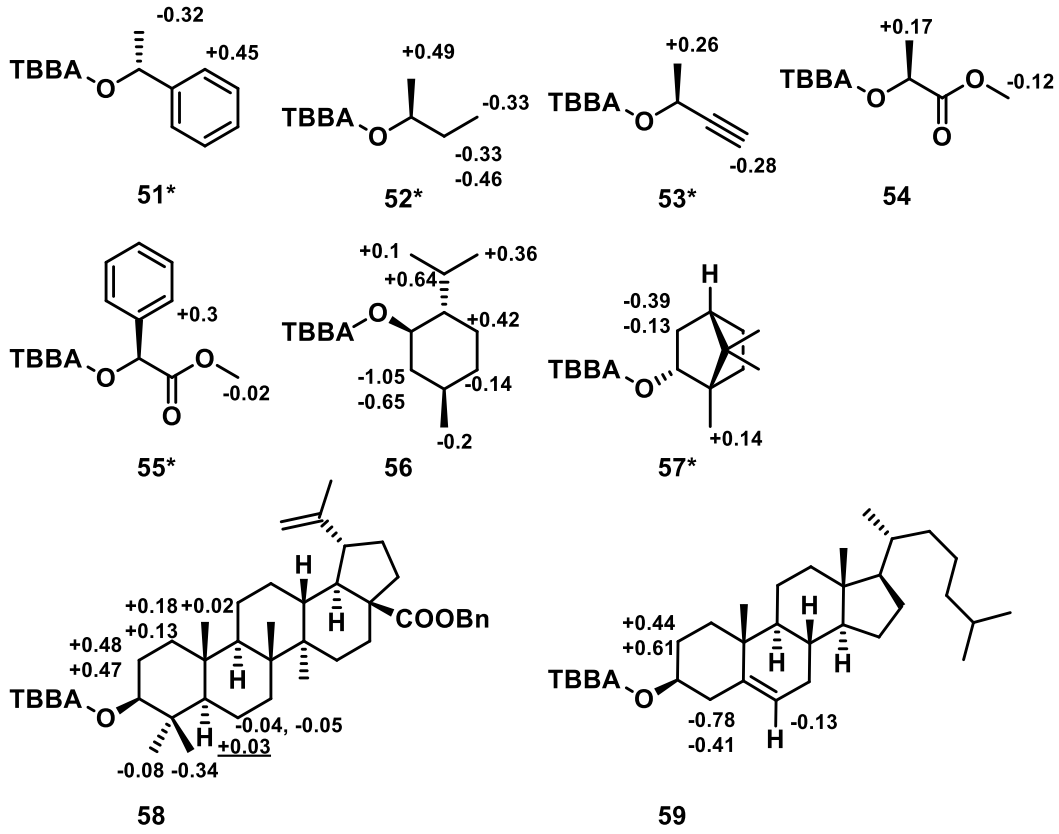

Figure 9 observed $\Delta\delta^{PM}$ for esters **51-59**

*compound was prepared by undergraduate student David Profous

Further substitution of the aliphatic chains for the carboxymethyl in **54** caused further decrease of the observed $\Delta\delta^{PM}$. The $\Delta\delta^{PM}$ of the methyl group decreased from the +0.49 and +0.26 for **52** and **53** to +0.17, but stayed similar to the alanine derivative **49**. Interestingly, the $\Delta\delta^{PM}$ of the methylester was -0.12 which was significantly higher compared to alanine **49** (-0.05) and phenylalanine **50** (-0.01). The difference was also comparable to MPA ester 0.075 ppm for methyl and 0.17 ppm for methylester.[100] Further substitution of the methyl group for phenyl significantly reduced the $\Delta\delta^{PM}$ of the methylester: -0.02 in **55** compared to -0.12 in **54.** The $\Delta\delta^{PM}$ of the phenyl is slightly lower compared to the phenyl substituted ester **51**. The difference are also smaller compared to MPA and 9-AMAA esters.[91,100]

In addition, L-menthol TBBA esters **56** were prepared because menthol often serves as a model compound for new CDAs.[86,160–162] The observed $\Delta\delta^{PM}$ of the isopropyl group (+0.1 and +0.36) were smaller compared to 9-AMAA with the $\Delta\delta^{PM}$ of the methyl group at position 4 was slightly higher compared to 9-AMAA (0.2 vs 0.1 ppm).[89] The $\Delta\delta^{PM}$ at the position 3 (-1.05 and -0.65 ppm) were unexpectedly high and even the differences at more remote positions 5 (-0.14) and 6 (+0.42) exceeded

0.1 ppm. Interestingly, the structurally similar borneol **57** displayed smaller $\Delta\delta^{PM}$ compared to menthol **56**. The difference at position 3 was -0.13 and -0.39 ppm and the methyl group at positon 1 displayed +0.14 ppm which was on the same level as MPA ester and smaller compared to 9-AMAA ester.[91]

Lastly, two natural products derivaves were tested: benzylbetulinate **58** and cholesterol **59**. The derivative **58** displayed high $\Delta\delta^{PM}$ on the A-ring (+0.48, +0.47, +0.18 and +0.13) and the adjacent methyl groups (-0.08 and -0.34). The differences were observable even at remote positions 6 (-0.04 and 0.05) and methyl at position 25 (+0.02). This was likely due to high rigidity of the steroidal structure which allows clear projection of the shielding effect on the remote positions. The proton at position 5 displays anomalous sign of the $\Delta\delta^{PM}$*;* however, this anomaly can be ignored due the low magnitude of the difference and the fact that the remaining protons differences show homogenous signs. Cholesterol **59** was previously derivatized with MTPA.[158] TBBA differences on the A-ring (+0.44, +0.61, -0.41 and -0.78) were significantly higher compared to MTPA (-0.06, +0.09 and +0.09).

^{13}C NMR analysis

In addition, ^{13}C NMR spectra were analyzed as well. Compared to ^{1}H, the use of ^{13}C for the configuration assignment is limited. This limitation comes from the two major factors: a) larger amounts of sample and time are required to obtain high quality ^{13}C NMR spectra and b) the $\Delta\delta^{RS}$ values observed in ^{13}C spectra are in most cases small when the whole scale (0-200 ppm) of ^{13}C NMR spectra is considered.[87] Nevertheless, modern NMR techniques allow to obtain high quality NMR spectra even from tiny amounts of sample.

To our delight, analyzed $^{13}C\Delta\delta^{PM}$ data followed the general trend observed in ^{1}H spectra. The easily distinguishable methyl groups in compounds **39**-**43**, **48**-**49** showed $^{13}C\Delta\delta^{PM}$ absolute values between 0.14 and 0.4 ppm. The methylene signals in **51**-**54** displayed differences 0.3 and 0.33 ppm. On the other hand, the methylene carbons in **50** were shifted by 0.08 ppm. Most importantly, the alkynyl carbon in **53** without protons demonstrated a difference of 0.45 ppm. Furthermore, in accordance with the general trend, the more remote methylester signals in **48**-**50, 54- 55** displayed low $^{13}C\Delta\delta^{PM}$ values ranging from 0.04 (compounds **13**, **14**) to 0.06 (compounds **18**, **19**) ppm. Despite the fact that observed values are small when the entire ^{13}C NMR chemical shift range is considered, in most cases, the $\Delta\delta^{PM}$ value was high enough to assign the absolute configuration, especially, when results were coupled with ^{1}H chemical shifts data.

Conformational model for assignment of absolute configuration by ^{1}H or ^{13}C NMR

Not only the NMR differences were higher compared to most of the common reagents, but more importantly, they followed the clear trend. Based on the data, conformational model was devised, which allows for assignment of the absolute configuration of tested compounds (Figure 10).

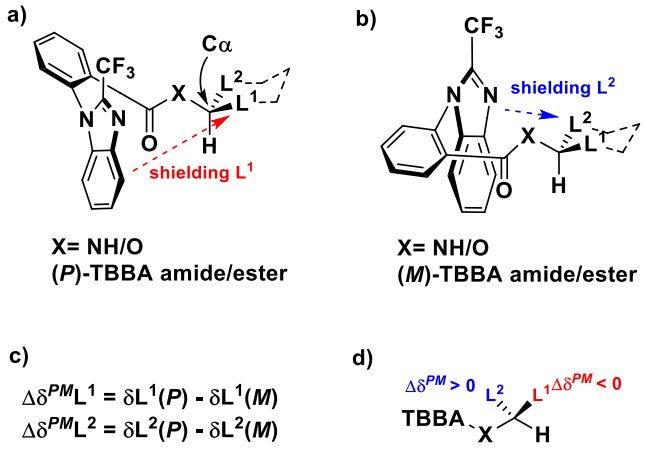

Figure 10 Model for assignment of the absolute configuration if chiral secondary alcohols and primary amines a) (*P*)-TBBA amide/ester b) (*M*)-TBBA amide/ester c) calculation of $\Delta\delta^{PM}$ d) simplified model

In this proposed model, the benzimidazole and phenyl rings are perpendicular to each other. The carbonyl group is oriented opposite compared to the trifluoromethyl group. The proton at Cα is in *syn*-periplanar position to the carbonyl group which orients one of the the substituents L^1 and L^2 in front of the benzimidazole ring, which projects the shielding effect on this substituent (figure 10a/10b). This projected shielding effect causes the chemical shift of the substituent to be shifted upfield. In the example on Figure 10, assuming the displayed configuration, substituent L^1 in the (*P*)-derivative (Figure 10a) is going to have lower chemical shift compared to the L^1 in the (*M*)-derivative (Figure 10b). Analogously, the chemical shift of the L^2 substituent in the (*P*)-derivative is going to be higher compared to the same substituent in the (*M*)-derivative.

These changes on chemical shifts can be expressed as the $\Delta\delta^{PM}$ parameter, which was calculated according to equation shown in Figure 10c. Based on the observed $\Delta\delta^{PM}$ values, the substituents L^1 and L^2 can then be located in space and absolute configuration can be deduced. If the substituent has a negative $\Delta\delta^{PM}$ value (as does L^1 in Figure 10), it is located above the plane of coplanar amide/ester function and Cα. If the substituent posess a positive $\Delta\delta^{PM}$ value (as does L^2 in Figure 10), it is located bellow the plane. The simplified model is shown in Figure 10d.

To further confirm our model, series of in-silico simulations using Spartan 16 software were performed. The populations of theoretical conformers were calculated with the molecular mechanics model MMFF. Depending on the total number of theoretical conformers, this was followed by sorting of the conformation candidates with relative energies lower than 10−20 kJ/mol. The energies of sorted candidates at the ground state in the nonpolar solvent were calculated using density functional theory (B3LYP, 6-31G*) to find the lowest energy conformer.

The calculation revealed that over 99% of diastereomer **(*P*)-39** was distributed over four conformers with Boltzmann weights of 0.414, 0.276, 0.186, and 0.120. The most stable conformer (Figure 11a) (Boltzman weight 0.414) is not relevant for the NMR experiments, since the molecule is rotated in a way where both substituents are located in the shielding zone of the benzimidazole. This means, the shielding effect is not produced selectively and, in the end, both substituents would have their chemical shifts moved upfield and therefore no difference in the NMR spectra can be expected. We assumed the second most stable theoretical conformer (Figure 11b) of **(*P*)-39** (Boltzmann weight 0.276, $\Delta G = +1.01$ kJ/mol) was the most NMR-significant one since the anisotropic effect of the benzimidazole moiety is preferentially space-oriented and efficient toward the methyl group. As proposed in the model, the Cα and carbonyl group are *syn*-periplanar.

The Remaining two conformers (Figure 11c/d) with Boltzman weights 0.186 and 0.120 ($\Delta G = +1.99$ kJ/mol and 3.06 kJ/mol) were not NMR relevant since both of the substituents are located outside of the shielding zone and therefore, no observable change in the NMR spectra can be expected.

Compound (*P*)-39

a)

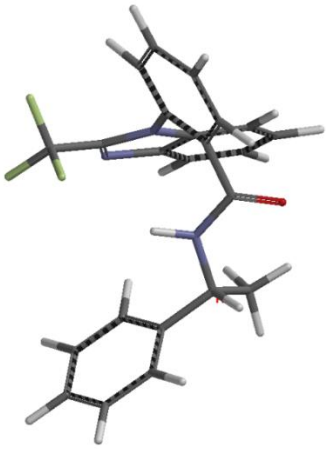

Most stable conformer

Boltzman weight: 0.414

NMR insignificant: non-selective shielding of both substituents at the same time

b)

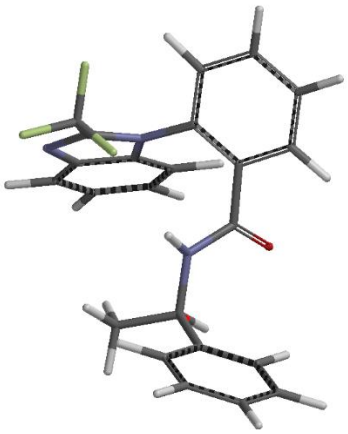

2nd most stable ΔG= +1.01 kJ/mol

Boltzman weight: 0.276

NMR relevant:selective shielding on methyl substituent

c)

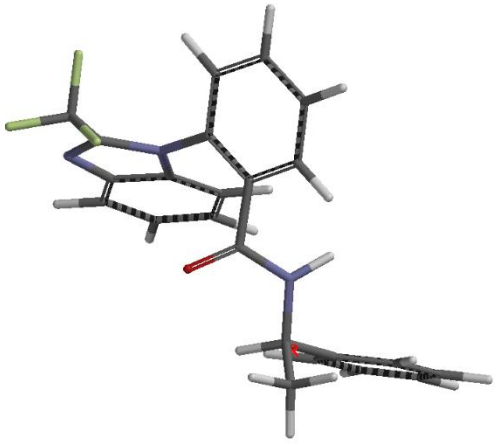

3rd most stable ΔG= +1.99 kJ/mol

Boltzman weight: 0.186

NMR insignificant: shielding effect is not produced on any of the substituents

d)

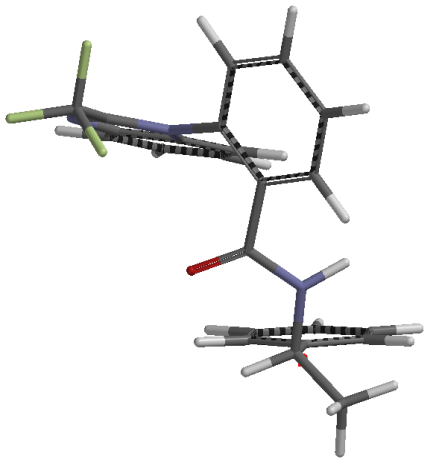

4th most stable ΔG= +3.06 kJ/mol

Boltzman weight: 0.120

NMR insignificant: shielding effect is not produced on any of the substituents

Figure 11 Conformers of compounds (***P*)-39**

The calculations revealed that the most of the conformation equilibria of the diastereomer **(*M*)-39** consisted of only two conformers (total Boltzman weight 0.978). The major conformer (Bolzman weight 0.60), which is similar to **(*P*)-39,** is not NMR relevant since none of the substituents are located in the shielding zone of the benzimidazole ring. The less stable conformer (Figure 12b) (Boltzman weight 0.378, ΔG= +1.15 kJ/mol) was considered as the NMR relevant conformer with the phenyl ring being directly in the shielding zone of the benzimidazole with complete accordance to the experimental data.

Compound (*M*)-39

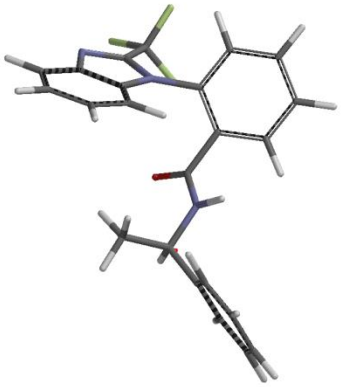

a) Most stable conformer

Boltzman weight: 0.60

NMR insignificant: shielding effect is not produced on any of the substituents

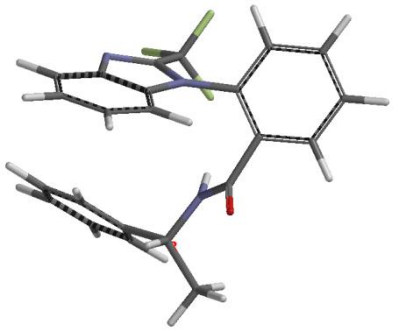

b) 2nd most stable ΔG= +1.15 kJ/mol

Boltzman weight: 0.378

NMR relevant: shielding effect produced selectively on phenyl substituent

Figure 12 Conformers of compounds (***M)*-39**

^{19}F-NMR analysis

Attempts to correlate the ^{19}F spectra with the absolute configuration were conducted as well. The ΔCF_3 was calculated analogously to the $\Delta\delta^{PM}$ parameter using following equations:

$$\Delta CF_3 = \delta L1^{19F}(P) - \delta L1^{19F}(M)$$

by substracting the chemical shift of the ^{19}F spectrum of the (*M*)-diastereomer from the ^{19}F spectrum of the (*P*)-diastereomer. The results are summarized in Figure 13 and 14.

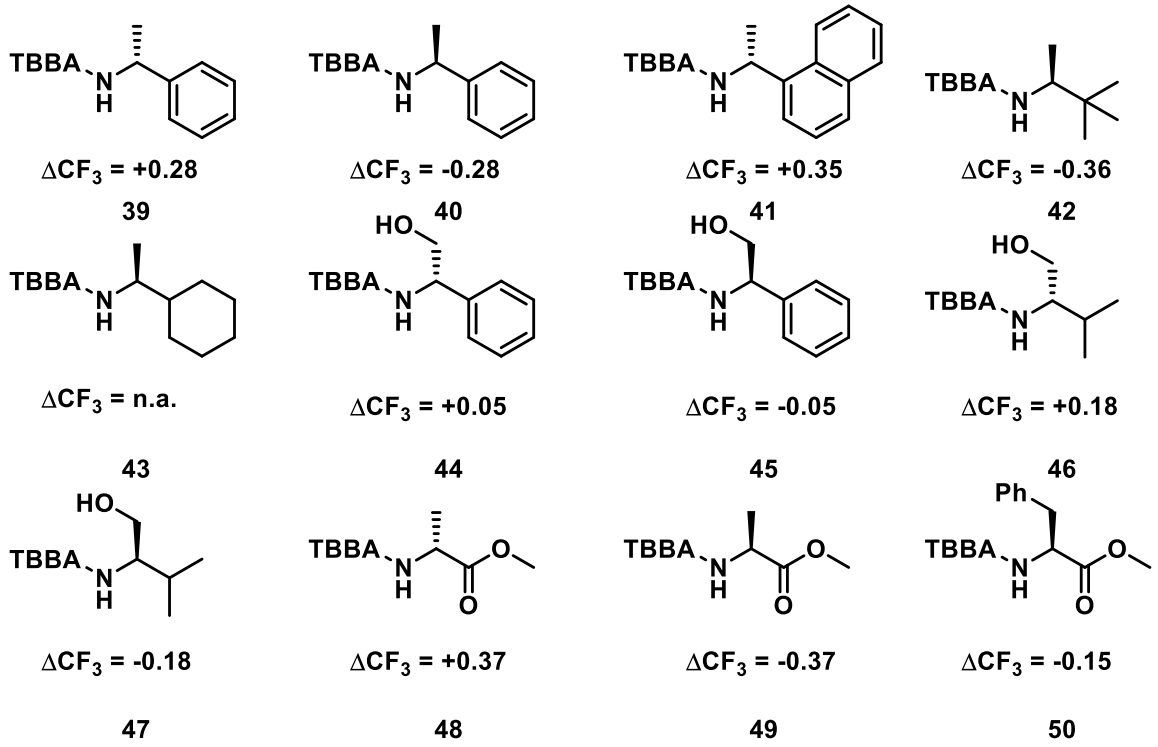

Figure 13 Observed ΔCF_3 for amides **39-50,** na: not available

At first, the ^{19}F NMR spectra of the TBBA-amides **39-50** were analyzed (Figure 13). The amides **39** and **40** displayed 0.28 ppm difference and, as expected, the sign was reversed for the **40** compared to **39**. Changing the phenyl ring of **39** for a larger napthtyl ring in **41** slightly increased the ΔCF_3 to +0.35 ppm. Moreover, the positive sign was same as observed for **39** with the same absolute configuration. Further changing the aromatic moiety for aliphatic in **42** did not have a significant effect on the ΔCF_3. Addition of polar hydroxyl group proved significant difference and lowered the ΔCF_3 to 0.05 in **44** and **45** and to 0.18 in **46** and **47**. Modification of the structure by addition of the carboxymethyl group in **48** and **49** displayed a similar ΔCF_3 to aryl derivatives **39-41.** Substitution of the methyl group to benzyl in **50** slightly lowered the ΔCF_3 from -0.37 to -0.15 in **49**.

Interestingly, compound **51** displayed a significantly lower ΔCF_3 compared to aza-analogue **39**: +0.02 vs +0.28. The structure exchange of the phenyl group for ethyl in **52** displayed a slightly higher ΔCF_3 (-0.18) as was observed in similar aliphatic aza-derivative **42.** The substitution of the ethyl group for the ethynyl in ester **53** displayed not only smaller ΔCF_3 (+0.07), but also the positive sign of the ΔCF_3, which was in the stark contrast to other compounds, where the trend would suggest negative ΔCF_3 for compound **53.** Further addition of carboxymethyl group in **54** showed a similar ΔCF_3 in magnitude as alkynyl derivative **53** although this time with expected negative sign of the ΔCF_3. Substitution of the methyl group for phenyl inat **55** showed comparable ΔCF_3 (-0.17) to **52**. The addition of carboxymethyl group caused significant change in the magnitude of the ΔCF_3 value as compared to **51** (-0.17 vs 0.02).

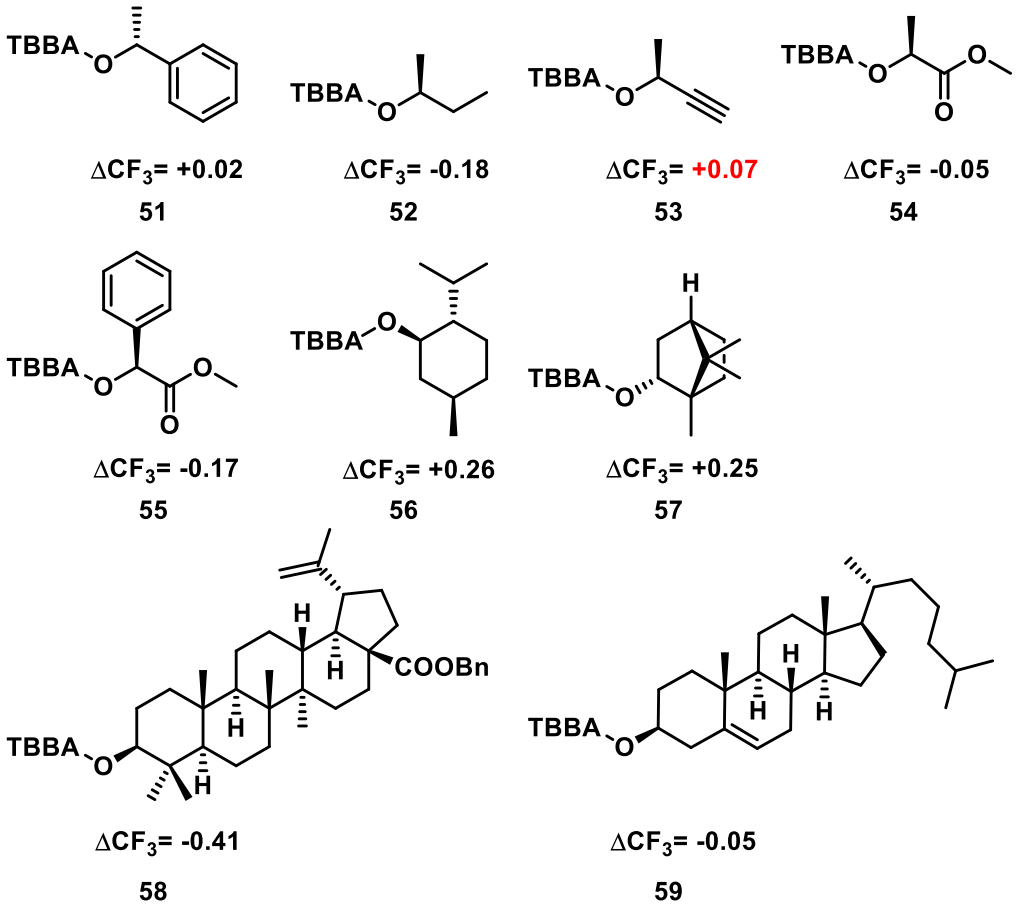

Figure 14 observed ΔCF_3 for esters **51-59**

Menthol **56** and borneol **57** displayed very similar ΔCF_3 +0.26 and +0.25 ppm, respectively, which were higher differences than previously described for the esters **51-55** and comparable to most of the analyzed amides. The two terpene derivatives **58** and **59**, although similar in structure, displayed a highly dissimilar ΔCF_3: -0,41 for **50** and -0.05 for **51**. To our delight, compounds **51-59** displayed homogenous sign distribution of the ΔCF_3 differences with the exception of the compound **53**. The simple model was proposed in Figure 15.

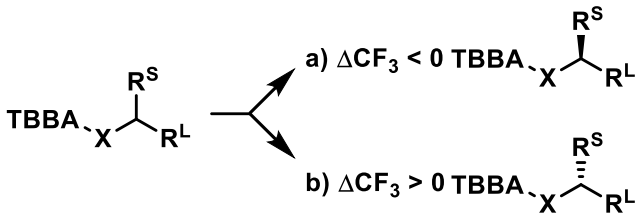

Figure 15 First proposed model for observed ΔCF_3

Assuming the large substituent (R^L) is positioned in the plane, the small substituent is positioned in front of the plane if the $\Delta CF_3 < 0$ (Figure 15a) and vice versa, if the $\Delta CF_3 > 0$, then the small substituent

is positioned behind the plane (Figure 15b). Unfortunately, this simplification only reliably works for acyclic compounds. In the case of cyclic esters **56-59** the large substituent R^L is clearly identified. The approximate size-priority of substituents is from R^L to R^S: *tert*-butyl > ester > aryl > isopropyl > benzyl > hydroxymethylene > methyl.

The difference in the ^{19}F spectra are likely caused by shielding or deshielding of the trifluoromethyl group by the substituents L^1 and L^2 of the analyte. The shielding cones are displayed in Figure 16.[163,164]

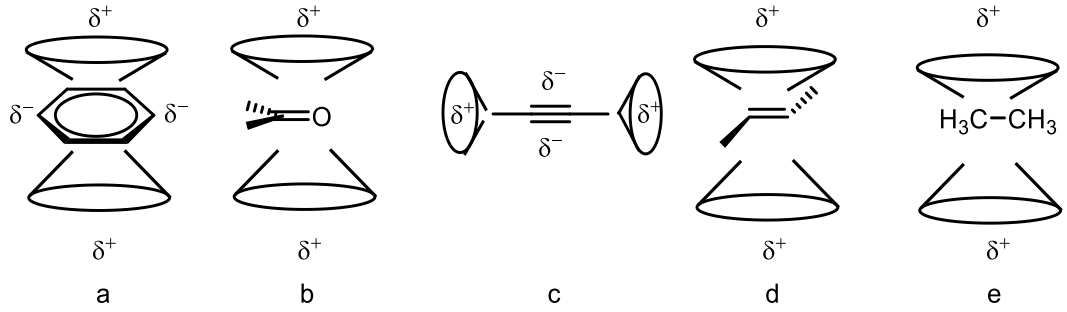

Figure 16: shielding cones a) aryl b) carbonyl group c) alkyne d) alkene e) alkane

δ^+: shielding δ^-: deshielding

Those shielding effects projected by substituents shield or deshield the CF_3 group (Figure 17) and, then, it is observed as a difference of the ^{19}F chemical shifts (Figure 13 and 14).

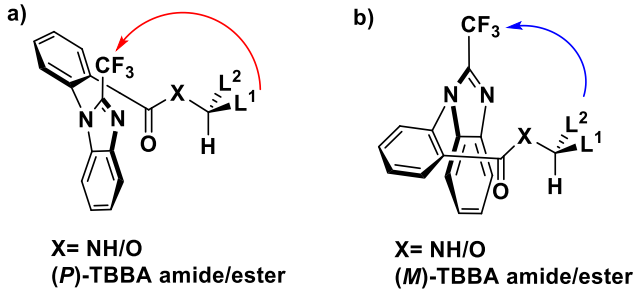

Figure 17 Possible explanation for observed ΔCF_3 differences

This model explains the observed differences of ^{19}F spectra and, furthermore, reveals the origin of the anomalous value for alkyne **53**, where the anisotropic effect of the alkyne is different. This difference is displayed in Figure 18, where the shielding effects of amide (***P*)-40** and ester (***P*)-53** are compared.

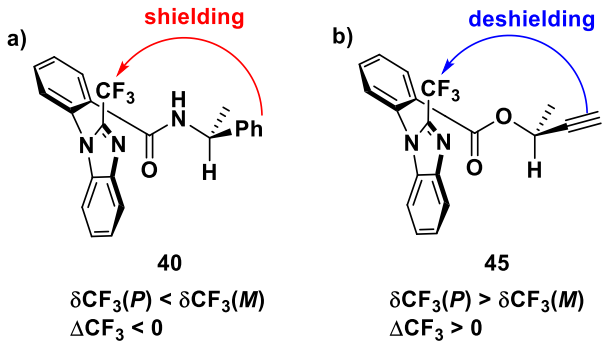

Figure 18 Possible explanation for observed ΔCF_3 values of compounds **40** and **45**

As can be seen in Figure 18, the same arrangement of the substituents in space causes the different chemical shifts of ^{19}F spectra. The phenyl ring causes shielding of the CF_3 group in the (***P***)**-40** and, therefore, it resonates upfield. For this reason, a lower chemical shift was observed compared to the (***M***)**-40** and, as a result, the negative ΔCF_3 was obtained after subtraction. The alkyne moiety in (***P***)**-53**, although located at the same position in space as the phenyl ring in (***P***)**-40**, causes deshielding of the CF_3 group. Then the higher chemical shift is observed, therefore a positive ΔCF_3 is obtained.

Since the simple alkyl group cause the shielding effect as well,[164,165] the observed ΔCF_3 in aliphatic derivatives **42, 46, 47, 52, 56-59** can be also explained. Our explanation is based on the hypothesis that the branched or longer aliphatic chains project stronger shielding effect compared to unbranched or shorter chains. The lack of branching or multiple bonds on the A-ring of the cholesterol derivative is the likely cause of the low observed ΔCF_3 (-0.05).

In the end, the use of ^{19}F NMR is more complicated than ^{1}H or ^{13}C NMR because the observed ΔCF_3 values depend not only on the absolute configuration of the analyte but also on the structure of present functional groups. Furthermore, only one data point is obtained for each diastereomer and, therefore, their comparisons always yield configuration with no space for self-correction. This is not the case of ^{1}H or ^{13}C analysis where multiple signals could be analyzed and any anomalous data can be resolved.This was shown in the case of MTPA which displayed lower than 50% reliability when using ^{19}F spectra.[86]

Analysis of β-chiral alcohols and amines

After the analysis of α-chiral compounds was finished, we turned our attention towards more complex β-chiral compounds. The analysis of this type of compounds is more complicated due to following reasons:[69,71,92,166]

a) Additional carbon in the structure highly increases the conformational flexibility; therefore, the NMR relevant conformer is less prevalent compared to α-chiral compounds.

b) The chiral center is located further away from the group projecting the anisotropic shielding effect.

For those reasons, the observed $\Delta\delta^{RS}$ values are smaller compared to the α-chiral derivatives and the only CDA that is able to produce sufficient and reliable differentiation is 9-AMAA.While MPA or MTPA work in some cases, the differentiation is significantly smaller compared to 9-AMAA and in some cases no differences in chemical shifts are observed.[69,71]

The advantage of TBBA compared to MPA or MTPA lies in lower conformational flexibility, which should allow more selective projection of the anisotropic shielding effect. Furthermore, the size of the benzimidazole ring is approximately in the middle between phenyl and napthyl rings of MPA/MTPA and 9-AMAA. The library of 18 esters (Figure 19) was prepared with the alcohols chosen to match the already prepared 9-AMAA esters to allow direct comparison of TBBA and 9-AMAA.[69,71] The analysis was conducted in the same manner as for the α-chiral alcohols and amines.

^{1}H NMR analysis

At first, (*S*)-2-methylbutan-1-ol **60** was used as the simplest alcohol available. The methyl group displayed $\Delta\delta^{PM}$ -0.11 ppm for the methyl group and +0.06 ppm for the ethyl group. Those values were comparable to 9-AMAA which yielded a lower difference (-0.01 ppm) on the methyl group but slightly higher (+0.08 ppm) for the ethyl group. The observed differences were significantly higher than those of MPA (+0.02, -0.01) and MTPA (+0.00 and -0.01) esters.[71]

Substitution of the ethyl group for bromomethylene in **61** did not have significant effect and yielded high $\Delta\delta^{PM}$ for ester **53**. The observed differences, -0.12 for methyl and +0.23 for methylene, were similar to 9-AMAA with the difference at the methylene protons being higher compared to 9-AMAA (+0.23 vs +0.09). Further substitution of the bromide for carboxymethyl group in **62** displayed similar $\Delta\delta^{PM}$ on the methyl group (-0.11). This difference was very similar to **60** and **61** and very close to 9-AMAA (+0.1). As expected, the more remote carboxymethyl group showed lower $\Delta\delta^{PM}$ of +0.06 which was slightly lower than 9-AMAA (+0.1). In comparison to those of MTPA (-0.01 and +0.01) and MPA (+0.02 and -0.04), the TBBA ΔδPM values18 were significantly higher.[71]

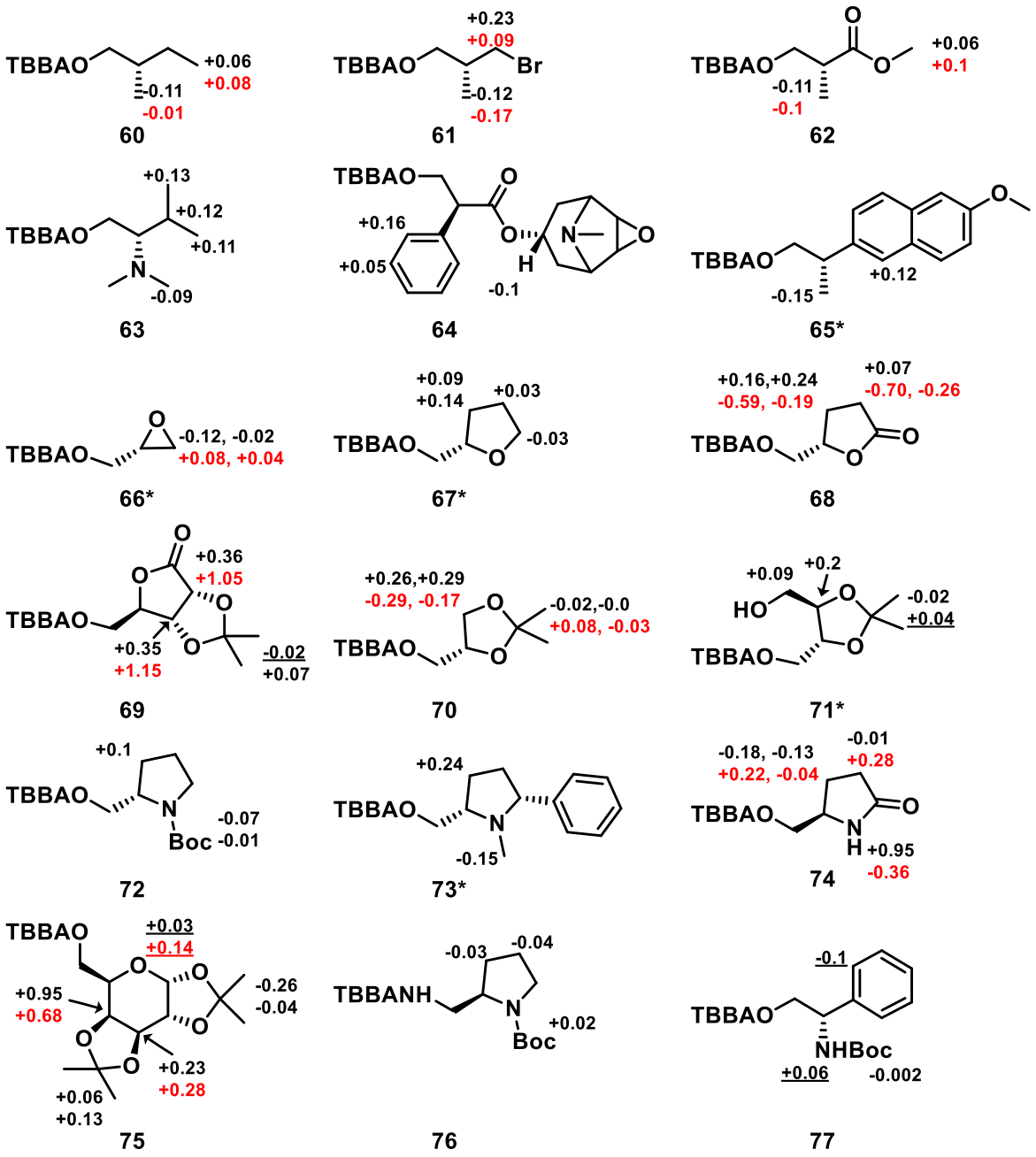

Figure 19 Observed $\Delta\delta^{PM}$ for compounds **60-77,** black: TBBA, red: 9-AMAA, anomalous values are underlined.

*Compound was prepared by undergraduate student David Profous.

** 9-AMAA esters **66**, **70**, **64** were prepared from the starting materials with opposite absolute configuration compared to TBBA esters. Therefore, the sign of the $\Delta\delta^{RS}$ is opposite compared to TBBA.

Branched alkyl chain in **63** slightly increased the observed $\Delta\delta^{PM}$ of the isopropyl (+0.11, +0.12 and +0.13) compared to the unbranched ethyl in **60**. The difference at the dimethylamino group was slightly lower as expected due to the methyl groups being located further away from the chiral center compared

to the methyl group in **60**, **61,** and **62**. Although, it was reported, that the presence of polar groups can change the conformation equilibirium,[92] it does not seem to be the case of compounds **62** and **63** since the observed $\Delta\delta^{PM}$ values are fairly high and distortion of the conformations was expected to significantly lower the observed $\Delta\delta^{PM}$.

Aromatic derivatives **64** and **65** were tested as well. In the case of **64**, partial (aprox. 10%) racemization was observed during the preparation of the ester, nevertheless it still allowed for NMR analysis. Protons in the *ortho* position of the phenyl ring displayed +0.16 ppm difference while the protons at the meta position displayed lower +0.05 ppm difference. The proton in the scopine moiety displayed $\Delta\delta^{PM}$ of -0.1 ppm which is comparable to the methylester **62.** Naproxol **65** showed -0.15 ppm difference at the methyl group and +0.12 at the *ortho* position, which is comparable to scopolamine derivative **64** and methyl substituted compounds **60**-**62**. The $\Delta\delta^{PM}$ values of (*S*)-glycidol TBBA ester **66** (-0.12 and -0.02 ppm) were comparable to those of the 9-AMMA ester, although a different conformational model was used.[92] While only one substituent was analyzed for **66**, the +0.2 ppm difference at position 2 suggested that a similar modification of the conformational model could be applied in the case of TBBA.

The $\Delta\delta^{PM}$ differences of tetrahydrofurane **67** at position 3 were +0.09 and +0.14 ppm and further decreased at positions 4 (+0.03 ppm) and 5 (-0.03 ppm). Tetrahydrofuranone **68** showed smaller $\Delta\delta^{PM}$ differences (+0.24 and +0.07 ppm) compared to those of 9-AMAA (-0.59 and -0.7 ppm) and slightly higher differences compared to those of **67**. This was evidently caused by the presence of the carbonyl group which alters the bond angles in the furanone ring. Ribonic-γ-lactone **69** displayed +0.36 and +0.35 ppm differences at the most relevant positions (smaller differences compared to those of the 9-AMAA ester)[71], and one of the acetonic methyl groups showed an anomalous negative sign. However, the magnitude of this difference was small and thus it can be ignored

The $\Delta\delta^{PM}$ values of the methylene group in glycerol **70** were +0.26 and +0.29 ppm for TBBA but only -0.05 and -0.07 for MPA and -0.01 and -0.03 ppm for MTPA. The values of the 9-AMAA ester (-0.29 and -0.17 ppm) [71] were similar to those of TBBA. Tartaric acid derivative **71** showed $\Delta\delta^{PM}$ values of +0.2 and +0.09 ppm. The difference of the CH proton was comparable to those of protons at the same positions in **67**, **68** and **69.**

The protons at position 3 of Boc-prolinol **72** displayed a difference of +0.1 ppm. Two values of -0.07 and -0.01 ppm of $\Delta\delta^{PM}$ were observed for the Boc group due to signal splitting into two singlets corresponding to 3 and 6 protons in the case of diastereomer (*P*)-**72**. The splitting was not observed at (*M*)-**72**. This phenomenon was likely caused by the partial presence (on average) of one methyl group slightly outside of the shielding cone. The $\Delta\delta^{PM}$ values of **72** were slightly lower than those of other ring structures, such as **67-71.**

Interestingly, the *N*-methylprolinol derivative **73** showed significantly higher $\Delta\delta^{PM}$ compared to *N*-boc derivative 72. As expected, the $\Delta\delta^{PM}$ of the methyl group is higher compared to boc because the

protons are closer to the chiral center and therefore located more inside the shielding cone compared to the boc group. Interestingly, the $\Delta\delta^{PM}$ at the position 3 is more than double of the in the boc-derivative **72**. The pyroglutaminol ester **74** showed significant $\Delta\delta^{PM}$ at the position 1 (+0.95) which is higher in magnitude than 9-AMAA (-0.35). The differences at position 3 (-0.18 and -0.13) were similar to 9-AMAA (+0.22 and anomalous +0.04) while the difference at position 4 was significantly smaller (-0.01 vs +0.28).

The protected galactopyranose ester **75** showed high $\Delta\delta^{PM}$ of +0.95 ppm at position 5 and +0.23 ppm at position 4, which were comparable to those of the 9-AMAA ester (+0.68 and +0.28 ppm).[18] Unfortunately, the anomalous $\Delta\delta^{PM}$ value at position 2, as was also observed for the 9-AMAA ester, could slightly complicate the assignment. Nevertheless, the small anomalous value of the TBBA ester at position 2 could be ignored since the most relevant signals displayed correct values.[24]

Generally, acetonide methyls were variously located in or out of the shielding zone. Thus, the sign distribution of the galactopyranoside acetonide methyl groups in **75** showed major differences in $\Delta\delta^{PM}$ values (-0.04, -0.26, +0.06 and +0.13) for the acetonide methyls, unlike derivatives **69**, **70**, and **71**. Similar to **69**, one of the acetonide methyl groups of **70** showed an anomalous positive $\Delta\delta^{PM}$ value, whereas **70** did not. However, one of the methyls on **70** showed a $\Delta\delta^{PM}$ value close to zero.

To preliminarily prove whether the method can be extended to β-chiral primary amines, amide **76** was prepared and compared with ester **72.** Boc-pyrrolidine **76** showed significantly smaller $\Delta\delta^{PM}$ differences at the relevant protons (-0.03, -0.04, and +0.02) than those of **72**, **73**, and **74.** The smaller $\Delta\delta^{PM}$ values observed for compounds **72** and **76** were likely caused by the large Boc protecting group. As expected, the $\Delta\delta^{PM}$ of *N*-substituents decreased with increasing distance from the nitrogen atom (+0.95 ppm for **74**, -0.15 for **73,** and -0.01 and -0.07 ppm for **72**).

Interestingly, (*S*)-Boc-Phenylglycinol **77** was not in accordance with the proposed model, and the opposite configuration was observed. This limitation of the method was likely caused by the sterically demanding Boc group, which impacts the conformational equilibrium. This seemed to be in agreement with the fairly low $\Delta\delta^{PM}$ values for Boc-substituted derivatives **72** and **76**.

Conformational model for assignment of absolute configuration by 1H or 13C NMR

Based on the experimental data, conformational model (Figure 20) for assignment of the absolute configuration was proposed. At first, the proton at the chiral center (Cα) is in *anti*-periplanar conformation to the carbonyl group. This allows the benzimidazole to project the shielding effect towards the L^2 substituent (Figure 20a). Naturally, in the (*M*)-diastereomer (Figure 20b), the shielding effect is produced towards the substituent L^1. Analogously to the α-chiral compounds, the $\Delta\delta^{PM}$ parameter is calculated following the equation in Figure 20c. The simplified model is shown in Figure 20d: if the substituent has $\Delta\delta^{PM}$ less than zero, it is located above of the carbonyl-Cα plane while if the $\Delta\delta^{PM}$ is higher than zero, the substituent is located under the plane.

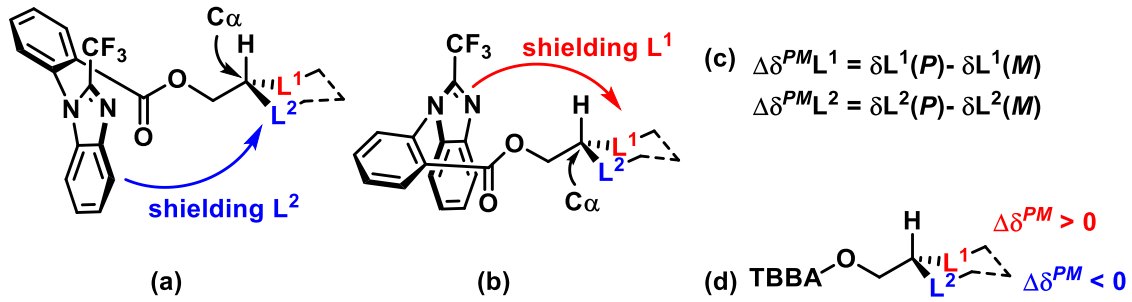

Figure 20 Conformational model for assignment of absolute configuration of chiral primary alcohols a) (*P*)-TBBA ester b) (*M*)-TBBA ester c) calculation of $\Delta\delta^{PM}$ d) simplified model.

To further strenghten the proposed model, DFT calculations were performed using Spartan 16 software using ester **60** as the model compound. The populations of theoretical conformers were calculated with the molecular mechanics model MMFF. Depending on the total number of theoretical conformers, this was followed by sorting of the conformation candidates with relative energies lower than 10−20 kJ/mol. The energies of sorted candidates at the ground state in the nonpolar solvent were calculated using density functional theory (B3LYP, 6-31G*) to find the lowest energy conformer.

a)

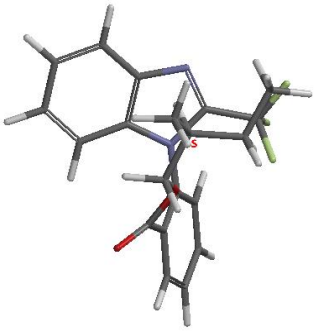

Most stable conformer

NMR relevant conformer

(0.358)

b)

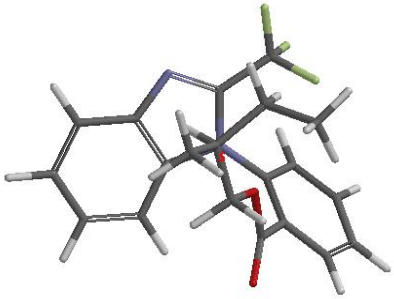

2nd most stable conformer

NMR-relevant

(0.091) ΔG= 3.39 kJ/mol

Figure 21 Conformers of **(*P*)-60**

a) b) c)

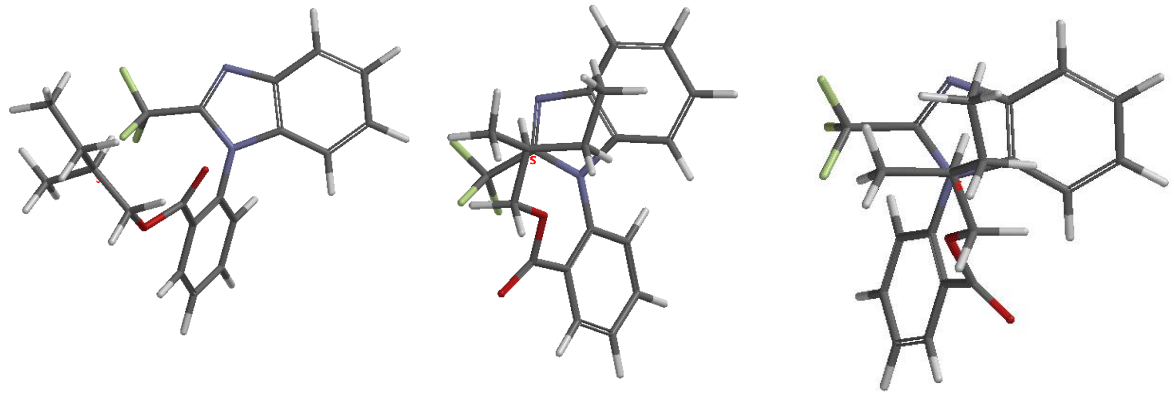

Most stable conformer

NMR irrelevant conformer

(0.173)

2nd most stable conformer

NMR relevant conformer

(0.163) ΔG= 0.12 kJ/mol

3rd most stable conformer

NMR relevant conformer

(0.092) ΔG= 1.56 kJ/mol

Figure 22 Conformers of (***M***)**-60**

As expected, the number of conformers is higher compared to α-chiral alcohols or amines. The most relevant conformers for diastereomer (***P***)**-60** are shown in Figure 21. The most stable conformer (Boltzman weight 0.358) is shown in Figure 21a. The proton at Cα is in *anti*-periplanar position to the carbonyl group which allows the methyl group to be shielded by the benzimidazole ring. The *anti*-periplanar conformation is slightly distorted and the Cα proton is also partially located in the shielding zone of the benzimidazole. The second most stable conformer with Boltzman weight 0.091 (Figure 21b) has the methyl and ethyl substituents located in a same manner as the most stable conformer. The difference is caused by the rotation of the ethyl group.

In the case of (***M***)**-60** diastereomer the conformation equilibrium is more complex since the most abundant conformer (Figure 22a) with Boltzman weight 0.173 is not NMR relevant. None of the substituents of the alcohol are outside of the shielding zone. The second most stable conformer (Boltzman weight 0.162 kJ/mol) is the most NMR relevant although the conformation is different compared to the described model (Figure 22b). The proton at Cα is rotated approximately 60° from the *anti*-periplanar conformation to the carbonyl group which moves the methyl group to the *syn*-periplanar conformation with the carbonyl group. Nevertheless, the ethyl group remains in the shielding zone of the benzimidazole. This conformational changes were already described by Seco[92] although for compounds possessing polar groups such as methoxy or Boc-amino. Further 60° rotation around the *Cα-CH*$_2$CO bond leads to the third most stable conformer of diastereomer (***M***)**-60** which is also NMR-relevant with the ethyl group being located inside the shielding zone of the benzimidazole (Figure 22c).

Furthermore, the in-silico study was performed on compound **77** because the opposite configuration was obtained using the proposed model and further inquiry into the conformations of compound **77** was required. The preliminary in silico modelling using B3LYP-G-31* suggested few explanations for the deviation from the expected conformational model (figure 23a).

At first, a steric interaction between bulky Boc-group and the benzimidazole demanded a rotation which put the bulky Boc group on the opposite side of the benzimidazole. This is the major conformer (Boltzman weight 0.292) observed in the (***P)*-77** diastereomer (Figure 23b). In the (***M*)-77** diastereomer, the situation is similar with the hydrogen atom being *syn*-periplanar with the carbonyl oxygen (boltzman weight 0.761). The conformation is further stabilized by hydrogen bonds between the trifluoromethyl group or the benzimidazole nitrogen (Figure 23c). The expected conformers with *N*-Boc group located in the periplanar position[92] (Figure 23d, 23e) were observed only as minor (Boltzman weight 0.094 and 0.146 respectively) conformers.

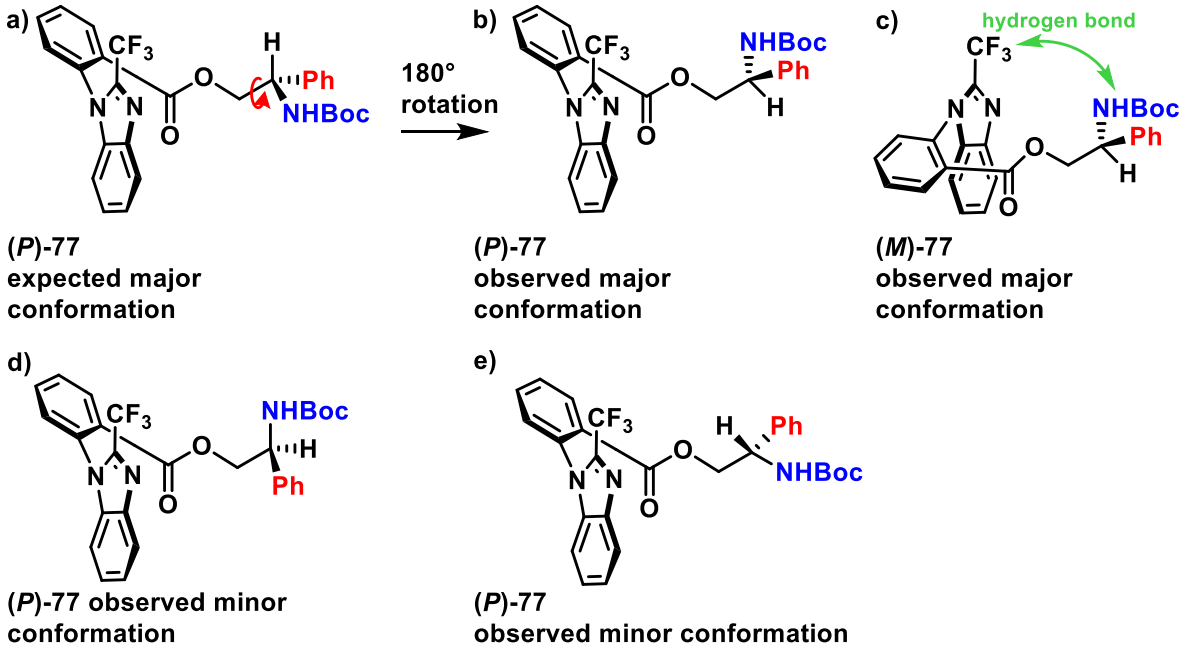

Figure 23 conformers observed in the B3LYP-G-31*

While the in-silico modeling provided some insight into the conformation of the compound **77** and its deviation from the proposed model, further experiments were performed to obtain more experimental evidence on this conformational change.

Investigation of the Boc-protected aminoalcohols

At first, small library of Boc-protected aminoalcohols was synthesized to confirm, if the unexpected conformations of compound **77** are only anomaly or if there is an ongoing trend (Figure 24)

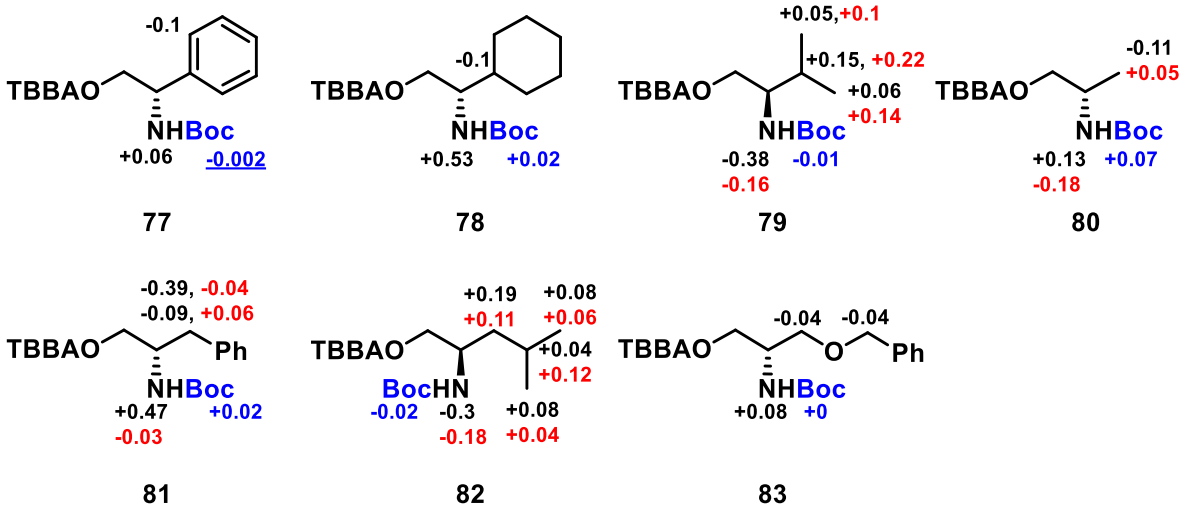

Figure 24 Analyzed Boc-aminoalcohols and their $\Delta\delta^{PM}$ values. Underlined values follow the previously proposed model. 9-AMAA values[71] are shown in red. 9-AMMA esters **71** and **74** were prepared from alcohol with opposite configuration compared to TBBA ester. $\Delta\delta^{PM}$ of the Boc group is displayed in blue for higher clarity

As described above, the (*S*)-Boc-Phenylglycinol ester **77** displayed -0.1 ppm difference at the ortho position of the phenyl ring and +0.06 of the NH. Using those values and the previously described model (Figure 20) yielded opposite configuration. The protons in the *tert*-butyl moiety in the Boc protecting group displayed $\Delta\delta^{PM}$ of -0.002 which is in accordance with the proposed model, but the difference is on the edge of the limitations of the NMR measurements.

Boc-cyclohexylglycinol **78** showed reliable distribution of $\Delta\delta^{PM}$: +0.53 for NH, +0.02 for Boc and -0.1 ppm for the proton at position 1 but when those values were used for the configuration assignment, opposite than expceted configuration was obtained as in the case of phenylglycinol **77**.

Reduction of size of the substituent by substitution of the cyclohexyl ring to isopropyl in **79** had only a minor effect on the observed $\Delta\delta^{PM}$ values. The NH proton displayed -0.38 ppm which is higher compared to the 9-AMAA derivative ($\Delta\delta^{RS}$ -0.16). The Boc protons displayed higher $\Delta\delta^{PM}$ (-0.01) compared to **79** and slightly smaller compared to **77**. The observed differences of the isopropyl moiety (+0.05, +0.15 and +0.06) were slightly smaller compared to 9-AMAA derivative (+0.1, +0.22 and +0.14).[71,92] The Boc-aminopropanol **80** showed lower $\Delta\delta^{PM}$ compared to **78** or **79**. The methyl group

displayed -0.11 ppm difference which is higher compared to 9-AMAA (0.05) while the observed $\Delta\delta^{PM}$ of the Boc-amino group were slightly lower (+0.13 for TBBA and -0.18 for 9-AMAA).[71]

Further modification of the structure by addition of the phenylring in phenylalaninol **81** displayed high $\Delta\delta^{PM}$ +0.47 for the aminogroup which is significantly higher than the 9-AMAA ester (-0.03). The protons at the benzylic position displayed -0.39 and -0.09 ppm difference. Interestingly, the 9-AMAA ester displayed anomalous value of one of the protons at the benzylic position. Substitution of the phenyl ring for isopropyl in **82** cause a significant change of the observed $\Delta\delta^{PM}$ values compared to the phenylalanine derivative **81**. The amino group displayed -0.3 ppm difference which is smaller compared to derivatives 7**8**, **79,** and **81.** The proton in *tert*-butyl group displayed -0.02 ppm difference which is in the same magnitude compared to previously described Boc-aminoalcohols **78-81**. Compared to 9-AMAA, compound **82** showed differences of a roughly same magnitude.

Last, the introduction of the more polar benzylether group of Boc-benzylserinol derivative **83** caused an interesting drop of observed $\Delta\delta^{PM}$ values. No $\Delta\delta^{PM}$ was observed in the case of boc group, while the NH proton displayed +0.08 ppm which is comparable to phenylglycinol derivative **77**. The protons at benzyl and position 3 displayed small -0.04 ppm differences. The exact cause of this small differences is unknown but possibly the preference for specific conformers is low in compound **83** due to the similar sizes of Boc-amino group and the benzylether moiety.

Analysis of phenylglycinol derivatives

Because the Boc-protected aminoaclohols clearly displayed preference for different conformation states compared to the previously developed model for β-chiral alcohols, the library was further expanded with various *N*-substitued phenylglycinols to further investigate the conformational model. At first, the *N*-methyl phenylglycinol derivatives were prepared to investigate the presence of the hydrogen bond.

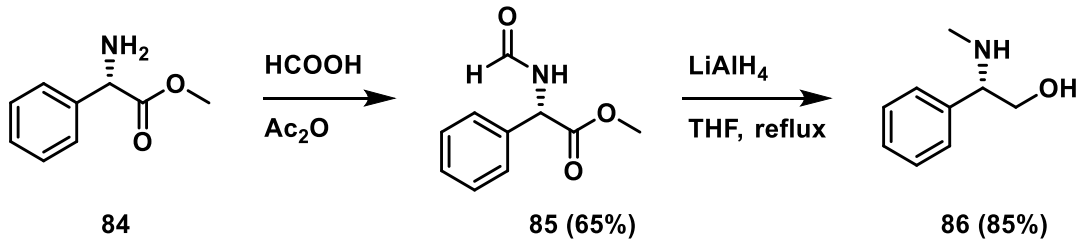

84 **85 (65%)** **86 (85%)**

Scheme 14 Synthesis of *N*-methyl phenylglycinol

Various methods to prepare key *N*-methylphenylglycinol **86** such as direct methylation of phenylglycinol with MeI, direct methylation of *N*-Boc-phenylglycinol with MeI; however, they did not yield any product at all. $LiAlH_4$ reduction of *N*-carbamates did not provide any product although the method was reported multiple times in the literature.[167,168] For this reason, a multistep sequence was

used (Scheme 14).[169,170] Starting from phenylglycine methylester **84** which was formylated using Ac_2O and HCOOH in 65% yield. Compound **85** was then reduced using $LiAlH_4$ in refluxing THF in high yield (85%).[171] Intermediate **86** was then converted into various *N*-methylphenylglycinols (Scheme 15).

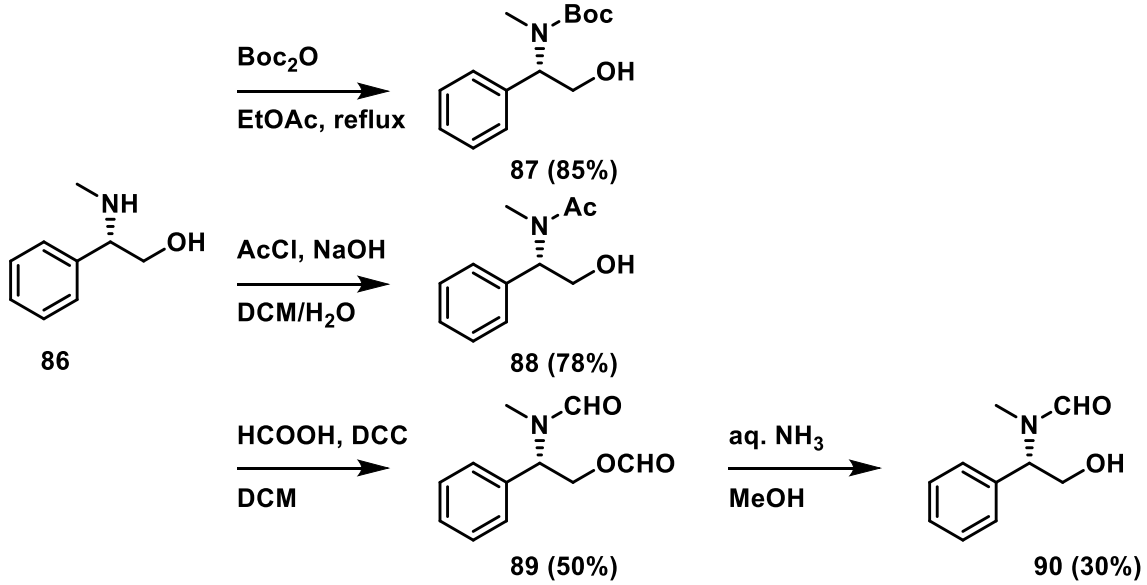

Scheme 15 Synthesis of *N*-methyl phenylglycinol derivatives

Boc-protection using Boc_2O in refluxing ethylacetate yielded derivative **87**.[171] Acylation of **86** using biphasic system DCM:H_2O yielded acetylated derivative **88**, which was isolated as a mixture of amidic rotamers in 10:4 ratio.[172] Formylation with already used Ac_2O+HCOOH system yielded a complex mixture of products. Luckily, HCOOH and DCC[173] yielded product **89**. Although the mono-formylated compound **90** was observed on TLC, the conversion of **86** to **89** was very fast and **90** was impossible to isolate from the reaction mixture in useful yields. Therefore, the reaction was let to finish and compound **89** was isolated with the idea of subsequent ester hydrolysis in the separate step. Hydrolysis of **89** using aq. NaOH yielded complex mixture of products. The use of aq. ammonia solution fully hydrolyzed the ester while keeping the amide bond intact. As in the case of **88**, compounds **89** and **90** were isolated as amidic bond rotamers.

N-acetyl phenylglycinol **93** was prepared in a similar manner as formyl derivative **90** by hydrolysis of ester **92**.[174] Dibenzyl **94**[175] and pthalimide **95**[176] protected phenylglycinols were prepared according to the literature procedures (Scheme 16).

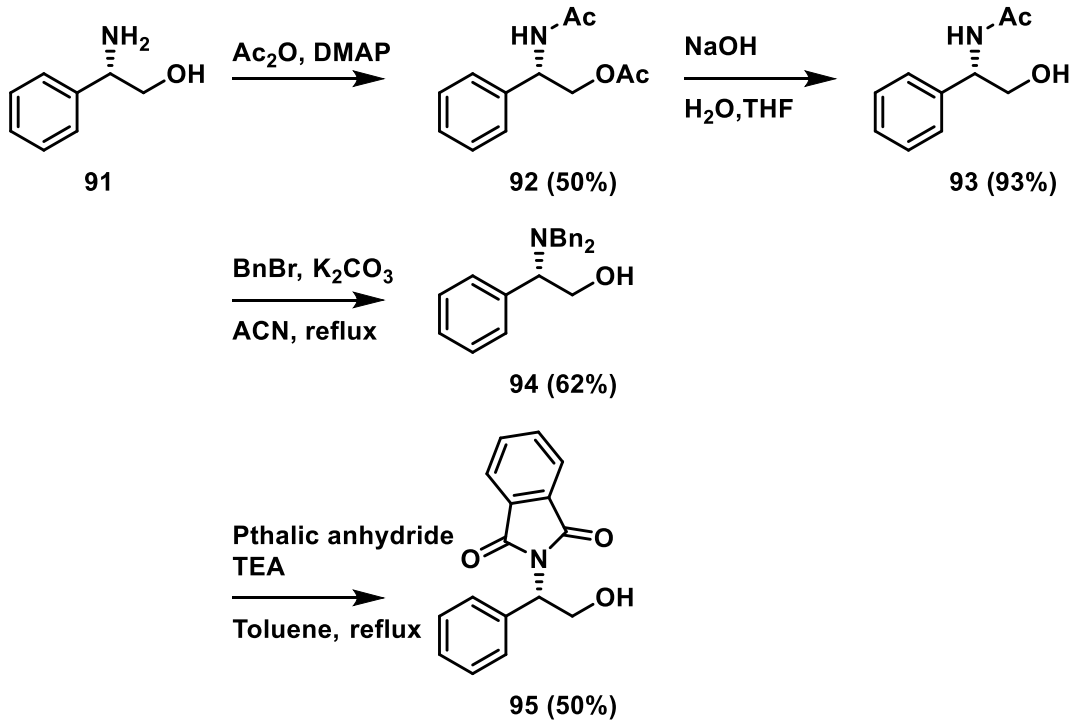

Scheme 16 Synthesis of phenylglycinol deriatives

With the protected alcohols **87**, **88**, **90**, **93-95** in hand, the library of TBBA esters was expanded (Figure 25). The *N*-Methyl-*N*-Boc derivative **96** displayed +0.1 ppm difference at the methyl group while -0.01 ppm at the Boc and *ortho*-protons. The observed $\Delta\delta^{PM}$ was smaller compared to the non-methylated compound **77**. Importantly, the configuration obtained using the $\Delta\delta^{PM}$ for compound **96** was opposite as in the case of compound **77**. The dimethylderivative **97**, showed -0.1 ppm difference for the dimethylamino group and +0.08 and +0.03 for *ortho* and *meta* protons on the phenyl ring. The obtained configuration was correct as was expected due to the similarity to compound **63** (Figure 19). This observation revealed no significant effect on the phenyl ring on the conformations as was reported in literature.[157]

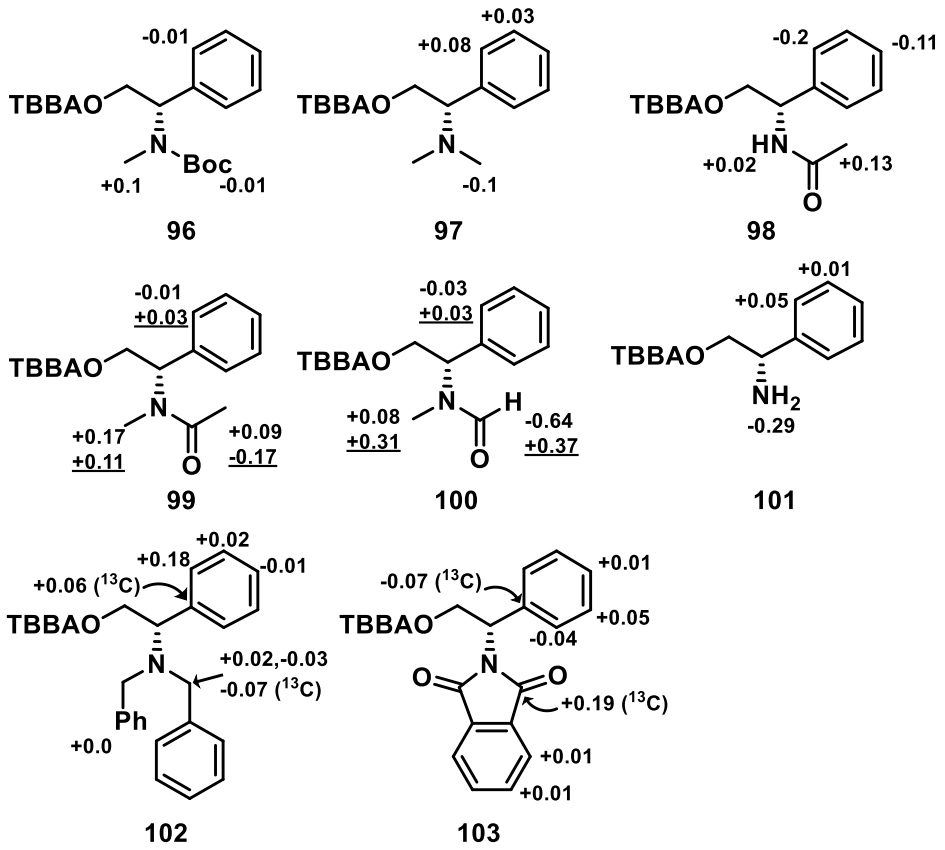

Figure 25 Observed $\Delta\delta^{PM}$ in derivatives **96-103**, minor rotamers are underlined

N-acetyl ester **98** showed +0.13 and +0.02 $\Delta\delta^{PM}$ at the acetyl group and amide proton respectively. The phenyl ring displayed -0.2 ppm difference at the *ortho*-position and -0.11 ppm at the *meta* and *para* positions and again. The magnitude of observed $\Delta\delta^{PM}$ in **98** was comparable to alcohols **60-83** (Figures 19 and 24). Based on calculated $\Delta\delta^{PM}$ opposite configuration was obtained as in the case of compounds **77-83** and **96**. This further suggests the hydrogen bond plays an effect, although it is not the sole reason for the preference of a different conformer since the *N*-methyl derivative **96** also yielded opposite configuration.

The *N*-methylation had a significant effect on the observed $\Delta\delta^{PM}$. First, ester **99** was isolated as a mixture of amide bond rotamers as was parent alcohol **88** which complicated the analysis. The major rotamer showed +0.17 and + 0.09 $\Delta\delta^{PM}$ for both methyl and acetyl protons while the phenyl displayed small -0.01 ppm difference at the *ortho* position. The minor rotamer showed +0.11 and -0.17 ppm for the methyl and acetyl protons and +0.03 ppm for the proton the *ortho* position of the phenyl ring. Using the observed $\Delta\delta^{PM}$ values for the configuration assignment, one can see that the major rotamer yields the opposite configuration while the minor rotamer gives ambiguous results.

Susbstitution of the acetyl for sterically less demanding formyl in ester **100** showed similar results as the acetamide **99**. The product was again isolated as a mixture of two rotamers. The major rotamer

displayed unsusually high $\Delta\delta^{PM}$ of the formyl group: -0.64 ppm. The methyl group showed $\Delta\delta^{PM}$: +0.08 ppm and the proton in ortho position of the phenyl ring displayed -0.03 ppm difference. Although the formyl group displayed high $\Delta\delta^{PM}$, the remaining two protons (methyl and ortho-Ph) showing anomalous sign of their $\Delta\delta^{PM}$ make the correct assignment inconclusive. The minor rotamer displayed +0.31 and +0.37 ppm for the methyl and formyl group, respectively, while the proton at the *ortho* position of the phenyl ring showed +0.03 ppm difference. This anomalous value again makes the configuration assignment inconclusive.

The *N*-unprotected ester **101** was prepared by removal of the Boc-group of compound **77** using 20% TFA in dichloromethane. The removal of the protecting group had a significant effect on the observed $\Delta\delta^{PM}$ values. The unprotected amino group displayed -0.29 ppm while the *ortho* and *para* protons displayed +0.05 and +0.01 ppm respectively. Those observed $\Delta\delta^{PM}$ values match the previously developed conformational model as in the case of the dimethyl derivative **97** and correct configuration was obtained.

Furthermore, dibenzyl **102** and pthalimide **103** protected phenylglycinols were prepared as well. Those two groups could be used as ammonia equivalents[177,178] and for this reason, the analysis of those derivatives is of high interest. The dibenzyl derivative **102** displayed positive $\Delta\delta^{PM}$ values on the phenyl ring: +0.18 ppm for the *ortho* proton, +0.02 ppm for the *meta* proton and anomalous -0.01 ppm for the proton in the most remote *para* position. The dibenzyl group showed 0 ppm difference in the aromatic rings while both positive (+0.02) and negative (-0.03) $\Delta\delta^{PM}$ values in the benzylic position. Although the anomalous value in the *para* position of the phenyl ring could be ignored, as being low in magnitude and far away from the chiral center, this logic cannot be applied in the case of the benzylic protons. Both $\Delta\delta^{PM}$ values at the benzylic position are similar in the absolute magnitude and the protons are located directly adjacent to the chiral center. Because of this discrepancy the ^{13}C NMR spectra were analyzed as well. The quarterary carbon in the phenyl ring displayed $\Delta\delta^{PM}$ of +0.06 ppm while the carbon at the benzylic position displayed difference of -0.07 ppm. Combining ^{1}H and ^{13}C NMR data and the conformational model developed for the β-chiral compounds, then the correct configuration was obtained.

The pthalimide derivative **103** displayed similar behavior. The protons in pthalimide moiety displayed +0.01 ppm difference while the protons in the phenyl ring showed anomalous behavior: the $\Delta\delta^{PM}$ for the protons in the *ortho* position was -0.04 ppm while the *meta* and *para* protons showed positive +0.05 and +0.01 $\Delta\delta^{PM}$. As in the case of **102,** ^{13}C NMR was analyzed to resolve the observed anomalous $\Delta\delta^{PM}$ values. The ^{13}C NMR showed +0.19 ppm difference for the carbonyl carbons and -0.07 ppm for the quarternary carbon in the phenyl ring. Using those values and the previously developed model, the incorrect absolute configuration is obtained for the pthalimide **103**.

Investigation of the possible bonding interactions

Based on those experiments we suspected hydrogen bond between boc hydrogen and fluorine which would favor an opposite conformation. Furthermore, the interaction between fluorine and boc carbonyl [179,180] could not be ruled out as well as repulsion between partially negatively charged carbonyl oxygen and trifluoromethyl group. NMR experiments were conducted with compounds **77-83** and **96** as model substrates. At first, the NMR spectra were measured in acetone-D_6 which was considered as a competing hydrogen bond acceptor and therefore could cause the change in the conformation equilibrium by removing the possible conformation-stabilizing H-F interaction. Furthermore, methyl trifluoroacetate (TFAOMe) was added as a source of external trifluoromethyl group which could interact with the Boc carbonyl group of the substrates. Observed $\Delta\delta^{PM}$ values are depicted in Figure 26.

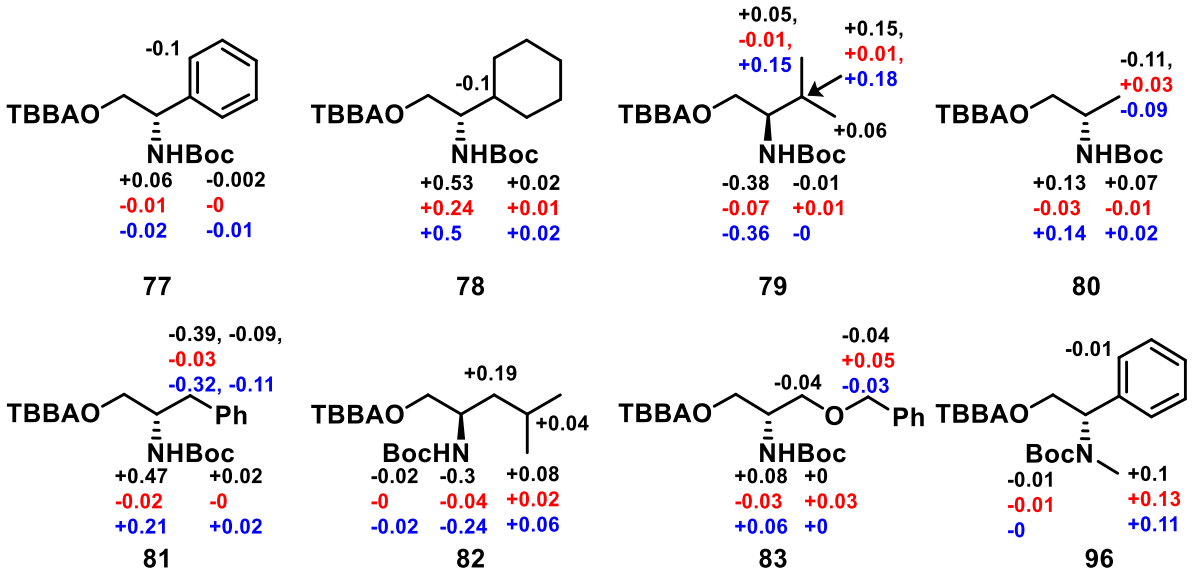

Figure 26 Observed $\Delta\delta^{PM}$ for compounds **77-83** and **96** in various solvents, black: $CDCl_3$, red: acetone-D_6, blue: $CDCl_3$+ TFAOMe

The observed $\Delta\delta^{PM}$ of **77** in acetone-D_6 displayed the correct signs, although the observed difference was small and close to the limits of the instrumentation. Similar situation was observed after the addition of TFAOMe into the $CDCl_3$ sample. Interestingly, in the case of derivative **78**, the sign of the $\Delta\delta^{PM}$ stayed the same as in the original spectra, although the magnitude of the difference was smaller. The $\Delta\delta^{PM}$ in the case of **79** became irregular in acetone-D_6. At first, the $\Delta\delta^{PM}$ of the methyls in the isopropyl group become negative while the CH in the isopropyl group displayed positive +0.01 ppm difference. Similar irregularity was observed on the Boc-amino group which displayed negative -0.07 ppm difference of the NH while the Boc group displayed positive +0.01 ppm difference. The observed $\Delta\delta^{PM}$ after the addition of TFAOMe into the $CDCl_3$ sample displayed very similar values compared to the original $CDCl_3$ spectra without the additive.

Complete inversion of the $\Delta\delta^{PM}$ sign was observed in **80** when the spectrum was measured in acetone-D_6 although the difference was close to zero. The spectra of **80** with TFAOMe in $CDCl_3$ displayed almost identical $\Delta\delta^{PM}$ as the original sample. Similar effect was observed in the case of compound **81**. No inversion of $\Delta\delta^{PM}$ was observed in the case of compound **82**. The observed $\Delta\delta^{PM}$ in acetone-D_6 were, nevertheless, significantly smaller compared to spectra in $CDCl_3$ (eg. -0.04 vs -0.3 ppm for NH). The addition of TFAOMe did not have a significant effect. Partial inversion was observed in the case of compound **83**. The $\Delta\delta^{PM}$ at the benzylic position and NH were inverted in acetone-D6 compared to $CDCl_3$. Nevertheless, the Boc-group displayed non-inverted positive $\Delta\delta^{PM}$ And no significant change was observed after the addition of TFAOMe. Elimination of intramolecular hydrogen bond formation in the case of compound **96** led to marginal $\Delta\delta^{PM}$ differences between the NMR spectra in $CDCl_3$ and acetone-D_6 solutions. .

Those results suggest the hydrogen bond might be present in the compounds although it is not likely the only cause of the obtained opposite configuration in the Boc-protected aminoalcohols. This can be seen in the examples in Figure 26. Conducting the NMR measurement in acetone-D_6 had significant effect on the observed $\Delta\delta^{PM}$, although not all of the derivatives displayed fully inverted $\Delta\delta^{PM}$. This suggests the presence of other interactions. The previously mentioned F…CO interaction is less likely because the addition of TFAOMe (as an external CF_3 source) had only a marginal effect on the chemical shifts., Steric effects very likely play an important role as well, although sterically demanding dibenzyl derivative **102** (Figure 25) followed the proposed model. It displayed an anomalous value at one of the benzylic protons while ^{13}C spectra showed the expected sign. Pthalimide **103** (Figure 25) displayed a mix of positive and negative $\Delta\delta^{PM}$ values which would make the assignment of absolute configuration impossible or at least very speculative. It does not contain acidic NH within its structure. The sterically less demanding derivatives **97** and **101** (Figure 25) fully followed the proposed model. The *N*-methyl derivatives **96**, **99**, and **100** display a mix of positive and negative $\Delta\delta^{PM}$ values due to the complex conformational equilibrium with various amide rotamers. Very likely all those effects are combined and play a role in the conformational equilibrium. In the case of Boc-protected or acetylated aminoalcohols, the hydrogen bond is the reason for preference of different conformers. However, based on the structure of the specific substrate, the electronic repulsion could predominate.

19F NMR analysis of β-chiral alcohols and amines

Similar to the α-chiral derivatives, ^{19}F NMR spectra were analyzed as well (Figure 27) to see whether a suitable model might be developed. At first, compounds **60**-**77** were analyzed because they followed the proposed model for β-chiral compounds (with the exception of compounds **77**). Similar assumptions were made about shielding cones (Figure 16) as in the case of α-chiral derivatives. In general, approximately a half of the compounds follow the general model and display ΔCF_3 differences between 0-0.6 ppm.

The valinol derivative **63** displays 0 ppm difference between the (*P*)- and (*M*)- diastereomer, likely due to similarities between the isopropyl group and dimethylamino group. Scopolamine ester **64** displayed a negative ΔCF_3 value. This suggests that the carbonyl group produces a stronger shielding effect compared to the phenyl ring. Furthermore, the phenyl ring might be oriented in a way that projects the deshielding effect towards the CF_3 group. Similar anomalous ΔCF_3 is observed in the case of naproxol ester **65** which should project shielding effect on the CF_3 group in the (*M*)-diastereomer to yield a positive ΔCF_3 difference; however, a negative difference was observed. Ester **66** also displays anomalous ΔCF_3 with the expected shielding coming from CH_2 group is projected towards the trifluoromethyl group in the the (*M*)- instead of (*P*)-diastereomer. Likely, the small size of the ring affects the direction of the shielding cone.

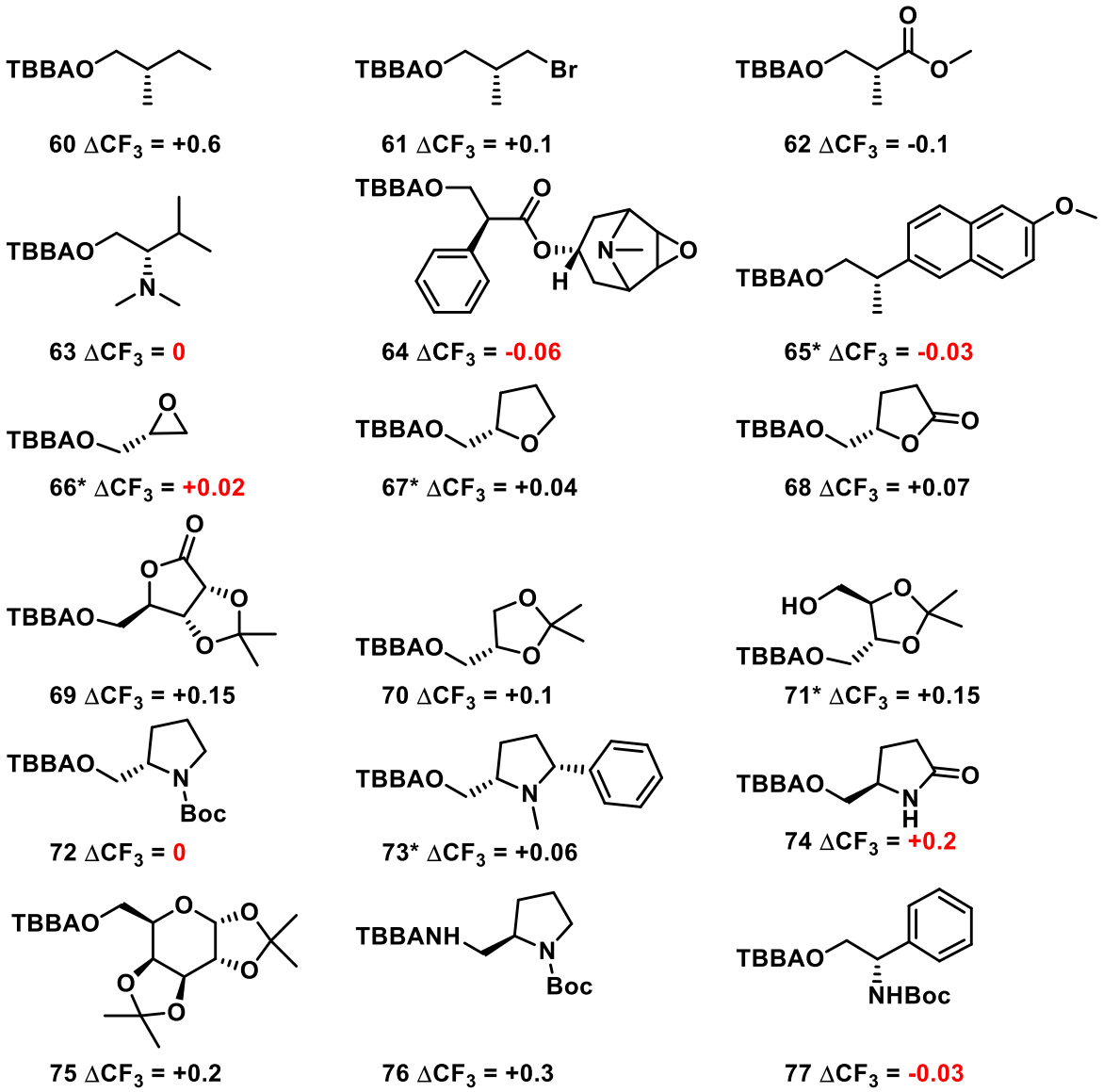

Figure 27 Observed ΔCF_3 for compounds **60-77.** Differences not matching the expected model are shown in red

The five-membered rings **67-71** follow the model and the expected ΔCF_3 values are observed even in the case of **69** or **71** which include more functional groups. Boc-protected ester **72** displayed 0 ppm ΔCF_3 difference. Possibly the sterically demanding Boc-group changes the conformation equilibrium which is in an agreement with fairly low observed $\Delta\delta^{PM}$ in the ^{1}H NMR spectra. Phenyl-substituted pyrrolidine **73** followed the model, although the phenyl ring could influence the conformations and therefore ^{19}F NMR spectrum as well. Pyroglutamol ester **74** displayed positive +0.2 ppm difference which is not in agreement with the model. In this case, the presence of hydrogen bond between NH and CF_3 group or other acceptors cannot be ruled out which could explain the high observed $\Delta\delta^{PM}$ (+0.95) in ^{1}H NMR spectra (see Figure 19; compound **74**). The Boc-phenylglycinol ester **77** does not follow the proposed model, although the negative ΔCF_3 value is in an agreement with the different conformational model (vide infra).

The ^{19}F NMR spectra of the rest of the prepared derivatives (Boc-protected aminoalcohols and Phenylglycinol derivatives) were analyzed as well. However, in those cases, almost a half (6 out of 14) of prepared derivatives display inconsistent chemical shift differences in the ^{19}F spectra and these differences cannot be easily translated to the absolute configuration of the chiral center as in the case of α-chiral derivatives (Figure 28).

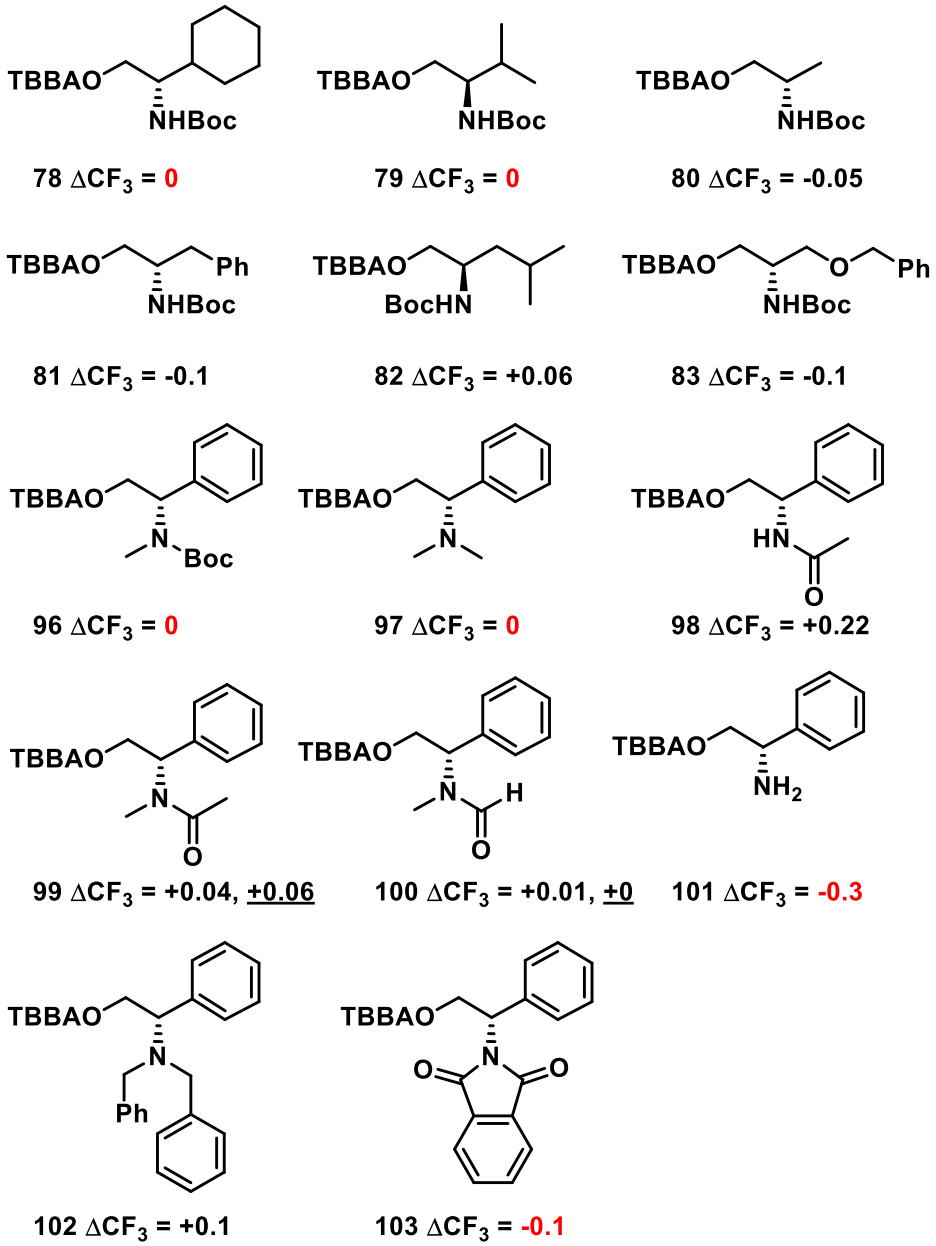

Figure 28 Observed ΔCF_3 of compounds **78-83** and **96-103** Differences not matching the expected model are shown in red

Computational investigation of the conformation of N-boc aminoalcohols

Last, more complex, in-silico modeling was performed using Spartan software. Conformer distribution was calculated with density functional theory (ωB97X-V/6-311+G(2df,2p)[6-311G*]) using ωB97X-D/6-31G* geometry[181] for Boc-derivatives **77**, **80**, and **81** as model substrates. In general, a lower number of conformers was observed compared to preliminary calculactions with B3LYP 6-31G*. This is likely due to the method which included three subsequent re-calculations and subsequent removal of high energy conformers.

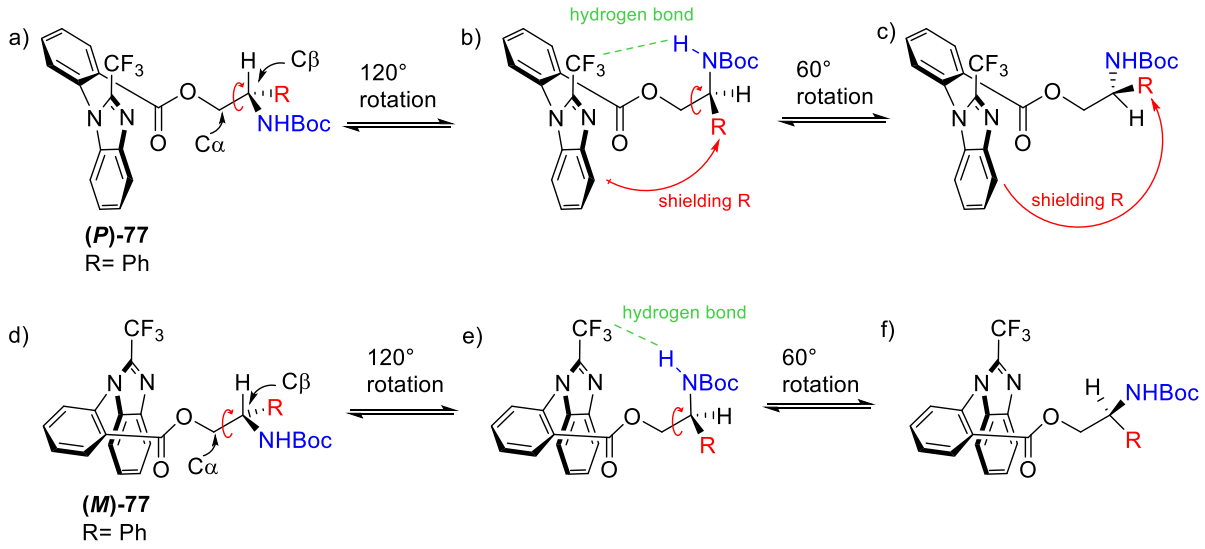

Figure 29 Supposed effect of the NHBoc group on the general simplified conformational model of **(*P*)-77** and **(*M*)-77** a) expected major conformer of **(*P*)-77** b) conformer after 120° rotation around Cα-Cβ bond, c) conformer after further 60° rotation around Cα-Cβ bond, d) expected major conformer of **(*M*)-77**, e) conformer after 120° rotation around Cα-Cβ bond, f) conformer after further 60° rotation around Cα-Cβ bond

Two major conformers (Boltzman weight 0.518 and 0.482) were identified in (***P*)-77**. Rotation around Cα-Cβ bond was observed in all cases (Figure 29). Interestingly, different hydrogen bonds were observed compared to B3LYP-G-31*: between NH and the benzimidazole nitrogen. The only observed conformer for (***M*)-77** similarly had Cα proton and carbonyl in a syn-periplanar conformation while the shielding effect was produced mostly towards the NH. The Boc group was positioned outside the shielding cone which explains the negligible observed $\Delta\delta^{PM}$ (Figure 30).

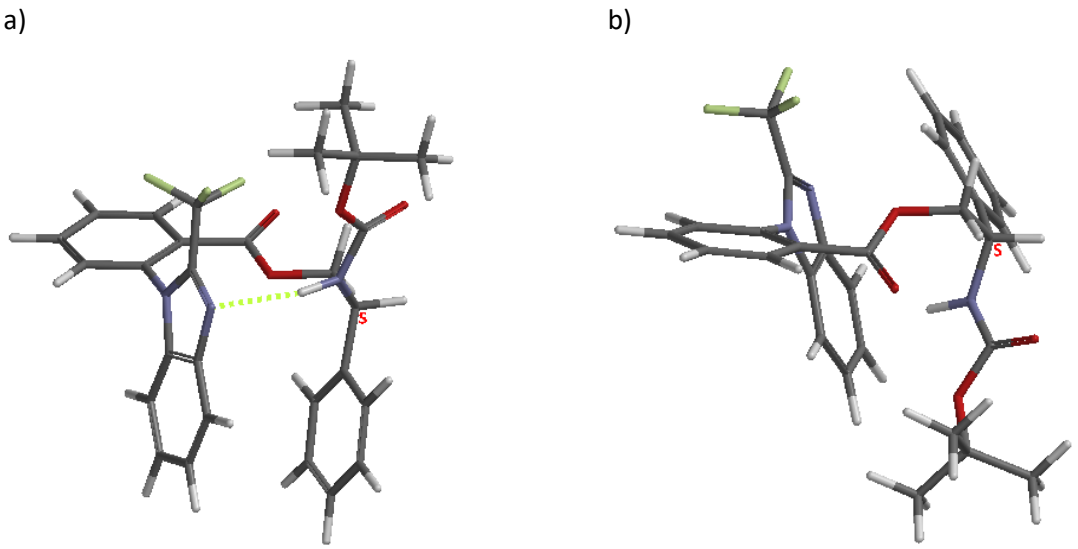

Figure 30: Major conformers of **(*P*)-77** (a) and **(*M*)-77** (b)

Two major conformers were identified in **(*P*)-80** again with the proton and the carbonyl group in *syn*-periplanar conformation. The hydrogen bond between NH and the benzimidazole nitrogen further locks the conformation and the shielding effect is projected to the methyl group in accordance with experimental data (Figure 31). Four conformers were identified in (***M***)-**80**. Interestingly, the major conformer (boltzman weight 0.555) approximately follows the proposed model with the help of NH-benzimidazole hydrogen bond, the shielding effect is produced on the methyl substituent (Figure 31b). The remaining conformers with boltzman weights 0.222, 0.142, and 0.121 produce the shielding effect on the NH in accordance with experimental data, although only the least probable conformer has the proton in *syn*-periplanar conformation with the carbonyl group. The other two conformers are bent from the periplanar conformation.

a) b)

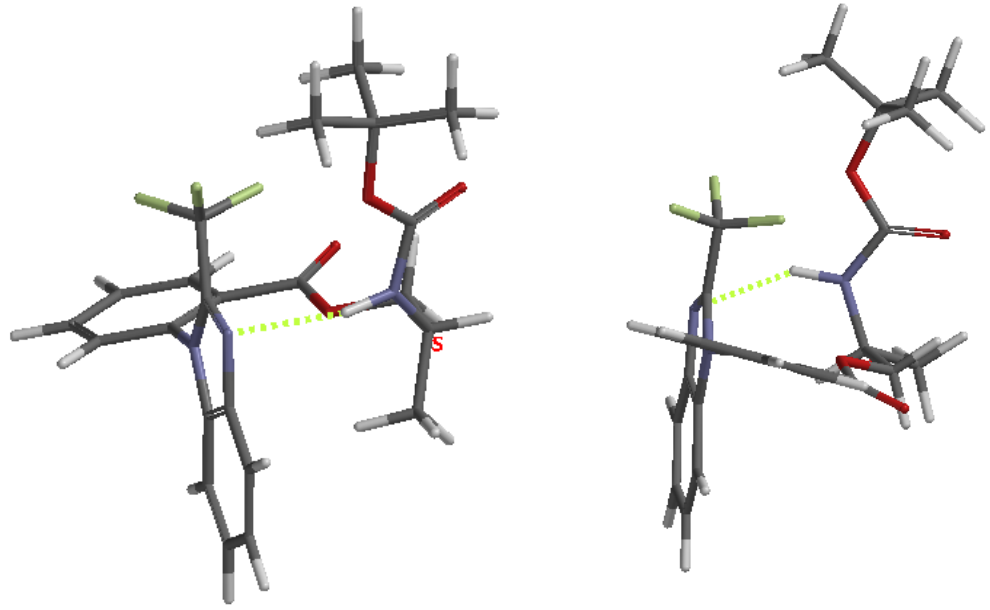

Figure 31 Major conformers for **(*P*)-80** (a) and **(*M*)-80**

Only one conformer for compound **(*P*)-81** was identified with the CH being positioned in *syn*-periplanar conformation with the carbonyl group. The benzyl group is situated directly in front of the benzimidazole ring in accordance with the experimental data. This conformation explains observed the relatively high -0.39 $\Delta\delta^{PM}$. Again, the hydrogen bond between NH and imidazole was suggested (Figure 32a). The major conformer in **(*M*)-81** (boltzman weight 0.594) follows the previously proposed model for β-chiral compounds (Figure 32b) and, therefore, the shielding effect is projected towards the benzyl group. This could explain why one of the benzylic protons have relatively high $\Delta\delta^{PM}$ while the other value (-0.09) is comparatively smaller. Out of the remaining four conformers, three were formed by the similar bond rotation and have the CH and carbonyl in the *syn*-periplanar conformation. This leads to the space arrangement, where the shielding effect is produced directly towards the NH which

demonstrates itself in high $\Delta\delta^{PM}$ (+0.47) for the NH. The Boc group is located further away from the shielding cone and, therefore, the $\Delta\delta^{PM}$ of the Boc group is relatively small.

a) b)

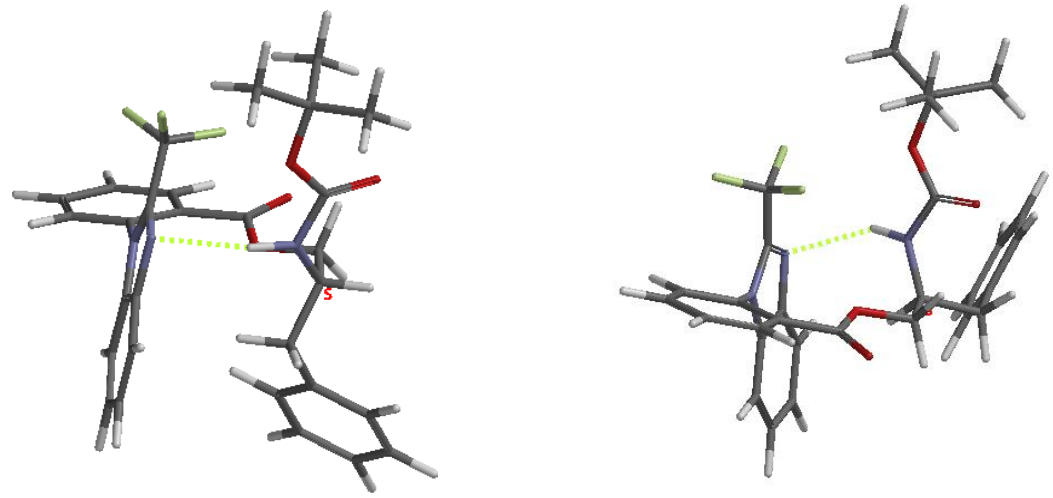

Figure 32 Major conformers of **(*P*)-81** (a) and **(*M*)-81** (b)

Then, we turned our attention towards *N*-methylated derivative **96.** As expected, no hydrogen bonds were observed and the number of conformers increased significantly. The major conformer in **(*P*)-96** projects the shielding effect mainly on the phenyl ring and the *N*-methyl, while the Boc group is located outside of the shielding cone of the benzimidazole (Figure 33a). Interestingly, the boc group is partially shielded by the phenyl ring of TBBA. Contrary, the methyl group is further deshilded by the phenyl ring of phenylglycinol. The situation is similar in the case of ***(M)-96*** with less deshielding being observed on the methyl group (Figure 33b). The high number of conformers (five for **(*P*)-96** and especially eleven for **(*M*)-96**) with different shielding / deshielding effects explains the relatively low $\Delta\delta^{PM}$.

a) b)

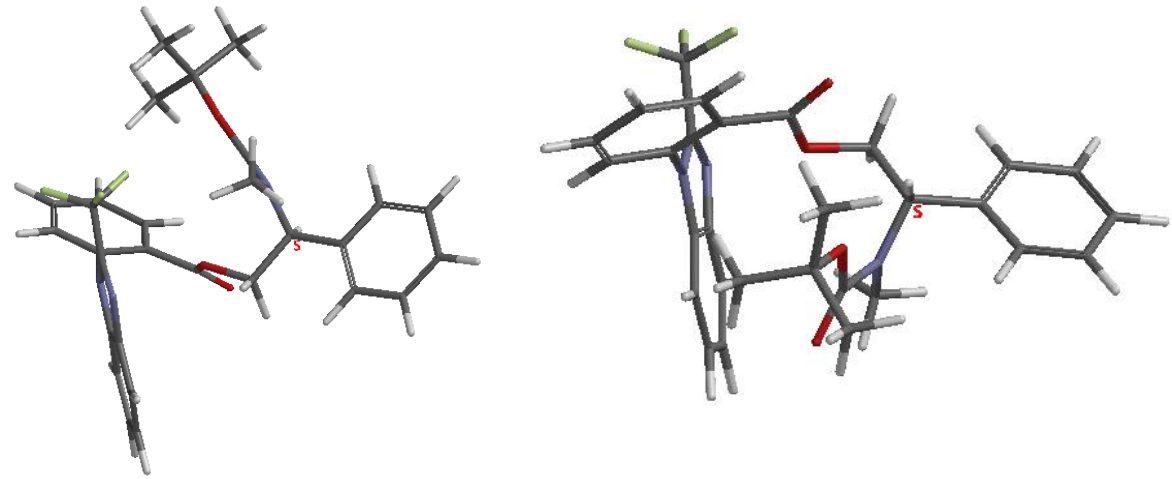

Figure 33 Major conformers of **(*P*)-96** (a) and **(*M*)-96** (b)

Removal of protecting groups in **101** simplified the conformational equilibrium with the major conformer in **(*P*)-101** has the phenyl group in *syn*-periplanar conformation to the carbonyl similar to already reported examples.[92] While this is a deviation from the proposed model, simple rotation by 60° yields the conformation proposed in the model and has no effect on the sign of the $\Delta\delta^{PM}$. The remaining two conformers (total boltzman weight 0.113) are formed by the rotation around O-CH_2 bond which moves the phenyl ring into the shielding zone of the benzimidazole. This explains the relatively low $\Delta\delta^{PM}$ observed for compound **101**. The **(*M*)-101** occupies similar conformation with the phenyl group in the *syn*-periplanar conformation; nevertheless, the phenyl ring is located in the shielding cone of the benzimidazole due to slight distortions. Interestingly, the hydrogen bond between the NH group and CF_3 was proposed by the calculations, however, no effect of the hydrogen bond on the $\Delta\delta^{PM}$ was observed. Possibly, the lack of carbonyl substituent on the aminogroup allows for higher flexibility of the aminogroup which is located just outside of the shielding zone of the benzimidazole (Figure 34).

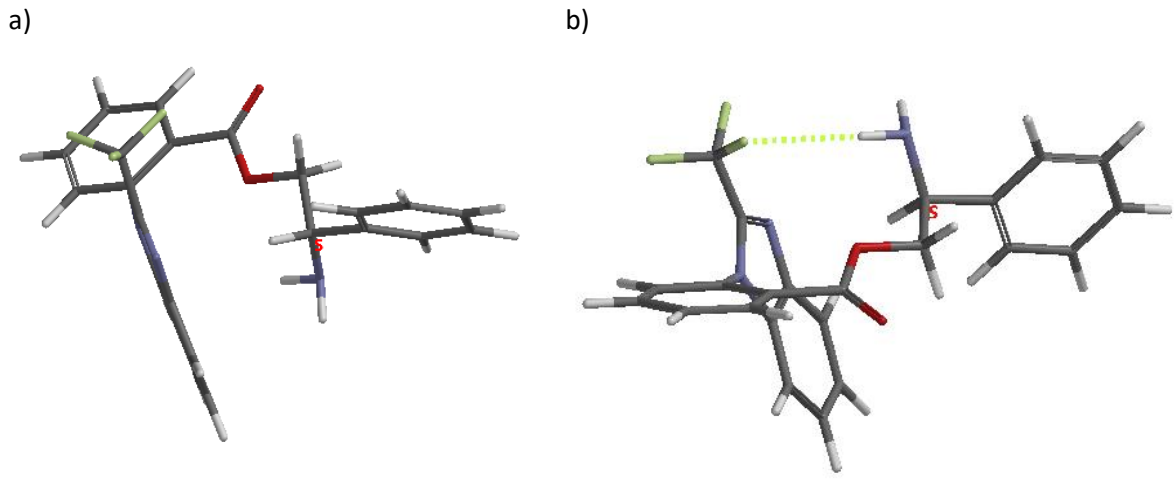

Figure 34 Major conformers of **(*P*)-101** (a) and **(*M*)-101** (b)

The pthalimide protected derivative **103** showed highly anomalous $\Delta\delta^{PM}$ with most of them being positive. The major conformer of (***M***)**-103** has phenyl group located in *syn*-periplanar position with the carbonyl group which could explain both positive and negative $\Delta\delta^{PM}$ observed in the case of compound **103**. Furthermore, the high rigidity of the pthalimide and high steric demand impacts the conformation in such a way where both phenyl and pthalimide moiety are partially located in the shielding cone of the benzimidazole (Figure 35).

a) b)

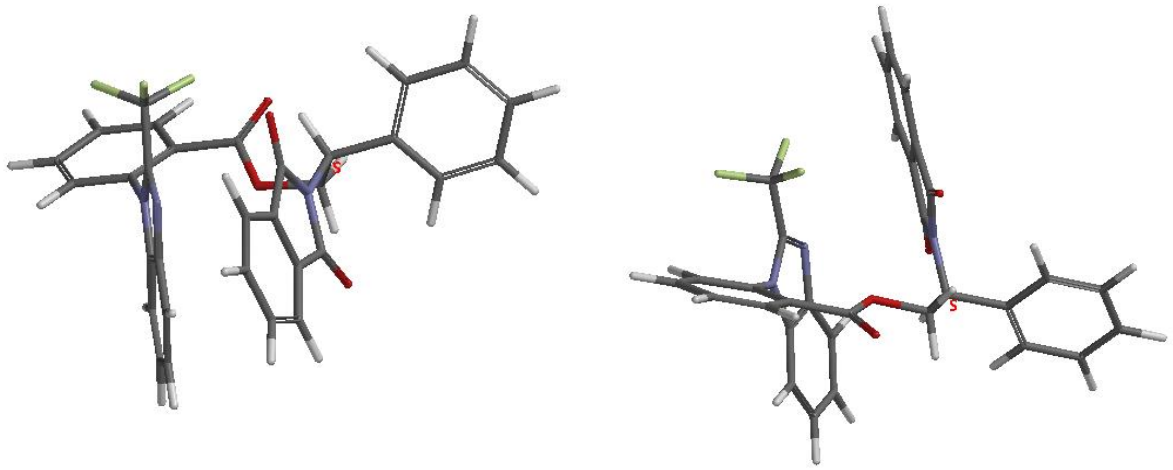

Figure 35 Major conformers of **(*P*)-103** (a) and **(*M*)-103** (b)

Based on the experimental results and the in-silico modeling we propose alternative conformation model for *N*-Boc aminoalcohols (Figure 36).

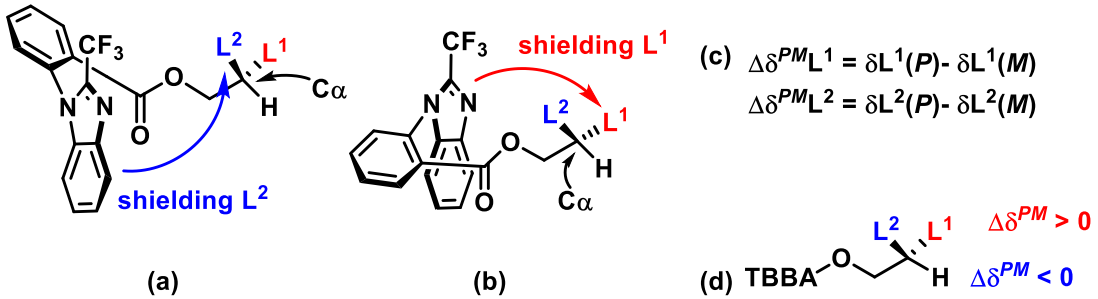

Figure 36 Conformational model for analysis of the Boc-substituted derivatives

In this model, the proton at Cα and the ester carbonyl group are in *syn*-periplanar conformation which moves one of the substituents into the shielding zone of the benzimidazole (Figure 30a/b). Compared to the previously devised model for β-chiral esters, the rotation around Cα-CH_2O bond causes the shielding effect to be projected towards the opposite substituents. The shielding/deshielding $\Delta\delta^{PM}$ is calculated in a same way as in the other models (Figure 28c) and the simplified model is shown in Figure 28d. Importantly, the model is suitable for compounds containing NHCOR (ie. Amide, carbamate) as one of the substituents. The presence of the more acidic hydrogen causes likely the formation of hydrogen bonds which change the preferred conformer and the observed $\Delta\delta^{PM}$ values.

In case of *N*-disubstituted derivatives with R-NCOR´, the conformation equilibrium is more complex due to the formation of amide bond rotamers and the observed $\Delta\delta^{PM}$ does not allow clear configuration assignment.

Synthesis of deuterated TBBA

Later, the deuterated version of TBBA **104** was prepared using high-pressure hydrogen deuterium exchange (Scheme 17).[182] Possibly the H → D exchange could simplify the analysis of the ^{1}H NMR spectra of the TBBA derivatives.

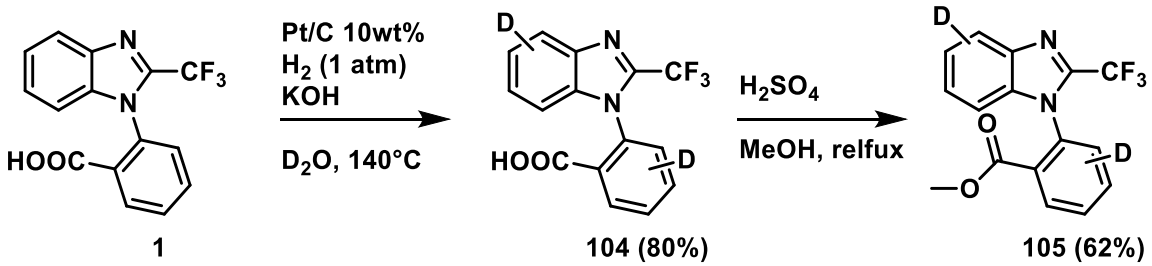

Scheme 17 Synthesis of deuterated derivatives **104** and **105**

At first, TBBA **1** was dissolved in D_2O in the presence of 1eq. of KOH due to the low solubility of TBBA in water. Heating for 24 hours in autoclave in the presence of Pt catalyst and hydrogen atmosphere yielded TBBA-D_6 **104.** The extent of deuteration was confirmed by HRMS and 6 deuterium atoms were exchanged (Figure 37). Furthermore, the deuterated compound **104** was converted into the methylester **105**. Integration of the ^{1}H NMR spectra suggested 25% deuterium incorporation at two positions, 90% incorporation at another two positions and full deuteration on the remaining 4. This suggests presence of multiple derivatives with various extent of deuteration.

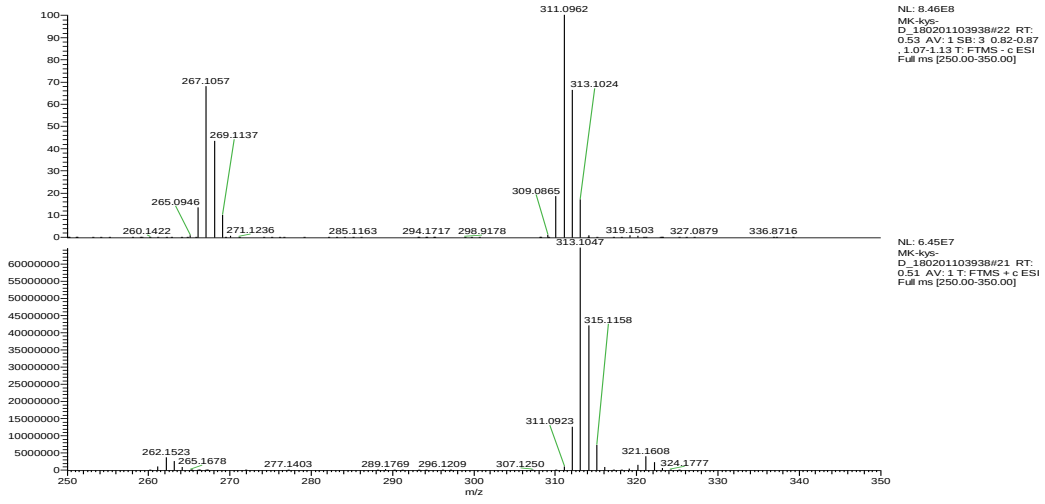

Figure 37 HRMS spectra of **104, top: ESI(-), bottom: ESI(+)**

Possibly increase of reaction time could yield fully deuterated derivative, however because the reaction could be performed only at low scale and the conditions were not compatible with the use of enantiopure TBBA, this approach was abandoned.

Conclusion

In conclusion, the novel CDA for absolute configuration assignment by NMR was developed. The conformational model was validated on a set of seventeen α-chiral esters and amides which allows the configuration assignment by means of ^{1}H, ^{13}C, and ^{19}F NMR spectroscopy.

A similar model was developed for β-chiral compounds and was validated on a set of eighteen compounds. Seventeen of them fully followed the model while in one case, an opposite configuration was obtained. Further investigation of fifteen derivatives revealed the different conformation preference for *N*-Boc aminoalcohols and *N*-acyl aminoalcohols. This conformational preference is likely caused by the hydrogen bond between NH and CF_3 or benzimidazole nitrogen as suggested by in silico modelling. This was confirmed by ^{1}H NMR spectra measured in acetone-D_6 as an external hydrogen bond acceptor which caused significant changes in the observed $\Delta\delta^{PM}$ compared to $CDCl_3$. Based on experimental data and in silico modelling, alternative conformational model was proposed for the aminoalcohols with the *N*-carbonyl moiety. Unfortunately, compounds of the R-N-COR or RCO-N-OCR type of functional groups did not follow any proposed models and provided highly anomalous $\Delta\delta^{PM}$.

The removal of the protecting group changed the conformation equilibrium again. The unprotected compound followed the general model for β-chiral compounds which allows for two subsequent analyses one of the protected compound using the modified model and another one using deprotected aminoalcohol ester and the unmodified model. Unfortunately, the ^{19}F NMR yields ambiguous results and, therefore, cannot be recommended for this type of compounds.

Results and discussion: Project catalysis

Design of the ligand

Two structures of the ligand (Figure 38) were envisioned at first. The benzimidazol-2-one/thione **106** which was reported multiple times as a ligand for Pd-catalyzed or organocatalytic reactions.[60,183–185] The benzimidazole-pyridine ligand **107** is based on pyridine-oxazoline catalyst developed by Kočovský.[125]

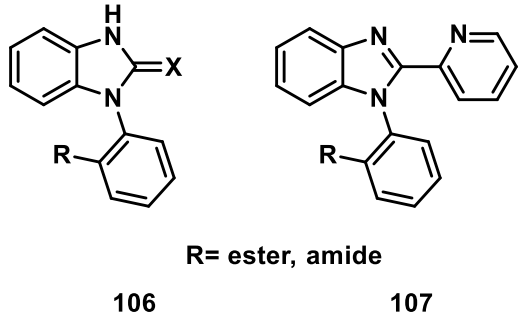

Figure 38 Proposed structures of the ligands

While the synthesis of the ligand **106**, could be conducted under copper-catalyzed Chan-lam arylation,[131] a different approach was chosen for the following reasons: a) the arylation yielded a significant amount of bisarylated product,[131] b) the subsequent oxidation of the methyl group to the carboxyl was expected to be problematic based on the previous attempts, and c) the requirement to use column chromatography could be problematic for obtaining enough material to develop a chiral resolution method. For those reasons, the cyclization-based synthesis was developed (Scheme 18).

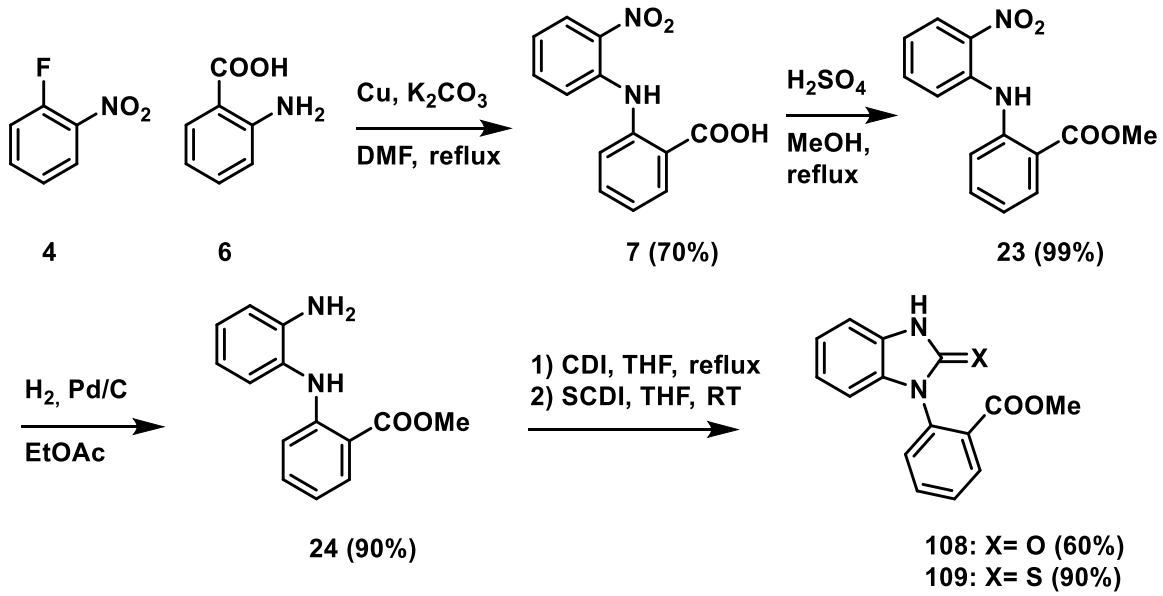

Scheme 18 Synthesis of **108** and **109**

Synthesis of benzimidazolone based ligand

The synthesis started with copper catalyzed arylation of anthranilic acid **6** to yield nitroacid **7**, which was converted to methylester **23** using common acid catalyzed esterification. The esterification was followed by catalytic hydrogenation in ethylacetate to yield diaminoester **24**. The final product **108** was formed by cyclization with carbonyldiimidazole (CDI) in refluxing THF and sulfur analog **109** with thiocarbonyldiimidazole in THF at room temperature. The purification of **108** required column chromatography since multiple byproducts were observed. For this reason, further optimization was performed to see if better conditions could be devised.

Later it was decided to further modify the structure by various alkylations on the benzimidazole nitrogen. Based on the previous results,[186] the direct alkylation was expected to yield a mixture of products; nevertheless, two attempts were made to see if direct alkylation was possible or not to yield **110**.

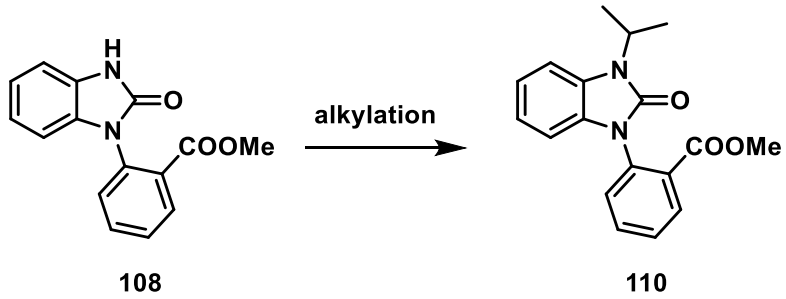

108 **110**

Scheme 19 Proposed synthesis of **110**

At first, the mitsunobu conditions were used (DIAD, PPh_3, THF). The starting material was not fully consumed overnight while two products were detected in HPLC-MS analysis in the approximately same amount. Further addition of more PPh_3, DIAD and alcohol did not improve the conversion. The products were not isolated since their separation by column chromatography was not possible. The structure of *N*- and *O*-isopropyl regioisomers was suggested on the basis of the LCMS analysis (Figure 39). Similar results were obtained with isopropyl iodide and sodium hydride as a base in THF. For this reason, alternative approach was developed.

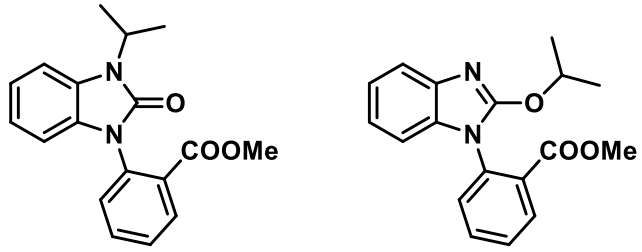

110 **111**

Figure 39 Proposed structure of the products of alkylation of **108**

In this approach, the isopropyl group was introduced earlier in the sequence followed by cyclization by suitable reagent. The approach is depicted in Scheme 20. The synthesis started as before but reduced intermediate **24** was alkylated using various conditions.

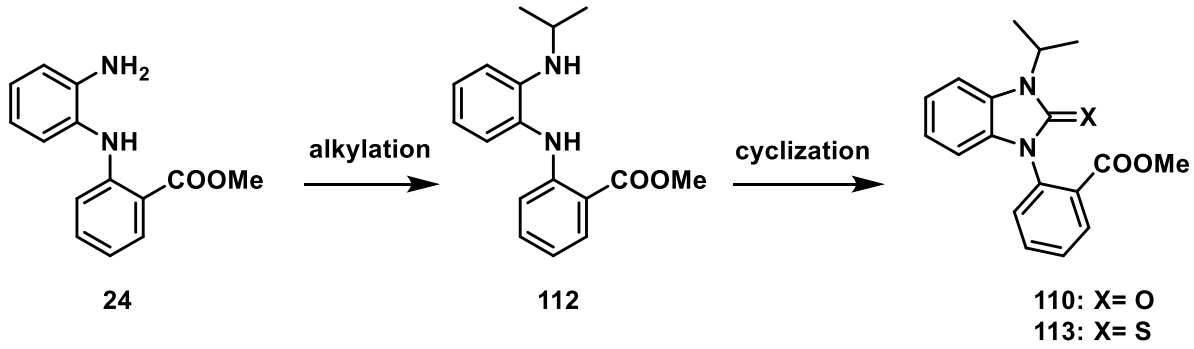

Scheme 20 Proposed synthesis of **110** and **113**

Table 17 Initial attempts to synthesize **112**

Entry	**Conditions**	**Result**
1[187]	Acetone, DCE, $NaBH(OAc)_3$, HOAc	15% conversion*
2	Acetone, THF, $NaBH_4$	No reaction

* By HPLC

The results of direct alkylation are summarized in Table 17. The reductive amination with $NaBH(OAc)_3$ in the presence of acetic acid in dichloroethane showed low conversion (entry 1) while the use of $NaBH_4$ as a reducing agent did not yield any product at all (entry 2). Possibly, the residual water in acetone was the cause for low conversion and therefore other reducting agents were investigated. Due to good experience with catalytic hydrogenation of nitro group, it was assumed the possibility of reductive alkylation via *in situ* formed imine **114**. This idea was expanded to development of one pot protocol of direct conversion of nitroester **23** to isopropyl derivative **112** (Scheme 21).

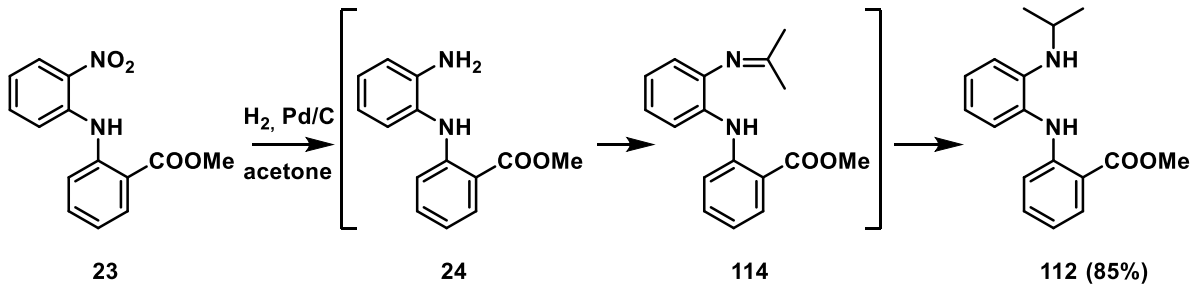

Scheme 21 One pot reduction/reductive amination

This protocol consisted of *in situ* preparation of amino ester **24** from nitroester **23** followed by imine **114** formation which would be reduced by catatalytic hydrogenation to yield isopropylamine **112**. The optimization procedures are summarized in Table 18.

Table 18 Optimization of the reductive amination

Entry	Eq. catalyst	concentration	additive	results
1	5%	0.025M	--	50% conversion
2	5%	0.05M	HOAc cat.(3 "drops")	60% yield
3	5%	0.05M	HOAc 1.5 eq.	97% isolated yield
4	2.5%	0.05M	HOAc 1.5 eq	94% isolated yield
5	2.5%	0.075M	HOAc 1.5 eq	95% isolated yield

At first, the reduction was conducted in acetone instead of ethylaceate and partial conversion was observed in HPLC-MS after 24 hours (entry 1). No byproducts were observed suggesting the low conversion was due to slow formation of imine **114**. Addition of catalytic amount of acetic acid and increase in the reaction concentration improved the reaction rate and the starting material was fully converted into product. The product was fully isolated in 60% yield after column chromatography. Because the reaction was conducted on a small scale (20 mg), the exact amount of acetic acid in the reaction was not known. Therefore, the reaction was conducted on a larger scale and a more exact amount of acid was added. The use of 1.5 equivalent of acid (entry 3) further increased the conversion of the starting material into the product. Furthermore, full conversion was observed and the product was isolated by simple filtration through pad of celite and evaporation of the solvent. Residual acetic acid remained in the evaporation residue. For this reason, the oily residue was dissolved in ethylacetate and extracted with carbonate solution and evaporated again to yield the product in the high yield (entry 3).

Further, the amount of the catalyst was reduced to 2.5 mol% (entry 4), which did not have any effect on the isolated yield. The concentration of the reaction mixture was further increased to 0.075M and again, no effect on isolated yield was observed (entry 5). This reaction was scaled up to the 9 g scale. The cyclization of the isopropyl ester **112** to benzimidazole derivaties **110** and **113** were then performed (Scheme 22).

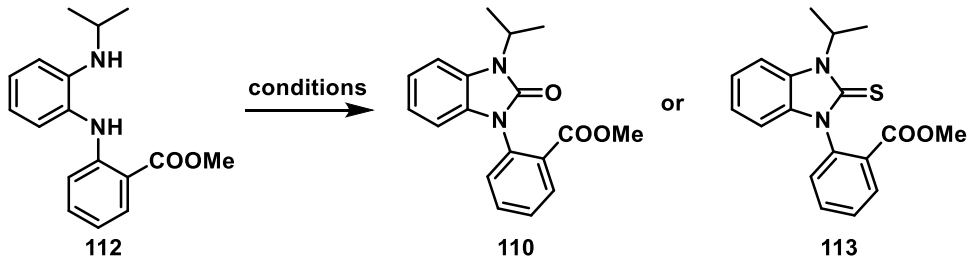

112 110 113

Scheme 22 Synthesis of benzimidazole derivatives **110** and **113**

The previously used conditions were not suitable for the synthesis of **110** or **113** and therefore new set of optimizations was performed. The performed reactions leading to **110** are summarized in Table 19.

Table 19 Cyclization to **110**

Entry	**conditions**	**results**
1	CDI, THF, reflux	10 % conversion*
2	Ethylchloroformate, TEA, DCM	No reaction
3	Triphosgene, DCM, RT	40% conversion*
4	Triphosgene, pyridine, DCM, RT	85% isolated yield
5	Triphosgene, DIEA, DCM, RT	85% isolated yield
6	Triphosgene, TEA, DCM, RT	85% isolated yield
7	Phosgene (15% in toluene), TEA, DCM	90% isolated yield
8	Triphosgene, TEA, DCM, RT, scale-up	95% isolated yield

* by HPLC

The previously used cyclization using CDI in refluxing THF provided only low conversion of the starting material (entry 1). The reaction between starting material **103** and ethylchloroformate in DCM at room temperature did not yield any product at all (entry 2), not even the ethylacarbamate intermediate was detected. Possibly residual moisture was the cause of no observed reaction.

For this reason, more reactive triphosgene was used. The reaction without any external base resulted in 40% HPLC conversion (entry 3). Likely, HCl formed in situ from the reaction was protonating the amine which made it unreactive. The addition of an external base proved beneficial (entries 4-6). Three bases were investigated: pyridine (entry 4), diisopropylethylamine (entry 5), and triethylamine (entry 6). No measurable difference between those bases was observed. Triethylamine was used for the scale-up reaction: pyridine being UV active complicates the TLC/HPLC analysis and the price of DIEA was higher compared to TEA. Furthermore, a phosgene solution in toluene was used which was deemed assumed to be more reactive compared to triphosgene (entry 7). The product was isolated in 80% yield, which was comparable to isolated yields using triphosgene (entries 4-6). Although the yield using phosgene was slightly higher (90%) compared to triphosgene, triphosgene was used for the scale-up reaction due to safety concerns and ease of handling. The product of the scale-up reaction (entry 8) was isolated in 95% yield.

The cyclization leading to **113** was also more complex. The results are summarized in Table 20. The reaction with thiocarbonyldiimidazole in THF at room temperature did show any conversion of the starting material (entry 1). Increasing the reaction temperature to reflux did not offer any improvements (entry 2). Further addition of the base (entry 3) did not show any conversion as well. For this reason, more reactive, although toxic, thiophosgene was used. At first, traces of product were observed when using triethylamine as a base at room temperature (entry 4). Increasing the temperature to reflux provided slight improvement and the product was isolated in 35% yield after column chromatography. Interestingly, using inorganic base[183] further improved the reaction yield to 50% after column chromatography. The reaction was later scaled-up to a 2.4 gram scale and improved purification by crystallization from EtOH was developed which improved the yield to 75%.

Table 20 Cyclization to **113**

entry	**conditions**	**Result**
1	SCDI, THF, RT	No reaction
2	SCDI, THF, reflux	No reaction
3	SCDI, TEA, THF, reflux	No reaction
4	Thiophosgene, TEA, THF, RT	Traces*
5	Thiophosgene, TEA, THF reflux	35%*
6[183]	Thiophosgene, $NaHCO_3$, THF	50%*
7[183]	Thiophosgene, $NaHCO_3$, THF, scale-up	75%*

* by HPLC

Several other derivatives were prepared using similar methodology (Scheme 23). The nitro acid **7** was converted into acyl chloride using $SOCl_2$ in toluene at reflux. This acyl chloride was treated with various amines in the presence of triethylamine in $CHCl_3$. This acylation yielded amides **115a-d** in high yields (from 90% to quantitative). The nitro amides **115a-d** were alkylated using the previously described reductive alkylation with acetone, acetic acid, and palladium on carbon using hydrogen gas as a reducing agent. The alkylated amides **116a-d** were isolated in 50-60% yield after column chromatography. The reaction was slower with the amide compared to the ester alkylation and therefore unreacted starting material had to be removed via chromatography. The cyclization with triphosgene in DCM was performed as previously described for the methyl ester **110** and the products **117a-d** were isolated in high yields.

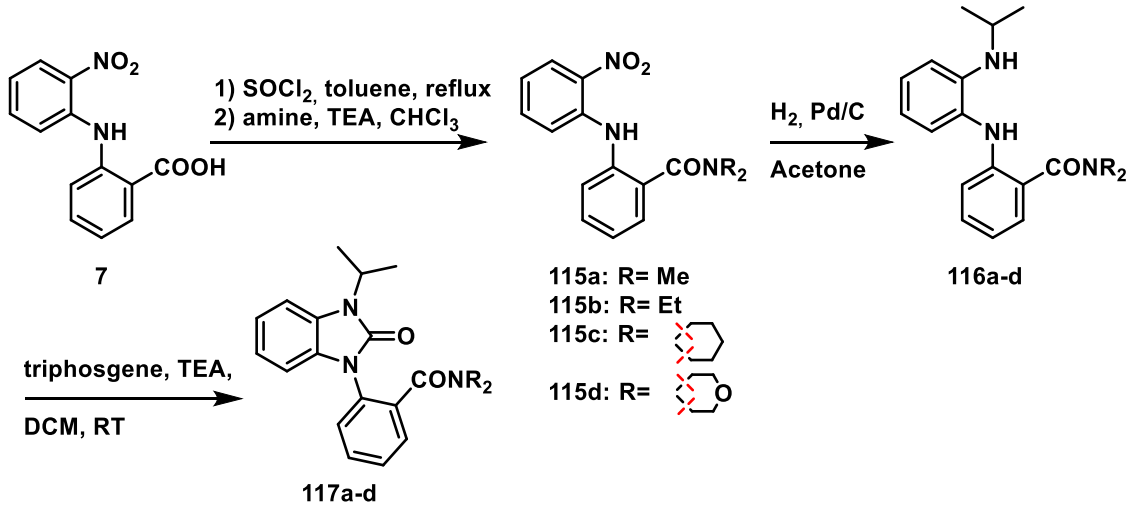

Scheme 23 Synthesis of amide derivatives

This approach was later found out unsuitable. Firstly, the prepared amides would not be possible to separate into enantiomers with the exception of chiral HPLC which is not suitable for larger amounts of the compound and second, the synthesis of each derivative required multiple steps. It was modified into a more diversity-oriented approach which would allow to prepare the various derivatives in single step. The alternative synthesis was devised: the methylester were hydrolyzed to yield free acid **118** or **119**

(Scheme 24) which could be separated into enantiomers by crystallization and further diversified using common esterification or amidation methods.

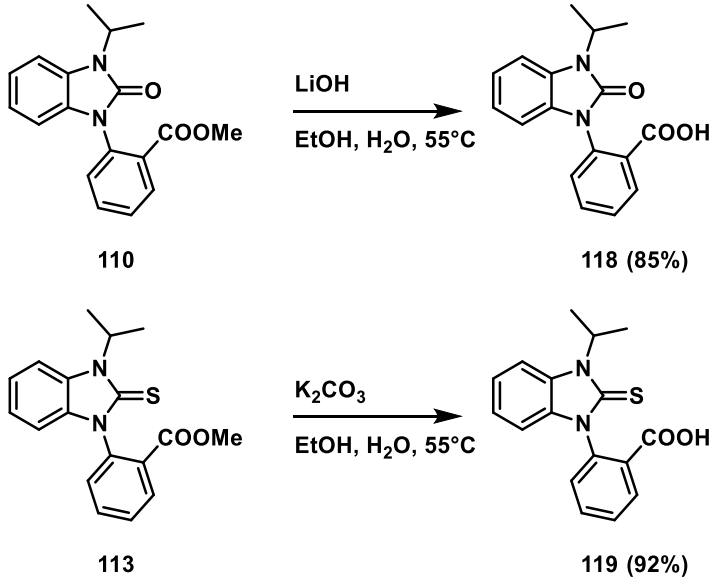

Scheme 24 Synthesis of carboxylic acids **118** and **119**

Ester **110** was hydrolyzed using LiOH in EtOH / H_2O mixture at 55 °C and after neutralization the acid was isolated in 85% yield. Multiple approaches were tested for hydrolysis of the ester **113**. The hydrolysis is summarized in Table 21.

Table 21 Hydrolysis of **110**

entry	**conditions**	**results**
1	LiOH, EtOH, H_2O, 55°C	55% isolated yield
2[188]	TMSOK, THF, RT	95% isolated yield (as K^+ salt)
3	K_2CO_3, EtOH, H_2O, reflux	87% isolated yield
4	K_2CO_3, EtOH, H_2O, reflux, scale-up	92% isolated yield

At first, the same conditions were used as for the hydrolysis of **110** (entry 1). After acidification and extraction, the product was isolated in 55% yield. TMSOK in THF[188] was used alternatively and the product was isolated as a potassium salt of the acid as was clear from a different NMR spectra of the product (Figure 40). The yield of the salt was 95% (entry 2). The hydrolysis was further conducted using K_2CO_3 in EtOH / H_2O mixture at reflux (entry 3). The product was isolated in 87% yield and in 92% after scale up to 1.5 g scale (entry 4).

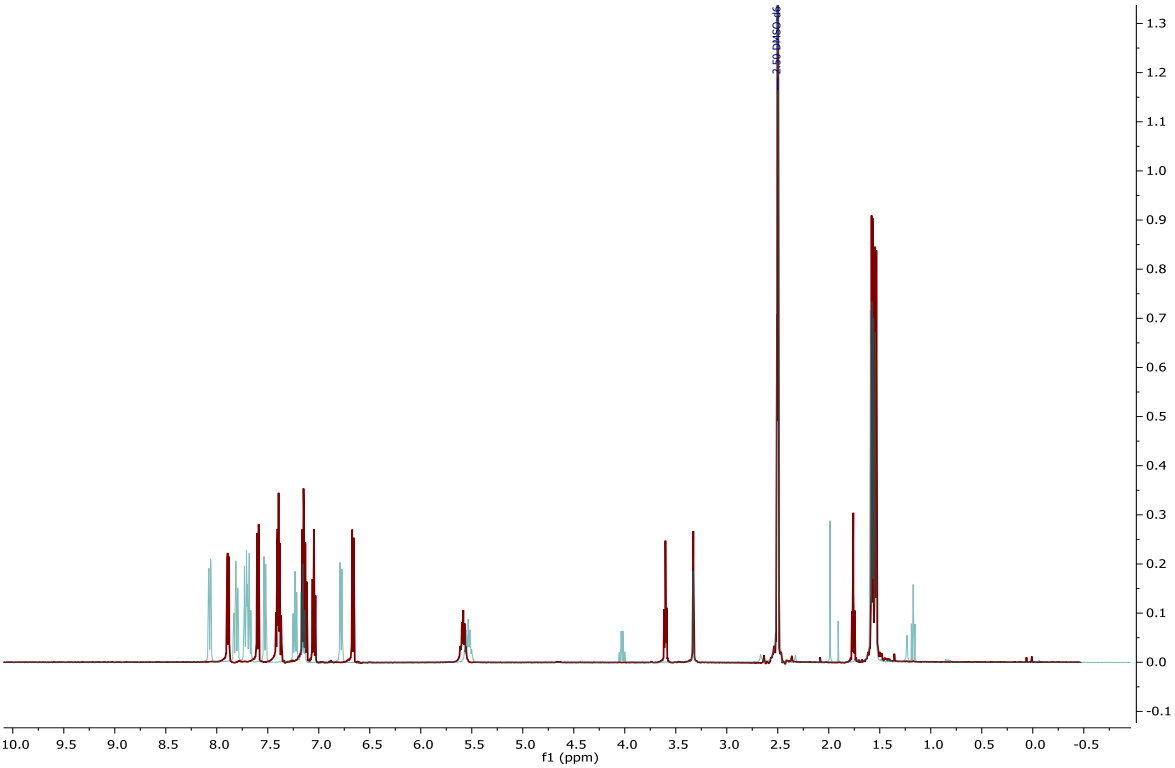

Figure 40 red: Potassium salt of **119**, blue: acid **119**

The acid **118** was further modified by common acylation reaction (Scheme 25). Multiple conditions were tested (Table 22). Simple aniline acylation was used as a model reaction. DCC, DMAP yielded product **120** in 40% yield after column chromatography (entry 1). T3P in EtOAc and in DMF (entries 2 and 3) yielded the product **120** in 53 and 51% yield after simple extractive workup. The acid activation using carbonyldiimidazole (entry 4) and thiocarbonyldiimidazole (entry 5) did not yield any product at all. The use of more reactive HATU activator yielded product in 56% yield (entry 6) Last, the use of EDCl/HOBt in DMF provided the anilide **120** in 60% yield after column chromatography (entry 7).

The acid **118** was also converted into the (*S*)-phenylglycinol amide **121** in 77% yield after extractive workup (Scheme 25). No separation of diastereomers was observed by HPLC or TLC. Interestingly, the NMR of the product **121** displayed a mixture of diastereomers in approximately 10:3 ratio suggesting a kinetic resolution (Figure 41). Unfortunately, no HPLC or TLC separation was observed for oxazoline **122** which made this approach unsuitable for the preparative separation of the enantiomers.

Table 22

entry	**conditions**	**results**
1	DCC, DMAP, DCM	42% isolated yield
2	T3P, EtOAc, Pyridine	53% isolated yield
3	T3P, DMF, Pyridine	51% isolated yield
4	CDI, THF	No reaction
5	SCDI, THF	No reaction
6	HATU, DIEA, DMF	56% isolated yield
7	EDCl, HOBt, DMF	60% isolated yield

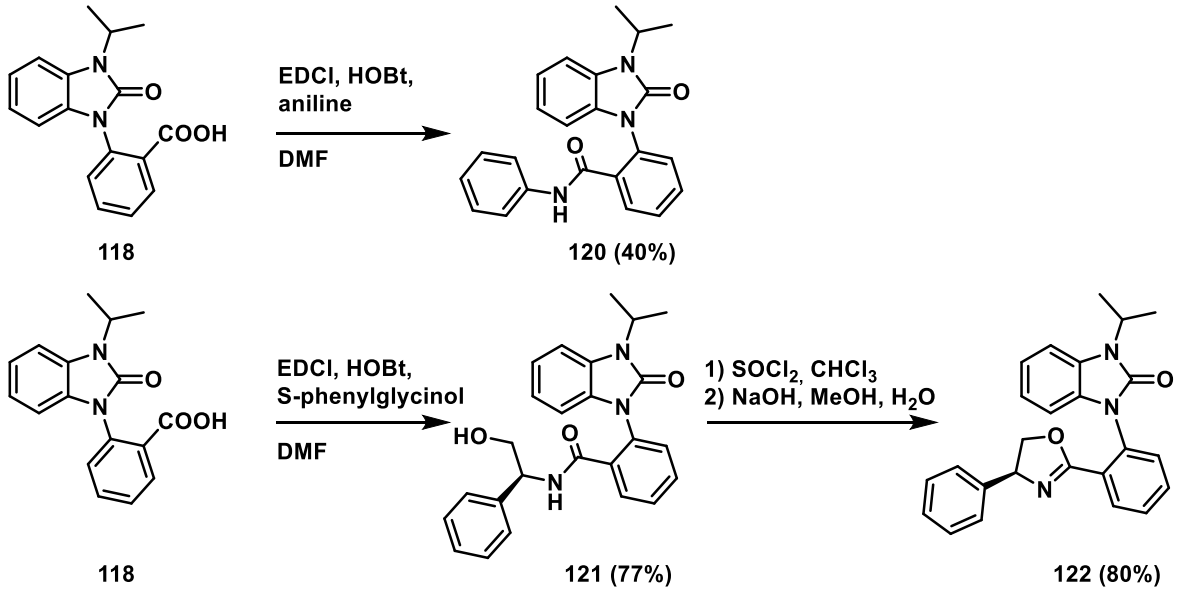

Scheme 25 Derivatization of **118**

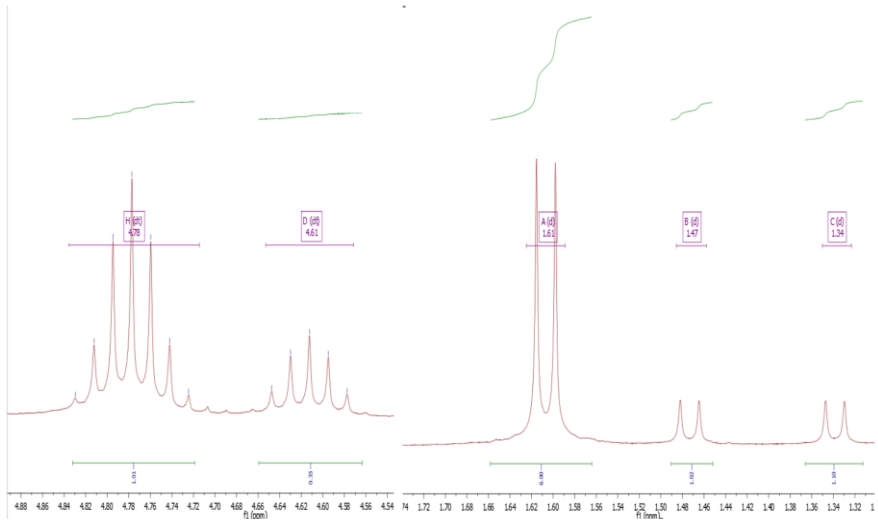

Figure 41 Detail of NMR spectra of **121**

Analogous procedure was designed towards thio derivative **123**. Two approaches were attempted (Scheme 26). The two-step protocol including previously described hydrolysis of the methylester **113** followed by acylation of (*S*)-phenylglycinol or direct one step amidation of the methyester. While the hydrolysis of ester **113** to acid **119** was already developed, the direct amidation could save time and possibly increase the final yield of amide **123**.

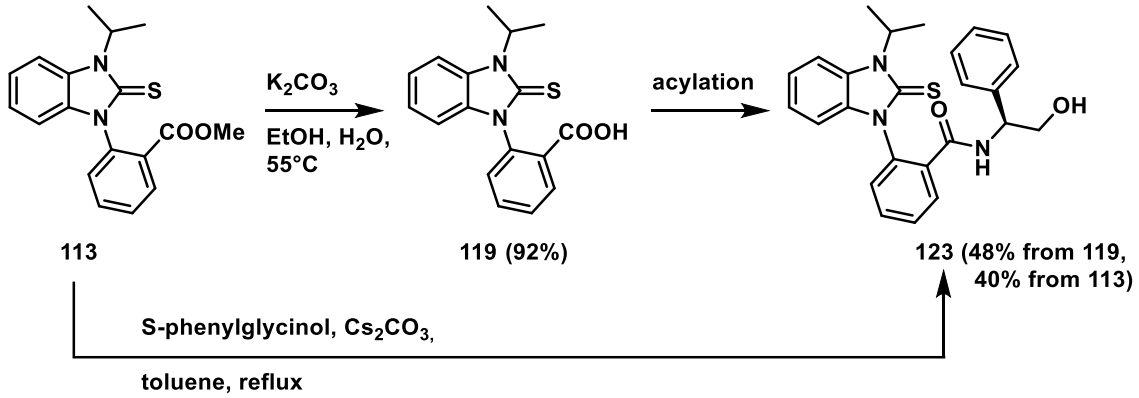

Scheme 26 Synthesis of **123**

Multiple conditions were tried for the direct amidation of ester **113** (Table 23). At first, heating of the ester in the presence of potassium phosphate and (*S*)-phenylglycinol in isopropyl alcohol (entry 1) resulted in hydrolysis of the ester to acid **119.** Traces of amide 123 were observed by TLC and HPLC. The use of Cesium carbonate in toluene improved the reaction and the amide was isolated in 70% yield. Importantly, separation of the diastereomers was possible using column chromatography. The scale-up of the reaction from 0.5 mmol to 2 mmol (entry 3) did not yield any product at all and full hydrolysis to acid **119** was observed. The cause was thought to be presence of water or hydroxide in old Cs_2CO_3. The use of fresh Cs_2CO_3 from a new bottle proved beneficial and the reaction worked as expected (entry 4). Nevertheless, because the amidation was complicated by this, the two-step procedure was adopted instead.

Table 23 Direct amidation of ester **113** to amide **123**

Entry	**Conditions**	**Result**
1	K_2PO_4, (*S*)-phenylglycinol, isopropyl alcohol, reflux	Hydrolysis to acid
2	Cs_2CO_3, (*S*)-phenylglycinol, toluene, reflux	70% isolated **123**
3	Cs_2CO_3, (*S*)-phenylglycinol, toluene, reflux, scale-up	Hydrolysis to acid
4	"Fresh" Cs_2CO_3, S-phenylglycinol, toluene, reflux,	50% isolated **123**

The acylation was performed under multiple conditions. The acylation was conducted using T3P or EDCl as activating agents. The use of T3P yielded a mixture of products (Table 24, entry 1) as did acylation with EDCl in DMF without any additive (entry 2). Addition of HOBt (entry 3) or DMAP (entry 4) was advantageous and the product was isolated in high yield.

Table 24 Acylation of **119**

Entry	**Conditions**	**Result**
1	T3P, Pyridine, EtOAc, RT	Mixture of products
2	EDCl, DMF, RT	Mixture of products
3	EDCl, HOBt, DMF, RT	95%
4	EDCl, DMAP, DMF, RT	70%

Phenylglycinol amide **123** was then converted into oxazoline **124,** (Scheme 27) assuming better separation of the diastereomers. Unfortunately, the oxazolines **124** provided worse separation compared to **123**.

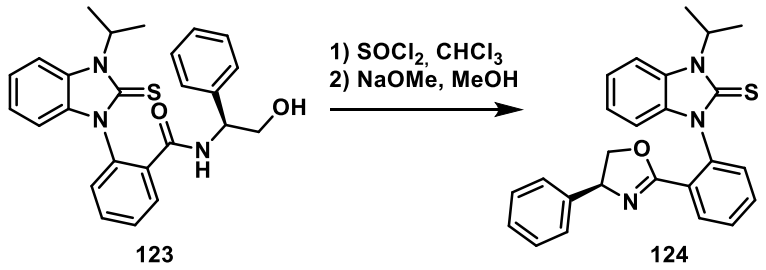

Scheme 27 Synthesis of **124**

Last, *N*-heterocyclic carbene precursors **125** and **126** were prepared. At first the precursor **125** was prepared by cyclization of **112** (scheme 28). The cyclization was conducted using triethylorthoformate as a solvent and $HClO_4$ as a catalyst. The product was isolated in 70% yield.[189]

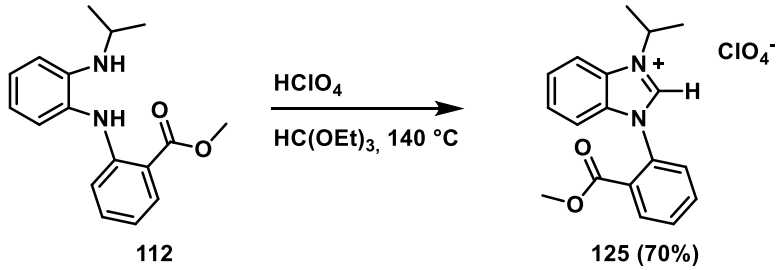

Scheme 28 Synthesis of **125**

An alternative approach was the oxidation of derivatives **113** or **123** with mCPBA and $HClO_4$ in THF[60] (Scheme 29) to yield NHC precursor **125.** Compound **123** decomposed during oxidation. Unfortunately, the literature revealed racemization[60] of the prepared NHC even under mild conditions; therefore, this approach was abandoned.

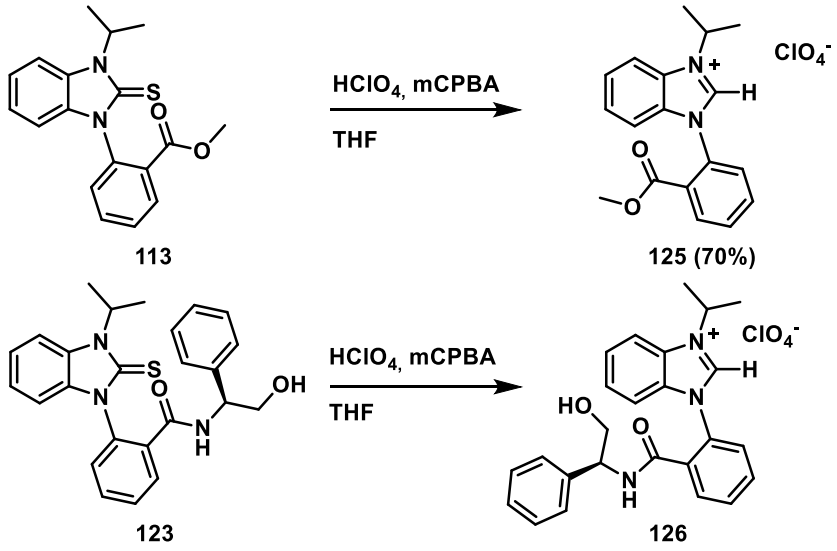

Scheme 29 Synthesis of NHC precursors

Synthesis of pyridine based ligand

Because the preliminary results (vide infra) did not show any catalytic activity of the compounds **111** and **113**, alternative structure **127** was developed. Two possible synthethic disconnections were envisioned (Figure 42). The first possible pathway was metal catalyzed arylation reaction between 2-pyridylbenzimidazole and suitable aryl halide (disconnection **127a**). The second option was cyclization of diamine such as **24** with suitable pyridine derivative (disconnection **127b**). The racemate **127** would be then resolved by a suitable method. This resolved core structure would then be modified to yield a library of various ligands.

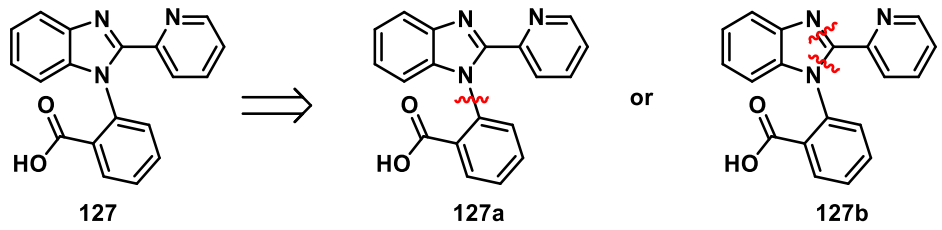

Figure 42 Disconnections leading to compound **127**

N-arylation based synthesis

At first, the arylation between 2-pyridylbenzimidazole **128** and iodobenzoic acid or its ester **129** (Scheme 30) was attempted. Several reaction conditions were tested. (Table 25).

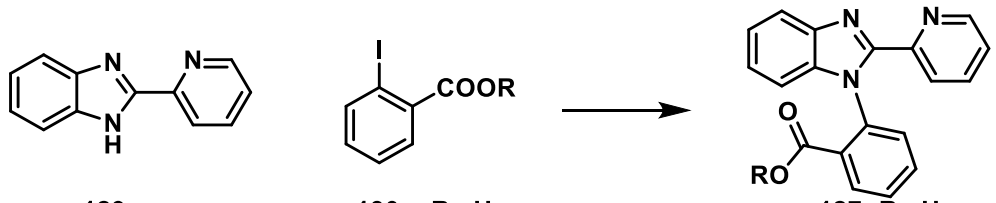

129 **130a: R= H, 130b: R= Me** **127: R= H 128: R= Me**

Scheme 30 Arylation of **129**

At first, the copper catalyzed arylation with L-proline as a catalyst was performed. The reaction was conducted in DMSO at 80°C (entry 1). Unfortunately, no product was observed under those conditions using iodobenzoic acid as an aryl halide partner. The presence of the free carboxylic acid group was thought to be problematic for the reaction; therefore, it was protected as a methylester. Nevertheless, under the same conditions using methyleter **130b** (entry 2), no product was observed in HPLC analysis of the reaction mixture. Different reaction conditions (CuI, 1,10-phen, Cs_2CO_3, DMF, reflux) were tried as well (entries 3-4); however, even under those more forcing conditions, no product was observed.

Table 25 Arylation of **129**

entry	conditions	result
1	CuI, L-proline, K_2CO_3, DMSO, 80°C, **130a** [190]	No reaction
2	CuI, L-proline, K_2CO_3, DMSO, 80°C, **130b**	No reaction
3	CuI, 1,10-phenantroline, Cs_2CO_3, DMF, argon, reflux, **130a** [191]	No reaction
4	CuI, 1,10-phenantroline, Cs_2CO_3, DMF, argon, reflux, **130b** [191]	No reaction

Cyclization approach

Alternatively, the cyclization of diamine **24** was developed at the same time (Scheme 32) and since it yielded better results, the arylation based synthesis was abandoned. Diamine **24** was prepared as previously described and subjected to various cyclization conditions (Table 26).

Table 26 One step cyclization

Entry	Conditions	result
1	PyCOOH, HOAc, reflux	Traces
2	PyCHO, H_2O_2, ACN, HCl[192]	Traces
3	PyCHO, H_2O_2, ACN, pTSA	No reaction
4	PyCHO, H_2O_2, ACN, TFA	No reaction
5	PyCHO, $Na_2S_2O_5$, DMA, 100°C[193]	Traces
6	PyCHO, DMSO, 100°C[194]	No reaction
7	PyCHO, HOAc, reflux	Traces
8	PyCHO, Oxone, DMF, H_2O	50% isolated
9	PyCHO, EtOH, then I_2, K_2CO_3, DCM	80% isolated
10	PyCHO, EtOH, then I_2, K_2CO_3, DCM, scale-up	30% isolated

The cyclization in refluxing acetic acid yielded traces of the product (entry 1) while the rest of the mixture consisted of two byproducts. The suggested structures of byproducts **131** and **132** are depicted in Figure 43. Structure **131** was assumed on the basis of mass from the MS spectra. The structure **132** was suggested as a reasonable product of cyclization of compound **131**. The compound did not ionize well in the MS; therefore, its m/z was not detected, therefore the structure is a suggestion based on the known reactivity.

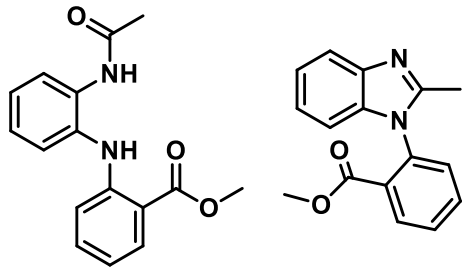

131 **132**

Figure 43 Proposed structures of byproducts **131** and **132**

The cyclization using pyridine-carbaldehyde with aq. HCl as a catalyst and H_2O_2 as an oxidant[192] (entry 2) yielded traces of the product together with a mixture of the staring material and hydrolyzed methylester derivatives. Because of the observed hydrolysis of the methylester, the aq. HCl was substituted for pTSA (entry 3). In this case, no reaction at all was observed. This was in accordances with the proposed reaction mechanism which involves formation of HOCl in situ as an active oxidant. The same was observed in the case of TFA being used as an acid catalyst for the reaction (entry 4).

The reaction of pyridine-carbaldehyde with $Na_2S_2O_5$ as a catalyst in dimethyacetamide at high temperature only yielded traces of the product (entry 5). The cyclization of diamine **24** with pyridine-carbaldehyde in DMSO at elevated temperature, which was used in one of research groups in our department with success,[194] did not yield any product at all (entry 6). The cyclization of pyridine-carbaldehyde in refluxing acetic acid with access of air as an oxidant showed traces of the product in HPLC analysis (entry 7).

Finally, the oxone mediated cyclization (entry 8) yielded the product in reasonable yield (50%).[195] Furthermore, the two stage procedure (entry 9) consisting of *in situ* formation of the imine followed by iodine-mediated cyclization yielded product **128** in slightly higher 80% yield. Unfortunately, the scale-up of the reaction did not proceed well and the product was isolated only in 30% yield (entry 10).

While it was possible to prepare the product **128** via direct cyclization, the problems with scale up and reproducibility forced us to explore another procedure. The two-step procedure was envisioned

which included the acylation of **24** with pyridine-2-carboxylic acid followed by dehydrative cyclization of intermediate **133** towards final product **128** (Scheme 31).

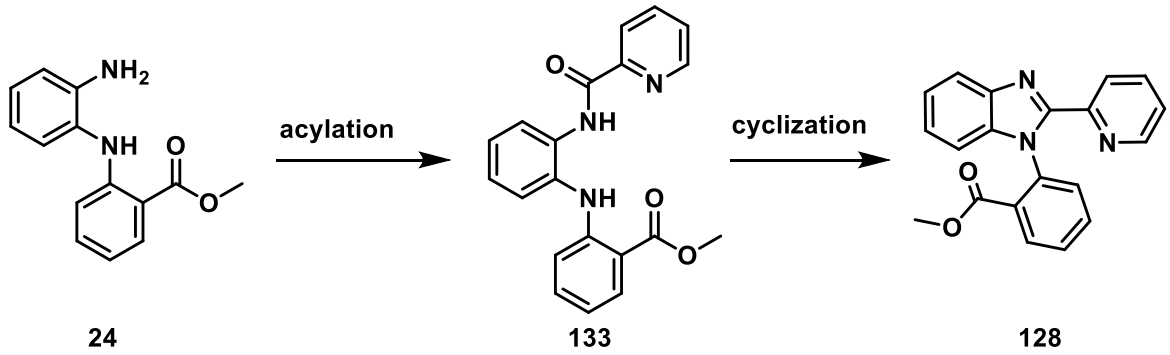

Scheme 31 Synthesis of **128** *via* acylation/cyclization sequence

The acylation was attempted under common conditions. At first, EDCl+DMAP were tried (Table 27, entry 1). Incomplete conversion of the staring material was observed. The use of T3P in EtOAc/pyridine yielded full conversion of the starting material into the product (entry 2) and product **133** was isolated in 80% yield. The reaction was further scaled up up to 58 mmol scale (20 grams) and the product was isolated in high yield after simple acid/base extraction (entries 2-6).

Table 27 Acylation of **24**

Entry	Conditions	result
1	EDCl, DMAP, DMF	50% (incomplete conversion)
2	T3P, Pyridine, EtOAc, 1 mmol scale	80% isolated
3	T3P, Pyridine, EtOAc, 4 mmol scale	66% isolated
4	T3P, Pyridine, EtOAc, 12 mmol scale	77% isolated
5	T3P, Pyridine, EtOAc, 15 mmol scale	90% isolated
6	T3P, Pyridine, EtOAc, 58 mmol scale	80% isolated

The cyclization proved to be more complex. The optimization of the procedure is summarized in Table 28. At first, acid catalyzed cyclization using HCl in acetic acid was investigated. Performing the reaction at room temperature (entry 1) did not yield any product and only starting material was observed. Increasing the temperature to reflux, provided full cyclization although the product was hydrolyzed to free acid **127** (entry 2). Reducing the temperature to 65°C reduced the rate of hydrolysis to approximately 30%. The product was isolated by crystallization from ethylacetate/hexane mixture (entry 3) in 55% yield.

Conducting the reaction in neat acetic acid at reflux with the intention to limit the ester hydrolysis by the water present in conc. HCl did not yield any conversion of the starting material (entry 4). Similar behavior was observed when HCl was substituted for pTSA (entry 5). Acetic anhydride was than used as a dehydrative agent (entry 6), but no product was observed. Use of sulfuric acid as a dehydrative

agent (entry 7) and as a strong acid catalyst yielded only sulfonated starting material. PPA (entry 8) provided full conversion, although approximately 70% of the ester was hydrolyzed into acid **127**. Using H_3PO_4 instead of PPA (entry 9) provided full conversion and limited ester hydrolysis to aprox. 30%. T3P in DMF was also used as a dehydrating agent, although only low conversion was observed (entry 10).

The use of $BF_3.OEt_2$ in refluxing dioxane[196] (entry 11) provided the product in 60% yield. More careful control of the reaction temperature and ensuring the refluxing of the reaction mixture enabled full conversion of the starting material to the product. The reaction was also scaled up to 46 mmol. The product was isolated in high yields between 70-86% (entries 12-15). Last, a slight modification of the reaction workup yielded product **128** in the almost quantitative yield even at a large scale (entry 16).

Table 28 Optimization of cyclization conditions

Entry	**conditions**	**result**
1	HOAc, HCl (10:1) RT	No reaction
2	HOAc, HCl (10:1) reflux	Hydrolysis to acid **127**
3	HOAc, HCl (10:1) 65°C	55% isolated after recrystallization
4	HOAc, 100°C	No reaction
5	pTSA, HOAc, 70°C	No reaction
6	Ac_2O, reflux	No reaction
7	HOAc, H_2SO_4, reflux	Sulfonated starting material observed
8	PPA, 150°C	70% hydrolysis to **127**
9	H_3PO_4, reflux	70% **128**, 30% hydrolysis to **127**
10	T3P, DMF, RT	5% conversion
11	$BF_3.OEt_2$, dioxane, 90°C, 0.5 mmol scale	80% conversion, 60% isolated
12	$BF_3.OEt_2$, dioxane, reflux, 2 mmol scale	73% isolated after recrystallization
13	$BF_3.OEt_2$, dioxane, reflux, 11 mmol scale	77% isolated after recrystallization
14	$BF_3.OEt_2$, dioxane, reflux, 10 mmol scale	68% isolated after recrystallization
15	$BF_3.OEt_2$, dioxane, reflux, 46 mmol scale	86% isolated after recrystallization
16	$BF_3.OEt_2$, dioxane, reflux, 31 mmol scale	Quantitative, different workup

The substitution of K_2CO_3 for Na_2CO_3 in the quench of the reaction proved crucial. The formed $NaBF_4$[197] is significantly more soluble in water (1080 g/L)[198] compared to KBF_4 (5.5 g/L)[198] while being less soluble in organic solvents. This allowed the precipitation of the $NaBF_4$ from the reaction mixture after quench and the residual $NaBF_4$ was removed after extraction with water. The removal of residual salts from the product, allowed for isolation of the product as a solid material compared to the oils which required purification by recrystallization (entries 12-15).

Nitrile derivative **133** was also prepared. The nitrile group would allow synthesis of various other derivatives. Most importantly, diastereomeric oxazoline **134** (Figure 44) could be prepared in one step from the nitrile, which would allow for separation of the atropoisomers by the same method as was used for separation of TBBA.

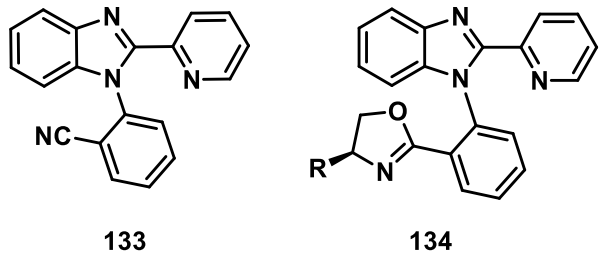

Figure 44 Structure of nitrile **133** and oxazoline **134**

The synthesis of **133** was similar to synthesis of **128**. At first, 2-aminobenzonitrile was arylated with 2-fluoronitrobenze using DMSO and KOH. The reaction proceeded well at room temperature and product **135** was isolated by simple precipitation from water.[199] The nitro group was reduced using H_2 and Pd/C catalyst in EtOH and reduced derivative **136** was acylated with pyridine-2-carboxylic acid using T3P in EtOAc/pyridine. Amide **137** was isolated in 75% yield. The $BF_3.OEt_2$ promoted cyclization to yield product **133** which was isolated by simple precipitation from the reaction mixture after the quench of the BF_3 (Scheme 32).

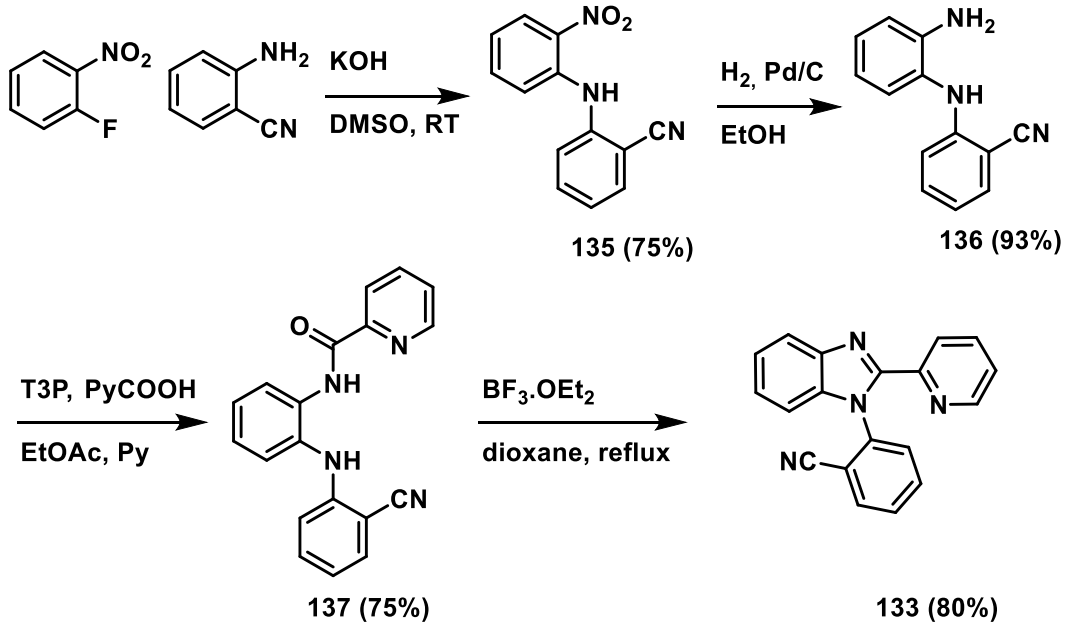

Scheme 32 Synthesis of nitrile **133**

Resolution of pyridine catalyst 128

Via diastereomeric oxazolines

At first, the same procedures as in the case of TBBA was performed.The oxazoline was prepared by direct reaction of the nitrile **133** with (*S*)-phenylglycinol in the presence of $ZnCl_2$ in chlorobenzene at 140°C (Scheme 33).[200] The reaction proceeded without formation of any byproducts; however, 7 days of heating were required to fully convert nitrile **133** to oxazoline **134**. Unfortunately, diestereomers were

impossible to separate on TLC or column chromatography but separation of small amounts was possible by HPLC.

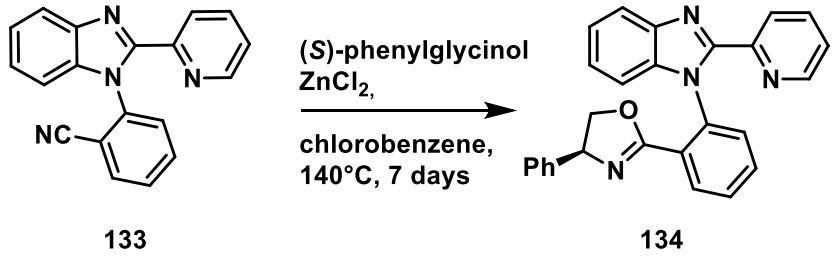

Scheme 33 Synthesis of oxazoline **134**

Resolution via diastereomeric salt formation

The resolution via formation of oxazolines was possible, but only small amounts. Therefore, further structural diversification was not possible. For this reason, resolution of ester **128** was developed. The results are displayed in Tables 29 and 30.

Table 29 Resolution of **128** with LTA mix

Entry	Resolving agent	Solvent and concentration	yield	%ee
1	LTA* mix	EtOAc 0.75M	0	
2	LTA mix	MeOH 0.75M	37%	85%
3	LTA mix	MeOH 0.375M **	83%	42%
4	LTA mix	BuOH 0.6M	87%	57%
5	LTA mix	BuOH 0.375M **	73%	63%
6	LTA mix	ACN 0.16M	42%	85%
7	LTA mix	ACN 0.045	60%	90%
8	LTA mix	ACN 0.21	65%	67%
9	LTA mix	ACN 0.045M **	45%	87%
10	LTA mix	ACN 0.1M	56%	84%
11	LTA mix	ACN 0.0.05	54%	93%

* equimolar mixture of L-dibenzoyltartrate, L-dianisoyltartrate and L-ditoluoyl tartrate
** recrystallization of the previous batch

Initially, the "Dutch resolution" procedure[140–142,201] was used using LTA mix (L-dibenzoyl tartrate (L-DBT), L-ditoluolyl tartrate (L-DTT), and L-dianisoyl tartrate (L-DAT). At first, the resolution was attempted in ethylacetate and methanol (entries 1 and 2). No precipitate was observed for EtOAc, but the product was isolated in methanol in 37% yield and 85% ee. Recrystallization from MeOH reduced the enantiomeric purity (entry 3). Crystallization from BuOH provided the product in high yield; however, the enantiomeric purity was only 57% (entry 4). Recrystallization (entry 5) improved the enantiomeric purity to 63%.

Using acetonitrile as a solvent (entry 6) yielded the product in 42% yield and 85% enantiomeric purity which was slightly better compared to crystallization from MeOH. The recrystallization (entry 7)

improved the enantiomeric purity to 90%. Increasing the concentration to 0.21M (entry 8) slightly improved the yield, but the enantiomeric purity dropped to 67%. Recrystallization from acetonitrile improved the enantiomeric purity to 87% (entry 9). Reducing the concentration even further to 0.1M (entry 10) yielded the product in high enantiomeric purity (84%) and 56% yield. Further dilution of the crystallization to 0.05M (entry 11) had positive effect on enantiomeric purity (93%) while the yield was same as when the more concentrated solution was crystallized (54%).

Next, because the LTA mix worked well, each of the tartaric acid derivatives were used alone to further optimize the procedure. The results are presented in Table 30.

Table 30 Use of acylated tartrates as a single resolving agent for resolution of **128**

Entry	**Resolving agent**	**Solvent and concentration**	**yield**	**%ee**
1	L-DBT	ACN, 0.06M	88%	77%
2	L-DTT	ACN, 0.15M	---	
3	L-DAT	ACN, 0.125M	74%	74%
4	L-DBT	MeOH 0.187M	75%	75%
5	L-DBT	ACN, 0.1M	61%	80%
6	L-DBT	ACN, 0.115M	71%	80%

The use of L-dibenzoyltartrate in acetonitrile (entry 1) yielded the product in high yield and enantiomeric purity. No precipitation was observed when L-ditoluolyltartrate was used (entry 2) while the L-dianisoyltartrate provided the product in slightly lower yield and enantiomeric purity (entry 3). Using methanol as a solvent had a negative effect for the yield although the enantiomeric purity stayed the same (entry 4). Furhter increase of concentration compared to entry 1 had also a negative effect on the yield although the enantiomeric purity was slightly higher (entries 5 and 6). In the end, the enantioenriched product was recrystallized although in some cases the drop of enantiomeric purity was observed. The likely cause was poor solubility of the salt in acetonitrile and required prolonged heating.

The alternative protocol was developed, when the enantioenriched salt after single crystallization from acetonitrile was neutralized with NaOH. Freebase **128** was crystallized from EtOAc or EtOAc/hexane mixture which yielded the product in 99%+ enantiomeric purity. This modification was then used to resolve the racemate on gram scale.

Modifications of the structure of the ligand 128

For further modifications, ester **128** was hydrolyzed to acid **127** using LiOH (Scheme 34). The hydrolysis of the ester proceeded well at room temperature and the product was isolated by simple evaporation and acidification of the reaction mixture which caused precipitation of the product. Unfortunately, the acid was found to be racemic after further derivatization to amide **138** and **139** (scheme 35).

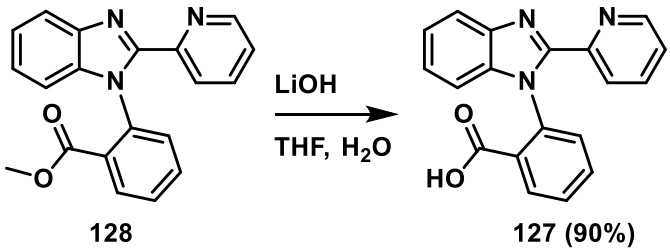

Scheme 34 Hydrolysis of ester **128**

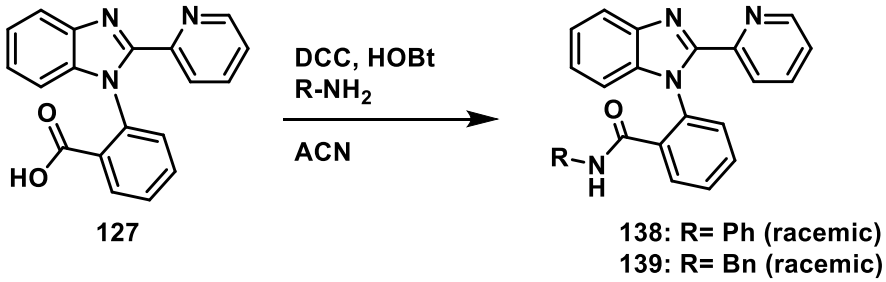

Scheme 35 Amidation of **127**

At this time, it was not known whether the racemization occurred during the hydrolysis step or during the amidation. Direct analysis of acid **127** on chiral SFC was not possible due to problematic separation of the enantiomers. For this reason, indirect analysis via the amides was used. Literature search suggested that the racemization might have occurred during the acidification of the reaction mixture by formation of hydrogen bond between the carboxyl group and pyridine nitrogen which lowers the rotational barrier (Scheme 36).[21]

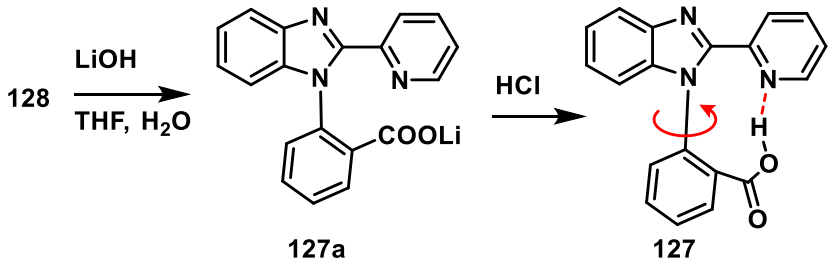

Scheme 36 Acid promoted racemization of acid **127**

For this reason, the hydrolysis of the ester was modified and the acidification step was omitted. Acid **127** was isolated as a lithium salt **127a** after simple evaporation of the reaction mixture. The lithium salt was then amidated using DCC, HOBt in acetonitrile to yield benzylamide **139** in good yield and reasonable enantiomeric purity (77% ee). This drop in enantiomeric purity suggested, that the acid catalyzed racemization was a valid hypothesis, although it did not rule out the possibility of partial racemization during hydrolysis and partial racemization during the amidation.

Multiple other amides were prepared (Figure 45) as racemates and some were separated on preparative HPLC with chiral stationary phase by Ondřej Kurka, Ph.D. from Department of Analytical

chemistry at our university. This separation yielded enough material for reduction experiments (vide infra). However, due to a lack of time and COVID-19 only ligands **138** and **139** were separated. Ligands **138-142** were prepared by simple amidation using DCC/HOBt while the ligand **143** was prepared by two step synthesis. First, *ortho*-phenylene diamine was acylated with acid **127** using DCC/HOBt and then the amide was cyclized into benzimidazole using $BF_3.OEt_2$ mediated cyclization.[196]

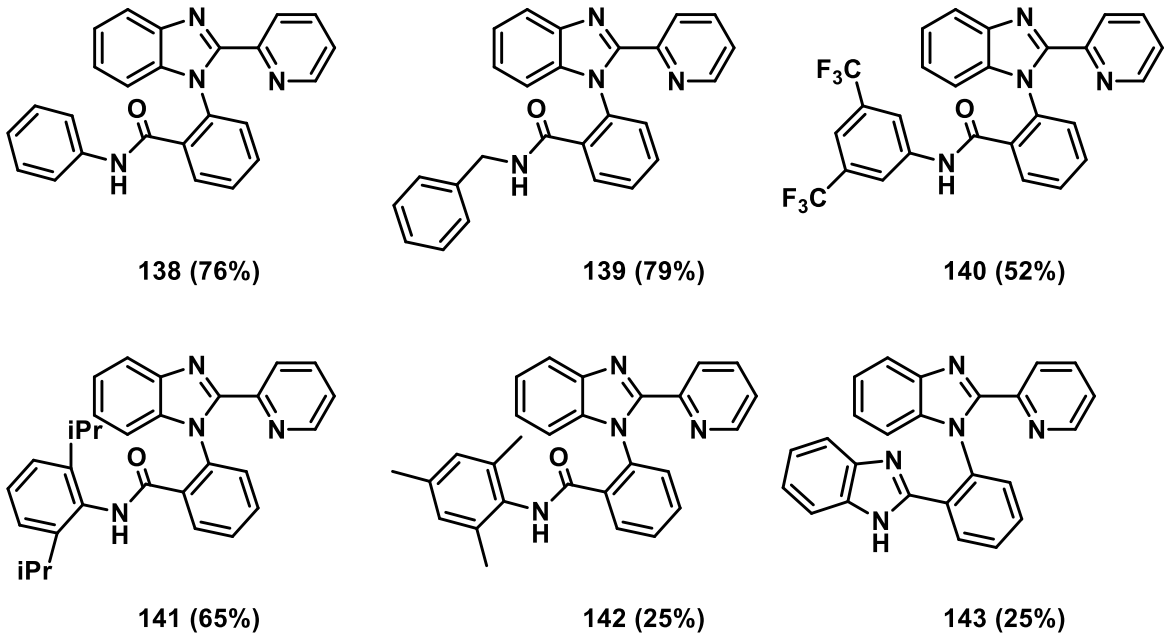

Figure 45 Prepared amide ligands

Further modifications of the structure were attempted. Addition of phenyllithium yielded triarylmethanol derivative **144** in high yield and purity. Interestingly, no racemization was observed during this reaction (Scheme 36). Reduction of methylester **128** with $LiAlH_4$ in diethylether provided hydroxymethyl ligand **145** with no loss of enantiomeric purity. Transesterification using NaH and isopropylalcohol yilded ligand **146** again with no loss of enantiomeric purity. The oxidation towards N-oxide **147** provided only racemic product. The exact mechanism of the racemization is unknown, We speculate that the possible nucleophilic attack of the N-oxide oxygen on the carbonyl followed by decomposition of the tetrahedral intermediate back to **147** with rotation around the chiral axis.

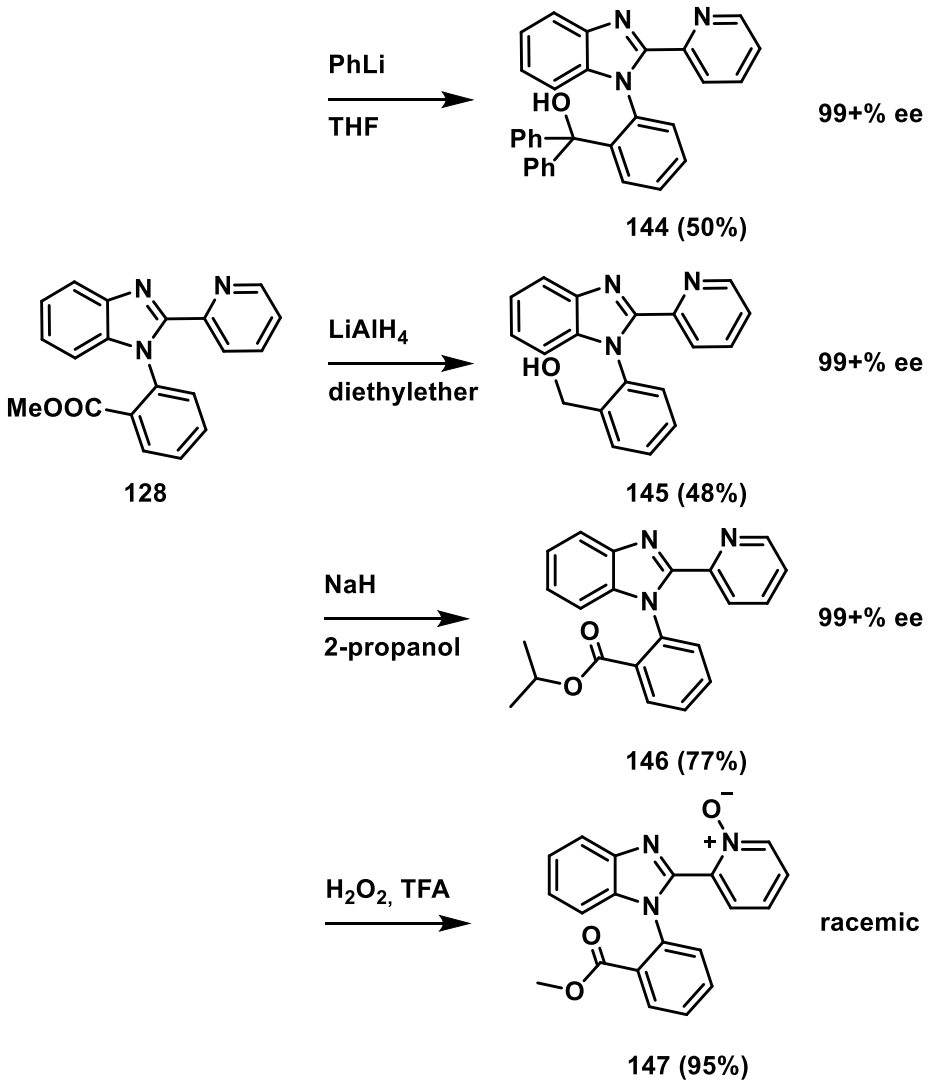

Scheme 36 Structural modifications of ligand **128**

Alternative diversification methods were explored. The synthesis of acyl azide **148** was envisioned via hydrazine derivative **149**. The azide could then act as a leaving group in amidation reactions,[202] or it could be converted into amine via Curtius rearrangement or the intermediate isocyanide might be trapped by nucleophiles and yield variously substituted ureas. Importantly, use of the azide as a leaving group could provide access to various amides without the need of preparation of acid **127.** Possibly, no racemization would be observed in the preparation of hydrazide **149** due to higher steric requirements compared to carboxyl anion and because no racemization was observed during transesterification to isopropylester **146**

At first, the methylester **128** was transformed into hydrazine derivative **149** by reaction with hydrazine hydrate in methanol. Unfortunatelly, partial racemization was observed and hydrazide **149** was isolated in 70% ee. (Scheme 37)

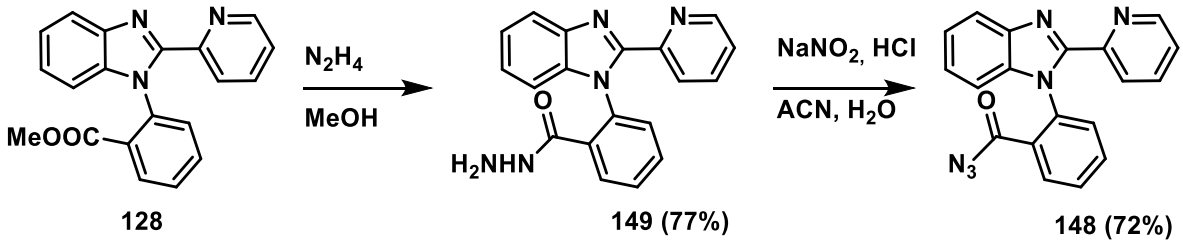

Scheme 37 Synthesis of azide **148**

Azide **148** was prepared in quantitative yields using acid catalyzed azidation with $NaNO_2$ (Scheme 37). Since the racemization occurred in the synthesis of **149**, only a racemic variant of the reaction was continued due to a low amount of the available material. Simple resolution of the hydrazide **149** was attempted using LTA mix in acetonitrile with no success. Possibly the presence of the additional basic groups distorted the formation of the crystals and precipitation of the material. Alternative procedure was envisioned during writing the thesis: synthesis of active ester such as nitrophenyl or pentrafluorophenyl which could be resolved by crystallization and then directly used as acylation reagents[203] to yield various amides or esters, possibly with no loss of enantiomeric purity.

Azide **148** was then converted into series of derivatives. At first, the amiation with benzylamine and DMAP as a catalyst.[202] After 24 hours, the conversion of the starting material was 85% and the product was isolated in 60% yield. Furthermore, the azide was converted into urea derivative **150** by heating in toluene in the presence of the amine nucleophile (Scheme 38).

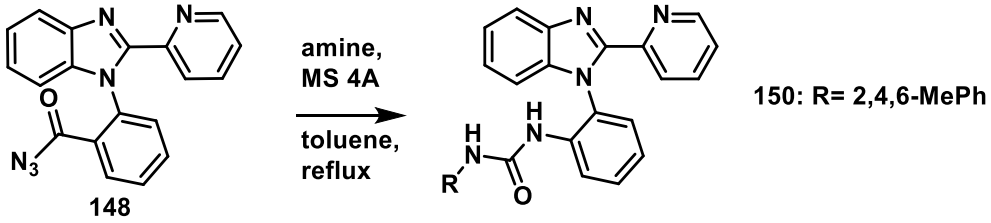

Scheme 38 Synthesis of urea derivative **150**

Atroposelective approach towards ligand 128

Alongside with diastereomeric salt resolution, an atroposelective synthesis was attempted with menthol as a chiral auxiliary. Possibly, the sterically demanding menthol would direct the final cyclization towards one of the atroposiomers or diastereomers might offer separation by chromatography. At first, nitroacid **7** was converted into menthol ester **151**, which was further reduced with hydrogen gas to yield the aminoester **152**. Acylation with pyridine-2-carboxylic acid using T3P in EtOAc/pyridine, as previously described, yielded acylated deriavative **153** in 87% yield. The final cyclization using $BF_3.OEt_2$ yielded the product **154** in 80% yield. Unfortunately, separation of

diastereomers was not possible and NMR analysis revealed only low levels of atroposelectivity of the products being isolated in 10:8 ratio (Scheme 39).

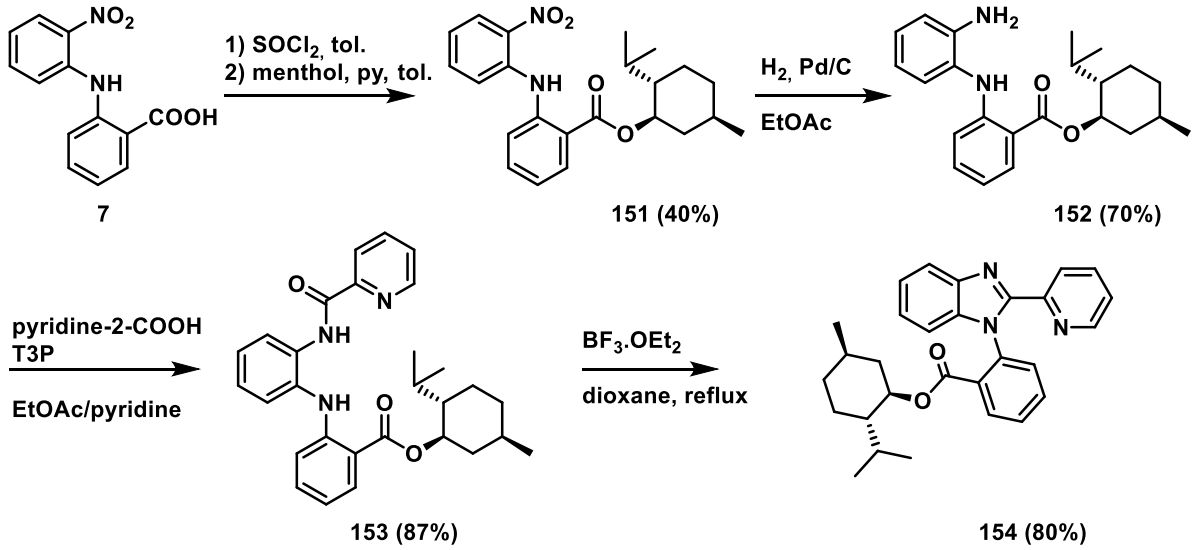

Scheme 39 Attempted atroposelective cyclization with menthol as an auxiliary

Reduction experiments

At first, reduction attempts to reduce acetophenone into 1-phenylethan-1-ol **155** failed and no conversion was observed (Scheme 40).

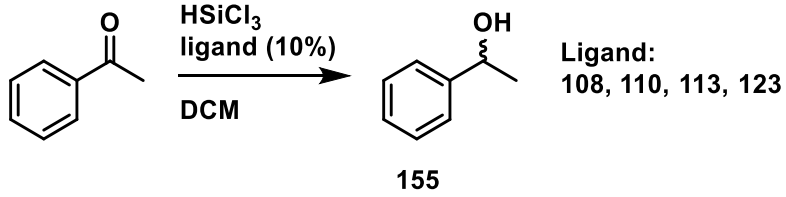

Scheme 40: Reduction of acetophenone

Afterwards, we turned our attention towards reduction of imines. Imine **156** was used as a model substrate for reduction (Scheme 41). Multiple ligands were tested and the results are summarized in Table 31.

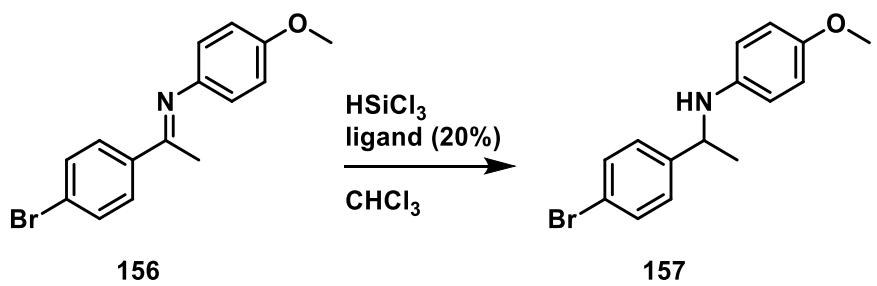

Scheme 41: Model reaction of imine reduction for ligand screening

Table 31: Ligand screening

entry	ligand	Loading (mol%)	solvent	Er.	yield
1	108	20	$CHCl_3$	--	--
2	110	20	$CHCl_3$	--	--
3	113	20	$CHCl_3$	--	--
4	128	20	$CHCl_3$	67/33	70%
5	134	20	$CHCl_3$	65/35	65%
6	138	20	$CHCl_3$	81/19	70%
7	139	20	$CHCl_3$	80/20	70%
8	144	20	$CHCl_3$	82/18	65%
9	128	20, TES used instead of $HSiCl_3$	$CHCl_3$	--	--

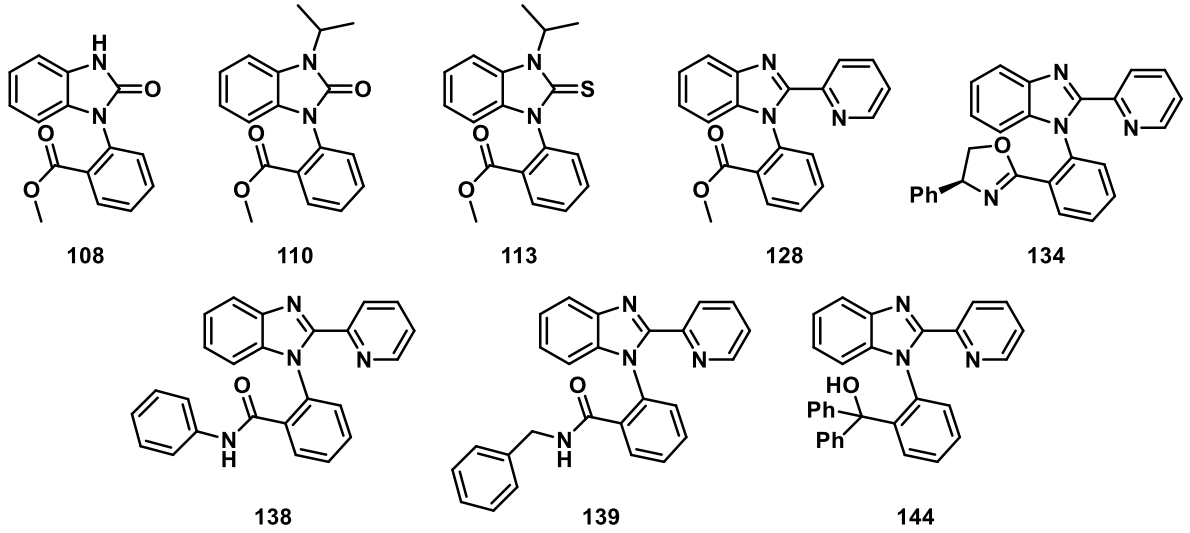

At first, the benzimidazole-2-on derivatives **108** and **110** (entries 1 and 2) were tested; however, no conversion of the starting material was observed. The same was observed in the case of thio analogue **113** (entry 3). Fortunatelly, the methylester **128** yielded the product in 70% yield and moderate enantioselectivity (30%ee, 65:35 er.) (entry 4). The oxazoline ligand **134** yielded the product in similar yield and similar enantioselectivity (entry 5). The use of anilide **138** and benzylamide **139** as a ligand, significantly improved the enantioselectivity towards 60% ee (entries 6 and 7). Similar results were obtained when triarylmethanol ligand **144** was used (entry 8). Using triethylsilane instead of trichlorosilane (entry 9) did not show any conversion of the starting material as expected. This might likely be caused by lower electrophility of the silicon atom compared to the trichlorosilane. This lower electrophility then does not allow coordination of the ligand and formation of the active reducing agent.

Further experiments were highly complicated by the available amounts of the ligand. For this reason, we used methylester **128** as a model ligand for optimization of the procedure and then the optimized conditions were used with other ligands.

. At first, the reduction using 20 mol% ligand loading was reproduced (Table 32, entry 1). The product was isolated with similar enantiomeric purity as in the initial experiment. Reducing the ligand loading to 10% (entry 2), 5% (entry 3), or 1% (entry 4) did not have a significant impact on the

enantioselectivity contrary to the expectations. Furthermore, it seemed that the reduction of the ligand loading proved to be beneficial (compare entry 1 and 4).

Table 32: Effect of ligand loading on the reduction

entry	**ligand**	**Loading (mol%)**	**solvent**	**Er.**
1	128	20	$CHCl_3$	69/31
2	128	10	$CHCl_3$	72/28
3	128	5	$CHCl_3$	73/27
4	128	1	$CHCl_3$	74/26
5	138	1	$CHCl_3$	75/25
6	139	1	$CHCl_3$	75/25
7	144	1	$CHCl_3$	Slow reaction

The amide ligands **138** and **139** yielded the product with slightly higher enantiomeric purity compared to the 20% loading (entries 5 and 6). Last, the reduction utilizing triarylmethanol ligand **144** proceeded significantly slower and the product was not isolated (entry 7).

Next, the solvent effect was tested (Table 33). At first, reaction was conducted in dichloromethane (entry 2). Slight improvement in enantioselectivity was observed compared to chloroform (entry 1). Changing solvent to toluene unexpectedly improved the enantioselectivity of the reduction to 60% enantiomeric excess (85:15 enantiomeric ratio) (entry 3). Similar results were obtained after reproducing the experiment (entry 4). The expected role of π-π interactions to stabilize the transition state[119] was not shown and quite possibly, in the case of ligands **129-136** if the interaction is present, it has negative instead of positive effect on the enantioselectivity.

Table 33: Solvent effect on the reduction

Entry	**ligand**	**Loading (mol%)**	**solvent**	**Er.**
1	128	1	$CHCl_3$	74/26
2	128	1	DCM	77/23
3	128	1	toluene	85/15
4	128	1	toluene	83/17
5	138	1	toluene	80/20
6	139	1	toluene	76/25
7	144	1	toluene	85/15
8	146	1	toluene	72/28
9	128	5	toluene	63/37

In the case of ligands **138** and **139** (entries 5 and 6)**,** no improvement in enantioselectivity was observed compared to ligand **128** (entry 3) suggesting the possibility of a different transition state or different interactions playing a key role. Possibly, the amide NH might be involved in the reaction. Furthermore, similar enantioselectivity of the reaction was observed for ligand **144** (entry 7) compared to ligand **128** (entry 3). More importantly, significant improvement in the rate of the reaction was observed. While any reaction was observed barely in chloroform (Table 32, entry 7) after 24 hours, in toluene (Table 33, entry 7) a full conversion was observed together with high enantioselectivity.

Isopropyl ester **146** (entry 8) showed lower levels of enantioselectivity as the methylester (entry 3) similar to benzylamide **139** (entry 6). Last, 5 mol% of ligand **128** were used (entry 9) to confirm the positive effect of the reduced loading. The product was isolated in enantiomeric ratio 63/37 which is significantly worse compared to 1% loading (entry 1, 74/26 er)

Last, other imines **158-163** (Figure 46) were tested with using the optimized conditions (1 mol% of ligand, toluene, RT).

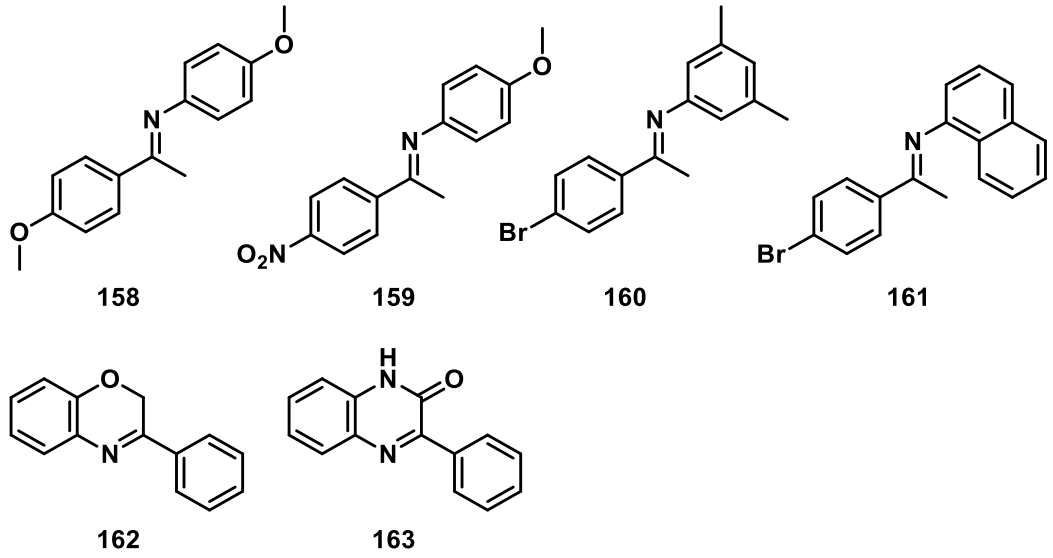

Figure 46: Structures of prepared imines

The results are summarized in Table 34. The reduction of dimethoxyimine **158** yielded the resulting amine in 60% yield and moderate enantioselectivity (er 73/27) (entry 1). The reduction of the nitro-methoxy derivative **159** proceed in similar manner with moderate enantioselectivity (e.r. 78/22) and yield 65% (entry 2). Unfortunately, only decomposition to the acetophenone and aniline was observed in the case of compounds **160** and **161**. The exact cause is unknown since the reaction was also attempted in dry solvents with molecular sieves. Possibly, the higher steric hinderance on the aniline part plays a role. Last, the cyclic imines **162** and **163** were reduced. The imine **162** was reduced with low enantioselectivity (er. 65/35) (entry 5). The reduction of imine **163** did not proceed, possibly due to the low solubility of the imine in toluene. Further addition of chloroform to dissolve the starting material did not have significant effect and no conversion was observed (entry 6).

Table 34: Reduction of imines under optimazed conditions

entry	imine	er	yield
1	158	73/27	60 %
2	159	78/22	65 %
3	160	Decomposition	
4	161	Decomposition	
5	162	65/35	70 %
6	163	No reaction	

Nonlinear effect

Preliminary experiments were conducted to get some insight into the reaction mechanism and transition state. At first, results in Table 32 (lowering the loading of ligand increases the enantiomeric purity of the product) indicate that only one molecule of the ligand is likely involved in the transition state. Further experiments with variable enantiomeric purity of ligand **128** were performed (Table 35). At first, the reductions with racemic (entry 1) and enantiopure ligand 128 (entry 7) were conducted. Further, lowering the enantiomeric purity of the ligand, caused variation of the enantiomeric purity of the product (entries 2-6).

Table 35: Study of nonlinear effect with ligand **128**

entry	%Ee ligand (1 mol%)	%Ee product 157
1	0	0
2	19.5	10
3	32.5	13
4	45	21
5	65	10
6	78	17
7	97	67

As can be seen in Figure 47, there is a clear nonlinear relationship (NLE) between %ee of the ligand and enantiomeric purity of the product. This negative nonlinear effect ((−)-NLE) [204,205] suggests more than one molecule of the ligand is involved in the transition state.[204] This is in direct contradiction with previous results with lower ligand loadings providing higher %ee. Possibly, two competing processes are occurring at the same time: a) coordination of a single molecule of the ligand to $HSiCl_3$ which further provides product with higher %ee and b) coordination of two molecules of the ligand to $HSiCl_3$ which also forms catalytically active species; however, reaction catalyzed by these species provide a product with lover %ee. Those two competing processes could explain the unusuall local minimum in the %ee product vs %ee ligand dependency (Figure 47)

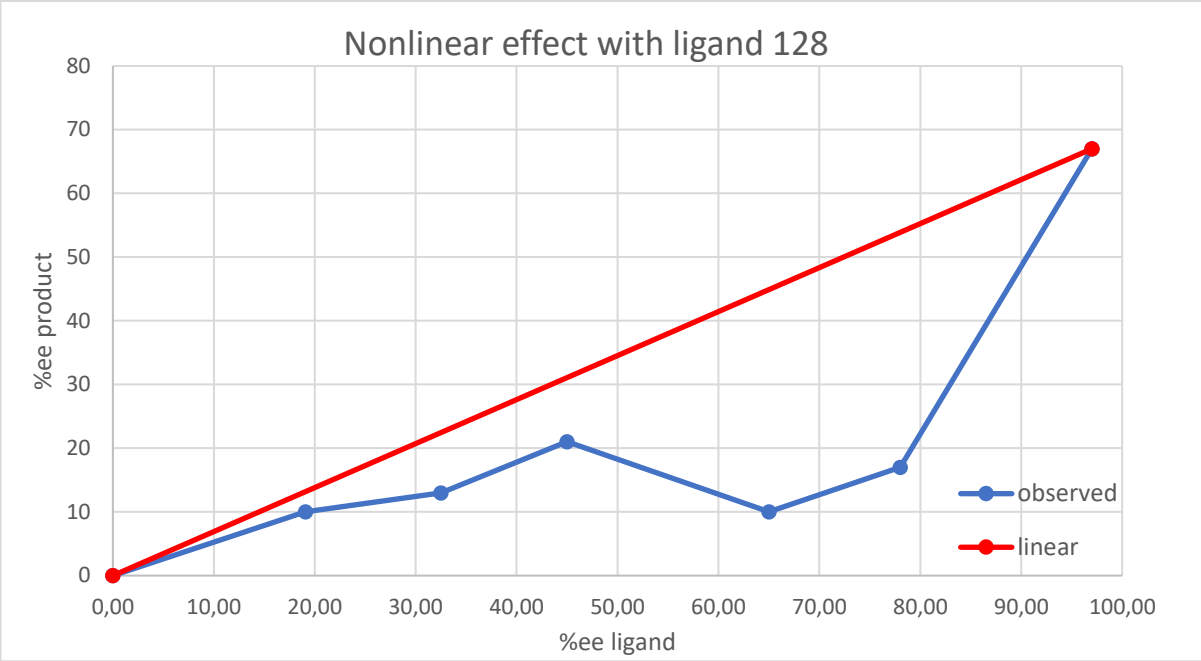

Figure 47: Nonlinear effect of imine reduction with ligand **128**

The magnitude of the NLE highly depends on the specific conditions of the reaction such as temperature, concentration, loading of the ligand etc.; therefore, these presented results shall be considered only preliminary and indicate much more complicated kinetic of the reduction mechanism. Furthermore, due to the extremely low loading of the ligand and scale of the reaction, the experiment might be tainted by higher error due to required manipulations.

Compared to literature examples, the presented ligands provide lower enantioselectivity. Most of the examples found in literature provided products with higher enantioselectivity er. 90/10 (80%ee) or higher.[119,120,125,206,207] Further structural optimization and modifications are required to improve the enantiomeric excess of the product to already known ligands.

Conclusion

In conclusion, this thesis deals with two projects. At first, the novel chiral derivatization agent, 2-(2-(trifluoromethyl)-1*H*-benzo[*d*]imidazol-1-yl)benzoic acid (TBBA) was developed for assignment of absolute configuration of chiral alcohols and amines. Racemic TBBA was prepared by the conventional methods and subsequent chiral resolution was carried out *via* conversion into a diastereomeric pair of oxazolines. Atroposelective synthesis t of TBBA was attempted as well but only with partial success.

Eighteen chiral secondary alcohols and α-chiral primary amines with the known absolute configuration were used to evaluate TBBA. All model compounds followed the proposed general conformational model for assignment of absolute configuration.

Furthermore, eighteen β-chiral primary alcohols and amines with the known absolute configuration were tested as well. Seventeen of them fully followed the devised conformational model while one, (*S*)-*N*-Boc-Phenylglycinol, offered the opposite absolute configuration.

Further investigation of this irregularity involved synthesis of six other Boc-protected aminoalcohols derivatives and eight (*S*)-phenylglycinols to probe limitations of TBBA. Syntheiss of multiple *N*-substituted derivatives revealed strong influence of the *N*-carbonyl functionality. Hydrogen bond was revelaed by B3LYP-G-31* and ωB97X-D/6-31G* in silico modelling. The hydrogen bond was further confirmed by ^{1}H experiments in acetone-D_6 which acts as an H-bond acceptor. Significant differences in the $\Delta\delta^{PM}$ were observed in acetone-D_6 compared to $CDCl_3$. The influence of the hydrogen bond is further increased by the presence of *N*-carbonyl moiety due to the repulsion between CF_3 and carbonyl oxygen.

The aim of the second project was to develop novel axially chiral ligands for asymmetric reduction of imines using $HSiCl_3$ as a cheap hydride source. 2-(2-Pyridyl)benzimidazole-based ligand was prepared and resolved into enantiomers on a multigram scale. Other structural modifications were attempted; however, racemization was observed in the case of acylation reaction. New ligands were prepared as racemates and some of them were resolved by chiral semipreparative HPLC. Unfortunately, external reasons did not allow for resolution of all prepared racemates.

Several reduction experiments were performed and revealed methyl 2-(2-(pyridin-2-yl)-1*H*-benzo[*d*]imidazol-1-yl)benzoate as the best ligand when used in toluene at low catalytic loadings. Multiple imines were reduced in moderate enantioselectivity and preliminary experiments revealed a possible negative nonlinear effect observed on a model substrate. Some of the prepared imines were not reduced due to their poor solubility in toluene. This project remained unfinished due to time reasons.

Eperimental part

GENRAL METHODS: All reactions were carried out under normal coditions without any specific precautions to exclude moisture or air from the reaction unless otherwise stated. Reaction workup and column chromatography were performed with commercial grade solvents without further purification. ^{1}H NMR, ^{13}C NMR, and ^{19}F NMR spectra were measured on a Jeol ECA400II (400 MHz) or Jeol ECX-500SS (500 MHz) instrument in $CDCl_3$, DMSO-D_6 or acetone-D_6 as a solvent. ^{1}H and ^{13}C spectra were calibrated using residual nondeutertated solvent as an internal reference (7.26 and 77.16 ppm for $CDCl_3$, 2.50 and 39.52 ppm for DMSO-D_6, 2.050 and 29.840 for acetone-D_6). ^{19}F spectra were calibrated by the addition of $CFCl_3$ as an internal reference (δ = 0.0 ppm). All ^{13}C NMR spectra were measured with broadband ^{1}H decoupling. ^{1}H NMR data are reported as follows: δ, chemical shift; coupling constants (J are given in hertz, Hz) and integration. Abbreviations to denote the multiplicity of a particular signal were s (singlet), d (doublet), t (triplet), q (quartet), m (multiplet), app (appears as) and br (broad).

Analytical thin-layer chromatography (TLC) was performed using Kieselgel 60 F_{254} plates (Merck). Compounds were detected by UV light (255 nm) and then by basic $KMnO_4$ solution. Flash chromatography was performed using silica gel (35−70 μm particle size). HRMS analysis was performed using an LC-MS Orbitrap Elite high-resolution mass spectrometer with electrospray ionization (Dionex Ultimate 3000, Thermo Exactive plus, MA, USA). The samples were dissolved in MeOH or acetonitrile and injected to the mass spectrometer over autosampler after HPLC separation: precolumn Phenomenex Gemini (C18, 50 × 2 mm, 2.6 μm), mobile phase isokrat MeOH/water/HCOOH 95:5:0.1.

SFC chiral analyses were performed using an Acquity UPC^2 system (Waters) consisting of a binary solvent manager, sample manager, column manager, column heater, convergence manager, PDA detector 2998, QDa mass detector and chiral analytical columns (4.6 mm × 100 mm, 3 μm particle size). The chromarographic runs were performed at a flow rate of 2.2 mL/min, column temperature of 38 °C, and ABPR 2000 psi.

Dry solvents (THF, diethylether, DMF, DCM, ethanol) were dried over activated alumina and used as received from solvent purification system. Toluene was dried over activated molecular sieved or used as received from supplier. Acetonitrile was dried over activated molecular sieves.

2-(2-(trifluoromethyl)-1*H*-benzo[*d*]imidazol-1-yl)benzoic acid (1)

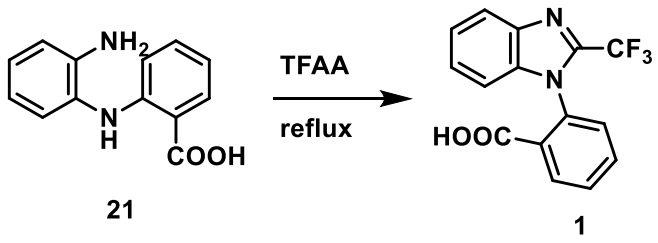

21 1

To 2-((2-aminophenyl)amino)benzoic acid **21** (11.4 g, 49.9 mmol, 1 eq.) trifluoroacetic anhydride was added (100 mL, c= 0,5 mmol/mL). After effervescence ended, a solution was refluxed for 70 minutes. The reaction mixture was then cooled to room temperature and added dropvise into ice-cold water (2.7 L) with rapid stirring by overhead stirrer. A white precipitate was collected by filtration and dried in vacuum at 90°C. Yield 14.5 g (94%), a pale yellow solid. **^{1}H NMR** (400 MHz, DMSO-D6) δ 13.19 (d, J = 84.5 Hz, 1H), 8.18 (dd, J = 7.7, 1.6 Hz, 1H), 7.92 – 7.89 (m, 1H), 7.88 (dd, J = 7.6, 1.7 Hz, 1H), 7.81 (td, J = 7.6, 1.3 Hz, 1H), 7.74 (dd, J = 7.7, 0.8 Hz, 1H), 7.44 – 7.38 (m, 2H), 7.06 – 7.02 (m, 1H). **^{13}C NMR {^{1}H}** (101 MHz, DMSO-D6) δ 165.21, 140.19, 139.98 (q, J = 38.9 Hz), 137.36, 133.78, 133.27, 131.88, 130.94, 130.18, 129.36, 125.97, 123.72, 120.79, 118.84 (q, J = 272.2 Hz), 111.13. 19F NMR (376 MHz, DMSO-D6) δ -60.52, HRMS ESI[M+H]$^{+}$ calculated for $C_{15}H_{10}O_2N_2F_3$+H: 307.0689, found: 307.0685, Mp: 218-220°C

2-methyl-*N*-(2-nitrophenyl)aniline (2)

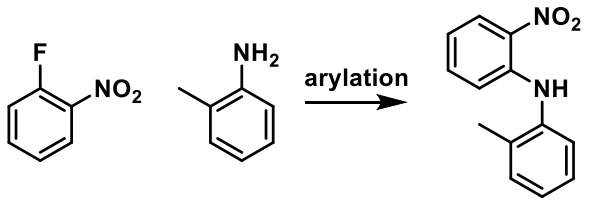

4 5 2

O-Toluidine (825 µL, 7.5 mmol, 1 eq), 2-fluoronitrobenzene (755 µL mmol, 1eq) and trimethylamine (1 mL, 10 mmol, 1.3 eq) were heated without solvent in pressure tube at 150°C for 20 hours. After 20 hours, the mixture was cooled to room temperature and poured into MeOH (10 mL). This mixture was cooled in ice bath and the precipitate was collected by filtration. Isolated 3.11 g (60%). **^{1}H NMR** (400 MHz, DMSO-d_6) δ 9.34 (s, 3H), 8.13 (dd, *J* = 8.6, 1.6 Hz, 3H), 7.45 (dddd, *J* = 8.6, 6.9, 1.6, 0.5 Hz, 5H), 7.40 – 7.35 (m, 6H), 7.31 – 7.22 (m, 11H), 6.80 (ddd, *J* = 8.4, 6.9, 1.3 Hz, 3H), 6.67 (dd, *J* = 8.7, 1.2 Hz, 4H), 2.18 (s, 3H). **^{13}C NMR {^{1}H}** (101 MHz, DMSO-D_6) δ 143.3, 137.2, 136.3, 134.4, 132.1, 131.2, 127.1, 126.7, 126.7, 126.2, 117.0, 115.8, 17.5.

***N*1-(o-tolyl)benzene-1,2-diamine (3)**

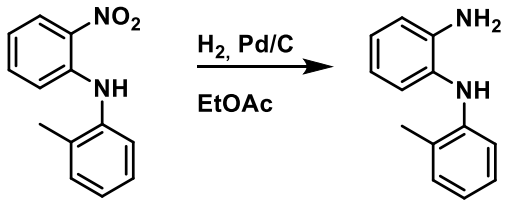

2

Three necked flask fitted with stirbar, rubber septa and valve was charged with 170 mg of 10% Pd/C (0.164 mmol, 0.025 eq). **2** (1.5 g, 6.57 mmol, 1 eq) was added followed by EtOAc (30 mL). The last open neck was fitted with rubber balloon and the whole apparatus was purged with argon / vacuum cycle three times. After the evacuation of the flask, hydrogen gas was introduced and the suspension was

rapidly stirred at room temperature for 22 hours. After 22 hours, the flask was opened to air, the suspension was filtered through pad of silica and the filtrate was evaporated yielding 1.22 g (95%) of oil which solidified by standing on air. **^{1}H NMR** (400 MHz, DMSO) δ 7.07 (d, *J* = 7.2 Hz, 1H), 6.95 (t, *J* = 7.8 Hz, 1H), 6.86 – 6.77 (m, 2H), 6.73 (d, *J* = 7.7 Hz, 1H), 6.67 (dd, *J* = 8.5, 6.6 Hz, 1H), 6.58 – 6.49 (m, 1H), 6.47 (d, *J* = 8.2 Hz, 1H), 6.32 (s, 1H), 4.72 (s, 2H), 2.21 (s, 3H). **^{13}C NMR {^{1}H}** (101 MHz, DMSO) δ 143.9, 142.3, 130.3, 128.3, 126.4, 125.0, 124.0, 123.6, 118.6, 116.6, 115.1, 114.6, 17.9.

1-(o-tolyl)-2-(trifluoromethyl)-1*H*-benzo[*d*]imidazole (3a)

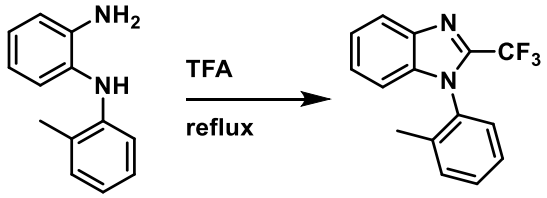

3 **3a**

3 (600 mg, 3 mmol, 1 eq) was dissolved in TFA (6 mL) and refluxed for 18 hours. After 18 hours, the reaction was cooled to room temperature and the TFA was evaporated. The oily residue was dissolved in DCM (20 mL) and washed with 10% aq K_2CO_3 (3x 20 mL). The organic layer was dried with $MgSO_4$ and evaporated to yield 400 mg of oil (65%). **^{1}H NMR** (400 MHz, DMSO-d_6) δ 7.95 (dt, *J* = 4.9, 3.0 Hz, 1H), 7.61 – 7.50 (m, 3H), 7.49 – 7.41 (m, 3H), 7.07 – 7.01 (m, 1H), 1.88 (s, 3H). **^{13}C NMR {^{1}H}** (101 MHz, DMSO-D_6) δ 140.2, 139.58 (q, J = 38.6 Hz), 136.3, 135.8, 132.6, 131.3, 130.6, 128.6, 127.4, 126.3, 124.1, 121.2, 118.73 (q, J = 273.7 Hz), 111.3, 16.4. **^{19}F NMR** (376 MHz, DMSO-D_6) δ -60.8.

Oxidation of 3a to 1

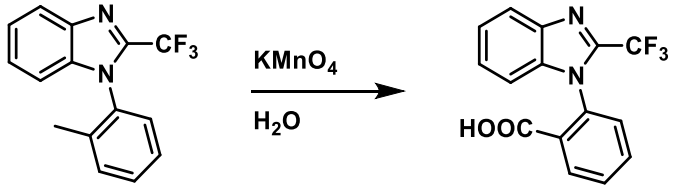

3a **1**

3a (400 mg, 1.45 mmol, 1 eq) was suspended in water (50 mL), $KMnO_4$ (1420 mg, 9 mmol, 6eq) was added and the reaction was refluxed for 24 hours. After 24 hours, HPLC analysis revealed incomplete confersion therefore $KMnO_4$ (1400 mg, 9 mmol, 6eq) was added and the reaction was futher refluxed for 24 hours. The reaction was then cooled to room temperature and extracted with DCM (3x 50 mL). The DCM extracts were combined and washed with water (3x 50) and 10% NaOH (3x 50). The alkaline extracts were combined, acidified with conc. HCl, extracted with DCM (3x 50) and the organic extracts were combined, dried with $MgSO_4$ and evaporated to yield 150 mg of 1 as an oil (30%).

2-((2-nitrophenyl)amino)benzoic acid (7)

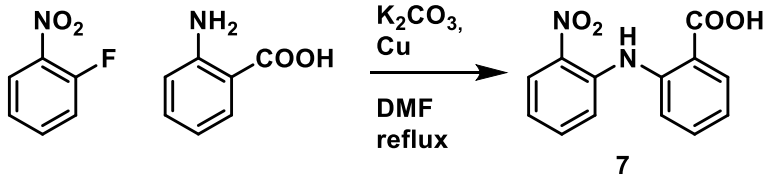

7

Anthranilic acid (16.8 g; 120 mmol) was dissolved in DMF (30 mL). 2-fluoronitrobenzene (12.75 mL; 120 mmol, 1eq), K_2CO_3 (16.5 g; 120 mmol; 1 eq) and copper (160 mg; 0.8 mmol, 0.02 eq) were added

respectively. The suspension was refluxed for 17 hrs. After 17 hrs, reaction mixture was cooled down to room temperature. The formed muddy solid was suspended in cold water (150 ml). This suspension was acidified using glacial acetic acid (150 mL). The precipitated solid was broken down into suspension using sonification and spatula until fine suspension was formed. This suspension was filtered and washed with water. The solid was then recrystallized from glacial acetic acid (125 mL), filtered, washed thoroughly with water and dried in oven (90 °C). Yield: 22g (70%), brown solid. **^{1}H NMR** (400 MHz, DMSO-D6) δ 13.46 (s, 1H), 11.11 (s, 1H), 8.13 (dd, *J* = 8.4, 1.4 Hz, 1H), 8.00 – 7.95 (m, 1H), 7.67 – 7.58 (m, 2H), 7.56 – 7.49 (m, 2H), 7.13 – 7.05 (m, 2H). **^{13}C NMR {^{1}H}** (101 MHz, DMSO-D6) δ 168.76, 142.12, 138.11, 137.20, 135.48, 133.65, 131.80, 126.31, 121.67, 120.66, 119.20, 118.60, 118.27. **HRMS** ESI[M+H]$^{+}$ calculated for $C_{13}H_{11}O_4N_2$: 259.0713, found: 259.0712 **Mp**: 218-221°C.

(*P*/*M*)-(*S*)-4-Phenyl-2-(2-(2-(trifluoromethy)-1*H*-benzo[*d*]imidazol-1-yl)phenyl)-4,5-dihydrooxazole (*P*/*M*-15)

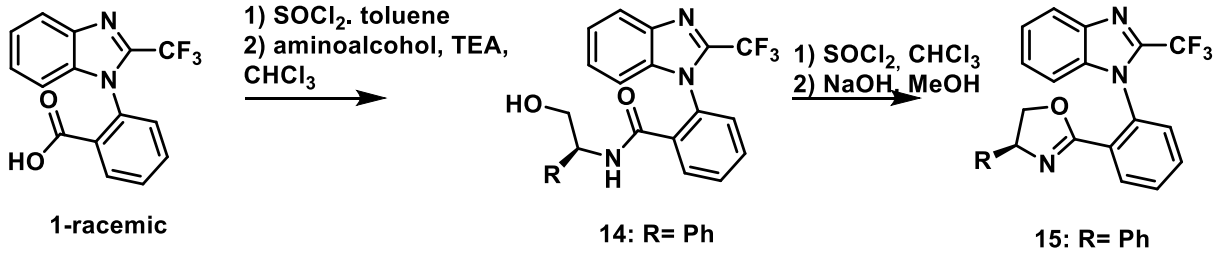

Racemic 2-(2-(trifluoromethyl)-1*H*-benzo[*d*]imidazol-1-yl)benzoic acid **rac-1** (1.8 g, 6 mmol, 1 eq.) was suspended in toluene (90 mL) and $SOCl_2$ (2.2 mL, 30 mmol, 5 eq.) was added. A mixture was refluxed for 20 minutes (all solids dissolved). After cooling to RT, the solvent was evaporated yielding a dark oily residue. This residue was twice dissolved in $CHCl_3$ (25 mL) and evaporated to remove all residual $SOCl_2$.

The resulting oil was dissolved in $CHCl_3$ (25 mL) and after cooling to 5°C (ice/water bath), a solution was added dropvise into a cooled solution of (*S*)-(+)-phenylglycinol (904 mg, 6.6 mmol, 1.1 eq.) and triethylamine (910 µL, 6.6 mmol, 1.1 eq.) in $CHCl_3$ (12 mL). This mixture was stirred on an ice bath for 90 min. After 90 min., the solution was washed with 10% (v/v) aq. HCl (2 x 30 mL) and 10% (m/m) aq. K_2CO_3 (2 x 30 mL) and dried over $MgSO_4$.

Afterwards, the drying agent was removed by filtration and $SOCl_2$ (2.2 mL, 30 mmol, 5 eq.) was added to the filtrate. The solution was stirred at room temperature in an open flask for 90 minutes (monitored by TLC, hexane:EtOAc 2:1; Rf= 0.75). After the reaction was completed, the solution was evaporated, redissolved in $CHCl_3$, and evaporated again to yield a dark oily residue.

This residue was dissolved in MeOH (32 mL) and solution of NaOH (1.2 g, 30 mmol, 5 eq.) in water (12 mL) was added dropwise and the reaction was stirred for 2 hrs (monitored by TLC, hexane:EtOAc 2:1, Rf= 0.62 or Hex:EtOAc 5:1, Rf= 0.32 and 0.22). After completion of the reaction, methanol was evaporated using RVO and H_2O (50 mL) was added. A cloudy solution was extracted with $CHCl_3$ (50 and 2x 30 mL). Organic layers were combined and dried over $MgSO_4$ and evaporated to yield 1.94 g of an oily mixture of diastereomers. The mixture was purified by column chromatography (10x6 cm, petrolether: ethyl acetate 6:1) yielding 807 mg (65% from rac. acid) of (***P***)-**15a** and 676 mg (55% from rac. acid) of (***M***)-**15** as yellow oils.

(***P***)-**15 ^{1}H NMR** (400 MHz, $CDCl_3$) δ 8.24 (dd, *J* = 7.6, 1.9 Hz, 1H), 7.90 (d, *J* = 7.3 Hz, 1H), 7.76 – 7.65 (m, 2H), 7.54 (dd, *J* = 7.4, 1.3 Hz, 1H), 7.43 – 7.33 (m, 2H), 7.16 – 7.08 (m, 3H), 7.02 (dd, *J* = 7.3, 1.2 Hz, 1H), 6.63 (td, *J* = 7.4, 3.2 Hz, 2H), 5.06 (dd, *J* = 9.9, 9.1 Hz, 1H), 4.28 (dd, *J* = 10.3, 8.4 Hz, 1H), 3.83 (t, *J* = 8.6 Hz, 1H). **^{13}C NMR {^{1}H}** (101 MHz, $CDCl_3$) δ 161.23 (s), 141.67 (s), 141.49 (q, *J* = 40.7 Hz), 141.03 (s), 137.61 (s), 133.58 (s), 132.35 (s), 131.58 (s), 130.47 (s), 129.95 (s), 128.57 (s),

127.29 (s), 126.62 (s), 126.17 (s), 125.64 (s), 123.74 (s), 121.51 (s), 119.05 (q, *J* = 271.7 Hz), 110.96 (s), 74.36 (s), 69.74 (s). **^{19}F NMR** (376 MHz, $CDCl_3$) δ -61.52 (s). **HRMS** ESI[M+H]$^+$ calculated for $C_{23}H_{16}ON_3F_3$+H: 408.1318, found: 408.1320 $[\alpha]_D^{26}$ = -82.31° (c= 0.39 MeOH).

(*M*)-15 ^{1}H NMR (400 MHz, $CDCl_3$) δ 8.22 (dd, *J* = 7.7, 1.7 Hz, 1H), 7.95 – 7.89 (m, 1H), 7.77 – 7.65 (m, 2H), 7.53 (dd, *J* = 7.6, 1.2 Hz, 1H), 7.43 – 7.33 (m, 2H), 7.25 – 7.18 (m, 3H), 7.08 – 7.02 (m, 1H), 6.88 – 6.82 (m, 2H), 5.02 (t, *J* = 9.4 Hz, 1H), 4.40 (dd, *J* = 10.2, 8.5 Hz, 1H), 3.50 (t, *J* = 8.7 Hz, 1H). **^{13}C NMR {^{1}H}** (101 MHz, $CDCl_3$) δ 162.29 (s), 141.52 (q, *J* = 39.9 Hz), 141.33 (s), 140.86 (s), 137.66 (s), 133.40 (s), 132.41 (s), 131.87 (s), 130.46 (s), 129.68 (s), 128.67 (s), 127.66 (s), 127.07 (s), 126.68 (s), 125.77 (s), 123.88 (s), 121.50 (s), 119.00 (q, *J* = 272.1 Hz), 111.08 (s), 75.02 (s), 69.84 (s). **^{19}F NMR** (376 MHz, $CDCl_3$) δ -61.34 (s). **HRMS** ESI[M+H]$^+$ calculated for $C_{23}H_{16}ON_3F_3$+H: 408.1318, found: 408.1323 $[\alpha]_D^{26}$ = +82.50° (c= 0.44 MeOH).

Hydrolysis of (*P*)-15a to (*P*)-1-carboxyphenyl(2-trifluoromethy)benzimidazole (*P-1)*

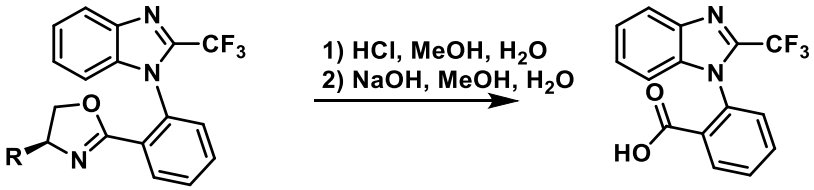

15a: R= Ph **1**

(***S,P***)-4-phenyl-2-(2-(2-(trifluoromethyl)-1H-benzo[d]imidazol-1-yl)phenyl)-4,5-dihydrooxazole (***P***)-**15a** (807 mg, 2 mmol, 1 eq.) was dissolved in MeOH (20 mL) and 10% (v/v) HCl (7.2 mL) was added. The solution was stirred at room temperature for 90 minutes when HPLC analysis showed complete ring opening. After 90 minutes, NaOH (1.6g, 40 mmol, 20 eq.) was added as a 10% aq. solution (16 mL). The reaction was stirred for another 3 hours until HPLC analysis showed a complete conversion. The solution was then diluted with water (15 mL), methanol was evaporated using RVO and a resulting solution was extracted with DCM (3x20 mL). The alkaline aq. phase was then added dropvise to ice cold 10% (v/v) HCl (30 mL) with rapid stirring. A white precipitate was collected by filtration and dried on air to give 393 mg of a white solid (64%). The compound was identical as racemic acid **rac-1** (with regards to spectrocsopic properties NMR, MS, MP). $[\alpha]_D^{24}$ = -46.02° (c= 1, MeOH). Enantiomeric purity was determined by chiral SFC: isocratic elution with 90% CO_2, 10% MeOH 0.1% TFA, column CHIRALPAK 1A3.

Hydrolysis of (*M*)-*15a* to (*M*)-1-carboxyfenyl(2-trifluoromethy)benzimidazole (*M*-1)

Following the above described procedure, starting with 676 mg of oxazoline (***M***)-**15**. 324 mg of white solid (64%) $[\alpha]_D^{24}$ = +45.54° (c= 1, MeOH).

2-((2-Aminophenyl)amino)benzoic acid (21)

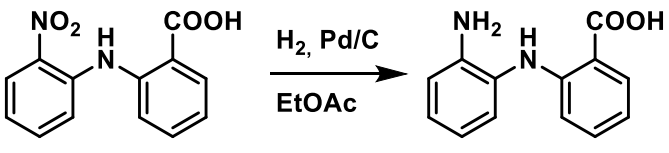

(7) **(21)**

A two liter three-necked flask was charged with 2-((2-nitrophenyl)amino)benzoic acid **7** (16.8 g, 65 mmol, 1 eq.) and 10% Pd/C (1.3 g, 0.01 eq.). A solid mixture was suspended in ethylacetate (1 L). The flask was fitted with a large stir bar, rubber balloon, valve and rubber septa, and flushed with nitrogen and vacuum multiple times to remove air. To an evacuated aparatus, a hydrogen gas was introduced and the reaction mixure was rapidly stirred at room temperature (500 rpm). The reaction was monitored by

TLC (hexane:ethyl aceate 1:1, UV and nynhydrin detection) (a sample can be taken via syringe through rubber septum). After two hours, the mixture was filtered through pad of celite. Celite was washed twice with ethylacetate and a filtrate was evaporated. Yield 14.3 g (96%), a yellow to brown solid. **^{1}H NMR** (400 MHz, DMSO-D6) δ 9.02 (s, 1H), 7.86 (dd, J = 7.9, 1.4 Hz, 1H), 7.28 (ddd, J = 8.5, 7.2, 1.5 Hz, 1H), 7.03 (dd, J = 7.7, 1.1 Hz, 1H), 6.99 – 6.93 (m, 1H), 6.80 (dd, J = 8.0, 1.2 Hz, 1H), 6.66 (td, J = 7.6, 0.9 Hz, 1H), 6.62 – 6.56 (m, 2H). **^{13}C NMR {^{1}H}** (101 MHz, DMSO-D6) δ 170.60, 149.73, 144.68, 134.57, 132.07, 126.82, 126.65, 125.26, 117.08, 116.38, 115.94, 113.75, 111.79, **HRMS** ESI$[M+H]^+$ calculated for $C_{13}H_{10}O_2N_2$+H: 229.0972, found: 229.0973, **Mp**: 195-200°C.

methyl 2-((2-(2,2,2-trifluoroacetamido)phenyl)amino)benzoate (22)

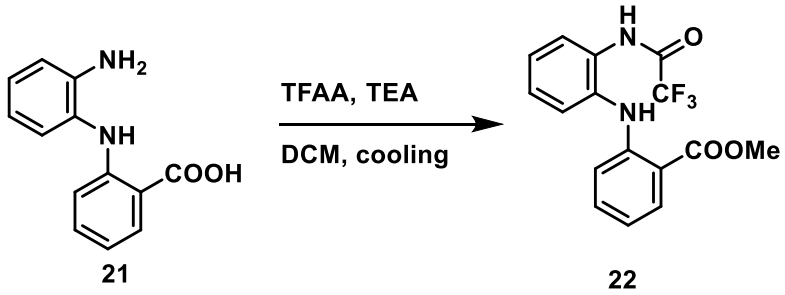

21 22

21 (228 mg, 1 mmol, 1 eq) was dissolved in DCM (6 mL) and trimethylamine (157 µL, 1.1 mmol, 1.1 eq) was added. This solution was cooled in ice bath and TFAA (200 µL, 1.1 mmol, 1.1 eq) in DCM (4 mL) was added dropwise. Reaction mixture was stirred for 40 minutes. After 40 minutes, water (5 mL) was added and the precipitate was filtered and dried. Isolated 120 mg (37 %) ^{1}H NMR (400 MHz, DMSO-d_6) δ 11.25 – 10.97 (m, 1H), 9.80 – 9.51 (m, 1H), 7.89 (d, *J* = 7.4 Hz, 1H), 7.55 – 7.51 (m, 1H), 7.44 – 7.32 (m, 3H), 7.18 (q, *J* = 7.7 Hz, 1H), 7.10 – 7.02 (m, 1H), 6.78 (t, *J* = 7.5 Hz, 1H).

methyl 2-((2-nitrophenyl)amino)benzoate (23)

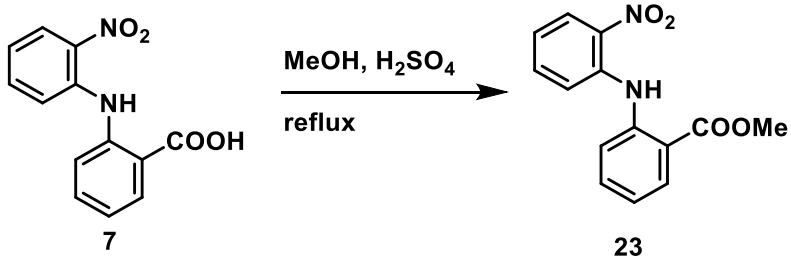

7 23

7 (10 g, 38.7 mmol) was dissolved in MeOH (200 mL) and conc. H_2SO_4 (3 mL) was added. The mixture was refluxed for 24 hrs. During this time, orange precipitate started to appear. After 24 hrs, the reaction was cooled down to room temperature and the precipitate was filtered, washed with MeOH and dried. Yield 10.5 g (99%) of orange solid. **^{1}H NMR** (400MHz ,DMSO-d_6) δ = 10.90 (s, 1 H), 8.15 (td, *J* = 1.1, 8.3 Hz, 1 H), 8.00 - 7.95 (m, 1 H), 7.63 - 7.63 (m, 0 H), 7.66 - 7.52 (m, 4 H), 7.16 - 7.05 (m, 2 H), 3.89 - 3.88 (m, 3 H) **^{13}C NMR {^{1}H}** (101MHz ,DMSO-d_6) δ = 167.0, 141.8, 138.1, 137.0, 135.5, 134.0, 131.4, 126.3, 122.0, 120.7, 119.2, 119.0, 117.7, 52.3 **HRMS** ESI$[M+H]^+$ calculated for $C_{14}H_{13}O_4N_2$: 273.0870, found: 273.0872

methyl 2-((2-aminophenyl)amino)benzoate (24)

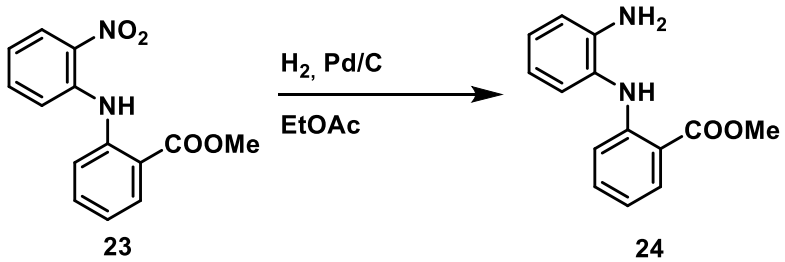

23 24

Three necked 2L flask fitted with stirbar, rubber septa and valve was charged with 4400 mg of 10% Pd/C (4.135 mmol, 0.05 eq). **23** (22.5 g, 82.7 mmol, 1 eq) was added followed by EtOAc (830 mL). The last open neck was fitted with rubber balloon and the whole apparatus was purged with argon / vacuum cycle three times. After the evacuation of the flask, hydrogen gas was introduced and the suspension was rapidly stirred at room temperature for 18 hours (Hydrogen gas was reintroduced if necessary). After 18 hours, the flask was opened to air, the suspension was filtered through pad of silica and the filtrate was evaporated yielding 18.1 g (90%) of gray solid.**^{1}H NMR** (400 MHz, $CDCl_3$) δ 8.76 (s, 1H), 7.86 (dd, *J* = 8.0, 1.6 Hz, 1H), 7.31 (ddd, *J* = 8.6, 7.1, 1.7 Hz, 1H), 7.03 (dd, *J* = 7.8, 1.4 Hz, 1H), 6.98 (td, *J* = 7.7, 1.5 Hz, 1H), 6.80 (dd, *J* = 8.0, 1.4 Hz, 1H), 6.68 (ddd, *J* = 8.1, 7.1, 1.1 Hz, 1H), 4.89 (s, 2H), 3.85 (s, 3H). **^{13}C NMR {^{1}H}** (101 MHz, $CDCl_3$) δ 168.2, 149.0, 144.3, 134.4, 131.0, 126.5, 126.4, 124.5, 116.6, 116.0, 115.5, 113.4, 110.5, 51.8. **HRMS** ESI$[M+H]^+$ calculated for $C_{14}H_{15}O_2N_2$: 243.1128, found: 243.1129

methyl 2-((2-(2,2,2-trifluoroacetamido)phenyl)amino)benzoate (25)

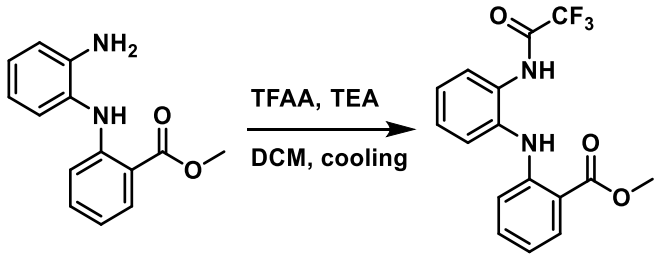

24 **25**

24 (242 mg, 1 mmol, 1 eq) was dissolved in DCM (10 mL), trimethylamine (155 µL, 1.1 mmol, 1.1 eq) was added and the reaction was cooled in ice bath. Trifluoroacetic acid anhydride (200 µL, 1.1 mmol, 1.1 eq) was added dropwise and the reaction mixture was stirred for 1 hour in ice bath. After 1 hours, water (10 mL) was added and the organic layer was separated. The organic layer was futher washed with 10% HCl (1x 10 mL), 10% K_2CO_3 (1x 10 mL), dried with $MgSO_4$ and evaporated to yield 282 mg of product (67%) **^{1}H NMR** (400 MHz, CDCl3) δ 9.11 (s, 1H), 8.50 (s, 1H), 8.33 (dd, *J* = 8.1, 1.4 Hz, 1H), 8.02 (dd, *J* = 8.0, 1.7 Hz, 1H), 7.43 – 7.21 (m, 5H), 6.90 – 6.77 (m, 1H), 6.54 (dd, *J* = 8.4, 1.1 Hz, 1H), 3.95 (s, 3H). **^{13}C NMR {^{1}H}** (101 MHz, $CDCl_3$) δ 169.2, 148.9, 134.8, 132.7, 131.8, 131.2, 127.5, 127.4, 126.9, 121.4, 118.6, 114.4, 114.3, 112.7, 52.2.

methyl 2-(2-(trifluoromethyl)-1H-benzo[d]imidazol-1-yl)benzoate (26)

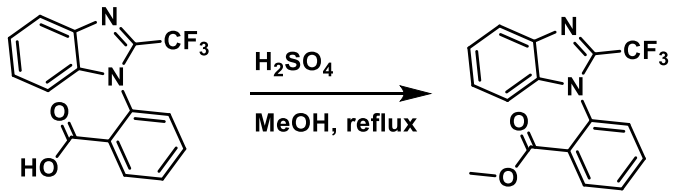

1 **26**

1 (150 mg, 0.5 mmol, 1 eq) was dissolved in MeOH (20 mL) and conc. H_2SO_4 (0.5 mL) was added and the reaction was refluxed for 16 hours. After 16 hours, the solvent was evaporated and the resiude was diluted with water (10 mL) and basified with 10% aq. K_2CO_3 (25 mL) followed by extraction with EtOAc (3x 20 mL). The combined organic extracts were washed with 10% K_2CO_3 (25 mL), brine, dried with $MgSO_4$ and evaporated to yield 130 mg of yellow oil (80%). **^{1}H NMR** (400 MHz, $CDCl_3$) δ 8.22 (dd, *J* = 7.7, 1.8 Hz, 1H), 7.96 – 7.92 (m, 1H), 7.77 (td, *J* = 7.6, 1.7 Hz, 1H), 7.70 (td, *J* = 7.7, 1.4 Hz, 1H), 7.50 (dd, *J* = 7.7, 1.1 Hz, 1H), 7.42 – 7.37 (m, 1H), 7.35 (td, *J* = 7.7, 7.2, 1.4 Hz, 1H), 6.99 – 6.96 (m, 1H), 3.46 (s, 3H). **^{13}C NMR.{^{1}H}** (101 MHz, $CDCl_3$) δ 164.5, 141.09 (q, J = 38.3 Hz), 140.7, 137.6, 134.1, 133.6, 132.3, 130.5, 130.0, 128.9, 125.9, 123.9, 121.4, 118.92 (q, J = 271.8 Hz), 110.7, 52.4

Atroposelective cyclization to (1)

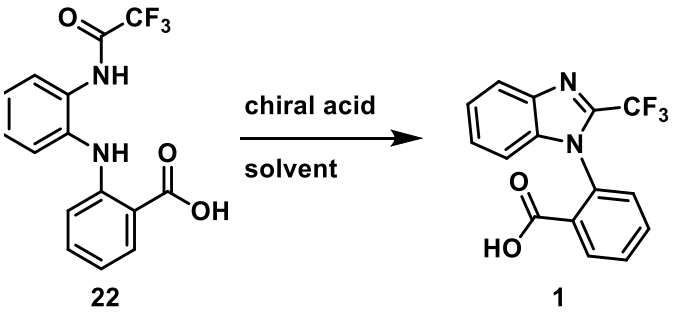

22 1

22 (68 mg, 0.2 mmol, 1 eq) was dissolved in toluene (2 mL) and acid (10 mol%) was added. The mixture was heated to desired temperature for 24 hours. After 24 hours, sample was taken and analyzed by chiral SFC. In the case of L-dibenzoyltartaric acid (entry 2) precipitate was formed which was removed by filtration and analyzed separately.

entry	acid	Solvent	Er
1	10-CSA	THF (65°C)	25 / 75
2	L-dibenzoyltartaric acid	THF (65°C)	26 / 74 (solution) 50 / 50 (precipitate)
3	L-dianisoyltartaric acid	THF (65°C)	26 / 74
4	L-ditoluolyltartaric acid	THF (65°C)	26 / 74
5	L-proline	THF (65°C)	40 / 60
6	R-Mandelic acid	THF (65°C)	28 / 72
7	S-TRIP	THF (65°C)	nd
8	10-CSA	Toluene (80°C)	nd
9	L-dibenzoyltartaric acid	Toluene (80°C)	nd
10	L-dianisoyltartaric acid	Toluene (80°C)	nd
11	L-ditoluolyltartaric acid	Toluene (80°C)	nd
12	L-proline	Toluene (80°C)	nd
13	R-Mandelic acid	Toluene (80°C)	nd
14	TBBA	Toluene (80°C)	nd
15	S-TRIP	Toluene (80°C)	nd

Atroposelective cyclization to (26)

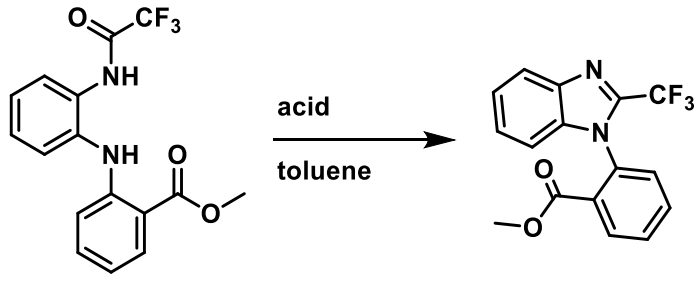

25 26

25 (68 mg, 0.2 mmol, 1 eq) was dissolved in toluene (2 mL) and acid (10 mol%) was added. The mixture was heated to desired temperature for 24 hours. After 24 hours, sample was taken and analyzed by chiral SFC. Unfortunately, no product was detected.

entry	acid	Solvent + temperature	results
1	10-CSA	Toluene (80°C)	nd
2	L-dibenzoyltartaric acid	Toluene (80°C)	nd
3	L-dianisoyltartaric acid	Toluene (80°C)	nd
4	L-ditoluolyltartaric acid	Toluene (80°C)	nd
5	L-proline	Toluene (80°C)	nd
6	R-Mandelic acid	Toluene (80°C)	nd
7	TBBA	Toluene (80°C)	nd
8	S-TRIP	Toluene (80°C)	nd
9	10-CSA	Toluene (120°C)	nd
10	L-dibenzoyltartaric acid	Toluene (120°C)	nd
11	S-TRIP	Toluene (120°C)	nd

Lewis acid catalyzed cyclization to (26)

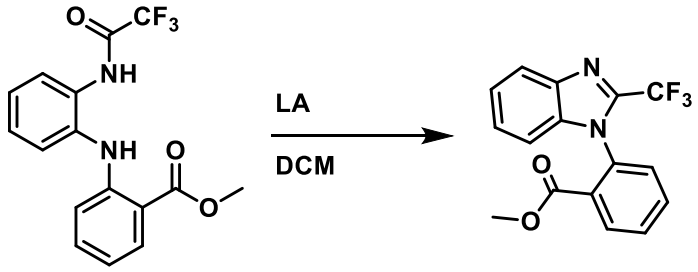

25 **26**

25 (85 mg, 0.25 mmol, 1 eq) was dissolved in dry DCM (2.5 mL), 4A molecular sieves were added and the mixture was cooled in ice bath. After the cooling, lewis acid (0.5 mmol, 2 eq) was added. Reaction was stirred for 5 hours. After 5 hours, water (2 mL) was added and the mixture was filtered through celite. The organic layer was separated, dried with $MgSO_4$ and evaporated. The residue was analyzed by HPLC.

entry	Lewis acid	solvent	results
1	$SnCl_4$, 2 eq.	DCM	Complex mixture
2	$TiCl_4$, 2 eq. (1M solution)	DCM	79%
3	$Ti(OiPr)_4$, 2 eq.	DCM	Complex mixture, low conversion
4	$TiCl_4$ 0.2 eq	DCM	Traces of product
5	$TiCl_4$ 0.5 eq	DCM	Traces of product
6	$TiCl_4$ 1 eq	DCM	65 % isolated

$TiCl_4$ catalyzed cyclization to (26)

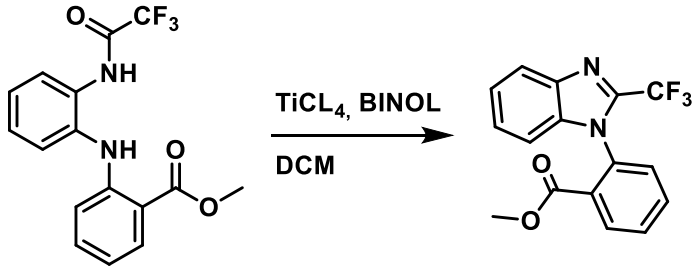

25 26

(*R*)-BINOL (81 mg) was dissolved in dry DCM (2 mL) and molecular sieves were added. $TiCl_4$ (1M in DCM, 300 µL, 1 eq) was added and the solution immediately turned red. This solution was stirred at room temperature for 1 hours. **25** was dissolved in dry DCM (1 mL) and to this solution the $TiCl_4$-BINOL solution was added (670 µL or 1300 µL). The reaction was stirred for 24 hours and after 24 hours was analyzed by HPLC. Due to low conversion no isolation was attempted.

entry	**Eq. TiCl4**	**solvent**	**result**
1	1 + 1eq. (*R*)-BINOL	DCM	10% conversion
2	2 + 2eq. (*R*)-BINOL	DCM	20% conversion, 50:50 er.

(2-((2-aminophenyl)amino)phenyl)methanol (29)

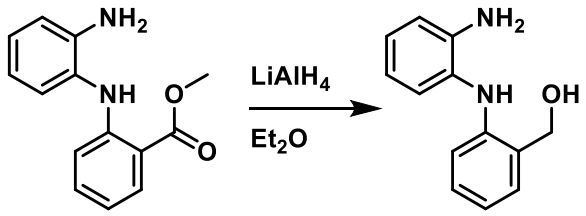

24 29

24 (968 mg, 4 mmol, 1eq) was added over 20 minutes as a solid into the suspension of $LiAlH_4$ (608 mg, 16 mmol, 4 eq) in dry diethylether (72 mL). This suspension was stirred at room temperature for 30 minutes. After 30 minutes, the reaction was cooled in ice bath and water (1.3 mL) was added. The mixture was stirred in ice bath for 30 minutes forming brown suspension. After 30 minutes, 15% aq. NaOH (610 µL) and water (1.2 mL) were added and the reaction was stirred for 10 minutes. After 10 minutes, celite was added and the solids were removed by filtration. The filtrate was evaporated and purified by column chromatography (Hexane: EtOAc 2:1) to yield 500 mg of oil which solidified by standing on air (60%). **^{1}H NMR** (400 MHz, $CDCl_3$) δ 7.19 – 7.12 (m, 2H), 7.11 – 7.08 (m, 1H), 7.02 (ddd, *J* = 7.9, 7.4, 1.5 Hz, 1H), 6.82 – 6.76 (m, 3H), 6.70 (d, *J* = 7.7 Hz, 1H), 6.39 (s, 1H), 4.75 (s, 2H), 3.24 (s, 2H). **^{13}C NMR {^{1}H}** (101 MHz, $CDCl_3$) δ 144.9, 141.2, 129.5, 129.5, 128.7, 125.9, 125.5, 125.0, 119.5, 118.9, 116.5, 114.5, 64.7.

2,2,2-trifluoro-*N*-(2-((2-(hydroxymethyl)phenyl)amino)phenyl)acetamide (30a)

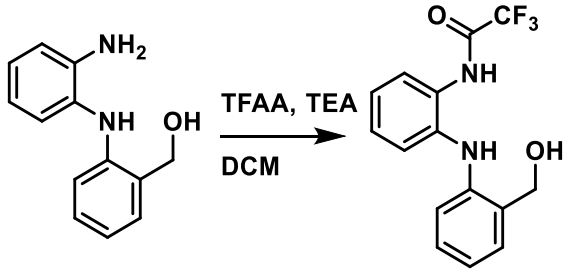

29 **30a**

29 (50 mg, 0.23 mmol, 1 eq) was dissolved in dry DCM (2.5 mL). Triethylamine (49 µL, 0.35 mmol, 1.5 eq) was added and the mixture was cooled in ice bath. TFAA (49 µL, 0.35 mmol, 1.5 eq) dissolved in dry DCM (0.5 mL) was slowly added and the reaction was stirred at room temperature for 2 hours. After 2 hours, reaction was diluted with DCM (5mL) and the solution was washed with 10% K_2CO_3 (3x 5 mL) and 10% HCl (1x 5 mL), dried with MgSO4 and evaporated. The residue was purified by column chromatography (hexane:EtOAc 4:1) to yield 40 mg (56%) of product as oil.**^{1}H NMR** (400 MHz, $CDCl_3$) δ 8.40 (s, 1H), 8.11 – 8.06 (m, 1H), 7.22 (dt, *J* = 6.3, 3.2 Hz, 3H), 7.19 – 7.12 (m, 3H), 6.86 (td, *J* = 7.4, 1.0 Hz, 2H), 6.64 – 6.59 (m, 1H), 4.80 (s, 2H).

***N*-(2-((2-(((tert-butyldiphenylsilyl)oxy)methyl)phenyl)amino)phenyl)-2,2,2-trifluoroacetamide (30b)**

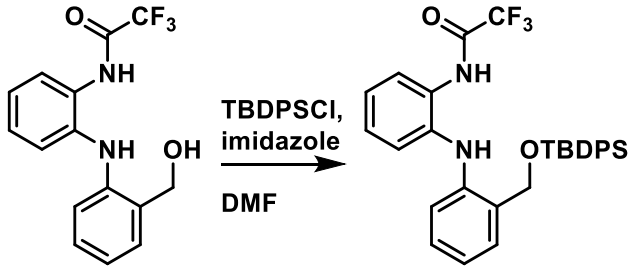

30a **30b**

30a (184 mg, 0.6 mmol, 1eq) was dissolved in dry DMF (6 mL). Imidazole (98 mg, 1.44 mmol, 2.4 eq) was added followed by TBDPSCl (182 µL, 0.71 mmol, 1.2 eq). Reaction was stirred at room temperature for 4 hours After 4 hours, reaction was diluted with water (20 mL) and extracted into ethylacetate (3x 20 mL). Combined organic extracts were washed with 10% HCl (2x 20 mL), 10% aq. K_2CO_3 (2x 20 mL) and brine. Organic extracts were dried with $MgSO_4$ and evaporated. The residue was purified bycolumn chromatography (Hex:EtoAc 350:15) to yield 157 mg of the product (50%). **^{1}H NMR** (400 MHz, $CDCl_3$) δ 10.57 (s, 1H), 7.63 (d, *J* = 6.8 Hz, 4H), 7.53 (d, *J* = 7.5 Hz, 1H), 7.43 (dq, *J* = 14.3, 7.1 Hz, 6H), 7.25 (d, *J* = 7.8 Hz, 1H), 7.17 (t, *J* = 7.5 Hz, 1H), 7.12 (t, *J* = 7.7 Hz, 1H), 7.06 (t, *J* = 7.4 Hz, 1H), 6.91 (t, *J* = 7.6 Hz, 1H), 6.82 (q, *J* = 8.1 Hz, 3H), 4.81 (s, 2H), 1.02 (s, 9H). **^{13}C NMR {^{1}H}** (101 MHz, $CDCl_3$) δ 155.17 (q, J = 36.4 Hz), 139.9, 139.5, 135.0, 132.9, 132.0, 129.9, 128.0, 127.9, 127.5, 127.2, 126.5, 124.6, 122.1, 120.6, 119.9, 119.3, 115.88 (d, J = 288.9 Hz), 62.1, 26.7, 18.9.

Cyclization to 31a

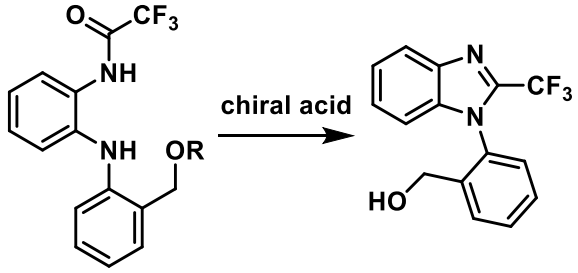

30a **31a**

30a (135 mg, 0.45 mmol, 1eq) was dissolved in toluene (6 mL) and this solution was separated into 6 reaction vials. To each vial, catalytical amount of the acid was added and the reaction was heated to 65°C for 24 hours. After 24 hours, the reaction was cooled to room temperature, washed with K_2CO_3 (1x 1.5 mL), brine, died with MgSO4 and evaporated. **^{1}H NMR** (400 MHz, $CDCl_3$) δ 7.95 (d, *J* = 8.1 Hz, 1H), 7.78 (d, *J* = 7.3 Hz, 1H), 7.67 – 7.62 (m, 2H), 7.53 – 7.48 (m, 2H), 7.44 – 7.35 (m, 6H), 7.33 (d, *J* = 7.9 Hz, 2H), 7.02 (d, *J* = 7.4 Hz, 2H), 4.33 (q, *J* = 13.7 Hz, 2H).

Entry	acid	Solvent + temperature	results
1	L-dibenzoyltartaric acid	Toluene 65°C	No reaction
2	L-dianysoyltartaric acid	Toluene 65°C	No reaction
3	L-ditoluolyltartaric acid	Toluene 65°C	No reaction
4	(*S*)-TRIP	Toluene 65°C	Er. 73/27
5	10-CSA	Toluene 65°C	Er. 32/68*
6	(*S*)-TRIP	Toluene 85°C	decomposition

* overlapping peaks allowed only approximate integration.

***N*1-(2-(((tert-butyldiphenylsilyl)oxy)methyl)phenyl)benzene-1,2-diamine (32)**

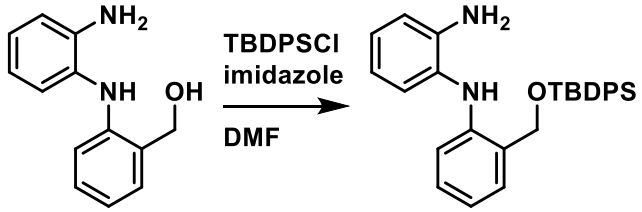

29 **32**

29 (241 mg, 1 mmol, 1eq) was dissolved in dry DMF (5 mL) and imidazole (163 mg, 2.4 mmol, 2,4 eq) was added followed by TBDPSCl (308 µL, 1.2 mmol, 1.2 eq). Reaction was stirred at room temperature for 18 hours. Afterwards, water (20 mL) was added and the solution was extracted with EtOAc (3x 20 mL). Organic extracts were combined and washed with 10% aq. HCl (2x 20 mL) and 10% aq K_2CO_3 (2x 20 mL), brine and dried with $MgSO_4$ and evaporated. The residue was purified by column chromatography (Hexane:EtOAc 20:1) to isolate 350 mg of product (75%) **^{1}H NMR** (400 MHz, $CDCl_3$) δ 7.73 – 7.63 (m, 5H), 7.51 – 7.35 (m, 8H), 7.09 – 7.03 (m, 1H), 6.81 (ddd, *J* = 17.9, 8.0, 1.1 Hz, 3H), 6.71 (dd, *J* = 7.9, 1.3 Hz, 1H), 6.55 – 6.45 (m, 2H), 6.42 (s, 1H), 4.86 (s, 2H), 4.62 (s, 2H), 1.05 (s, 9H). **^{13}C NMR {^{1}H}** (101 MHz, $CDCl_3$) δ 142.6, 142.4, 136.4, 135.0, 134.5, 133.0, 129.9, 129.2, 127.9, 127.8, 127.6, 127.5, 126.4, 124.3, 123.7, 118.7, 116.7, 115.1, 114.9, 62.8, 26.7, 18.9.

2-(((tert-butyldiphenylsilyl)oxy)methyl)aniline (34)

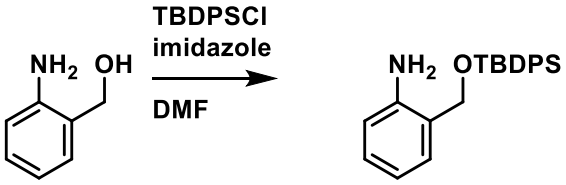

34

2-hydroxymethylaniline (123 mg, 1 mmol, 1 eq) was dissolved in dry DMF. Imidazole (163 mg, 2.5 mmol, 2.4 qe) was added followed by TBDPSCl (308 µL, 1.2 mmol, 1.2 eq). Reaction was stirred at room temperature for 18 hours. Afterwards, water (20 mL) was added and the solution was extracted with EtOAc (3x 20 mL). Organic extracts were combined and washed with sat. aq. NH_4Cl (2x 20 mL) and brine and dried with $MgSO_4$ and evaporated to yield 270 mg of oil (75%) **^{1}H NMR** (400 MHz, $CDCl_3$) δ 7.65 (d, *J* = 7.1 Hz, 4H), 7.52 – 7.35 (m, 7H), 7.14 (d, *J* = 7.5 Hz, 1H), 6.98 (t, *J* = 7.6 Hz, 1H), 6.65 (d, *J* = 7.8 Hz, 1H), 6.57 (t, *J* = 7.3 Hz, 1H), 4.87 (s, 2H), 4.66 (s, 2H), 1.03 (s, 9H). **^{13}C NMR {^{1}H}** (101 MHz, $CDCl_3$) δ 145.6, 135.0, 134.5, 133.0, 129.9, 127.9, 127.6, 127.5, 126.3, 123.8, 116.0, 114.7, 63.2, 26.7, 18.9.

2,2,2-trifluoro-*N*-(2-iodophenyl)acetamide (37)

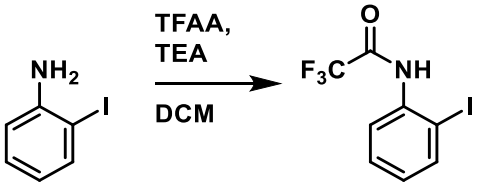

37

2-iodoaniline (219 mg, 1 mmol, 1 eq) and triethylamine (193 µL, 1.5 mmol , 1.5 eq) were dissolved in dry DCM (4 mL) and the solution was cooled in ice bath. TFAA (168 µL, 1.2 mmol, 1.2 eq) was added dropwise and the reaction was stirred for 16 hours at room temperature. After 16 hours, TLC (hexane: EtOAc 5:1) revelaed unreacted starting material. TEA (193 µL, 1.5 mmol , 1.5 eq) and TFAA (140 µL, 1 mmol, 1 eq) were subsequently added and the reaction was stirred at room temperature for 4 hours. After 4 hurs, the reaction was diluted with DCM (10 mL) and washed with 10% aq. K_2CO_3 (3x 15 mL) 10% HCl (3x 15 mL). The organic layer was dried with MgSO4 and evaporated to yield 155 mg (50%) **^{1}H NMR** (400 MHz, DMSO-d_6) δ 11.24 (s, 1H), 7.96 (dd, *J* = 7.9, 1.4 Hz, 1H), 7.48 (td, *J* = 7.6, 1.5 Hz, 1H), 7.38 (dd, *J* = 7.9, 1.7 Hz, 1H), 7.15 (td, *J* = 7.6, 1.7 Hz, 1H).

Coupling leading to (30a)

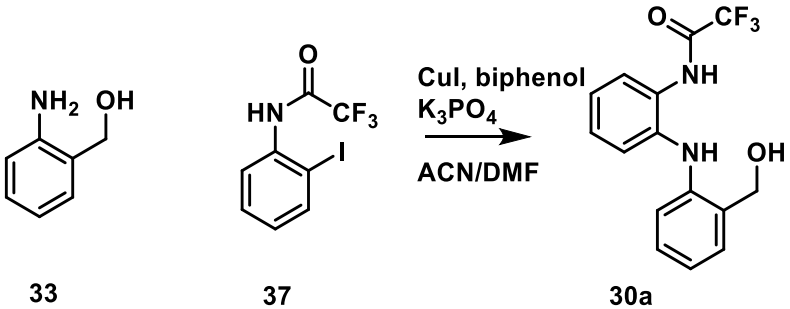

33 **37** **30a**

5 mL flame dried schlenk tube with teflon coated stirrbar was charged with **33 (**70 mg, 0.22 mmol, 1eq), biphenol (3.72 mg, 0.01 mmol, 0.1 eq) and K_3PO_4 (102 mg, 0.22 mmol, 2.2 eq). The schlenk tube was evacuated and backfilled with argon three times. Separate flask was charged with **37** (54 mg, 0.44 mmol, 2 eq) and evacuated and backfilled with argon three times. Dry acetonitrile (dried over activated mol. Sieves for 3 days, 500 µL) and dry DMF (1 mL) were added and the subsequent cloudy solution was added to the schlenk flask containing compound **33**. Reaction was heated to 65 °C for 18 hours. After 18 hours, reaction was cooled to room temperature, diluted with EtOAc (10 mL) and washed with sat.

aq. $NaHCO_3$ (3x 10 mL), 10% HCl (3x 10 mL) and brine. The organic layer was evaporated and purified by column chromatography (Hexane: EtOAc 5:1) to yield 15 mg of the product (25%).

Coupling leading to and (30b)

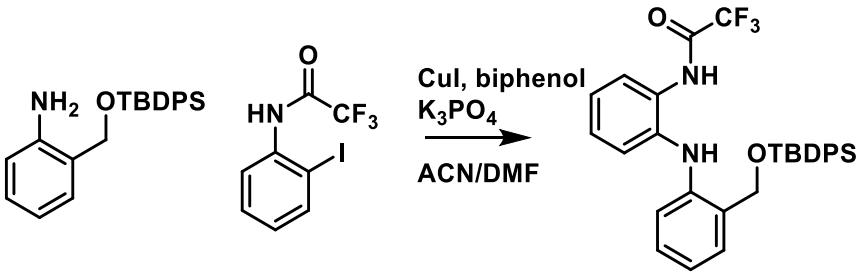

34 **37** **30b**

5 mL flame dried schlenk tube with teflon coated stirrbar was charged with **34 (**31mg, 0.1 mmol, 1eq), biphenol (1.86 mg, 0.01 mmol, 0.1 eq) and K_3PO_4 (47 mg, 0.22 mmol, 2.2 eq). The schlenk tube was evacuated and backfilled with argon three times. Separate flask was charged with **37** (72mg, 0.2 mmol, 2 eq) and evacuated and backfilled with argon three times. Dry acetonitrile (dried over activated mol. Sieves for 3 days, 500 µL) and dry DMF (1 mL) were added and the subsequent cloudy solution was added to the shclenk flask containing compound **34**. Reaction was heated to 65°C for 18 hours. Neither TLC or HPLC analysis showed any conversion of starting material.

2,5-dioxopyrrolidin-1-yl 2-(2-(trifluoromethyl)-1H-benzo[d]imidazol-1-yl)benzoate (38)

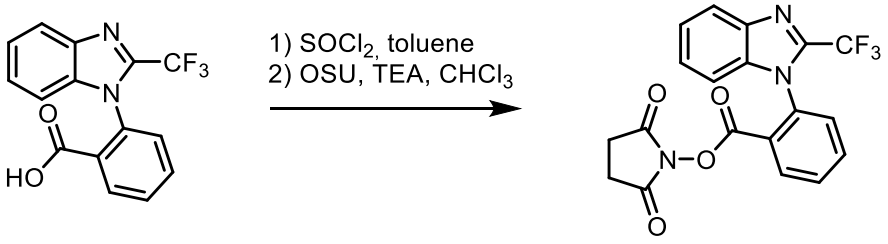

1 **38**

1 (1 g, 3.26 mmol, 1 eq) was dissolved in toluene (45 mL) and $SOCl_2$ (1.22 mL, 16.8 mmol, 5 eq) was added. This mixture was refluxed until the acid was not fully dissolved. Afterwards, the reaction mixture was evaporated, dissolved in $CHCl_3$ and evaporated again. The residue was dissolved in dry DCM (10 mL) and was added slowly into the suspension of N-hydroxysuccinimide (375 mg, 3.58 mmol, 1.1 eq) and trimethylamine (450 µL, 3.58 mmol, 1.1 eq) in dry DCM (10 mL). After the addition was complete, the reaction was stirred at room temperature for 18 hours. After 18 hours, the reaction was extracted with water (3x 20 mL), dried with MgSO4 and evaporated to yield 1.26 g (95%). **^{1}H NMR** (400 MHz, $CDCl_3$) δ 8.40 (dd, *J* = 7.9, 1.5 Hz, 1H), 7.91 (dddd, *J* = 7.8, 6.0, 3.1, 1.4 Hz, 2H), 7.79 (td, *J* = 7.8, 1.3 Hz, 1H), 7.58 (d, *J* = 7.8 Hz, 1H), 7.42 – 7.35 (m, 2H), 7.03 – 6.98 (m, 1H), 2.69 (s, 4H). **^{13}C NMR** (101 MHz, $CDCl_3$) δ 168.5, 159.0, 140.8, 140.8 (q, J = 38.6 Hz) 137.3, 135.7, 135.3, 132.9, 131.0, 130.9, 126.3, 124.2, 121.5, 118.80 (q, J = 272.2 Hz), 110.8, 25.5. **^{19}F NMR** (376 MHz, $CDCl_3$) δ -61.3.

General procedure for TBBA-amide formation

(*P*)-(*R*)-*N*-(1-Phenylethyl)-2-(2-(trifluoromethyl)-1*H*-benzo[*d*]imidazol-1-yl)benzamide (*M*)-39

(*P*)-1-Carboxyphenyl(2-trifluoromethy)benzimidazole **(*P*)-1** (40 mg, 0.13 mmol, 1 eq) was dissolved in DMF (0.8 mL). EDCl (51 mg, 0.26 mmol, 2 eq) and then HOBt (40 mg, 0.26 mmol, 2 eq) were subsequently added into the solution. Afterwards, (*R*)-(+)-1-Phenylethylamine (18.2 µL, 0.143 mmol, 1.1 eq) was added into the mixture and the reaction was stirred at room temperature (23-25°C) until a complete conversion of the starting material was detected by HPLC analysis (90-120 min). After completion, the reaction was diluted with 4 ml of EtOAc forming a cloudy white solution, which was

extracted with 10% HCl (2x 4ml), sat. $NaHCO_3$ (2x 4 ml), and brine (4 ml). The organic layer was dried over Na_2SO_4 and evaporated to give 24 mg of a white solid (47%). **^{1}H NMR** (400 MHz, $CDCl_3$) δ 7.83 – 7.78 (m, 1H), 7.67 – 7.60 (m, 2H), 7.39 (ddd, *J* = 15.5, 10.2, 6.3 Hz, 3H), 7.26 – 7.19 (m, 3H), 7.09 (d, *J* = 7.7 Hz, 1H), 7.00 – 6.95 (m, 2H), 5.59 (d, *J* = 7.4 Hz, 1H), 4.84 (p, *J* = 7.0 Hz, 1H), 0.92 (d, *J* = 6.8 Hz, 3H). **^{13}C{^{1}H} NMR** (101 MHz, $CDCl_3$) δ 164.4, 142.1, 140.6, 137.5, 135.3, 131.7, 131.5, 130.8, 129.9, 129.5, 128.8, 127.7, 126.5, 126.05, 124.5, 121.7, 119.0 (q, *J* = 272.0 Hz), 49.4, 20.7 **^{19}F NMR** (376 MHz, $CDCl_3$) δ -61.21 **^{15}N NMR** (50.664 MHz, $CDCl_3$): δ -128.8, -226.4, -247.3 (^{1}J=89.5 Hz) **HRMS** (ESI) m/z: $[M+H]^+$ calculated for $C_{23}H_{19}ON_3F_3$: 410.1475, found: 410.1472, $[\alpha]_D^{22}$ = -21.89° (c= 0.50, MeOH).

(*M*)-(*R*)-*N*-(1-Phenylethyl)-2-(2-(trifluoromethyl)-1*H*-benzo[*d*]imidazol-1-yl)benzamide (*M*)-39, From 40 mg of **(*M*)-1** and R-(+)-1-Phenylethylamine, 43 mg of a white solid (81%). **^{1}H NMR** (400 MHz, $CDCl_3$) δ 7.96 (d, *J* = 8.1 Hz, 1H), 7.91 – 7.86 (m, 1H), 7.70 – 7.62 (m, 2H), 7.47 – 7.34 (m, 3H), 7.19 – 7.10 (m, 3H), 7.06 (d, *J* = 8.2 Hz, 1H), 6.73 – 6.69 (m, 2H), 5.48 (d, *J* = 7.0 Hz, 1H), 4.86 (p, *J* = 7.0 Hz, 1H), 1.12 (d, *J* = 6.8 Hz, 3H). **^{13}C{^{1}H} NMR** (101 MHz, $CDCl_3$) δ 164.3, 141.9, 140.7, 137.5, 135.3, 131.8, 131.3, 130.9, 130.2, 129.5, 128.7, 127.55, 126.5, 125.8, 124.5, 122.0, 118.8 (q, *J* = 272.3 Hz), 111.1, 49.5, 21.1 **^{19}F NMR** (376 MHz, $CDCl_3$) δ -61.49 **^{15}N NMR** (50.664 MHz, $CDCl_3$): δ -129.5, -226.2, -247.4 (^{1}J=89.1 Hz) **HRMS** (ESI) m/z: $[M+H]^+$ calculated for $C_{23}H_{19}ON_3F_3$: 410.1475, found: 410.1475, $[\alpha]_D^{22}$ = +159.59° (c= 0.73, MeOH).

***(P)*-(S)-N-(1-phenylethyl)-2-(2-(trifluoromethyl)-1H-benzo[d]imidazol-1-yl)benzamide (*P*)-40** From 40 mg of *1-P* and S-(-)-1-Phenylethylamine, 25 mg of white solid (47%). **^{1}H NMR** (400 MHz, $CDCl_3$) δ 7.96 (d, *J* = 8.2 Hz, 1H), 7.90 – 7.85 (m, 1H), 7.68 – 7.62 (m, 2H), 7.41 (ddt, *J* = 20.8, 16.0, 4.0 Hz, 3H), 7.19 – 7.09 (m, 3H), 7.06 (d, *J* = 8.2 Hz, 1H), 6.71 (dd, *J* = 7.7, 1.8 Hz, 2H), 5.52 (d, *J* = 7.0 Hz, 1H), 4.85 (p, *J* = 7.0 Hz, 1H), 1.12 (d, *J* = 6.8 Hz, 3H). **^{13}C NMR** (101 MHz, $CDCl_3$) δ 164.2 (s), 141.9 (s), 141.1 (s), 140.7 (s), 137.5 (s), 135.4 (s), 131.8 (s), 131.4 (s), 130.9 (s), 130.2 (s), 129.5 (s), 128.8 (s), 127.6 (s), 126.55 (s), 125.8 (s), 124.5 (s), 121.9 (s), 118.9 (q, *J* = 271.7 Hz), 111.1 (s), 49.5 (s), 21.1 (s). **^{19}F NMR** (376 MHz, $CDCl_3$) δ -61.49 (s). **HRMS** (ESI) $[M+H]^+$ calculated for $C_{23}H_{18}ON_3F_3$+H: 410.1475, found: 410.1473, $[\alpha]_D^{22}$ = -157.10° (c= 0.92, MeOH).

***(M)*-(S)-N-(1-phenylethyl)-2-(2-(trifluoromethyl)-1H-benzo[d]imidazol-1-yl)benzamide (*M*)-40** From 40 mg of *1-M* and S-(-)-1-Phenylethylamine, 38 mg of white solid (70%) **^{1}H NMR** (400 MHz, $CDCl_3$) δ 7.94 (dd, *J* = 7.0, 1.5 Hz, 1H), 7.85 – 7.80 (m, 1H), 7.68 – 7.63 (m, 2H), 7.45 – 7.36 (m, 3H), 7.26 – 7.20 (m, 3H), 7.10 (dd, *J* = 7.1, 1.5 Hz, 1H), 6.99 (dd, *J* = 7.5, 1.7 Hz, 2H), 5.58 (d, *J* = 7.4 Hz, 1H), 4.85 (p, *J* = 7.0 Hz, 1H), 0.93 (d, *J* = 6.8 Hz, 3H). **^{13}C NMR** (101 MHz, $CDCl_3$) δ 164.5 (s), 142.05 (s), 140.5 (s), 137.5 (s), 135.3 (s), 131.7 (s), 131.5 (s), 130.8 (s), 129.8 (s), 129.5 (s), 128.8 (s), 127.7 (s), 126.5 (s), 126.0 (s), 124.5 (s), 121.65 (s), 119.0 (q, *J* = 272.5 Hz), 111.4 (s), 49.4 (s), 20.7 (s). **^{19}F NMR** (376 MHz, $CDCl_3$) δ -61.20 (s). **HRMS** (ESI) $[M+H]^+$ calculated for $C_{23}H_{18}ON_3F_3$+H: 410.1475, found: 410.1478, $[\alpha]_D^{22}$ = +19.76° (c= 0.49, MeOH).

(*P*)-(*R*)-N-(1-(naphthalen-1-yl)ethyl)-2-(2-(trifluoromethyl)-1H-benzo[d]imidazol-1-yl)benzamide (*P*)-41 From 15 mg of **(*P*)-1** and (*R*)-(+)-1-(1-Naphthyl)ethylamine, 17 mg of oil (74%). Purified by column chromatography (hexane:ethylacetate 3:1, column dimesions 1x10 cm). **^{1}H NMR** (500 MHz, $CDCl_3$) δ (ppm) = 7.90 (d, *J* = 7.5 Hz, 1H), 7.84 (d, *J* = 7.6 Hz, 1H), 7.75 (dd, *J* = 12.6, 5.3 Hz, 1H), 7.61 (pd, *J* = 7.4, 1.4 Hz, 1H), 7.51 – 7.43 (m, 1H), 7.38 (dt, *J* = 15.5, 7.3 Hz, 1H), 7.20 (d, *J* = 7.1 Hz, 1H), 7.11 (d, *J* = 7.6 Hz, 1H), 5.76 – 5.65 (m, 1H), 1.16 (d, *J* = 6.5 Hz, 1H). **^{13}C{1H} NMR** (126 MHz, $CDCl_3$) δ (ppm) = 164.4, 140.6, 140.6 (app.d, *J* = 38.2 Hz), 137.7, 137.4, 135.6, 134.0, 131.7, 131.0, 130.8, 129.7, 128.9, 128.7, 126.8, 126.4, 126.0, 125.3, 124.4, 123.1, 122.6, 121.7, 119.0 (q, *J* =, 272.0 Hz), 111.5, 45.1, 19.9. **^{19}F NMR** (376 MHz, $CDCl_3$) δ (ppm) = -61.19. **HRMS** (ESI) m/z: $[M+H]^+$ calculated for $C_{27}H_{21}F_3N_3O$: 460.1637 found: 460.1632, $[\alpha]_D^{22}$ −95.00° (c= 0.1 $CHCl_3$).

(*M*)-(*R*)-N-(1-(naphthalen-1-yl)ethyl)-2-(2-(trifluoromethyl)-1H-benzo[d]imidazol-1-yl)benzamide (*M*)-41

From 15 mg of **(*M*)-2** and (*R*)-(+)-1-(1-Naphthyl)ethylamine, 15.5 mg of oil (68%). Purified by column chromatography (hexane: ethylacetate 3:1, column dimesions 1x10 cm). **^{1}H NMR** (500 MHz, $CDCl_3$) δ (ppm) = 7.88 (d, *J* = 8.2 Hz, 1H), 7.86 – 7.81 (m, 1H), 7.80 (d, *J* = 7.9 Hz, 1H), 7.71 (d, *J* = 8.2 Hz, 1H), 7.65 – 7.59 (m, 1H), 7.47 – 7.43 (m, 1H), 7.43 – 7.40 (m, 1H), 7.39 (dd, *J* = 5.9, 3.2 Hz, 1H), 7.37 – 7.33 (m, 1H), 7.27 (dd, *J* = 7.0, 1.0 Hz, 1H), 7.24 (d, *J* = 7.1 Hz, 1H), 6.98 (d, *J* = 8.2 Hz, 1H), 6.86 (d, *J* = 7.1 Hz, 1H), 5.72 (p, *J* = 6.8 Hz, 1H), 5.58 (d, *J* = 7.8 Hz, 1H), 1.26 (d, *J* = 6.7 Hz, 1H). **^{13}C{1H} NMR** (126 MHz, $CDCl_3$) δ (ppm) = 164.1 (s), 141.1 (d, *J* = 38.6 Hz), 140.7, 137.5, 137.40, 135.3, 133.9, 131.8, 131.62, 130.9 , 130.7, 130.0, 129.7, 128.8, 128.5, 126.7, 126.3, 126.0, 125.2, 124.4, 123.0, 122.2, 121.8, 119.0 (q), 110.9, 44.9, 20.3. **^{19}F NMR** (376 MHz, $CDCl_3$) δ (ppm) = -61.54. **HRMS** (ESI) m/z: $[M+H]^+$ calculated for $C_{27}H_{21}F_3N_3O$: 460.1637 found: 460.1632, $[\alpha]_D^{22}$ +68.00° (c= 0.1 $CHCl_3$).

(*P*)-(*S*)-N-(3,3-dimethylbutan-2-yl)-2-(2-(trifluoromethyl)-1H-benzo[d]imidazol-1-yl)benzamide (*P*)-42

From 15 mg of **(*P*)-1** and (*S*)-(+)-3,3-dimethyl-2-butylamine, 16.2 mg of oil (83%). Purified by column chromatography (hexane: ethylacetate 4:1, column dimesions 1x10 cm). **^{1}H NMR** (500 MHz, $CDCl_3$) δ(ppm) = 7.96 – 7.93 (m, 1H), 7.91 (dd, *J* = 7.6, 1.7 Hz, 1H), 7.71 – 7.63 (m, 2H), 7.44 – 7.38 (m, 3H), 7.14 – 7.10 (m, 1H), 5.16 (d, *J* = 9.2 Hz, 1H), 3.69 (dq, *J* = 9.5, 6.8 Hz, 1H), 0.70 (d, *J* = 6.8 Hz, 3H), 0.48 (s, 9H). **^{13}C{1H}** (126 MHz, $CDCl_3$) δ 164.7, 141.05 (q, *J* = 39.4 Hz), 140.85, 137.5, 135.9, 131.6, 131.1, 131.0, 130.4 129.6, 126.6, 124.7, 122.0, 118.94 (q, *J* = 272.1 Hz), 111.2, 53.6, 33.6, 25.7, 15.7, **^{19}F NMR** (376 MHz, $CDCl_3$) δ (ppm) = -61.42, **HRMS** (ESI) m/z: $[M+H]^+$ calculated for $C_{21}H_{23}F_3N_3O$: 390.1793 found: 390.1788, $[\alpha]_D^{22}$ -80.00° (c= 0.1 $CHCl_3$).

(*M*)-(*S*)-N-(3,3-dimethylbutan-2-yl)-2-(2-(trifluoromethyl)-1H-benzo[d]imidazol-1-yl)benzamide (*M*)-42

Using method B, from 15 mg of **(*M*)-1** and (*S*)-(+)-3,3-dimethyl-2-butylamine, 14,6 mg of oil (75 %). Purified by column chromatography (hexane: ethylacetate 4:1, column dimesions 1x10 cm). **^{1}H NMR** (500 MHz, $CDCl_3$) δ 7.94 – 7.90 (m, 1H), 7.88 – 7.85 (m, 1H), 7.67 (pd, *J* = 7.5, 1.7 Hz, 2H), 7.43 – 7.37 (m, 4H), 7.14 – 7.10 (m, 1H), 5.21 (d, *J* = 9.2 Hz, 1H), 3.65 (dq, *J* = 9.6, 6.8 Hz, 1H), 0.66 (s, 9H), 0.42 (d, *J* = 6.8 Hz, 3H). **^{13}C{1H} NMR** (126 MHz, $CDCl_3$) δ 164.9, 140.7, 140.5 (q, *J* = 38.4 Hz), 137.6, 135.9, 131.6, 131.2, 130.9, 130.00, 129.6, 126.6, 124.6, 121.7, 119.1 (q, *J* = 271.7 Hz), 111.6, 53.5, 33.8, 25.9, 15.1 **^{19}F NMR** (376 MHz, $CDCl_3$) δ (ppm) = -61.06. **HRMS** (ESI) m/z: $[M+H]^+$ calculated for $C_{21}H_{23}F_3N_3O$: 390.1793 found: 390.1790, $[\alpha]_D^{22}$ = +155.56° (c= 0.09 $CHCl_3$).

(*P*)-(*S*)-*N*-(1-Cyklohexylethyl)-2-(2-(trifluoromethyl)-1*H*-benzo[*d*]imidazol-1-yl)benzamide (*P*)-43

From 20 mg **(P)-1**, (*S*)-1-cyklohexylethanamine (7,5 µl; 0,05 mmol; 0,8 ekv) purified by column chromatography (Hex/EtOAc 3:1) 17 mg of yellow oild (81%).**^{1}H NMR** (500 MHz, $CDCl_3$) δ (ppm) = 7.96 – 7.93 (m, 1H), 7.91 – 7.89 (m, 1H), 7.70 – 7.61 (m, 2H), 7.44 – 7.37 (m, 3H), 7.13 – 7.11 (m, 1H), 5.16 (d, *J* = 8.2 Hz, 1H), 3.70 – 3.64 (m, 1H), 1.55 – 1.47 (m, 3H), 1.18 (dd, *J* = 12.8, 1.8 Hz, 1H), 1.10 (dd, *J* = 12.7, 1.9 Hz, 1H), 0.98 – 0.78 (m, 5H), 0.77 (d, *J* = 6.8 Hz, 3H), 0.52 – 0.43 (m, 1H), 0.37 (dt, *J* = 12.2, 7.8 Hz, 1H). **^{13}C NMR** (126 MHz, $CDCl_3$) δ (ppm) = 164.6, 140.9 (app. d, *J* = 38.0 Hz), 140.8, 137.5, 135.8, 131.6, 131.1, 130.9, 130.4, 129.5, 126.6, 124.6, 121.9, 119.0 (app. d, *J* = 272.2 Hz), 111.4, 50.0, 42.6, 28.6, 28.3, 26.2, 26.1, 26.1, 17.4. **HRMS** (ESI) m/z calc for $C_{23}H_{25}F_3N_3O$ $[M^+H]^+$ 416.1950, found 416.1945. $[\propto]_d^{22}$: -120.00° (c = 0,13 MeOH).

(*M*)-(*S*)-*N*-(1-Cyklohexylethyl)-2-(2-(trifluoromethyl)-1*H*-benzo[*d*]imidazol-1-yl)benzamide (*M*)-43

From 20 mg **(P)-1**, (*S*)-1-cyklohexylethanamine (7,5 µl; 0,05 mmol; 0,8 ekv) purified by column chromatography (Hex/EtOAc 3:1) 15 mg of yellow oild (72%).**^{1}H NMR** (500 MHz, $CDCl_3$) δ (ppm) = 7.94 – 7.92 (m, 1H), 7.86 – 7.84 (m, 1H), 7.69 – 7.62 (m, 2H), 7.43 – 7.38 (m, 3H), 7.12 – 7.09 (m, 1H), 5.21 (d, *J* = 8.6 Hz, 1H), 3.71 – 3.64 (m, 1H), 1.65 – 1.54 (m, 3H), 1.45 – 1.38 (m, 1H), 1.34 – 1.30 (m, 1H), 1.08 – 0.97 (m, 4H), 0.78 – 0.70 (m, 1H), 0.60 (ddd, *J* = 14.8, 11.8, 5.2 Hz, 1H), 0.54 (d, *J* =

6.7 Hz, 3H). **^{13}C NMR** (126 MHz, $CDCl_3$) δ (ppm) =164.8, 140.7, 140.7 (q, *J* = 38.5 Hz), 135.9, 131.5, 131.4, 130.9, 130.0, 129.6, 126.5, 124.5, 121.7, 119.0 (q, *J* = 272.0 Hz), 111.4, 49.9, 42.8, 28.9, 28.6, 26.3, 26.1, 26.1, 17.0. **HRMS** (ESI) m/z calc. for $C_{23}H_{25}F_3N_3O$ $[M^+H]^+$ 416.1950, found 416.1944. $[\propto]_d^{22}$: +41.67° (c = 0,12 MeOH).

(*P*)-(*S*)-*N*-(2-Hydroxy-1-phenylethyl)-2-(2-(trifluoromethyl)-1*H*-benzo[*d*]imidazol-1-yl)benzamide (*P*)-44

From 40 mg of **(*P*)-1** and (*S*)-(+)-2-Phenylglycinol, 41 mg of oil (74%). **^{1}H NMR** (400 MHz, $CDCl_3$) δ 7.93 – 7.85 (m, 2H), 7.70 – 7.64 (m, 2H), 7.41 (dddd, *J* = 13.4, 8.6, 6.1, 2.8 Hz, 3H), 7.25 – 7.20 (m, 3H), 7.12 (dd, *J* = 6.9, 1.8 Hz, 1H), 6.23 (d, *J* = 7.1 Hz, 1H), 4.79 (dt, *J* = 7.3, 4.6 Hz, 1H), 3.48 – 3.39 (m, 1H), 3.27 (dd, *J* = 11.0, 4.1 Hz, 1H). **^{13}C{^{1}H} NMR** (101 MHz, $CDCl_3$) δ 165.5, 140.9 (q, *J* = 38.1 Hz), 140.6, 138.4, 137.4, 134.9, 131.9, 131.6, 130.9, 130.0, 129.6, 128.5, 128.0, 126.5, 124.5, 121.65, 119.0 (q, *J* = 272.2 Hz), 111.4, 65.6, 55.6 **^{19}F NMR** (376 MHz, $CDCl_3$) δ -61.29 **HRMS** (ESI) m/z: $[M+H]^+$ calculated for $C_{23}H_{19}O_2N_3F_3$: 426.1424, found: 426.1423, $[\alpha]_D^{24}$ = -32.50° (c= 0.76, MeOH).

(*M*)-(*S*)-*N*-(2-Hydroxy-1-phenylethyl)-2-(2-(trifluoromethyl)-1*H*-benzo[*d*]imidazol-1-yl)benzamide (*M*)-44

From 40 mg of **(*M*)-1** and (*S*)-(+)-2-Phenylglycinol, 39 mg of oil (70%). **^{1}H NMR** (400 MHz, $CDCl_3$) δ 7.91 (td, *J* = 8.3, 1.1 Hz, 2H), 7.70 – 7.63 (m, 2H), 7.45 – 7.39 (m, 2H), 7.36 (dt, 1H), 7.18 – 7.11 (m, 1H), 7.07 (d, *J* = 8.1 Hz, 2H), 6.71 (dd, *J* = 7.8, 1.5 Hz, 2H), 6.12 (d, *J* = 6.9 Hz, 1H), 4.79 (dt, *J* = 6.9, 5.0 Hz, 1H), 3.55 (dd, *J* = 5.4, 11.2 Hz, 1H), 3.51 (dd, *J* = 4.6, 11.2 Hz, 1H). **^{13}C{^{1}H} NMR** (101 MHz, $CDCl_3$) δ 165.4, 141.0 (q, *J* = 38.7 Hz), 140.8, 140.8, 138.1, 137.4, 134.8, 132.0, 131.55, 130.95, 130.3, 129.6, 128.9, 127.9, 126.5, 126.4, 124.5, 121.8, 119.5 (q, *J* = 272.7 Hz), 111.2, 65.8, 55.95 **^{19}F NMR** (376 MHz, $CDCl_3$) δ -61.36 **HRMS** (ESI) m/z: $[M+H]^+$ calculated for $C_{23}H_{19}O_2N_3F_3$: 426.1424, found: 426.1423, $[\alpha]_D^{25}$ = +130.50° (c= 0.8 MeOH).

***(P)*-(R)-N-(2-hydroxy-1-phenylethyl)-2-(2-(trifluoromethyl)-1H-benzo[d]imidazol-1-yl)benzamide (P)-45**:

From 40 mg of *(P)-1* and (R)-(+)-2-Phenylglycinol, 46 mg of white foam (83%). **^{1}H NMR** (500 MHz, $CDCl_3$) δ 7.96 – 7.91 (m, 1H), 7.71 – 7.66 (m, 1H), 7.46 – 7.41 (m, 1H), 7.37 (t, *J* = 7.7 Hz, 1H), 7.21 – 7.13 (m, 2H), 7.08 (d, *J* = 8.1 Hz, 1H), 6.73 – 6.69 (m, 1H), 6.06 (d, *J* = 6.8 Hz, 1H), 4.83 – 4.79 (m, 1H), 3.55 (qd, *J* = 11.2, 4.9 Hz, 1H). **^{13}C NMR** (126 MHz, $CDCl_3$) δ 165.46 (s), 141.0 (q, *J* = 38.5 Hz), 140.8 – 140.76 (m), 138.05 (s), 137.4 (s), 134.8 (s), 132.1 (s), 131.5 (s), 131.0 (s), 130.3 (s), 129.6 (s), 128.9 (s), 128.0 (s), 126.5 (s), 126.4 (s), 124.6 (s), 121.9 (s), 118.9 (q, *J* = 271.9 Hz), 111.2 (s), 65.9 (s), 56.0 (s). **^{19}F NMR** (471 MHz, $CDCl_3$) δ -61.36 (s). **HRMS** (ESI) $[M+H]^+$ calculated for $C_{23}H_{18}O_2N_3F_3$+H: 426.1424, found: 426.1427, $[\alpha]_D^{25}$ = -138.50° (c= 0.12 MeOH).

***(M)*-(R)-N-(2-hydroxy-1-phenylethyl)-2-(2-(trifluoromethyl)-1H-benzo[d]imidazol-1-yl)benzamide (M)-45**

From 40 mg of *(M)-1* and (R)-(+)-2-Phenylglycinol, 38 mg of white foam (70%). **^{1}H NMR** (500 MHz, $CDCl_3$) δ 7.90 (d, *J* = 7.5 Hz, 1H), 7.89 – 7.86 (m, 1H), 7.70 – 7.65 (m, 2H), 7.46 – 7.36 (m, 3H), 7.25 – 7.20 (m, 3H), 7.12 (d, *J* = 7.3 Hz, 1H), 6.98 – 6.94 (m, 2H), 6.25 (d, *J* = 7.2 Hz, 1H), 4.79 (dt, *J* = 7.4, 4.6 Hz, 1H), 3.44 (dd, *J* = 11.1, 5.0 Hz, 2H), 3.26 (dd, *J* = 11.1, 4.2 Hz, 1H). **^{13}C NMR** (126 MHz, $CDCl_3$) δ 165.5 (s), 140.8 (q, *J* = 38.3 Hz), 140.6 (s), 138.4 (s), 137.4 (s), 134.9 (s), 132.0 (s), 131.6 (s), 130.9 (s), 130.05 (s), 129.6 (s), 128.9 (s), 128.8 (s), 128.0 (s), 127.9 (s), 126.7 (s), 126.5 (s), 124.6 (s), 121.6 (s), 119.0 (q, *J* = 271.9 Hz), 111.4 (s), 65.6 (s), 55.6 (s). **^{19}F NMR** (471 MHz, $CDCl_3$) δ -61.31 (s). **HRMS** (ESI) $[M+H]^+$ calculated for $C_{23}H_{18}O_2N_3F_3$+H: 426.1424, found: 426.1427, $[\alpha]_D^{22}$ = +35.84° (c= 0.12, MeOH).

***(P)*-(*S*)-*N*-(1-Hydroxy-3-methylbutan-2-yl)-2-(2-(trifluoromethyl)-1*H*-benzo[*d*]imidazol-1-yl)benzamide (*P*)-46**

From 40 mg of **(*P*)-1** and (*S*)-(+)-2-amino-3-methylbutanol, 21 mg of white solid (41%) after purification by preparative HPLC **^{1}H NMR** (400 MHz, $CDCl_3$) δ 7.94 – 7.90 (m, 1H), 7.89 – 7.85 (m, 1H), 7.71 – 7.64 (m, 2H), 7.45 – 7.38 (m, 3H), 7.15 – 7.09 (m, 1H), 5.70 (d, *J* = 8.6 Hz, 1H), 3.53 (ddd, *J* = 11.6, 8.5, 4.2 Hz, 1H), 3.24 (dd, *J* = 11.0, 4.6 Hz, 1H), 2.96 (dd, *J* = 11.0, 3.7 Hz, 1H), 1.63 (dq, *J* = 13.7, 6.9 Hz, 1H), 0.72 (d, *J* = 6.8 Hz, 3H), 0.67 (d, *J* = 6.8 Hz, 3H). **^{13}C{^{1}H} NMR** (101 MHz, $CDCl_3$) δ 165.9, 141.0, 140.6, 137.4, 135.4, 131.8, 131.3, 130.9, 130.0, 129.5, 126.6, 124.6. 121.5, 119.0 (q, *J* = 272.0 Hz), 111.5, 62.8, 56.8, 28.8, 19.3, 18.5 **^{19}F NMR** (376 MHz, $CDCl_3$) δ -61.18. **HRMS** (ESI) m/z: $[M+H]^+$ calculated for $C_{20}H_{21}O_2N_3F_3$: 392.1580, found: 392.1577, $[\alpha]_D^{22}$ = +99.6° (c= 0.25, MeOH).

(*M*)-(*S*)-*N*-(1-Hydroxy-3-methylbutan-2-yl)-2-(2-(trifluoromethyl)-1*H*-benzo[*d*]imidazol-1-yl)benzamide (*M*)-46

From 40 mg of **(*M*)-1** and (*S*)-(+)-2-amino-3-methylbutanol, 22 mg of a white solid (41%) after purification by preparative HPLC. **^{1}H NMR** (400 MHz, $CDCl_3$) δ 7.96 – 7.90 (m, 1H), 7.90 – 7.84 (m, 1H), 7.70 – 7.63 (m, 2H), 7.46 – 7.36 (m, 3H), 7.14 – 7.08 (m, 1H), 5.65 (d, *J* = 8.4 Hz, 1H), 3.60 – 3.52 (m, 1H), 3.33 (ddd, *J* = 15.0, 11.1, 4.5 Hz, 2H), 1.53 (dq, *J* = 13.6, 6.8 Hz, 1H), 0.53 (d, *J* = 6.8 Hz, 3H). **^{13}C{^{1}H} NMR** (101 MHz, $CDCl_3$) δ 166.1, 141.1 (q, *J* = 38.5 Hz), 140.8, 137.5, 135.4, 131.8, 131.4, 130.9, 129.9, 129.6, 126.4, 124.5, 118.9 (q, *J* = 272.1 Hz), 111.2, 63.0, 57.0, 28.7, 19.1, 18.14 **^{19}F NMR** (376 MHz, $CDCl_3$) δ -61.36. **HRMS** (ESI) m/z: $[M+H]^+$ calculated for $C_{20}H_{21}O_2N_3F_3$: 392.1580, found: 392.1581, $[\alpha]_D^{22}$ = +81.63° (c= 0.49, MeOH).

***(P)*-(R)-N-(1-hydroxy-3-methylbutan-2-yl)-2-(2-(trifluoromethyl)-1H-benzo[d]imidazol-1-yl)benzamide (*P*)-47**

From 40 mg of *(P)-1* and (R)-(-)-2-amino-3-methylbutanol, 30 mg of yellow oil (60 %) after purification by preparative HPLC **^{1}H NMR** (500 MHz, $CDCl_3$) δ 7.93 (dd, *J* = 6.5, 2.3 Hz, 1H), 7.88 (dd, *J* = 6.0, 3.3 Hz, 1H), 7.70 – 7.65 (m, 2H), 7.45 – 7.37 (m, 4H), 7.11 (dd, *J* = 6.5, 2.3 Hz, 1H), 5.64 (d, *J* = 8.3 Hz, 1H), 3.60 – 3.53 (m, 1H), 3.38 (dd, *J* = 11.1, 5.2 Hz, 1H), 3.29 (dd, *J* = 11.1, 3.8 Hz, 1H), 1.53 (dq, *J* = 13.6, 6.8 Hz, 1H), 0.62 (d, *J* = 6.8 Hz, 3H), 0.53 (d, *J* = 6.8 Hz, 3H). **^{13}C NMR** (126 MHz, $CDCl_3$) δ 166.0 (s), 141.1 (q, *J* = 38.8 Hz), 140.8(s), 137.4 (s), 135.3 (s), 131.8 (s), 131.4 (s), 130.9 (s), 129.9 (s), 129.6 (s), 126.3 (s), 124.5 (s), 121.8 (s), 118.9 (q, *J* = 272.2 Hz), 111.2 (s), 63.1 (s), 57.0 (s), 28.7 (s), 19.05 (s), 18.14 (s). **^{19}F NMR** (471 MHz, $CDCl_3$) δ -61.36 (s). **HRMS** (ESI) $[M+H]^+$ calculated for $C_{20}H_{20}O_2N_3F_3$+H: 392.1580, found: 392.1579, $[\alpha]_D^{22}$ = -86.0° (c= 0.3, MeOH).

***(M)*-(R)-N-(1-hydroxy-3-methylbutan-2-yl)-2-(2-(trifluoromethyl)-1H-benzo[d]imidazol-1-yl)benzamide (*M*)-47**

From 40 mg of *(M)-1* and (R)-(-)-2-amino-3-methylbutanol, 25 mg of white solid (50 %) after purification by preparative HPLC. **^{1}H NMR** (500 MHz, $CDCl_3$) δ 7.91 (dd, *J* = 6.6, 2.1 Hz, 1H), 7.87 – 7.84 (m, 1H), 7.69 – 7.64 (m, 2H), 7.45 – 7.36 (m, 3H), 7.11 (dd, *J* = 6.6, 2.1 Hz, 1H), 5.77 (d, *J* = 8.7 Hz, 1H), 3.52 (ddd, *J* = 12.4, 8.5, 4.2 Hz, 1H), 3.25 (dd, *J* = 10.9, 4.6 Hz, 1H), 2.97 (dd, *J* = 11.0, 3.7 Hz, 1H), 1.63 (dq, *J* = 13.7, 6.9 Hz, 1H), 0.71 (d, *J* = 6.8 Hz, 3H), 0.65 (d, *J* = 6.8 Hz, 3H). **^{13}C NMR** (126 MHz, $CDCl_3$) δ 165.9 (s), 140.8 (q, *J* = 38.3 Hz), 140.6 (s), 137.4 (s), 135.4 (s), 131.75 (s), 131.3 (s), 130.9 (s), 129. 9 (s), 129.5 (s), 126.5 (s), 124.6 (s), 121.5 (s), 119.0 (q, *J* = 271.9 Hz), 111.5 (s), 62.7 (s), 56.7 (s), 28.8 (s), 19.3 (s), 18.5 (s). **^{19}F NMR** (471 MHz, $CDCl_3$) δ -61.24 (s). HRMS (ESI) $[M+H]^+$ calculated for $C_{20}H_{20}O_2N_3F_3$+H: 392.1580, found: 392.1585, $[\alpha]_D^{22}$ = -104.76° (c= 0.21, MeOH).

(*P*)-Methyl (2-(2-(trifluoromethyl)-1*H*-benzo[*d*]imidazol-1-yl)benzoyl)-D-alaninate (*P*)-48

From 40 mg of **(*P*)-1**, D-AlaOMe.HCl and 1.1 eq of triethylamine. 25 mg of white solid (50 %). **^{1}H NMR** (500 MHz, $CDCl_3$) δ 7.92 (dd, *J* = 6.5, 2.4 Hz, 1H), 7.86 (dd, *J* = 5.7, 3.6 Hz, 1H), 7.71 – 7.66 (m, 2H), 7.48 – 7.44 (m, 1H), 7.42 – 7.35 (m, 2H), 7.09 (dd, *J* = 6.5, 2.4 Hz, 1H), 6.12 (d, *J* = 6.9 Hz, 1H), 4.35 (p, *J* = 7.1 Hz, 1H), 3.65 (s, 3H), 0.85 (d, *J* = 7.2 Hz, 3H). **^{13}C{^{1}H} NMR** (126 MHz, $CDCl_3$)

δ 172.7, 164.7, 140.6 (q, *J* = 38.6 Hz), 134.7, 132.0, 131.8, 130.9, 129.75, 129.6, 126.4, 124.4, 121.6, 119.0 (q, *J* = 272.1 Hz), 111.5, 52.7, 48.3, 17.7. **^{19}F NMR** (471 MHz, $CDCl_3$) δ -61.26 **HRMS** (ESI) m/z: $[M+H]^+$ calculated for $C_{19}H_{17}O_3N_3F_3$: 392.1217, found: 392.1211, $[\alpha]_D^{22}$ = -59.03° (c= 0.31 MeOH).

(*M*)-Methyl (2-(2-(trifluoromethyl)-1*H*-benzo[*d*]imidazol-1-yl)benzoyl)-D-alaninate (*M*)-48
From 40 mg of **(*M*)-1**, D-AlaOMe.HCl and 1.1 eq of triethylamine. 30 mg of white solid (60 %). **^{1}H NMR** (500 MHz, $CDCl_3$) δ 7.95 – 7.90 (m, 1H), 7.87 – 7.83 (m, 1H), 7.70 – 7.66 (m, 2H), 7.47 – 7.43 (m, 1H), 7.42 – 7.36 (m, 2H), 7.09 (dd, *J* = 5.8, 3.3 Hz, 1H), 6.10 (d, *J* = 6.9 Hz, 1H), 4.35 (p, *J* = 7.1 Hz, 1H), 3.59 (s, 3H), 1.03 (d, *J* = 7.0 Hz, 3H). **^{13}C{^{1}H} NMR** (126 MHz, $CDCl_3$) δ 172.6, 164.6, 141.2 (q, *J* = 38.7 Hz), 140.7, 137.55, 134.7, 132.0, 132.0, 130.9, 129.7, 129.7, 126.3, 124.4, 121.7, 118.9 (q, *J* = 272.1 Hz), 111.1, 52.6, 48.35, 18.1 **^{19}F NMR** (471 MHz, $CDCl_3$) δ -61.63 **HRMS** (ESI) m/z: $[M+H]^+$ calculated for $C_{19}H_{17}O_3N_3F_3$: 392.1217, found: 392.1219, $[\alpha]_D^{22}$ = +142.09° (c= 0.24 MeOH).

(*P*)-methyl (2-(2-(trifluoromethyl)-1H-benzo[d]imidazol-1-yl)benzoyl)-L-alaninate (*P*)-49
From 40 mg of ***(P)*-1**, L-AlaOMe.HCl and 1.1 eq. of triethylamine, 16 mg of white solid (33 %) after purification by preparative HPLC. **^{1}H NMR** (400 MHz, $CDCl_3$) δ 7.95 – 7.90 (m, 1H), 7.87 – 7.83 (m, 1H), 7.71 – 7.65 (m, 2H), 7.47 – 7.43 (m, 1H), 7.42 – 7.36 (m, 2H), 7.11 – 7.06 (m, 1H), 6.10 (d, *J* = 7.0 Hz, 1H), 4.41 – 4.29 (m, 1H), 3.59 (s, 3H), 1.03 (d, *J* = 7.1 Hz, 3H). **^{13}C NMR** (101 MHz, $CDCl_3$) δ 172.6 (s), 164.6 (s), 141.1 (q, *J* = 38.5 Hz), 140.7 (s), 137.5 (s), 134.7 (s), 131.99 (s), 131.96 (s), 130.8 (s), 129.7 (s), 129.6 (s), 126.3 (s), 124.3 (s), 121.7 (s), 118.9 (q, *J* = 272.2 Hz), 111.18 (s), 52.6 (s), 48.3 (s), 18.1 (s). **^{19}F NMR** (376 MHz, $CDCl_3$) δ -61.63 (s). **HRMS** (ESI) $[M+H]^+$ calculated for $C_{19}H_{16}O_3N_3F_3$+H: 392.1217, found: 392.1213, $[\alpha]_D^{22}$ = -138.71° (c= 0.31 MeOH).

(*M*)-methyl (2-(2-(trifluoromethyl)-1H-benzo[d]imidazol-1-yl)benzoyl)-L-alaninate (*M*)-49
From 40 mg of (***M*)-1**, L-AlaOMe.HCl and 1.1 eq. of triethylamine. 18 mg of white solid (36%). **^{1}H NMR** (400 MHz, $CDCl_3$) δ 7.91 (dd, *J* = 6.2, 2.8 Hz, 1H), 7.85 (dd, *J* = 5.8, 3.5 Hz, 1H), 7.71 – 7.65 (m, 2H), 7.47 – 7.43 (m, 1H), 7.42 – 7.34 (m, 2H), 7.08 (dd, *J* = 6.0, 3.0 Hz, 1H), 6.14 (d, *J* = 6.8 Hz, 1H), 4.34 (p, *J* = 7.1 Hz, 1H), 3.64 (s, 3H), 0.85 (d, *J* = 7.1 Hz, 3H). **^{13}C NMR** (101 MHz, $CDCl_3$) δ 172.7 (s), 164.7 (s), 140.6 (q, *J* = 38.5 Hz), 140.6 (s), 137.6 (s), 134.7 (s), 132.0 (s), 131.8 (s), 130.9 (s), 129.7 (s), 129.6 (s), 126.3 (s), 124.4 (s), 121.6 (s), 119.0 (q, *J* = 271.8 Hz), 111.5 (s), 52.7 (s), 48.3 (s), 17.7 (s). **^{19}F NMR** (376 MHz, $CDCl_3$) δ -61.25 (s). **HRMS** ESI$[M+H]^+$ calculated for $C_{19}H_{16}O_3N_3F_3$+H: 392.1217, found: 392.1221, $[\alpha]_D^{22}$ = +55.06° (c= 0.18 MeOH).

(*P*)-methyl (2-(2-(trifluoromethyl)-1H-benzo[d]imidazol-1-yl)benzoyl)-L-phenylalaninate (*P*)-50
From 15 mg of **(*P*)-1** and L-PheOMe.HCl and 2.2 eq. of triethylamine, 17,5 mg of oil (75 %). Purified by column chromatography (hexane:ethylacetate 3:1, column dimesions 1x10 cm). **^{1}H NMR** (500 MHz, $CDCl_3$) δ 7.94 – 7.91 (m, 1H), 7.70 – 7.63 (m, 5H), 7.43 – 7.36 (m, 5H), 7.25 – 7.22 (m, 4H), 7.09 – 7.06 (m, 1H), 6.94 (dd, *J* = 7.3, 2.1 Hz, 3H), 6.10 (d, *J* = 7.5 Hz, 1H), 4.68 (dt, *J* = 7.6, 5.8 Hz, 1H), 3.58 (s, 4H), 2.91 (dd, *J* = 5.8, 2.2 Hz, 3H). **^{13}C NMR {1H}** (126 MHz, $CDCl_3$) δ 171.2, 164.8, 141.0 (q, *J* = 39.6 Hz), 140.7, 137.8, 135.6, 134.6, 132.3, 132.0, 130.8, 130.0, 129.3, 129.2, 128.7, 127.3, 126.2, 124.3, 121.6, 119.0 (q, *J* = 271.5 Hz), 111.4, 53.5, 52.5, 37.8. **^{19}F NMR** (376 MHz, $CDCl_3$) δ (ppm) = -61.58., **HRMS** (ESI) m/z: $[M+H]^+$ calculated for $C_{25}H_{21}F_3N_3O_3$: 468.1535 found: 468.1529, $[\alpha]_D^{22}$ = -75.00°(c= 0.12 MeOH).

(*M*)-methyl (2-(2-(trifluoromethyl)-1H-benzo[d]imidazol-1-yl)benzoyl)-L-phenylalaninate (*M*)-50
From 15 mg of **(*M*)-1** and L-PheOMe.HCl and 2.2 eq. of triethylamine, 19 mg of oil (81 %). Purified by column chromatography (hexane: ethylacetate 3:1, column dimesions 1x10 cm). **^{1}H NMR** (500 MHz, $CDCl_3$) δ 7.93 (d, *J* = 7.8 Hz, 1H), 7.76 – 7.74 (m, 1H), 7.69 – 7.63 (m, 2H), 7.43 – 7.33 (m, 4H), 7.25 – 7.20 (m, 3H), 7.03 (d, *J* = 7.9 Hz, 1H), 6.90 (dd, *J* = 7.3, 2.0 Hz, 2H), 6.04 (d, *J* = 7.5 Hz, 1H), 4.65 (dt, *J* = 7.6, 6.1 Hz, 1H), 3.59 (s, 3H), 2.84 – 2.75 (m, 2H). **^{13}C NMR{1H}** (126 MHz, $CDCl_3$) δ 171.5, 164.9, 141.1 (q, *J*=38.5 Hz), 140.7, 137.6, 135.5, 134.4, 132.2, 132.1, 130.8, 130.0, 129.5, 129.1, 128.8, 127.3, 127.3, 126.2, 124.3, 121.7, 119.0 (q, *J* = 272.2 Hz), 111.3., 53.6, 52.4, 37.8., **^{19}F NMR** (376 MHz,

$CDCl_3$) δ (ppm) = -61.43, **HRMS** (ESI) m/z: $[M+H]^+$ calculated for $C_{25}H_{21}F_3N_3O_3$: 468.1535 found: 468.1528, $[\alpha]_D^{22}$ = +33.00°(c= 0.09 MeOH).

General procedure for TBBA-ester formation

***(P)-(S)*-1-Methoxy-1-oxopropan-2-yl 2-(2-(trifluoromethyl)-1*H*-benzo[*d*]imidazol-1-yl)benzoate (*P*)-54:** (*P*)-1-Carboxyphenyl(2-trifluoromethy)benzimidazole **(*P*)-1** (40 mg; 0.13 mmol; 1 eq) and (−)-methyl L-lactate (13μL; 14 mg; 0.13 mmol; 1 eq) were dissolved in dry DCM (2 mL). DCC (27 mg; 0.13 mmol; 1 eq) and then DMAP (16 mg; 0.13 mmol; 1 eq) were subsequently added into the solution. The solution was then stirred at room temperature for 16 hours. After 16 hours, a solid precipitate was filtered-off via syringe filter. The mixture was then adsorbed on celite and purified via column chromatography (hexane: ethylacetate 6:1, column dimensions: 1x10 cm). 46 mg of white foamy solid (88 %) **^{1}H NMR** (400 MHz, $CDCl_3$) δ 8.32 – 8.28 (m, 1H), 7.93 – 7.88 (m, 1H), 7.79 (td, *J* = 7.6, 1.7 Hz, 1H), 7.72 (td, *J* = 7.7, 1.4 Hz, 1H), 7.49 (dd, *J* = 7.7, 1.2 Hz, 1H), 7.41 – 7.33 (m, 2H), 7.05 – 7.00 (m, 1H), 4.91 (q, *J* = 7.1 Hz, 0H), 3.49 (s, 2H), 0.99 (d, *J* = 5.2 Hz, 1H). **^{13}C{^{1}H} NMR** (101 MHz, $CDCl_3$) δ 170.2, 163.6, 141.2, 140.8, 140.7, 137.9, 134.1, 134.1, 133.1, 130.8, 130.3, 128.7, 125.9, 124.0, 121.3, 120.3, 117.6, 69.6, 52.3, 16.3 **^{19}F NMR** (376 MHz, $CDCl_3$) δ -62.03 **HRMS** (ESI) m/z: $[M+H]^+$ calculated for $C_{19}H_{16}O_4N_2F_3$: 393.1057 found: 393.1058, $[\alpha]_D^{22}$ = −36.7° (c= 0.46 $CHCl_3$).

(*P*)-(R)-1-phenylethyl 2-(2-(trifluoromethyl)-1H-benzo[d]imidazol-1-yl)benzoate (*P*)-51 Using general procedure, from 15 mg of **(*P*)-1** and (*R*)-1-Phenylethanol, 18 mg of oil (88 %). Purified by column chromatography (hexane: ethylacetate 10:1, column dimesions 1x10 cm). **^{1}H NMR** (400 MHz, $CDCl_3$) δ 8.23 – 8.19 (m, 1H), 7.98 – 7.93 (m, 1H), 7.75 (td, *J* = 7.6, 1.8 Hz, 1H), 7.68 (td, *J* = 7.6, 1.4 Hz, 1H), 7.48 – 7.44 (m, 1H), 7.44 – 7.38 (m, 1H), 7.38 – 7.33 (m, 1H), 7.29 – 7.24 (m, 4H), 7.07 – 7.02 (m, 2H), 7.02 – 6.98 (m, 1H), 5.68 (q, *J* = 6.6 Hz, 1H), 0.80 (d, *J* = 6.6 Hz, 3H). **^{13}C NMR {1H}** (101 MHz, $CDCl_3$) δ 163.9, 140.9 (q, *J* = 38.4 Hz), 140.7, 140.2, 137.8, 133.6, 133.5, 132.7, 130.6, 130.0, 129.8, 128.5, 128.2, 126.4, 126.0, 124.0, 121.5, 118.9 (q, *J* = 272.2 Hz), 110.9, 74.1, 20.5, ^{19}F NMR (376 MHz, $CDCl_3$) δ (ppm) = -62.00, **HRMS** (ESI-TOF) m/z: $[M+H]^+$ calculated for $C_{23}H_{18}F_3N_2O_2$: 411.1320 found: 411.1317, $[\alpha]_D^{22}$ = -131.18°(c= 0.17 $CHCl_3$).

(*M*)-(R)-1-phenylethyl 2-(2-(trifluoromethyl)-1H-benzo[d]imidazol-1-yl)benzoate (*M*)-51 Using general procedure, from 15 mg of **(*M*)-1** and (*R*)-1-Phenylethanol, 19 mg of oil (93 %). Purified by column chromatography (hexane: ethylacetate 10:1, column dimesions 1x10 cm). ^{1}H NMR (400 MHz, $CDCl_3$) δ 8.28 – 8.25 (m, 1H), 7.96 (dt, *J* = 8.1, 1.0 Hz, 1H), 7.75 (td, *J* = 7.6, 1.8 Hz, 1H), 7.69 (td, *J* = 7.6, 1.4 Hz, 1H), 7.47 – 7.41 (m, 2H), 7.34 (ddd, *J* = 8.3, 7.2, 1.1 Hz, 1H), 7.16 – 7.11 (m, 1H), 7.06 (ddt, *J* = 8.3, 6.6, 1.4 Hz, 2H), 6.97 – 6.93 (m, 1H), 6.58 – 6.54 (m, 2H), 5.74 (q, *J* = 6.7 Hz, 1H), 1.11 (d, *J* = 6.7 Hz, 3H). **^{13}C NMR {1H}** (101 MHz, $CDCl_3$) δ 163.8, 141.1 (q, *J* = 38.6 Hz), 140.8, 140.4, 138.0, 133.7, 133.2, 130.7, 130.2, 129.9, 128.4, 128.0, 126.1, 126.0, 124.1, 121.6, 119.0 (q, *J* = 272.2 Hz), 111.2, 74.2, 21.3, **^{19}F NMR** (376 MHz, $CDCl_3$) δ (ppm) = -62.02, **HRMS** (ESI-TOF) m/z: $[M+H]^+$ calculated for $C_{23}H_{18}F_3N_2O_2$: 411.1320 found: 411.1317, $[\alpha]_D^{22}$ = +3.64°(c= 0.11 $CHCl_3$).

(*P*)-(S)-sec-butyl 2-(2-(trifluoromethyl)-1H-benzo[d]imidazol-1-yl)benzoate (*P*)-52 Using general procedure, from 15 mg of **(*P*)-1** and (*S*)-(+)-2-Butanol, 11.5 mg of oil (64 %). Purified by column chromatography (hexane: ethylacetate 9:1, column dimesions 1x10 cm). **^{1}H NMR** (400 MHz, $CDCl_3$) δ 8.28 (dd, *J* = 7.6, 1.8 Hz, 1H), 7.94 (d, *J* = 7.8 Hz, 1H), 7.74 (dqd, *J* = 15.0, 7.5, 1.6 Hz, 2H), 7.48 (dd, *J* = 7.6, 1.2 Hz, 1H), 7.37 (tdd, *J* = 15.0, 7.3, 1.1 Hz, 2H), 6.99 (d, *J* = 7.5 Hz, 1H), 4.73 – 4.63 (m, 1H), 0.88 (d, *J* = 6.3 Hz, 3H), 0.87 – 0.80 (m, 1H), 0.77 – 0.64 (m, 1H), 0.35 (t, *J* = 7.5 Hz, 3H). **^{13}C NMR {1H}** (101 MHz,) δ 164.1, 141.1 (q, *J* = 39.4 Hz), 140.7, 138.1, 133.7, 133.5, 132.9, 130.7, 130.2, 125.9, 124.0, 121.5, 119.0 (q, *J* = 271.9 Hz), 111.1, 74.2, 28.1, 18.9, 9.4, **^{19}F NMR** (376 MHz, $CDCl_3$) δ (ppm) = -62.04. **HRMS** (ESI) m/z: $[M+H]^+$ calculated for $C_{19}H_{18}F_3N_2O_2$: 363.1320 found: 363.1313, $[\alpha]_D^{22}$ = -88.57°(c= 0.07 $CHCl_3$).

(*M*)-(S)-sec-butyl 2-(2-(trifluoromethyl)-1H-benzo[d]imidazol-1-yl)benzoate (*M*)-52 Using general procedure, from 15 mg of **(*M*)-1** and (*S*)-(+)-2-Butanol, 10 mg of oil (55 %). Purified by column chromatography (hexane: ethylacetate 9:1, column dimesions 1x10 cm). **^{1}H NMR** (400 MHz, $CDCl_3$) δ 8.25 (dd, *J* = 7.6, 1.8 Hz, 1H), 7.94 (d, *J* = 7.9 Hz, 1H), 7.76 (td, *J* = 7.6, 1.8 Hz, 1H), 7.71 (td, *J* = 7.6, 1.4 Hz, 1H), 7.49 (d, *J* = 7.5 Hz, 1H), 7.42 – 7.30 (m, 1H), 6.97 (d, *J* = 7.9 Hz, 1H), 4.73 – 4.54 (m, 1H), 1.29 – 1.07 (m, 1H), 0.68 (t, *J* = 7.4 Hz, 1H), 0.39 (d, *J* = 6.3 Hz, 1H). **^{13}C NMR {1H}** (101 MHz, $CDCl_3$) δ 164.3, 141.1 (q, *J* = 38.6 Hz), 140.7, 138.0, 133.6, 133.5, 132.8, 130.7, 130.2, 130.0, 126.0, 124.1, 121.5, 119.0 (q, *J* = 271.9 Hz), 111.0, 74.2, 28.3, 18.1, 9.7, **^{19}F NMR** (376 MHz, $CDCl_3$) δ = -61.86, **HRMS** (ESI-TOF) m/z: $[M+H]^+$ calculated for $C_{19}H_{18}F_3N_2O_2$: 363.1320 found: 363.1315, $[\alpha]_D^{22}$ = +141.67°(c= 0.06 $CHCl_3$).

(*P*)-(S)-but-3-yn-2-yl 2-(2-(trifluoromethyl)-1H-benzo[d]imidazol-1-yl)benzoate (*P*)-53 Using general procedure, from 15 mg of **(*P*)-1** and (*S*)-But-3-yn-2-nol, 15 mg of oil (84 %). Purified by column chromatography (hexane:ethylacetate 7:1, column dimesions 1x10 cm). **^{1}H NMR** (400 MHz, $CDCl_3$) δ 8.26 (dd, *J* = 7.7, 1.2 Hz, 1H), 7.94 (d, *J* = 7.8 Hz, 1H), 7.76 (dtd, *J* = 15.2, 7.6, 1.0 Hz, 2H), 7.50 (d, *J* = 7.7 Hz, 1H), 7.37 (td, *J* = 14.3, 7.2 Hz, 2H), 6.99 (d, *J* = 8.1 Hz, 1H), 5.21 (qd, *J* = 6.7, 2.0 Hz, 1H), 2.07 (d, *J* = 2.1 Hz, 1H), 1.08 (d, *J* = 6.8 Hz, 3H). **^{13}C NMR {1H}** (101 MHz,) δ 163.4, 141.0 (q, *J* = 39.1 Hz), 140.8, 138.0, 134.0, 133.9, 132.8, 130.7, 130.2, 129.3, 126.0, 124.0, 121.6, 119.0 (q, *J* = 271.9 Hz), 111.0, 80.6, 73.1, 61.4, 20.5, **^{19}F NMR** (376 MHz, $CDCl_3$) δ = -61.99 **HRMS** (ESI) m/z: $[M+H]^+$ calculated for $C_{19}H_{14}F_3N_2O_2$: 359.1007 found: 359.1001, $[\alpha]_D^{22}$ = -156.67°(c= 0.09 $CHCl_3$).

(*M*)-(S)-but-3-yn-2-yl 2-(2-(trifluoromethyl)-1H-benzo[d]imidazol-1-yl)benzoate (*M*)-53 Using general procedure, from 15 mg of **(*M*)-1** and (*S*)-But-3-yn-2-nol, 16 mg of oil (89 %). Purified by column chromatography (hexane:ethylacetate 7:1, column dimesions 1x10 cm). **^{1}H NMR** (400 MHz, $CDCl_3$) δ 8.27 (dd, *J* = 7.8, 1.7 Hz, 1H), 7.95 (d, *J* = 7.6 Hz, 1H), 7.76 (dtd, *J* = 25.7, 7.5, 1.5 Hz, 2H), 7.50 (d, *J* = 7.5 Hz, 1H), 7.40 (td, *J* = 7.3, 7.3, 1.3 Hz, 1H), 7.35 (td, *J* = 8.1, 1.3 Hz, 1H), 6.97 (dd, *J* = 7.4, 0.9 Hz, 1H), 5.19 (qd, *J* = 6.7, 2.1 Hz, 1H), 2.35 (d, *J* = 2.2 Hz, 1H), 0.82 (d, *J* = 6.7 Hz, 4H), **^{13}C NMR {1H}** (101 MHz, $CDCl_3$) δ 163.4, 141.2 (q, *J* = 38.6 Hz), 140.8, 137.9, 134.00 (s), 133.93 (s), 132.8, 130.7, 130.2, 129.3, 126.0, 124.0, 121.6, 119.0 (q, *J* = 272.0 Hz), 110.8, 80.9, 73.5, 61.4, 20.1. **^{19}F NMR** (376 MHz, $CDCl_3$) δ = -62.06. **HRMS** (ESI-TOF) m/z: $[M+H]^+$ calculated for $C_{19}H_{14}F_3N_2O_2$: 359.1000 found: 359.1001, $[\alpha]_D^{22}$ = -61.25°(c= 0.08 $CHCl_3$).

(*M*)-(*S*)-1-Methoxy-1-oxopropan-2-yl 2-(2-(trifluoromethyl)-1*H*-benzo[*d*]imidazol-1-yl)benzoate (*M*)-54: (*M*)-1-Carboxyphenyl(2-trifluoromethy)benzimidazole **(*M*)-1** (40 mg, 0.13 mmol, 1 eq) and (−)-methyl L-lactate (13μL, 14 mg, 0.13 mmol, 1 eq) purified via column chromatography (hexane:ethylacetate 6:1, column dimensions: 1x10 cm). 43 mg of a white foamy solid (85 %). **^{1}H NMR** (400 MHz, $CDCl_3$) δ 8.31 – 8.25 (m, 1H), 7.95 – 7.89 (m, 1H), 7.80 (td, *J* = 7.6, 1.7 Hz, 1H), 7.73 (td, *J* = 7.7, 1.4 Hz, 1H), 7.50 (d, *J* = 7.7 Hz, 1H), 7.43 – 7.30 (m, 1H), 7.01 – 6.95 (m, 1H), 4.86 (q, *J* = 7.1 Hz, 1H), 3.61 (s, 2H), 0.82 (d, *J* = 7.1 Hz, 1H). **^{13}C{^{1}H} NMR** (101 MHz, $CDCl_3$) δ 170.2, 163.7, 141.1 (q, *J* = 38.6 Hz), 140.6, 137.9, 134.1, 134.0, 133.0, 130.8, 130.3, 128.8, 125.9, 124.0, 121.5, 118.9 (q, *J* = 271.9 Hz), 111.0, 69.5, 52.4, 16.0 **^{19}F NMR** (376 MHz, $CDCl_3$) δ -61.98 **HRMS** (ESI) m/z: $[M+H]^+$ calculated for $C_{19}H_{16}O_4N_2F_3$: 393.1057 found: 393.1057, $[\alpha]_D^{22}$ = +68.14° (c= 0.43 $CHCl_3$).

(*P*)-(S)-2-methoxy-2-oxo-1-phenylethyl 2-(2-(trifluoromethyl)-1H-benzo[d]imidazol-1-yl)benzoate (*P*)-55 Using general procedure, from 20 mg of **(*P*)-1** and Methyl-(*S*)-(+)-mandelate, 22 mg of white solid (75 %). Purified by column chromatography (hexane:ethylacetate 7:1, column dimesions 1x10 cm). **^{1}H NMR** (400 MHz, $CDCl_3$) δ 8.36 (dd, *J* = 7.7, 1.7 Hz, 1H), 7.84 – 7.80 (m, *J* = 2.5, 1.7 Hz, 1H), 7.78 (dd, *J* = 7.6, 1.8 Hz, 1H), 7.73 (td, *J* = 7.6, 1.4 Hz, 1H), 7.44 (dd, *J* = 7.6, 1.0 Hz, 1H), 7.40 – 7.31 (m, 3H), 7.28 – 7.22 (m, 3H), 7.03 – 6.97 (m, 3H), 5.79 (s, 1H), 3.58 (s, 3H), **^{13}C NMR {1H}** (101 MHz, $CDCl_3$) δ 168.5, 163.8, 140.9 (q, *J* = 38.9 Hz), 140.7, 137.6, 134.10, 134.07, 132.8, 130.7, 130.3, 129.4, 128.8, 128.7, 127.7, 126.7, 125.9, 123.9, 121.6, 118.9 (q, *J* = 271.7 Hz), 110.9, 75.5, 52.7, **^{19}F NMR** (376 MHz, $CDCl_3$) δ -62.10, **HRMS** (ESI-TOF) m/z: $[M+H]^+$ calculated for $C_{24}H_{18}F_3N_2O_4$: 455.1213 found: 455.1230, $[\alpha]_D^{22}$ = +32.73°(c= 0.22 $CHCl_3$).

(*M*)-(S)-2-methoxy-2-oxo-1-phenylethyl 2-(2-(trifluoromethyl)-1H-benzo[d]imidazol-1-yl)benzoate (*M*)-55 Using general procedure, from 20 mg of **(*M*)-1** and Methyl-(*S*)-(+)-mandelate, 24 mg of white solid (82 %). Purified by column chromatography (hexane:ethylacetate 7:1, column dimesions 1x10 cm). **^{1}H NMR** (400 MHz, $CDCl_3$) δ 8.32 (dd, *J* = 7.7, 1.7 Hz, 1H), 7.82 (d, *J* = 8.0 Hz, 1H), 7.78 (td, *J* = 7.6, 1.7 Hz, 1H), 7.72 (td, *J* = 7.6, 1.4 Hz, 1H), 7.45 (d, *J* = 7.0 Hz, 1H), 7.43 – 7.27 (m, 4H), 7.25 – 7.20 (m, *J* = 10.3, 4.7 Hz, 2H), 6.97 – 6.91 (m, 3H), 5.77 (s, 1H), 3.60 (s, 3H). **^{13}C NMR {1H}** (101 MHz, $CDCl_3$) δ 168.5, 163.6, 140.7, 140.7 (q, *J* = 38.3 Hz), 137.6, 134.3, 134.2, 133.0, 132.8, 130.7, 130.4, 129.5, 128.9, 128.8, 128.4, 127.7, 126.7, 125.9, 123.9, 121.6, 118.9 (q, *J* = 271.9 Hz), 111.0 (s), 75.6, 52.9, **^{19}F NMR** (376 MHz, $CDCl_3$) δ -61.93, **HRMS** (ESI-TOF) m/z: $[M+H]^+$ calculated for $C_{24}H_{18}F_3N_2O_4$: 455.1213 found: 455.1230, $[\alpha]_D^{22}$ = +130.0°(c= 0.24 $CHCl_3$).

***(P)*-(1*R*,2*S*,5*R*)-2-Isopropyl-5-methylcyclohexyl 2-(2-(trifluoromethyl)-1*H*-benzo[*d*]imidazol-1-yl)benzoate (*P*)-56:** (*P*)-1-Carboxyphenyl(2-trifluoromethy)benzimidazole **(*P*)-1** (40 mg, 0.13 mmol, 1 eq) and (1*R*,2*S*,5*R*)-(−)-Menthol (20 mg, 0.13 mmol, 1 eq) purified via column chromatography (hexane:ethylacetate 30:1, column dimensions: 1x10 cm). 49 mg of a white foamy solid (86 %). **^{1}H NMR** (500 MHz, $CDCl_3$) δ 8.15 (dd, *J* = 7.6, 1.7 Hz, 1H), 7.87 (dd, *J* = 8.1, 1.0 Hz, 1H), 7.69 (ddd, *J* = 7.6, 7.5, 1.7 Hz, 1H), 7.64 (ddd, *J* = 7.6, 7.5, 1.4 Hz, 1H), 7.42 (d, *J* = 7.5 Hz, 1H), 7.32 (ddd, *J* = 8.1, 7.3, 1.2 Hz, 1H), 7.26 (td, *J* = 8.1, 7.3, 1.1 Hz, 1H), 6.89 (dt, *J* = 8.1, 1.0 Hz, 1H), 4.45 (ddd, *J* = 10.8, 10.8, 4.5 Hz, 1H), 1.46 (m, 1H), 1.42 (m, 1H), 1.40 (m, 1H), 1.09 (m,1H), 1.01 (m,1H), 0.76 (m,1H), 0.74 (m,1H), 0.72 (d, *J* = 7.0 Hz, 3H), 0.55 (d, *J* = 6.5 Hz, 3H), 0.50 (d, *J* = 7.0 Hz, 3H), -0.54 (q, *J* = 12.0, 12.0, 11.2 Hz, 1H). **^{13}C{^{1}H} NMR** (126 MHz, $CDCl_3$) δ 141.1 (q, *J* = 38.4 Hz), 140.8, 138.0, 133.3, 132.6, 130.5, 130.2, 129.9, 125.9, 123.9, 121.5, 118.9 (q, *J* = 272.0 Hz), 110.9, 75.7, 46.3, 39.0, 33.8, 31., 24.6, 22.7, 21.8, 20.7, 15.7 **^{19}F NMR** (376 MHz, $CDCl_3$) δ -61.74 **HRMS** (ESI) m/z: $[M+H]^+$ calculated for $C_{25}H_{28}O_2N_2F_3$: 445.2097.1057 found: 445.2099, $[\alpha]_D^{22}$ = −133.68° (c= 0.19 MeOH).

***(M)*-(1*R*,2*S*,5*R*)-2-Isopropyl-5-methylcyclohexyl 2-(2-(trifluoromethyl)-1*H*-benzo[*d*]imidazol-1-yl)benzoate (*M*)-57:** *(M)*-1-Carboxyphenyl(2-trifluoromethy)benzimidazole **(*M*)-1** (40 mg, 0.13 mmol, 1 eq) and (1*R*,2*S*,5*R*)-(−)-Menthol (20 mg, 0.13 mmol, 1 eq) purified via column chromatography (hexane:ethylacetate 30:1, column dimensions: 1x10 cm). 48 mg of a white foamy solid (85 %). **^{1}H NMR** (500 MHz, $CDCl_3$) δ 8.24 (dd, *J* = 7.5, 1.9 Hz, 1H), 7.89 (dd, *J* = 7.9, 1.2 Hz, 1H), 7.69 (ddd, *J* = 7.6, 7.5, 1.7 Hz, 1H), 7.65 (ddd, *J* = 7.6, 7.5, 1.4 Hz, 1H), 7.38 (d, *J* = 7.6 Hz, 1H), 7.33 (ddd, *J* = 7.9, 7.3, 1.2 Hz, 1H), 7.38 (ddd, *J* = 8.2, 7.3, 1.3 Hz, 1H), 6.93 (dt, *J* = 8.2, 1.0 Hz, 1H), 4.55 (ddd, *J* = 11.0, 11.0, 4.4 Hz, 1H), 1.66 (m, 1H), 1.45 (m, 1H), 1.34 (m, 1H), 1.23 (m,1H), 0.82 (m,1H), 0.75 (m,1H), 0.75 (d, *J* = 6.5 Hz, 3H), 0.70 (m,1H), 0.58 (m, 1H), 0.40 (d, *J* = 7.0 Hz, 3H), 0.36 (d, *J* = 7.0 Hz, 3H), 0.32 (m, 1H), **^{13}C{^{1}H} NMR** (126 MHz, $CDCl_3$) δ 164.0, 141.0 (q, *J* = 38.3 Hz), 140.7, 138.0, 133.7, 133.4, 133.0, 130.7, 130.2, 130.1, 125.9, 124.0, 121.5, 119.0 (q, *J* = 272.0 Hz), 111.1, 75.8, 46.3, 40.1, 34.0, 31.4, 25.5, 22.7, 21.9, 20.8, 15.5. **^{19}F NMR** (376 MHz, $CDCl_3$) δ -61.38 **HRMS** (ESI) m/z: $[M+H]^+$ calculated for $C_{25}H_{28}O_2N_2F_3$: 445.2097.1057 found: 445.2101, $[\alpha]_D^{22}$ = −3.29° (c= 0.15 MeOH).

(*P*)-(1S,2R,4S)-1,7,7-trimethylbicyclo[2.2.1]heptan-2-yl 2-(2-(trifluoromethyl)-1H-benzo[d]imidazol-1-yl)benzoate (*P*)-57 Using general procedure, from 15 mg of **(*P*)-1** and (-)-Borneol, 17 mg of oil (77 %). Purified by column chromatography (hexane:ethylacetate 8.5:1, column dimesions 1x10 cm). **^{1}H NMR** (400 MHz, $CDCl_3$) δ 8.22 – 8.19 (m, 1H), 7.97 – 7.92 (m, 1H), 7.72 (dqd, *J* = 14.8, 7.5, 1.7 Hz, 2H), 7.42 (dd, *J* = 9.5, 1.4 Hz, 1H), 7.42 – 7.33 (m, 2H), 7.04 – 7.01 (m, 1H), 4.84 (ddd, *J* = 10.0, 3.6, 2.2 Hz, 1H), 2.07 – 1.97 (m, 1H), 1.53 (tdd, *J* = 12.0, 8.0, 4.4 Hz, 1H), 1.46 (t, *J* = 4.5 Hz, 1H), 1.17 (ddd, *J* = 13.8, 9.5, 4.6 Hz, 1H), 1.09 – 1.00 (m, 1H), 0.76 (s, *J* = 4.4 Hz, 3H), 0.75 (s, 3H), 0.74 – 0.67 (m, 1H), 0.64 (s, 3H), 0.24 (dd, *J* = 13.9, 3.6 Hz, 1H). **^{13}C NMR{1H}** (101 MHz, $CDCl_3$) δ 165.3, 140.8 (q, *J* = 38.6 Hz), 140.8, 137.7, 133.4, 133.3, 132.5, 130.6, 130.1, 130.0, 126.1, 124.1, 121.7, 119.0 (q, *J* = 272.0 Hz), 110.9, 82.2, 48.7, 47.9, 44.6, 35.8, 27.8, 26.9, 19.7, 18.8, 13.4, **^{19}F NMR** (376 MHz, $CDCl_3$) δ= -61.65, **HRMS** (ESI) m/z: $[M+H]^+$ calculated for $C_{25}H_{26}F_3N_2O_2$: 443.1946 found: 443.1941, $[\alpha]_D^{22}$ = -142.5°(c= 0.08 $CHCl_3$).

(*M*)-(1S,2R,4S)-1,7,7-trimethylbicyclo[2.2.1]heptan-2-yl 2-(2-(trifluoromethyl)-1H-benzo[d]imidazol-1-yl)benzoate (*M*)-57 Using general procedure, from 15 mg of **(*M*)-1** and (-)-Borneol, 15 mg of oil (68 %). Purified by column chromatography (hexane: ethylacetate 8.5:1, column dimesions 1x10 cm). **^{1}H NMR** (400 MHz, $CDCl_3$) δ 8.24 (dd, *J* = 7.5, 2.0 Hz, 1H), 7.96 – 7.92 (m, 1H), 7.73 (pd, *J* = 7.5, 1.6 Hz, 2H), 7.44 – 7.33 (m, 3H), 7.08 – 7.02 (m, 1H), 4.95 – 4.90 (m, 1H), 2.14 (ddt, *J* = 14.0, 10.0, 4.0 Hz, 1H), 1.56 – 1.47 (m, 2H), 1.06 – 0.84 (m, 2H), 0.78 (s, *J* = 17.4 Hz, 3H), 0.73 (s, 3H) overalps with 0.75– 0.70 (m, 1H), 0.57 (dd, *J* = 13.8, 3.6 Hz, 1H), 0.50 (s, 3H). **^{13}C NMR {1H}** (101 MHz, $CDCl_3$) δ 165.0, 140.9 (q, *J* = 38.3 Hz), 140.8, 137.7, 133.5, 133.4, 132.6, 130.6, 130.1, 126.1, 124.1, 121.7, 119.0 (q, *J* = 271.9 Hz), 111.1, 81.8, 48.9, 48.00, 44.7, 36.1, 27.9, 26.8, 19.7, 18.8, 13.2, **^{19}F NMR** (376 MHz, $CDCl_3$) δ (ppm) = -61.90, **HRMS** (ESI) m/z: [M+H]+ calculated for $C_{25}H_{26}F_3N_2O_2$: 443.1946 found: 443.1942, $[\alpha]_D^{22}$ = -3.33°(c= 0.09 $CHCl_3$).

***(P)*-(3*S*,8*S*,9*S*,10*R*,13*R*,14*S*,17*R*)-10,13-Dimethyl-17-((*R*)-6-methylheptan-2-yl)-2,3,4,7,8,9,10,11,12,13,14, 15,16,17-tetradecahydro-1*H*-cyclopenta[*a*]phenanthren-3-yl 2-(2-(trifluoromethyl)-1*H*-benzo[*d*]imidazol-1-yl)benzoate (*P*)-58**

(*P*)-1-Carboxyphenyl(2-trifluoromethy)benzimidazole **(*P*)-1** (40 mg, 0.13 mmol, 1 eq) and cholesterol (50 mg, 0.13 mmol, 1 eq) purified via column chromatography (hexane:ethylacetate 9:1, column dimensions: 1x10 cm). 64 mg of white foamy solid (72 %). **^{1}H NMR (**500MHz, $CDCl_3$)**:** δ 8.20 (dd, *J* = 7.6, 1.6 Hz, 1H), 7.88 (dd, *J* = 7.8, 1.3 Hz, 1H), 7.69 (ddd, *J* = 7.6, 7.5, 1.8 Hz, 1H), 7.64 (ddd, *J* = 7.6, 7.5, 1.5 Hz, 1H), 7.44 (d, *J* = 7.5 Hz, 1H), 7.33 (ddd, *J* = 7.8, 7.5, 1.1 Hz, 1H), 7.28 (td, *J* = 7.8, 7.5, 1.1 Hz, 1H), 6.91 (dd, *J* = 7.8, 1.3 Hz, 1H), 5.04 (m, 1H), 4.34 (dddd, *J* = 10.8, 10.8, 4.5 Hz, 1H), 0.50 (d, *J* = 7.0 Hz, 3H), 0.50 (d, *J* = 7.0 Hz, 3H), 0.50 (d, *J* = 7.0 Hz, 3H), 0.69 (s, 3H), 0.59 (s, 3H), 0.70 - 1.92 (overlapping multiplets) **^{13}C{^{1}H} NMR,** 126MHz, $CDCl_3$**:** δ 163.9, 141.2 (q, *J* =38.5), 140.6, 139.3, 138.1, 133.6, 133.6, 132.9, 130.7, 130.1, 130.0, 126.0, 124.0, 122.6, 121.4, 119.0 (q, *J* = 272.2), 111.0, 75.3, 56.7, 56.2, 50.0, 42.4, 39.8, 39.6, 36.7, 36.6, 36.5, 36.3, 35.9, 31.9, 31.8, 28.3, 29.1, 26.9, 24.4, 23.9, 23.0, 22.7, 21.0, 19.2, 18.8, 11.9 **^{19}F NMR** (376 MHz, $CDCl_3$) δ -61.98 **HRMS** (ESI) m/z: $[M+H]^+$ calculated for $C_{42}H_{54}O_2N_2F_3$: 675.4132, found: 675.4137 $[\alpha]_D^{22}$ = -96.41° (c= 0.64 $CHCl_3$).

***(M)*-(3*S*,8*S*,9*S*,10*R*,13*R*,14*S*,17*R*)-10,13-Dimethyl-17-((*R*)-6-methylheptan-2-yl)-2,3,4,7,8,9,10,11,12,13,14, 15,16,17-tetradecahydro-1*H*-cyclopenta[*a*]phenanthren-3-yl 2-(2-(trifluoromethyl)-1*H*-benzo[*d*]imidazol-1-yl)benzoate (*M*)-58**

(M)-1-Carboxyphenyl(2-trifluoromethy)benzimidazole **(*M*)-1** (40 mg, 0.13 mmol, 1 eq) and cholesterol (50 mg, 0.13 mmol, 1 eq) purified via column chromatography (hexane:ethylacetate 9:1, column dimensions: 1x10 cm). 57 mg of a white foamy solid (64 %). **^{1}H NMR** (500MHz, $CDCl_3$): δ 8.19 (dd, *J* = 7.6, 1.9 Hz, 1H), 7.88 (dd, *J* = 7.8, 1.3 Hz, 1H), 7.69 (ddd, *J* = 7.6, 7.5, 1.7 Hz, 1H), 7.64 (ddd, *J* = 7.6, 7.5, 1.4 Hz, 1H), 7.43 (d, *J* = 7.5 Hz, 1H), 7.33 (ddd, *J* = 7.8, 7.4, 1.2 Hz, 1H), 7.28 (ddd, *J* = 7.6, 7.4, 1.3 Hz, 1H), 6.91 (dt, *J* = 7.6, 1.0 Hz, 1H), 5.17 (ddd, *J* = 11.0, 11.0, 4.4 Hz, 1H), **^{13}C{^{1}H} NMR** (126MHz, $CDCl_3$): δ 163.9, 141.2 (q, *J* =38.4), 140.7, 139.2, 138.1, 133.6, 133.5, 132.8, 130.7, 130.1, 130.1, 126.0, 124.0, 123.0, 122.8, 121.5, 119.0 (q, *J* =272.1), 111.0, 75.3, 56.8, 56.2, 50.0, 42.4, 39.8, 39.6, 37.2, 36.7 36.5, 36.3, 35.9, 31.9, 31.8, 28.3, 28.1, 26.2, 25.7, 24.4, 23.9, 23.0, 22.7, 21.0, 19.3, 18.8, 12.0 **^{19}F NMR** (376 MHz, $CDCl_3$) δ -61.98 **HRMS** (ESI) m/z: $[M+H]^+$ calculated for $C_{42}H_{54}O_2N_2F_3$: 675.4132, found: 675.4132 $[\alpha]_D^{22}$ = +69.83° (c= 0.57 $CHCl_3$).

***(P)*-Benzyl (1*R*,3a*S*,5a*R*,5b*R*,7a*R*,9*S*,11a*R*,11b*R*,13a*R*,13b*R*)-5a,5b,8,8,11a-pentamethyl-1-(prop-1-en-2-yl)-9-((2-(2-(trifluoromethyl)-1*H*-benzo[*d*]imidazol-1-yl)benzoyl)oxy)icosahydro-3a*H*-cyclopenta[*a*]chrysene-3a-carboxylate (*P*)-59**

(P)-1-Carboxyphenyl(2-trifluoromethy)benzimidazole **(*P*)-1** (40 mg, 0.13 mmol, 1 eq) and benzyl betulinate (71 mg, 0.13 mmol, 1 eq) purified via column chromatography (hexane:ethylacetate 12:1, column dimensions: 1x10 cm). 37 mg of a white foamy solid (35 %). **^{1}H NMR** (500MHz, $CDCl_3$): δ 8.13 (dd, *J* = 7.5, 1.5 Hz, 1H), 7.86 (dd, *J* = 7.8, 1.0 Hz, 1H), 7.67 (ddd, *J* = 7.6, 7.5, 1.7 Hz, 1H), 7.62 (ddd, *J* = 7.6, 7.5, 1.4 Hz, 1H), 7.39 (d, *J* = 7.6 Hz, 1H), 7.32 (overlap, 1H), 7.29 (overlap, 1H), 7.21-7.30 (m, 5H), 6.96 (dt, *J* = 7.8, 1.3 Hz, 1H), 5.05 (d, 12.3 Hz, 1H), 5.00 (d, 12.3 Hz, 1H), 4.63 (d, 1.8

Hz, 1H), 4.51 (d, 1.8 Hz, 1H), 4.44 (dd, *J* = 11.9, 4.6 Hz, 1H), 2.92 (m, 1H), 2.16 (m, 1H), 2.05 (m, 1H), 1.68 (s, 3H), 0.81 (s, 3H), 0.62 (s, 3H), 0.58 (s, 3H), 0.52 (s, 3H), 0.11 (s, 3H), 0.70 - 1.92 (overlapping multiplets). **^{13}C{^{1}H} NMR** (126 MHz, $CDCl_3$)**:** δ 175.9, 164.4, 150.6, 141.9 (q, *J* =38.6), 140.8, 137.8, 136.60, 133.6, 133.2, 132.4, 130.6, 130.4, 130.0, 128.60 (2C), 128.4 (2C), 128.2, 125.8, 124.0, 121.5, 119.0 (q, *J* =272.1), 111.2, 109.7, 82.7, 65.8, 56.6, 55.4, 50.4, 49.5, 47.0, 42.4, 40.7, 38.4, 38.2, 37.8, 37.0, 34.2, 32.2, 30.7, 29.8, 29.6, 27.7, 25.5, 23.3, 20.9, 19.4, 18.1, 16.1, 15.8 14.7 **^{19}F NMR** (376 MHz, $CDCl_3$) δ -61.86 **HRMS** (ESI) m/z: $[M+H]^+$ calculated for $C_{52}H_{62}O_4N_2F_3$: 835.4656 found 835.4623 $[\alpha]_D^{22}$ = +4.05° (c= 0.37 $CHCl_3$).

(*M*)-Benzyl (1*R*,3a*S*,5a*R*,5b*R*,7a*R*,9*S*,11a*R*,11b*R*,13a*R*,13b*R*)-5a,5b,8,8,11a-pentamethyl-1-(prop-1-en-2-yl)-9-((2-(2-(trifluoromethyl)-1*H*-benzo[*d*]imidazol-1-yl)benzoyl)oxy)icosahydro-3a*H*-cyclopenta[*a*]chrysene-3a-carboxylate (*M*)-59

(*M***)**-1-Carboxyphenyl(2-trifluoromethy)benzimidazole **(*M*)-1** (40 mg, 0.13 mmol, 1 eq) and benzyl betulinate (71 mg, 0.13 mmol, 1 eq) purified via column chromatography (hexane:ethylacetate 12:1, column dimensions: 1x10 cm). 67 mg of white foamy solid (62 %). **^{1}H NMR** (500MHz, $CDCl_3$): δ 8.10 (dd, *J* = 7.6, 1.7 Hz, 1H), 7.86 (dd, *J* = 8.0, 1.0 Hz, 1H), 7.67 (ddd, *J* = 7.6, 7.5, 1.4 Hz, 1H), 7.62 (ddd, *J* = 7.6, 7.5, 1.2 Hz, 1H), 7.39 (d, *J* = 7.5 Hz, 1H), 7.31 (ddd, *J* = 8.0, 7.5, 1.2 Hz, 1H), 7.26 (overlap, 1H), 7.20-7.31 (m, 5H), 6.92 (dt, *J* = 8.0, 1.0 Hz, 1H), 4.63 (d, 1H), 5.06 (d, 12.2 Hz, 1H), 5.00 (d, 12.2 Hz, 1H), 4.63 (d, 1.8 Hz, 1H), 4.51 (d, 1.8 Hz, 1H), 4.33 (dd, *J* = 11.0, 4.9 Hz, 1H), 2.93 (m, 1H), 2.18 (m, 1H), 2.06 (m, 1H), 1.59 (s, 3H), 0.80 (s, 3H), 0.62 (s, 3H), 0.58 (s, 3H), 0.52 (s, 3H), 0.45 (s, 3H), 0.70 - 1.86 (overlapping multiplets). **^{13}C{^{1}H} NMR** (126MHz, $CDCl_3$)**:** δ 175.8, 164.7, 150.7, 140.84, 140.76 (q, *J* =38.5), 137.6, 136.6, 133.4, 133.3, 132.3, 130.5, 130.1, 129.9, 128.6 (2C), 128.4 (2C), 128.5, 126.0, 124.0, 121.6, 119.0 (q, *J* =271.8), 110.9, 109.8, 82.9, 65.8, 56.6, 55.4, 50.4, 49.5, 47.0, 42.4, 40.7, 38.4, 38.2, 37.7, 37.04, 37.00, 34.2, 32.2, 30.7, 29.8, 29.6, 27.9, 25.5, 22.5, 20.9, 19.5, 18.1, 16.3, 16.1, 15.9, 14.7 **^{19}F NMR** (376 MHz, $CDCl_3$) δ -61.45 **HRMS** (ESI) m/z: $[M+H]^+$ calculated for $C_{52}H_{62}O_4N_2F_3$: 835.4656, found: 835.4619, $[\alpha]_D^{22}$ = +100.77° (c= 0.52 $CHCl_3$).

(*P*)-(S)-2-Methylbutyl 2-(2-(trifluoromethyl)-1H-benzo[d]imidazol-1-yl)benzoate (*P*)-60

Purified by CC (Hexane:EtOAc 8:1), Yield: 10 mg, (53%), clear oil **^{1}H NMR** (400 MHz, $CDCl_3$) δ 8.27 – 8.22 (m, 1H), 7.96 – 7.92 (m, 1H), 7.73 (dtd, *J* = 21.4, 7.6, 1.6 Hz, 2H), 7.46 (dd, *J* = 7.6, 1.4 Hz, 1H), 7.37 (tdd, *J* = 14.9, 7.2, 1.3 Hz, 2H), 7.00 (ddd, *J* = 7.7, 1.5, 0.8 Hz, 1H), 3.77 (dd, *J* = 10.8, 6.0 Hz, 1H), 3.67 (dd, *J* = 10.8, 6.9 Hz, 1H), 1.20 (td, *J* = 13.1, 6.8 Hz, 1H), 1.11 – 0.99 (m, 1H), 0.92 – 0.80 (m, 1H), 0.72 (t, *J* = 7.4 Hz, 3H), 0.49 (d, *J* = 6.7 Hz, 3H). **^{13}C{^{1}H} NMR** (101 MHz, $CDCl_3$) δ 164.7, 141.1 (q, J = 39.4 Hz), 140.9, 137.8, 133.9, 133.5, 132.7, 130.6, 130.1, 129.6, 126.0, 124.0, 121.6, 119.0 (q, *J* = 271.8 Hz), 110.9, 70.7, 33.8, 25.8, 15.9, 11.0. **^{19}F NMR** (376 MHz, $CDCl_3$) δ -61.4. **HRMS** (ESI) m/z: $[M + H]^+$ calcd. for $C_{20}H_{20}F_3N_2O_2$: 377.1471; found: 377.1470, $[\alpha]_d^{22}$ -47.14° (c= 0.10, $CHCl_3$).

(*M*)-(*S*)-2-Methylbutyl 2-(2-(trifluoromethyl)-1*H*-benzo[*d*]imidazol-1-yl)benzoate (*M*)-60

Purified by CC (Hexane:EtOAc 8:1), Yield: 14 mg (74%), clear oil **^{1}H NMR** (400 MHz, $CDCl_3$) δ 8.26 – 8.22 (m, 1H), 7.96 – 7.92 (m, 1H), 7.76 (td, *J* = 7.6, 1.8 Hz, 1H), 7.70 (td, *J* = 7.6, 1.5 Hz, 1H), 7.46 (dd, *J* = 7.6, 1.4 Hz, 1H), 7.41 – 7.32 (m, 2H), 7.00 (ddd, *J* = 7.7, 1.5, 0.8 Hz, 1H), 3.71 (qd, *J* = 10.8, 6.5 Hz, 2H), 1.18 (dddd, *J* = 13.3, 7.8, 6.6, 5.5 Hz, 1H), 0.97 – 0.86 (m, 2H), 0.85 – 0.71 (m, 2H), 0.66 (t, *J* = 7.3 Hz, 3H), 0.60 (d, *J* = 6.8 Hz, 3H). **^{13}C{^{1}H} NMR** (101 MHz, $CDCl_3$) δ 164.7, 141.1 (q, J = 38.6 Hz), 140.8, 137.8, 137.7, 133.9, 133.5, 132.7, 130.6, 130.1, 129.6, 126.0, 124.0, 121.6, 119.0 (q, J = 272.0 Hz), 110.9, 70.7, 33.7, 25.7, 16.0, 11.0. **^{19}F NMR** (376 MHz, $CDCl_3$) δ -62.0. **HRMS** (ESI) m/z: $[M + H]^+$ calcd. for $C_{20}H_{20}F_3N_2O_2$: 377.1471; found: 377.1470, $[\alpha]_d^{22}$ +57.00° (c= 0.14, $CHCl_3$).

(*P*)-(*R*)-3-Bromo-2-methylpropyl 2-(2-(trifluoromethyl)-1*H*-benzo[*d*]imidazol-1-yl)benzoate (*P*)-61

Purified by CC (Hexane:EtOAc 10:1) Yield: 13.3 mg (60%), clear oil **^{1}H NMR** (400 MHz, $CDCl_3$) δ 8.25 (ddd, *J* = 7.8, 1.7, 0.5 Hz, 1H), 7.96 – 7.93 (m, 1H), 7.78 (td, *J* = 7.6, 1.8 Hz, 1H), 7.72 (td, *J* = 7.6, 1.4 Hz, 1H), 7.48 (dd, *J* = 7.7, 1.4 Hz, 1H), 7.48 (dd, *J* = 7.7, 1.4 Hz, 1H), 7.43 – 7.34 (m, 2H), 7.00 (ddd, *J* = 7.7, 1.5, 0.8 Hz, 1H), 3.85 (dd, *J* = 6.3, 0.8 Hz, 2H), 2.96 (qd, *J* = 10.3, 5.3 Hz, 2H), 1.67 (dqd, *J* = 13.3, 6.7, 1.4 Hz, 1H), 0.68 (d, *J* = 6.8 Hz, 3H). **^{13}C NMR{^{1}H}** (101 MHz, $CDCl_3$) δ 164.4, 141.0 (q, J = 38.5 Hz), 140.8, 137.7, 133.9, 133.8, 132.8, 130.7, 130.2, 129.1, 126.2, 124.2, 121.7, 119.0 (q, J = 271.5 Hz), 110.8, 68.1, 36.3, 34.2, 15.4 **^{19}F NMR** (376 MHz, $CDCl_3$) δ -61.9. **HRMS** (ESI- TOF) m/z: $[M + H]^+$ calcd. for $C_{19}H_{17}BrF_3N_2O_2$: 441.0420; found: 441.0422, $[\alpha]_d^{22}$ -70.77° (c= 0.13, $CHCl_3$).

(*M*)-(*R*)-3-Bromo-2-methylpropyl 2-(2-(trifluoromethyl)-1*H*-benzo[*d*]imidazol-1-yl)benzoate (*M*)-61

Purified by CC (Hexane:EtOAc 10:1) Yield: 10 mg (45%), clear oil **^{1}H NMR** (400 MHz, $CDCl_3$) δ 8.26 (dd, *J* = 7.8, 1.6 Hz, 1H), 7.97 – 7.93 (m, 5H), 7.79 (td, *J* = 7.6, 1.8 Hz, 1H), 7.73 (td, *J* = 7.6, 1.4 Hz, 1H), 7.49 (dd, *J* = 7.7, 1.3 Hz, 1H), 7.40 (pd, *J* = 7.2, 1.4 Hz, 1H), 7.05 – 6.99 (m, 1H), 3.89 (dd, *J* = 11.1, 7.6 Hz, 1H), 3.81 (dd, *J* = 11.1, 5.2 Hz, 1H), 2.83 (dd, *J* = 10.3, 4.8 Hz, 1H), 2.63 (dd, *J* = 10.3, 5.1 Hz, 1H), 1.55 (dtdd, *J* = 11.9, 6.8, 5.1, 1.7 Hz, 1H), 0.76 (d, *J* = 6.8 Hz, 3H). **^{13}C{^{1}H} NMR** (101 MHz, $CDCl_3$) δ 164.4, 141.1 (d, J = 40.0 Hz), 140.7, 137.7, 133.9, 133.8, 132.9, 130.8, 130.1, 129.2, 126.2, 124.3, 121.7, 119.0 (q, *J* = 271.9 Hz), 110.9, 67.9, 36.4, 33.9, 15.4. **^{19}F NMR** (471 MHz, $CDCl_3$) δ -62.0. **HRMS** (ESI- TOF) m/z: $[M + H]^+$ calcd. for $C_{19}H_{17}BrF_3N_2O_2$: 441.0420; found: 441.0421, $[\alpha]_d^{22}$ +25° (c= 0.1, $CHCl_3$).

(*P*)-(*R*)-3-Methoxy-2-methyl-3-oxopropyl 2-(2-(trifluoromethyl)-1*H*-benzo[*d*]imidazol-1-yl)benzoate (*P*)-62

Purified by CC (Hexane:EtOAc 4:1) Yield: 11.2 mg (55%), white foam **^{1}H NMR** (400 MHz, $CDCl_3$) δ 8.23 – 8.19 (m, 1H), 7.95 (ddd, *J* = 8.1, 1.3, 0.8 Hz, 1H), 7.77 (td, *J* = 7.6, 1.7 Hz, 1H), 7.70 (td, *J* = 7.7, 1.4 Hz, 1H), 7.48 (dd, *J* = 7.7, 1.3 Hz, 1H), 7.40 (ddd, *J* = 8.1, 7.2, 1.4 Hz, 1H), 7.35 (td, *J* = 7.7, 7.2, 1.4 Hz, 1H), 4.14 (dd, *J* = 11.0, 7.2 Hz, 1H), 3.86 (dd, *J* = 11.0, 6.1 Hz, 1H), 3.63 (s, 3H), 2.27 (td, *J* = 7.2, 6.1 Hz, 1H), 0.83 (d, *J* = 7.2 Hz, 3H). **^{13}C NMR{^{1}H}** (101 MHz, $CDCl_3$) δ 173.8, 164.1, 141.1 (q, J = 39.0 Hz) 140.8, 137.7, 134.0, 133.8, 132.7, 130.7, 130.1, 129.0, 126.1, 124.1, 121.6, 118.9 (q, J = 272.1 Hz) 110.8, 66.7, 52.0, 38.5, 13.7. **^{19}F NMR** (471 MHz, $CDCl_3$) δ -62.1.**HRMS** (ESI) m/z: $[M + H]^+$ calcd. for $C_{20}H_{18}F_3N_2O_4$: 407.1213; found: 407.1212, $[\alpha]_d^{22}$ -70.0° (c= 0.11, $CHCl_3$).

(*M*)-(*R*)-3-Methoxy-2-methyl-3-oxopropyl 2-(2-(trifluoromethyl)-1*H*-benzo[*d*]imidazol-1-yl)benzoate (*M*)-62

Purified by CC (Hexane:EtOAc 4:1) Yield: 10 mg (50%), white foam **^{1}H NMR** (400 MHz, $CDCl_3$) δ 8.23 – 8.20 (m, 1H), 7.96 – 7.93 (m, 1H), 7.77 (td, *J* = 7.6, 1.7 Hz, 1H), 7.70 (td, *J* = 7.7, 1.4 Hz, 1H), 7.47 (dd, *J* = 7.7, 1.3 Hz, 1H), 7.40 (ddd, *J* = 8.1, 7.2, 1.3 Hz, 1H), 7.35 (td, *J* = 7.7, 7.2, 1.3 Hz, 1H), 6.97 (ddd, *J* = 7.9, 1.3, 0.8 Hz, 1H), 4.12 (dd, *J* = 11.0, 7.2 Hz, 1H), 3.96 (dd, *J* = 11.0, 5.8 Hz, 1H), 3.57 (s, 3H), 2.33 (td, *J* = 7.2, 5.8 Hz, 1H), 0.94 (d, *J* = 7.2 Hz, 3H). **^{13}C NMR{^{1}H}** (101 MHz, $CDCl_3$) δ 173.7, 164.0, 141.0 (q, J = 38.4 Hz), 140.8, 137.7, 134.1, 133.8, 132.7, 130.7, 130.1, 129.0, 126.0, 124.0, 121.6, 119.0 (q, J = 271.9 Hz) 110.8, 66.6, 52.0, 38.5, 13.8. **^{19}F NMR** (471 MHz, $CDCl_3$) δ -62.0. **HRMS** (ESI) m/z: $[M + H]^+$ calcd. for $C_{20}H_{18}F_3N_2O_4$: 407.1213; found: 407.1214, $[\alpha]_d^{22}$ +49.0° (c= 0.10, $CHCl_3$).

(*P*)-(S)-2-(Dimethylamino)-3-methylbutyl 2-(2-(trifluoromethyl)-1H-benzo[d]imidazol-1-yl)benzoate (*P*)-63

Purified by HPLC, Yield: 8 mg (38%), clear oil **^{1}H NMR** (500 MHz, $CDCl_3$) δ 8.22 (dd, *J* = 7.9, 1.5 Hz, 1H), 7.96 (dt, *J* = 8.2, 1.1 Hz, 1H), 7.77 (td, *J* = 7.6, 1.7 Hz, 1H), 7.71 (td, *J* = 7.7, 1.4 Hz, 1H), 7.47 (dd, *J* = 7.7, 1.3 Hz, 1H), 7.40 (ddd, *J* = 8.2, 7.2, 1.3 Hz, 1H), 7.38 – 7.34 (m, 1H), 7.00 (ddd, *J* = 8.0, 0.8 Hz, 1H), 4.07 (dd, *J* = 12.1, 5.5 Hz, 1H), 4.01 (dd, *J* = 12.1, 3.4 Hz, 1H), 2.04 (s, 6H), 1.78 – 1.73 (m, 1H), 1.63 (dq, *J* = 13.9, 6.8 Hz, 1H), 0.87 (d, *J* = 6.7 Hz, 3H), 0.74 (d, *J* = 6.7 Hz, 3H). **^{13}C NMR{^{1}H}**

(126 MHz, $CDCl_3$) δ 164.3, 141.5, 141.2, 140.9, 140.9, 140.6, 137.8, 134.0, 133.6, 132.5, 130.7, 130.1, 129.4, 126.0, 124.1, 121.7, 119.0 (q, J = 272.0 Hz), 111.0, 68.2, 63.1, 41.6, 31.1, 28.2, 19.2. **^{19}F NMR** (376 MHz, $CDCl_3$) δ -61.9. **HRMS** (ESI) m/z: $[M + H]^+$ calcd. for $C_{22}H_{25}F_3N_3O_2$: 420.1893; found: 420.1891, $[\alpha]_d^{22}$ -878.75° (c= 0.08, $CHCl_3$).

(*M*)-(*S*)-2-(Dimethylamino)-3-methylbutyl 2-(2-(trifluoromethyl)-1*H*-benzo[*d*]imidazol-1-yl)benzoate (*M*)-63

Purified by HPLC, Yield: 5 mg (23%), clear oil **^{1}H NMR** (500 MHz, $CDCl_3$) δ 8.23 – 8.21 (m, 1H), 7.97 – 7.94 (m, 1H), 7.77 (td, *J* = 7.6, 1.7 Hz, 1H), 7.71 (td, *J* = 7.7, 1.4 Hz, 1H), 7.48 (dd, *J* = 7.6, 1.1 Hz, 1H), 7.40 (ddd, *J* = 8.2, 7.2, 1.3 Hz, 1H), 7.35 (ddd, *J* = 8.3, 7.2, 1.2 Hz, 1H), 7.00 (ddd, *J* = 8.0, 0.8 Hz, 1H), 4.03 (d, *J* = 4.5 Hz, 2H), 2.13 (s, 6H), 1.77 (br.s, 1H), 1.55 – 1.46 (m, 1H), 0.76 (d, *J* = 6.7 Hz, 3H), 0.61 (d, *J* = 6.7 Hz, 3H). **^{13}C NMR{^{1}H}** (126 MHz, $CDCl_3$) δ 164.4, 141.06 (app. d, J = 38.6 Hz), 140.9, 137.7, 134.0, 133.6, 132.5, 130.7, 130.1, 129.4, 126.0, 124.1, 121.7, 119.00 (app. d, J = 272.1 Hz), 110.9, 68.1, 63.2, 41.6, 31.1, 28.2, 20.6, 19.3. **^{19}F NMR** (376 MHz, $CDCl_3$) δ -61.9. **HRMS** (ESI) m/z: $[M + H]^+$ calcd. for $C_{22}H_{25}F_3N_3O_2$: 420.1893; found: 420.1892, $[\alpha]_d^{22}$ -56.0° (c= 0.05, $CHCl_3$).

(*P*)-(2*S*)-3-((9-Methyl-3-oxa-9-azatricyclo[3.3.1.02,4]nonan-7-yl)oxy)-3-oxo-2-phenylpropyl 2-(2-(trifluoromethyl)-1*H*-benzo[*d*]imidazol-1-yl)benzoate (*P*)-64

Following literature procedure:[1] Scopolamine hydrobromide trihydrate (80 mg, 0.18 mmol) was dissolved in DI water (5 mL) and 10% NaOH solution was added dropwise (4 drops) until pH of the solution was around 10. The solution was extracted 3× with diethylether. Oganic layers were washed with brine, dried with $MgSO_4$ and evaporated to yield scopolamine freebase. Scopolamine freebase was then esterified according to general procedure.

Purified by CC (gradient Hexane:EtOAc 1:2 → EtOAc) Yield 12 mg (40%), light yellow oil **^{1}H NMR** (500 MHz, $CDCl_3$) δ 8.13 (dd, *J* = 7.8, 1.7 Hz, 1H), 7.96 (dt, *J* = 8.2, 0.9 Hz, 1H), 7.76 (td, *J* = 7.7, 1.6 Hz, 1H), 7.68 (td, *J* = 7.7, 1.3 Hz, 1H), 7.46 (dd, *J* = 7.9, 1.0 Hz, 1H), 7.41 (ddd, *J* = 8.2, 7.2, 1.2 Hz, 1H), 7.36 – 7.33 (m, 1H), 7.31 – 7.24 (m, 3H), 7.06 (dd, *J* = 7.6, 1.9 Hz, 2H), 6.95 (dt, *J* = 8.2, 0.9 Hz, 1H), 4.82 (t, *J* = 5.5 Hz, 1H), 4.48 (dd, *J* = 11.1, 8.7 Hz, 1H), 4.15 (dd, *J* = 11.1, 6.1 Hz, 1H), 3.31 (dd, *J* = 8.7, 6.1 Hz, 1H), 3.26 (d, *J* = 3.0 Hz, 1H), 3.08 (s, 1H), 2.90 (s, 1H), 2.48 (d, *J* = 3.0 Hz, 1H), 2.44 (s, 3H), 2.12 – 2.05 (m, 1H), 1.93 (dt, *J* = 14.8, 4.1 Hz, 1H), 1.52 (d, *J* = 15.1 Hz, 1H), 1.19 (d, *J* = 15.3 Hz, 1H). **^{13}C NMR{^{1}H}** (126 MHz, $CDCl_3$) δ 169.5, 163.9, 141.1 (app. d, *J* = 38.4 Hz), 140.8, 137.7, 134.9, 134.1, 133.9, 132.6, 130.7, 130.1, 129.2, 128.4, 127.9, 126.1, 124.0, 121.5, 118.95 (app. d, *J* = 272.1 Hz), 110.9, 67.1, 65.3, 58.0, 57.9, 56.4, 55.9, 50.3, 42.5, 31.1, 30.8. **^{19}F NMR** (471 MHz, $CDCl_3$) δ -61.94. **HRMS** (ESI) m/z: $[M+H]^+$ calcd. for $C_{32}H_{29}O_5N_3F_3$: 592.2054 found: 592.2054.

(*M*)-(2*S*)-3-((9-Methyl-3-oxa-9-azatricyclo[3.3.1.02,4]nonan-7-yl)oxy)-3-oxo-2-phenylpropyl 2-(2-(trifluoromethyl)-1*H*-benzo[*d*]imidazol-1-yl)benzoate (*M*)-64

Purified by CC (gradient Hexane:EtOAc 1:2 → EtOAc) Yield 10 mg (34%), light yellow oil **^{1}H NMR** (500 MHz, $CDCl_3$) δ 8.16 (dd, *J* = 7.8, 1.4 Hz, 1H), 7.98 (dt, *J* = 8.2, 0.9 Hz, 1H), 7.77 (td, *J* = 7.7, 1.7 Hz, 1H), 7.69 (td, *J* = 7.7, 1.3 Hz, 1H), 7.48 (d, *J* = 7.7 Hz, 1H), 7.45 (ddd, *J* = 8.3, 7.2, 1.1 Hz, 1H), 7.37 (ddd, *J* = 8.2, 7.2, 1.1 Hz, 1H), 7.25 (d, *J* = 2.3 Hz, 3H), 6.96 (dt, *J* = 8.2, 1.0 Hz, 1H), 6.94 – 6.91 (m, 2H), 4.91 (t, *J* = 5.5 Hz, 1H), 4.56 (dd, *J* = 11.0, 9.4 Hz, 1H), 3.88 (dd, *J* = 11.1, 5.4 Hz, 1H), 3.40 (d, *J* = 2.9 Hz, 1H), 3.13 (s, 1H), 3.09 (dd, *J* = 9.4, 5.4 Hz, 1H), 2.90 (s, 1H), 2.46 (s, 1H), 2.45 (s, 3H), 2.11 (d, *J* = 15.4 Hz, 1H), 1.94 (d, *J* = 15.1 Hz, 1H), 1.69 (d, *J* = 15.0 Hz, 1H), 1.18 (d, *J* = 15.3 Hz, 1H). **^{13}C NMR{^{1}H}** (126 MHz, $CDCl_3$) δ 169.6, 164.0, 141.16 (app.d, J = 38.7 Hz), 140.8, 137.8, 137.8, 134.7, 134.0, 133.9, 132.7, 130.7, 130.1, 128.9, 128.3, 127.8, 126.2, 124.2, 121.5, 120.0 (q, J = 272.2 Hz) 110.9, 67.1, 65.4, 58.1, 57.9, 56.5, 55.9, 50.2, 42.3, 30.8, 30.7. **^{19}F NMR** (471 MHz, $CDCl_3$) δ -61.88. **HRMS** (ESI) m/z: $[M+H]^+$ calcd. for $C_{32}H_{29}O_5N_3F_3$: 592.2054 found: 592.2055.

(*P*)-(*S*)-2-(6-Methoxynaphthalen-2-yl)propyl 2-(2-(trifluoromethyl)-1*H*-benzo[*d*]imidazol-1-yl)benzoate (*P*)-65

Purified by CC (Hexane:EtOAc 6,5:1) Yield: 11 mg (44%), clear foam **^{1}H NMR** (500 MHz, $CDCl_3$) δ 8.13 (dd, *J* = 7.9, 1.6 Hz, 1H), 7.96 (dt, *J* = 8.2, 0.9 Hz, 1H), 7.74 (td, *J* = 7.7, 1.6 Hz, 1H), 7.69 – 7.61 (m, 3H), 7.47 (dd, *J* = 7.7, 0.8 Hz, 1H), 7.44 – 7.35 (m, 2H), 7.31 (ddd, *J* = 8.2, 7.2, 1.1 Hz, 1H), 7.15 (dd, *J* = 8.5, 1.8 Hz, 1H), 7.12 (dd, *J* = 8.9, 2.5 Hz, 1H), 7.08 (d, *J* = 2.5 Hz, 1H), 6.96 (dt, *J* = 8.2, 0.9 Hz, 1H), 4.08 (dd, *J* = 10.8, 6.5 Hz, 1H), 3.99 (dd, *J* = 10.8, 8.1 Hz, 1H), 3.90 (s, 3H), 2.76 – 2.68 (m, 1H), 0.93 (d, *J* = 7.0 Hz, 3H). **^{13}C NMR{^{1}H}** (126 MHz, $CDCl_3$) δ 164.4, 157.6, 141.1 (q, *J* = 38.7 Hz), 140.9, 137.8, 134.0, 133.6, 132.6, 130.6, 130.0, 129.4, 129.3, 129.1, 127.1, 126.2, 126.0, 125.5, 124.1, 121.6, 119.0 (q, *J* = 271.9 Hz), 119.0, 110.9, 105.7, 70.7, 55.4, 38.6, 17.9. **^{19}F NMR** (471 MHz, $CDCl_3$) δ -61.96 **HRMS** (ESI) m/z: $[M+H]^+$ calcd. for $C_{29}H_{24}F_3O_3N_2$: 505.1734; found: 505.1736 $[\propto]_d^{22}$**:** -75.46(c= 0.11 $CHCl_3$).

(*M*)-(*S*)-2-(6-Methoxynaphthalen-2-yl)propyl 2-(2-(trifluoromethyl)-1*H*-benzo[*d*]imidazol-1-yl)benzoate (*M*)-65

Purified by CC (Hexane:EtOAc 6,5:1) Yield: 12 mg (50%), clear foam **^{1}H NMR** (500 MHz, $CDCl_3$) δ 8.13 (dd, *J* = 7.9, 1.6 Hz, 1H), 7.97 (dt, *J* = 8.2, 0.9 Hz, 1H), 7.74 (td, *J* = 7.7, 1.6 Hz, 1H), 7.66 (td, *J* = 7.7, 1.3 Hz, 1H), 7.61 (t, *J* = 8.8 Hz, 2H), 7.47 (d, *J* = 7.8 Hz, 1H), 7.41 (ddd, *J* = 8.3, 7.2, 1.1 Hz, 1H), 7.34 (ddd, *J* = 8.2, 7.2, 1.1 Hz, 1H), 7.30 (d, *J* = 1.1 Hz, 1H), 7.11 (dd, *J* = 8.8, 2.6 Hz, 1H), 7.07 (d, *J* = 2.5 Hz, 1H), 7.05 (dd, *J* = 8.4, 1.8 Hz, 1H), 6.96 (dt, *J* = 8.2, 0.9 Hz, 1H), 4.09 (dd, *J* = 10.9, 6.5 Hz, 1H), 3.99 (dd, *J* = 10.9, 7.9 Hz, 1H), 3.90 (s, 3H), 2.73 – 2.61 (m, 1H), 1.08 (d, *J* = 7.0 Hz, 3H). **^{13}C NMR{^{1}H}** (126 MHz, $CDCl_3$) δ 164.4, 157.6, 141.2 (q, *J* = 38.4 Hz), 140.9, 137.8, 137.8, 134.0, 133.6, 132.6, 130.6, 130.0, 129.3, 129.2, 129.1, 127.1, 126.2, 126.1, 125.4, 124.1, 121.6, 119.0 (q, *J* = 272.1 Hz), 118.9, 110.9, 105.7, 70.7, 55.4, 38.5, 18.1. **^{19}F NMR** (471 MHz, $CDCl_3$) δ -61.93. **HRMS** (ESI) m/z: $[M+H]^+$ calcd. for $C_{29}H_{24}F_3O_3N_2$: 505.1734; found: 505.1734 $[\propto]_d^{22}$**:** +61.88 (c= 0.12 $CHCl_3$).

(*P*)-(*R*)-Oxiran-2-ylmethyl 2-(2-(trifluoromethyl)-1*H*-benzo[*d*]imidazol-1-yl)benzoate (*P*)-66 *

Purified by CC (Hexane:EtOAc 3:1) Yield: 7 mg (38%), clear oil **^{1}H NMR** (500 MHz, $CDCl_3$) δ 8.27 (dd, *J* = 7.8, 1.7 Hz, 1H), 7.96 – 7.93 (m, 1H), 7.80 (td, *J* = 7.7, 1.7 Hz, 1H), 7.73 (td, *J* = 7.7, 1.3 Hz, 1H), 7.52 (dd, *J* = 7.8, 0.8 Hz, 1H), 7.38 (dtd, *J* = 15.1, 7.2, 1.2 Hz, 2H), 6.98 (ddd, *J* = 7.9, 1.2, 0.7 Hz, 1H), 3.91 (qd, *J* = 12.0, 5.1 Hz, 2H), 2.71 (dtd, *J* = 6.0, 4.2, 2.5 Hz, 1H), 2.59 – 2.56 (m, 1H), 2.20 (dd, *J* = 4.8, 2.6 Hz, 1H). **^{13}C NMR{^{1}H}** (126 MHz, $CDCl_3$) δ 163.9, 140.9 (app. d, *J* = 38.2 Hz), 140.9, 137.8, 134.2, 134.0, 132.8, 130.7, 130.2, 128.8, 126.1, 124.1, 121.6, 119.0 (app. d, *J* = 272.4 Hz), 110.8, 66.4, 48.4, 44.8. **^{19}F NMR** (376 MHz, $CDCl_3$) δ -62.06. **HRMS** (ESI) m/z: $[M+H]^+$ calcd. for $C_{18}H_{14}F_3N_2O_3$: 363.0957; found: 363.0950 $[\propto]_d^{22}$**:**-25,71° (c= 0.07 $CHCl_3$).

**S-alcohol was used. The priority of substituents changed after esterification.*

(*M*)-(*R*)-Oxiran-2-ylmethyl 2-(2-(trifluoromethyl)-1*H*-benzo[*d*]imidazol-1-yl)benzoate (*M*)-66 *

Purified by CC (Hexane:EtOAc 3:1) Yield: 6 mg (33%), clear oil **^{1}H NMR** (500 MHz, $CDCl_3$) δ 8.31 – 8.24 (m, 1H), 7.94 (ddd, *J* = 8.1, 1.3, 0.8 Hz, 1H), 7.77 (dtd, *J* = 35.3, 7.6, 1.5 Hz, 2H), 7.52 (d, *J* = 7.8 Hz, 1H), 7.44 – 7.33 (m, 2H), 7.00 (ddd, *J* = 7.8, 1.4, 0.8 Hz, 1H), 3.98 (dd, *J* = 12.0, 4.2 Hz, 1H), 3.88 (dd, *J* = 12.1, 5.8 Hz, 1H), 2.59 (tt, *J* = 4.8, 2.4 Hz, 1H), 2.56 (tdd, *J* = 5.9, 3.7, 2.1 Hz, 1H), 2.32 (dd, *J* = 4.8, 2.6 Hz, 1H). **^{13}C NMR{^{1}H}** (126 MHz, $CDCl_3$) δ 163.9, 141.1 (app. d, *J* = 38.2 Hz), 140.8, 137.8, 134.2, 134.0, 132.8, 130.8, 130.2, 128.8, 126.1, 124.1, 121.6, 119.00 (q, *J* = 271.8 Hz), 110.9, 66.4, 48.4, 44.8. **^{19}F NMR** (376 MHz, $CDCl_3$) δ -62.08. **HRMS** (ESI) m/z: $[M+H]^+$ calcd. for $C_{18}H_{14}F_3N_2O_3$: 363.0957; found: 363.0950. $[\propto]_d^{22}$**:** +20,00° (c= 0.06 $CHCl_3$).

**S-alcohol was used. The priority of substituents changed after esterification.*

(*P*)-(*S*)-(Tetrahydrofuran-2-yl)methyl 2-(2-(trifluoromethyl)-1*H*-benzo[*d*]imidazol-1-yl)benzoate (*P*)-67

Purified by CC (Hexane:EtOAc 3,5:1) Yield: 15 mg (77%), clear oil **^{1}H NMR** (400 MHz, $CDCl_3$) δ 8.26 (dd, *J* = 7.8, 1.6 Hz, 1H), 7.98 – 7.91 (m, 1H), 7.73 (dtd, *J* = 25.4, 7.6, 1.5 Hz, 2H), 7.47 (dd, *J* = 7.7, 1.3 Hz, 1H), 7.42 – 7.33 (m, 2H), 7.02 – 6.98 (m, 1H), 3.89 (d, *J* = 0.5 Hz, 1H), 3.87 (s, 1H), 3.72 – 3.65 (m, 1H), 3.61 – 3.54 (m, 1H), 3.48 (ddd, *J* = 12.4, 6.8, 5.7 Hz, 1H), 1.79 – 1.66 (m, 3H), 1.29 –

1.20 (m, 1H). **^{13}C NMR{^{1}H}** (101 MHz, $CDCl_3$) δ 164.2, 141.1 (q, *J*= 38.4 Hz), 140.8, 137.8, 134.1, 133.7, 132.7, 130.6, 130.1, 129.2, 126.0, 124.0, 121.5, 119.0 (q, *J* = 272.0 Hz), 110.9, 75.8, 68.3, 67.4, 28.0, 25.5. **^{19}F NMR** (376 MHz, $CDCl_3$) δ -62.0 **HRMS** (ESI) m/z: $[M+H]^+$ calcd. for $C_{20}H_{18}F_3N_2O_3$: 391.1270; found: 391.1264. $[\propto]_d^{22}$**:** -68,46° (c= 0.13 $CHCl_3$).

(*M*)-(*S*)-(Tetrahydrofuran-2-yl)methyl 2-(2-(trifluoromethyl)-1*H*-benzo[*d*]imidazol-1-yl)benzoate (*M*)-67

Purified by CC (Hexane:EtOAc 3,5:1) Yield 11 mg (56%), clear oil **^{1}H NMR** (400 MHz, $CDCl_3$) δ 8.26 (dd, *J* = 7.7, 1.8 Hz, 1H), 7.97 – 7.91 (m, 1H), 7.73 (dtd, *J* = 25.6, 7.6, 1.5 Hz, 2H), 7.47 (dd, *J* = 7.7, 1.3 Hz, 1H), 7.37 (dtd, *J* = 15.0, 7.2, 1.3 Hz, 2H), 7.02 – 6.96 (m, 1H), 3.88 (ddd, *J* = 16.2, 11.3, 5.6 Hz, 2H), 3.72 – 3.59 (m, 3H), 1.77 – 1.66 (m, 2H), 1.63 – 1.54 (m, 1H), 1.12 (ddd, *J* = 15.6, 12.4, 7.5 Hz, 1H). **^{13}C NMR{^{1}H}** (101 MHz, $CDCl_3$) δ 164.2, 141.3 (app.d, *J*= 38.6 Hz), 140.9, 140.8, 137.7, 134.1, 133.7, 132.7, 130.6, 130.1, 129.1, 125.9, 124.0, 121.5, 119.0 (q, J = 272.0 Hz), 110.9, 75.9, 68.3, 67.3, 28.0, 25.5. **^{19}F NMR** (376 MHz, $CDCl_3$) δ -62.04. **HRMS** (ESI) m/z: $[M + H]^+$ calcd. For $C_{20}H_{18}F_3N_2O_3$: 391.1270; found:391.1264 $[\boldsymbol{\alpha}]_{\boldsymbol{d}}^{\boldsymbol{22}}$ +86.67° (c= 0.12 $CHCl_3$).

(*P*)-(*S*)-(5-Oxotetrahydrofuran-2-yl)methyl 2-(2-(trifluoromethyl)-1*H*-benzo[*d*]imidazol-1-yl)benzoate (*P*)-68

Purified by CC (Hexane:EtOAc 2:1) Yield 9 mg (44%), clear oil **^{1}H NMR** (500 MHz, $CDCl_3$) δ 8.24 (dd, *J* = 7.7, 1.5 Hz, 1H), 7.97 – 7.92 (m, 1H), 7.81 (td, *J* = 7.7, 1.6 Hz, 1H), 7.73 (td, *J* = 7.7, 1.3 Hz, 1H), 7.51 (d, *J* = 7.2 Hz, 1H), 7.40 (pd, *J* = 7.2, 1.3 Hz, 1H), 7.01 (dd, *J* = 7.0, 1.5 Hz, 1H), 4.12 – 4.07 (m, 1H), 4.07 – 4.04 (m, 2H), 2.45 – 2.41 (m, 2H), 2.13 – 2.06 (m, 1H), 1.71 – 1.64 (m, 1H).**^{13}C NMR{^{1}H}** (126 MHz, $CDCl_3$) δ 176.1, 163.7, 140.9 (q, J = 38.4 Hz)140.7, 137.7, 134.2, 134.2, 132.7, 130.9, 130.3, 128.4, 126.3, 124.3, 121.5, 119.0 (q, J = 272.0 Hz) 111.0, 76.6, 66.1, 28.0, 23.9. **^{19}F NMR** (376 MHz, $CDCl_3$) δ -61.97. **HRMS** (ESI) m/z: $[M+H]^+$ calcd. for $C_{20}H_{16}F_3N_2O_4$: 405.1057; found: 405.1056 $[\propto]_d^{22}$: -62.50° (c= 0.04 $CHCl_3$).

(*M*)-(*S*)-(5-Oxotetrahydrofuran-2-yl)methyl 2-(2-(trifluoromethyl)-1*H*-benzo[*d*]imidazol-1-yl)benzoate (*M*)-68

Purified by CC (Hexane:EtOAc 2:1)Yield 8.5 mg (42%), clear oil **^{1}H NMR** (500 MHz, $CDCl_3$) δ 8.26 – 8.23 (m, 1H), 7.97 – 7.94 (m, 1H), 7.81 (td, *J* = 7.7, 1.7 Hz, 1H), 7.73 (td, *J* = 7.7, 1.3 Hz, 1H), 7.51 (dd, *J* = 7.8, 1.2 Hz, 1H), 7.44 – 7.39 (m, 1H), 7.37 (td, *J* = 7.7, 7.2, 1.3 Hz, 1H), 7.00 (ddd, *J* = 8.0, 1.3, 0.8 Hz, 1H), 4.32 (tdd, *J* = 7.4, 5.8, 4.3 Hz, 1H), 4.10 (dd, *J* = 12.0, 4.3 Hz, 1H), 4.03 (dd, *J* = 12.0, 5.8 Hz, 1H), 1.93 (dddd, *J* = 13.1, 9.8, 7.3, 5.0 Hz, 1H), 1.47 – 1.40 (m, 1H). **^{13}C NMR{^{1}H}** (126 MHz, $CDCl_3$) δ 176.0, 163.8, 141.20 (q, J = 38.2, 37.7 Hz) , 140.8, 137.7, 134.2, 132.8, 130.8, 130.2, 128.4, 128.2, 126.2, 124.2, 121.7, 118.9 (q, J = 272.2 Hz), 110.8, 76.7, 65.9, 28.0, 23.9. **^{19}F NMR** (376 MHz, $CDCl_3$) δ -62.04. **HRMS** (ESI) m/z: $[M+H]^+$ calcd. for $C_{20}H_{16}F_3N_2O_4$: 405.1057; found: 405.1055 $[\propto]_d^{22}$: -153.0° (c= 0.09 $CHCl_3$).

(*P*)-((3a*R*,4*R*,6a*R*)-2,2-Dimethyl-6-oxotetrahydrofuro[3,4-*d*][1,3]dioxol-4-yl)methyl 2-(2-(trifluoromethyl)-1*H*-benzo[*d*]imidazol-1-yl)benzoate (*P*)-69

Purified by CC (Hexane:EtOAc 3:1) Yield: 21 mg (88%), clear oil **^{1}H NMR** (500 MHz, $CDCl_3$) δ 8.04 (ddd, *J* = 7.8, 1.6, 0.3 Hz, 1H), 7.97 – 7.94 (m, 1H), 7.83 (td, *J* = 7.7, 1.6 Hz, 1H), 7.74 (td, *J* = 7.7, 1.3 Hz, 1H), 7.44 – 7.37 (m, 2H), 7.01 – 6.98 (m, 1H), 4.63 (d, *J* = 5.7 Hz, 1H), 4.56 (t, *J* = 3.2 Hz, 1H), 4.45 (dd, *J* = 5.7, 0.5 Hz, 1H), 4.23 – 4.16 (m, 2H), 1.46 (s, 3H), 1.37 (s, 3H). **^{13}C NMR{^{1}H}** (126 MHz, $CDCl_3$) δ 173.2, 163.0, 140.7, 140.6 (q, J = 38.6, 38.0 Hz), 137.7, 134.5, 134.5, 131.7, 131.1, 130.5, 127.9, 126.4, 124.3, 121.7, 119.0 (q, *J* = 271.7 Hz), 114.2, 110.8, 79.6, 75.0, 64.2, 26.8, 25.5. **^{19}F NMR** (471 MHz, $CDCl_3$) δ -61.95. **HRMS** (ESI) m/z: $[M+H]^+$ calcd. for $C_{23}H_{20}O_6N_2F_3$: 477.1268 found: 477.1268 $[\boldsymbol{\alpha}]_{\boldsymbol{d}}^{\boldsymbol{22}}$ -33.81° (c=0.21 $CHCl_3$).

(*M*)-((3a*R*,4*R*,6a*R*)-2,2-Dimethyl-6-oxotetrahydrofuro[3,4-*d*][1,3]dioxol-4-yl)methyl 2-(2-(trifluoromethyl)-1*H*-benzo[*d*]imidazol-1-yl)benzoate (*M*)-69

Purified by CC (Hexane:EtOAc 3:1) Yield: 21 mg (88%), clear oil **^{1}H NMR** (500 MHz, $CDCl_3$) δ 8.12 (ddd, *J* = 7.8, 1.6, 0.4 Hz, 1H), 7.97 (ddd, *J* = 8.1, 1.4, 0.8 Hz, 1H), 7.83 (td, *J* = 7.7, 1.6 Hz, 1H), 7.74 (td, *J* = 7.7, 1.3 Hz, 1H), 7.53 (dd, *J* = 7.8, 1.2 Hz, 1H), 7.43 (ddd, *J* = 8.0, 7.2, 1.4 Hz, 1H), 7.41 – 7.37 (m, 1H), 6.99 (ddd, *J* = 7.8, 1.4, 0.8 Hz, 1H), 4.54 (t, *J* = 3.5 Hz, 1H), 4.34 (dd, *J* = 12.4, 3.7 Hz, 1H), 4.27 (d, *J* = 5.7 Hz, 1H), 4.11 – 4.08 (m, 1H), 4.08 – 4.07 (m, 1H), 1.41 (s, 3H), 1.30 (s, 3H). **^{13}C**

NMR{^{1}H} (126 MHz, $CDCl_3$) δ 173.0, 163.2, 141.32 (q, J = 38.9 Hz), 140.9, 137.4, 134.5, 134.5, 134.3, 132.4, 131.0, 130.3, 127.8, 126.3, 124.4, 121.9, 118.88 (app.d *J* = 272.1 Hz), 114.1, 110.5, 79.7, 74.8, 64.0, 26.8, 25.7. **^{19}F NMR** (471 MHz, $CDCl_3$) δ -62.10 **HRMS** (ESI) m/z:[M+H]+ calcd. for $C_{23}H_{20}O_6N_2F_3$: 477.1268 found: 477.1270 $[\alpha]_d^{22}$ +28.57° (c= 0.21 $CHCl_3$).

(*P*)-(*S*)-(2,2-Dimethyl-1,3-dioxolan-4-yl)methyl 2-(2-(trifluoromethyl)-1*H*-benzo[*d*]imidazol-1-yl)benzoate* (*P*)-70

Purified by CC (Hexane:EtOAc 4:1) Yield: 9 mg (42%), clear oil **^{1}H NMR** (500 MHz, $CDCl_3$) δ 8.26 (dd, *J* = 7.8, 1.6 Hz, 1H), 7.96 – 7.93 (m, 1H), 7.80 – 7.76 (m, 1H), 7.72 (td, *J* = 7.7, 1.3 Hz, 1H), 7.50 – 7.47 (m, 1H), 7.40 (ddd, *J* = 8.2, 7.2, 1.3 Hz, 1H), 7.36 (td, *J* = 7.7, 7.2, 1.2 Hz, 1H), 3.88 (qd, *J* = 11.2, 5.9 Hz, 2H), 3.75 (dd, *J* = 8.6, 6.3 Hz, 1H), 3.61 (p, *J* = 6.0 Hz, 1H), 3.37 (dd, *J* = 8.6, 5.2 Hz, 1H), 1.29 (s, 3H), 1.23 (s, 3H). **^{13}C NMR{^{1}H}** (126 MHz,$CDCl_3$) δ 164.1, 141.0 (q, J = 38.5 Hz), 140.8, 137.7, 134.0, 133.9, 132.8, 130.7, 130.2, 128.9, 126.1, 124.2, 121.6, 119.0 (q, J = 271.8 Hz) 110.9, 109.7, 72.8, 66.4, 66.0, 26.8, 25.2. **^{19}F NMR** (376 MHz, $CDCl_3$) δ -62.0. **HRMS** (ESI- TOF) m/z: $[M + H]^+$ calcd. for $C_{21}H_{20}F_3N_2O_4$: 421.1370; found: 421.1371, $[\alpha]_d^{22}$ -78.89° (c= 0.9, $CHCl_3$).

**R-alcohol was used. The priority of substituents changed after esterification.*

(*M*)-(*S*)-(2,2-Dimethyl-1,3-dioxolan-4-yl)methyl 2-(2-(trifluoromethyl)-1*H*-benzo[*d*]imidazol-1-yl)benzoate*(*M*)-70

Purified by CC (Hexane:EtOAc 4:1) Yield: 11 mg (50%), clear oil **^{1}H NMR** (500 MHz, $CHCl_3$) δ 8.28 (dd, *J* = 7.8, 1.6 Hz, 1H), 7.95 (d, *J* = 8.1 Hz, 1H), 7.78 (td, *J* = 7.6, 1.7 Hz, 1H), 7.72 (td, *J* = 7.7, 1.3 Hz, 1H), 7.48 (dd, *J* = 7.7, 1.0 Hz, 1H), 7.41 (ddd, *J* = 8.2, 7.2, 1.2 Hz, 1H), 7.36 (td, *J* = 7.8, 7.3, 1.2 Hz, 1H), 6.98 (dt, *J* = 8.0, 0.9 Hz, 1H), 3.94 (dd, *J* = 11.1, 5.4 Hz, 1H), 3.85 (dd, *J* = 11.1, 6.5 Hz, 1H), 3.72 (ddd, *J* = 11.7, 6.3, 5.4 Hz, 1H), 3.49 (dd, *J* = 8.7, 6.3 Hz, 1H), 3.06 (dd, *J* = 8.7, 5.2 Hz, 1H), 1.29 (s, 3H), 1.25 (s, 3H). **^{13}C NMR{^{1}H}** (126 MHz, $CDCl_3$) δ 164.0, 141.1 (q, J = 38.7 Hz), 140.8, 137.7, 134.0, 134.0, 132.9, 130.7, 130.2, 128.9, 126.1, 124.2, 121.6, 119.0 (q, J = 271.9 Hz), 110.9, 109.7, 72.8, 66.3, 65.9, 26.9, 25.2. **^{19}F NMR** (376 MHz, $CDCl_3$) δ -62.1. **HRMS** (ESI- TOF) m/z: $[M + H]^+$ calcd. for $C_{21}H_{20}F_3N_2O_4$: 421.1370; found 421.1370, $[\alpha]_d^{22}$ +27.3° (c= 0.11, $CHCl_3$).

**R-alcohol was used. The priority of substituents changed after esterification.*

(*P*)-((4*R*,5*R*)-5-(Hydroxymethyl)-2,2-dimethyl-1,3-dioxolan-4-yl)methyl 2-(2-(trifluoromethyl)-1*H*-benzo[*d*]imidazol-1-yl)benzoate (*P*)-71

Purified by CC (Hexane:EtOAc 2,5:1) Yield: 10 mg (44%), clear oil **^{1}H NMR** (500 MHz, $CDCl_3$) δ 8.24 (dd, *J* = 7.8, 1.6 Hz, 1H), 7.94 (d, *J* = 8.0 Hz, 1H), 7.75 (dtd, *J* = 36.6, 7.7, 1.4 Hz, 2H), 7.51 (d, *J* = 7.5 Hz, 1H), 7.44 – 7.32 (m, 2H), 7.00 (d, *J* = 8.0 Hz, 1H), 4.13 (dd, *J* = 11.9, 3.6 Hz, 1H), 3.93 (dd, *J* = 11.9, 5.7 Hz, 1H), 3.71 (ddd, *J* = 7.9, 5.7, 3.6 Hz, 1H), 3.67 – 3.60 (m, 2H), 3.52 – 3.44 (m, 1H), 1.33 (s, 3H), 1.30 (s, 3H). **^{13}C NMR{^{1}H}** (126 MHz, $CDCl_3$) δ 164.0, 141.1 (app. d, *J* = 38.3 Hz), 140.8, 137.7, 134.2, 134.0, 132.5, 130.7, 130.2, 128.8, 126.1, 124.1, 119.0 (app. d, *J* = 272.0 Hz), 110.9, 109.9, 78.1, 74.9, 65.3, 62.0, 31.1, 27.1, 27.0. **^{19}F NMR** (376 MHz, $CDCl_3$) δ -61.9. **HRMS** (ESI) m/z: $[M+H]^+$ calcd. for $C_{22}H_{22}F_3N_2O_5$: 451.1481; found: 451.1475 $[\propto]_d^{22}$**:** -46,00° (c= 0.09 $CHCl_3$).

(*M*)-((4*R*,5*R*)-5-(Hydroxymethyl)-2,2-dimethyl-1,3-dioxolan-4-yl)methyl 2-(2-(trifluoromethyl)-1*H*-benzo[*d*]imidazol-1-yl)benzoate (*M*)-71

Purified by CC (Hexane:EtOAc 2,5:1) Yield: 12 mg (53%), clear oil **^{1}H NMR** (500 MHz, $CDCl_3$) δ 8.24 (dd, *J* = 7.8, 1.3 Hz, 1H), 7.95 (d, *J* = 8.0 Hz, 1H), 7.79 (td, *J* = 7.6, 1.0 Hz, 1H), 7.72 (t, *J* = 7.7 Hz, 1H), 7.50 (d, *J* = 7.7 Hz, 1H), 7.38 (dt, *J* = 15.0, 7.2 Hz, 2H), 6.99 (d, *J* = 8.1 Hz, 1H), 4.13 (dd, *J* = 11.9, 3.5 Hz, 1H), 3.97 (dd, *J* = 11.9, 5.5 Hz, 1H), 3.76 – 3.67 (m, 1H), 3.58 – 3.50 (m, 1H), 3.46 – 3.37 (m, 2H), 1.35 (s, 3H), 1.26 (s, 3H). **^{13}C NMR{^{1}H}** (126 MHz, $CDCl_3$) δ 164.0, 141.2 (app. d, *J* = 38.0 Hz), 140.9, 137.7, 134.2, 134.0, 132.6, 130.7, 130.2, 128.8, 126.1, 124.1, 121.6, 118.9 (app. d, *J* = 271.6 Hz), 110.8, 109.8, 77.9, 74.9, 65.0, 61.9, 29.8, 27.0. **^{19}F NMR** (376 MHz, $CDCl_3$) δ -62.05. **HRMS** (ESI) m/z: $[M+H]^+$ calcd. for $C_{22}H_{22}F_3N_2O_5$: 451.1481; found: 451.1475 $[\propto]_d^{22}$**:** +33,63° (c= 0.11 $CHCl_3$).

(*P*)-*tert*-Butyl (*S*)-2-(((2-(2-(trifluoromethyl)-1*H*-benzo[*d*]imidazol-1-yl)benzoyl)oxy)methyl)pyrrolidine-1-carboxylate (*P*)-72

Purified by CC (Hexane:EtOAc 4:1) Yield: 8 mg (30%), clear oil **^{1}H NMR** (500 MHz, $CDCl_3$) δ 8.25 (d, *J* = 7.4 Hz, 1H), 7.94 (d, J = 8.2 Hz, 1H), 7.81 – 7.68 (m, 2H), 7.48 (d, *J* = 7.1 Hz, 1H), 7.42 – 7.38 (m, 1H), 7.35 (td, *J* = 7.7, 7.3, 1.2 Hz, 1H), 6.99 (d, *J* = 8.0 Hz, 1H), 4.15 – 3.97 (m, 1H), 3.83 – 3.64 (m, 1H), 3.20 (d, *J* = 23.9 Hz, 3H), 1.75 – 1.59 (m, 4H), 1.40 (s, 3H), 1.34 (s, 6H). **^{13}C NMR{^{1}H}** (126 MHz, $CDCl_3$) δ 164.2, 154.3, 141.27 (d, J = 38.7 Hz), 140.8, 137.7, 133.9, 133.8, 132.8, 130.7, 130.2, 129.1, 126.1, 124.1, 121.6, 119.0 (q, J = 272.1 Hz), 110.8, 79.9, 65.7, 55.1, 46.4, 29.8, 28.5, 22.7. **^{19}F NMR** (471 MHz, $CDCl_3$) δ -61.3. **HRMS** (ESI) m/z: $[M+H]^+$ calcd. for $C_{25}H_{27}F_3N_3O_4$: 490.1948; found: 490.1950 $[\propto]_d^{22}$**:** -913.7° (c= 0.08 $CHCl_3$).

(*M*)-*tert*-Butyl (*S*)-2-(((2-(2-(trifluoromethyl)-1*H*-benzo[*d*]imidazol-1-yl)benzoyl)oxy)methyl)pyrrolidine-1-carboxylate (*M*)-72

Purified by CC (Hexane:EtOAc 4:1) Yield: 14 mg (58%), clear oil **^{1}H NMR** (500 MHz, $CDCl_3$) δ 8.25 (d, *J* = 7.4 Hz, 1H), 7.94 (d, *J* = 8.2 Hz, 1H), 7.81 – 7.68 (m, 2H), 7.48 (d, *J* = 7.1 Hz, 1H), 7.42 – 7.38 (m, 1H), 7.35 (td, *J* = 7.7, 7.3, 1.2 Hz, 1H), 6.99 (d, *J* = 8.0 Hz, 1H), 4.15 – 3.97 (m, 1H), 3.83 – 3.64 (m, 1H), 3.20 (d, *J* = 23.9 Hz, 3H), 1.75 – 1.59 (m, 4H), 1.40 (s, 3H), 1.34 (s, 6H). **^{13}C NMR{^{1}H}** (126 MHz, $CDCl_3$) δ 164.2, 154.3, 141.27 (d, J = 38.7 Hz), 140.8, 137.7, 133.9, 133.8, 132.8, 130.7, 130.2, 129.1, 126.1, 124.1, 121.6, 118.99 (q, J = 272.1 Hz), 110.8, 79.9, 65.7, 55.1, 46.4, 29.8, 28.5, 22.7. **^{19}F NMR** (471 MHz, $CDCl_3$) δ -61.3. **HRMS** (ESI) m/z: $[M+H]^+$ calcd. for $C_{25}H_{27}F_3N_3O_4$: 490.1948; found: 490.1949 $[\propto]_d^{22}$**:** -32.86° (c= 0.14 $CHCl_3$).

(*P*)-((2*S*,5*R*)-1-Methyl-5-phenylpyrrolidin-2-yl)methyl 2-(2-(trifluoromethyl)-1*H*-benzo[*d*]imidazol-1-yl)benzoate (*P*)-73

Purified by CC (Hexane:EtOAc 6:1) Yield: 15 mg (62%), clear foam **^{1}H NMR** (400 MHz, $CDCl_3$) δ 8.30 – 8.24 (m, 1H), 7.99 – 7.94 (m, 1H), 7.75 (dtd, *J* = 23.0, 7.6, 1.6 Hz, 2H), 7.51 – 7.47 (m, 1H), 7.37 (dtd, *J* = 9.2, 7.2, 1.2 Hz, 2H), 7.29 – 7.23 (m, 4H), 7.22 – 7.17 (m, 1H), 7.01 (ddd, *J* = 8.0, 1.3, 0.8 Hz, 1H), 3.88 (ddd, *J* = 18.2, 10.8, 5.9 Hz, 2H), 3.21 (dd, *J* = 9.8, 6.3 Hz, 1H), 2.15 – 2.07 (m, 1H), 1.94 (s, 3H), 1.98 – 1.89 (m, 4H), 1.67 (ddd, *J* = 17.2, 12.6, 8.7 Hz, 1H), 1.53 (ddd, *J* = 18.8, 12.1, 9.3 Hz, 1H), 1.34 – 1.27 (m, 1H). **^{13}C NMR{^{1}H}** (126 MHz, $CDCl_3$) δ 164.5, 143.4, 141.1 (q, *J* = 38.4 Hz), 140.9, 137.8, 134.0, 133.6, 132.7, 130.7, 130.1, 129.5, 128.4, 127.3, 127.1, 126.1, 124.1, 121.6, 119.0 (q, *J* = 271.9 Hz), 110.9, 72.1, 68.6, 63.6, 39.5, 34.4, 27.5. **^{19}F NMR** (376 MHz, $CDCl_3$) δ -61.92. **HRMS** (ESI) m/z: $[M+H]^+$ calcd. for: $C_{27}H_{25}F_3N_3O_2$: 480.1899 found: 480.1891 $[\propto]_d^{22}$:-463.34 (c= 0.15 $CHCl_3$).

(*M*)-((2*S*,5*R*)-1-Methyl-5-phenylpyrrolidin-2-yl)methyl 2-(2-(trifluoromethyl)-1*H*-benzo[*d*]imidazol-1-yl)benzoate (*M*)-73

Purified by CC (Hexane:EtOAc 6:1) Yield: 18 mg (75%), clear foam **^{1}H NMR** (400 MHz, $CDCl_3$) δ 8.31 – 8.27 (m, 1H), 7.98 – 7.95 (m, 1H), 7.75 (dtd, *J* = 22.3, 7.5, 1.6 Hz, 2H), 7.48 (dd, *J* = 7.6, 1.4 Hz, 1H), 7.38 (dddd, *J* = 21.8, 8.3, 7.2, 1.2 Hz, 2H), 7.29 – 7.17 (m, 6H), 3.94 (ddd, *J* = 18.1, 10.9, 5.7 Hz, 2H), 3.22 (dd, *J* = 9.3, 6.6 Hz, 1H), 2.33 – 2.22 (m, 1H), 2.08 (s, 3H), 1.92 – 1.80 (m, 1H), 1.48 – 1.33 (m, 2H), 1.09 – 0.98 (m, 1H). **^{13}C NMR{^{1}H}** (126 MHz, $CDCl_3$) δ 164.5, 143.5, 141.1 (q, *J* = 38.5 Hz), 140.9, 137.8, 134.0, 133.7, 132.8, 130.7, 130.11, 129.5, 128.4, 127.3, 127.1, 126.0, 124.1, 121.6, 119.0 (q, *J* = 272.1 Hz), 111.0, 72.0, 68.4, 63.8, 39.6, 34.3, 27.2. **^{19}F NMR** (376 MHz, $CDCl_3$) δ -61.98. **HRMS** (ESI) m/z: $[M+H]^+$ calcd. for $C_{27}H_{25}F_3N_3O_2$: 480.1899 found: 480.1891 $[\propto]_d^{22}$**:** +61.88 (c= 0.16 $CHCl_3$).

(*P*)-(*R*)-(5-Oxopyrrolidin-2-yl)methyl 2-(2-(trifluoromethyl)-1*H*-benzo[*d*]imidazol-1-yl)benzoate (*P*)-74

Purified by CC (EtOAc) Yield: 8 mg (40%), clear oil **^{1}H NMR** (400 MHz, $CDCl_3$) δ 8.25 (dd, *J* = 7.8, 1.7 Hz, 1H), 7.97 (dt, *J* = 8.1, 1.0 Hz, 1H), 7.82 (td, *J* = 7.6, 1.7 Hz, 1H), 7.74 (td, *J* = 7.7, 1.4 Hz, 1H), 7.53 (dd, *J* = 7.8, 0.8 Hz, 1H), 7.46 – 7.41 (m, 1H), 7.39 (td, *J* = 7.7, 7.3, 1.2 Hz, 1H), 5.37 (s, 1H), 3.97 (dd, *J* = 11.3, 4.4 Hz, 1H), 3.66 (dd, *J* = 11.3, 7.4 Hz, 1H), 3.29 (ddd, *J* = 12.9, 7.7, 5.1 Hz, 1H), 2.14 (ddd, *J* = 9.1, 7.1, 3.2 Hz, 2H), 1.87 (dddd, *J* = 13.3, 9.1, 8.0, 6.7 Hz, 1H). **^{13}C NMR{^{1}H}** (101 MHz, $CDCl_3$) δ 177.5, 164.2, 141.2 (q, J = 38.2 Hz), 140.7, 137.8, 134.3, 133.9, 133.0, 130.9, 130.2, 128.5,

126.3, 124.4, 121.7, 118.9 (q, J = 272.0 Hz),110.8, 68.2, 52.2, 29.1, 23.1. **^{19}F NMR** (471 MHz, $CDCl_3$) δ -62.0. **HRMS** (ESI) m/z: $[M + H]^+$ calcd. for $C_{20}H_{17}F_3N_3O_3$: 404.1217; found: 404.1216, $[\alpha]_d^{22}$ -63.75° (c= 0.08, $CHCl_3$).

(*M*)-(*R*)-(5-Oxopyrrolidin-2-yl)methyl 2-(2-(trifluoromethyl)-1*H*-benzo[*d*]imidazol-1-yl)benzoate (*M*)-74

Purified by CC (EtOAc) Yield: 8 mg (40%), clear oil **^{1}H NMR** (400 MHz, $CDCl_3$) δ 8.33 – 8.24 (m, 1H), 8.00 – 7.96 (m, 1H), 7.82 (td, *J* = 7.6, 1.7 Hz, 1H), 7.75 (td, *J* = 7.7, 1.4 Hz, 1H), 7.52 (dd, *J* = 7.7, 1.3 Hz, 1H), 7.51 – 7.43 (m, 2H), 7.06 – 7.02 (m, 1H), 4.42 (s, 1H), 3.86 (dd, *J* = 11.2, 3.7 Hz, 1H), 3.70 (dd, *J* = 11.2, 8.8 Hz, 1H), 3.11 – 3.03 (m, 1H), 2.18 – 2.13 (m, 2H), 2.02 (dq, *J* = 13.1, 7.9 Hz, 1H). **^{13}C NMR{^{1}H}** (101 MHz, $CDCl_3$) δ 177.2, 164.1, 141.3 (q, J = 38.9 Hz), 140.6, 137.8, 134.3, 133.7, 133.2, 131.0, 130.2, 128.6, 126.5, 124.7, 121.8, 118.9 (q, J = 272.0 Hz), 110.8, 68.8, 51.9, 29.0, 22.9. **^{19}F NMR** (471 MHz, $CDCl_3$) δ -62.2. **HRMS** (ESI) m/z: $[M + H]^+$ calcd. for $C_{20}H_{17}F_3N_3O_3$: 404.1217; found: 404.1217, $[\alpha]_d^{22}$ -77.50° (c= 0.08, $CHCl_3$).

(*P*)-((3a*R*,5*R*,5a*S*,8a*S*,8b*R*)-2,2,7,7-Tetramethyltetrahydro-5*H*-bis([1,3]dioxolo)[4,5-*b*:4',5'-*d*]pyran-5-yl)methyl 2-(2-(trifluoromethyl)-1*H*-benzo[*d*]imidazol-1-yl)benzoate (*P*)-75

Purified by CC (Hexane:EtOAc 4:1) Yield 8 mg (30%), clear oil **^{1}H NMR** (500 MHz, $CDCl_3$) δ 8.27 (dd, *J* = 7.9, 1.6 Hz, 1H), 7.93 (dt, *J* = 8.2, 0.9 Hz, 1H), 7.76 (td, *J* = 7.6, 1.7 Hz, 1H), 7.70 (td, *J* = 7.7, 1.4 Hz, 1H), 7.45 (dd, *J* = 7.7, 1.1 Hz, 1H), 7.37 (ddd, *J* = 8.2, 7.2, 1.2 Hz, 1H), 7.32 (ddd, *J* = 8.2, 7.2, 1.2 Hz, 1H), 6.98 – 6.96 (m, 1H), 5.43 (d, *J* = 5.0 Hz, 1H), 4.49 (dd, *J* = 7.9, 2.5 Hz, 1H), 4.24 (dd, *J* = 5.0, 2.5 Hz, 1H), 4.20 (dd, *J* = 11.3, 6.1 Hz, 1H), 4.03 (dd, *J* = 11.2, 6.9 Hz, 1H), 3.81 (dd, *J* = 7.9, 1.9 Hz, 1H), 3.64 (td, *J* = 6.4, 1.8 Hz, 1H), 1.37 (s, 3H), 1.34 (s, 3H), 1.29 (s, 6H). **^{13}C NMR{^{1}H}** (126 MHz, $CDCl_3$) δ 163.9, 141.11 (q, J = 38.4 Hz), 140.8, 137.7, 134.2, 133.7, 132.7, 130.7, 130.2, 128.9, 125.9, 124.0, 121.6, 119.0 (q, J = 271.9 Hz)7, 113.6, 110.8, 109.6, 108.8, 96.2, 70.6, 70.6, 70.5, 65.4, 64.1, 26.1, 26.0, 25.0, 24.5. **^{19}F NMR** (376 MHz, $CDCl_3$) δ -61.9. **HRMS** (ESI) m/z: $[M + H]^+$ calcd. For $C_{27}H_{28}F_3N_2O_7$: 549.1843; found: 549.1843, $[\propto]_d^{22}$**:** -125.0° (c=0.08 $CHCl_3$).

(*M*)-((3a*R*,5*R*,5a*S*,8a*S*,8b*R*)-2,2,7,7-Tetramethyltetrahydro-5*H*-bis([1,3]dioxolo)[4,5-*b*:4',5'-*d*]pyran-5-yl)methyl 2-(2-(trifluoromethyl)-1*H*-benzo[*d*]imidazol-1-yl)benzoate (*M*)-75

Purified by CC (Hexane:EtOAc 4:1), Yield 8 mg (30%), clear oil **^{1}H NMR** (500 MHz, $CDCl_3$) δ 8.32 – 8.30 (m, 1H), 7.97 – 7.94 (m, 1H), 7.77 (td, *J* = 7.6, 1.7 Hz, 1H), 7.71 (td, *J* = 7.7, 1.4 Hz, 1H), 7.47 (dd, *J* = 7.7, 1.3 Hz, 1H), 7.43 – 7.39 (m, 1H), 7.37 (ddd, *J* = 8.3, 7.2, 1.3 Hz, 1H), 7.02 (ddd, *J* = 8.0, 1.2, 0.8 Hz, 2H), 5.40 (d, *J* = 5.0 Hz, 1H), 4.28 (dd, *J* = 7.9, 2.4 Hz, 1H), 4.21 (dd, *J* = 5.0, 2.4 Hz, 1H), 4.10 (dd, *J* = 11.0, 7.3 Hz, 1H), 4.02 (dd, *J* = 11.0, 6.3 Hz, 1H), 3.53 – 3.49 (m, 1H), 2.86 (dd, *J* = 7.9, 1.9 Hz, 1H), 1.60 (s, 3H), 1.32 (s, 3H), 1.32 (s, 3H), 1.15 (s, 3H). **^{13}C NMR{^{1}H}** (126 MHz, $CDCl_3$) δ 163.9, 141.13 (q, J = 38.5 Hz), 140.8, 137.8, 134.0, 133.8, 133.1, 130.7, 130.1, 129.0, 125.9, 123.8, 122.0, 119.0 (q, J = 272.6 Hz), 111.0, 109.2, 109.0, 96.2, 70.6, 69.8, 65.0, 63.8, 26.2, 25.9, 25.1, 24.3. **^{19}F NMR** (376 MHz, $CDCl_3$) δ -62.1. **HRMS** (ESI) m/z: $[M + H]^+$ calcd. for $C_{27}H_{28}F_3N_2O_7$: 549.1843; found: 549.1845, $[\propto]_d^{22}$**:** -832.5° (c=0.08 $CHCl_3$).

(*P*)-*tert*-Butyl-(*R*)-2-((2-(2-(trifluoromethyl)-1*H*-benzo[*d*]imidazol-1-yl)benzamido)methyl)pyrrolidine-1-carboxylate (*P*)-76

TBBA (20 mg, 0.065 mmol, 1 eq.) was dissolved in dry DMF (1.5 mL). Amine (13mg, 0.065 mmol,1 eq.) was added followed by HOBt.H_2O (20 mg, 0.13 mmol, 2 eq.) and EDCl (26 mg, 0.13 mmol, 2 eq.). Reaction was stirred at room temperature for 3 hrs. After 3 hrs. the solution was diluted with EtOAc (5 mL) and washed 3× with 10% HCl and 10% K_2CO_3 and once with brine. Oganic layer was dried with $MgSO_4$ and purified by column chromatography (hexane:EtOAc 2:1) Yield 15mg (62%), clear oil **^{1}H NMR** (500 MHz, $CDCl_3$) δ 7.91 (dd, *J* = 6.9, 1.8 Hz, 1H), 7.85 – 7.78 (m, 1H), 7.68 – 7.60 (m, 2H), 7.45 – 7.41 (m, 1H), 7.39 – 7.32 (m, 2H), 7.05 (dd, *J* = 6.8, 1.8 Hz, 1H), 3.76 (s, 1H), 3.32 (dt, *J* = 10.8, 7.8 Hz, 1H), 3.26 – 3.19 (m, 1H), 3.16 (dt, *J* = 13.6, 4.3 Hz, 1H), 3.04 (s, 1H), 1.84 – 1.77 (m, 3H), 1.75 – 1.69 (m, 2H), 1.46 (s, 9H).**^{13}C NMR{^{1}H}** (126 MHz, $CDCl_3$) δ 165.6, 156.8, 141.1 (q, *J* = 38.3 Hz), 140.6, 137.8, 134.9, 132.6, 131.5, 130.5, 129.7, 129.1, 125.8, 123.9, 121.5, 119.1 (q, *J* = 272.1 Hz),

111.4, 80.3, 56.2, 47.2, 46.7, 29.6, 28.5, 23.8. **^{19}F NMR** (376 MHz, $CDCl_3$) δ -61.5. **HRMS** (ESI) m/z: $[M + H]^+$ calcd. For $C_{25}H_{28}O_3N_4F_3$: 489.2108; found: 489.2111 $[\alpha]_d^{22}$ -8.67° (c=0.15 $CHCl_3$).

(*M*)-*tert*-Butyl-(*R*)-2-((2-(2-(trifluoromethyl)-1*H*-benzo[*d*]imidazol-1-yl)benzamido)methyl)pyrrolidine-1-carboxylate (*M*)-76

Following same procedure as for compound (*P*)-76.

Purified by CC (hexane:EtOAc 2:1) Yield 12 mg (50%), clear oil **^{1}H NMR** (500 MHz, $CDCl_3$) δ 7.91 (dd, *J* = 6.7, 2.0 Hz, 1H), 7.83 – 7.77 (m, 1H), 7.67 – 7.60 (m, 2H), 7.45 – 7.41 (m, 1H), 7.35 (tt, *J* = 7.2, 5.9 Hz, 2H), 7.09 – 7.05 (m, 1H), 3.90 (s, 1H), 3.33 (dt, *J* = 10.9, 7.8 Hz, 1H), 3.27 (dt, *J* = 11.0, 6.2 Hz, 1H), 3.15 (s, 1H), 3.13 – 3.08 (m, 1H), 1.84 (s, 2H), 1.79 – 1.73 (s, 2H), 1.44 (s, 9H). **^{13}C NMR{^{1}H}** (126 MHz, $CDCl_3$) δ 165.6, 157.0, 141.2 (q, J = 38.0 Hz) 140.6, 137.8, 135.0, 132.7, 131.5, 130.6, 129.9, 128.8, 125.8, 123.9, 121.5, 119.0 (q, J = 272.3 Hz) 111.4, 80.3, 56.2, 47.2, 46.6, 29.5, 28.5, 23.8. **^{19}F NMR** (376 MHz, $CDCl_3$) δ -61.8. **HRMS** (ESI) m/z: $[M + H]^+$ calcd. For $C_{25}H_{28}O_3N_4F_3$: 489.2108; found: 489.2112 $[\alpha]_d^{22}$ -14.17° (c= 0.12 $CHCl_3$).

(*P*)-(*S*)-2-((*tert*-Butoxycarbonyl)amino)-2-phenylethyl 2-(2-(trifluoromethyl)-1*H*-benzo[*d*]imidazol-1-yl)benzoate (*P*)-77

Purified by CC (hexane: EtOAc 5:1) Yield 15 mg (57%), amorphous solid **^{1}H NMR** (400 MHz, $CDCl_3$) δ 8.19 (dd, *J* = 7.8, 1.5 Hz, 1H), 7.95 (d, *J* = 7.8 Hz, 1H), 7.77 (td, *J* = 7.7, 1.7 Hz, 1H), 7.69 (td, *J* = 7.7, 1.3 Hz, 1H), 7.51 – 7.46 (m, 1H), 7.43 – 7.37 (m, 1H), 7.37 – 7.32 (m, 1H), 7.30 – 7.23 (m, 3H), 7.12 – 7.08 (m, 2H), 6.98 – 6.93 (m, 1H), 4.75 (s, 2H), 4.29 – 4.21 (m, 1H), 4.08 (d, *J* = 10.6 Hz, 1H), 1.39 (s, 9H). **^{13}C NMR{^{1}H}** (101 MHz, $CDCl_3$) δ 163.9, 155.2, 141.14 (q, *J* = 38.6 Hz), 140.8, 138.3, 137.6, 134.3, 133.9, 132.7, 130.7, 130.2, 128.8, 128.6, 128.0, 126.5, 126.1, 124.1, 121.6, 118.96 (q, *J* = 272.2 Hz), 110.8, 80.0, 67.3, 53.7, 28.4. **^{19}F NMR** (376 MHz, $CDCl_3$) δ -62.01 **HRMS** (ESI) m/z: $[M + H]^+$ calcd. For $C_{28}H_{27}N_3O_4F_3$; 526.1948; found: 526.1951 $[\alpha]_d^{22}$ +52.86° (c= 0.15 $CHCl_3$). **^{1}H NMR** (400 MHz, Acetone-D_6) δ 8.24 (dd, *J* = 7.8, 1.6 Hz, 1H), 7.94 (t, *J* = 7.4 Hz, 1H), 7.87 (dq, *J* = 7.2, 3.6 Hz, 1H), 7.82 (t, *J* = 7.7 Hz, 1H), 7.74 (d, *J* = 7.8 Hz, 1H), 7.41 (td, *J* = 6.7, 6.0, 4.0 Hz, 2H), 7.38 – 7.21 (m, 5H), 7.05 – 7.01 (m, 1H), 6.48 (d, *J* = 6.6 Hz, 1H), 4.95 (s, 1H), 4.28 – 4.14 (m, 2H), 1.38 (s, 9H). **^{1}H NMR** (400 MHz, $CDCl_3$+TFAOMe) δ 8.19 (dd, *J* = 7.8, 1.5 Hz, 1H), 7.95 (d, *J* = 7.9 Hz, 1H), 7.77 (td, *J* = 7.7, 1.7 Hz, 1H), 7.68 (td, *J* = 7.7, 1.3 Hz, 1H), 7.48 (d, *J* = 7.6 Hz, 1H), 7.40 (td, *J* = 8.1, 7.7, 1.3 Hz, 1H), 7.37 – 7.32 (m, 1H), 7.29 – 7.22 (m, 3H), 7.10 (dd, *J* = 7.9, 1.7 Hz, 2H), 6.96 (d, *J* = 8.0 Hz, 1H), 4.77 (s, 2H), 4.25 (s, 1H), 4.08 (d, *J* = 11.5 Hz, 1H), 1.38 (s, 9H).

(*M*)-(*S*)-2-((*tert*-Butoxycarbonyl)amino)-2-phenylethyl 2-(2-(trifluoromethyl)-1*H*-benzo[*d*]imidazol-1-yl)benzoate (*M*)-77

Purified by CC (hexane: EtOAc 5:1) Yield 21 mg (80%), amorphous solid **^{1}H NMR** (400 MHz, $CDCl_3$) δ 8.16 (br. d, 1H), 7.97 – 7.92 (m, 1H), 7.79 – 7.73 (m, 1H), 7.68 (td, *J* = 7.7, 1.3 Hz, 1H), 7.50 – 7.44 (m, 1H), 7.42 – 7.32 (m, 2H), 7.32 – 7.22 (m, 3H), 7.26 (s, 4H), 7.16 – 7.10 (m, 2H), 6.97 – 6.93 (m, 1H), 4.79 (br. s, 1H), 4.68 (br. s, 1H), 4.27 (br. s, 1H), 4.08 (br. d, *J* = 11.0 Hz, 1H), 1.39 (s, 9H). **^{13}C NMR{^{1}H}** (101 MHz, $CDCl_3$) δ 163.8, 155.1, 141.0 (app. d, *J* = 38.7 Hz), 140.7, 138.2, 137.6, 134.2, 133.8, 132.5, 130.6, 130.1, 128.8, 128.6, 127.9, 126.4, 126.0, 124.0, 121.7, 118.9 (app. d, *J* = 272.0 Hz), 110.7, 79.9, 67.2, 53.5, 28.3. **^{19}F NMR** (376 MHz, $CDCl_3$) δ .-61.98 **HRMS** (ESI) m/z: $[M + H]^+$ calcd. For $C_{28}H_{27}N_3O_4F_3$; 526.1948; found: 526.1949. $[\alpha]_d^{22}$ -34.0° (c= 0.21 $CHCl_3$). **^{1}H NMR** (400 MHz, Acetone-D_6) δ 8.25 (ddd, J = 7.9, 1.6, 0.4 Hz, 1H), 7.95 (dd, J = 7.7, 1.6 Hz, 1H), 7.90 – 7.87 (m, 1H), 7.82 (td, J = 7.7, 1.2 Hz, 1H), 7.74 (dd, J = 7.7, 1.0 Hz, 1H), 7.45 – 7.37 (m, 2H), 7.34 – 7.29 (m, 4H), 7.28 – 7.24 (m, 1H), 7.02 – 6.99 (m, 1H), 6.49 (s, 1H), 4.91 (s, 1H), 4.23 (q, J = 9.7, 8.4 Hz, 1H), 4.15 (dd, J = 10.5, 5.0 Hz, 1H), 1.38 (s, 9H). **^{1}H NMR** (400 MHz, $CDCl_3$+TFAOMe) δ 8.18 – 8.14 (m, 1H), 7.94 (d, J = 7.9 Hz, 1H), 7.76 (td, J = 7.7, 1.7 Hz, 1H), 7.68 (td, J = 7.7, 1.3 Hz, 1H), 7.47 (d, J = 7.3 Hz, 1H), 7.40 (ddd, J = 8.1, 7.2, 1.3 Hz, 1H), 7.35 (td, J = 7.7, 7.2, 1.2 Hz, 1H), 7.31 – 7.24 (m, 3H), 7.12 (d, J = 7.0 Hz, 2H), 6.97 – 6.93 (m, 1H), 4.79 (s, 1H), 4.69 (d, J = 7.3 Hz, 1H), 4.26 (s, 1H), 4.09 (d, J = 10.9 Hz, 1H), 1.39 (s, 9H).

(*S*)-2-(6-Methoxynaphthalen-2-yl)propan-1-ol

(*S*)-2-(6-Methoxynaphthalen-2-yl)propanoic acid (150 mg, 0.652 mmol, 1 eq.) was slowly added into the suspension of $LiAlH_4$ (38 mg, 1.95 mmol, 3 eq.) in dry THF (12 ml). This mixture was stirred at room temperature for 16 hours. After 16 hours, EtOAc (30 ml) was added followed by deionized water (25 ml) and EtOAc (30 ml). Layers were separated and aq. layer was further extracted with EtOAc (3x 30ml). Combined organic phases were extracted with brine, dried with $MgSO_4$ and evaporated yielding white solid (123 mg, 87%) **^{1}H NMR** (400 MHz, $CDCl_3$) δ 7.74 – 7.68 (m, *J* = 8.5, 6.2 Hz, 2H), 7.61 (d, *J* = 1.2 Hz, 1H), 7.35 (dd, *J* = 8.5, 1.8 Hz, 1H), 7.17 – 7.11 (m, 1H), 3.92 (s, 3H), 3.77 (d, *J* = 6.8 Hz, 2H), 3.09 (h, *J* = 6.9 Hz, 1H), 1.36 (d, *J* = 7.0 Hz, 3H). **^{13}C NMR{^{1}H}** (101 MHz, $CDCl_3$) δ 157.6, 138.8, 133.7, 129.2, 129.2, 127.4, 126.4, 126.0, 119.0, 105.8, 68.8, 55.5, 42.5, 17.8. **HRMS** (ESI) m/z: $[M+H]^+$ calcd. for: $C_{14}H_{17}O_2$: 217.1229 found: 217.1223 $[\propto]_d^{22}$**:** -19.86 (c= 0.7 $CHCl_3$).

***P*-(*S*)-2-((tert-butoxycarbonyl)amino)-2-cyclohexylethyl 2-(2-(trifluoromethyl)-1H-benzo[d]imidazol-1-yl)benzoate (*P*)-78**

Purified by CC (Hexane:EtOAc 7:1), Yield: 12 mg (45%) **^{1}H NMR** (400 MHz, $CDCl_3$) δ 8.31 – 8.26 (m, 1H), 7.98 – 7.94 (m, 1H), 7.77 (td, *J* = 7.6, 1.7 Hz, 1H), 7.70 (td, *J* = 7.6, 1.4 Hz, 1H), 7.46 – 7.43 (m, 1H), 7.38 (ddd, *J* = 8.4, 4.9, 1.4 Hz, 2H), 7.03 – 6.97 (m, 1H), 4.13 (d, *J* = 9.5 Hz, 1H), 4.11 – 4.07 (m, 1H), 3.97 (dd, *J* = 11.5, 3.5 Hz, 1H), 3.41 – 3.33 (m, 1H), 1.55 (t, *J* = 15.2 Hz, 3H), 1.42 (s, 9H), 1.07 – 0.93 (m, 3H), 0.85 – 0.73 (m, 2H), 0.63 – 0.52 (m, 1H). **^{13}C NMR{^{1}H}** (101 MHz, $CDCl_3$) δ 164.4, 155.8, 141.21 (q, *J* = 38.6 Hz), 140.8, 137.7, 133.9, 133.8, 133.1, 130.7, 130.1, 128.9, 126.2, 124.3, 121.7, 119.0 (q, *J* = 272.2 Hz), 111.0, 79.4, 66.0, 54.0, 37.9, 29.6, 29.1, 28.5, 26.2, 25.7, 25.7. **^{19}F NMR** (376 MHz, $CDCl_3$) δ -61.9. **HRMS** (ESI) m/z: $[M + H]^+$ calcd. For $C_{28}H_{33}N_3O_4F_3$: 532.2418; found: 532.2418. $[\boldsymbol{\alpha}]_{\boldsymbol{d}}^{\mathbf{22}}$ -60.83° (c= 0.12, $CHCl_3$) **^{1}H NMR** (400 MHz, Acetone-D_6) δ 8.31 (dd, J = 7.9, 1.6 Hz, 1H), 7.94 (td, J = 7.7, 1.6 Hz, 1H), 7.92 – 7.86 (m, 1H), 7.83 (td, J = 7.7, 1.2 Hz, 1H), 7.73 (d, J = 7.8 Hz, 1H), 7.47 – 7.40 (m, 2H), 7.09 (ddt, J = 7.8, 5.3, 2.2 Hz, 1H), 5.45 (d, J = 10.1 Hz, 1H), 4.03 (d, J = 5.3 Hz, 2H), 3.47 (h, J = 5.4, 4.8 Hz, 1H), 1.69 – 1.49 (m, 5H), 1.39 (s, 9H), 1.18 – 1.05 (m, 4H), 1.01 – 0.85 (m, 2H). **^{1}H NMR** (400 MHz, $CDCl_3$+TFAOMe) δ 8.30 – 8.26 (m, 1H), 7.97 (d, J = 7.6 Hz, 1H), 7.77 (td, J = 7.6, 1.7 Hz, 1H), 7.70 (td, J = 7.6, 1.4 Hz, 1H), 7.45 (d, J = 6.4 Hz, 1H), 7.43 – 7.35 (m, 2H), 7.01 (d, J = 7.5 Hz, 1H), 4.13 (d, J = 9.7 Hz, 1H), 4.11 – 4.07 (m, 1H), 3.99 – 3.94 (m, 1H), 3.41 – 3.32 (m, 1H), 1.59 (d, J = 26.5 Hz, 4H), 1.42 (s, 9H), 1.35 (d, J = 10.9 Hz, 1H), 1.10 – 0.95 (m, 3H), 0.86 – 0.73 (m, 2H), 0.65 – 0.54 (m, 1H).

***M*-(*S*)-2-((tert-butoxycarbonyl)amino)-2-cyclohexylethyl 2-(2-(trifluoromethyl)-1H-benzo[d]imidazol-1-yl)benzoate (*M*)-78**

Purified by CC (Hexane:EtOAc 7:1), Yield: 6 mg (22%) **^{1}H NMR** (400 MHz, $CDCl_3$) δ 8.29 (dd, *J* = 7.6, 1.5 Hz, 1H), 8.00 – 7.95 (m, 1H), 7.76 (td, *J* = 7.6, 1.8 Hz, 1H), 7.71 (td, *J* = 7.6, 1.5 Hz, 1H), 7.47 – 7.37 (m, 3H), 7.05 – 7.02 (m, 1H), 4.15 (dd, *J* = 11.6, 4.5 Hz, 1H), 3.90 (dd, *J* = 11.6, 3.4 Hz, 1H), 3.55 (d, *J* = 9.6 Hz, 1H), 3.33 (dd, *J* = 10.6, 6.4 Hz, 1H), 1.67 (d, *J* = 19.2 Hz, 2H), 1.51 – 1.39 (m, 2H), 1.40 (s, 9H), 1.23 – 1.12 (m, 2H), 1.12 – 0.98 (m, 1H), 0.87 – 0.74 (m, 2H), 0.74 – 0.65 (m, 1H). **^{13}C NMR{^{1}H}** (101 MHz, $CDCl_3$) δ 164.6, 155.6, 141.12 (q, J = 39.3, 38.6 Hz), 140.7, 137.7, 137.7, 137.7, 133.8, 133.6, 133.2, 130.8, 130.3, 129.0, 126.4, 124.3, 121.8, 118.9 (q, J = 272.1 Hz), 110.9, 79.3, 66.2, 53.7, 37.8, 29.7, 29.2, 28.5, 26.2, 25.7, 25.6. **^{19}F NMR** (376 MHz, $CDCl_3$) δ -61.9. **HRMS** (ESI) m/z: $[M + H]^+$ calcd. For $C_{28}H_{33}N_3O_4F_3$: 532.2418; found: 532.2420. $[\boldsymbol{\alpha}]_{\boldsymbol{d}}^{\mathbf{22}}$ -63.08° (c= 0.6, $CHCl_3$) **^{1}H NMR** (400 MHz, Acetone-D_6) δ 8.31 (dd, J = 7.9, 1.6 Hz, 1H), 7.94 (td, J = 7.7, 1.6 Hz, 1H), 7.92 – 7.87 (m, 1H), 7.84 (td, J = 7.7, 1.2 Hz, 1H), 7.73 (d, J = 7.8 Hz, 1H), 7.48 – 7.41 (m, 2H), 7.10 – 7.06 (m, 1H), 5.21 (d, J = 9.4 Hz, 1H), 4.08 – 3.99 (m, 2H), 3.47 (h, J = 5.1, 4.5 Hz, 1H), 1.71 – 1.50 (m, 5H), 1.38 (s, 9H), 1.23 – 1.06 (m, 4H), 0.92 (dddd, J = 24.9, 16.3, 12.5, 3.6 Hz, 2H). **^{1}H NMR** (400 MHz, $CDCl_3$+TFAOMe) δ 8.29 (dd, J = 7.6, 1.5 Hz, 1H), 8.00 – 7.96 (m, 1H), 7.76 (td, J = 7.6, 1.8 Hz, 1H), 7.71 (td, J = 7.6, 1.5 Hz, 1H), 7.42 (p, J = 7.1 Hz, 3H), 7.05 – 7.02 (m, 1H), 4.15 (dd, J = 11.5, 4.4 Hz, 1H), 3.90 (dd, J = 11.6, 3.4 Hz, 1H), 3.55 (d, J = 9.7 Hz, 1H), 3.37 – 3.29 (m, 1H), 1.72 – 1.58 (m, 3H), 1.46 (d, J = 8.4 Hz, 2H), 1.40 (s, 9H), 1.20 – 1.00 (m, 3H), 0.89 – 0.65 (m, 3H).

***P*-(*R*)-2-((tert-butoxycarbonyl)amino)-3-methylbutyl 2-(2-(trifluoromethyl)-1H-benzo[d]imidazol-1-yl)benzoate (*P*)-79**

Purified by CC (Hexane:EtOAc 4:1), Yield: 12 mg (50%) **^{1}H NMR** (400 MHz, $CDCl_3$) δ 8.27 (dd, *J* = 7.6, 1.3 Hz, 1H), 7.96 (dd, *J* = 6.9, 1.5 Hz, 1H), 7.77 (td, *J* = 7.6, 1.8 Hz, 1H), 7.71 (td, *J* = 7.6, 1.4 Hz, 1H), 7.46 – 7.35 (m, 3H), 7.05 – 7.00 (m, 1H), 4.10 (dd, *J* = 11.5, 5.1 Hz, 1H), 3.92 (dd, *J* = 11.4, 4.0 Hz, 1H), 3.76 (d, *J* = 9.6 Hz, 1H), 3.34 (tt, *J* = 8.5, 4.4 Hz, 1H), 1.40 (s, 9H), 0.74 (dd, *J* = 13.3, 6.7 Hz, 6H). **^{13}C NMR{^{1}H}** (101 MHz, $CDCl_3$) δ 164.4, 155.6, 141.04 (q, J = 38.4, 37.9 Hz), 140.8, 137.7, 133.8, 133.0, 130.7, 130.2, 129.0, 126.3, 124.2, 121.8, 118.9 (q, J = 272.1 Hz), 110.9, 79.4, 66.3, 54.6, 28.8, 28.5, 19.4, 18.6. **^{19}F NMR** (376 MHz, $CDCl_3$) δ -62.0. δ **HRMS** (ESI) m/z: $[M + H]^+$ calcd. For $C_{25}H_{29}N_3O_4F_3$: 492.2105; found: 492.2107. $[\alpha]_d^{22}$ -19.13° (c= 0.12 $CHCl_3$) **^{1}H NMR** (400 MHz, Acetone-D_6) δ 8.31 (dd, J = 7.8, 1.6 Hz, 1H), 7.95 (td, J = 7.7, 1.6 Hz, 1H), 7.91 – 7.86 (m, 1H), 7.83 (td, J = 7.7, 1.1 Hz, 1H), 7.75 – 7.72 (m, 1H), 7.46 – 7.39 (m, 2H), 7.09 – 7.04 (m, 1H), 5.51 (d, J = 9.5 Hz, 1H), 4.07 – 3.97 (m, 2H), 3.53 – 3.43 (m, 1H), 1.51 – 1.44 (m, 1H), 1.38 (s, 9H), 0.79 (d, J = 6.8 Hz, 6H). **^{1}H NMR** (400 MHz, $CDCl_3$+TFAOMe) δ 8.29 – 8.23 (m, 1H), 7.96 (dd, J = 7.0, 1.5 Hz, 1H), 7.76 (td, J = 7.6, 1.8 Hz, 1H), 7.71 (td, J = 7.6, 1.4 Hz, 1H), 7.51 – 7.33 (m, 3H), 7.04 – 7.00 (m, 1H), 4.10 (dd, J = 11.5, 5.0 Hz, 1H), 3.92 (dd, J = 11.4, 4.0 Hz, 1H), 3.76 (d, J = 9.6 Hz, 1H), 3.34 (tt, J = 9.9, 4.8 Hz, 1H), 1.40 (s, 9H), 1.09 (dq, J = 14.1, 7.1 Hz, 1H), 0.74 (dd, J = 13.3, 6.7 Hz, 6H).

***M*-(*R*)-2-((tert-butoxycarbonyl)amino)-3-methylbutyl 2-(2-(trifluoromethyl)-1H-benzo[d]imidazol-1-yl)benzoate (*M*)-79**

Purified by CC (Hexane:EtOAc 4:1), Yield: 12 mg (50%) **^{1}H NMR** (400 MHz, $CDCl_3$) δ 8.27 (d, *J* = 7.8 Hz, 1H), 7.96 (ddd, *J* = 8.1, 1.4, 0.8 Hz, 1H), 7.77 (td, *J* = 7.6, 1.7 Hz, 1H), 7.70 (td, *J* = 7.7, 1.4 Hz, 1H), 7.45 (d, *J* = 7.3 Hz, 1H), 7.41 (ddd, *J* = 8.0, 7.2, 1.4 Hz, 1H), 7.42 – 7.31 (m, 1H), 7.00 (ddd, *J* = 7.9, 1.5, 0.8 Hz, 1H), 4.14 (d, *J* = 9.6 Hz, 1H), 4.08 (dd, *J* = 11.5, 5.8 Hz, 1H), 3.95 (dd, *J* = 11.5, 3.9 Hz, 1H), 3.43 – 3.30 (m, 1H), 1.41 (s, 9H), 0.68 (dd, *J* = 19.0, 6.7 Hz, 6H). **^{13}C NMR{^{1}H}** (101 MHz, $CDCl_3$) δ 164.3, 155.8, 141.1 (q, *J* = 38.6 Hz), 140.8, 137.7, 133.9, 133.8, 133.0, 130.7, 130.2, 128.9, 126.1, 124.1, 121.7, 119.0 (q, *J* = 272.2 Hz), 110.9, 79.4, 66.2, 54.7, 28.6, 28.4, 19.3, 18.6. **^{19}F NMR** (376 MHz, $CDCl_3$) δ -62.0. **HRMS** (ESI) m/z: $[M + H]^+$ calcd. For $C_{25}H_{29}N_3O_4F_3$: 492.2105; found: 492. 2104. $[\alpha]_d^{22}$ +84.35° (c= 0.12 $CHCl_3$) **^{1}H NMR** (400 MHz, Acetone-D_6) δ 8.31 (dd, J = 7.9, 1.6 Hz, 1H), 7.94 (td, J = 7.7, 1.6 Hz, 1H), 7.91 – 7.86 (m, 1H), 7.83 (td, J = 7.7, 1.2 Hz, 1H), 7.74 (d, J = 7.8 Hz, 1H), 7.46 – 7.39 (m, 2H), 7.11 – 7.05 (m, 1H), 5.58 (d, J = 9.4 Hz, 1H), 4.03 (d, J = 5.3 Hz, 2H), 3.54 – 3.45 (m, 1H), 1.50 – 1.43 (m, 1H), 1.38 (s, 9H), 0.80 (dd, J = 6.8, 2.4 Hz, 6H). **^{1}H NMR** (400 MHz, $CDCl_3$+TFAOMe) δ 8.26 (d, J = 7.7 Hz, 1H), 7.94 (dd, J = 7.2, 1.1 Hz, 1H), 7.75 (td, J = 7.6, 1.7 Hz, 1H), 7.69 (td, J = 7.6, 1.4 Hz, 1H), 7.44 (d, J = 7.6 Hz, 1H), 7.42 – 7.31 (m, 2H), 6.98 (dd, J = 7.2, 1.1 Hz, 1H), 4.12 (d, J = 9.3 Hz, 1H), 4.06 (dd, J = 11.4, 5.8 Hz, 1H), 3.98 – 3.88 (m, 1H), 3.40 – 3.30 (m, 1H), 1.40 (s, 9H), 0.91 (dt, J = 13.7, 6.9 Hz, 1H), 0.67 (dd, J = 19.0, 6.7 Hz, 6H).

***P*-(*S*)-2-((tert-butoxycarbonyl)amino)propyl 2-(2-(trifluoromethyl)-1H-benzo[d]imidazol-1-yl)benzoate (*P*)-80**

Purified by CC (Hexane:EtOAc 4:1), Yield: 10 mg (40%) **^{1}H NMR** (400 MHz,) δ 8.27 (dd, *J* = 7.7, 1.6 Hz, 1H), 7.98 – 7.94 (m, 1H), 7.77 (td, *J* = 7.6, 1.7 Hz, 1H), 7.74 – 7.68 (m, 1H), 7.47 (dt, *J* = 5.4, 2.7 Hz, 1H), 7.44 – 7.34 (m, 2H), 7.03 – 6.98 (m, 1H), 4.06 (br.s, 1H), 3.92 (ddd, *J* = 12.8, 10.6, 3.4 Hz, 2H), 3.66 (br.s, *J* = 14.9 Hz, 1H), 1.41 (s, 9H), 0.69 (d, *J* = 5.0 Hz, 3H). **^{13}C NMR{^{1}H}** (101 MHz, $CDCl_3$) δ 164.3, 155.1, 140.73 (q, J = 39.3 Hz), 140.70, 137.7, 133.9, 133.8, 132.9, 130.7, 130.2, 128.9, 126.2, 124.2, 121.7, 118.9 (q, J = 272.9 Hz), 110.9, 68.6, 68.5, 45.2, 45.2, 28.5, 16.8. **^{19}F NMR** (376 MHz, $CDCl_3$) δ -62.0. **HRMS** (ESI) m/z: $[M + H]^+$ calcd. For $C_{23}H_{25}N_3O_4F_3$: 464.1795; found: 464.1795. $[\alpha]_d^{22}$ -56.0° (c= 0.1 $CHCl_3$) **^{1}H NMR** (400 MHz, Acetone-D_6) δ 8.32 (dd, J = 7.9, 1.6 Hz, 1H), 7.95 (td, J = 7.7, 1.6 Hz, 1H), 7.90 – 7.86 (m, 1H), 7.84 (td, J = 7.7, 1.2 Hz, 1H), 7.76 – 7.72 (m, 1H), 7.45 – 7.37 (m, 2H), 7.11 – 7.05 (m, 1H), 5.64 (d, J = 5.6 Hz, 1H), 3.97 – 3.86 (m, 2H), 3.77 – 3.68 (m, 1H), 1.37 (s, 9H), 0.93 (d, J = 6.8 Hz, 3H). **^{1}H NMR** (400 MHz, $CDCl_3$+TFAOMe) δ 8.27 (dd, J = 7.7, 1.5 Hz, 1H), 7.97 – 7.93 (m, 1H), 7.77 (td, J = 7.6, 1.7 Hz, 1H), 7.71 (td, J = 7.7, 1.4 Hz, 1H), 7.47

(d, J = 7.7 Hz, 1H), 7.43 – 7.34 (m, 2H), 7.00 (ddd, J = 7.6, 1.5, 0.7 Hz, 1H), 4.08 (d, J = 5.8 Hz, 1H), 3.96 – 3.86 (m, 2H), 3.66 (s, 1H), 1.41 (s, 9H), 0.69 (d, J = 5.3 Hz, 3H).

***M*-(*S*)-2-((tert-butoxycarbonyl)amino)propyl 2-(2-(trifluoromethyl)-1H-benzo[d]imidazol-1-yl)benzoate (*M*)-80**

Purified by CC (Hexane:EtOAc 4:1), Yield: 14 mg (60%) **^{1}H NMR** (400 MHz, $CDCl_3$) δ 8.25 (dd, *J* = 7.8, 1.6 Hz, 1H), 7.95 (dt, *J* = 6.9, 4.0 Hz, 1H), 7.76 (td, *J* = 7.6, 1.7 Hz, 1H), 7.70 (td, *J* = 7.7, 1.4 Hz, 1H), 7.45 (d, *J* = 7.7 Hz, 1H), 7.43 – 7.33 (m, 2H), 7.01 – 6.97 (m, 1H), 3.96 (br.s., *J* = 20.9 Hz, 2H), 3.84 (dd, *J* = 11.0, 4.2 Hz, 1H), 3.66 (s, 1H), 1.39 (s, 9H), 0.78 (s, 3H). **^{13}C NMR{^{1}H}** (101 MHz, $CDCl_3$) δ 164.3, 155.0, 141.09 (q, *J* = 37.8 Hz), 140.8, 137.7, 133.9, 133.8, 132.9, 130.7, 130.2, 129.0, 126.2, 124.2, 121.7, 119.0 (q, *J* = 272.0 Hz), 110.8, 68.7, 28.5, 17.1. **^{19}F NMR** (376 MHz, $CDCl_3$) δ -61.95. **HRMS** (ESI) m/z: $[M + H]^+$ calcd. For $C_{23}H_{25}N_3O_4F_3$: 464.1795; found: 464.1793. $[\alpha]_d^{22}$ +13.57° (c= 0.14 $CHCl_3$) **^{1}H NMR** (400 MHz, Acetone-d6) δ 8.33 (dd, J = 7.8, 1.6 Hz, 1H), 7.95 (td, J = 7.7, 1.6 Hz, 1H), 7.90 – 7.87 (m, 1H), 7.84 (td, J = 7.7, 1.2 Hz, 1H), 7.77 – 7.72 (m, 1H), 7.45 – 7.38 (m, 2H), 7.09 – 7.04 (m, 1H), 5.67 (d, J = 5.6 Hz, 1H), 3.92 (dd, J = 6.8, 3.9 Hz, 2H), 3.71 (dt, J = 9.5, 5.4 Hz, 1H), 1.38 (s, 9H), 0.90 (d, J = 6.4 Hz, 3H). **^{1}H NMR** (400 MHz, $CDCl_3$+TFAOMe) δ 8.25 (dd, J = 7.7, 1.7 Hz, 1H), 7.96 – 7.93 (m, 1H), 7.76 (td, J = 7.6, 1.7 Hz, 1H), 7.70 (td, J = 7.7, 1.4 Hz, 1H), 7.46 – 7.44 (m, 1H), 7.37 (pd, J = 7.2, 1.3 Hz, 2H), 7.01 – 6.97 (m, 1H), 3.94 – 3.91 (m, 2H), 3.84 (dd, J = 11.0, 4.4 Hz, 1H), 3.66 (s, 1H), 1.39 (s, 9H), 0.78 (s, 3H).

***P*-(*S*)-2-((tert-butoxycarbonyl)amino)-3-phenylpropyl 2-(2-(trifluoromethyl)-1H-benzo[d]imidazol-1-yl)benzoate (*P*)-81**

Purified by CC (Hexane:EtOAc 4:1), Yield: 21 mg (95%) **^{1}H NMR** (400 MHz, $CDCl_3$) δ 8.28 (d, *J* = 7.5 Hz, 1H), 7.99 – 7.93 (m, 1H), 7.79 (td, *J* = 7.6, 1.7 Hz, 1H), 7.72 (td, *J* = 7.7, 1.4 Hz, 1H), 7.48 (d, *J* = 7.7 Hz, 1H), 7.43 – 7.36 (m, 2H), 7.24 – 7.13 (m, 3H), 7.08 – 7.03 (m, 1H), 6.90 (d, *J* = 6.9 Hz, 2H), 4.19 (d, *J* = 7.4 Hz, 1H), 3.94 (d, *J* = 4.5 Hz, 2H), 3.81 (br. s, 1H), 2.37 (dd, *J* = 13.5, 6.3 Hz, 1H), 2.04 (dd, *J* = 13.0, 8.0 Hz, 1H), 1.40 (s, 9H). **^{13}C NMR{^{1}H}** (101 MHz, $CDCl_3$) δ 164.3, 155.2, 141.2 (q, *J* = 39.3 Hz), 140.8, 137.7, 137.1, 133.9, 133.9, 133.1, 130.8, 130.2, 129.2, 128.8, 128.6, 126.7, 126.3, 124.3, 123.0, 119.0 (q, *J* = 271.7 Hz), 110.9, 79.6, 66.5, 50.5, 37.0, 28.4. **^{19}F NMR** (376 MHz, $CDCl_3$) δ -61.9., **HRMS** (ESI) m/z: $[M + H]^+$ calcd. For $C_{29}H_{29}N_3O_4F_3$: 440.2105; found: 440.2108. $[\alpha]_d^{22}$ -26.19° (c= 0.21 $CHCl_3$) **^{1}H NMR** (400 MHz, Acetone-D_6) δ 8.34 (dd, J = 7.9, 1.4 Hz, 1H), 7.95 (td, J = 7.7, 1.6 Hz, 1H), 7.91 – 7.87 (m, 1H), 7.84 (td, J = 7.7, 1.2 Hz, 1H), 7.75 (d, J = 7.8 Hz, 1H), 7.44 – 7.39 (m, 2H), 7.24 (t, J = 7.2 Hz, 2H), 7.19 – 7.09 (m, 4H), 5.66 (d, J = 8.4 Hz, 1H), 4.00 – 3.97 (m, 2H), 3.93 (dd, J = 11.6, 6.0 Hz, 1H), 2.59 (q, J = 7.3, 6.8 Hz, 2H), 1.33 (s, 9H). **^{1}H NMR** (400 MHz, $CDCl_3$+TFAOMe) δ 8.27 (d, J = 7.4 Hz, 1H), 7.99 – 7.94 (m, 1H), 7.79 (td, J = 7.6, 1.7 Hz, 1H), 7.72 (td, J = 7.7, 1.4 Hz, 1H), 7.48 (d, J = 7.4 Hz, 1H), 7.43 – 7.36 (m, 2H), 7.19 (dt, J = 11.8, 6.8 Hz, 3H), 7.09 – 7.03 (m, 1H), 6.90 (d, J = 6.8 Hz, 2H), 4.19 (d, J = 9.1 Hz, 1H), 3.94 (d, J = 4.5 Hz, 2H), 3.81 (s, 1H), 2.37 (dd, J = 13.8, 6.5 Hz, 1H), 2.04 (t, J = 9.9 Hz, 1H), 1.40 (s, 9H).

***M*-(*S*)-2-((tert-butoxycarbonyl)amino)-3-phenylpropyl 2-(2-(trifluoromethyl)-1H-benzo[d]imidazol-1-yl)benzoate (*M*)-81**

Purified by CC (Hexane:EtOAc 4:1), Yield: 15 mg (40%) **^{1}H NMR** (400 MHz, $CDCl_3$) δ 8.26 (dd, *J* = 7.8, 1.6 Hz, 1H), 7.98 – 7.92 (m, 1H), 7.79 (td, *J* = 7.6, 1.7 Hz, 1H), 7.75 – 7.70 (m, 1H), 7.48 (dd, *J* = 7.7, 0.9 Hz, 1H), 7.43 – 7.36 (m, 2H), 7.26 – 7.15 (m, 3H), 7.05 – 6.97 (m, 3H), 3.96 (br.s., *J* = 11.2 Hz, 2H), 3.89 (dd, *J* = 11.3, 4.2 Hz, 1H), 3.72 (br.s., *J* = 23.2 Hz, 1H), 2.54 – 2.30 (m, 2H), 1.38 (s, 9H). **^{13}C NMR{^{1}H}** (101 MHz, $CDCl_3$) δ 164.3, 155.1, 141.13 (q, *J* = 38.5 Hz), 140.7, 137.7, 137.2, 133.9, 133.8, 132.9, 130.8, 130.2, 129.2, 128.9, 128.7, 126.7, 126.4, 124.3, 121.8, 119.0 (q, *J* = 272.1 Hz), 110.8, 79.6, 66.6, 50.5, 37.2, 28.4. **^{19}F NMR** (376 MHz, $CDCl_3$) δ -61.8. **HRMS** (ESI) m/z: $[M + H]^+$ calcd. For $C_{29}H_{29}N_3O_4F_3$: 440.2105; found: 440.2109. $[\alpha]_d^{22}$ +21.0° (c= 0.15 $CHCl_3$) **^{1}H NMR** (400 MHz, Acetone-D_6) δ 8.34 (dd, J = 7.8, 1.5 Hz, 1H), 7.96 (td, J = 7.7, 1.6 Hz, 1H), 7.89 – 7.83 (m, 2H), 7.75 (dd, J = 7.8, 1.1 Hz, 1H), 7.44 – 7.38 (m, 2H), 7.24 (tt, J = 8.1, 1.7 Hz, 2H), 7.20 – 7.16 (m, 1H), 7.16 – 7.11 (m, 2H), 7.10 – 7.07 (m, 1H), 5.68 (d, J = 8.1 Hz, 1H), 3.99 (qd, J = 11.0, 5.3 Hz, 2H), 3.93 – 3.86

(m, 1H), 2.62 (d, J = 7.1 Hz, 2H), 1.33 (s, 9H). **^{1}H NMR** (400 MHz, $CDCl_3$) δ 8.26 (dd, J = 7.8, 1.6 Hz, 1H), 7.97 – 7.94 (m, 1H), 7.79 (td, J = 7.6, 1.7 Hz, 1H), 7.73 (td, J = 7.6, 1.4 Hz, 1H), 7.48 (dd, J = 7.7, 1.0 Hz, 1H), 7.43 – 7.36 (m, 2H), 7.23 (tt, J = 8.0, 2.0 Hz, 2H), 7.20 – 7.15 (m, 1H), 7.05 – 6.98 (m, 3H), 3.98 (d, J = 12.6 Hz, 2H), 3.89 (dd, J = 11.3, 4.2 Hz, 1H), 3.74 (s, 1H), 2.53 – 2.43 (m, 1H), 2.36 (dd, J = 11.5, 8.9 Hz, 1H), 1.38 (s, 9H).

***P*-(*R*)-2-((tert-butoxycarbonyl)amino)-4-methylpentyl 2-(2-(trifluoromethyl)-1H-benzo[d]imidazol-1-yl)benzoate (*P*)-82**

Purified by CC (Hexane:EtOAc 5:1), Yield: 13 mg (50%) **^{1}H NMR** (500 MHz, $CDCl_3$) δ 8.28 (d, *J* = 7.4 Hz, 1H), 7.96 (dd, *J* = 7.2, 1.1 Hz, 1H), 7.77 (td, *J* = 7.6, 1.7 Hz, 1H), 7.71 (td, *J* = 7.7, 1.3 Hz, 1H), 7.41 (ddd, *J* = 18.2, 16.2, 7.7 Hz, 3H), 7.01 (dd, *J* = 7.1, 1.1 Hz, 1H), 3.99 (dd, *J* = 11.0, 4.2 Hz, 1H), 3.90 (dd, *J* = 11.3, 3.6 Hz, 1H), 3.70 (d, *J* = 8.5 Hz, 1H), 3.60 (dd, *J* = 7.4, 3.5 Hz, 1H), 1.46 – 1.41 (m, 1H), 1.40 (s, 9H), 0.96 – 0.87 (m, 1H), 0.85 (d, *J* = 6.6 Hz, 3H), 0.81 (d, *J* = 7.0 Hz, 3H). **^{13}C NMR{^{1}H}** (126 MHz, $CDCl_3$) δ 164.5, 155.2, 141.1 (q, *J* = 38.3 Hz), 140.7, 137.7, 133.8, 133.0, 130.7, 130.2, 129.0, 126.3, 124.3, 121.8, 119.0 (q, *J* = 272.2 Hz), 115.7, 110.9, 79.4, 68.3, 47.5, 39.9, 28.5, 24.8, 22.8, 22.0. **^{19}F NMR** (376 MHz, $CDCl_3$) δ -61.88 **HRMS** (ESI) m/z: $[M + H]^+$ calcd. For $C_{26}H_{31}N_3O_4F_3$: 506.2161; found: 506.2162. $[\boldsymbol{\alpha}]_{\boldsymbol{d}}^{\mathbf{22}}$ -10.77° (c= 0.13, $CHCl_3$) **^{1}H NMR** (400 MHz, Acetone-D_6) δ 8.33 (dd, J = 7.8, 1.5 Hz, 1H), 7.94 (td, J = 7.7, 1.6 Hz, 1H), 7.91 – 7.86 (m, 1H), 7.86 – 7.81 (m, 1H), 7.73 (d, J = 7.8 Hz, 1H), 7.46 – 7.39 (m, 2H), 7.09 – 7.04 (m, 1H), 5.47 (d, J = 8.8 Hz, 1H), 3.93 (dt, J = 9.0, 4.2 Hz, 2H), 3.79 (dq, J = 8.5, 4.6, 3.8 Hz, 1H), 1.63 – 1.52 (m, 1H), 1.38 (s, 9H), 1.25 – 1.17 (m, 1H), 1.04 (ddd, J = 13.6, 8.9, 4.6 Hz, 1H), 0.85 (dd, J = 11.3, 6.6 Hz, 6H). **^{1}H NMR** (400 MHz, $CDCl_3$+TFAOMe) δ 8.28 (d, J = 7.7 Hz, 1H), 7.97 (d, J = 7.7 Hz, 1H), 7.77 (td, J = 7.6, 1.8 Hz, 1H), 7.71 (td, J = 7.6, 1.4 Hz, 1H), 7.46 – 7.36 (m, 3H), 7.02 (d, J = 7.8 Hz, 1H), 4.02 – 3.98 (m, 1H), 3.90 (dd, J = 11.2, 3.6 Hz, 1H), 3.71 (d, J = 9.1 Hz, 1H), 3.64 – 3.57 (m, 1H), 1.45 – 1.42 (m, 1H), 1.40 (s, 9H), 0.89 (d, J = 5.4 Hz, 1H), 0.83 (dd, J = 15.6, 6.6 Hz, 7H).

***M*-(*R*)-2-((tert-butoxycarbonyl)amino)-4-methylpentyl 2-(2-(trifluoromethyl)-1H-benzo[d]imidazol-1-yl)benzoate (*M*)-82**

Purified by CC (Hexane:EtOAc 5:1), Yield: 8 mg (30%) **^{1}H NMR** (500 MHz, $CDCl_3$) δ 8.29 (d, *J* = 7.6 Hz, 1H), 7.98 – 7.95 (m, 1H), 7.77 (td, *J* = 7.6, 1.6 Hz, 1H), 7.71 (td, *J* = 7.7, 1.3 Hz, 1H), 7.45 (d, *J* = 7.7 Hz, 1H), 7.43 – 7.39 (m, 1H), 7.37 (ddd, *J* = 8.3, 7.2, 1.3 Hz, 1H), 7.02 – 7.00 (m, 1H), 3.96 (t, *J* = 5.9 Hz, 3H), 3.64 (dq, *J* = 8.8, 4.7 Hz, 1H), 1.42 (s, 9H), 1.39 – 1.34 (m, 1H), 0.77 (d, *J* = 7.0 Hz, 3H), 0.74 (d, *J* = 6.6 Hz, 3H), 0.72 – 0.64 (m, 1H). **^{13}C NMR{^{1}H}** (126 MHz, $CDCl_3$) δ 164.4, 155.4, 141.2 (q, *J* = 38.1 Hz), 140.8, 137.7, 133.9, 133.8, 133.1, 130.7, 130.1, 129.0, 126.2, 124.2, 121.8, 119.0 (q, *J* = 272.3 Hz), 111.0, 79.4, 68.2, 47.6, 39.6, 28.5, 24.7, 22.9, 22.0. **^{19}F NMR** (376 MHz, $CDCl_3$) δ -61.94 **HRMS** (ESI) m/z: $[M + H]^+$ calcd. For $C_{26}H_{31}N_3O_4F_3$: 506.2161; found: 506.2163. $[\boldsymbol{\alpha}]_{\boldsymbol{d}}^{\mathbf{22}}$ +85.00° (c= 0.8, $CHCl_3$) **^{1}H NMR** (400 MHz, Acetone-D_6) δ 8.32 (dd, J = 7.8, 1.6 Hz, 1H), 7.94 (td, J = 7.7, 1.5 Hz, 1H), 7.91 – 7.86 (m, 1H), 7.86 – 7.81 (m, 1H), 7.74 (d, J = 7.8 Hz, 1H), 7.46 – 7.39 (m, 2H), 7.11 – 7.07 (m, 1H), 5.51 (d, J = 8.8 Hz, 1H), 3.93 (d, J = 5.4 Hz, 2H), 3.77 (dt, J = 10.4, 5.2 Hz, 1H), 1.67 – 1.52 (m, 1H), 1.38 (s, 9H), 1.24 – 1.13 (m, 1H), 1.01 (ddd, J = 13.7, 9.1, 4.6 Hz, 1H), 0.86 – 0.80 (m, 6H). **^{1}H NMR** (400 MHz, $CDCl_3$+TFAOMe) δ 8.29 (d, J = 7.3 Hz, 1H), 7.98 – 7.93 (m, 1H), 7.77 (td, J = 7.6, 1.7 Hz, 1H), 7.71 (td, J = 7.6, 1.4 Hz, 1H), 7.45 (d, J = 7.6 Hz, 1H), 7.44 – 7.35 (m, 3H), 7.01 (dt, J = 7.7, 0.9 Hz, 1H), 3.97 – 3.93 (m, 3H), 3.69 – 3.58 (m, 1H), 1.42 (s, 9H), 0.76 (dd, J = 12.2, 6.6 Hz, 7H), 0.70 (d, J = 12.0 Hz, 1H).

***P*-(*S*)-3-(benzyloxy)-2-((tert-butoxycarbonyl)amino)propyl 2-(2-(trifluoromethyl)-1H-benzo[d]imidazol-1-yl)benzoate (*P*)-83**

Purified by CC (Hexane:EtOAc 3:1), Yield: 23 mg (80%) **^{1}H NMR** (400 MHz, $CDCl_3$) δ 8.23 (d, *J* = 7.9 Hz, 1H), 7.94 (d, *J* = 7.6 Hz, 1H), 7.77 (td, *J* = 7.7, 1.6 Hz, 1H), 7.68 (td, *J* = 7.7, 1.2 Hz, 1H), 7.45 (d, *J* = 7.6 Hz, 1H), 7.42 – 7.37 (m, 1H), 7.35 (dd, *J* = 8.0, 1.1 Hz, 2H), 7.33 – 7.26 (m, 3H), 7.23 – 7.19 (m, 2H), 6.95 (d, *J* = 7.7 Hz, 1H), 4.54 (d, *J* = 10.8 Hz, 1H), 4.32 (s, *J* = 12.7 Hz, 2H), 4.15 (dd, *J* = 10.9, 5.5 Hz, 1H), 4.02 (dd, *J* = 11.1, 5.3 Hz, 1H), 3.78 – 3.69 (m, 1H), 3.13 – 2.99 (m, 2H), 1.41 (s,

9H). **^{13}C NMR{^{1}H}** (101 MHz, $CDCl_3$) δ 164.0, 155.3, 141.09 (q, J = 37.8 Hz)140.7, 137.8, 137.6, 134.0, 133.8, 132.9, 130.7, 130.1, 128.9, 128.5, 127.9, 127.8, 126.1, 124.2, 121.7, 118.9 (q, J = 272.1 Hz), 110.9, 79.7, 73.3, 68.4, 65.0, 49.0, 28.4. **^{19}F NMR** (376 MHz, $CDCl_3$) δ -62.0. **HRMS** (ESI) m/z: $[M + H]^+$ calcd. For $C_{30}H_{31}N_3O_5F_3$; 570.2210; found: 570.2214. $[\alpha]_d^{22}$ -29.13° (c= 0.23 $CHCl_3$) **^{1}H NMR** (400 MHz, Acetone-D_6) δ 8.28 (ddd, J = 7.8, 1.6, 0.3 Hz, 1H), 7.94 (td, J = 7.7, 1.6 Hz, 1H), 7.90 – 7.86 (m, 1H), 7.82 (td, J = 7.7, 1.3 Hz, 1H), 7.73 (d, J = 7.8 Hz, 1H), 7.44 – 7.37 (m, 2H), 7.33 – 7.23 (m, 5H), 7.08 – 7.01 (m, 1H), 5.65 (d, J = 8.5 Hz, 1H), 4.42 (s, 2H), 4.14 – 4.05 (m, 2H), 3.93 – 3.83 (m, 1H), 3.36 – 3.25 (m, 2H), 1.38 (s, 9H). **^{1}H NMR** (400 MHz, $CDCl_3$+TFAOMe) δ 8.22 (d, J = 7.6 Hz, 1H), 7.94 (dt, J = 8.5, 0.8 Hz, 1H), 7.76 (td, J = 7.6, 1.7 Hz, 1H), 7.68 (td, J = 7.7, 1.3 Hz, 1H), 7.45 (d, J = 7.3 Hz, 1H), 7.42 – 7.36 (m, 1H), 7.35 (dd, J = 8.0, 1.3 Hz, 1H), 7.33 – 7.25 (m, 3H), 7.23 – 7.19 (m, 2H), 6.95 (d, J = 7.6 Hz, 1H), 4.55 (d, J = 8.5 Hz, 1H), 4.32 (s, 2H), 4.15 (dd, J = 10.8, 5.8 Hz, 1H), 4.02 (dd, J = 9.9, 3.9 Hz, 1H), 3.75 (s, 1H), 3.15 – 2.99 (m, 2H), 1.41 (s, 9H).

***M*-(*S*)-3-(benzyloxy)-2-((tert-butoxycarbonyl)amino)propyl 2-(2-(trifluoromethyl)-1H-benzo[d]imidazol-1-yl)benzoate (*M*)-83**

Purified by CC (Hexane:EtOAc 3:1), Yield: 28 mg (95%) **^{1}H NMR** (400 MHz, $CDCl_3$) δ 8.22 (d, *J* = 7.6 Hz, 1H), 7.94 (d, *J* = 8.0 Hz, 1H), 7.77 (td, *J* = 7.6, 1.6 Hz, 1H), 7.69 (t, *J* = 7.5 Hz, 1H), 7.45 (dd, *J* = 7.8, 1.1 Hz, 1H), 7.39 (ddd, *J* = 8.1, 5.8, 1.3 Hz, 1H), 7.37 – 7.33 (m, 1H), 7.33 – 7.26 (m, 3H), 7.23 – 7.18 (m, *J* = 6.3 Hz, 2H), 6.95 (d, *J* = 7.8 Hz, 1H), 4.49 (d, *J* = 8.0 Hz, 1H), 4.34 (dd, *J* = 24.6, 11.4 Hz, 2H), 4.09 (t, *J* = 13.1 Hz, 1H), 3.99 (dt, *J* = 13.5, 6.7 Hz, 1H), 3.77 (s, 1H), 3.12 (d, *J* = 31.8 Hz, 2H), 1.41 (s, 9H). **^{13}C NMR{^{1}H}** (101 MHz, $CDCl_3$) δ 164.0, 155.2, 141.0 (q, J = 38.6 Hz), 140.7, 137.9, 137.7, 133.9, 133.8, 132.9, 130.7, 130.2, 128.9, 128.5, 127.9, 127.7, 126.2, 124.2, 121.7, 118.9 (q, J = 272.1 Hz), 110.8, 79.7, 73.2, 68.3, 64.7, 48.9, 28.4. **^{19}F NMR** (376 MHz,) δ -61.9. **HRMS** (ESI) m/z: $[M + H]^+$ calcd. For $C_{30}H_{31}N_3O_5F_3$; 570.2210; found: 570.2215. $[\alpha]_d^{22}$ +9.29° (c= 0.28 $CHCl_3$) **^{1}H NMR** (400 MHz, Acetone-D_6) δ 8.28 – 8.25 (m, 1H), 7.92 (td, J = 7.7, 1.6 Hz, 1H), 7.86 – 7.83 (m, 1H), 7.80 (td, J = 7.8, 1.2 Hz, 1H), 7.71 (dd, J = 7.9, 0.9 Hz, 1H), 7.41 – 7.34 (m, 2H), 7.29 – 7.19 (m, 5H), 6.99 (dd, J = 6.4, 2.3 Hz, 1H), 5.68 (d, J = 8.7 Hz, 1H), 4.41 – 4.27 (m, 2H), 4.05 (qd, J = 11.1, 6.3 Hz, 2H), 3.76 (p, J = 7.4, 6.3 Hz, 1H), 3.26 – 3.10 (m, 2H), 1.35 (s, 9H). **^{1}H NMR** (400 MHz, $CDCl_3$+TFAOMe) δ 8.21 (d, J = 7.5 Hz, 1H), 7.94 (d, J = 7.9 Hz, 1H), 7.77 (td, J = 7.7, 1.6 Hz, 1H), 7.68 (t, J = 7.4 Hz, 1H), 7.45 (dd, J = 7.8, 1.0 Hz, 1H), 7.41 – 7.36 (m, 1H), 7.36 – 7.33 (m, 1H), 7.32 – 7.26 (m, 3H), 7.21 (d, J = 6.4 Hz, 2H), 6.95 (d, J = 7.9 Hz, 1H), 4.49 (d, J = 8.3 Hz, 1H), 4.34 (q, J = 11.4 Hz, 2H), 4.11 (s, 1H), 4.01 (dd, J = 6.7, 4.2 Hz, 1H), 3.75 (s, 1H), 3.11 (d, J = 33.7 Hz, 2H), 1.41 (s, 9H).

Methyl (*S*)-2-formamido-2-phenylacetate (85)

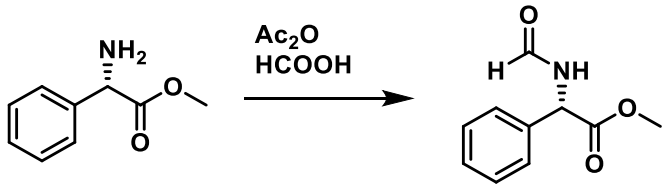

85

Following literature procedure.[170] (*S*)-phenylglycine methylester hydrochloride (603 mg, 3 mmol, 1 eq.) was dissolved in DI water (10 ml) and aq. K_2CO_3 solution was added (10ml, 10 weight %). The solution was extracted with diethylether (3x 20 mL), dried with $MgSO_4$ and evaporated to yield of freebase (*S*)-phenylglycine methylester (360 mg of clear oil (70%)). This oil was dissolved in formic acid (30 mL) and cooled in ice bath. Acetic anhydride (8.3 mL) was added dropwise while cooling. After the addition was complete, the reaction was stirred for 16 hours. After 16 hours, DI water was added (20 mL) and the solution was stirred for 20 minutes and evaporated. The oily residue was dissolved in EtOAc (50 mL) and extracted with 10% aq. HCl (3x 50 mL) and 10% aq. K_2CO_3 (3x 50 mL), dried with $MgSO_4$ and evaporated to yield clear oil which solidified upon standing on room temperature or under high vacuum. Yield: 371 mg of white solid (75%). Reaction was reproduced on 10 mmol scale, yielding 1.2g (65%) of white solid. **^{1}H NMR** (400 MHz, $CDCl_3$) δ 8.25 (s, 1H), 7.38 – 7.33 (m, 5H), 6.60 (s, 1H),

5.67 (d, *J* = 7.4 Hz, 1H), 3.75 (s, 3H).**^{13}C NMR {^{1}H}** (101 MHz, $CDCl_3$) δ 171.1, 160.2, 136.2, 129.2, 128.9, 127.3, 55.2, 53.1. **HRMS** (ESI- TOF) m/z:[M + H]$^+$ calcd. for $C_{10}H_{12}N_3O_1$: 194.0812; found: 194.0813, $[\alpha]_d^{22}$ +87.62° (c= 0.42, $CHCl_3$)

(*S*)-2-(methylamino)-2-phenylethan-1-ol (86)

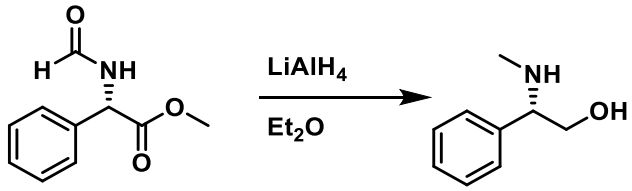

85 86

Modified literature procedure.[170] Methyl (*S*)-2-formamido-2-phenylacetate (400 mg, 2 mmol, 1 eq.) was added portionwise to a suspension of $LiAlH_4$ (380 mg, 10 mmol, 5eq.) in dry THF (15 mL) at 5°C (ice/water bath). After addition was completed, the mixture was refluxed for 16 h. After reaction competion (TLC: EtOAc:MeOH 2:1), reaction was cooled to room temperature and further cooled in ice bath and aq. NaOH solution (15% by weight, 0.75 ml/ mmol $LiALH_4$) was added dropwise. The resultion susspension was filtered through celite and washed thoroughly with EtOAc, dried by $MgSO_4$ and evaporated. The residual oil was purified by collum chromatography (EtOAc:MeOH 2:1) yielding 242 mg of white solid (80%). Reaction was reproduced on 6.2 mmol scale, yielding white solid which was suspended in chloroform, filtered and after evaporation 800 mg (85%) of white solid was obtained. **^{1}H NMR** (400 MHz, $CDCl_3$) δ 7.39 – 7.34 (m, 2H), 7.32 – 7.27 (m, 3H), 3.75 (dd, *J* = 10.1, 4.1 Hz, 1H), 3.71 – 3.66 (m, 1H), 3.61 (dd, *J* = 10.0, 8.0 Hz, 1H), 2.69 (s, 2H), 2.36 (s, 3H).**^{13}C NMR {^{1}H}** (101 MHz, $CDCl_3$) δ 179.1, 129.4, 129.2, 128.2, 66.2, 64.5, 31.5, 23.8. HRMS (ESI- TOF) m/z:[M + H]$^+$ calcd. for $C_9H_4N_1O_1$: 152.1070; found: 152.1070, $[\alpha]_d^{22}$ +39.89° (c= 0.88, $CHCl_3$)

tert-Butyl (*S*)-(2-hydroxy-1-phenylethyl)(methyl)carbamate (87)

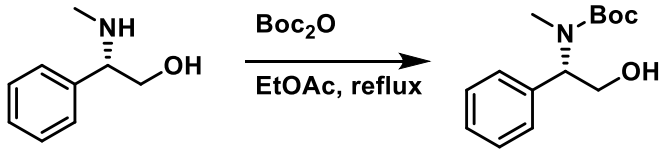

86 87

Following literature procedure.[171] (*S*)-2-(methylamino)-2-phenylethan-1-ol (40 mg, 0.25 mmol, 1 eq.) was dissolved in EtOAc (10 mL) and Boc_2O was added at once and the mixture was refluxed for 16 hours. After 16 hours, the reaction was cooled to room temperature washed twice with water and once with brine, dried with $MgSO_4$ and evaporated, yileding 53 mg of oil (85%) **^{1}H NMR** (400 MHz, $CDCl_3$) δ 7.36 – 7.20 (m, 5H), 5.32 – 5.24 (m, 1H), 4.11 – 4.01 (m, 2H), 2.69 (s, 1H), 1.51 (s, 3H), 1.47 (s, 9H). **^{13}C NMR {^{1}H}** (101 MHz, $CDCl_3$) δ 146.9, 128.8, 127.8, 127.5, 85.3, 80.4, 60.6, 28.6, 27.6. HRMS (ESI- TOF) m/z:[M + H]$^+$ calcd. for $C_{14}H_{22}N_1O_3$: 252.1594; found: 252.1595, $[\alpha]_d^{22}$ +55.17° (c= 0.6, $CHCl_3$)

(*S*)-*N*-(2-hydroxy-1-phenylethyl)-N-methylacetamide (88)

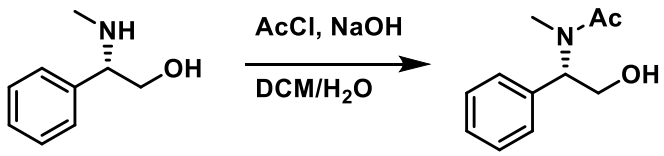

86 88

Following literature procedure.[172] *(S)-N*-methyl-phenylglycinol (50 mg, 0.33 mmol, 1 eq.) was dissolved in DCM (1.5 mL) and acetylchloride was added (30 µL, 0.4 mmol, 1.2 eq.) followed by dropwise addition of 0.5M NaOH (840 µL, 0.4 mmol, 1.2 eq.). The biphasic systém was stirred rapidly for 1 hour. After 1 hr the mixture was diluted with water (10 mL) and extracted with DCM (3 × 10 mL). Organic layeres were combined, dried with MgSO4 and purified by collumn chromatography (EtOAc:MeOH 20:1) to yield 50 mg of white solid (78%) as a mixture of rotamers in aprox. 10:4 ratio. Peaks belonging to major rotamer are designated M, peaks belonging to minor rotamer are designated m. **^{1}H NMR** (400 MHz, $CDCl_3$) δ 7.41 – 7.19 (m, 10H, both rotamers), 5.83 (dd, *J* = 9.3, 4.9 Hz, 1H, M), 5.09 (dd, *J* = 9.2, 4.9 Hz, 1H, m), 4.23 – 4.02 (m, 4H, both rotamers), 2.78 (s, 4H, both rotamers), 2.42 (dd, *J* = 7.2, 4.7 Hz, 1H, M), 2.28 (s, 3H, m), 2.19 (s, 3H, M), 2.15 – 2.05 (m, 1H, m). **^{13}C NMR{^{1}H}** (126 MHz, $CDCl_3$) δ 172.8 M, 172.4 m, 137.2 M, 137.0 m, 129.1 m, 128.8 M, 128.2 m, 127.93 M, 127.89 M, 127.0 m, 62.6 m, 61.9 M, 61.5 m, 58.4 M, 32.0 M, 28.1 m, 22.5 M, 22.2 m. **HRMS** (ESI) m/z:$[M+H]^+$ calcd. for: $C_{11}H_{16}NO_2$: 194,1176 found: 194,1176 $[\alpha]_d^{22}$-440,0°(c= 0.13 $CHCl_3$)

(S)-2-(N-methylformamido)-2-phenylethyl formate (89)

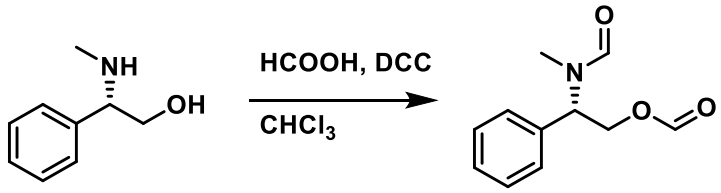

86 89

Following literature procedure.[173]HCOOH (150 µL, 4 mmol, 4 eq.) solution in $CHCl_3$ (2 mL) was added dropwise while cooling into the DCC (412 mg, 2 mmol, 2 eq.) solution in $CHCl_3$ (3 mL). After 5 minues, the white suspension was added dropwise into the solution of (*S*)-N-methyl-phenylglycinol (151 mg, 1 mmol, 1 eq.) in mixure of $CHCl_3$ (3 mL) and pyridine (1.5 mL) and stirred in ice bath for 16 hours. After 16 hours, the reaction mixture was evaporated, suspended in diethylether (10 mL) filtered and the filtrate was evaporated. The residue was then redissolved in ethylacetate and extracted twice with 10% HCl and 10% K_2CO_3 and brine, dried with $MgSO_4$ and purified by collumn chromatography (Hexane:EtOAc 1:1) to yield 100 mg of oil (50%) as a mixture of two rotamers in aprox. 10:6 ratio. Peaks belonging to major rotamer are designated M, peaks belonging to minor rotamer are designated m. **^{1}H NMR** (500 MHz, $CDCl_3$) δ 8.31 (s, 1H, M), 8.18 (s, 1H, m), 8.10 (s, 1H, M), 8.08 (s, 1H, m), 7.43 – 7.31 (m, 5H, both rotamers), 7.29 – 7.22 (m, 5H, both rotamers), 5.91 (dd, *J* = 9.5, 5.3 Hz, 1H, m), 4.91 (dd, *J* = 10.0, 4.6 Hz, 1H, M), 4.79 – 4.72 (m, 1H, both rotamers), 4.67 – 4.62 (m, 1H, both rotamers), 2.76 (s, 3H, m), 2.69 (s, 3H, M). **^{13}C NMR {^{1}H}** (126 MHz, $CDCl_3$) δ 163.5 m, 163.1 M, 160.6 m, 160.4 M, 135.2 m, 134.8 M, 129.3, 129.1, 128.9, 128.6, 127.9, 127.2, 60.8 M, 59.6 m, 52.7 M, 49.3 m, 34.1, 30.6. **HRMS** (ESI) m/z:$[M+H]^+$ calcd. for: $C_{11}H_{14}NO_3$: 208.0968 found: 208.0967 $[\alpha]_d^{22}$+89.47 (c= 0.19 $CHCl_3$)

(S)-*N*-(2-hydroxy-1-phenylethyl)-*N*-methylformamide (90)

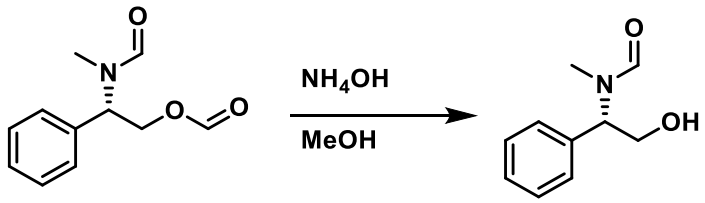

89 90

(*S*)-2-(*N*-methylformamido)-2-phenylethyl formate (80 mg, 0.38 mmol, 1 eq.) was dissolved in MeOH (8 mL) and NH_3 was added (25% aq. solution, 90 µL, 1.15 mmol, 3 eq) and the reaction was stirred at room temperature for 2 hours. After two hours, the solution was evaporated, dissolved in EtOAc,

extracted with brine three times. Organic layer was separated, dried with $MgSO_4$ and evaporated. The residue was purified by collumn chromatography (EtOAc) to yield 21 mg (30%) of clear oil as a mixture of two rotamers in aprox. 10:6 ratio. **^{1}H NMR** (500 MHz, $CDCl_3$) δ 8.33 (s, 1H, M), 8.21 (s, 1H, m), 7.40 – 7.22 (m, 10H, both rotamers), 5.41 (dd, *J* = 8.4, 5.4 Hz, 1H, m), 4.68 (dd, *J* = 8.7, 5.3 Hz, 1H, M), 4.17 – 4.08 (m, 4H, both rotamers), 2.80 (s, 3H, m), 2.70 (s, 3H, M). **^{13}C NMR {^{1}H}** (126 MHz, $CDCl_3$) δ 164.3, 163.9, 136.2, 136.1, 129.1, 129.0, 128.5, 128.3, 127.9, 127.4, 63.5, 61.6, 60.7, 58.7, 32.1, 26.6. **HRMS** (ESI) m/z:$[M+H]^+$ calcd. for: $C_{10}H_{14}O_2N_1$: 180.1019 found: 180.1019, $[\alpha]_d^{22}$+41.51 (c= 0.21 $CHCl_3$)

(*S*)-2-acetamido-2-phenylethyl acetate (92)

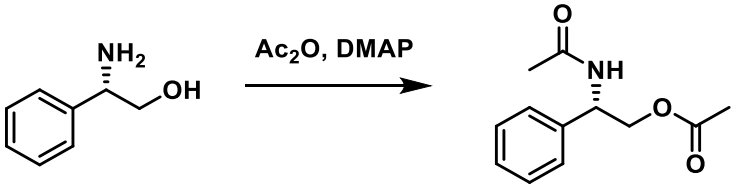

92

(*S*)-phenylglycinol (670 mg, 5 mmol, 1 eq.) and DMAP (70 mg, 0.5 mmol, 0.1 eq.) was dissolved in Ac_2O (7 mL) and stirred at room temperatur efor 2.5 hr. After 2.5 hrs the soution was added dropwise into 10% K_2CO_3 aq. Solution (15 mL). The solution was furhter neutralized with solid K_2CO_3 until pH=7 and then extracted into DCM (3 × 30 mL). Organic layers were combined and dried with MgSO4 and evaporated to yield white solid (573 mg, 50%) **^{1}H NMR** (500 MHz, $CDCl_3$) δ 7.37 – 7.33 (m, 2H), 7.31 – 7.27 (m, 3H), 6.09 (d, *J* = 6.4 Hz, 1H), 5.29 (td, *J* = 7.6, 4.7 Hz, 1H), 4.43 (dd, *J* = 11.5, 7.2 Hz, 1H), 4.26 (dd, *J* = 11.5, 4.7 Hz, 1H), 2.05 (s, 3H), 2.02 (s, 3H). **^{13}C NMR {^{1}H}** (126 MHz, $CDCl_3$) δ 171.4, 169.7, 138.5, 129.0, 128.1, 126.8, 66.2, 52.7, 23.5, 21.0. **HRMS** (ESI) m/z:$[M+H]^+$ calcd. for: $C_{12}H_{16}NO_3$: 222.1130 found: 222.1125 $[\alpha]_d^{22}$+80,77° (c= 0.13 $CHCl_3$)

(S)-*N*-(2-hydroxy-1-phenylethyl)acetamide (93)

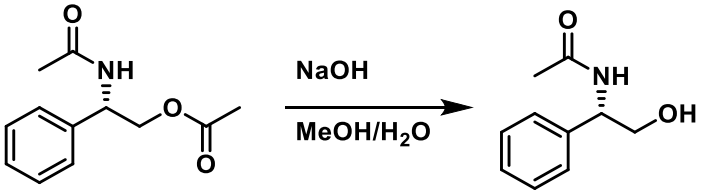

92 **93**

(*S*)-2-acetamido-2-phenylethyl acetate 300 mg, 1.35 mmol, 1 eq.) was dissolved in MeOH (15 mL) and NaOH solution (270 mg, 6.75 mmol, 5eq. dissolved in 5 mL of DI water) and stirred at room temperature for 12 hours. After 12 hours, the mixture was filtered through pad of celite, washed with 30 mL of EtOAc:MeOH (1:1) and the filtrate was dried with MgSO4 and evaporated yielding white solid (228 mg, 93%) **^{1}H NMR** (500 MHz, $CDCl_3$) δ 7.37 – 7.33 (m, 2H), 7.31 – 7.27 (m, 3H), 6.38 (d, *J* = 3.5 Hz, 1H), 5.04 (dt, *J* = 7.1, 5.1 Hz, 1H), 3.85 (d, *J* = 5.1 Hz, 2H), 3.12 (s, 1H), 2.02 (s, 3H). **^{13}C NMR {^{1}H}** (126 MHz, $CDCl_3$) δ 171.0, 139.1, 129.0, 128.0, 126.9, 66.6, 56.1, 23.4. **HRMS** (ESI) m/z:$[M+H]^+$ calcd. for: $C_{10}H_{14}NO_2$: 180.1019 found: 180.1019 $[\alpha]_d^{22}$+45,26°(c= 0.19 $CHCl_3$)

(*S*)-2-(dibenzylamino)-2-phenylethan-1-ol (94)

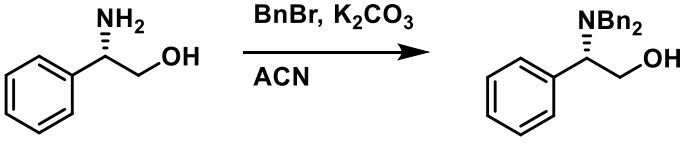

94

Following literature procedure.[175] (*S*)-phenylglycinol (137 mg, 1 mmol, 1eq.) was dissolved in acetonitrile (7 mL), K_2CO_3 (280 mg, 2 mmol, 2 eq.) was added followed by benzyl bromide (250 µL,

2.1 mmol, 2.1 eq.). The reaction was stirred at 60°C for 24 hrs. After the reaction was complete (TLC Hexane:EtOAc 4:1), the reaction was filtered and the filtrate was evaporated and purified by collumn chromatography (Hexane:EtOAc, gradient from 10:1 to 8:1). Isolated as a colorless oil (199 mg, 62%) **^{1}H NMR** (400 MHz, $CDCl_3$) δ 7.48 – 7.34 (m, 3H), 7.34 (d, *J* = 4.4 Hz, 8H), 7.27 (q, *J* = 3.9, 3.2 Hz, 4H), 4.14 (t, *J* = 10.6 Hz, 1H), 3.96 – 3.93 (m, 1H), 3.62 (dd, *J* = 10.8, 5.2 Hz, 1H), 3.16 (d, *J* = 13.4 Hz, 1H). **^{13}C NMR {^{1}H}** (101 MHz, $CDCl_3$) δ 139.3, 135.3, 129.4, 129.1, 128.7, 128.5, 128.2, 127.4, 63.2, 60.6, 53.7. **HRMS** (ESI- TOF) m/z:[M + H]+ calcd. for $C_{22}H2_4N_1O_1$: 318.1852; found: 318.1853, $[\boldsymbol{\alpha}]_{\boldsymbol{d}}^{\mathbf{22}}$ +122.33° (c= 0.6, $CHCl_3$)

(*S*)-2-(2-hydroxy-1-phenylethyl)isoindoline-1,3-dione (95)

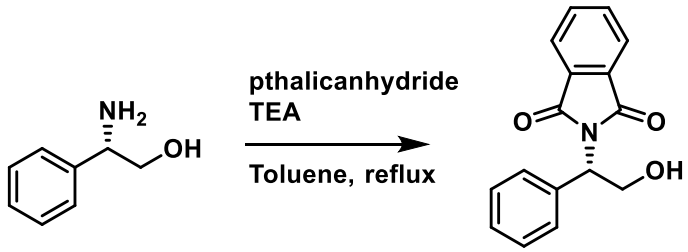

95

Following literature procedure.[176] (*S*)-phenylglycinol (420 mg, 3 mmol, 1 eq.) was suspended in toluene (10 mL), pthalic anhydride (450 mg, 3 mmol, 1 eq.) was added, followed by triethylamine (50 µL, 0.3 mmol, 0.1 eq.). Reaction was refluxed for 16 hrs. The reaction was then cooled to the room temperature, evaporated and the residue was redissolved in EtOAc (25 mL) and extracted with 10% aq. HCl (3× 25 mL) and 10% aq. K_2CO_3 (3× 25 mL). Combined organic layers were washed with brine, dried with $MgSO_4$ and evaporated. The residue was purified by collumn chromatography (Hexane:EtOAc 2:1). 390mg (50%). **^{1}H NMR** (400 MHz, $CDCl_3$) δ 7.83 (dd, *J* = 5.6, 3.2 Hz, 2H), 7.71 (td, *J* = 5.3, 2.1 Hz, 2H), 7.46 (dd, *J* = 6.9, 1.5 Hz, 2H), 7.39 – 7.23 (m, 3H), 5.47 (dd, *J* = 9.0, 5.0 Hz, 1H), 4.65 (dd, *J* = 11.7, 8.9 Hz, 1H), 4.24 (dd, *J* = 11.7, 5.0 Hz, 1H). **^{13}C NMR {^{1}H}** (101 MHz, $CDCl_3$) δ 169.0, 137.0, 134.3, 132.0, 128.9, 128.3, 128.0, 123.6, 62.5, 57.7. **HRMS** (ESI- TOF) m/z:[M + H]+ calcd. for $C_{16}H_{14}N_1O_3$: 268.0968; found: 268.0967, $[\boldsymbol{\alpha}]_{\boldsymbol{d}}^{\mathbf{22}}$ -45.17° (c= 0.29, $CHCl_3$)

(*S*)-2-(dimethylamino)-2-phenylethan-1-ol

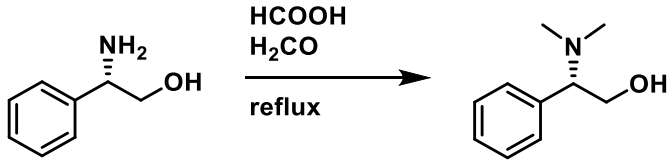

Following literature procedure.[208] (*S*)-phenylglycinol (550 mg, 4 mmol, 1 eq.) was dissolved in HCOOH (0.6 mL) and formaldehyde was added (38% aq. solution, 0.6 mL) and the reaction was heated at 90°C for 16 hours. After 16 hrs the solution was cooled to room temperature, bazified with NH_3 solution (25% aq. solution, 0.5 mL) and extracted 3 times with DCM. The organic phases were combined and dried with $MgSO_4$, evaporated and purified by collumn chromatography (EtOAc:MeOH 20:1) yielding 400 mg (60%) of brown oil which solidifed by standing at room temperature. **^{1}H NMR** (400 MHz, $CDCl_3$) δ 7.41 – 7.28 (m, 3H), 7.25 – 7.16 (m, 2H), 3.93 (dd, *J* = 10.7, 9.0 Hz, 1H), 3.68 (dd, *J* = 10.6, 5.3 Hz, 1H), 3.57 (dd, *J* = 9.0, 5.3 Hz, 1H), 2.21 (s, 3H). **^{13}C NMR {^{1}H}** (101 MHz, $CDCl_3$) δ 135.9, 129.1, 128.3, 128.0, 70.3, 61.4, 41.5. **HRMS** (ESI) m/z:$[M+H]^+$ calcd. for: $C_{10}H_{16}NO$: 166.1266 found: 166.1266 $[\boldsymbol{\alpha}]_{\boldsymbol{d}}^{\mathbf{22}}$+32.5° (c= 0.36 $CHCl_3$)

Compounds **96-103** were prepared by following the general procedure for TBBA ester formation

***P*-(*S*)-2-((tert-butoxycarbonyl)(methyl)amino)-2-phenylethyl 2-(2-(trifluoromethyl)-1H-benzo[d]imidazol-1-yl)benzoate (*P*)-96**

Purified by CC (Hexane:EtOAc 5:1), Yield: 19 mg (70%) **^{1}H NMR** (400 MHz, $CDCl_3$) δ 8.21 (d, *J* = 6.3 Hz, 1H), 7.99 – 7.91 (m, 1H), 7.77 (t, *J* = 7.5 Hz, 1H), 7.67 (t, *J* = 7.5 Hz, 1H), 7.49 (d, *J* = 7.6 Hz, 1H), 7.42 – 7.33 (m, 2H), 7.32 – 7.23 (m, 3H), 7.10 (br.s, 2H), 7.00 – 6.97 (m, 1H), 5.42 (d, *J* = 197.9 Hz, 1H), 4.46 (s, 2H), 2.51 (s, 3H), 1.41 (s, 9H). **^{13}C NMR {^{1}H}** (126 MHz, $CDCl_3$) δ 163.5, 141.09 (q, J = 38.6 Hz), 140.8, 137.6, 136.8, 134.5, 133.8, 132.6, 130.6, 130.2, 128.8, 128.6, 127.9, 127.3, 127.0 126.0, 124.0, 121.7, 119.0 (q, J = 273.3 Hz), 110.8, 80.2, 62.8, 55.4, 29.8, 28.5. **^{19}F NMR** (471 MHz, $CDCl_3$) δ -61.4. **HRMS** (ESI) m/z:[M + H]+ calcd. For $C_{29}H_{29}N_3O_4F_3$; 540.2105; found: 540.2109. $[\alpha]_d^{22}$ -10.53° (c= 0.095 $CHCl_3$) **^{1}H NMR** (400 MHz, Acetone-D_6) δ 8.24 (dd, J = 7.8, 1.6 Hz, 1H), 7.99 – 7.92 (m, 1H), 7.90 – 7.85 (m, 1H), 7.83 (t, J = 7.4 Hz, 1H), 7.75 (d, J = 7.9 Hz, 1H), 7.45 – 7.38 (m, 2H), 7.34 (tt, J = 8.1, 1.9 Hz, 2H), 7.30 – 7.25 (m, 1H), 7.23 (d, J = 7.1 Hz, 2H), 7.08 – 7.03 (m, 1H), 5.47 (d, J = 109.5 Hz, 1H), 4.51 (s, 2H), 2.58 (s, 3H), 1.40 (s, 9H). **^{1}H NMR** (400 MHz, $CDCl_3$+TFAOMe) δ 8.18 (d, J = 7.7 Hz, 1H), 7.94 – 7.88 (m, 1H), 7.75 (t, J = 7.6 Hz, 1H), 7.65 (t, J = 7.6 Hz, 1H), 7.47 (d, J = 7.8 Hz, 1H), 7.40 – 7.30 (m, 2H), 7.28 – 7.20 (m, 4H), 7.07 (d, J = 4.2 Hz, 2H), 6.95 (d, J = 8.2 Hz, 1H), 5.39 (d, J = 194.0 Hz, 1H), 4.51 – 4.24 (m, 2H), 2.49 (s, 3H), 1.37 (s, 9H).

***M*-(*S*)-2-((tert-butoxycarbonyl)(methyl)amino)-2-phenylethyl 2-(2-(trifluoromethyl)-1H-benzo[d]imidazol-1-yl)benzoate (*M*)-96**

Purified by CC (Hexane:EtOAc 5:1), Yield: 22 mg (81%) **^{1}H NMR** (500 MHz, $CDCl_3$) δ 8.21 (dd, *J* = 7.8, 1.5 Hz, 1H), 7.93 (d, *J* = 7.7 Hz, 1H), 7.77 (t, *J* = 7.5 Hz, 1H), 7.68 (s, 1H), 7.49 (d, *J* = 7.8 Hz, 1H), 7.40 – 7.33 (m, 2H), 7.31 – 7.22 (m, 3H), 7.09 (d, *J* = 30.8 Hz, 2H), 6.96 (d, *J* = 8.2 Hz, 1H), 5.44 (d, *J* = 182.5 Hz, 1H), 4.50 (dd, *J* = 11.4, 5.6 Hz, 1H), 4.34 (d, *J* = 60.2 Hz, 1H), 2.42 (s, 3H), 1.41 (s, 9H). **^{13}C NMR{^{1}H}** (126 MHz, $CDCl_3$) δ 163.5, 155.8, 140.92 (q, J = 39.1 Hz), 140.8, 137.7, 136.9, 134.5, 133.9, 132.5, 130.6, 130.2, 128.8, 128.7, 127.9, 127.3, 127.0, 126.1, 124.0, 121.6, 119.00 (app. d, J = 271.9 Hz), 110.8, 80.2, 63.3, 56.9, 29.3, 28.5. **^{19}F NMR** (471 MHz, $CDCl_3$) δ -61.4. **HRMS** (ESI) m/z:[M + H]+ calcd. For $C_{29}H_{29}N_3O_4F_3$; 540.2105; found: 540.2108. $[\alpha]_d^{22}$ +12.27° (c= 0.22 $CHCl_3$) **^{1}H NMR** (400 MHz, Acetone-D_6) δ 8.24 (dd, J = 7.8, 1.6 Hz, 1H), 7.98 – 7.91 (m, 1H), 7.90 – 7.79 (m, 2H), 7.74 (d, J = 7.8 Hz, 1H), 7.43 – 7.36 (m, 2H), 7.35 – 7.24 (m, 3H), 7.20 (d, J = 7.0 Hz, 2H), 7.01 (d, J = 8.2 Hz, 1H), 5.44 (d, J = 103.3 Hz, 1H), 4.52 (dd, J = 11.5, 5.4 Hz, 1H), 4.45 (d, J = 9.8 Hz, 1H), 2.45 (s, 3H), 1.41 (s, 9H). **^{1}H NMR** (400 MHz, $CDCl_3$+TFAOMe) δ 8.17 (d, J = 7.8 Hz, 1H), 7.89 (d, J = 7.0 Hz, 1H), 7.74 (t, J = 7.4 Hz, 1H), 7.65 (t, J = 7.7 Hz, 1H), 7.46 (d, J = 7.6 Hz, 1H), 7.33 (p, J = 7.2 Hz, 2H), 7.28 – 7.18 (m, 3H), 7.03 (s, 2H), 6.92 (d, J = 7.3 Hz, 1H), 5.40 (d, J = 139.4 Hz, 1H), 4.51 – 4.20 (m, 2H), 2.38 (s, 3H), 1.37 (s, 9H).

***P*-(*S*)-2-(dimethylamino)-2-phenylethyl 2-(2-(trifluoromethyl)-1H-benzo[d]imidazol-1-yl)benzoate (*P*)-97**

Purified by HPLC, Yield: 14 mg (50%) **^{1}H NMR** (500 MHz, $CDCl_3$) δ 8.06 (dd, *J* = 7.8, 1.6 Hz, 1H), 7.99 – 7.97 (m, 1H), 7.73 (td, *J* = 7.7, 1.6 Hz, 1H), 7.65 (td, *J* = 7.7, 1.3 Hz, 1H), 7.47 – 7.44 (m, 1H), 7.42 (ddd, *J* = 8.2, 7.2, 1.2 Hz, 1H), 7.36 (td, *J* = 7.7, 7.2, 1.1 Hz, 1H), 7.30 – 7.22 (m, 3H), 7.12 – 7.09 (m, 2H), 6.98 (dt, *J* = 8.1, 0.9 Hz, 1H), 4.29 (dd, *J* = 11.5, 6.5 Hz, 1H), 4.13 (dd, *J* = 11.5, 6.1 Hz, 1H), 2.98 (t, *J* = 6.3 Hz, 1H), 1.96 (s, 6H). **^{13}C NMR{^{1}H}** (126 MHz, $CDCl_3$) δ 164.0, 141.1 (q, J = 38.5 Hz), 140.8, 137.8, 137.7, 134.0, 133.6, 132.5, 130.6, 130.0, 129.1, 128.4, 128.4, 127.8, 126.0, 124.0, 121.6, 118.9 (q, J = 272.1 Hz), 111.0, 68.3, 66.6, 42.7. **^{19}F NMR** (471 MHz, $CDCl_3$) δ -61.3. **HRMS** (ESI) m/z:[M + H]+ calcd. For $C_{25}H_{23}N_3O_2F_3$: 454.1737; found: 454.1735. $[\alpha]_d^{22}$ -53.57° (c= 0.14, $CHCl_3$)

***M*-(*S*)-2-(dimethylamino)-2-phenylethyl 2-(2-(trifluoromethyl)-1H-benzo[d]imidazol-1-yl)benzoate (*M*)-97**

Purified by HPLC, Yield: 14 mg (50%) **^{1}H NMR** (500 MHz, $CDCl_3$) δ 8.08 (dd, *J* = 7.9, 1.6 Hz, 1H), 7.96 (dt, *J* = 8.2, 0.9 Hz, 1H), 7.74 (td, *J* = 7.7, 1.6 Hz, 1H), 7.65 (td, *J* = 7.7, 1.3 Hz, 1H), 7.45 (dd, *J* =

7.8, 0.9 Hz, 1H), 7.40 (ddd, *J* = 8.3, 7.2, 1.1 Hz, 1H), 7.33 (ddd, *J* = 8.2, 7.2, 1.1 Hz, 1H), 7.27 – 7.21 (m, 3H), 7.04 – 7.00 (m, 2H), 6.94 (dt, *J* = 8.2, 1.0 Hz, 1H), 4.34 (dd, *J* = 11.5, 6.6 Hz, 1H), 4.14 (dd, *J* = 11.5, 5.9 Hz, 1H), 3.09 (t, *J* = 6.2 Hz, 1H), 2.06 (s, 6H). **^{13}C NMR{^{1}H}** (126 MHz, $CDCl_3$) δ 164.0, 141.10 (q, J = 38.5 Hz), 140.8, 137.7, 137.5, 134.1, 133.6, 132.5, 130.6, 130.0, 129.1, 128.4, 127.8, 126.0, 124.0, 121.6, 119.0 (q, J = 272.3 Hz), 110.9, 68.4, 66.5, 42.8. **^{19}F NMR** (471 MHz, $CDCl_3$) δ -61.3. **HRMS** (ESI) m/z:[M + H]+ calcd. For $C_{25}H_{23}N_3O_2F_3$: 454.1737; found: 454.1737. $[\alpha]_d^{22}$ +44.29° (c= 0.14, $CHCl_3$)

***P*-(*S*)-2-acetamido-2-phenylethyl 2-(2-(trifluoromethyl)-1H-benzo[d]imidazol-1-yl)benzoate (*P*)-98**

Purified by CC, yield 5 mg (21%) **^{1}H NMR** (500 MHz, $CDCl_3$) δ 8.23 (ddd, *J* = 7.8, 1.7, 0.3 Hz, 1H), 7.94 (dt, *J* = 8.2, 1.0 Hz, 1H), 7.78 (td, *J* = 7.7, 1.7 Hz, 1H), 7.71 (td, *J* = 7.7, 1.3 Hz, 1H), 7.47 (dd, *J* = 7.8, 1.2 Hz, 1H), 7.41 (ddd, *J* = 8.2, 7.2, 1.2 Hz, 1H), 7.35 (ddd, *J* = 8.3, 7.2, 1.1 Hz, 1H), 7.20 – 7.17 (m, 3H), 6.96 – 6.94 (m, 1H), 6.92 – 6.89 (m, 2H), 5.58 (d, *J* = 8.4 Hz, 1H), 5.10 (ddd, *J* = 8.2, 7.0, 4.0 Hz, 1H), 4.39 (dd, *J* = 11.7, 7.0 Hz, 1H), 4.12 (dd, *J* = 11.7, 4.0 Hz, 1H), 1.99 (s, 3H). **^{13}C NMR{^{1}H}** (126 MHz, $CDCl_3$) δ 169.8, 164.4, 141.25 (q, J = 38.8, 38.8, 38.4 Hz), 140.7, 134.1, 134.0, 133.1, 130.8, 130.1, 128.8, 128.4, 127.9, 126.4, 126.3, 124.4, 121.5, 118.9 (q, J = 273.0 Hz), 111.0, 67.4, 52.1, 23.3. **^{19}F NMR** (376 MHz, $CDCl_3$) δ -61.67 **HRMS** (ESI) m/z:[M + H]+ calcd. For $C_{25}H_{21}N_3O_3F_3$: 468.1530; found: 468.1530. $[\alpha]_d^{22}$ +12.73° (c= 0.05, $CHCl_3$)

***M*-(*S*)-2-acetamido-2-phenylethyl 2-(2-(trifluoromethyl)-1H-benzo[d]imidazol-1-yl)benzoate (*M*)-98**

Purified by CC, yield 10 mg (42%) **^{1}H NMR** (500 MHz, $CDCl_3$) δ 8.16 (dd, *J* = 7.8, 1.6 Hz, 1H), 7.95 (d, *J* = 8.1 Hz, 1H), 7.78 (td, *J* = 7.7, 1.6 Hz, 1H), 7.70 (td, *J* = 7.7, 1.3 Hz, 1H), 7.48 (d, *J* = 7.1 Hz, 1H), 7.42 (ddd, *J* = 8.3, 7.3, 1.2 Hz, 1H), 7.36 (td, *J* = 7.7, 7.2, 1.1 Hz, 1H), 7.31 – 7.25 (m, 4H), 7.13 – 7.10 (m, 2H), 6.98 – 6.96 (m, 1H), 5.56 (d, *J* = 7.9 Hz, 1H), 5.06 (d, *J* = 11.9 Hz, 1H), 4.46 (dd, *J* = 11.7, 7.0 Hz, 1H), 3.99 (dd, *J* = 11.7, 4.2 Hz, 1H), 1.86 (s, 3H). **^{13}C NMR{^{1}H}** (126 MHz, $CDCl_3$) δ 169.7, 164.4, 141.2 (app. d, *J* = 38.6 Hz), 140.8, 137.7, 134.1, 134.1, 132.7, 130.8, 130.2, 128.9, 128.4, 128.1, 126.6, 126.2, 124.2, 121.8, 118.9 (q, *J* = 271.9 Hz), 110.8, 67.1, 52.4, 23.3. **^{19}F NMR** (376 MHz, $CDCl_3$) δ -61.89 **HRMS** (ESI) m/z:[M + H]+ calcd. For $C_{25}H_{21}N_3O_3F_3$: 468.1530; found: 468.1532. $[\alpha]_d^{22}$ +60.0° (c= 0.1, $CHCl_3$)

***P*-(*S*)-2-(N-methylacetamido)-2-phenylethyl 2-(2-(trifluoromethyl)-1H-benzo[d]imidazol-1-yl)benzoate (*P*)-99**

Purified by CC (Hexane:EtOAc 1:1), yield 17 mg (70%) **^{1}H NMR** (500 MHz, $CDCl_3$) δ 8.19 (dd, *J* = 7.9, 1.5 Hz, 1H, both rotamers), 7.94 (d, *J* = 8.2 Hz, 1H, both rotamers), 7.77 (td, *J* = 7.7, 1.6 Hz, 1H, both rotamers), 7.70 (td, *J* = 7.7, 1.3 Hz, 1H, both rotamers), 7.49 (d, *J* = 8.0 Hz, 1H, both rotamers), 7.43 – 7.39 (m, 1H, both rotamers), 7.39 – 7.34 (m, 1H, both rotamers), 7.32 – 7.27 (m, 3H, both rotamers), 7.10 (dd, *J* = 7.3, 1.5 Hz, 1H, both rotamers), 7.05 – 7.01 (m, 1H, m), 7.00 – 6.97 (m, 1H, M), 6.09 (t, *J* = 7.5 Hz, 1H, M), 4.86 (dd, *J* = 8.8, 6.2 Hz, 1H, m), 4.55 (dd, *J* = 11.7, 6.0 Hz, 1H, m), 4.44 (d, *J* = 7.0 Hz, 2H, M), 4.29 (dd, *J* = 11.7, 8.9 Hz, 1H, m), 2.62 (s, 3H, m), 2.59 (s, 1H, M), 2.06 (s, 3H, M), 1.96 (s, 3H, m). **^{13}C NMR{^{1}H}** (126 MHz, $CDCl_3$) δ 171.6, 171.2, 163.8, 163.6, 141.03 (q, J = 38.5 Hz), 140.8, 137.6, 136.3, 135.7, 134.4, 134.3, 133.9, 132.5, 132.5, 130.9, 130.9, 130.4, 130.2, 129.2, 128.9, 128.5, 128.5, 128.2, 128.1, 127.6, 126.6, 126.6, 126.2, 126.1, 124.2, 124.1, 121.8, 121.6, 119.0 (d, J = 272.1 Hz), 110.9, 110.7, 63.8, 62.5, 58.6, 53.4, 30.8, 28.2, 22.2, 21.8. **^{19}F NMR** (471 MHz, $CDCl_3$) δ -61.36, -61.44. **HRMS** (ESI) m/z:[M + H]+ calcd. For $C_{26}H_{23}N_3O_3F_3$: 482.1686; found: 482.1685. $[\alpha]_d^{22}$ -392.36° (c= 0.17, $CHCl_3$)

***M*-(*S*)-2-(N-methylacetamido)-2-phenylethyl 2-(2-(trifluoromethyl)-1H-benzo[d]imidazol-1-yl)benzoate (*M*)-99**

Purified by CC (Hexane:EtOAc 1:1), yield 12 mg (50%) **^{1}H NMR** (500 MHz, $CDCl_3$) δ 8.19 (dd, *J* = 7.8, 1.6 Hz, 1H, M), 8.16 (dd, *J* = 7.9, 1.6 Hz, 1H, m), 8.00 – 7.91 (m, 1H, M), 7.92 (dt, *J* = 8.2, 1.0 Hz,

1H, m), 7.81 (td, *J* = 7.7, 1.6 Hz, 1H, m), 7.77 (td, *J* = 7.7, 1.6 Hz, 1H, M), 7.73 (td, *J* = 7.7, 1.3 Hz, 1H, m), 7.69 (td, *J* = 7.7, 1.3 Hz, 1H, M), 7.52 (dd, *J* = 7.9, 1.2 Hz, 1H, m), 7.48 (dd, *J* = 7.7, 1.3 Hz, 1H, M), 7.43 – 7.24 (m, 10H, both rotamers), 7.15 – 7.06 (m, 2H, M), 7.00 (ddd, *J* = 7.9, 1.6, 0.8 Hz, 1H, m), 6.99 – 6.97 (m, 1H, M), 6.95 (dt, *J* = 8.0, 1.1 Hz, 1H, m), 6.02 (dd, *J* = 9.2, 5.5 Hz, 1H, M), 4.97 (dd, *J* = 9.2, 5.7 Hz, 1H, m), 4.55 (dd, *J* = 11.5, 5.5 Hz, 1H, M), 4.49 (dd, *J* = 11.7, 5.7 Hz, 1H, m), 4.40 (dd, *J* = 11.5, 9.2 Hz, 1H, M), 4.28 (dd, *J* = 11.7, 9.3 Hz, 1H, m), 2.51 (s, 3H, m), 2.42 (s, 3H, M), 2.13 (s, 2H, m), 1.97 (s, 3H, M). **^{13}C NMR{^{1}H}** (126 MHz, $CDCl_3$) δ 171.3, 171.3, 163.8, 163.6, 141.20 (d, J = 38.3 Hz), 140.9, 140.7, 136.4, 135.7, 134.4, 134.3, 133.9, 132.7, 132.3, 130.9, 130.8, 130.1, 129.1, 128.9, 128.5, 128.4, 128.1, 127.6, 126.6, 126.3, 125.9, 124.2, 124.0, 121.7, 121.5, 118.97 (q, J = 272.5 Hz), 110.8, 63.7, 62.9, 58.6, 53.8, 31.0, 28.0, 22.3, 21.7. **^{19}F NMR** (471 MHz, $CDCl_3$) δ -61.4, -61.5. **HRMS** (ESI) m/z:[M + H]+ calcd. For $C_{26}H_{23}N_3O_3F_3$: 482.1686; found: 482.1685. $[\alpha]_d^{22}$ +127.5° (c= 0.12, $CHCl_3$)

_P_-(_S_)-2-(N-methylformamido)-2-phenylethyl 2-(2-(trifluoromethyl)-1H-benzo[d]imidazol-1-yl)benzoate (_P_)-100

Purified by CC (Hexane:EtOAc 2:1), yield 18 mg (78%) **^{1}H NMR** (500 MHz, $CDCl_3$) δ 8.20 (dt, *J* = 7.8, 1.9 Hz, 1H, both rotamers), 8.08 (s, 1H,m), 7.98 – 7.96 (m, 1H, M), 7.95 (dt, *J* = 8.2, 0.9 Hz, 1H, m), 7.81 (td, *J* = 7.7, 1.6 Hz, 1H, M), 7.77 (td, *J* = 7.6, 1.7 Hz, 1H, m), 7.75 – 7.72 (m, 1H, M), 7.72 – 7.69 (m, 1H, m), 7.54 (s, 1H, M), 7.52 (dd, *J* = 7.8, 1.2 Hz, 1H, M), 7.48 (dd, *J* = 7.9, 1.4 Hz, 1H, m), 7.47 – 7.44 (m, 2H,M), 7.43 – 7.36 (m, 2H, m), 7.35 – 7.27 (m, 5H, both rotamers), 7.17 – 7.08 (m, 1H, M), 7.06 – 6.96 (m, 1H, both rotamers), 6.98 (dd, *J* = 1.4, 0.7 Hz, 1H, m), 5.77 (dd, *J* = 10.0, 5.3 Hz, 1H, m), 4.60 (dd, *J* = 11.7, 10.0 Hz, 1H, M), 4.53 – 4.43 (m, 2H, m), 4.28 (dd, *J* = 11.7, 4.7 Hz, 1H, M), 4.15 (dd, *J* = 10.0, 4.6 Hz, 1H, M), 2.56 (s, 3H, m), 2.51 (s, 3H, M). **^{13}C NMR{^{1}H}** (126 MHz, $CDCl_3$) δ 163.8, 163.6, 163.5, 162.8, 141.26 (q, J = 34.0), 140.8, 140.7, 137.8, 137.6, 135.0, 134.6, 134.3, 134.2, 134.0, 132.8, 132.6, 130.9, 130.9, 130.2, 130.2, 129.2, 129.0, 128.8, 128.5, 128.4, 128.2, 127.7, 127.0, 126.4, 126.1, 124.3, 124.1, 121.6, 118.9 (q, J = 271.8 Hz), 111.0, 110.9, 62.4, 61.8, 59.4, 52.6, 30.1, 25.9. **^{19}F NMR** (471 MHz, $CDCl_3$) δ -61.3, -61.5. **HRMS** (ESI) m/z:[M + H]+ calcd. For $C_{25}H_{21}N_3O_3F_3$: 468.1530; found: 468.1531. $[\alpha]_d^{22}$ +23.33° (c= 0.18, $CHCl_3$)

_M_-(_S_)-2-(N-methylformamido)-2-phenylethyl 2-(2-(trifluoromethyl)-1H-benzo[d]imidazol-1-yl)benzoate (_M_)-100

Purified by CC (Hexane:EtOAc 2:1), yield 16 mg (70%) **^{1}H NMR** (500 MHz, $CDCl_3$) δ 8.29 – 8.21 (m, 1H, m), 8.17 (s, 1H, m), 8.21 – 8.12 (m, 1H, m), 7.97 – 7.94 (m, 1H, m), 7.94 – 7.92 (m, 1H, M), 7.81 (td, *J* = 7.7, 1.6 Hz, 1H, M), 7.77 (td, *J* = 7.7, 1.7 Hz, 1H, m), 7.73 (dd, *J* = 7.8, 1.3 Hz, 1H, M), 7.75 – 7.66 (m, 2H, m), 7.52 (dd, *J* = 7.8, 1.1 Hz, 1H, M), 7.47 (dd, *J* = 7.8, 1.3 Hz, 1H, m), 7.44 – 7.27 (m, 10H, both rotamers), 7.10 (m, 2H, m), 7.05 (dd, m, 2H, M), 7.01 (ddd, J = 7.8, 1.4, 0.7 Hz, 1H, m), 6.98 (d, m, 1H, M), 5.71 (dd, *J* = 10.4, 4.8 Hz, 1H, m), 4.68 – 4.55 (m, 1H, M), 4.61 – 4.58 (m, 1H, m), 4.43 (dd, *J* = 9.8, 1.7 Hz, 1H, m), 4.43 (ddd, *J* = 11.6, 10.2, 8.2 Hz, 1H, m), 4.33 (dd, *J* = 7.1, 4.7 Hz, 1H, M), 2.43 (s, 3H, M), 2.25 (s, 3H, m). **^{13}C NMR{^{1}H}** (126 MHz, $CDCl_3$) δ 163.7, 163.7, 163.3, 162.8, 141.32 (app. d, J = 38.5 Hz), 140.9, 140.7, 137.7, 135.0, 134.7, 134.4, 134.3, 134.2, 134.0, 133.0, 132.4, 130.9, 130.9, 130.3, 130.1, 129.2, 129.0, 128.8, 128.5, 128.4, 128.2, 127.7, 127.0, 126.3, 126.0, 124.2, 124.0, 121.6, 121.5, 118.97 (q, J = 272.0 Hz), 111.1, 110.9, 62.5, 61.8, 59.4, 52.5, 29.8, 26.0. **^{19}F NMR** (471 MHz, $CDCl_3$) δ -61.4, -61.5. **HRMS** (ESI) m/z:[M + H]+ calcd. For $C_{25}H_{21}N_3O_3F_3$: 468.1530; found: 468.1531. $[\alpha]_d^{22}$ +67.50° (c= 0.16, $CHCl_3$)

_P_-(_S_)-2-amino-2-phenylethyl 2-(2-(trifluoromethyl)-1H-benzo[d]imidazol-1-yl)benzoate (_P_)-101

Compound **(_P_)-77** (15 mg, 0.028 mmol) was dissolved in dry DCM (2 mL) and TFA (250 μL) was added. Reaction was stirred at room temperature for 20 minutes. The solution was evaporated by stream of nitrogen, dissolved in EtOAc (2 mL) and extracted with sat. $NaHCO_3$. Organic layer was dried with MgSO4 and evaporated to yield 8.5 mg of oil (70%) **^{1}H NMR** (500 MHz, $CDCl_3$) δ 8.28 – 8.25 (m, 1H), 8.01 – 7.98 (m, 1H), 7.79 (td, *J* = 7.6, 1.7 Hz, 1H), 7.73 (td, *J* = 7.7, 1.3 Hz, 1H), 7.51 (dd, *J* = 7.8,

1.2 Hz, 1H), 7.45 – 7.38 (m, 2H), 7.29 – 7.20 (m, 3H), 7.19 – 7.17 (m, 2H), 7.07 – 7.05 (m, 1H), 3.97 – 3.83 (m, 2H), 3.55 (dd, *J* = 9.0, 3.9 Hz, 1H), 1.07 (br.s, 2H). **^{13}C NMR{^{1}H}** (126 MHz, $CDCl_3$) δ 164.3, 141.31 (app. d, J = 38.7 Hz), 140.8, 137.9, 133.9, 133.8, 133.1, 130.8, 130.1, 129.2, 128.7, 127.9, 126.8, 126.3, 124.3, 121.7, 119.0 (q, J = 272.0 Hz), 111.0, 71.6, 54.2. **^{19}F NMR** (471 MHz, $CDCl_3$) δ -61.5. **HRMS** (ESI) m/z:[M + H]+ calcd. For $C_{23}H_{19}N_3O_2F_3$: 426.1424; found: 426.1424. $[\alpha]_d^{22}$ +70.59° (c= 0.09, $CHCl_3$)

***M*-(*S*)-2-amino-2-phenylethyl 2-(2-(trifluoromethyl)-1H-benzo[d]imidazol-1-yl)benzoate (*M*)-101**
Compound **(*M*)-77** (21 mg, 0.04 mmol) was dissolved in dry DCM (2 mL) and TFA (250 µL) was added. Reaction was stirred at room temperature for 20 minutes. The solution was evaporated by stream of nitrogen, dissolved in EtOAc (2 mL) and extracted with sat. $NaHCO_3$. Organic layer was dried with MgSO4 and evaporated to yield 10 mg of oil (58%) **^{1}H NMR** (500 MHz, $CDCl_3$) δ 8.22 (dd, *J* = 7.8, 1.6 Hz, 1H), 8.00 – 7.98 (m, 1H), 7.79 (td, *J* = 7.7, 1.6 Hz, 1H), 7.72 (td, *J* = 7.7, 1.3 Hz, 1H), 7.51 (d, *J* = 7.7 Hz, 1H), 7.44 (ddd, *J* = 8.2, 7.3, 1.1 Hz, 1H), 7.38 (td, *J* = 7.8, 7.3, 1.1 Hz, 1H), 7.28 – 7.20 (m, 3H), 7.14 – 7.11 (m, 2H), 7.03 – 7.00 (m, 1H), 3.94 – 3.89 (m, 1H), 3.86 (dd, *J* = 10.9, 8.9 Hz, 1H), 3.57 (dd, *J* = 8.7, 4.0 Hz, 1H), 1.36 (br.s, 2H). **^{13}C NMR{^{1}H}** (126 MHz, $CDCl_3$) δ 164.4, 141.21 (q, J = 38.1 Hz), 140.8, 137.8, 133.8, 132.8, 130.7, 130.1, 129.2, 128.7, 127.9, 126.7, 126.2, 124.3, 121.7, 119.00 (q, J = 272.1 Hz), 110.9, 71.6, 54.2. **^{19}F NMR** (471 MHz, $CDCl_3$) δ -61.2. **HRMS** (ESI) m/z:[M + H]+ calcd. For $C_{23}H_{19}N_3O_2F_3$: 426.1424; found: 426.1422. $[\alpha]_d^{22}$ +48.0° (c= 0.1, $CHCl_3$)

***P*-(*S*)-2-(dibenzylamino)-2-phenylethyl 2-(2-(trifluoromethyl)-1H-benzo[d]imidazol-1-yl)benzoate (*P*)-102**
Purified by collumn chromatography (Hexane:EtOAc 6:1) 12 mg (40%) **^{1}H NMR** (500 MHz, $CDCl_3$) δ 8.05 (dd, *J* = 7.8, 1.4 Hz, 1H), 7.86 (d, *J* = 8.1 Hz, 1H), 7.75 (td, *J* = 7.7, 1.6 Hz, 1H), 7.65 (td, *J* = 7.7, 1.3 Hz, 1H), 7.46 – 7.44 (m, 2H), 7.35 – 7.31 (m, 3H), 7.31 – 7.26 (m, 9H), 7.23 (ddd, *J* = 12.0, 7.3, 2.2 Hz, 3H), 7.13 (d, *J* = 6.9 Hz, 2H), 6.87 (dt, *J* = 8.2, 0.9 Hz, 1H), 4.53 (dd, *J* = 11.4, 6.7 Hz, 1H), 4.33 (dd, *J* = 11.4, 7.4 Hz, 1H), 3.78 (t, *J* = 7.0 Hz, 1H), 3.66 (d, *J* = 13.8 Hz, 2H), 3.23 (d, *J* = 13.8 Hz, 2H). **^{13}C NMR{^{1}H}** (126 MHz, $CDCl_3$) δ 163.8, 140.95 (q, J = 38.5 Hz), 140.7, 139.7, 137.6, 136.5, 134.3, 133.6, 132.3, 130.5, 130.2, 129.0, 128.9, 128.7, 128.4, 128.3, 127.7, 127.1, 125.9, 123.9, 121.6, 118.9 (q, J = 272.0 Hz), 110.7, 64.3, 60.4, 54.2. **^{19}F NMR** (471 MHz, $CDCl_3$) δ -61.3. **HRMS** (ESI) m/z:[M + H]+ calcd. For $C_{37}H_{31}N_3O_2F_3$: 606.2363; found: 606.2364. $[\alpha]_d^{22}$ +11.67° (c= 0.12, $CHCl_3$)

***M*-(*S*)-2-(dibenzylamino)-2-phenylethyl 2-(2-(trifluoromethyl)-1H-benzo[d]imidazol-1-yl)benzoate (*M*)-102**
Purified by collumn chromatography (Hexane:EtOAc 6:1) 14 mg (46%) **^{1}H NMR** (500 MHz, $CDCl_3$) δ 8.04 (dd, *J* = 7.9, 1.6 Hz, 1H), 7.87 (d, *J* = 8.2 Hz, 1H), 7.74 (td, *J* = 7.7, 1.6 Hz, 1H), 7.65 (td, *J* = 7.7, 1.3 Hz, 1H), 7.47 – 7.44 (m, 2H), 7.37 – 7.31 (m, 2H), 7.31 – 7.26 (m, 10H), 7.23 (ddd, *J* = 13.0, 5.0, 2.8 Hz, 4H), 7.10 (d, *J* = 7.1 Hz, 2H), 6.89 (dt, *J* = 8.2, 0.9 Hz, 1H), 4.51 (dd, *J* = 11.4, 6.7 Hz, 1H), 4.42 (dd, *J* = 11.4, 7.5 Hz, 1H), 3.88 (t, *J* = 7.0 Hz, 1H), 3.65 (d, *J* = 13.8 Hz, 2H), 3.27 (d, *J* = 13.8 Hz, 2H). **^{13}C NMR{^{1}H}** (126 MHz, $CDCl_3$) δ 163.7, 141.03 (q, J = 38.3 Hz), 140.8, 139.7, 137.6, 136.5, 134.4, 133.6, 132.3, 130.5, 130.1, 128.9, 128.8, 128.7, 128.4, 128.3, 127.7, 127.1, 125.9, 123.9, 121.6, 119.0 (q, J = 272.0 Hz), 110.7, 64.1, 60.3, 54.2. **^{19}F NMR** (471 MHz, $CDCl_3$) δ -61.4. **HRMS** (ESI) m/z:[M + H]+ calcd. For $C_{37}H_{31}N_3O_2F_3$: 606.2363; found: 606.2365. $[\alpha]_d^{22}$ +72.86° (c= 0.14, $CHCl_3$)

***P*-(*S*)-2-(1,3-dioxoisoindolin-2-yl)-2-phenylethyl 2-(2-(trifluoromethyl)-1H-benzo[d]imidazol-1-yl)benzoate (*P*)-103**
Purified by collumn chromatography (Hexane:EtOAc 2:1) 13 mg (46%) **^{1}H NMR** (500 MHz, $CDCl_3$) δ 8.09 (dd, *J* = 7.9, 1.6 Hz, 1H), 7.87 (d, *J* = 8.1 Hz, 1H), 7.81 (dd, *J* = 5.5, 3.0 Hz, 2H), 7.74 – 7.72 (m, 1H), 7.77 – 7.67 (m, 2H), 7.63 (td, *J* = 7.7, 1.1 Hz, 1H), 7.42 (d, *J* = 7.7 Hz, 1H), 7.37 – 7.33 (m, 3H), 7.31 – 7.24 (m, 4H), 6.92 (d, *J* = 8.2 Hz, 1H), 5.32 (dd, *J* = 9.8, 5.5 Hz, 1H), 4.94 (dd, *J* = 11.4, 9.8 Hz, 1H), 4.72 (dd, *J* = 11.5, 5.5 Hz, 1H). **^{13}C NMR{^{1}H}** (126 MHz, $CDCl_3$) δ 167.9, 163.7, 140.85 (q, J = 38.4 Hz), 140.7, 134.2, 134.2, 133.8, 132.5, 131.9, 130.6, 130.2, 128.6, 128.1, 126.0, 124.0, 123.5,

121.7, 118.8 (q, J = 273.0 Hz), 110.6, 63.6, 53.6. **^{19}F NMR** (471 MHz, $CDCl_3$) δ -61.5. **HRMS** (ESI) m/z:[M + H]+ calcd. For $C_{31}H_{21}N_3O_4F_3$: 566.1479; found: 566.1481. $[\alpha]_d^{22}$ -49.26° (c= 0.13, $CHCl_3$)

***M*-(*S*)-2-(1,3-dioxoisoindolin-2-yl)-2-phenylethyl 2-(2-(trifluoromethyl)-1H-benzo[d]imidazol-1-yl)benzoate (*M*)-103**

Purified by collumn chromatography (Hexane:EtOAc 2:1) 14 mg (49%) **^{1}H NMR** (500 MHz, $CDCl_3$ δ 8.11 (dd, *J* = 7.9, 1.4 Hz, 1H), 7.91 (dt, *J* = 8.2, 0.8 Hz, 1H), 7.82 – 7.78 (m, 2H), 7.75 – 7.72 (m, 1H), 7.72 – 7.70 (m, 2H), 7.63 (td, *J* = 7.7, 1.3 Hz, 1H), 7.43 (d, *J* = 7.4 Hz, 1H), 7.34 – 7.30 (m, 3H), 7.29 – 7.24 (m, 3H), 7.20 (ddd, *J* = 8.2, 7.2, 1.0 Hz, 1H), 6.87 (dt, *J* = 8.2, 0.9 Hz, 1H), 5.19 (dd, *J* = 9.8, 5.5 Hz, 1H), 5.02 (dd, *J* = 11.4, 9.8 Hz, 1H), 4.62 (dd, *J* = 11.5, 5.5 Hz, 1H). **^{13}C NMR{^{1}H}** (126 MHz, $CDCl_3$) δ 167.9, 163.7, 140.95 (q, J = 38.8 Hz), 140.7, 137.6, 136.0, 134.2, 134.2, 133.9, 132.6, 131.9, 130.6, 130.2, 128.9, 128.6, 128.6, 128.0, 125.9, 123.9, 123.5, 121.8, 118.88 (q, J = 271.5 Hz), 110.5, 63.8, 53.6. **^{19}F NMR** (471 MHz, $CDCl_3$) δ -61.4. **HRMS** (ESI) m/z:[M + H]+ calcd. For $C_{31}H_{21}N_3O_4F_3$: 566.1479; found: 566.1481. $[\alpha]_d^{22}$ +21.43° (c= 0.14, $CHCl_3$)

2-(2-(trifluoromethyl)-1H-benzo[d]imidazol-1-yl)benzoic acid-D (104)

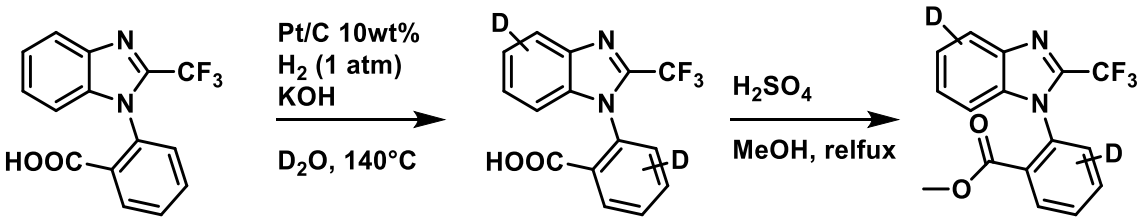

In autoclave TBBA **1** (150 mg, 0.5 mmol, 1 eq) was suspended in D_2O (10 mL) and NaOH (20 mg, 0.5 mmol, 1 eq) was added and the mixture was stirred until dissolution. After dissolution, 10% Pt/C (100 mg, 0.05 mmol, 0.1 eq) and the autoclave was closed and purged three times with vacuum/argon. After final evacuation, H_2 (1 atm, 10 psi) was introduced. The reaction was heated for 24 hours to 160°C. **!!Careful: During the heating the internal pressure increased to 40 psi!!** After 24 hours, the reaction was cooled to room temperature, the Pt catalyst was removed by filtration through celite. The celite was washed with small amount 10% NaOH and the filtrate was acidified with conc. HCl (few drops) while cooling and stirring. Precipitated material was isolated by filtration (120 mg, 80%).

methyl 2-(2-(trifluoromethyl)-1H-benzo[d]imidazol-1-yl)benzoate-D (105)

104 (120 mg, 0.4 mmol, 1 eq) was dissolved in MeOH (7.5 mL) and conc. H_2SO_4 (4 drops) was added. The mixture was refluxed for 16 hours. After 16 hours, reaction was cooled to room temperature and evaporated. The residue was dissolved in EtOAc (10 mL) and washed with K_2CO_3 (3x 10 mL), brine, dried with $MgSO_4$ and evaporated. Yield 100 mg (62%).**^{1}H NMR** (400 MHz, $CDCl_3$) δ 8.22 (s, 0.8H), 7.50 (s, 0.11H), 7.39 (s, 0.14H), 7.02 – 6.93 (m, 0.75H), 3.45 (s, 3H).

methyl 2-(2-oxo-2,3-dihydro-1*H*-benzo[*d*]imidazol-1-yl)benzoate (108)

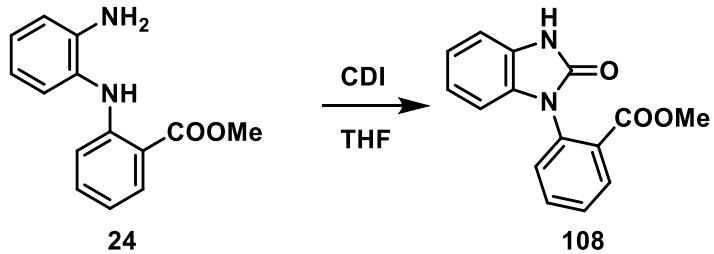

24 (1.6 g, 6.6 mmol, 1eq) was dissolved in THF, CDI (2.4 g, 13.2 mmol, 2 eq) was added and the mixture was stirred at room temperature for 18 hours. After 18 hours, 16 mL of 1M HCl was added slowly. The mixture was further diluted with water (60 mL) and extracted with EtOAc (3x60 mL), dried with MgSO4

and evaporated. The residue was purified by column chromatography (Petrolether:etoac 3:1 → EtOAc). Yield 60% **^{1}H NMR** (400 MHz, DMSO-D_6) δ 11.10 (s, 1H), 7.97 (dd, *J* = 8.0, 1.5 Hz, 1H), 7.83 – 7.76 (m, 1H), 7.64 – 7.58 (m, 3H), 7.09 – 7.02 (m, 3H), 7.01 – 6.94 (m, 2H), 6.82 – 6.76 (m, 1H), 3.60 (s, 1H). **^{13}C NMR {^{1}H}** (101 MHz, DMSO-D_6) δ 166.1, 153.9, 134.0, 133.9, 131.5, 131.0, 129.2, 129.2, 129.0, 128.9, 122.2, 121.3, 109.7, 108.2, 52.7.

methyl 2-(2-thioxo-2,3-dihydro-1*H*-benzo[*d*]imidazol-1-yl)benzoate (109)

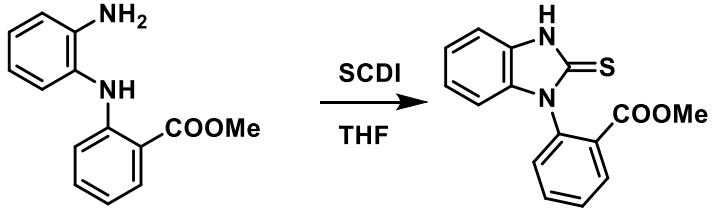

24 **109**

24 (242 mg, 1 mmol, 1 eq) was dissolved in THF (10 mL). Thiocarbonyldiimidazole (213 mg, 1.2 mmol, 1.2 eq) was added and the mixture was stirred at room temperature for 4 hours. After 4 hours, the reaction was quenched with 10% HCl (10 mL), water (20 mL) was added and the solution was extracted with EtOAc (3x30 mL). Organic layers were combined, washed with brine, dried with MgSO4 and evaporated to yield 253 mg (90%) of solid. **^{1}H NMR** (400 MHz, DMSO-D_6) δ 8.06 (dd, *J* = 7.8, 1.5 Hz, 1H), 7.85 (td, *J* = 7.7, 1.6 Hz, 1H), 7.70 (td, *J* = 7.7, 1.2 Hz, 1H), 7.56 (dd, *J* = 7.8, 1.1 Hz, 1H), 7.28 – 7.19 (m, 3H), 7.12 (td, *J* = 7.7, 1.3 Hz, 1H), 6.76 (d, *J* = 7.9 Hz, 1H), 3.54 (s, 3H). **^{13}C NMR {^{1}H}** (101 MHz, DMSO-D_6) δ 169.5, 164.7, 134.7, 134.1, 133.8, 131.2, 131.2, 130.1, 129.6, 129.3, 123.2, 122.6, 109.7, 109.2, 52.3.

methyl 2-(3-isopropyl-2-oxo-2,3-dihydro-1*H*-benzo[*d*]imidazol-1-yl)benzoate (110)

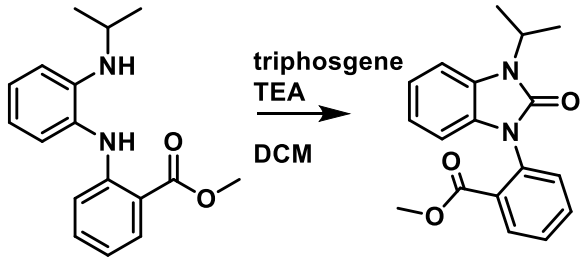

112 **110**

112 (2020 mg, 7.11 mmol, 1 eq) was dissolved in dry DCM (35 mL) and trimethylamine (2.95 mL, 21.3 mmol, 3 eq) was added. Triphosgene (3200 mg, 10.6 mmol, 1.5 eq) was dissolved in DCM (35 mL) and slowly added into the solution of the starting material over 15 minutes. After the addition was complete, the reaction was stirred for 45 minutes. After 45 minutes, the reaction was washed with 10% HCl (3x 50 mL), water (3x 50 mL). Organic layer was dried with $MgSO_4$ and purified by column chromatography (hexane:EtOAc 3:1) to yield 1.5 g of oil (70%). **^{1}H NMR** (400 MHz, DMSO-D_6) δ 7.98 (dd, *J* = 8.1, 1.6 Hz, 1H), 7.81 (td, *J* = 7.8, 2.0 Hz, 1H), 7.62 (dt, *J* = 7.3, 3.4 Hz, 2H), 7.40 (d, *J* = 7.9 Hz, 1H), 7.11 (t, *J* = 7.7 Hz, 1H), 7.01 (t, *J* = 7.7 Hz, 1H), 6.83 (d, *J* = 7.4 Hz, 1H), 4.65 (hept, *J* = 7.0 Hz, 1H), 3.56 (s, 3H), 1.50 (dd, *J* = 6.9, 2.8 Hz, 6H). **^{13}C NMR {^{1}H}** (101 MHz, DMSO-D_6) δ 165.5, 152.1, 133.4, 131.1, 129.4, 128.8, 128.5, 128.3, 121.5, 120.8, 109.1, 107.8, 52.1, 44.6, 19.8, 19.7.

methyl 2-((2-(isopropylamino)phenyl)amino)benzoate (112)

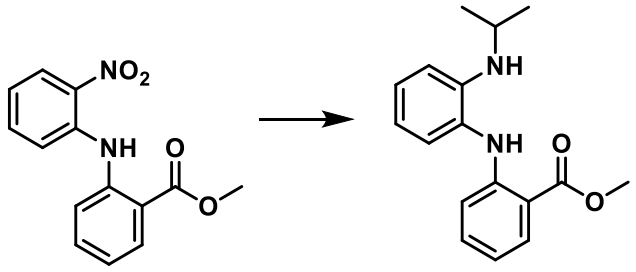

23 **112**

3-necked round-bottomed flask equipped with stirrbar, valve and rubber septa was charged with 10% palladium on charcoal (200 mg, 5%). Methyl 2-((2-nitrophenyl)amino)benzoate **23** (1088 mg, 4 mmol, 1 eq) was dissolved in acetone (160 ml, 0.025 M) and glacial acetic acid was added (400 µL, 6.3 mmol, 1.6 eq). This solution was added to the flask and it was closed with balloon. The system was evacuated and purged with nitrogen 4 times. After the last purge, the flask was evacuated and filled with hydrogen gas. The suspension was stirred overnight for 16 hours. After the reaction was complete, celite was added and the suspension was filtered. The solid was washed with aprox. 100 ml of acetone and the combined organic layers were evaporated. The oily residue was purified by column chromatography (dry loading, column size: 10 x 3.5 cm, mobile phase: hexane:ethylacetate 35:1, fraction size: 20 ml, product was collected in fractions 10-22) yielding 960 mg (85%) of yellow oil that solidified on air. **^{1}H NMR** (400 MHz, DMSO-D_6) δ 8.72 (s, 1H), 7.87 (dd, *J* = 8.0, 1.7 Hz, 1H), 7.31 (ddd, *J* = 8.6, 7.1, 1.7 Hz, 1H), 7.12 – 7.07 (m, 1H), 7.05 (dd, *J* = 7.7, 1.3 Hz, 1H), 6.75 (d, *J* = 7.3 Hz, 1H), 6.73 – 6.67 (m, 1H), 6.61 (td, *J* = 7.5, 1.3 Hz, 1H), 6.55 (dd, *J* = 8.5, 1.0 Hz, 1H), 4.42 (d, *J* = 8.4 Hz, 1H), 3.86 (s, 3H), 3.68 – 3.55 (m, 1H), 1.10 (d, *J* = 6.3 Hz, 6H). **^{13}C NMR {^{1}H}** (101 MHz, DMSO-D_6) δ 168.21, 149.08, 143.65, 134.37, 131.03, 126.92, 126.41, 125.52, 116.36, 116.14, 113.74, 111.85, 110.87, 51.85, 43.22, 22.46.

methyl 2-(3-isopropyl-2-thioxo-2,3-dihydro-1*H*-benzo[*d*]imidazol-1-yl)benzoate (113)

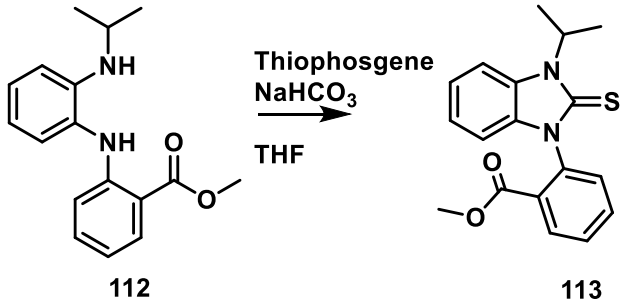

112 **113**

Two-necked flask was charged with **112** (2400 mg, 8.5 mmol, 1eq) THF (70 mL) was added followed by $NaHCO_3$. The flask was fitted with addition funnel and whole setup was flushed with argon. The addition funnel was charged with $CSCl_2$ (1460 mg, 12.7 mmol, 1.5 eq) in THF (20 mL). The flask was heated to 55°C and then the $CSCl_2$ solution was added dropwise over 10 minutes. After the addition was complete, the reaction was further stirred at 55°C for 90 minutes. Afterwards, the reaction was cooled to room temperature and water (50 mL) was added. THF layer was separated, washed with brine and evaporated to yield oily residue, which was dried overnight at high vacuum. The remaining oil (2.63 g) was crystalized from EtOH (20 mL) to yield 2 g brown crystalline solid (75%). **^{1}H NMR** (400 MHz, DMSO-d_6) δ 8.07 (dd, *J* = 1.6, 0.3 Hz, 1H), 7.86 (td, *J* = 7.7, 1.6 Hz, 1H), 7.75 (dt, *J* = 8.1, 0.9 Hz, 1H), 7.71 (td, *J* = 7.7, 1.3 Hz, 1H), 7.59 (dd, *J* = 7.9, 0.9 Hz, 1H), 7.26 (td, *J* = 8.0, 7.4, 1.2 Hz, 1H), 7.17 (td, *J* = 7.7, 1.0 Hz, 1H), 6.82 (dq, *J* = 8.0, 0.4 Hz, 1H), 5.53 (hept, *J* = 7.0 Hz, 1H), 3.47 (s, 3H), 1.58 (t, *J* = 7.1 Hz, 6H). **^{13}C NMR {^{1}H}** (101 MHz, DMSO-D_6) δ 169.1, 164.7, 135.1, 133.8, 133.2, 131.5, 130.1, 130.0, 129.7, 129.2, 127.8, 122.8, 110.9, 109.4, 52.3, 48.6, 19.5, 19.3.

General procedure for synthesis of amides 115a-d

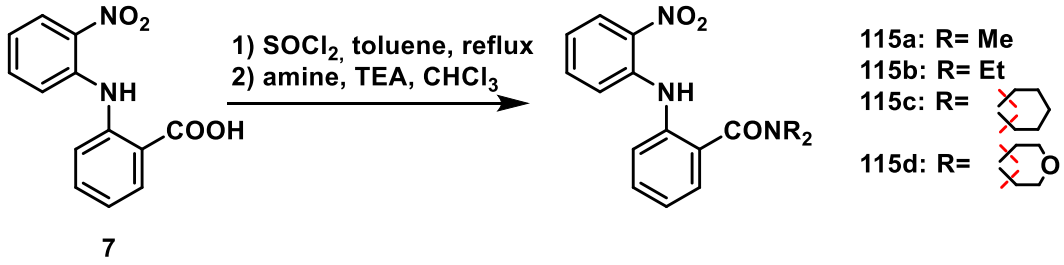

7

Acid **7** (500 mg, 2 mmol, 1 eq) was dissolved in toluene (12 mL) and $SOCl_2$ (1.2 mL, 10 mmol, 5 eq) was added and the reaction was refluxed for 2 hours. After two hours, the reaction was evaporated and dissolved in $CHCl_3$ (10 mL). This solution was added dropwised into solution of amine (2.2 mmol, 1.1 eq) and triethylamine (310 µL, 2.2 mmol, 1.1 eq) cooled in ice bath. This reaction was stirred at room temperature for 2 hours. After 2 hours, the reaction was washed with 10% aq HCl (3x 30 mL), 10% aq K_2CO_3 (3x30 mL), dried with $MgSO_4$ and evaporated.

115a: 511 mg (90%) **^{1}H NMR** (400 MHz, $CDCl_3$) δ 9.60 (s, 1H), 8.17 (dd, *J* = 8.6, 1.6 Hz, 1H), 7.44 (dd, *J* = 8.1, 1.0 Hz, 1H), 7.42 – 7.34 (m, 3H), 7.29 – 7.20 (m, 2H), 6.80 (ddd, *J* = 8.4, 6.9, 1.3 Hz, 1H), 1.09 (d, *J* = 28.3 Hz, 6H).

115b: 560 mg (90%) **^{1}H NMR** (400 MHz, $CDCl_3$) δ 9.77 (s, 1H), 8.19 (dd, *J* = 8.6, 1.6 Hz, 1H), 7.47 – 7.30 (m, 5H), 7.21 (td, *J* = 7.6, 1.2 Hz, 1H), 6.81 (ddd, *J* = 8.4, 6.9, 1.4 Hz, 1H), 3.02 (d, *J* = 32.1 Hz, 6H). **^{13}C NMR{^{1}H}** (101 MHz, $CDCl_3$) δ 169.3, 141.8, 136.5, 135.6, 134.4, 131.0, 130.2, 128.5, 126.8, 124.9, 123.5, 118.4, 116.7, 39.0, 35.0.

115c: 680 mg (quant.) **^{1}H NMR** (400 MHz, $CDCl_3$) δ 9.67 (s, 1H), 8.19 (dd, *J* = 8.6, 1.5 Hz, 1H), 7.48 – 7.33 (m, 4H), 7.29 (dd, *J* = 8.6, 1.2 Hz, 1H), 7.24 – 7.19 (m, 1H), 6.81 (ddd, *J* = 8.4, 6.9, 1.4 Hz, 1H), 3.68 (s, 2H), 3.31 (s, 2H), 1.54 (d, *J* = 68.7 Hz, 6H). **^{13}C NMR{^{1}H}** (101 MHz, $CDCl_3$) δ 167.8, 142.1, 136.1, 135.6, 134.3, 131.7, 130.0, 128.2, 126.8, 125.2, 123.8, 118.3, 116.6, 48.4, 42.9, 26.6, 25.7, 24.6.

115d: 664 mg (quant) **^{1}H NMR** (400 MHz, $CDCl_3$) δ 9.73 (s, 1H), 8.20 (dd, *J* = 8.5, 1.6 Hz, 1H), 7.48 – 7.34 (m, 4H), 7.30 – 7.20 (m, 2H), 6.84 (ddd, *J* = 8.4, 7.0, 1.2 Hz, 1H), 3.94 – 3.31 (m, 8H). **^{13}C NMR{^{1}H}** (101 MHz, $CDCl_3$) δ 168.1, 141.8, 136.6, 135.7, 134.5, 130.5, 130.3, 128.5, 126.9, 125.2, 123.9, 118.6, 116.6, 66.9, 47.8, 42.4.

General procedure for synthesis of amines 116a-d by reductive amination

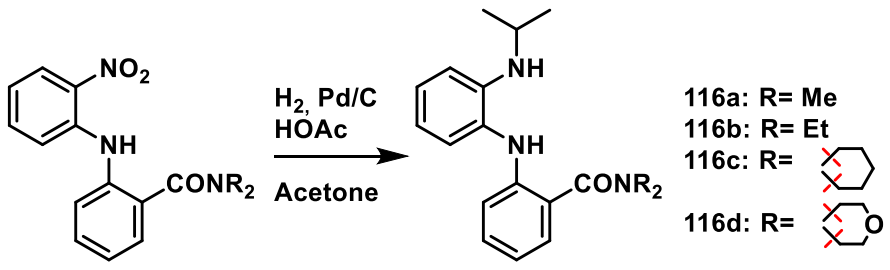

115a-d

116a-d

Three necked 250 mL flask fitted with stirrbar, rubber septa and valve was charged with starting material **115a-d** (2 mmol, 1 eq), Pd/C (100 mg, 0.05 eq), acetone (80 mL) and acetic acid (200 µL, 3.5 mmol, 1.75 eq). The flask was fitted with balloon and purged with argon/vacuum three times. After the final evacuation, hydrogen gas was introduced and the reaction as stirred rapidly at room temperature for 18 hours. After 18 hours, reaction was filtered through pad of celite, evaporated and the residue was dissolved in EtOAc (50 mL) and washed with K_2CO_3 (3x30 mL) brine and dried with $MgSO_4$. The residue was purified by column chromatography.

116a: Hexane:EtOAc (3:1), 260 mg (50%) **^{1}H NMR** (400 MHz, DMSO-D_6) δ 7.16 – 7.11 (m, 2H), 7.05 – 6.98 (m, 1H), 6.96 (dd, *J* = 7.7, 1.4 Hz, 1H), 6.79 – 6.68 (m, 3H), 6.58 (td, *J* = 7.5, 1.4 Hz, 1H), 6.52 (dd, *J* = 8.6, 1.0 Hz, 1H), 4.27 (d, *J* = 8.1 Hz, 1H), 3.57 (dt, *J* = 7.8, 6.3 Hz, 1H), 2.95 (s, 6H), 1.09 (d, *J* = 6.3 Hz, 6H). **^{13}C NMR{^{1}H}** (101 MHz, DMSO-D_6) δ 169.4, 143.4, 142.9, 129.8, 127.9, 127.8, 125.7, 125.3, 122.8, 117.7, 116.2, 114.8, 111.8, 43.3, 34.2, 22.6.

116b: Hexane:EtOAc (5:1), 330 mg (61%) **^{1}H NMR** (400 MHz, DMSO-D_6) δ 7.18 – 7.08 (m, 2H), 7.02 – 6.94 (m, 2H), 6.78 (td, *J* = 7.4, 1.1 Hz, 1H), 6.69 (dd, *J* = 8.1, 1.2 Hz, 1H), 6.58 (dtd, *J* = 7.5, 3.7, 1.4 Hz, 2H), 6.51 (s, 1H), 3.60 – 3.50 (m, 1H), 3.33 (s, 4H), 1.09 (d, *J* = 9.6 Hz, 12H). **^{13}C NMR{^{1}H}** (101 MHz, DMSO-D_6) δ 169.0, 142.7, 142.4, 129.5, 128.2, 127.1, 125.3, 124.4, 124.2, 118.2, 116.4, 115.2, 112.0, 43.4, 22.6, 13.7, 12.8.

116c: Hexane:EtOAc (5:1), 300mg (55%) **^{1}H NMR** (400 MHz, DMSO-D_6) δ 7.15 – 7.09 (m, 2H), 7.01 (td, *J* = 7.8, 1.5 Hz, 1H), 6.96 (dd, *J* = 7.7, 1.5 Hz, 1H), 6.75 (td, *J* = 7.4, 1.1 Hz, 1H), 6.70 (dd, *J* = 8.2, 1.2 Hz, 1H), 6.67 (s, 1H), 6.58 (td, *J* = 7.5, 1.4 Hz, 1H), 6.50 (d, *J* = 8.2 Hz, 1H), 4.26 (d, *J* = 8.1 Hz, 1H), 3.62 – 3.52 (m, 1H), 3.44 (s, 4H), 1.54 (d, *J* = 30.1 Hz, 6H), 1.08 (d, *J* = 6.3 Hz, 6H). **^{13}C NMR{^{1}H}** (101 MHz, DMSO-D_6) δ 167.9, 143.2, 142.8, 129.7, 127.9, 127.6, 125.6, 125.1, 123.1, 118.0, 116.3, 114.8, 111.8, 43.3, 25.6, 24.1, 22.6.

116d: Hexane:EtOAc (3:1), 370 mg (60%) **^{1}H NMR** (400 MHz, DMSO-D_6) δ 7.15 (td, *J* = 7.5, 1.4 Hz, 2H), 7.05 – 6.99 (m, 1H), 6.95 (dd, *J* = 7.7, 1.4 Hz, 1H), 6.79 – 6.74 (m, 2H), 6.70 (dd, *J* = 8.2, 1.1 Hz, 1H), 6.58 (td, *J* = 7.5, 1.4 Hz, 1H), 6.53 (dd, *J* = 8.8, 1.1 Hz, 1H), 4.31 (d, *J* = 8.7 Hz, 1H), 3.63 – 3.54 (m, 5H), 3.47 (s, 3H), 1.09 (d, *J* = 6.3 Hz, 6H). **^{13}C NMR{^{1}H}** (101 MHz, DMSO-D_6) δ 168.2, 143.4, 142.8, 130.0, 128.1, 127.8, 125.6, 125.2, 122.2, 118.0, 116.2, 115.1, 111.7, 66.0, 43.3, 22.6.

General procedure for cyclization to 117a-d

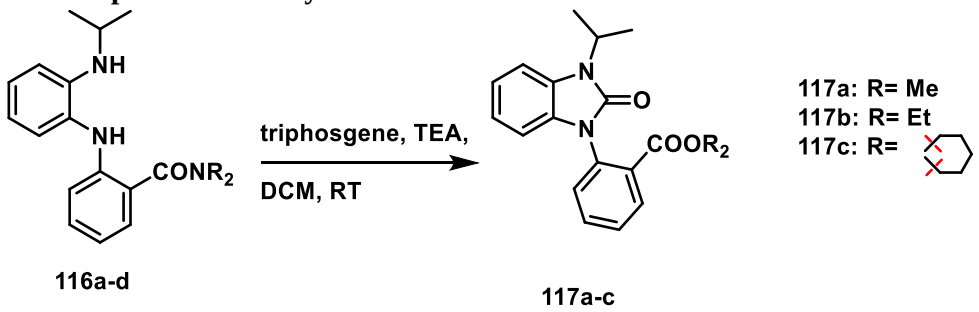

116a-d

117a-c

Diamine **116** (0.45 mmol, 1 eq) was dissolved in DCM (4.5 mL) and triethylamine (335 µL, 1.35 mmol, 3 eq) was added followed by addition of triphosgene (180 mg, 0.67 mmol, 1:5 eq) and the miture was stirred at room temperature for 1 hour. After 1 hour, the reaction was washed with 10% HCl (3x5 mL) and 10% K_2CO_3 (3x5 mL). The organic layer was evaporated and purified by column chromatography.

117a: Hexane::EtOAc 1:1.5, 120 mg (75%) **^{1}H NMR** (400 MHz, DMSO-D_6) δ 7.65 – 7.60 (m, 1H), 7.57 – 7.49 (m, 3H), 7.38 – 7.33 (m, 1H), 7.08 (td, *J* = 7.7, 1.2 Hz, 1H), 6.99 (td, *J* = 7.7, 1.1 Hz, 1H), 6.82 – 6.77 (m, 1H), 4.62 (hept, *J* = 6.9 Hz, 1H), 2.84 (s, 3H), 2.73 (s, 3H), 1.48 (t, *J* = 6.8 Hz, 6H). **^{13}C NMR{^{1}H}** (101 MHz, DMSO-D_6) δ 167.6, 135.2, 131.6, 130.1, 129.6, 128.7, 128.2, 128.2, 121.4, 120.7, 108.9, 108.4, 44.7, 34.3, 19.9, 19.6.

117b: Hexane:EtOAc 1:1, 120 mg (76%) **^{1}H NMR** (400 MHz, DMSO-D_6) δ 7.62 (td, *J* = 7.5, 1.8 Hz, 1H), 7.57 (td, *J* = 7.4, 1.5 Hz, 1H), 7.51 (ddd, *J* = 7.2, 3.3, 1.6 Hz, 2H), 7.34 (d, *J* = 7.7 Hz, 1H), 7.06 (td, *J* = 7.7, 1.2 Hz, 1H), 6.97 (td, *J* = 7.7, 1.0 Hz, 1H), 6.74 (d, *J* = 7.4 Hz, 1H), 4.63 (hept, *J* = 7.0 Hz, 1H), 3.57 – 3.21 (m, 2H), 2.93 (d, *J* = 44.1 Hz, 2H), 1.47 (t, *J* = 7.0 Hz, 6H), 0.99 (t, *J* = 7.1 Hz, 3H), 0.64 (s, 3H). **^{13}C NMR{^{1}H}** (101 MHz, DMSO-D_6) δ 166.9, 151.9, 136.3, 131.1, 131.1, 130.0, 129.8, 129.3, 128.7, 127.9, 127.5, 121.3, 120.6, 108.9, 44.5, 42.2, 37.5, 19.8, 19.8, 13.5, 11.4.

117c: Hexane:EtOAc 2:1, 134 mg (82%) **^{1}H NMR** (400 MHz, DMSO-D_6) δ 7.65 – 7.59 (m, 1H), 7.52 (dq, *J* = 15.6, 7.1 Hz, 3H), 7.35 (d, *J* = 7.8 Hz, 1H), 7.11 – 7.05 (m, 1H), 6.98 (t, *J* = 7.6 Hz, 1H), 6.79 (d, *J* = 7.7 Hz, 1H), 4.64 (hept, *J* = 6.8 Hz, 1H), 3.33 (s, 3H), 3.21 (s, 3H), 1.48 (dd, *J* = 10.1, 6.9 Hz, 6H), 1.42 (s, 4H).

2-(3-isopropyl-2-oxo-2,3-dihydro-1*H*-benzo[*d*]imidazol-1-yl)benzoic acid (118)

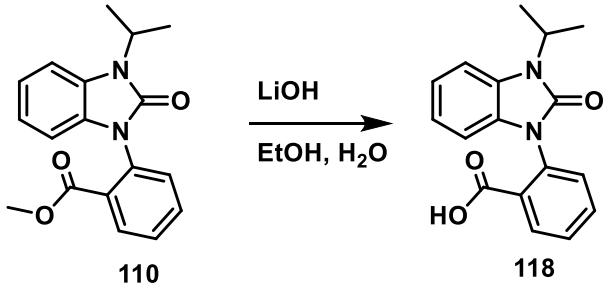

Starting material (2.14 g, 6.9 mmol, 1 eq) was dissolved in EtOH (35 mL) and water (20 mL). LiOH.H_2O (1.65 g, 69 mmol, 10 eq) was added and the suspension was heated to 55°C for 3.5 hrs. Afterwards, the mixture was cooled to room temperature, diluted with 50 mL of water and extracted with DCM (2x 25 mL). The aq. Layer was then acidified with HCl (5 mL) and extracted with EtOAc (3x 50 mL). Organic extracts were combined and dried with $MgSO_4$ and evaporated. The residue was dissolved in EtOH, evaporated and after drying under high vacuum 1.75 g of light foam was isolated (85%). **^{1}H NMR** (400 MHz, DMSO-D_6) δ 8.00 (dd, *J* = 7.8, 1.3 Hz, 1H), 7.77 (td, *J* = 7.6, 1.6 Hz, 1H), 7.63 – 7.56 (m, 2H), 7.39 – 7.36 (m, 1H), 7.08 (td, *J* = 7.7, 1.2 Hz, 1H), 6.99 (td, *J* = 7.7, 1.1 Hz, 1H), 6.77 (dd, *J* = 7.8, 0.8 Hz, 1H), 4.65 (hept, *J* = 6.9 Hz, 1H), 1.49 (t, *J* = 6.8 Hz, 6H). **^{13}C NMR{^{1}H}** (101 MHz, DMSO-D_6) δ 166.5, 152.4, 133.6, 133.0, 131.3, 129.9, 129.1, 128.6, 121.3, 120.8, 109.1, 107.8, 44.5, 19.9, 19.8.

2-(3-isopropyl-2-thioxo-2,3-dihydro-1*H*-benzo[*d*]imidazol-1-yl)benzoic acid (119)

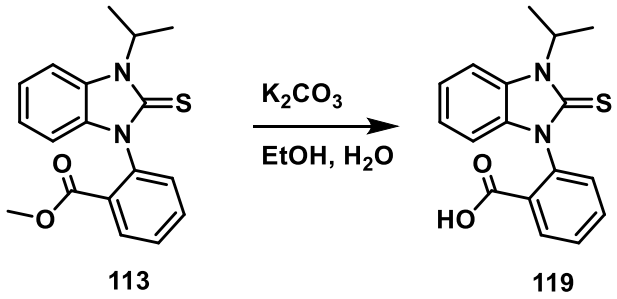

113 (1.53 g, 4.69 mmol, 1 eq) was dissolved in EtOH (30 mL) and water (37 mL) was added, followed by K_2CO_3 (6.5 g, 46.9 mmol, 10 eq). The mixture was refluxed for 18 hours. After 18 hours, the reaction was cooled to room temperature, ethanol was evaporated under reduced pressure and the remaining solution was acidified by HCl while cooling and stirring. The mixture was left stirring for 30 minutes and the precipitated solid was isolated by filtration yielding 1.3 g of white solid (92%). **^{1}H NMR** (400 MHz, DMSO-D_6) δ 8.07 (dd, *J* = 7.8, 1.5 Hz, 1H), 7.81 (td, *J* = 7.6, 1.6 Hz, 1H), 7.72 (d, *J* = 8.0 Hz, 1H), 7.68 (td, *J* = 7.7, 1.3 Hz, 1H), 7.53 (dd, *J* = 7.8, 1.1 Hz, 1H), 7.23 (td, *J* = 7.8, 1.2 Hz, 1H), 7.15 (td, *J* = 7.8, 1.0 Hz, 1H), 6.80 – 6.76 (m, 1H), 5.54 (hept, *J* = 7.1 Hz, 1H), 1.57 (dd, *J* = 12.3, 7.1 Hz, 5H). **^{13}C NMR{^{1}H}** (101 MHz, DMSO-D_6) δ 169.3, 165.7, 135.3, 133.5, 133.4, 131.5, 130.5, 130.2, 130.1, 129.6, 122.7, 122.6, 110.9, 109.5, 48.5, 19.6, 19.4.

2-(3-isopropyl-2-oxo-2,3-dihydro-1*H*-benzo[*d*]imidazol-1-yl)-*N*-phenylbenzamide (120)

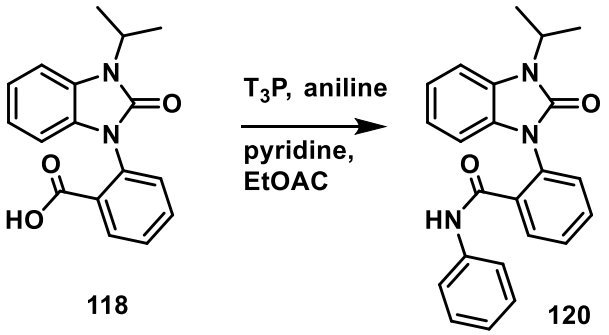

118 (50 mg, 0.17 mmol, 1 eq) was dissolved in EtOAc (600 µL), pyridine (282 µL was added) followed by T3P (50 wt% in EtOAc, 110 µL, 1 mmol, 1eq) and aniline (17.5 µL, 0.19 mmol, 1.1 eq). The mixture was stirred at room temperature for 4 hours. After 4 hours, the reaction was diluted with EtOAc (10 mL), extracted with 10% HCl (3x 10 mL), 10% K_2CO_3 (3x 10 mL) and brine (1x 10 mL). Organic layers were combined, dried with $MgSO_4$ and evaporated to yield 40 mg of oil (63%) **^{1}H NMR** (500 MHz, DMSO-D_6) δ 10.34 (s, 1H), 7.82 – 7.78 (m, 2H), 7.72 (td, *J* = 7.7, 1.5 Hz, 1H), 7.65 – 7.58 (m, 3H), 7.54 (d, *J* = 7.7 Hz, 2H), 7.34 (d, *J* = 7.8 Hz, 1H), 7.25 (t, *J* = 7.9 Hz, 2H), 7.07 (td, *J* = 7.7, 1.2 Hz, 1H), 7.05 – 7.01 (m, 2H), 6.99 (td, *J* = 7.7, 1.0 Hz, 1H), 6.89 – 6.85 (m, 2H), 4.59 (hept, *J* = 6.9 Hz, 1H), 1.43 (dd, *J* = 14.6, 6.9 Hz, 6H). **^{13}C NMR{^{1}H}** (101 MHz, $CDCl_3$) δ 165.0, 154.8, 154.3, 144.6, 138.4, 138.2, 131.7, 131.1, 130.5, 130.2, 129.5, 129.0, 128.5, 124.3, 122.3, 121.9, 119.6, 109.7, 45.8, 20.4.

(*R*)-*N*-(2-hydroxy-1-phenylethyl)-2-(3-isopropyl-2-oxo-2,3-dihydro-1*H*-benzo[*d*]imidazol-1-yl)benzamide (121)

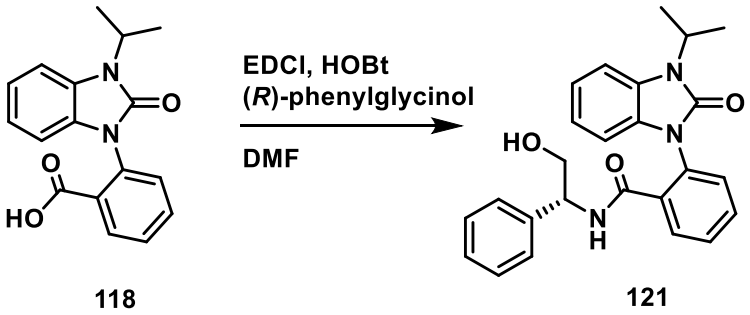

118 (150 mg, 0.5 mmol, 1eq) was dissolved in DMF (2.5 mL). EDCl (198 mg, 1 mmol, 2 eq) was added followed by HOBt (153 mg, 1 mmol, 2eq) and R-(-)-phenylglycinol (76 mg, 0.55 mmol, 1.1 eq). The reaction was stirred at room temperature for 18 hours. After 18 hours, the solution was diluted with EtOAc (15 mL), washed with 10% HCl (3x 15 mL), 10% K_2CO_3 (3x 15 mL) and brine (1x 15 mL). The EtOAc solution was dried with $MgSO_4$ and evaporated to yield 160 mg of light foam (77%). No chromatographic separation of the diastereomers was possible.

(*S*)-*N*-(2-hydroxy-1-phenylethyl)-2-(3-isopropyl-2-thioxo-2,3-dihydro-1*H*-benzo[*d*]imidazol-1-yl)benzamide (123)

Method 1)

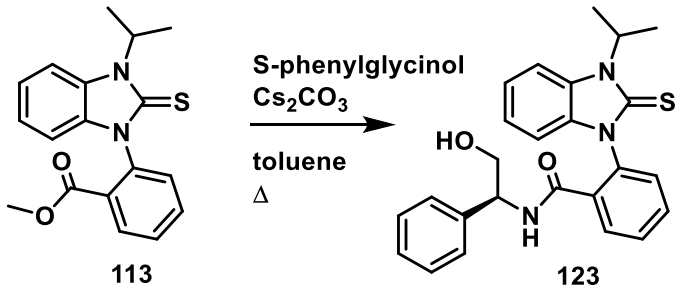

113 (650 mg, 2 mmol, 1 eq) was dissolved in toluene (5 mL), Cs_2CO_3 (650 mg, 2 mmol, 1 eq) was added followed by S-(+)-phenylglycinol (550 mmg, 2 mmol, 2 eq). Reaction mixture was heated to 100°C for 18 hours. After 18 hours, the mixture was cooled to room temperature, toluene (20 mL) and water (20 mL) were added and layers were separated. Organic layer was washed with water (1x20 mL) and brine (2x 20 mL), dried with MgSO4 and evaporated. The residue was purified by column chromatography (Hexane:EtOAc gradient 2:1 → 3:2 → 1:1). Two diastereomers were isolated as white foam: product eluting first: 210 mg (48%), product eluting second: 140 mg (32%).

Product eluting first: ^{1}H NMR (400 MHz, CDCl3) δ 7.78 – 7.69 (m, 1H), 7.71 – 7.56 (m, 3H), 7.52 (dt, *J* = 8.2, 0.8 Hz, 1H), 7.37 – 7.21 (m, 7H), 7.18 (td, *J* = 7.8, 1.0 Hz, 1H), 6.85 (dt, *J* = 7.9, 0.8 Hz, 1H), 5.72 (hept, *J* = 7.0 Hz, 1H), 5.00 (ddd, *J* = 8.5, 6.2, 4.6 Hz, 1H), 3.62 – 3.49 (m, 2H), 1.68 (dd, *J* = 7.1, 2.5 Hz, 6H). **^{13}C NMR{^{1}H}** (101 MHz, $CDCl_3$) δ 168.9, 166.7, 138.5, 137.2, 134.2, 132.7, 131.8, 130.5, 130.4, 129.7, 129.7, 128.8, 127.8, 127.0, 123.8, 123.6, 111.2, 110.9, 66.2, 56.3, 50.0, 20.3, 20.0.
Product eluting second: ^{1}H NMR (400 MHz, $CDCl_3$) δ 8.02 – 7.90 (m, 2H), 7.72 – 7.60 (m, 2H), 7.53 (dt, *J* = 8.2, 0.9 Hz, 1H), 7.35 – 7.23 (m, 2H), 7.16 (ddd, *J* = 8.4, 7.5, 1.0 Hz, 1H), 7.08 – 7.02 (m, 1H), 6.95 – 6.90 (m, 2H), 6.75 (ddd, *J* = 8.0, 1.0, 0.6 Hz, 1H), 6.68 – 6.64 (m, 2H), 5.59 (hept, *J* = 7.0 Hz, 1H), 4.88 (td, *J* = 6.1, 4.0 Hz, 1H), 3.83 (dd, *J* = 11.7, 3.9 Hz, 1H), 3.75 (dd, *J* = 11.7, 6.3 Hz, 1H), 1.64 (d, *J* = 7.1 Hz, 3H), 1.41 (d, *J* = 7.1 Hz, 3H).**^{13}C NMR{^{1}H}** (101 MHz, $CDCl_3$) δ 169.2, 166.5, 138.4, 136.3, 134.2, 132.5, 132.3, 131.2, 130.7, 130.5, 129.9, 128.3, 127.3, 126.4, 123.9, 123.6, 111.1, 110.9, 66.3, 57.0, 49.9, 20.3, 19.8.

Method 2)

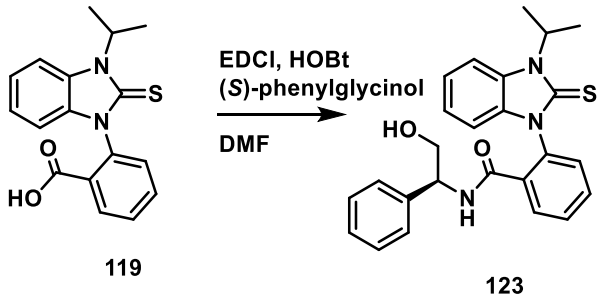

119 (100 mg, 0.3 mmol, 1eq) was dissolved in DMF (3 mL). EDCl (14 mg, 0.6 mmol, 2 eq) was added followed by HOBt.H_2O (92 mg, 0.6 mmol, 2 eq) and S-(+)-phenylglycinol (40 mg, 0.33 mmol, 1.1 eq). Reaction was stirred at room temperature for 18 hours. After 18 hours, reaction was diluted with EtOAc (15 mL), washed with 10% HCl (3x 15 mL), 10% K_2CO_3 (3x 15 mL) and brined. Organic layer was dried with MgSO4 and purified by collum chromatography. (Hexane:EtOAc gradient 2:1 → 3:2 → 1:1). Two diastereomers were isolated as white foam: product eluting first: 32 mg (44%), product eluting second: 30 mg (41%).

(*S*)-1-isopropyl-3-(2-(4-phenyl-4,5-dihydrooxazol-2-yl)phenyl)-1,3-dihydro-2*H*-benzo[*d*]imidazole-2-thione (124)

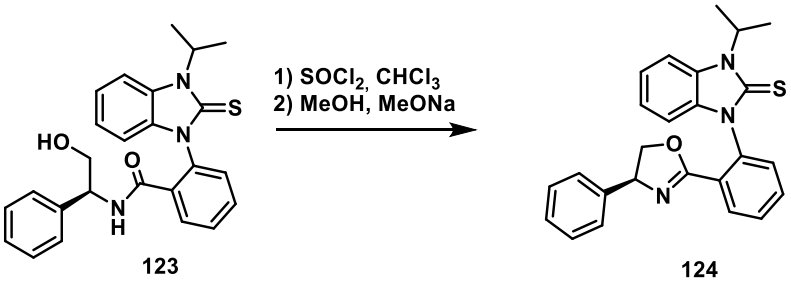

123 124

123 (215 mg, 0.5 mmol, 1eq) was dissolved in $CHCl_3$ (5 mL) and $SOCl_2$ (181 µL, 2.5 mmol, 5 eq) was added. The reaction was stirred at room temperature for 60 minutes. Afterwards, the mixture was evaporated, dissolved in $CHCl_3$ and evaporated again. The residues was dissolved in MeOH (5 mL) and sodium methoxide was added (135 mg, 2.5 mmol, 5 eq). The reaction was stirred at room temperature for 7 hours. After 7 hours, the reaction was diluted with water and extracted with DCM. No chromatographic separation was possible to separate the diastereomers.

3-isopropyl-1-(2-(methoxycarbonyl)phenyl)-1*H*-benzo[*d*]imidazol-3-ium perchlorate (125)

Method 1)

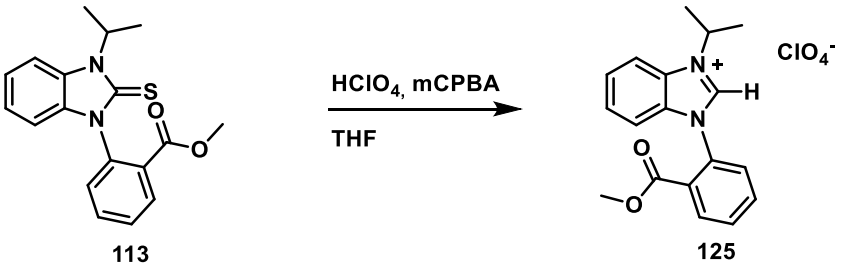

113 125

113 (163 mg, 0.5 mmol, 1 eq) was dissolved in THF (2 mL). The solution was cooled in acetone-dry ice bath (-78 °C). To the cooled solution, mCPBA (75%, 401 mg, 1.75 mmol, 3.5 eq) was added portionwise. To the resulting suspension, 70% aq. $HClO_4$ (214 µL, 2.5 mmol 5 eq) was added dropwise. The reaction was stirred in the bath for 3.5 hours and then it was warmed to room temperature and left stirring for 16 hours. The resulting suspension was filtered, washed with diethylether and water and dried to yield 73 mg of white solid (42%). **^{1}H NMR** (400 MHz, DMSO-D_6) δ 10.23 (s, 1H), 8.32 – 8.29 (m, 1H), 8.27 (d, *J* = 8.4 Hz, 1H), 8.04 (ddd, *J* = 7.9, 7.3, 1.6 Hz, 1H), 7.76 (ddd, *J* = 8.4, 7.3, 1.0 Hz, 1H), 7.67 (ddd, *J* = 8.3, 7.3, 1.0 Hz, 1H), 7.51 (dt, *J* = 8.3, 0.8 Hz, 1H), 5.23 (hept, *J* = 6.6 Hz, 1H), 3.60 (s, 3H), 1.69 (s (br, 6H). **^{13}C NMR{^{1}H}** (101 MHz, DMSO-D_6) δ 163.9, 142.1, 134.7, 132.6, 132.2, 132.1, 131.8, 130.0, 129.6, 127.6, 126.8, 126.7, 114.2, 113.1, 52.8, 50.9, 22.0, 21.5.

Method 2)

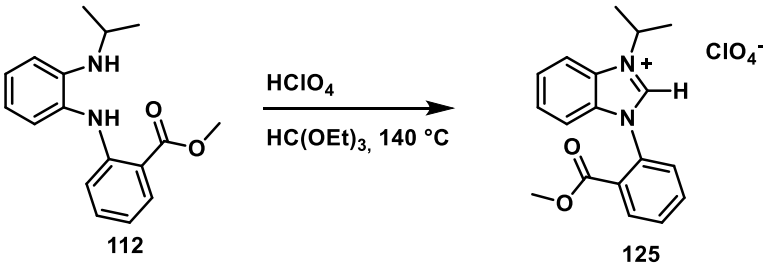

112 125

112 (142 mg, 0.5 mmol, 1eq) was suspended in HC(OEt)3 followed by addition of $HClO_4$ (90 µL, 2 eq). The reaction was heated in DrySyn heating block set up to 140°C. After 2 hours, the reaction was cooled to room temperature and evaporated. To the residue MeOH (2 mL) was added and the mixture was cooled in dry ice. The solid was filtered, washed with ether and dried. Yielding 121 mg (70%)

2-(2-(pyridin-2-yl)-1*H*-benzo[*d*]imidazol-1-yl)benzoic acid (127)

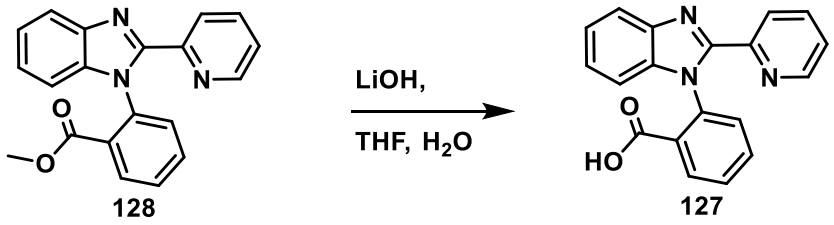

128 127

128 (1.65 g, 5 mmol, 1 eq) was dissolved in THF (45 mL) and water (36 mL). LiOH.H_2O (420 mg, 10 mmol, 2 eq) was added and the reaction was stirred at room temperature for 22 hours. Afterwards, the reaction was acidified with conc. HCl (863 µL, 10 mmol, 2 eq) and THF was evaporated under reduced pressure. The solid material was filtered and dried. Yield 1.42 g of brown solid, (90%). **^{1}H NMR** (400 MHz, DMSO-D_6) δ 12.55 (s, 1H), 8.25 (dt, *J* = 8.0, 1.1 Hz, 1H), 8.21 (ddd, *J* = 4.8, 1.9, 1.0 Hz, 1H), 8.02 (dd, *J* = 7.8, 1.6 Hz, 1H), 7.91 (td, *J* = 7.7, 1.8 Hz, 1H), 7.84 – 7.75 (m, 1H), 7.76 (dd, *J* = 7.7, 1.6 Hz, 1H), 7.64 (td, *J* = 7.6, 1.3 Hz, 1H), 7.53 (dd, *J* = 7.9, 1.2 Hz, 1H), 7.34 – 7.31 (m, 1H), 7.31 – 7.28 (m, 1H), 7.27 – 7.23 (m, 1H), 7.02 – 6.93 (m, 1H). **^{13}C NMR{^{1}H}** (101 MHz, DMSO-D_6) δ 206.4, 165.9, 150.3, 149.2, 148.3, 142.3, 137.9, 137.4, 136.9, 133.0, 131.1, 129.5, 129.4, 128.7, 124.0, 123.8, 123.6, 122.5, 119.5, 110.5, 30.6. **HRMS** ESI[M+H]$^+$ calculated for $C_{19}H_{14}O_2N_3$: 316.1081, found: 316.1078

methyl 2-(2-(pyridin-2-yl)-1*H*-benzo[*d*]imidazol-1-yl)benzoate (128)

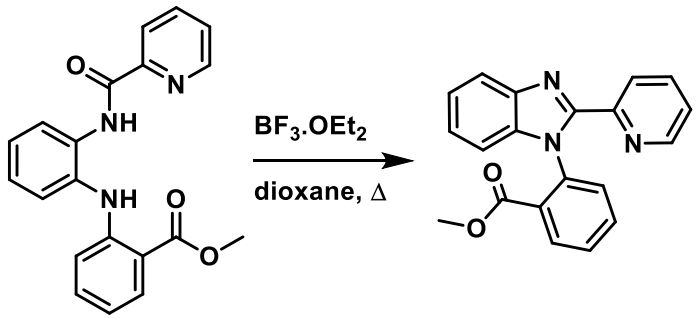

122 128

122 (10.7 g. 30.8 mmol, 1 eq) was dissolved in dioxane (150 mL) and BF_3.OEt_2 (9.75 mL, 77.1 mmol, 2,5 eq) was added. The reaction was refluxed for 16 hours. After 16 hours the reaction was cooled to room temperature and 10% aq Na_2CO_3 (50 mL) was added. The white precipitate was filtered away and the filtrate was concentrated under reduced pressure. The remaining solution was extracted with DCM (3x 20 mL). Combined organic extracts were dried with $MgSO_4$ and evaporated to yield 10g of gray solid (quantitative). **^{1}H NMR** (400 MHz, DMSO-D_6) δ 8.25 (d, *J* = 7.9 Hz, 1H), 8.22 – 8.18 (m, 1H), 7.99 (dd, *J* = 7.8, 1.5 Hz, 1H), 7.92 (td, *J* = 7.7, 1.6 Hz, 1H), 7.85 – 7.78 (m, 2H), 7.66 (td, *J* = 7.6, 1.1 Hz, 1H), 7.61 (d, *J* = 7.8 Hz, 1H), 7.36 – 7.23 (m, 3H), 7.00 (d, *J* = 7.7 Hz, 1H), 3.32 (s, 3H). **^{13}C NMR{^{1}H}** (101 MHz, DMSO-D_6) δ 165.3, 150.8, 149.5, 148.9, 142.8, 138.2, 137.8, 137.6, 134.0, 131.4, 130.1, 129.3, 128.8, 124.7, 124.4, 124.4, 123.2, 120.1, 111.0, 52.4. **HRMS** ESI[M+H]$^+$ calculated for $C_{20}H_{16}O_2N_3$: 330.1237, found: 330.1234

RESOLUTION OF 128

3900 mg of **128** (racemate) was suspended in acetonitrile (190 mL) and L-dibenzoyl-tartaric acid (4140 mg, 1 eq) was added. This mixture was refluxed until fully dissolved (15 min). After full dissolution, the mixture was allowed to cool to room temperature while stirring. After 2.5 hrs, the precipitate was filtered away. The filtrate was evaporated. The precipitate (A) contains product with aprox. 15:85 er., filtrate (B) contains in aprox. 95:5 er.

The precipitated material (A) was again recrystallized from acetonitrile (140 mL) by addition of the solid salt into boiling (prolonged heating causes racemization). After full dissolution, the mixture was left to cool to room temperature with stirring. After 2 hrs, the solid material was filtered away to yield solid in aprox. 2:98 er.

The evaporated filtrate (B) was dissolved in EtOAc and extracted twice with 10. aq. NaOH and once with brine and dried with $MgSO_4$. After removal of $MgSO_4$ by filtration, the solution was carefully concentrated under reduced pressure (to aprox. 10-20% of original volume) which induced precipitation of solid material which was collected by filtration to yield 890 mg (45%) of enantiopure ligand **128**.

methyl 2-((2-(picolinamido)phenyl)amino)benzoate (122)

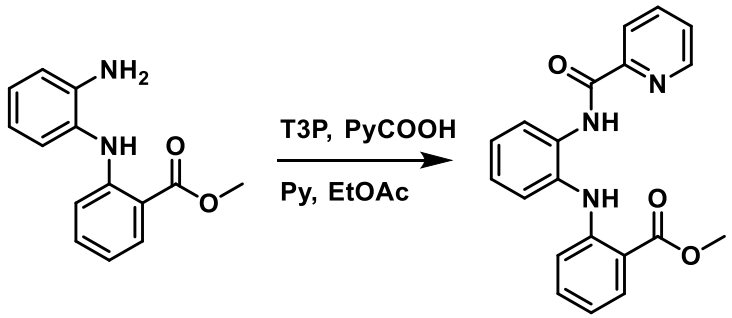

24 **122**

24 (14 g, 57.8 mmol, 1 eq) was dissolved in EtOAc (385 mL) and pyridine (192 mL) was added (Total volueme 578 mL, c= 0.1M). T3P (50%wt solution in EtOAc, 36.7g, 1 eq) was added followed by 2-picolinic acid. The reaction was stirred at room temperature for 16 hrs. After 16 hours, the reaction was washed with 10% HCl (3x 500 mL) and 10% K_2CO_3 (3x 500 mL), water (1x 500 mL) and brine. Organic layer was dried with $MgSO_4$ and evaporated to yield 16.1 g of gray solid (80%). **^{1}H NMR** (400 MHz, $CDCl_3$) δ 10.50 (s, 1H), 9.19 (s, 1H), 8.59 (dd, *J* = 8.5, 1.4 Hz, 1H), 8.41 (ddd, *J* = 4.7, 1.7, 0.9 Hz, 2H), 8.24 (dt, *J* = 7.8, 1.0 Hz, 1H), 8.00 (dd, *J* = 8.0, 1.6 Hz, 1H), 7.89 – 7.79 (m, 1H), 7.37 (ddd, *J* = 7.6, 4.8, 1.2 Hz, 1H), 7.35 – 7.30 (m, 2H), 7.23 (ddd, *J* = 8.7, 7.1, 1.7 Hz, 1H), 7.21 – 7.12 (m, 1H), 6.76 – 6.65 (m, 4H), 3.94 (s, *J* = 2.8 Hz, 3H). **^{13}C NMR{^{1}H}** (101 MHz, $CDCl_3$) δ 169.1, 162.3, 150.0, 149.5, 148.2, 137.5, 134.7, 134.7, 134.5, 131.5, 130.8, 127.2, 127.0, 126.3, 124.8, 122.3, 121.2, 117.4, 114.6, 112.2, 52.0. **HRMS** ESI$[M+H]^+$ calculated for $C_{20}H_{18}O_3N_3$: 348.1343, found: 348.1344

2-(2-(pyridin-2-yl)-1*H*-benzo[*d*]imidazol-1-yl)benzonitrile (133)

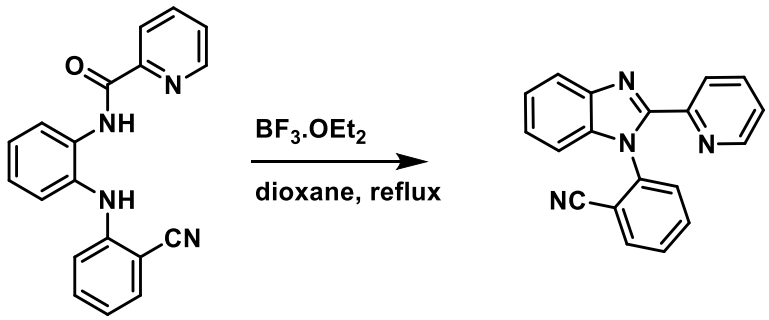

137 **133**

137 (245 mg, 0.5 mmol, 1 eq) was dissolved in dioxane (5 mL) and $BF_3.OEt_2$ (183 µL, 1.3 mmol, 2.5 eq) was added. The reaction was refluxed for 16 hours. After 16 hours, the reaction was cooled to room temperature, quenched with 10% aq. K_2CO_3 (5 mL) and further diluted with water (5 mL). The resultion solution was extracted with DCM (3x 10 mL). Combined organic extracts were dried with MgSO4, evaporated and purified by column chromatography (hexane:EtOAc 4:1) to yield 180 mg of product as gray solid (80%). **^{1}H NMR** (400 MHz, $CDCl_3$) δ 8.44 (dt, *J* = 8.0, 1.0 Hz, 1H), 8.20 (ddd, *J* = 4.8, 1.7, 0.9 Hz, 1H), 7.93 (dt, *J* = 8.1, 1.0 Hz, 1H), 7.84 – 7.75 (m, 3H), 7.60 (td, *J* = 7.7, 1.2 Hz, 1H), 7.55 (s,

1H), 7.38 (ddd, *J* = 8.1, 7.2, 1.2 Hz, 1H), 7.35 – 7.30 (m, 1H), 7.22 (ddd, *J* = 7.6, 4.8, 1.2 Hz, 1H), 7.08 (dt, *J* = 8.0, 0.9 Hz, 1H). **^{13}C NMR{^{1}H}** (101 MHz, $CDCl_3$) δ 150.3, 149.1, 148.5, 143.0, 141.3, 137.6, 137.0, 133.8, 133.6, 129.0, 128.8, 124.6, 124.4, 124.1, 123.8, 120.6, 115.8, 113.1, 110.4.

(*S*)-4-phenyl-2-(2-(2-(pyridin-2-yl)-1*H*-benzo[*d*]imidazol-1-yl)phenyl)-4,5-dihydrooxazole (134)

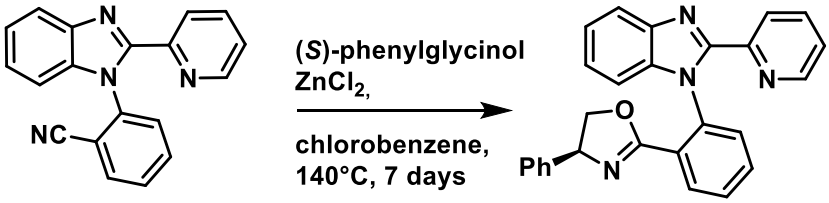

133 **134**

$ZnCl_2$ (40 mg, 0.06 mmol, 0.125 eq) was melted under vacuum with heatgun and let cool to room temperature. **133** (150 mg, 0.5 mmol, 1 eq) was dissolved in chlorobenzene (5 mL) and melted $ZnCl_2$ was added, followed by (*S*)-phenylglycinol. This mixture was refluxed for 7 days. After 7 days, the reaction was cooled to room temperature, partially evaporated and MeOH (5 mL) was added. This solution was then diluted with water (25 mL) and extracted with EtOAc (3x 20 mL). Combined extractes were washed with brine, dried with $MgSO_4$ and evaporated. The mixture was purified by preparative HPLC.

Product eluting first: ^{1}H NMR (400 MHz, $CDCl_3$) δ 8.31 (ddd, *J* = 4.8, 1.7, 0.9 Hz, 1H), 8.16 (dt, *J* = 8.0, 1.0 Hz, 1H), 8.10 (dd, *J* = 7.8, 1.6 Hz, 1H), 7.91 – 7.88 (m, 2H), 7.68 (dtd, *J* = 13.5, 7.7, 1.7 Hz, 3H), 7.55 (ddd, *J* = 14.9, 7.6, 1.3 Hz, 2H), 7.34 (ddd, *J* = 8.1, 7.2, 1.2 Hz, 1H), 7.31 – 7.26 (m, 1H), 7.20 – 7.15 (m, 6H), 7.12 – 7.09 (m, 2H), 6.84 – 6.80 (m, 3H), 4.90 (dd, *J* = 10.1, 8.7 Hz, 1H), 4.29 (dd, *J* = 10.2, 8.5 Hz, 1H), 3.57 (t, *J* = 8.6 Hz, 1H). **^{13}C NMR{^{1}H}** (101 MHz, CDCL3) δ 163.3, 151.2, 149.6, 148.9, 142.8, 141.7, 138.2, 137.3, 136.4, 131.9, 131.3, 129.7, 128.6, 128.6, 127.5, 126.7, 126.6, 124.1, 124.0, 123.7, 123.1, 120.2, 110.9, 74.8, 69.7.

Product eluting second: ^{1}H NMR (400 MHz, $CDCl_3$) δ 8.31 (ddd, *J* = 4.8, 1.8, 0.9 Hz, 1H), 8.22 (dt, *J* = 8.0, 1.0 Hz, 1H), 8.17 (dd, *J* = 7.8, 1.6 Hz, 1H), 7.90 – 7.87 (m, 1H), 7.70 (ddd, *J* = 6.8, 6.2, 1.6 Hz, 1H), 7.68 – 7.64 (m, 1H), 7.56 (td, *J* = 7.7, 1.4 Hz, 1H), 7.51 (dd, *J* = 8.0, 1.2 Hz, 1H), 7.35 (ddd, *J* = 8.1, 7.2, 1.2 Hz, 1H), 7.27 (ddd, *J* = 8.2, 7.2, 1.2 Hz, 1H), 7.19 (ddd, *J* = 7.6, 4.8, 1.2 Hz, 1H), 7.18 – 7.03 (m, 4H), 6.65 – 6.61 (m, 2H), 5.02 – 4.95 (m, 1H), 4.28 – 4.19 (m, 1H), 3.68 (t, *J* = 8.6 Hz, 1H). **^{13}C NMR{^{1}H}** (101 MHz, $CDCl_3$) δ 163.0, 151.1, 149.7, 148.9, 142.8, 141.9, 138.3, 137.4, 136.5, 132.0, 131.4, 129.6, 128.6, 128.5, 127.3, 126.4, 126.4, 124.1, 123.9, 123.7, 123.0, 120.1, 110.8, 74.7, 69.4.

2-((2-nitrophenyl)amino)benzonitrile (135)

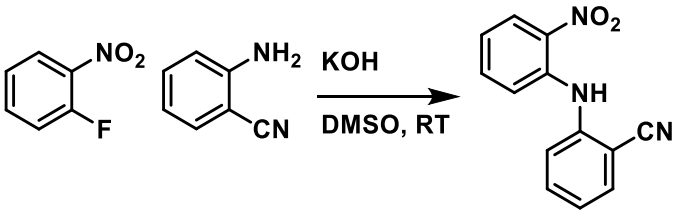

135

2-fluoronitrobenzene (3.75 mL, 35.6 mmol, 1 eq) was dissolved in DMSO (37 mL) and 2-aminobenzonitrile (4200 mg, 35.6 mmol, 1 eq) was added. To this solution solid KOH (4200 mg, 74.75 mmol, 2.1 eq) was added. The reaction was stirred at room temperature for 24 hours. After 24 hours, the reaction mixture was poured into cold water (150 mL). The precipitate was filtered and dried in oven overnignt. Yield 6.3 g (75%). **^{1}H NMR** (400 MHz, $CDCl_3$) δ 9.70 – 9.48 (m, 1H), 8.25 (dd, *J* = 8.5, 1.5 Hz, 1H), 7.71 (ddd, *J* = 7.8, 1.6, 0.5 Hz, 1H), 7.63 – 7.57 (m, 1H), 7.51 – 7.45 (m, 2H), 7.30 – 7.22 (m, 3H), 6.97 (ddd, *J* = 8.4, 7.1, 1.3 Hz, 1H). **^{13}C NMR{^{1}H}** (101 MHz, CDCL3) δ 142.7, 140.3, 135.7, 135.5, 134.1, 134.0, 127.0, 124.9, 122.8, 120.1, 117.1, 116.5, 107.4.

2-((2-aminophenyl)amino)benzonitrile (136)

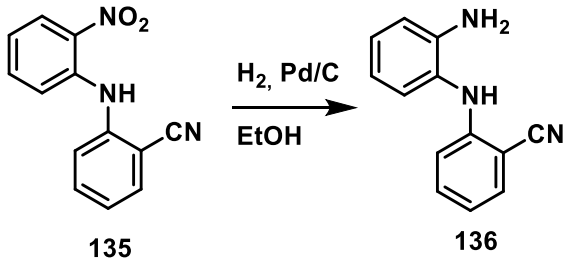

135 136

3-necked round-bottomed flask equipped with stirrbar, valve and rubber septa was charged with 10% palladium on charcoal (665 mg, 0.05 eq). **135** (3 g, 12.5 mmol, 1 eq) was added, followed by EtOH (200 mL). The system was evacuated and purged with nitrogen 4 times. After the last purge, the flask was evacuated and filled with hydrogen gas. The suspension was stirred 4 hours. After the reaction was complete, celite was added and the suspension was filtered. The filtrate was evaporated to yield 2.45 g of solid (93%) **^{1}H NMR** (400 MHz, $CDCl_3$) δ 7.47 (dd, *J* = 7.8, 1.6 Hz, 1H), 7.34 – 7.29 (m, 1H), 7.12 (ddd, *J* = 14.9, 7.7, 1.4 Hz, 2H), 6.83 (dd, *J* = 8.0, 1.3 Hz, 1H), 6.78 (tdd, *J* = 7.7, 2.0, 1.3 Hz, 2H), 6.56 (d, *J* = 8.5 Hz, 1H), 5.95 (s, 1H), 3.83 (s, 2H). **^{13}C NMR{^{1}H}** (101 MHz, $CDCl_3$) δ 148.9, 143.5, 134.3, 132.8, 128.2, 127.8, 124.8, 119.2, 118.4, 117.9, 116.4, 113.5, 96.9.

***N*-(2-((2-cyanophenyl)amino)phenyl)picolinamide (137)**

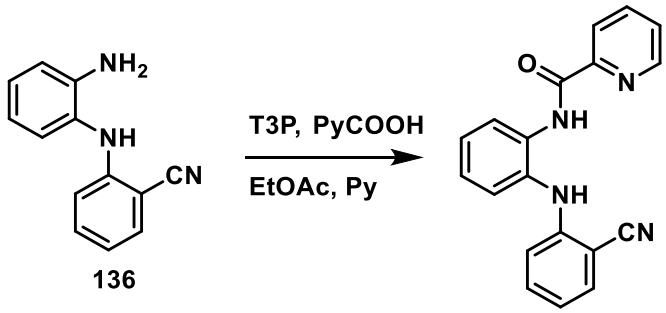

136 137

136 (2450 mg, 11.7 mmol, 1 eq) was dissolved in EtOAc (80 mL). Pyridine (40 mL) was added followed by T3P (50% wt in EtOAc, 7.45 mL, 11.7 mmol, 1 eq) and 2-picolinic acid (1570 mg, 12.9 mmol, 1.1 eq). The reaction was stirred for 16 hours at room temperature. After 16 hours, more T3P (50% wt in EtOAc, 7.45 mL, 11.7 mmol, 1 eq) was added to fully convert the starting material to the product. After 2 hours, the reaction was filtered to yield 1.15 g of the product. The filtrate was washed with 10% HCl (1x 100 mL). The organic extra was cooled in dry ice and the solid material was filtered to yield another 980 mg of solid material. The remaining solution was evaporated and recrystallized from EtOAc (42 mL). In total, 2.81 g of solid material was isolated (75%). **^{1}H NMR** (400 MHz, DMSO-D_6) δ 10.59 (s, 1H), 8.59 (ddd, *J* = 4.8, 1.7, 0.9 Hz, 1H), 8.19 (d, *J* = 6.8 Hz, 2H), 8.14 (dt, *J* = 7.8, 1.1 Hz, 1H), 8.05 (td, *J* = 7.7, 1.7 Hz, 1H), 7.64 (ddd, *J* = 7.6, 4.8, 1.3 Hz, 1H), 7.61 (dd, *J* = 7.8, 1.4 Hz, 1H), 7.39 – 7.27 (m, 3H), 7.22 (ddd, *J* = 8.6, 6.9, 1.5 Hz, 1H), 6.83 (td, *J* = 7.7, 1.0 Hz, 1H), 6.63 (d, *J* = 8.4 Hz, 1H). **^{13}C NMR{^{1}H}** (101 MHz, DMSO-D_6) δ 161.9, 149.2, 148.7, 148.4, 138.3, 134.3, 133.7, 133.1, 132.2, 127.2, 126.2, 125.9, 125.3, 122.4, 122.2, 119.2, 117.6, 115.2, 98.0.

General procedure for the amidation synthesis of 138-142.

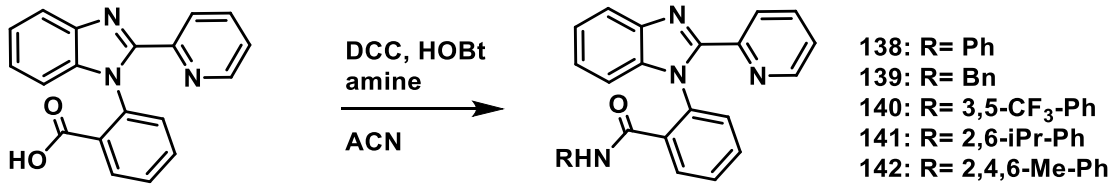

119

Acid **119** (100 mg, 0.22 mmol, 1 eq) was dissolved in acetonitrile (6 mL) HOBt.H_2O (38 mg, 0.25 mmol, 1.1 eq) was added followed by DCC (52 mg, 0.25 mmol, 1.1 eq) and amine (0.25 mmol, 1.1 eq). The reaction was stirred at room temperature for 16 hours. Afterwards, the precipitate was removed by filtration and the filtrate was evaporated. The residue was dissolved in EtOAc (20 mL) and washed with 10% K_2CO_3 (3x 20 mL). Organic layer was washed with brine, dried with MgSO4 and evaporated. The product was purified by suitable methods.

***N*-phenyl-2-(2-(pyridin-2-yl)-1*H*-benzo[*d*]imidazol-1-yl)benzamide (138):** The evaporated reside was dissolved in MeOH (1 mL) and water (1 mL) was added. After sonication, solid product precipitated and was filtered. Yield: 66 mg (76%). **^{1}H NMR** (400 MHz, DMSO-D_6) δ 10.40 (s, 1H), 8.45 (dd, *J* = 4.7, 1.5 Hz, 1H), 8.15 (d, *J* = 7.8 Hz, 1H), 7.91 (td, *J* = 7.8, 1.8 Hz, 1H), 7.82 (dd, *J* = 7.2, 2.1 Hz, 1H), 7.79 – 7.75 (m, 1H), 7.65 (pd, *J* = 7.6, 1.6 Hz, 2H), 7.46 – 7.38 (m, 2H), 7.33 – 7.25 (m, 2H), 7.22 (d, *J* = 8.2 Hz, 2H), 7.15 (t, *J* = 7.8 Hz, 2H), 7.06 – 7.01 (m, 1H), 6.96 (t, *J* = 7.1 Hz, 1H). **^{13}C NMR{^{1}H}** (101 MHz, DMSO-D_6) δ 164.6, 150.4, 148.7, 142.2, 138.5, 137.9, 137.6, 135.3, 134.8, 131.4, 129.0, 128.9, 128.9, 128.6, 123.9, 123.7, 122.8, 119.7, 119.5, 110.8. **HRMS** ESI[M+H]$^+$ calculated for $C_{25}H_{19}O_1N_4$: 391.1553, found: 391.1553

***N*-benzyl-2-(2-(pyridin-2-yl)-1*H*-benzo[*d*]imidazol-1-yl)benzamide (139)**: The evaporated reside was dissolved in MeOH (1 mL) and water (1 mL) was added. After sonication, solid product precipitated and was filtered. Yield: 70 mg (79%). **^{1}H NMR** (400 MHz, DMSO-D_6) δ 8.81 (t, *J* = 6.0 Hz, 1H), 8.28 (dd, *J* = 5.0, 1.8 Hz, 1H), 8.18 (d, *J* = 7.6 Hz, 1H), 7.93 (td, *J* = 7.7, 1.9 Hz, 1H), 7.82 (d, *J* = 8.0 Hz, 1H), 7.75 – 7.71 (m, 1H), 7.64 – 7.56 (m, 2H), 7.38 – 7.31 (m, 3H), 7.26 (td, *J* = 7.8, 1.0 Hz, 1H), 7.10 – 6.99 (m, 3H), 6.97 (d, *J* = 8.0 Hz, 1H), 6.70 (d, *J* = 7.1 Hz, 2H), 5.57 (d, *J* = 8.0 Hz, 1H), 4.16 – 4.02 (m, 2H). **^{13}C NMR{^{1}H}** (101 MHz, DMSO-D_6) δ 166.0, 150.6, 148.9, 148.6, 142.3, 138.7, 138.1, 137.4, 135.0, 131.0, 129.1, 128.9, 128.7, 128.0, 126.4, 124.4, 123.8, 122.7, 119.6, 110.9, 42.1. **HRMS** ESI[M+H]$^+$ calculated for $C_{26}H2_1O_1N_4$: 405.1710, found: 405.1710

***N*-(3,5-bis(trifluoromethyl)phenyl)-2-(2-(pyridin-2-yl)-1*H*-benzo[*d*]imidazol-1-yl)benzamide (140):** Residue was purified by column chromatography (Hexane:EtOAc 1:1). The fractions containing product were combined, evaporated and dissolved in small amount of DCM and the residual dicyclohexylurea was removed by filtration. Isolated 60 mg (52%) of oil **^{1}H NMR** (400 MHz, DMSO-D_6) δ 10.70 (s, 1H), 8.37 (ddd, *J* = 4.8, 1.5, 0.8 Hz, 1H), 8.06 (dt, *J* = 8.0, 1.0 Hz, 1H), 7.95 (s, 2H), 7.87 (dd, *J* = 7.5, 1.6 Hz, 1H), 7.81 – 7.77 (m, 1H), 7.77 – 7.75 (m, 1H), 7.74 (dd, *J* = 4.5, 2.8 Hz, 1H), 7.73 – 7.68 (m, 2H), 7.61 (dd, *J* = 7.7, 1.3 Hz, 1H), 7.35 – 7.26 (m, 3H), 7.12 (dd, *J* = 6.8, 1.8 Hz, 1H). **^{13}C NMR{^{1}H}** (101 MHz, DMSO-D_6) δ 165.4, 150.2, 148.8, 148.7, 142.2, 140.4, 137.7, 137.0, 135.5, 133.6, 131.9, 130.47 (q, J = 32.9 Hz), 129.0, 128.7, 128.6, 123.08 (q, J = 272.8 Hz), 124.12, 124.1, 123.9, 122.8 119.4 (d, J = 4.2 Hz), 116.5, 110.8. **^{19}F NMR** (376 MHz, $CDCl_3$) δ -63.1.

***N*-(2,6-diisopropylphenyl)-2-(2-(pyridin-2-yl)-1*H*-benzo[*d*]imidazol-1-yl)benzamide (141):** Residue was purified by column chromatography (Hexane:EtOAc 1.1:1). Yield: 155 mg (65%). **^{1}H NMR** (400 MHz, $CDCl_3$) δ 10.00 (s, 1H), 8.32 (d, *J* = 7.9 Hz, 1H), 8.32 – 8.26 (m, 1H), 7.98 (dd, *J* = 7.7, 1.4 Hz, 1H), 7.95 (d, *J* = 8.0 Hz, 1H), 7.89 (td, *J* = 7.8, 1.7 Hz, 1H), 7.60 (td, *J* = 7.5, 0.9 Hz, 1H), 7.40 (td, *J* = 7.6, 1.4 Hz, 2H), 7.33 (td, *J* = 7.8, 7.3, 1.0 Hz, 1H), 7.28 (ddd, *J* = 7.5, 5.0, 1.0 Hz, 1H), 7.21 – 7.11 (m, 2H), 7.08 (d, *J* = 7.4 Hz, 1H), 6.93 (d, *J* = 7.4 Hz, 1H), 6.90 – 6.83 (m, 1H), 3.18 (p, *J* = 6.9 Hz, 1H), 1.62 (dq, *J* = 16.5, 9.4, 8.1 Hz, 1H), 1.29 (d, *J* = 6.7 Hz, 3H), 1.20 (d, *J* = 6.8 Hz, 3H),

0.51 (d, *J* = 6.6 Hz, 3H), 0.36 (d, *J* = 6.7 Hz, 3H). **^{13}C NMR{^{1}H}** (101 MHz, $CDCl_3$) δ 167.0, 148.7, 147.2, 145.2, 138.7, 138.1, 137.2, 134.0, 131.2, 131.2, 131.0, 130.2, 129.9, 128.5, 128.2, 125.5, 125.3, 125.2, 125.2, 124.6, 124.1, 123.7, 123.0, 120.2, 111.9, 29.8, 29.2, 28.2, 23.8, 23.6, 23.0.

***N*-mesityl-2-(2-(pyridin-2-yl)-1*H*-benzo[*d*]imidazol-1-yl)benzamide (142):** Residue was purified by column chromatography (Hexane:EtOAc 1.5:1 → 1:1). Yield 69 (25%). **^{1}H NMR** (400 MHz, DMSO-D_6) δ 9.75 (s, 1H), 8.36 – 8.33 (m, 1H), 8.24 (d, *J* = 7.9 Hz, 1H), 7.97 (td, *J* = 7.8, 1.7 Hz, 1H), 7.87 (dd, *J* = 7.6, 1.5 Hz, 1H), 7.80 (d, *J* = 7.4 Hz, 1H), 7.68 (td, *J* = 7.6, 1.2 Hz, 1H), 7.62 (td, *J* = 7.7, 1.6 Hz, 1H), 7.41 – 7.35 (m, 2H), 7.31 (td, *J* = 8.1, 7.7, 1.4 Hz, 1H), 7.26 (td, *J* = 7.7, 7.3, 1.3 Hz, 1H), 6.97 (d, *J* = 7.4 Hz, 1H), 6.70 (s, 2H), 2.11 (s, 3H), 1.59 (br.s, 6H). **^{13}C NMR{^{1}H}** (101 MHz, DMSO-D_6) δ 164.5, 150.4, 148.9, 148.6, 137.6, 135.6, 134.9, 134.7, 131.6, 131.2, 129.4, 129.3, 128.8, 128.2, 124.5, 124.4, 123.9, 122.8, 119.6, 111.0, 20.4, 17.3.

1-(2-(1*H*-benzo[*d*]imidazol-2-yl)phenyl)-2-(pyridin-2-yl)-1*H*-benzo[*d*]imidazole (143)

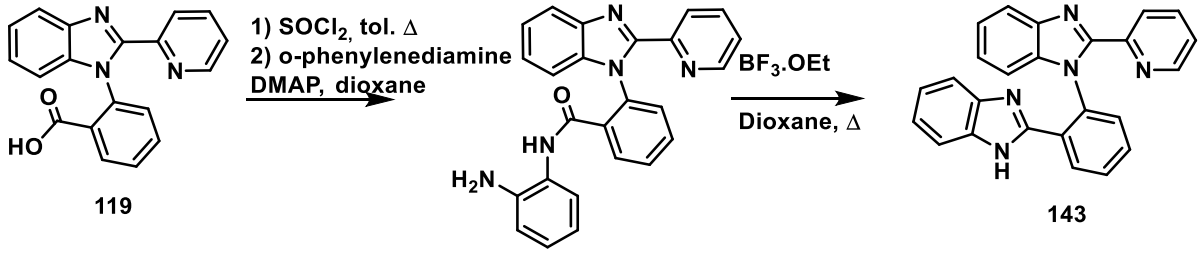

119 143

119 (160 mg, 0.5 mmol, 1eq) was dissolved in toluene, $SOCl_2$ (61 µL, 1 mmol, 2 eq) was added and the mixture was refluxed for 30 minutes. After 30 minutes, the reaction was cooled to room temperature, evaporated and the residue was suspended in dioxane (5 mL). This suspension was slowly added into the solution of o-phenylenediamine (60 mg, 0.55 mmol, 1.1 eq) and DMAP (70 mg, 0.55 mmol, 1.1eq) in dioxane (3 mL). THe reaction was stirred at room temperature for 20 hours. After 20 hours, reaction was filtered and $BF_3.OEt_2$ (250 µL, 2 mmol, 4 eq) was added to the filtrate. This mixture was then refluxed for 16 hours. After 16 hours, the reaction was cooled to room temperature, water (10 mL) was added followed by 10% aq. NaOH (10 mL). This mixture was extracted with EtOAc (3x 20 mL). Organic extracts were combined, washed with brine, dried with $MgSO_4$ and evaporated. The residue was then dissolved in EtOAc (1.5 mL) and precipitated with hexanes (7 ml). Yield: 50 mg (25%).
^{1}H NMR (400 MHz, DMSO-D_6) δ 12.21 (s, 1H), 8.23 (ddd, *J* = 4.8, 1.8, 0.9 Hz, 1H), 8.02 – 7.93 (m, 1H), 7.77 (ddt, *J* = 9.1, 7.9, 1.0 Hz, 2H), 7.73 – 7.64 (m, 2H), 7.63 (td, *J* = 7.7, 1.8 Hz, 1H), 7.62 – 7.53 (m, 1H), 7.32 – 7.19 (m, 4H), 7.20 (ddd, *J* = 8.3, 7.1, 1.2 Hz, 1H), 7.12 – 7.00 (m, 2H), 7.01 (ddd, *J* = 8.3, 7.1, 1.3 Hz, 1H), 6.49 (dd, *J* = 5.7, 3.5 Hz, 1H), 6.36 (dd, *J* = 5.7, 3.4 Hz, 1H).

diphenyl(2-(2-(pyridin-2-yl)-1*H*-benzo[*d*]imidazol-1-yl)phenyl)methanol (144)

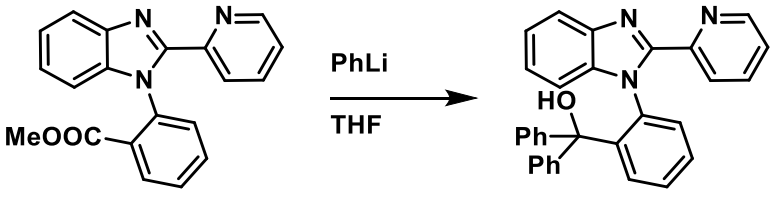

128 144

128 (110 mg, 0.33 mmol, 1 eq) was dissolved in dry THF (3 mL) and cooled in ice/salt/water bath to 0 °C and PhLi (1.9M in Bu_2O, 0.52 mL, 1 mmol, 3 eq) was added dropwise. The reaction was stirred in the ice bath for 30 minutes. Afterwards, 20% aq. NH_4Cl (2.5 mL) was added, followed by diethyleter (5 mL). Organic layer was separated and aq. layer was further extracted with diethyleter (3x 10 mL). Combined organic layers were dried with $MgSO_4$ and evaporated. The reside was purified by column chromatography (Hexane:EtOAc 1:1) to yield 75 mg of gray solid (50%) **^{1}H NMR** (400 MHz, DMSO-D_6) δ 8.21 (dd, *J* = 6.9, 1.8 Hz, 1H), 7.97 – 7.84 (m, 2H), 7.62 (d, *J* = 8.0 Hz, 1H), 7.58 (td, *J* = 6.8, 5.9, 4.0 Hz, 2H), 7.43 – 7.23 (m, 6H), 7.10 (t, *J* = 7.6 Hz, 1H), 7.09 – 6.94 (m, 4H), 6.95 – 6.83 (m, 4H),

6.76 – 6.68 (m, 4H), 6.41 (d, *J* = 8.1 Hz, 1H), 5.73 (s, 1H). **^{13}C NMR{^{1}H}** (101 MHz, DMSO-D_6) δ 154.5, 150.2, 149.9, 146.4, 146.3, 143.7, 138.9, 137.9, 137.7, 137.4, 131.8, 131.3, 128.9, 128.4, 128.3, 127.7, 127.4, 127.3, 127.0, 126.7, 126.6, 126.4, 126.3, 122.4, 121.4, 119.6, 118.6, 111.3, 81.5. **HRMS** ESI[M+H]$^+$ calculated for $C_{31}H_{24}O_1N_3$: 454.1914, found: 454.1914

(2-(2-(pyridin-2-yl)-1*H*-benzo[*d*]imidazol-1-yl)phenyl)methanol (145)

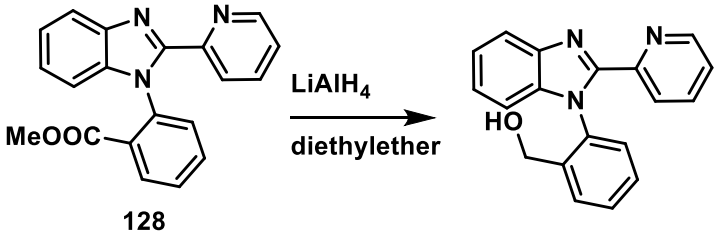

128 **145**

128 (55 mg, 0.16 mmol, 1 eq) was added slowly into the suspension of $LiAlH_4$ (25 mg, 0.65 mmol, 4 eq) in diethylether (4 mL). The reaction was stirred at room temperature for 2 hours. After 2 hours, water (25 µL) was added, followed by 10% aq NaOH (75 µL) and water (75 µL). The solid precipitate was filtered through celite. Celite was washed with diethylether and the filtrate was evaporated. The residue was purified by column chromatography (hexane:EtOAc 2:1) to yield 23 mg clear oil (48%). **^{1}H NMR** (400 MHz, $CDCl_3$) δ 8.27 (ddd, *J* = 4.9, 1.5, 0.9 Hz, 1H), 8.24 (dd, *J* = 7.9, 0.9 Hz, 1H), 7.92 (d, *J* = 8.1 Hz, 1H), 7.85 (td, *J* = 7.8, 1.7 Hz, 1H), 7.71 (dd, *J* = 7.7, 1.5 Hz, 1H), 7.51 (td, *J* = 7.6, 1.3 Hz, 1H), 7.37 (ddd, *J* = 8.1, 7.3, 1.2 Hz, 1H), 7.35 – 7.21 (m, 3H), 6.97 – 6.88 (m, 1H), 6.90 (dd, *J* = 7.8, 1.2 Hz, 1H), 5.41 (d, *J* = 9.1 Hz, 1H), 4.64 (d, *J* = 11.3 Hz, 1H), 4.39 (dd, *J* = 11.8, 6.4 Hz, 1H).

isopropyl 2-(2-(pyridin-2-yl)-1*H*-benzo[*d*]imidazol-1-yl)benzoate (146)

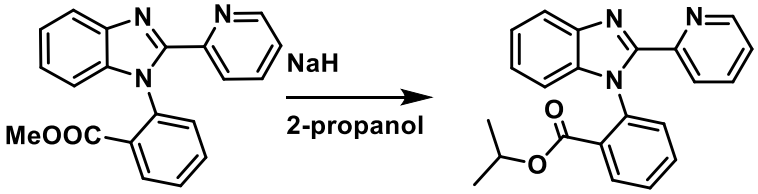

128 **146**

128 (50 mg, 0.15 mmol, 1 eq) was dissolved in 2-propanol and catalytic amount of NaH was added. The reaction was stirred at room temperature for 4 hours. After 4 hours, the reaction was quenched with conc. HCl (1 drop) and evaporated. The residue was dissolved in EtOAc (5 mL) and washed with 10% aq. K_2CO_3 (3x 5 mL), brined, dried with $MgSO_4$ and evaporated to yield 41 mg of clear foam (77%). **^{1}H NMR** (400 MHz, $CDCl_3$) δ 8.31 (d, *J* = 7.9 Hz, 1H), 8.24 (d, *J* = 4.3 Hz, 1H), 8.13 (dd, *J* = 7.8, 1.6 Hz, 1H), 7.91 (d, *J* = 8.0 Hz, 1H), 7.73 (td, *J* = 7.8, 1.8 Hz, 1H), 7.67 (td, *J* = 7.6, 1.7 Hz, 1H), 7.58 (td, *J* = 7.6, 1.3 Hz, 1H), 7.45 (dd, *J* = 7.8, 1.2 Hz, 1H), 7.35 – 7.30 (m, 1H), 7.27 – 7.22 (m, 1H), 7.16 (ddd, *J* = 7.4, 4.8, 0.9 Hz, 1H), 7.00 (d, *J* = 8.0 Hz, 1H), 4.72 (hept, *J* = 6.2 Hz, 1H), 0.76 (d, *J* = 6.2 Hz, 3H), 0.53 (d, *J* = 6.2 Hz, 3H). **^{13}C NMR{^{1}H}** (101 MHz, $CDCl_3$) δ 165.0, 150.6, 149.5, 148.6, 142.7, 138.6, 137.8, 136.4, 132.8, 131.7, 130.3, 129.9, 128.7, 124.0, 123.9, 123.6, 122.9, 120.0, 110.7, 21.1, 20.8.

2-(1-(2-(methoxycarbonyl)phenyl)-1*H*-benzo[*d*]imidazol-2-yl)pyridine 1-oxide (147)

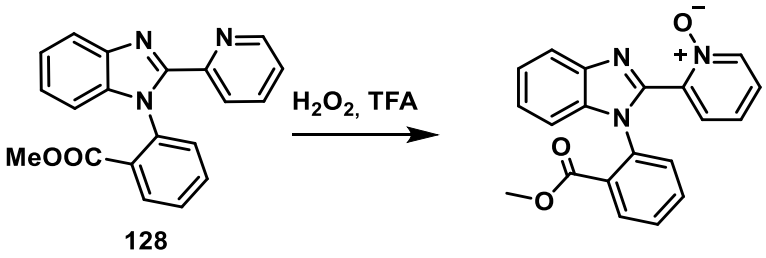

128 147

128 (110 mg, 0.33 mmol, 1 eq) was dissolved in TFA (830 µL) and 30% H_2O_2 (530 µL) was added. Reaction was stirred at room temperature for 22 hours. After 22 hours, the reaction was diluted with EtOAc (20 mL) and washed with 10% K_2CO_3 (3x 10 mL), saturated $Na_2S_2O_3$ (3x 10 mL), brine and dried with $MgSO_4$ and evaporated to yield 110 mg of solid (95 %). **^{1}H NMR** (400 MHz, $CDCl_3$) δ 8.03 – 8.00 (m, 1H), 7.96 – 7.92 (m, 1H), 7.92 – 7.88 (m, 1H), 7.79 – 7.76 (m, 1H), 7.70 – 7.65 (m, 2H), 7.51 (td, *J* = 7.6, 1.3 Hz, 1H), 7.36 – 7.27 (m, 2H), 7.29 – 7.19 (m, 2H), 7.12 (ddd, *J* = 7.7, 1.5, 0.7 Hz, 1H), 3.47 (s, 3H).

2-(2-(pyridin-2-yl)-1*H*-benzo[*d*]imidazol-1-yl)benzoyl azide (148)

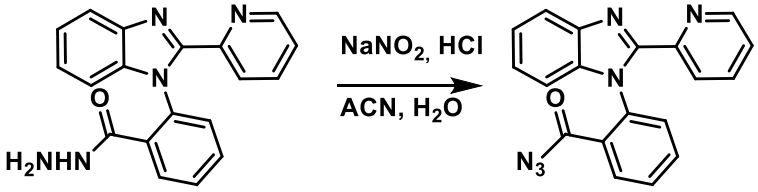

149 148

149 (76 mg, 0.23 mmol, 1 eq) was dissolved in acetonitrile (6 mL) and water (2 mL) and cooled in ice bath. Conc. HCl (348 µL, 1 mmol, 4 eq) was added. To this solution, solution of $NaNO_2$ (32 mg, 0.46 mmol, 2 eq) in water (2 mL) was added dropwise. The reaction slowly changed color from yellow to brown-orange. The mixture was stirred in the ice bath for 60 minutes. After 60 minutes, 10% aq. K_2CO_3 (10 mL) was added and the mixture separated into two layers. Organic layers was separated and the aquaeous layer was extracted with EtOAc (3x 10 mL). Combined organics were dried with $MgSO_4$ and evaporated to yield 56 mg of oil (72%). **^{1}H NMR** (400 MHz, DMSO-D_6) δ 8.31 – 8.27 (m, 1H), 8.22 – 8.18 (m, 1H), 8.06 (dd, *J* = 7.9, 1.4 Hz, 1H), 7.93 (td, *J* = 7.8, 1.8 Hz, 1H), 7.88 (td, *J* = 7.6, 1.6 Hz, 1H), 7.83 (d, *J* = 7.8 Hz, 1H), 7.70 (td, *J* = 7.7, 1.1 Hz, 1H), 7.62 (dd, *J* = 7.8, 0.9 Hz, 1H), 7.37 – 7.30 (m, 2H), 7.27 (t, *J* = 7.4 Hz, 1H), 6.99 (d, *J* = 7.8 Hz, 1H). **^{13}C NMR{^{1}H}** (101 MHz, DMSO-D_6) δ 170.4, 149.9, 148.9, 148.4, 142.3, 137.6, 137.2, 134.9, 131.0, 130.0, 129.1, 128.2, 124.2, 123.9, 123.8, 122.8, 119.6, 110.5.

2-(2-(pyridin-2-yl)-1*H*-benzo[*d*]imidazol-1-yl)benzohydrazide (149)

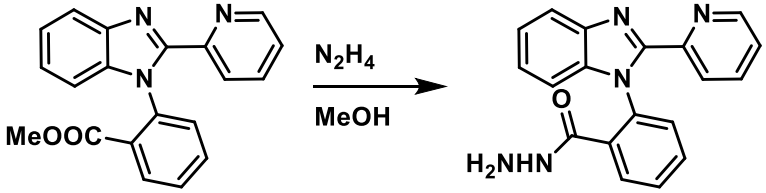

128 149

128 (1.95 g, 5.9 mmol, 1 eq) was dissolved in MeOH (53 mL) and hydrazine hydrate (35 mL) was added. The solution was stirred at room temperature for 16 hours. After 16 hours, MeOH was evaporated and the resulting suspension was filtered and dried to yield 1.5 g (77%) of yellow solid. **^{1}H NMR** (400 MHz, DMSO-D_6) δ 9.37 (s, 1H), 8.31 (ddd, *J* = 4.8, 1.7, 0.9 Hz, 1H), 8.18 (dt, *J* = 7.9, 1.0 Hz, 1H), 7.94 (td, *J* = 7.8, 1.8 Hz, 1H), 7.79 (d, *J* = 7.4 Hz, 1H), 7.64 – 7.60 (m, 1H), 7.60 – 7.55 (m, 2H), 7.40 – 7.34

(m, 2H), 7.30 (td, *J* = 7.6, 1.3 Hz, 1H), 7.25 (td, *J* = 7.6, 7.2, 1.3 Hz, 1H), 6.97 (dd, *J* = 7.6, 1.2 Hz, 1H), 4.05 (s, 2H). **^{13}C NMR{^{1}H}** (101 MHz, DMSO-D_6) δ 165.4, 150.8, 149.1, 148.7, 142.3, 137.9, 137.3, 135.2, 133.5, 131.1, 129.1, 128.8, 128.7, 124.4, 124.2, 123.7, 122.7, 119.6, 110.9.

1-mesityl-3-(2-(2-(pyridin-2-yl)-1*H*-benzo[*d*]imidazol-1-yl)phenyl)urea (150)

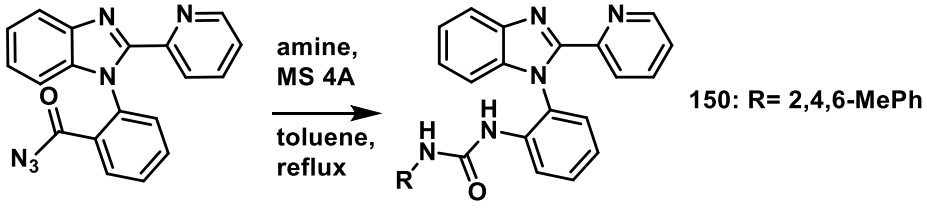

139

Freshly prepared azide **139** (155 mg, 0.5 mmol, 1 eq) was dissolved in dry toluene (20 mL, dried over activated sieves). Powdered molecular sieves (140 mg) were added followed by 2,4,6-trimethylaniline (1 mmol, 2 eq). The reaction was refluxed for 16 hours. After 16 hours, molecular sieves were removed by filtration through celite. The filtrate was evaporated and purified by column chromatography.Purified by gradient DCM → DCM:MeOH 20:1 to yield 177 mg of solid (82%) **^{1}H NMR** (400 MHz, DMSO-D_6) δ 8.30 (d, *J* = 21.9 Hz, 2H), 8.12 (d, *J* = 7.8 Hz, 1H), 7.99 – 7.91 (m, 1H), 7.86 (d, *J* = 7.9 Hz, 2H), 7.77 (s, 1H), 7.45 – 7.31 (m, 3H), 7.28 (t, *J* = 7.5 Hz, 1H), 7.01 (m, 3H), 6.78 (s, 2H), 2.16 (s, 3H), 1.91 (s, 6H).

(1*R*,2*S*,5*R*)-2-isopropyl-5-methylcyclohexyl 2-((2-nitrophenyl)amino)benzoate (151)

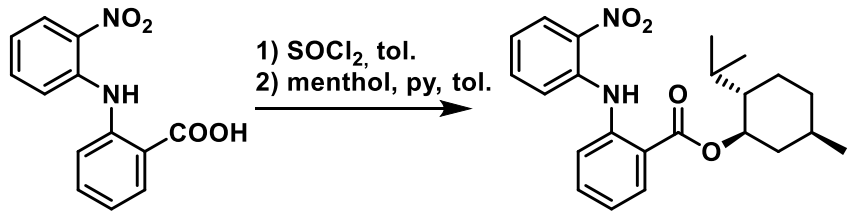

7 151

Acid **7** (256 mg, 1 mmol, 1 eq) was suspended in toluene (10 mL) and $SOCl_2$ (600 µL, 8.3 mmol, 8.3 eq) was added. The mixture was refluxed for 2 hours. After two hours, the raction was cooled to room temperature and evaporated. The intermediate acylchloride was dissolved in toluene (10 mL) and was added dropwise to solution of (1R,2S,5R)-menthol (125 mg, 0.8 mmol, 0.8 eq), pyridine (160 µL, 2 mmol, 2 eq) in toluene (5 mL). After the addition was complete, the mixture was refluxed for 24 hours. After 24 hours, the reaction mixture was cooled to room temperature, washed with 10% aq. K_2CO_3 (3x 10 mL), brine, dried with $MgSO_4$ and evaporated. The residue was purified by column chromatography (toluene) to yield 150 mg of dark oil (40%) **^{1}H NMR** (400 MHz, $CDCl_3$) δ 11.12 (s, 1H), 8.17 (dd, *J* = 8.4, 1.6 Hz, 1H), 8.05 (dd, *J* = 8.0, 1.6 Hz, 1H), 7.60 (dd, *J* = 8.6, 1.2 Hz, 1H), 7.51 (dd, *J* = 8.3, 1.1 Hz, 1H), 7.43 (ddt, *J* = 8.7, 7.2, 1.9 Hz, 2H), 7.05 (ddd, *J* = 8.2, 7.2, 1.2 Hz, 1H), 6.93 (ddd, *J* = 8.4, 7.1, 1.3 Hz, 1H), 5.01 (td, *J* = 10.9, 4.4 Hz, 1H), 2.15 (ddt, *J* = 9.5, 4.4, 2.7 Hz, 1H), 1.96 (pd, *J* = 7.0, 2.7 Hz, 1H), 1.79 – 1.68 (m, 2H), 1.67 – 1.47 (m, 2H), 1.11 (dt, *J* = 12.5, 5.3 Hz, 2H), 0.99 – 0.94 (m, 1H), 1.01 – 0.86 (m, 6H), 0.79 (d, *J* = 6.9 Hz, 3H). **^{13}C NMR{^{1}H}** (101 MHz, $CDCl_3$) δ 166.7, 142.5, 137.5, 134.8, 133.3, 132.1, 126.8, 121.9, 119.9, 119.4, 119.2, 119.0, 75.5, 47.2, 41.0, 34.4, 31.6, 26.6, 23.6, 22.1, 20.9, 16.6.

(1*R*,2*S*,5*R*)-2-isopropyl-5-methylcyclohexyl 2-((2-aminophenyl)amino)benzoate (152)

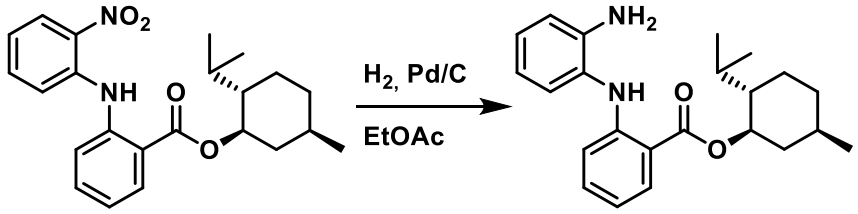

151 152

3-necked round-bottomed flask equipped with stirrbar, valve and rubber septa was charged with 10% palladium on charcoal (46 mg, 0.05 eq). **153** (350 mg, 0.88 mmol, 1 eq) was added, followed by EtOAc (10 mL). The system was evacuated and purged with nitrogen 4 times. After the last purge, the flask was evacuated and filled with hydrogen gas. The suspension was stirred for 4 hours. After the reaction was complete, celite was added and the suspension was filtered. The filtrate was evaporated to yield 220 mg (70 %) of oily product. **^{1}H NMR** (400 MHz, $CDCl_3$) δ 9.08 (s, 1H), 7.97 (dd, *J* = 8.1, 1.6 Hz, 1H), 7.27 (ddd, *J* = 8.6, 7.1, 1.7 Hz, 1H), 7.16 (dd, *J* = 7.8, 1.4 Hz, 1H), 7.09 (ddd, *J* = 7.9, 7.4, 1.5 Hz, 1H), 6.86 (dd, *J* = 8.0, 1.3 Hz, 1H), 6.79 (td, *J* = 7.6, 1.4 Hz, 1H), 6.69 (ddd, *J* = 8.1, 7.1, 1.1 Hz, 1H), 6.65 (dd, *J* = 8.5, 0.8 Hz, 1H), 4.93 (td, *J* = 10.9, 4.4 Hz, 1H), 3.91 (s, 2H), 2.19 – 2.13 (m, 1H), 2.04 – 1.99 (m, 1H), 1.78 – 1.70 (m, 2H), 1.58 (ddd, *J* = 15.1, 7.7, 3.2 Hz, 2H), 1.20 – 1.07 (m, 2H), 0.97 – 0.92 (m, 7H), 0.82 (d, *J* = 7.0 Hz, 3H). **^{13}C NMR{^{1}H}** (101 MHz, $CDCl_3$) δ 168.3, 149.6, 142.8, 134.3, 131.5, 127.6, 127.0, 126.5, 119.3, 116.5, 116.3, 113.9, 111.8, 74.5, 47.3, 41.2, 34.4, 31.6, 26.6, 23.7, 22.2, 20.9, 16.6.

(1*R*,2*S*,5*R*)-2-isopropyl-5-methylcyclohexyl 2-((2-(picolinamido)phenyl)amino)benzoate (153)

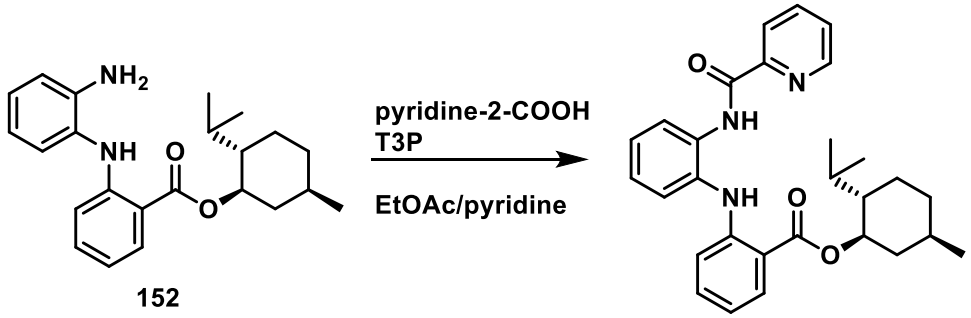

152 153

Ester **154** (120 mg, 0.32 mmol, 1eq) was dissolved in EtOAc (2 mL), pyridine (1 mL) was added followed by T3P (50% wt in EtOAc, 203 µL, 1eq) and 2-picolinic acid (44 mg, 0.36 mmol, 1.1 eq). Reaction was stirred at room temperature for 16 hours. After 16 hours, it was diluted with EtOAc (10 mL) an dextracted with 10% HCl (3x 10 mL), brine, dried with $MgSO_4$ and evaporated to yield 131 mg (87%). **^{1}H NMR** (400 MHz, $CDCl_3$) δ 10.53 (s, 1H), 9.32 (s, 1H), 8.60 (dd, *J* = 8.2, 1.4 Hz, 1H), 8.39 (ddd, *J* = 4.7, 1.7, 0.9 Hz, 1H), 8.25 (dt, *J* = 7.8, 1.1 Hz, 1H), 8.06 – 7.98 (m, 1H), 7.84 (td, *J* = 7.7, 1.7 Hz, 1H), 7.40 – 7.35 (m, 2H), 7.32 (td, *J* = 7.8, 1.4 Hz, 1H), 7.28 – 7.19 (m, 1H), 7.24 – 7.12 (m, 1H), 6.78 – 6.68 (m, 2H), 4.95 (td, *J* = 10.9, 4.4 Hz, 1H), 2.21 – 2.11 (m, 1H), 2.09 – 1.99 (m, 1H), 1.74 (d, *J* = 11.4 Hz, 2H), 1.62 – 1.51 (m, 2H), 1.15 (q, *J* = 13.7, 12.5 Hz, 2H), 0.98 – 0.90 (m, 7H), 0.82 (d, *J* = 6.9 Hz, 3H). **^{13}C NMR{^{1}H}** (101 MHz, $CDCl_3$) δ 162.3, 150.0, 149.5, 148.1, 137.5, 134.5, 134.2, 131.4, 130.7, 126.9, 126.7, 126.3, 124.7, 122.3, 121.1, 117.3, 114.4, 112.7, 74.7, 47.3, 41.2, 34.4, 31.6, 26.7, 23.7, 22.2, 20.9, 16.7.

(1*R*,2*S*,5*R*)-2-isopropyl-5-methylcyclohexyl 2-(2-(pyridin-2-yl)-1*H*-benzo[*d*]imidazol-1-yl)benzoate (154)

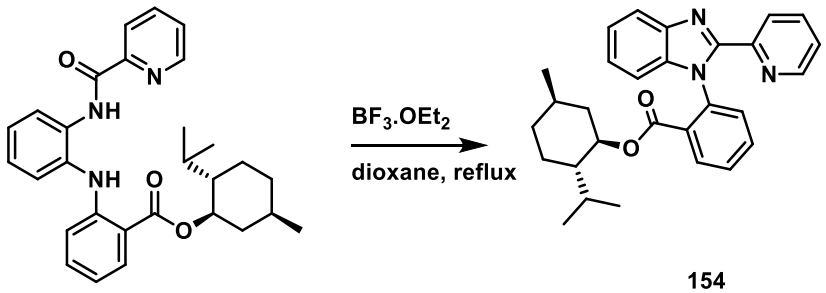

153 154

155 (245 mg, 0.5 mmol, 1 eq) was dissolved in dioxane (5 mL) and $BF_3.OEt_2$ (183 µL, 1,3 mmol, 2.5 eq) and the reaction mixture was refluxed for 18 hours. After 18 hours, 10% aq. K_2CO_3 (5 mL) and water (5 mL) were added. The resulting solution was extracted with DCM (3x 10 mL). Combined organic extracts were dried with MgSO4, evaporated and purified by column chromatography (hexane:EtOAc 4:1) to yield 180 mg of product as oil (80%). Isolated as a mixture of diastereomers in 1.25:1 ratio. **^{1}H NMR** (400 MHz, $CDCl_3$) δ 8.35 (dq, *J* = 8.0, 1.0 Hz, 1H), 8.32 (dq, *J* = 8.0, 1.0 Hz, 1H), 8.27 – 8.11 (m, 4H), 7.93 – 7.84 (m, 2H), 7.76 – 7.52 (m, 7H), 7.47 – 7.39 (m, 1H), 7.44 – 7.35 (m, 1H), 7.36 – 7.25 (m, 2H), 7.28 – 7.15 (m, 2H), 7.19 – 7.07 (m, 2H), 7.02 – 6.93 (m, 1H), 6.97 – 6.88 (m, 1H), 4.53 – 4.38 (m, 2H), 1.53 – 1.33 (m, 6H), 1.32 – 1.08 (m, 5H), 0.93 – 0.75 (m, 5H), 0.69 (d, *J* = 6.5 Hz, 4H), 0.62 (d, *J* = 6.4 Hz, 3H), 0.49 (d, *J* = 7.0 Hz, 4H), 0.44 (d, *J* = 6.9 Hz, 3H), 0.40 – 0.33 (m, 7H), -0.29 (q, *J* = 12.6 Hz, 1H). **^{13}C NMR{^{1}H}** (101 MHz, $CDCl_3$) δ 165.1, 164.9, 150.4, 149.6, 148.6, 148.5, 142.8, 142.6, 138.8, 138.7, 138.2, 138.0, 136.3, 132.9, 132.8, 132.1, 131.8, 130.1, 129.9, 129.7, 128.7, 123.9, 123.9, 123.6, 123.5, 123.0, 120.0, 110.8, 110.7, 75.0, 74.9, 46.4, 46.2, 39.8, 39.2, 34.0, 33.9, 31.2, 31.0, 25.6, 25.4, 22.8, 21.9, 20.7, 15.8, 15.7.

GENERAL PROCEDURE FOR SYNTHESIS OF KETIMINES

1-(4-bromophenyl)-*N*-(4-methoxyphenyl)ethan-1-imine (156)
^{1}H NMR (400 MHz, $CDCl_3$) δ 7.87 – 7.80 (m, 2H), 7.61 – 7.54 (m, 2H), 6.95 – 6.88 (m, 2H), 6.80 – 6.71 (m, 2H), 3.82 (s, 3H), 2.24 (s, 3H). **^{13}C NMR{^{1}H}** (101 MHz, $CDCl_3$) δ 164.8, 156.3, 144.4, 138.6, 131.6, 128.9, 125.1, 120.9, 114.4, 55.6, 17.3.

***N*-1-bis(4-methoxyphenyl)ethan-1-imine (158)**
^{1}H NMR (400 MHz, CDCl3) δ 7.99 – 7.88 (m, 2H), 7.00 – 6.89 (m, 2H), 6.95 – 6.85 (m, 2H), 6.79 – 6.69 (m, 2H), 3.87 (s, 3H), 3.82 (s, 3H), 2.22 (s, 3H). **^{13}C NMR{^{1}H}** (101 MHz, CDCL3) δ 164.9, 161.6, 155.9, 145.2, 132.6, 128.9, 121.0, 114.4, 113.7, 55.6, 55.5, 17.2.

***N*-(4-methoxyphenyl)-1-(4-nitrophenyl)ethan-1-imine (159)**
^{1}H NMR (400 MHz, CDCl3) δ 8.31 – 8.26 (m, 2H), 8.15 – 8.11 (m, 2H), 6.96 – 6.92 (m, 2H), 6.80 – 6.75 (m, 2H), 3.83 (s, 3H), 2.32 (s, 3H). **^{13}C NMR{^{1}H}** (101 MHz, CDCL3) δ 196.8, 156.7, 145.5, 144.0, 128.2, 123.7, 120.9, 114.5, 55.7, 17.6.

1-(4-bromophenyl)-*N*-(3,5-dimethylphenyl)ethan-1-imine (160)
^{1}H NMR (400 MHz, $CDCl_3$) δ 7.85 – 7.83 (m, 0H), 7.82 – 7.81 (m, 1H), 7.61 – 7.54 (m, 1H), 7.56 – 7.54 (m, 1H), 6.73 (tt, *J* = 1.5, 0.7 Hz, 1H), 6.41 – 6.39 (m, 2H), 2.31 (t, *J* = 0.9 Hz, 6H), 2.21 (s, 3H). **^{13}C NMR{^{1}H}** (101 MHz, $CDCl_3$) δ 164.0, 151.5, 138.8, 138.6, 131.6, 128.9, 125.2, 125.1, 117.0, 21.5, 17.3.

1-(4-bromophenyl)-*N*-(naphthalen-1-yl)ethan-1-imine (161)

^{1}H NMR (400 MHz, $CDCl_3$) δ 8.01 – 7.96 (m, 2H), 7.88 – 7.84 (m, 1H), 7.75 – 7.71 (m, 1H), 7.65 – 7.60 (m, 3H), 7.52 – 7.39 (m, 3H), 6.77 (dd, *J* = 7.2, 1.1 Hz, 1H), 2.19 (s, 3H). **^{13}C NMR{^{1}H}** (101 MHz, $CDCl_3$) δ 165.5, 147.8, 138.3, 134.4, 131.8, 129.1, 128.2, 126.3, 126.0, 126.0, 125.6, 125.5, 123.6, 123.6, 113.5, 17.7.

3-phenyl-2*H*-benzo[*b*][1,4]oxazine (162)

2-aminophenol (109 mg, 1 mml, 1 eq) was dissolved in DCM (20 mL). Then, 20% aq. K_2CO_3 (20 mL) was added followed by nBu_4NHSO_4 (17 mg, 0.05 mmol, 0.05 eq) and bromoacetophenone (200 mg, 1 mmol, 1 eq). The reaction was stirred at room temperature for 18 hours. After 18 hours, the layers were separated and the organic layer was evaporated. The residue was purified by column chromatography (Hexane:EtOAc 10:1) to yield 126 mg of light solid (60%).**^{1}H NMR** (400 MHz, $CDCl_3$) δ 7.95 – 7.90 (m, 2H), 7.51 – 7.46 (m, 3H), 7.44 (dd, *J* = 7.7, 1.6 Hz, 1H), 7.15 (ddd, *J* = 7.9, 7.4, 1.7 Hz, 1H), 7.03 (td, *J* = 7.6, 1.4 Hz, 1H), 6.92 (dd, *J* = 7.9, 1.4 Hz, 1H), 5.08 (s, 2H). **^{13}C NMR{^{1}H}** (101 MHz, $CDCl_3$) δ 158.8, 146.5, 135.6, 133.9, 131.3, 129.6, 128.9, 128.8, 128.5, 128.0, 126.6, 122.5, 115.7, 63.1.

3-phenylquinoxalin-2(1*H*)-one (163)

Methylbenzylformate (164 mg, 1 mmol, 1 eq) was dissolved in THF (9 mL) and pyridine (1 mL). Benzene-1,2-diamine (108 mg, 1 mmol, 1 eq) was added and the mixture was refluxed for 90 minutes. After 90 minutes, the reaction mixture was cooled to room temperature, evaporated and the residue was suspended in diethylether. The suspension was filtered and dried. Isolated 160 mg (72%).

^{1}H NMR (400 MHz, DMSO-D_6) δ 12.56 (s, 1H), 8.36 – 8.26 (m, 2H), 7.87 – 7.81 (m, 1H), 7.59 – 7.46 (m, 4H), 7.37 – 7.31 (m, 2H). **^{13}C NMR{^{1}H}** (101 MHz, $CDCl_3$) δ 158.8, 146.5, 135.6, 133.9, 131.3, 129.6, 128.9, 128.8, 128.0, 126.6, 122.5, 116.3, 115.7, 63.1.

GENERAL PROCEDURE FOR REDUCTION OF KETIMINES

Reduction with racemic ligand to provide racemic mixture as a reference for chiral SFC

Ketimine (0.115 mmol, 1 eq) was dissolved in chlorofom (1 mL) and ligand (0.023 mmol, 0.2 eq) was added. To this solution, trichlorosilane (34 μL, 0.45 mmol, 3 eq) and the reaction was stirred at room temperature for 18 hours. After 18 hours, sat. $NaHCO_3$ solution (1 mL) was added and the biphasic system was shaken. The resulting gel-like precipitate was filtered and the organic layer was separated. The aquaeous layer was extracted with EtOAc (2x 2 mL). Organic extracts were combined, washed with brine, dried with $MgSO_4$ and evaporated. The residue was purified by column chromatography.

Reduction with chiral ligand

Ketimine (0.115 mmol, 1 eq) was dissolved in dry toluene (1 mL) and ligand (0.001 mmol, 0.01 eq as a toluene solution with such concentration to add between 50-100 μL of the solution) was added. To this solution, trichlorosilane (34 μL, 0.45 mmol, 3 eq) and the reaction was stirred at room temperature for 18 hours. After 18 hours, sat. $NaHCO_3$ solution (1 mL) was added and the biphasic system was shaken. The resulting gel-like precipitate was filtered and the organic layer was separated. The aquaeous layer was extracted with EtOAc (2x 2 mL). Organic extracts were combined, washed with brine, dried with $MgSO_4$ and evaporated. The residue was purified by column chromatography.

***N*-(1-(4-bromophenyl)ethyl)-4-methoxyaniline (157)**

^{1}H NMR (400 MHz, $CDCl_3$) δ 7.45 – 7.40 (m, 2H), 7.26 – 7.22 (m, 2H), 6.72 – 6.66 (m, 2H), 6.46 – 6.39 (m, 2H), 4.36 (q, *J* = 6.7 Hz, 1H), 3.70 (s, 3H), 1.47 (d, *J* = 6.8 Hz, 3H). **^{13}C NMR {^{1}H}** (101 MHz, $CDCl_3$) δ 152.3, 144.8, 141.3, 131.9, 127.9, 120.6, 114.9, 114.8, 55.9, 54.0, 25.2.

4-methoxy-*N*-(1-(4-methoxyphenyl)ethyl)aniline (reduction of imine 158)
^{1}H NMR (400 MHz, $CDCl_3$) δ 8.20 – 8.16 (m, 2H), 7.56 – 7.52 (m, 2H), 6.71 – 6.66 (m, 2H), 6.43 – 6.38 (m, 2H), 4.50 (q, *J* = 6.7 Hz, 1H), 3.82 (s, 3H), 3.69 (s, 3H), 1.52 (d, *J* = 6.8 Hz, 3H). **^{13}C NMR{^{1}H}** (101 MHz, $CDCl_3$) δ 153.6, 152.5, 147.2, 140.8, 126.9, 124.2, 115.0, 114.7, 55.8, 54.2, 25.1.

4-methoxy-*N*-(1-(4-nitrophenyl)ethyl)aniline (reduction of imine 159)
^{1}H NMR (400 MHz, $CDCl_3$) δ 7.31 – 7.27 (m, 2H), 7.11 (d, *J* = 9.0 Hz, 2H), 6.79 – 6.75 (m, 2H), 6.68 – 6.64 (m, 2H), 4.40 (q, *J* = 6.9 Hz, 1H), 3.75 (s, 3H), 3.71 (s, 3H), 1.84 (d, *J* = 6.9 Hz, 3H). **^{13}C NMR{^{1}H}** (101 MHz, $CDCl_3$) δ 196.81, 156.70, 145.46, 143.97, 128.21, 123.69, 120.91, 114.52, 77.16, 55.66, 17.60.

3-phenyl-3,4-dihydro-2*H*-benzo[*b*][1,4]oxazine (reduction of imine 162)
^{1}H NMR (400 MHz, $CDCl_3$) δ 7.44 – 7.32 (m, 5H), 6.88 – 6.80 (m, 2H), 6.71 (ddd, *J* = 15.7, 7.8, 1.6 Hz, 2H), 4.52 (dd, *J* = 8.6, 3.0 Hz, 1H), 4.30 (dd, *J* = 10.6, 3.0 Hz, 1H), 4.01 (dd, *J* = 10.6, 8.6 Hz, 1H). **^{13}C NMR{^{1}H}** (101 MHz, $CDCl_3$) δ 143.7, 139.3, 134.0, 129.0, 128.5, 127.3, 121.6, 119.1, 116.7, 115.5, 71.1, 54.4.

3-phenyl-3,4-dihydroquinoxalin-2(1*H*)-one (reduction of imine 163 only with racemic ligand)
^{1}H NMR (400 MHz, DMSO-D_6) δ 10.39 (s, 1H), 7.35 – 7.30 (m, 4H), 7.28 – 7.24 (m, 1H), 6.81 – 6.75 (m, 2H), 6.75 – 6.71 (m, 1H), 6.64 (s, 1H), 6.59 (ddd, *J* = 7.8, 6.2, 2.5 Hz, 1H), 4.92 (s, 1H). **^{13}C NMR{^{1}H}** (101 MHz, DMSO-D_6) δ 165.8, 140.3, 133.8, 128.3, 127.5, 126.9, 123.0, 117.6, 114.7, 113.3, 59.3.

List of author´s publications

1 **Kriegelstein, M**.; Profous, D.; Lyčka, A.; Trávníček, Z.; Přibylka, A.; Volná, T.; Benická, S.; Cankař, P. Axially Chiral Trifluoromethylbenzimidazolylbenzoic Acid: A Chiral Derivatizing Agent for α-Chiral Primary Amines and Secondary Alcohols to Determine Absolute Configuration. *J. Org. Chem.* **2019**, *84* (18), 11911–11921.

2 **Kriegelstein, M**.; Profous, D.; Pribylka, A.; Cankař, P. The Assignment of Absolute Configuration of β-Chiral Primary Alcohols with Axially Chiral Trifluoromethylbenzimidazolylbenzoic Acid. *J. Org. Chem.* **2020**, *85* (20), 1–10.

3 **Kriegelstein, M**.; Profous, D.; Pribylka, A.; Cankař, P. Limitations of Trifluoromethylbenzoimidazolylbenzoic Acid as a Chiral Derivatizing Agent to Assign Absolute Configuration for β-Chiral Aminoalcohols *J. Org. Chem.* **Under review**

List of used literature sources

(1) Axial Chirality. *IUPAC Compend. Chem. Terminol.* **2008**, *2193*, 2201. https://doi.org/10.1351/goldbook.a00547.

(2) Bringmann, G.; Mortimer, A. J. P.; Keller, P. A.; Gresser, M. J.; Garner, J.; Breuning, M. Atroposelective Synthesis of Axially Chiral Biaryl Compounds. *Angew. Chemie - Int. Ed.* **2005**, *44* (34), 5384–5427. https://doi.org/10.1002/anie.200462661.

(3) Christie, G. H.; Kenner, J. The Molecular Configurations of Polynuclear Aromatic Compounds. Part I. The Resolution of γ-6 : 6′-Dinitro- and 4 : 6 : 4′ : 6′-Tetranitro-Diphenic Acids into Optically Active Components. *J. Chem. Soc. Trans.* **1922**, *121*, 614–620.

(4) Kuhn, R.; Albrecht, O. Über Ringneigung Beim A-Dinaphtyl. Zur Stereochemie Aromatischer Verbindungen. VII. *Justus Liebigs Ann. Chem.* **1928**, *465* (1), 282–287. https://doi.org/10.1002/jlac.19284650115.

(5) Stanley, W. M. Stereochemistry of Diphenyl Compounds. The Resolution of 8,8-Dicarboxy-1,1-Dinapthyl. *J. Am. Chem. Soc.* **1931**, *53* (1921), 1262–1267.

(6) Bock, L. H.; Adamsthe, R. The Stereochemistry of N-Phenylpyrroles. The Preparation and Resolution of N-2-Carboxyphenyl-2,5-Dimethyl-3-Carboxypyrrole. XIII. *J. Am. Chem. Soc.* **1931**, *53* (1), 374–376. https://doi.org/10.1021/ja01352a055.

(7) Bock, L. H.; Adams, R. Stereochemistry of Phenyl Pyrroles. XIX. *J. Am. Chem. Soc.* **1931**, *53* (9), 3519–3522. https://doi.org/10.1021/ja01360a047.

(8) Kumarasamy, E.; Raghunathan, R.; Sibi, M. P.; Sivaguru, J. Nonbiaryl and Heterobiaryl Atropisomers: Molecular Templates with Promise for Atropselective Chemical Transformations. *Chem. Rev.* **2015**, *115* (20), 11239–11300. https://doi.org/10.1021/acs.chemrev.5b00136.

(9) Bonne, D.; Rodriguez, J. A Bird's Eye View of Atropisomers Featuring a Five-Membered. *European J. Org. Chem.* **2018**, No. 20–21, 2417–2431. https://doi.org/10.1002/ejoc.201800078.

(10) Bott, G.; Field, L. D.; Sternhell, S. Steric Effects. A Study of a Rationally Designed System. *J. Am. Chem. Soc.* **1980**, *102* (17), 5618–5626. https://doi.org/10.1021/ja00537a036.

(11) Hainke, S.; Seitz, O. Binaphthyl-DNA: Stacking and Fluorescence of a Nonplanar Aromatic Base Surrogate in DNA. *Angew. Chemie - Int. Ed.* **2009**, *48* (44), 8250–8253. https://doi.org/10.1002/anie.200903194.

(12) Cooke, A. S.; Harris, M. M. Ground-State Strain and Other Factors Infuencing Optical Stability in the 1,1′-Binapthyl Series. *J. Chem. Soc.* **1963**, 2365–2373.

(13) Baker, R. W.; Brkic, Z.; Sargent, M. V; Skelton, B. W.; White, A. H. Atropoisomerism of 2,2′-Binapthalenes. *Aust. J. Chem.* **2000**, *53*, 925–938.

(14) Meyers, A. I.; Himmelsbach, R. J. Enantioselective Synthesis of 2,2',6-Trisubstituted Biphenyls. *J. Am. Chem. Soc.* **1985**, *107* (3), 682–685. https://doi.org/10.1021/ja00289a023.

(15) Meca, L.; Reha, D.; Havlas, Z. Racemization Barriers of 1,1′-Binaphthyl and 1,1′-Binaphthalene-2,2′-Diol: A DFT Study. *J. Org. Chem.* **2003**, *68* (14), 5677–5680. https://doi.org/10.1021/jo034344u.

(16) Gladiali, S.; Dore, A.; Fabbri, D.; de Lucchi, O.; Valle, G. Synthesis, Crystal Structure, Dynamic Behavior and Reactivity of Dinaphtho[2,1-b:1′,2′-d]Phospholes and Related Atropisomeric Phosphacyclic Derivatives. *J. Org. Chem.* **1994**, *59* (21), 6363–6371. https://doi.org/10.1021/jo00100a044.

(17) Bringmann, G.; Hartung, T.; Gobel, L.; Schupp, O.; Ewers, C. L. J.; Schoner, B.; Zagst, R.; Peters, K.; Schneringb, H. G. Von; Burschka, C. Synthesis and Structure of Benzonaphthopyranones, Useful Bridged Model Precursors for Stereoselective Biaryl Syntheses. *Liebigs Ann. der Chemie* **1992**, No. 4, 225–232.

(18) Hatsuda, M.; Hiramatsu, H.; Yamada, S. I.; Shimizu, T.; Seki, M. A Novel and Facile Racemization of Chiral 1,1′-Biaryl-2,2′-Dicarboxylic Acids. *J. Org. Chem.* **2001**, *66* (12), 4437–4439. https://doi.org/10.1021/jo0101196.

(19) Kannan, R.; Williams, D. H. Stereochemistry of the Cyclic Tripeptide Antibiotic WS-43708A. *J. Org. Chem.* **1987**, *52* (24), 5435–5437. https://doi.org/10.1021/jo00233a024.

(20) Brown, F. K.; Hempel, J. C.; Dixon, J. S.; Amato, S.; Mueller, L.; Jeffs, P. W. Structure of Biphenomycin A Derived from Two-Dimensional NMR Spectroscopy and Molecular Modeling. *J. Am. Chem. Soc.* **1989**, *111* (19), 7328–7333. https://doi.org/10.1021/ja00201a008.

(21) Dial, B. E.; Pellechia, P. J.; Smith, M. D.; Shimizu, K. D. Proton Grease: An Acid Accelerated Molecular Rotor. *J. Am. Chem. Soc.* **2012**, *134* (8), 3675–3678. https://doi.org/10.1021/ja2120184.

(22) Kyba, E. P.; Gokel, G. W.; Jong, F. De; Koga, K.; Sousa, L. R.; Siegel, M. G.; Kaplan, L.; Sogah, G. D. Y.; Cram, D. J. Host-Guest Complexation. 7. The Binaphthyl Structural Unit in Host Compounds. *J. Org. Chem.* **1977**, *42* (26), 4173–4184. https://doi.org/10.1021/jo00862a001.

(23) Lin, Y. L.; Lin, T. C.; Kuo, Y. H. Two Acetophenone Glucosides, Cynanonesides A and B, from Cynanchum Taiwanianum and Revision of the Structure for Cynandione A. *J. Nat. Prod.* **1997**, *60* (4), 368–370. https://doi.org/10.1021/np960256b.

(24) Bringmann, G.; Hartung, T. Novel Concepts in Directed Biaryl Synthesis, XXXVII. Synthesis and Enantiomerization of a Nonracemic 2-hydroxy-2′-biarylcarbaldehyde, a Probable Intermediate in the Atropo-enantioselective Ring Opening of Biaryl Lactones. *Liebigs Ann. der Chemie* **1994**, *1994* (3), 313–316. https://doi.org/10.1002/jlac.199419940314.

(25) Pummerer, R.; Prell, E.; Rieche, A. Darstellung von Binapthylendioxyd. *Berichte der Dtsch. Chem. Gesellschaft* **1926**, *797*, 2159–2161.

(26) Jacques, J.; Fouquey, C.; Viterbo, R. Enantiomeric Cyclic Binaphthyl Phosphoric Acids as Resolving Agents. *Tetrahedron Lett.* **1971**, *12* (48), 4617–4620. https://doi.org/10.1016/S0040-4039(01)97544-6.

(27) Tamai, Y.; Cho-Heung, P.; Iizuka, K.; Akamura, A.; Miyano, S. A Practical Method for Resolution of the Optical Isomers of 2,2′Dihydroxy-1,1′-Binapthalene. *Synthesis (Stuttg).* **1990**, 222.

(28) Brussee, J.; Jansen, A. C. A. A Highly Stereoselective Synthesis of s(-)-[1,1′-Binaphthalene]-2,2′-Diol. *Tetrahedron Lett.* **1983**, *24* (31), 3261–3262. https://doi.org/10.1016/S0040-4039(00)88151-4.

(29) Brussee, J.; Jansen, A. C. A.; te Koppele, J. M.; Gronenendijk, J. L. . On the Mechanism of the Formation of S(-)-(1,1′-Binapthalene)-2,2′-Diol via Copper(II) Amine Complexes. *Tetrahedron* **1985**, *41* (13), 3313–3319. https://doi.org/10.1016/S0040-4020(01)96682-7.

(30) Smrčina, M.; Poláková, J.; Vyskočil, Š.; Kočovský, P. Synthesis of Enantiomerically Pure Binaphthyl Derivatives. Mechanism of the Enantioselective, Oxidative Coupling of Naphthols and Designing a Catalytic Cycle. *J. Org. Chem.* **1993**, *58* (17), 4534–4538. https://doi.org/10.1021/jo00069a010.

(31) Brunel, J. M. BINOL: A Versatile Chiral Reagent. *Chem. Rev.* **2005**, *105*, 857–897. https://doi.org/10.1055/s-2006-956459.

(32) Hayashi, T.; Hayashizaki, K.; Kiyoi, T.; Ito, Y. Asymmetric Synthesis Catalyzed by Chiral Ferrocenylphosphine-Transition-Metal Complexes. 6. Practical Asymmetric Synthesis of 1,1'-Binaphthyls via Asymmetric Cross-Coupling with a Chiral [(Alkoxyalkyl)Ferrocenyl]Monophosphine/Nickel Catalyst. *J. Am. Chem. Soc.* **1988**, *110* (24), 8153–8156. https://doi.org/10.1021/ja00232a030.

(33) Terfort, A.; Brunner, H. Phosphane Ligands with Two Binding Sites of Differing Hardness for Enantioselective

Grignard Cross Coupling. *J. Chem. Soc. Perkin Trans. 1 Org. Bio-Organic Chem.* **1996**, 1467–1479.

(34) Dahlenburg, L.; Kurth, V. Chiral Bisphosphanes - Part XIII. Nickel, Palladium and Platinum Complexes Containing Optically Active Cyclopentane-Based P2 Ligands with Phosphorinane and Dicyclohexylphosphanyl Donor Functions. *Inorganica Chim. Acta* **2001**, *319* (1–2), 176–182. https://doi.org/10.1016/S0020-1693(01)00451-0.

(35) Cammidge, A. N.; Crépy, K. V. L. The First Asymmetric Suzuki Cross-Coupling Reaction. *Chem. Commun.* **2000**, No. 18, 1723–1724. https://doi.org/10.1039/b004513f.

(36) Yin, J.; Buchwald, S. L. A Catalytic Asymmetric Suzuki Coupling for the Synthesis of Axially Chiral Biaryl Compounds [29]. *J. Am. Chem. Soc.* **2000**, *122* (48), 12051–12052. https://doi.org/10.1021/ja005622z.

(37) Miyano, S.; Tobita, M.; Suzuki, S.; Nishikawa, Y.; Hashimoto, H. Partial Asymmetric Synthesis of Atropisomeric 1,1′-Binaphthyls Via the Ullmann Coupling Reaction of Chiral Alcohol Esters of 1-Bromo-2-Naphthoic Acid. *Chem. Lett.* **1980**, *9* (8), 1027–1030. https://doi.org/10.1246/cl.1980.1027.

(38) Meyers, A. I.; Nelson, T. D.; Moorlag, H.; Rawson, D. J.; Meier, A. Chiral Oxazoline Route to Enantiomerically Pure Biphenyls: Magnesio and Copper Mediated Asymmetric Hetero- and Homo-Coupling Reactions. *Tetrahedron* **2004**, *60* (20), 4459–4473. https://doi.org/10.1016/j.tet.2004.01.095.

(39) Meyers, A. I.; Meier, A.; Rawson, D. J. A Highly Stereoselective Synthesis of Axially Chiral Biaryls. Application to the Synthesis of a Potential Chiral Catalysts. *Tetrahedron Lett.* **1992**, *33* (7), 853–856. https://doi.org/10.1016/S0040-4039(00)91558-2.

(40) Ager, D. J.; Prakash, I.; Schaad, D. R. 1,2-Amino Alcohols and Their Heterocyclic Derivatives as Chiral Auxiliaries in Asymmetric Synthesis. *Chem. Rev.* **1996**, *96* (2), 835–876. https://doi.org/10.1021/cr9500038.

(41) Desimoni, G.; Faita, G.; Jørgensen, K. A. Update 1 of: C 2 -Symmetric Chiral Bis(Oxazoline) Ligands in Asymmetric Catalysis. *Chem. Rev.* **2011**, *111* (11), 284–437. https://doi.org/10.1021/cr100339a.

(42) Rae, J.; Frey, J.; Jerhaoui, S.; Choppin, S.; Wencel-Delord, J.; Colobert, F. Synthesis of Axially Chiral C-N Scaffolds via Asymmetric Coupling with Enantiopure Sulfinyl Iodanes. *ACS Catal.* **2018**, *8* (4), 2805–2809. https://doi.org/10.1021/acscatal.7b04343.

(43) Li, H.; Yan, X.; Zhang, J.; Guo, W.; Jiang, J.; Wang, J. Enantioselective Synthesis of C−N Axially Chiral N-Aryloxindoles by Asymmetric Rhodium-Catalyzed Dual C−H Activation. *Angew. Chemie - Int. Ed.* **2019**, *58* (20), 6732–6736. https://doi.org/10.1002/anie.201901619.

(44) Zhang, J.; Xu, Q.; Wu, J.; Fan, J.; Xie, M. Construction of N–C Axial Chirality through Atroposelective C–H Olefination of *N* -Arylindoles by Palladium/Amino Acid Cooperative Catalysis. *Org. Lett.* **2019**, acs.orglett.9b02243. https://doi.org/10.1021/acs.orglett.9b02243.

(45) Kwon, Y.; Chinn, A. J.; Kim, B.; Miller, S. J. Divergent Control of Point and Axial Stereogenicity: Catalytic Enantioselective C−N Bond-Forming Cross-Coupling and Catalyst-Controlled Atroposelective Cyclodehydration. *Angew. Chemie - Int. Ed.* **2018**, *57* (21), 6251–6255. https://doi.org/10.1002/anie.201802963.

(46) Kwon, Y.; Li, J.; Reid, J. P.; Crawford, J. M.; Jacob, R.; Sigman, M. S.; Toste, F. D.; Miller, S. J. Disparate Catalytic Scaffolds for Atroposelective Cyclodehydration. *J. Am. Chem. Soc.* **2019**, *141*, 6698–6705. https://doi.org/10.1021/jacs.9b01911.

(47) Bai, H. Y.; Tan, F. X.; Liu, T. Q.; Zhu, G. D.; Tian, J. M.; Ding, T. M.; Chen, Z. M.; Zhang, S. Y. Highly Atroposelective Synthesis of Nonbiaryl Naphthalene-1,2-Diamine N-C Atropisomers through Direct Enantioselective C-H Amination. *Nat. Commun.* **2019**, *10* (1), 1–9. https://doi.org/10.1038/s41467-019-10858-x.

(48) Yang, G. H.; Zheng, H.; Li, X.; Cheng, J. P. Asymmetric Synthesis of Axially Chiral Phosphamides via Atroposelective N-Allylic Alkylation. *ACS Catal.* **2020**, *10* (3), 2324–2333. https://doi.org/10.1021/acscatal.9b05443.

(49) Miyano, S.; Tobita, M.; Hashimoto, H. Asymmetric Synthesis of Axially Dissymmetric 1,1´-Binaphyls via an Intramoleclar Ullmann Couplling Reactio of (R) and (S)-2,2´-Bis(1-Bbromo-2-Napthylcabonyloxy)-1,1´-Binaptyl. *Bull. Chem. Soc. Jpn.* 1981, pp 3522–3526.

(50) Miyano, S.; Handa, S.; Shimizu, K.; Tagami, K.; Hashimoto, H. The Asymmetric Ullmann Coupling Reaction of Chiral Diol Esters. *Bulletin of the Chemical Society of Japan*. 1984, pp 1943–1947.

(51) Lipshutz, B. H.; Siegmann, K.; Garcia, E.; Kayser, F. Synthesis of Unsymmetrical Biaryls via "Kinetic" Higher Order Cyanocuprates: Scope, Limitations, and Spectroscopic Insights. *J. Am. Chem. Soc.* **1993**, *115* (20), 9276–9282. https://doi.org/10.1021/ja00073a051.

(52) Lipshutz, B. H.; Kayser, F.; Zi-Ping, L. Asymmeric Synthesis of Biaryls by Intraolecular Oxidative Couplings of Cyanocuprate Intermediates. *Angew. Chemie - Int. Ed.* **1994**, *60* (1), 6–8.

(53) Lin, G. Q.; Zhong, M. The First Asymmetric Synthesis of the Naturally Occurring (+)-Kotanin and the Assignment of Its Absolute Configuration. *Tetrahedron Asymmetry* **1997**, *8* (9), 1369–1372. https://doi.org/10.1016/S0957-4166(97)00117-1.

(54) Michaud, G.; Bulliard, M.; Ricard, L.; Genêt, J. P.; Marinetti, A. A Strategy for the Stereoselective Synthesis of Unsymmetric Atropisomeric Ligands: Preparation of NAPhePHOS, a New Biaryl Diphosphine. *Chem. - A Eur. J.* **2002**, *8* (15), 3327–3330. https://doi.org/10.1002/1521-3765(20020802)8:15<3327::AID-CHEM3327>3.0.CO;2-F.

(55) Bringmann, G.; Breuning, M.; Walter, R.; Wuzik, A.; Peters, K.; Peters, E.-M. Synthesis of Axially Chiral Biaryls by Atropo-Diastereoselective Cleavage of Configurationally Unstable Biaryl Lactones with Menthol-Derived O-Nucleophiles. *European J. Org. Chem.* **1999**, No. 11, 3047–3055. https://doi.org/https://doi.org/10.1002/(SICI)1099-0690(199911)1999:11<3047::AID-EJOC3047>3.0.CO;2-O.

(56) Bringmann, G.; Breuning, M.; Tasler, S.; Endress, H.; Ewers, C. L. J.; Göbel, L.; Peters, K.; Peters, E. M. Atropo-Diastereoselective Cleavage of Configurationally Unstable Biaryl Lactones with Alkali Metal Activated Primary 1-Arylethylamines. *Chem. - A Eur. J.* **1999**, *5* (10), 3029–3038. https://doi.org/10.1002/(SICI)1521-3765(19991001)5:10<3029::AID-CHEM3029>3.0.CO;2-5.

(57) Bringmann, G.; Breuning, M. Atropo-Enantioselective Reduction of Configurationally Unstable Biaryl Lactones with BINAL-H1. *Tetrahedron Asymmetry* **1999**, *10* (2), 385–390. https://doi.org/10.1016/S0957-4166(98)00503-5.

(58) Bringmann, G.; Breuning, M.; Henschel, P.; Hinrichs, J. Asymmetric Synthesis of (M)-2-Hydroxymethyl-1-(2-Hydroxy-4,6-Dimethylphenyl)Naphthalene Via a Configurationally Unstable Biaryl Lactone. *Org. Synth.* **2002**, *79* (September), 72. https://doi.org/10.15227/orgsyn.079.0072.

(59) Bringmann, G.; Hurtung, T. First Atropo-Enantioselective Ring Opening from Borane. *Angew. Chemie - Int. Ed.* **1992**, *31* (6), 761–762.

(60) Pesch, J.; Harms, K.; Bach, T. Preparation of Axially Chiral N,N???-Diarylimidazolium and N-Arylthiazolium Salts and Evaluation of Their Catalytic Potential in the Benzoin and in the Intramolecular Stetter Reactions. *European J. Org. Chem.* **2004**, No. 9, 2025–2035. https://doi.org/10.1002/ejoc.200300762.

(61) Stephens, P. J.; Devlin, F. J.; Pan, J.-J. The Determination of the Absolute Configurations of Chiral Molecules Using Vibrational Circular Dichroism (VCD) Spectroscopy. *Chirality* **2008**, *20*, 643–663.

(62) Brummel, B. R.; Lee, K. G.; McMillen, C. D.; Kolis, J. W.; Whitehead, D. C. One-Pot Absolute Stereochemical Identification of Alcohols via Guanidinium Sulfate Crystallization. *Org. Lett.* **2019**, *21* (23), 9622–9627. https://doi.org/10.1021/acs.orglett.9b03792.

(63) Rychkov, D. A.; Arkhipov, S. G.; Boldyreva, E. V. Simple and Efficient Modifications of Well Known Techniques for Reliable Growth of High-Quality Crystals of Small Bioorganic Molecules. *J. Appl. Crystallogr.* **2014**, *47* (4), 1435–1442. https://doi.org/10.1107/S1600576714011273.

(64) Spingler, B.; Schnidrig, S.; Todorova, T.; Wild, F. Some Thoughts about the Single Crystal Growth of Small Molecules. *CrystEngComm* **2012**, *14* (3), 751–757. https://doi.org/10.1039/c1ce05624g.

(65) Hoshino, M.; Khutia, A.; Xing, H.; Inokuma, Y.; Fujita, M. The Crystalline Sponge Method Updated. *IUCrJ* **2016**, *3*, 139–151. https://doi.org/10.1107/S2052252515024379.

(66) Seco, J. M.; Quiñoá, E.; Riguera, R. The Assignment of Absolute Configuration by NMR. *Chem. Rev.* **2004**, *104* (1), 17–117.

(67) Latypov, S. K.; Seco, J. M.; Quinoa, E.; Riguera, R. Are Both the (R)- and the (S)-MPA Esters Really Needed for the Assignment of the Absolute Configuration of Secondary Alcohols by NMR? The Use of a Single Derivative. *J. Am. Chem. Soc.* **1998**, *120* (5), 877–882. https://doi.org/10.1021/ja9700055.

(68) Latypov, S. K.; Seco, J. M.; Quiñoá, E.; Riguera, R. MTPA vs MPA in the Determination of the Absolute Configuration of Chiral Alcohols by 1H NMR. *J. Org. Chem.* **1996**, *61* (24), 8569–8577. https://doi.org/10.1021/jo960719i.

(69) Ferreiro, M. J.; Latypov, S. K.; Quiñoá, E.; Riguera, R. Determination of the Absolute Configuration and Enantiomeric Purity of Chiral Primary Alcohols by 1H NMR of 9-Anthrylmethoxyaceates. *Tetrahedron Asymmetry* **1996**, *7* (8), 2195–2198. https://doi.org/10.1063/1.1654326.

(70) Seco, J. M.; Quiñoá, E.; Riguera, R. Boc-Phenylglycine : The Reagent of Choice for the Assignment of the Absolute Configuration of α -Chiral Primary Amines by 1 H NMR Spectroscopy. *J. Org. Chem.* **1999**, *64* (13), 4669–4675.

(71) Latypov, S. K.; Ferreiro, M. J.; Quiñoá, E.; Riguera, R. Assignment of the Absolute Configuration of β-Chiral Primary Alcohols by NMR: Scope and Limitations. *J. Am. Chem. Soc.* **1998**, *120* (19), 4741–4751. https://doi.org/10.1021/ja972550b.

(72) Hoye, T. R.; Renner, M. K. MTPA (Mosher) Amides of Cyclic Secondary Amines : Conformational Aspects and a Useful Method for Assignment of Amine Configuration. *J. Org. Chem.* **1996**, *61* (7), 2056–2064. https://doi.org/10.1021/jo952043h.

(73) Hoye, T. R.; Renner, M. K. Applications of MTPA (Mosher) Amides of Secondary Amines : Assignment of Absolute Configuration in Chiral Cyclic Amines. *J. Org. Chem.* **1996**, *61* (7), 8489–8495. https://doi.org/10.1021/jo960373b.

(74) Izumi, S.; Moriyoshi, H.; Hirata, T. Identification of Absolute Configuration of Tertiary Alcohols by Comination of Mosher´s Method and Conformational Analysis. *Bull. Chem. Soc. Jpn.* **1994**, *67* (9), 2600–2602.

(75) Takahashi, H.; Kato, N.; Iwashima, M.; Ihuchi, K. Determination of Absolute Configurations of Tertiary Alcohols by NMR Spectroscopy. *Chem. Lett.* **1999**, *28* (11), 1181–1182.

(76) Porto, S.; Seco, J. M.; Ortiz, A.; Quiñoá, E.; Riguera, R. Chiral Thiols: The Assignment of Their Absolute Configuration by 1H NMR. *Org. Lett.* **2007**, *9* (24), 5015–5018. https://doi.org/10.1021/ol7022196.

(77) Louzao, I.; Seco, J. M.; Quiñoá, E.; Riguera, R. The Assignment of Absolute Configuration of Cyanohydrins by NMR. *Chem. Commun.* **2006**, No. 13, 1422–1424. https://doi.org/10.1039/b517917c.

(78) Louzao, I.; García, R.; Seco, J. M.; Quiñoá, E.; Riguera, R. Absolute Configuration of Ketone Cyanohydrins by 1H NMR: The Special Case of Polar Substituted Tertiary Alcohols. *Org. Lett.* **2009**, *11* (1), 53–56. https://doi.org/10.1021/ol8023314.

(79) Louzao, I.; Seco, J. M.; Quiñoá, E.; Riguera, R. The Use of a Single Derivative in the Configurational Assignment of Ketone Cyanohydrins. *European J. Org. Chem.* **2010**, No. 34, 6520–6524. https://doi.org/10.1002/ejoc.201001107.

(80) Leiro, V.; Freire, F.; Quiñoá, E.; Riguera, R. Absolute Configuration of Amino Alcohols by 1H-NMR. *Chem. Commun.* **2005**, *1* (44), 5554–5556. https://doi.org/10.1039/b510806c.

(81) Leiro, V.; Seco, J. M.; Quiñoá, E.; Riguera, R. Cross Interaction between Auxiliaries: The Chirality of Amino Alcohols by NMR. *Org. Lett.* **2008**, *10* (13), 2729–2732. https://doi.org/10.1021/ol8008528.

(82) Dale, J. A.; Dull, D. L.; Mosher, H. S. α-Methoxy-α-Trifluoromethylphenylacetic Acid, a Versatile Reagent for the Determination of Enantiomeric Composition of Alcohols and Amines'. *J. Org. Chem.* **1969**, *34* (9), 2543–2549.

(83) Sullivan, G. R.; Dale, J. A.; Mosher, H. S. Correlation of Configuration and 19F Chemical Shifts of α -Methoxy-α -Trifluoromethylphenylacetate Derivatives. *J. Org. Chem.* **1973**, *38* (12), 2143–2147. https://doi.org/10.1021/jo00952a006.

(84) Dale, J. A.; Mosher, H. S. Nuclear Magnetic Resonance Enantiomer Reagents. Configurational Correlations via Nuclear Magnetic Resonance Chemical Shifts of Diastereomeric Mandelate, O-Methylmandelate and α-Methoxy-α-Trifluormethylphenylacetate (MTPA) Esters. *J. Am. Chem. Soc.* **1973**, *95* (2), 512–519.

(85) Seco, J. M.; Quiñoá, E.; Riguera, R. The Assignment of Absolute Configuration by NMR. *Chem. Rev.* **2004**, *104* (1), 17–117. https://doi.org/10.1021/cr000665j.

(86) Ohtani, I.; Kusumi, T.; Kashman, Y.; Kakisawa, H. High-Field FT NMR Application of Mosher's Method. The Absolute Configurations of Marine Terpenoids. *J. Am. Chem. Soc.* **1991**, *113* (11), 4092–4096. https://doi.org/10.1021/ja00011a006.

(87) Seco, M.; Quiñoá, E.; Riguera, R.; Louzao, I. 13C NMR as a General Tool for the Assignment of Absolute Configuration. *Chem. Commun.* **2010**, *46*, 7903–7905. https://doi.org/10.1039/c0cc02774j.

(88) Trost, B. M.; Bunt, R. C.; Pulley, S. R. On the Use of O-Methylmandelic Acid for the Establishment of Absolute Configuration of α-Chiral Primary Amines. *J. Org. Chem.* **1994**, *59* (10), 4202–4205.

(89) Latypov, S. K.; Seco, J. M.; Quiñoá, E.; Riguera, R. Conformational Structure and Dynamics of Arylmethoxyacetates: DNMR Spectroscopy and Aromatic Shielding Effect. *J. Org. Chem.* **1995**, *60* (3), 504–515. https://doi.org/10.1021/jo00108a008.

(90) Chataigner, I.; Lebreton, J.; Durand, D.; Guingant, A.; Villiéras, J. A New Approach for the Determination of the Absolute Configuration of Secondary Alcohols by 1H NMR with O-Substituted Mandelate Derivatives. *Tetrahedron Lett.* **1998**, *39* (13), 1759–1762. https://doi.org/10.1016/S0040-4039(98)00059-8.

(91) Seco, J. M.; Latypov, S. K.; Quiñoá, E.; Riguera, R. Determining Factors in the Assignment of the Absolute Configuration of Alcohols by NMR . The Use of Anisotropic Effects on Remote Positions. *Tetrahedron* **1997**, *53* (25), 8541–8564.

(92) Freire, F.; Seco, J. M.; Quiñoá, E.; Riguera, R. Challenging the Absence of Observable Hydrogens in the Assignment of Absolute Configurations by NMR: Application to Chiral Primary Alcohols. *Chem. Commun.* **2007**, *1*

(14), 1456–1458. https://doi.org/10.1039/b617184b.

(93) Twibanire, J. D. A. K.; Grindley, T. B. Efficient and Controllably Selective Preparation of Esters Using Uronium-Based Coupling Agents. *Org. Lett.* **2011**, *13* (12), 2988–2991. https://doi.org/10.1021/ol201005s.

(94) Kobayashi, M. The Fucofuranoside Method for Determining the Absolute Configuration of the Tertiary Alcohols Substituted with Methyl and Two Methylene Groups. *Tetrahedron* **1998**, *54* (37), 10987–10998. https://doi.org/10.1016/S0040-4020(98)00645-0.

(95) Latypov, S. K.; Seco, J. M.; Quiñoá, E.; Riguera, R. Determination of the Absolute Stereochemistry of Chiral Amines by 1H NMR of Arylmethoxyacetic Acid Amides: The Conformational Model. *J. Org. Chem.* **1995**, *60* (6), 1538–1545. https://doi.org/10.1021/jo00111a011.

(96) Seco, J. M.; Quiñoá, E.; Riguera, R. Assignment of the Absolute Configuration of Polyfunctional Compounds by NMR Using Chiral Derivatizing Agents. *Chem. Rev.* **2012**, *112* (8), 4603–4641. https://doi.org/10.1021/cr2003344.

(97) Wang, F.; Cheng, X. L.; Li, Y. J.; Shi, S.; Liu, J. K. Ent-Pimarane Diterpenoids from Siegesbeckia Orientalis and Structure Revision of a Related Compound. *J. Nat. Prod.* **2009**, *72* (11), 2005–2008. https://doi.org/10.1021/np900449r.

(98) Zhang, Y.; Nakamura, S.; Pongpiriyadacha, Y.; Matsuda, H.; Yoshikawa, M. Absolute Structures of New Megastigmane Glycosides, Foliasalaciosides E1, E2, E3, F, G, H, and I from the Leaves of Salacia Chinensis. *Chem. Pharm. Bull.* **2008**, *56* (4), 547–553. https://doi.org/10.1248/cpb.56.547.

(99) Seco, J. M.; Quiñoá, E.; Riguera, R. Assignment of the Absolute Configuration of Polyfunctional Compounds by NMR Using Chiral Derivatizing Agents. *Chem. Rev.* **2012**, *112* (8), 4603–4641. https://doi.org/10.1021/cr2003344.

(100) Orlov, N. V; Ananikov, V. P. NMR Analysis of Chiral Alcohols and Amines: Development of an Enviromentaly Benign “in Tube” Procedure with High Efficiency and Improved Detection Limit. *Green Chem.* **2011**, *13* (7), 1735–1744.

(101) Porto, S.; Seco, J. M.; Espinosa, J. F.; Quiñoá, E.; Riguera, R. Resin-Bound Chiral Derivatizing Agents for Assignment of Configuration by NMR Spectroscopy. *J. Org. Chem.* **2008**, *73* (15), 5714–5722. https://doi.org/10.1021/jo800469c.

(102) Hawkins, J. M.; Watson, T. J. N. Asymmetric Catalysis in the Pharmaceutical Industry. *Angew. Chemie Int. Ed.* **2004**, *43* (25), 3224–3228. https://doi.org/10.1002/anie.200330072.

(103) Farina, V.; Reeves, J. T.; Senanayake, C. H.; Song, J. J. Asymmetric Synthesis of Active Pharmaceutical Ingredients. *Chem. Rev.* **2006**, *106* (7), 2734–2793. https://doi.org/10.1021/cr040700c.

(104) Noyori, R.; Hashiguchi, S. Asymmetric Transfer Hydrogenation Catalyzed by Chiral Ruthenium Complexes. *Acc. Chem. Res.* **1997**, *30* (2), 97–102. https://doi.org/10.1021/ar9502341.

(105) Ikariya, T.; Blacker, A. J. Asymmetric Transfer Hydrogenation of Ketones with Bifunctional Transition Metal-Based Molecular Catalysts. *Acc. Chem. Res.* **2007**, *40* (12), 1300–1308. https://doi.org/10.1021/ar700134q.

(106) Rossi, S.; Benaglia, M.; Massolo, E.; Raimondi, L. Organocatalytic Strategies for Enantioselective Metal-Free Reductions. *Catal. Sci. Technol.* **2014**, *4* (9), 2708–2723. https://doi.org/10.1039/c4cy00033a.

(107) Herrera, R. P. Organocatalytic Transfer Hydrogenation and Hydrosilylation Reactions. *Top. Curr. Chem.* **2016**, *374* (3), 1–40. https://doi.org/10.1007/s41061-016-0032-4.

(108) Denmark, S. E.; Fu, J. Catalytic Enantioselective Addition of Allylic Organometallic Reagents to Aldehydes and Ketones. *Chem. Rev.* **2003**, *103* (8), 2763–2793. https://doi.org/10.1021/cr020050h.

(109) Benkeser, R. A.; Smith, W. E. A New Method of Forming the Carbon-Silicon Bond. Reductive Silylation of Carbonyl Compounds. *J. Am. Chem. Soc.* **1969**, *91* (6), 1556–1557. https://doi.org/10.1021/ja01034a061.

(110) Fujita, M.; Hiyama, T. Fluoride Ion Catalyzed Reduction of Aldehydes and Ketones with Hydrosilanes. Synthetic and Mechanistic Aspects and an Application to the Threo-Directed Reduction of a-Substituted Alkanones. *J. Org. Chem.* **1988**, *53* (d), 5405–5415.

(111) Kobayashi, S.; Yasuda, M.; Hachiya, I. Trichlorosilane-Dimethylformamide (Cl3SiH-DMF) as an Efficient Reducing Agent. Reduction of Aldehydes and Imines and Reductive Amination of Aldehydes under Mild Conditions Using Hypervalent Hydridosilicates. *Chemistry Letters*. 1996, pp 407–408. https://doi.org/10.1246/cl.1996.407.

(112) Iseki, K.; Mizuno, S.; Kuroki, Y.; Kobayashi, Y. A Chiral Formamide: Design and Application to Catalytic Asymmetric Synthesis. *Tetrahedron Lett.* **1998**, *39* (18), 2767–2770. https://doi.org/10.1016/S0040-4039(98)00334-7.

(113) Denmark, S. E.; Coe, D. M.; Pratt, N. E.; Griedel, B. D. Asymmetric Allylation of Aldehydes with Chiral Lewis Bases. *J. Org. Chem.* **1994**, *59* (21), 6161–6163. https://doi.org/10.1021/jo00100a013.

(114) Verdaguer, X.; Lange, U. E. W.; Reding, M. T.; Buchwald, S. L. Highly Enantioselective Imine Hydrosilylation Using (S,S)-Ethylenebis(H5-Tetrahydroindenyl)Titanium Difluoride. *J. Am. Chem. Soc.* **1996**, *118* (28), 6784–6785. https://doi.org/10.1021/ja960808c.

(115) Reding, M. T.; Buchwald, S. L. Short Enantioselective Total Syntheses of the Piperidine Alkaloids (S)-Coniine and (2R,6R)-Trans-Solenopsin A via Catalytic Asymmetric Imine Hydrosilylation. *J. Org. Chem.* **1998**, *63* (18), 6344–6347. https://doi.org/10.1021/jo980808q.

(116) Lipshutz, B. H.; Shimizu, H. Copper(I)-Catalyzed Asymmetric Hydrosilylations of Imines at Ambient Temperatures. *Angew. Chemie - Int. Ed.* **2004**, *43* (17), 2228–2230. https://doi.org/10.1002/anie.200353294.

(117) Iwasaki, F.; Onomura, O.; Mishima, K.; Maki, T.; Matsumura, Y. Catalytic Activation of Trichlorosilane for Efficient and Stereoselective Reduction of Ketones. *Tetrahedron Lett.* **1999**, *40* (42), 7507–7511. https://doi.org/10.1016/S0040-4039(99)01554-3.

(118) Iwasaki, F.; Onomura, O.; Mishima, K.; Kanematsu, T.; Maki, T.; Matsumura, Y. First Chemo- and Stereoselective Reduction of Imines Using Trichlorosilane Activated with N-Formylpyrrolidine Derivatives. *Tetrahedron Lett.* **2001**, *42* (13), 2525–2527. https://doi.org/10.1016/S0040-4039(01)00219-2.

(119) Malkov, A. V.; Mariani, A.; MacDougall, K. N.; Kočovský, P. Role of Noncovalent Interactions in the Enantioselective Reduction of Aromatic Ketimines with Trichlorosilane. *Org. Lett.* **2004**, *6* (13), 2253–2256. https://doi.org/10.1021/ol049213+.

(120) Malkov, A. V.; Stončius, S.; MacDougall, K. N.; Mariani, A.; McGeoch, G. D.; Kočovský, P. Formamides Derived from N-Methyl Amino Acids Serve as New Chiral Organocatalysts in the Enantioselective Reduction of Aromatic Ketimines with Trichlorosilane. *Tetrahedron* **2006**, *62* (2–3), 264–284. https://doi.org/10.1016/j.tet.2005.08.117.

(121) Malkov, A. V.; Stončius, S.; Kočovský, P. Enantioselective Synthesis of 1,2-Diarylaziridines by the Organocatalytic Reductive Amination of α-Chloroketones. *Angew. Chemie - Int. Ed.* **2007**, *46* (20), 3722–3724. https://doi.org/10.1002/anie.200700165.

(122) Malkov, A. V.; Vranková, K.; Stončius, S.; Kočovský, P. Asymmetric Reduction of Imines with Trichlorosilane, Catalyzed by Sigamide, an Amino Acid-Derived Formamide: Scope and Limitations. *J. Org. Chem.* **2009**, *74* (16), 5839–5849. https://doi.org/10.1021/jo900561h.

(123) Malkov, A. V.; Figlus, M.; Stončius, S.; Kočovský, P. Organocatalysis with a Fluorous Tag: Asymmetric Reduction of Imines with Trichlorosilane Catalyzed by Amino Acid-Derived Formamides. *J. Org. Chem.* **2007**, *72* (4), 1315–1325. https://doi.org/10.1021/jo062215i.

(124) Malkov, A. V.; Figlus, M.; Kočovský, P. Polymer-Supported Organocatalysts: Asymmetric Reduction of Imines with Trichlorosilane Catalyzed by an Amino Acid-Derived Formamide Anchored to a Polymer. *J. Org. Chem.* **2008**, *73* (11), 3985–3995. https://doi.org/10.1021/jo800094q.

(125) Malkov, A. V.; Stewart Liddon, A. J. P.; Ramírez-López, P.; Bendová, L.; Haigh, D.; Kočovský, P. Remote Chiral Induction in the Organocatalytic Hydrosilylation of Aromatic Ketones and Ketimines. *Angew. Chemie - Int. Ed.* **2006**, *45* (9), 1432–1435. https://doi.org/10.1002/anie.200503941.

(126) Zheng, H.; Deng, J.; Lin, W.; Zhang, X. Enantioselective Hydrosilylation of Ketimines with Trichlorosilane Promoted by Chiral N-Picolinoylaminoalcohols. *Tetrahedron Lett.* **2007**, *48* (45), 7934–7937. https://doi.org/10.1016/j.tetlet.2007.09.064.

(127) Guizzetti, S.; Benaglia, M.; Cozzi, F.; Rossi, S.; Celentano, G. Enantioselective Catalytic Reduction of Ketoimines with Trichlorosilane Promoted by Readily Available Chiral Lewis Bases. *Chirality* **2009**, *21*, 233–238. https://doi.org/10.1002/chir.

(128) Pignataro, L.; Benaglia, M.; Cinquini, M.; Cozzi, F.; Celentano, G. Readily Available Pyridine- and Quinoline-N-Oxides as New Organocatalysts for the Enantioselective Allylation of Aromatic Aldehydes with Allyl(Trichloro)Silane. *Chirality* **2005**, *17* (7), 396–403. https://doi.org/10.1002/chir.20180.

(129) Wang, C.; Wu, X.; Zhou, L.; Sun, J. L-Valine Derived Chiral N-Sulfinamides as Effective Organocatalysts for the Asymmetric Hydrosilylation of N-Alkyl and N-Aryl Protected Ketimines. *Org. Biomol. Chem.* **2015**, *13* (2), 577–582. https://doi.org/10.1039/c4ob01257g.

(130) Warner, C. J. A.; Reeder, A. T.; Jones, S. P-Chiral Phosphine Oxide Catalysed Reduction of Prochiral Ketimines Using Trichlorosilane. *Tetrahedron Asymmetry* **2016**, *27* (2–3), 136–141. https://doi.org/10.1016/j.tetasy.2016.01.001.

(131) Janíková, K.; Jedinák, L.; Volná, T.; Cankař, P. Chan-Lam Cross-Coupling Reaction Based on the Cu2S/TMEDA

System. *Tetrahedron* **2018**, *74* (5), 606–617. https://doi.org/10.1016/j.tet.2017.12.042.

(132) René, O.; Souverneva, A.; Magnuson, S. R.; Fauber, B. P. Efficient Syntheses of 2-Fluoroalkylbenzimidazoles and -Benzothiazoles. *Tetrahedron Lett.* **2013**, *54* (3), 201–204. https://doi.org/10.1016/j.tetlet.2012.09.069.

(133) Wentzel, M. T.; Hewgley, J. B.; Kamble, R. M.; Wall, P. D.; Kozlowski, M. C. Copper-Catalyzed N-Arylation of Hindered Substrates under Mild Conditions. *Adv. Synth. Catal.* **2009**, *351* (6), 931–937. https://doi.org/10.1002/adsc.200800730.

(134) O'Neill, D. J.; Adedoyin, A.; Alfinito, P. D.; Bray, J. a; Cosmi, S.; Deecher, D. C.; Fensome, A.; Harrison, J.; Leventhal, L.; Mann, C.; McComas, C. C.; Sullivan, N. R.; Spangler, T. B.; Uveges, A. J.; Trybulski, E. J.; Whiteside, G. T.; Zhang, P. Discovery of Novel Selective Norepinephrine Reuptake Inhibitors: 4-[3-Aryl-2,2-Dioxido-2,1,3-Benzothiadiazol-1(3H)-Yl]-1-(Methylamino)Butan-2-Ols (WYE-103231). *J. Med. Chem.* **2010**, *53* (11), 4511–4521. https://doi.org/10.1021/jm100053t.

(135) Kommi, D. N.; Jadhavar, P. S.; Kumar, D.; Chakraborti, A. K. "All-Water" One-Pot Diverse Synthesis of 1,2-Disubstituted Benzimidazoles: Hydrogen Bond Driven 'Synergistic Electrophile–Nucleophile Dual Activation' by Water. *Green Chem.* **2013**, *15* (3), 798. https://doi.org/10.1039/c3gc37004f.

(136) Chauhan, S. M. S.; Singh, R.; Geetanjali. An Improved Synthesis of *N* -Substituted-2-Nitroanilines. *Synth. Commun.* **2003**, *33* (16), 2899–2906. https://doi.org/10.1081/SCC-120022180.

(137) Kalhapure, R. S.; Patil, B. P.; Jadhav, M. N.; Kawle, L. A.; Wagh, S. B. Synthesis of 11-(Piperazin-1-Yl)-5H-Dibenzo{[}b,e] {[}1,4]Diazepine on Kilo Scale. *E-Journal Chem.* **2011**, *8* (4), 1747–1749.

(138) Howe, G. W.; Vandersteen, A. A.; Kluger, R. How Acid-Catalyzed Decarboxylation of 2,4-Dimethoxybenzoic Acid Avoids Formation of Protonated CO2. *J. Am. Chem. Soc.* **2016**, *138* (24), 7568–7573. https://doi.org/10.1021/jacs.6b01770.

(139) Dickstein, J. S.; Mulrooney, C. A.; O'Brien, E. M.; Morgan, B. J.; Kozlowski, M. C. Development of a Catalytic Aromatic Decarboxylation Reaction. *Org. Lett.* **2007**, *9* (13), 2441–2444. https://doi.org/10.1021/ol070749f.

(140) Vries, T.; Wynberg, H.; Van Echten, E.; Koek, J.; ten Hoeve, W.; Kellog, R. M.; Broxterman, Q. B.; Minnaard, A.; Kaptein, B.; van der Sluis, S.; Hulshof, L. A.; Kooistra, J. The Family Approach to the Resolution of Racemates. *Chemtracts Org. Chem.* **1999**, *12* (17), 672–674.

(141) Nieuwenhuijzen, J. W.; Grimbergen, R. F. P.; Koopman, C.; Kellogg, R. M.; Vries, T. R.; Pouwer, K.; Van Echten, E.; Kaptein, B.; Hulshof, L. A.; Broxterman, Q. B. The Role of Nucleation Inhibition in Optical Resolutions with Families of Resolving Agents. *Angew. Chemie - Int. Ed.* **2002**, *41* (22), 4281–4286. https://doi.org/10.1002/1521-3773(20021115)41:22<4281::AID-ANIE4281>3.0.CO;2-F.

(142) Kellogg, R. M.; Nieuwenhuijzen, J. W.; Pouwer, K.; Vries, T. R.; Broxterman, Q. B.; Grimbergen, R. F. P.; Kaptein, B.; Crois, R. M.; de Wever, E.; Zwaagstra, K.; van der Laan, A. C. Dutch Resolution: Separationof Enantiomers with Families of Resolving Agents. A Status Report. *Synthesis (Stuttg).* **2003**, No. 10, 1626–1638. https://doi.org/10.1055/s-2003-40508.

(143) Wen, X.; Bakali, J. El; Deprez-Poulain, R.; Deprez, B. Efficient Propylphosphonic Anhydride (®T3P) Mediated Synthesis of Benzothiazoles, Benzoxazoles and Benzimidazoles. *Tetrahedron Lett.* **2012**, *53* (19), 2440–2443. https://doi.org/10.1016/j.tetlet.2012.03.007.

(144) Wehrmeister, H. L. Periodate Oxidations of Oxazolines. *J. Org. Chem.* **1961**, *26* (10), 3821–3824. https://doi.org/10.1021/jo01068a047.

(145) Davies, I. W.; Gerena, L.; Lu, N.; Larsen, R. D.; Reider, P. J. Concise Synthesis of Conformationally Constrained Pybox Ligands. *J. Org. Chem.* **1996**, *61* (96), 9629–9630. https://doi.org/10.1021/jo9616264.

(146) Zhu, S. F.; Xie, J. B.; Zhang, Y. Z.; Li, S.; Zhou, Q. L. Well-Defined Chiral Spiro Iridium/Phosphine-Oxazoline Cationic Complexes for Highly Enantioselective Hydrogenation of Imines at Ambient Pressure. *J. Am. Chem. Soc.* **2006**, *128* (39), 12886–12891. https://doi.org/10.1021/ja063444p.

(147) Reddy, L. R.; Saravanan, P.; Corey, E. J. A Simple Stereocontrolled Synthesis of Salinosporamide A. *J. Am. Chem. Soc.* **2004**, *126* (20), 6230–6231. https://doi.org/10.1021/ja048613p.

(148) Boisnard, S.; Neuville, L.; Bois-Choussy, M.; Zhu, J. Asymmetric Synthesis of Actinoidic Acid Derivatives. *Org. Lett.* **2000**, *2* (16), 2459–2462. https://doi.org/10.1021/ol006110s.

(149) Greene, T. W.; Wuts, P. G. M.; Protective, O. F. a; Groups, P.; Edition, T.; Greene, T. W.; Wuts, P. G. M. *Protective Groups in Organic Synthesis*, 2nd ed.; Willey, 2007. https://doi.org/10.1002/9780470053485.ch2.

(150) Profous, D. Syntéza Derivátů Odvozených Od 1-Arylbenzimidazolu Modifikovaných v Poloze 2 a Studium Jejich Reaktivity, Palacký University, 2018.

(151) Hong, B. T.; Chen, C. L.; Fang, J. M.; Tsai, K. C.; Wang, S. Y.; Huang, W. I.; Cheng, Y. S. E.; Wong, C. H. Oseltamivir Hydroxamate and Acyl Sulfonamide Derivatives as Influenza Neuraminidase Inhibitors. *Bioorganic Med. Chem.* **2014**, *22* (23), 6647–6654. https://doi.org/10.1016/j.bmc.2014.10.005.

(152) Jedinák, L.; Zátopková, R.; Zemánková, H.; Šustková, A.; Cankař, P. The Suzuki-Miyaura Cross-Coupling Reaction of Halogenated Aminopyrazoles: Method Development, Scope, and Mechanism of Dehalogenation Side Reaction. *J. Org. Chem.* **2017**, *82* (1), 157–169. https://doi.org/10.1021/acs.joc.6b02306.

(153) Heidlas, J. E.; Lees, W. J.; Pale, P.; Whitesides, G. M. Gram-Scale Synthesis of Uridine 5′-Diphospho-N-Acetylglucosamine: Comparison of Enzymic and Chemical Routes. *J. Org. Chem.* **1992**, *57* (1), 146–151. https://doi.org/10.1021/jo00027a028.

(154) Mühlberg, M.; Hoesl, M. G.; Kuehne, C.; Dernedde, J.; Budisa, N.; Hackenberger, C. P. R. Orthogonal Dual-Modification of Proteins for the Engineering of Multivalent Protein Scaffolds. *Beilstein J. Org. Chem.* **2015**, *11*, 784–791. https://doi.org/10.3762/bjoc.11.88.

(155) Neises, B.; Steglich, W. Simple Method for the Esterification of Carboxylic Acids. *Angew. Chemie Int. Ed. English* **1978**, *17* (7), 522–524. https://doi.org/10.1002/anie.197805221.

(156) Carpino, L. A.; El-Faham, A. The Diisopropylcarbodiimide/1-Hydroxy-7-Azabenzotriazole System: Segment Coupling and Stepwise Peptide Assembly. *Tetrahedron* **1999**, *55* (22), 6813–6830. https://doi.org/10.1016/S0040-4020(99)00344-0.

(157) Ohtani, I.; Hotta, K.; Ichikawa, Y.; Isobe, M. Application of Modified Mosher´s Method to α-Aromatic Secondary Alcohols. Exception of the Rule and Conformational Analyses. *Chem. Lett.* **1995**, *24* (6), 513–514.

(158) Omata, K.; Fujiwara, T.; Kabuto, K. Use of a Diamagnetic Lanthanide Complex for Extending the Scope of NMR Determination of Absolute Configuration by the Modified Mosher's Method. *Tetrahedron Asymmetry* **2002**, *13* (15), 1655–1662. https://doi.org/10.1016/S0957-4166(02)00414-7.

(159) García, R.; Seco, J. M.; Vázquez, S. A.; Quiñoá, E.; Riguera, R. Role of Barium(II) in the Determination of the Absolute Configuration of Chiral Amines by 1H NMR Spectroscopy. *J. Org. Chem.* **2006**, *71* (3), 1119–1130. https://doi.org/10.1021/jo0522207.

(160) Yukibaru, F.; Yaima, C.; Mizutani, J. A New Method for Establishment of Absolute Configurations of Secondary Alcohols by NMR Spectroscopy. *Tetrahedron Lett.* **1994**, *35* (4), 599–602.

(161) Bautista-Hernández, C. I.; Trejo-Carbajal, N.; Zúñiga-Estrada, E. A.; Aristeo-Dominguez, A.; Meléndez-Rodríguez, M.; Suárez-Castillo, O. R.; Sánchez-Zavala, M.; Cruz-Borbolla, J.; Morales-Ríos, M. S.; Joseph-Nathan, P. 2-Cyano-2-Indolylpropanoic Acid as a Chiral Derivatizing Agent for the Absolute Configuration Assignment of Secondary Alcohols and Primary Amines by 1H NMR and VCD. *Tetrahedron Asymmetry* **2017**, *28* (6), 762–782. https://doi.org/10.1016/j.tetasy.2017.04.011.

(162) Hoye, T. R.; Jeffrey, C. S.; Shao, F. Mosher Ester Analysis for the Determination of Absolute Configuration of Stereogenic (Chiral) Carbinol Carbons. *Nat. Protoc.* **2007**, *2* (10), 2451–2458. https://doi.org/10.1038/nprot.2007.354.

(163) Alkorta, I.; Elguero, J. Ab Initio Hybrid DFT-GIAO Calculations of the Shielding Produced by Carbon-Carbon Bonds and Aromatic Rings in 1H NMR Spectroscopy. *New J. Chem.* **1998**, *22* (4), 381–385. https://doi.org/10.1039/a708743h.

(164) Baranac-Stojanović, M. New Insight into the Anisotropic Effects in Solution-State NMR Spectroscopy. *RSC Adv.* **2014**, *4* (1), 308–321. https://doi.org/10.1039/c3ra45512b.

(165) Alkorta, I.; Elguero, J. Ab Initio Hybrid DFT-GIAO Calculations of the Shielding Produced by Carbon-Carbon Bonds and Aromatic Rings in 1H NMR Spectroscopy. *New J. Chem.* **1998**, *22* (4), 381–385. https://doi.org/10.1039/a708743h.

(166) Seco, J. M.; Quiñoá, E.; Riguera, R. The Assignment of Absolute Configuration by NMR. *Chem. Rev.* **2004**, *104* (1), 17–117. https://doi.org/10.1021/cr000665j.

(167) Matsui, T.; Kondo, T.; Nishita, Y.; Itadani, S.; Tsuruta, H.; Fujita, S.; Omawari, N.; Sakai, M.; Nakazawa, S.; Ogata, A.; Mori, H.; Kamoshima, W.; Terai, K.; Ohno, H.; Obata, T.; Nakai, H.; Toda, M. Highly Potent Inhibitors of TNF-α Production. Part II: Metabolic Stabilization of a Newly Found Chemical Lead and Conformational Analysis of an Active Diastereoisomer. *Bioorganic Med. Chem.* **2002**, *10* (12), 3787–3805. https://doi.org/10.1016/S0968-0896(02)00380-2.

(168) Ren, Y.; Su, Y.; Sun, L.; He, S.; Meng, L.; Liao, D.; Liu, X.; Ma, Y.; Liu, C.; Li, S.; Ruan, H.; Lei, X.; Wang, X.; Zhang, Z. Discovery of a Highly Potent, Selective, and Metabolically Stable Inhibitor of Receptor-Interacting Protein 1 (RIP1) for the Treatment of Systemic Inflammatory Response Syndrome. *J. Med. Chem.* **2017**, *60* (3), 972–986. https://doi.org/10.1021/acs.jmedchem.6b01196.

(169) Karim, A.; Mortreux, A.; Petit, F.; Buono, G.; Peiffer, G.; Siv, C. Synthese d'aminophosphinephosphinites Chiraux. Utilisation En Reduction Asymetrique Catalytique. *J. Organomet. Chem.* **1986**, *317* (1), 93–104. https://doi.org/10.1016/S0022-328X(00)99348-3.

(170) Boyle, G. A.; Govender, T.; Kruger, H. G.; Maguire, G. E. M. Synthesis of Chiral Pentacyclo-Undecane Ligands and Their Use in the Enantioselective Alkylation of Benzaldehyde with Diethylzinc. *Tetrahedron Asymmetry* **2004**, *15* (17), 2661–2666. https://doi.org/10.1016/j.tetasy.2004.07.038.

(171) Agami, C.; Couty, F.; Hamon, L.; Venier, O. Chiral Oxazolidinones from N-Boc Derivatives of β-Amino Alcohols. Effect of a N-Methyl Substituent on Reactivity and Stereoselectivity. *Tetrahedron Lett.* **1993**, *34* (28), 4509–4512. https://doi.org/10.1016/0040-4039(93)88071-P.

(172) Micouin, L.; Jullian, V.; Quirion, J. C.; Husson, H. P. Origins of Diastereoselectivity in the Alkylation of N-Substituted Lactams and Amides Derived from Optically Active Aminoalcohols. *Tetrahedron Asymmetry* **1996**, *7* (10), 2839–2846. https://doi.org/10.1016/0957-4166(96)00374-6.

(173) Waki, M.; Meienhofer, J. Efficient Preparation of N-Formylamino Acid Tert-Butyl Esters. *J. Org. Chem.* **1977**, *42* (11), 2019–2020. https://doi.org/https://doi.org/10.1021/jo00431a046.

(174) Profous, D. Využití TBBA pro Určení Absolutní Konfigurace Chirálních Aminů a Alkoholů, 2020.

(175) Andrés, J. M.; Barrio, R.; Martínez, M. A.; Pedrosa, R.; Pérez-Encabo, A. Synthesis of Enantiopure Syn-β-Amino Alcohols. A Simple Case of Chelation-Controlled Additions of Diethylzinc to α-(Dibenzylamino) Aldehydes. *J. Org. Chem.* **1996**, *61* (13), 4210–4213. https://doi.org/10.1021/jo960017t.

(176) Zheng, M.; Xue, W.; Xue, T.; Gong, H. Ester Formation via Nickel-Catalyzed Reductive Coupling of Alkyl Halides with Chloroformates. *Org. Lett.* **2016**, *18* (23), 6152–6155. https://doi.org/10.1021/acs.orglett.6b03158.

(177) Erhardt, P. W. Benzylamine and Dibenzylamine Revisited. Syntheses of N-Substituted Aryloxypropanol Amines Exemplifying a General Route to Secondary Aliphatic Amines. *Synth. Commun.* **1983**, *13* (2), 103–114. https://doi.org/10.1080/00397918308061967.

(178) Le, Z. G.; Chen, Z. C.; Hu, Y.; Zheng, Q. G. Organic Reactions in Ionic Liquids: N-Alkylation of Phthalimide and Several Nitrogen Heterocycles. *Synthesis (Stuttg).* **2004**, No. 2, 208–212. https://doi.org/10.1055/s-2003-44383.

(179) Holl, M. G.; Struble, M. D.; Siegler, M. A.; Lectka, T. The Close Interaction of a C-F Bond with a Carbonyl π–System: Attractive, Repulsive, or Both? *J. Fluor. Chem.* **2016**, *188*, 126–130. https://doi.org/10.1016/j.jfluchem.2016.06.016.

(180) Holl, M. G.; Pitts, C. R.; Lectka, T. Fluorine in a C−F Bond as the Key to Cage Formation. *Angew. Chemie - Int. Ed.* **2018**, *57* (11), 2758–2766. https://doi.org/10.1002/anie.201710423.

(181) Hehre, W.; Klunzinger, P.; Deppmeier, B.; Driessen, A.; Uchida, N.; Hashimoto, M.; Fukushi, E.; Takata, Y. Efficient Protocol for Accurately Calculating 13C Chemical Shifts of Conformationally Flexible Natural Products: Scope, Assessment, and Limitations. *J. Nat. Prod.* **2019**, *82* (8), 2299–2306. https://doi.org/10.1021/acs.jnatprod.9b00603.

(182) Sajiki, H.; Ito, N.; Esaki, H.; Maesawa, T.; Maegawa, T.; Hirota, K. Aromatic Ring Favorable and Efficient H-D Exchange Reaction Catalyzed by Pt/C. *Tetrahedron Lett.* **2005**, *46* (41), 6995–6998. https://doi.org/10.1016/j.tetlet.2005.08.067.

(183) Gao, Y. X.; Chang, L.; Shi, H.; Liang, B.; Wongkhan, K.; Chaiyaveij, D.; Batsanov, A. S.; Marder, T. B.; Li, C. C.; Yang, Z.; Huanga, Y. A Thiourea-Oxazoline Library with Axial Chirality: Ligand Synthesis and Studies of the Palladium-Catalyzed Enantioselective Bis(Methoxycarbonylation) of Terminal Olefins. *Adv. Synth. Catal.* **2010**, *352* (11–12), 1955–1966. https://doi.org/10.1002/adsc.201000070.

(184) Liang, B.; Liu, J.; Gao, Y. X.; Wongkhan, K.; Shu, D. X.; Lan, Y.; Li, A.; Batsanov, A. S.; Howard, J. A. H.; Marder, T. B.; Chen, J. H.; Yang, Z. Synthesis of Thiourea-Oxazolines, a New Class of Chiral S,N-Heterobidentate Ligands: Application in Pd-Catalyzed Asymmetric Bis(Methoxycarbonylation) of Terminal Olefins. *Organometallics* **2007**, *26* (19), 4756–4762. https://doi.org/10.1021/om700311x.

(185) Dai, M.; Liang, B.; Wang, C.; Chen, J.; Yang, Z. Synthesis of a Novel C2-Symmetric Thiourea and Its Application in the Pd-Catalyzed Cross-Coupling Reactions with Arenediazonium Salts under Aerobic Conditions. *Org. Lett.* **2004**, *6* (2), 221–224. https://doi.org/10.1021/ol036182u.

(186) Kriegelstein, M. Příprava Některých Derivátů 1-(1H-Indazol-3-Yl)-1H-Benzo[d]Imidazol-2(3H)-on Substituovaných v Poloze 5 a 6, 2016.

(187) Abdel-Magid, A. F.; Carson, K. G.; Harris, B. D.; Maryanoff, C. A.; Shah, R. D. Reductive Amination of Aldehydes and Ketones with Sodium Triacetoxyborohydride. Studies on Direct and Indirect Reductive Amination Procedures. *J. Org. Chem.* **1996**, *61* (11), 3849–3862. https://doi.org/10.1021/jo960057x.

(188) Lovrić, M.; Cepanec, I.; Litvić, M.; Bartolinčić, A.; Vinković, V. Scope and Limitations of Sodium and Potassium Trimethylsilanolate as Reagents for Conversion of Esters to Carboxylic Acids. *Croat. Chem. Acta* **2007**, *80* (1), 109–115.

(189) Grošelj, U.; Meden, A.; Stanovnik, B.; Svete, J. Synthesis of Novel C2-Symmetric 1,3-Bis{(1S,2R,3S,4R)-1,7,7-Trimethyl-3′H-Spiro[Bicyclo[2.2.1]Heptane-2,2′-Furan]-3-Yl}benzoimidazolium Tetrafluoroborates. *Tetrahedron Asymmetry* **2008**, *19* (3), 330–342. https://doi.org/10.1016/j.tetasy.2008.01.005.

(190) Huang, A.; Feng, L.; Qiao, Z.; Yu, W.; Zheng, Q.; Ma, C. Synthesis of Pyrrolobenzoxazepinones by CuI/L-Proline-Catalyzed Intramolecular Coupling Reactions. *Tetrahedron* **2013**, *69* (2), 642–646. https://doi.org/10.1016/j.tet.2012.11.009.

(191) Shan, G. G.; Li, H. Bin; Sun, H. Z.; Cao, H. T.; Zhu, D. X.; Su, Z. M. Enhancing the Luminescence Properties and Stability of Cationic Iridium(Iii) Complexes Based on Phenylbenzoimidazole Ligand: A Combined Experimental and Theoretical Study. *Dalt. Trans.* **2013**, *42* (31), 11056–11065. https://doi.org/10.1039/c3dt50358e.

(192) Bahrami, K.; Khodaei, M. M.; Kavianinia, I. A Simple and Efficient One-Pot Synthesis of 2-Substituted Benzimidazoles. *Synthesis (Stuttg).* **2007**, No. 4, 547–550. https://doi.org/10.1055/s-2007-965878.

(193) Yamashita, T.; Yamada, S.; Yamazaki, Y.; Tanaka, H. New Procedure for the Synthesis of 2-Alkylbenzimidazoles. *Synth. Commun.* **2009**, *39* (16), 2982–2988. https://doi.org/10.1080/00397910902730838.

(194) Vanda, D.; Soural, M.; Canale, V.; Chaumont-Dubel, S.; Satała, G.; Kos, T.; Funk, P.; Fülöpová, V.; Lemrová, B.; Koczurkiewicz, P.; Pękala, E.; Bojarski, A. J.; Popik, P.; Marin, P.; Zajdel, P. Novel Non-Sulfonamide 5-HT6 Receptor Partial Inverse Agonist in a Group of Imidazo[4,5-b]Pyridines with Cognition Enhancing Properties. *Eur. J. Med. Chem.* **2018**, *144*, 716–729. https://doi.org/10.1016/j.ejmech.2017.12.053.

(195) Beaulieu, P. L.; Hache, B.; Von moos, E. A Practical Oxone®-Mediated, High-Throughput, Solution-Phase Synthesis of Benzimidazoles from 1,2-Phenylenediamines and Aldehydes and Its Application to Preparative Scale Synthesis. *Synthesis (Stuttg).* **2003**, *2003* (11), 1683–1692. https://doi.org/10.1055/s-2003-40888.

(196) Tandon, V. K.; Kumar, M. BF3.Et2O Promoted One-Pot Expeditious and Convenient Synthesis of 2-Substituted Benzimidazoles and 3,1,5-Benzoxadiazepines. *Tetrahedron Lett.* **2004**, *45* (21), 4185–4187. https://doi.org/10.1016/j.tetlet.2004.03.117.

(197) Wamser, C. A. Equilibria in the System Boron Trifluoride-Water at 25°. *J. Am. Chem. Soc.* **1951**, *73* (1), 409–416. https://doi.org/10.1021/ja01145a134.

(198) Haynes, W. M. Physical Constants of Inorganic Compounds List of Abbreviations. In *CRC handbook of chemistry and physics, 94th Edition*; 2013; Vol. 94, pp 4.43-4.101.

(199) Gorvin, J. H. The Synthesis of Di and Triarylamines Throught Halogen Displacement by Base Activated Arylamines. *J. Chem. Soc. Perkin Trans. 1 Org. Bio-Organic Chem.* **1988**, No. 1, 1331–1335.

(200) Doherty, S.; Knight, J. G.; McRae, A.; Harrington, R. W.; Clegg, W. Oxazoline-Substituted Prolinamide-Based Organocatalysts for the Direct Intermolecular Aldol Reaction between Cyclohexanone and Aromatic Aldehydes. *European J. Org. Chem.* **2008**, No. 10, 1759–1766. https://doi.org/10.1002/ejoc.200700922.

(201) Yao, Q. J.; Zhang, S.; Zhan, B. B.; Shi, B. F. Atroposelective Synthesis of Axially Chiral Biaryls by Palladium-Catalyzed Asymmetric C−H Olefination Enabled by a Transient Chiral Auxiliary. *Angew. Chemie - Int. Ed.* **2017**, *56* (23), 6617–6621. https://doi.org/10.1002/anie.201701849.

(202) Larin, A. A.; Fershtat, L. L.; Ustyuzhanina, N. E.; Gening, M. L.; Nifantiev, N. E.; Makhova, N. N. New Hybrid Furoxan Structures with Antiaggregant Activity. *Mendeleev Commun.* **2018**, *28* (6), 595–597. https://doi.org/10.1016/j.mencom.2018.11.010.

(203) Valeur, E.; Bradley, M. Amide Bond Formation: Beyond the Myth of Coupling Reagents. *Chem Soc Rev* **2009**, *38* (2), 606–631. https://doi.org/10.1039/b701677h.

(204) Satyanarayana, T.; Abraham, S.; Kagan, H. B. Nonlinear Effects in Asymmetric Catalysis. *Angew. Chemie - Int. Ed.* **2009**, *48* (3), 456–494. https://doi.org/10.1002/anie.200705241.

(205) Guillaneux, D.; Shu-Hai, Z.; Odile, S.; Rainford, D.; Kagan, H. B. Nonlinear Effects in Asymmetric Catalysis. *J. Am. Chem. Soc.* **1994**, *116*, 9430–9439. https://doi.org/10.1021/ja00100a004.

(206) Malkov, A. V.; Vranková, K.; Sigerson, R. C.; Stončius, S.; Kočovský, P. New Organocatalysts for the Asymmetric Reduction of Imines with Trichlorosilane. *Tetrahedron* **2009**, *65* (45), 9481–9486. https://doi.org/10.1016/j.tet.2009.08.048.

(207) Chelouan, A.; Recio, R.; Borrego, L. G.; Álvarez, E.; Khiar, N.; Fernández, I. Sulfinamide Phosphinates as Chiral Catalysts for the Enantioselective Organocatalytic Reduction of Imines. *Org. Lett.* **2016**, *18* (13), 3258–3261.

https://doi.org/10.1021/acs.orglett.6b01509.

(208) Paolucci, C.; Rosini, G. Approach to a Better Understanding and Modeling of (S)-Dihydrofuran-2-Yl, (S)-Tetrahydrofuran-2-Yl-, and Furan-2-Yl-β-Dialkylaminoethanol Ligands for Enantioselective Alkylation. *Tetrahedron Asymmetry* **2007**, *18* (24), 2923–2946. https://doi.org/10.1016/j.tetasy.2007.11.034.

PALACKÝ UNIVERSITY

Olomouc

Faculty of Science

Department of Organic Chemistry

Derivatives of Benzoimidazolylbenzoic Acid as the Axially Chiral Derivatizing Agent and Organocatalyst

Ph.D Thesis

Mgr. Michal Kriegelstein

Supervisor: Doc. RNDr. Petr Cankař, Ph.D.

2019/2020

Author	Mgr. Michal Kriegelstein
	Faculty of Science, Palacky University
	Department of Organic Chemistry
Supervisor	Doc. RNDr. Petr Cankař, Ph.D.
	Faculty of Science, Palacky University
	Department of Organic Chemistry
Referees	Prof. RNDr. Milan Pour, Ph.D.
	Department of Inorganic and Organic Chemistry, Charles University in Prague, Faculty of Pharmacy Hradec Kralove, Heyrovskeho 1203, CZ-50005 Hradec Kralove, Czech Republic
	Prof. RNDr. Radek Marek, Ph.D.
	CEITEC − Central European Institute of Technology, National Centre for Biomolecular Research, Faculty of Science, and Department of Chemistry, Faculty of Science, Masaryk University, 625 00 Brno, Czech Republic

The defense of this thesis is going to take place on …….. Because of the unpredictability of the COVID-19 situation, the date or the platform of the defense can be changed.

I declare with my signature, that this is my original work. Further, I confirm that all used sources are refenced according to the department requirements.

Olomouc

……..

Mgr. Michal Kriegelstein

Abstract

The thesis deals with the synthesis of axially chiral benzimidazoles and their potential applications in the assignment of absolute configuration and organocatalysis. The introduction part is divided into the three chapters. The first chapter introduces the reader into an area of axially chiral compounds with focus on atropoisomers, especially those containing C-N bond as the chiral axis. The remaining two chapters introduce the reader into the two projects.

The first, and major, project deals with the design and development of the novel axially chiral derivatization agent (CDA) for the NMR assignment of absolute configuration of chiral compounds. While there are multiple methods that allow the configuration assignment, the common availability of NMR instruments makes this method very interesting for the general use. Many different CDAs have been reported together with their limitations in the past. In this chapter, the general principles of the method are summarized and the most relevant CDAs are discussed to show their limitations.

The second, minor, project deals with the development of a novel organocatalytic system for an asymmetric reduction of prochiral imines. The current methods are presented with focus on those using $HSiCl_3$ as a reducing agent due to its high availability and low price.

The results and discussion part is divided into two chapters, each dedicated to one of the projects. In this part, the results of each project are discussed, including various dead ends and unsuccessful attempts. A comparison to relevant data from the literature is included as well.

The experimental part includes experimental procedures for the conducted experiments which are not included in the publications that arised from this thesis.

Abstrakt

Tato disertační práce se zabývá syntézou axiálně chirálních benzimidazolů a jejich potenciálními aplikacemi v oblasi analýzy a katalýzy. Úvodní část je rozdělena do tří capitol, které uvedou čtenáře do problematiky v oblasti chirálních sloučenin se zaměřením na atroposiomery. Zbývající dvě kapitoly poskytují úvod do problematiky dvou projektů, kterými se tato práce zabývá.

Prvni project se zabývá vývojem nového chirálního derivatizačního činidla (CDA) pro určení absolutní konfigurace chirálních sloučenin pomocí NMR spektroskopie. Ačkoliv existuje celá řada metod, které jsou vhodné k tomuto účelu, snadnost a vysoká dostupnost NMR spektrometrů v chemických laboratořích je nespornou výhodou této metody. Několik různých CDA bylo již v minulosti popsáno a využito nicméně jejich využití není bez omezení. V této kapitole jsou popsány obecné principy těchto metod a nejpoužívanější CDA jsou popsána spolu s jejich limitacemi.

Druhý project se zabývá vývojem nového ligandu pro organokatalytické redukce prochirálních iminů. V této kapitole jsou popsány aktuální systémy pro organokatalytické redukce prochirálních iminů se zaměřením na využití $HSiCl_3$ jako redukčního činidla a to zejména z důvodu snadné dostpupnosti a nízké ceny tohoto činidla.

Následuje část výsledky a diskuse, která je rozdělená na dvě podkapitoly, ke každému projektu jedna. V této kapitole jsou prezentovány a diskutovány výsledky každého z projektů, která jsou dale srovnány s literaturou.

Následuje experimentální část, která popisuje jednotlivé experimenty.

Aims of this thesis

1) Development of a novel chiral derivatization agent for NMR spectroscopy

The synthesis and resolution of an axially chiral benzimidazole derivative as a chiral derivatization agent (CDA) and its study of capability to distinguish between the enantiomers of the analyte based on the ^{1}H, ^{13}C, or ^{19}F NMR spectra. The design of a conformational model for the assignment of absolute configuration deduced from the NMR data and in-silico modeling of model compounds.

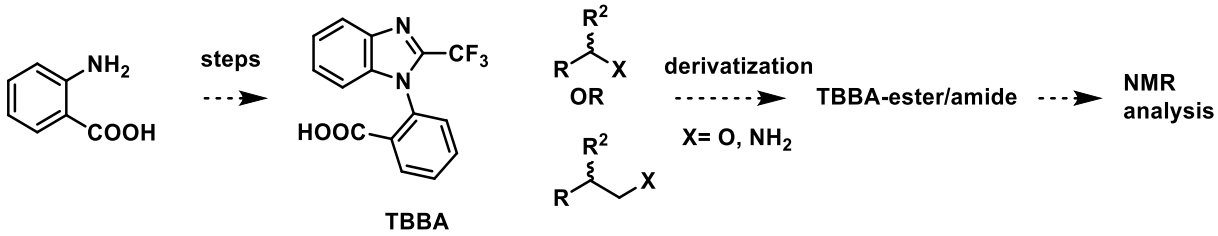

2) Design and development of an organocatalytic system for the asymmetric additions of organosilicon reagents to prochiral imines.

The synthesis and resolution of an axially chiral benzimidazole-pyridine ligand for the asymmetric reduction of prochiral imines by $HSiCl_3$ and the addition of allyl-$SiCl_3$. The optimization of the ligand for the highest enantiomeric purity of the product. The best ligand will be tested on a set of various model imines to further evaluate the applicability of the proposed catalytic system.

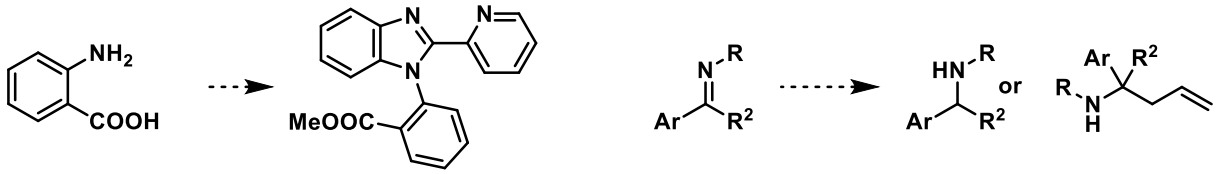

Introduction

Assignment of absolute configuration by NMR

The absolute configuration is one of the key characteristics of chiral compounds. There are several methods that allow the configuration assignment such as chiroptical methods[1] or X-ray crystallography,[2] however, the high availability of NMR instrumentation makes it competitive choice.

NMR spectroscopy can be used if several criteria are met. The most important is the requirement for suitable functional groups that allow for modification of the analyte with suitable chiral reagent. This modification can be either noncovalent using chiral solvating agents (CSA) or covalent using chiral derivatization agents (CDA). Since the experimental work described in this thesis deals with development of new CDA, this chapter will focus on the applications of various CDAs.

In theory, any chiral compound can be used as a CDA because covalent modification of given chiral analyte with chiral CDA will lead to diastereomeric compounds if we use different enantiomers of CDA. The diastereomers will differ in their NMR spectra unlike enantiomers but for compound to be used as a reliable CDA, the NMR difference in spectra of those diastereomers needs to be predictable which would lead to the assignment of the correct configuration of the analyte. This requirement disqualifies most of the chiral compounds. The "ideal" CDA should possess following structural features:[6]

a) A suitable functional group that allows covalent modification of the analyte – most often carboxylic acid but alcohols or amines could be used as well.
b) A suitable functional group that projects anisotropic effect on the analyte which causes the predictable change of NMR spectra ("shielding effect") - most often aromatic rings such as phenyl or anthryl.
c) A suitable polar group which "locks" the compound in preferred conformation which allows selective projection of the shielding effect on specific substituents of the analyte.

The structure of general CDA **I** is depicted on Figure 1. The X-group allows for modification of the analyte, Y-group projects the shielding effects towards the substituents R^3 **II** and R^4 **III** in the analyte which causes the selective change in the NMR spectra. R^1 and R^2 are other functional groups which play a role in maintaining the specific conformation of the diastereomers **II** and **III**.

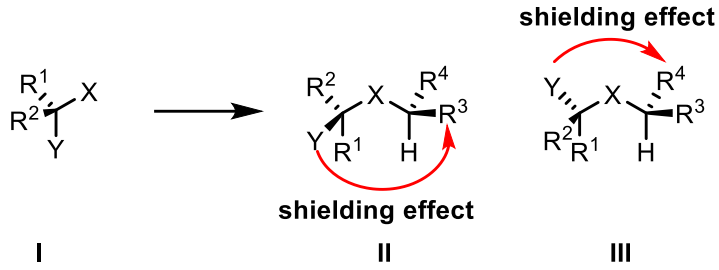

Figure 1 Schematic representation of the principle of the method

Most commonly, the analyte is modified separately with both enantiomers of the CDA and their NMR spectra are compared, although different approaches are available as well. The range of substrates includes α-chiral secondary alohols[8,9] and amines[10], β-chiral primary alchols[8,11], cyclic secondary amines,[12,13] tertiary alcohols,[14,15] thiols,[16] cyanohydrins[17–19] or polyfunctional aminoalcohols.[20,21] While the substrate scope is fairly broad, it is important to know, not every CDA is suitable for each of those analytes.

Mosher´s acid

Methoxytrifluoromethylphenylacetic acid (MTPA) or Mosher´s acid **IV** (Figure 2) is the most commonly used acid since its description by Dale and Mosher in 1973.[22–24] Analytes can be acylated with MTPA and a suitable activator or directly with acid chloride MTPA-Cl **V**

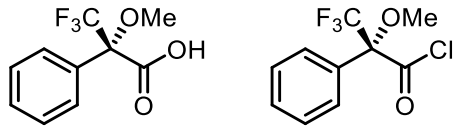

(*S*)-IV **(*R*)-V**

Figure 2 Structure of Mosher´s acid

At first, ^{19}F NMR was used by Mosher[23] with advantage due to simplified interpretation of ^{19}F spectra at that time. While the use of ^{19}F NMR allows straightforward assignment due to low number of signals in the spectra, the method was later rejected due to low reliability.[25]

The use of proton NMR is far more common than use of ^{19}F. The greatest advantage of ^{1}H over fluorine NMR lies in the number of data points gathered. The ^{19}F NMR always gives one or the other configuration and because only one signal is obtained; there is no room for self-correction. On the other hand, most organic molecules have multiple protons, which can be analyzed and therefore any anomalous behavior can be revealed.

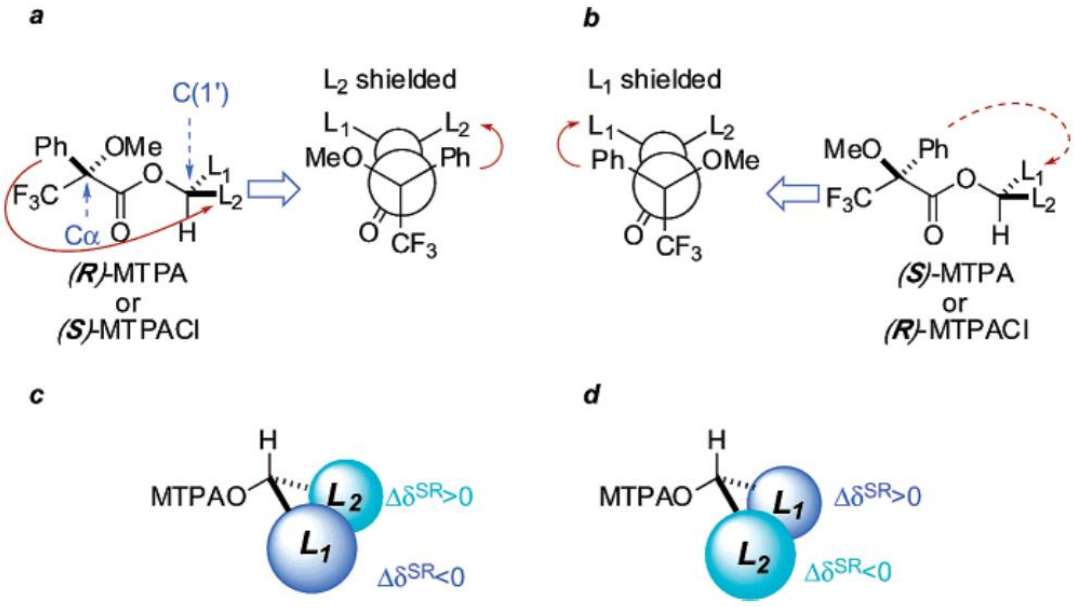

Figure 3 Conformational model for assignment of absolute configuration of chiral alcohols by Mosher´s acid (taken from [26])

The conformation is the same but the shielding effect is caused by the phenyl rings and is projected towards one of the substituents either L^1 or L^2. If (*R*)-MTPA is used, the shielding is projected towards the L^2 substituent (Figure 3a) and when opposite enantiomer, (*S*)-MTPA, is used, the shielding is projected towards the L^1 substituent (Figure 3b). This shielding is opposite if the alcohol has opposite configuration. The shielding towards the substituents can be calculated in similar fashion as in the case of ^{19}F:

$\Delta\delta^{SR}(L^1) = \delta L^1(S) - \delta L^1(R)$

$\Delta\delta^{SR}(L^2) = \delta L^2(S) - \delta L^2(R)$

Due to the shielding depicted in this example

$\Delta\delta^{SR}(L^1) < 0$

$\Delta\delta^{SR}(L^2) > 0$

After the calculation is done, the spatial arrangement of substituents L^1 and L^2 can be decoded using simplified models shown in Figure 3c/d. Naturally, all protons located in L^1 or L^2 substituent should have the same sign of

the $\Delta\delta^{SR}$ and it is advised to calculate as many $\Delta\delta^{SR}$ parameters as many protons as possible because of higher reliability of such assignment. ^{13}C NMR analysis can be performed in the same manner as ^{1}H although it has several limitations.[27]

Other reagents

Methoxyphenylacetic acid **VI** (MPA, Figure 3) was also reported by Mosher,[24] however its application was limited due to observed racemization during the acylation step. This difficulties were later solved by Trost[28] by use of different acylation conditions.

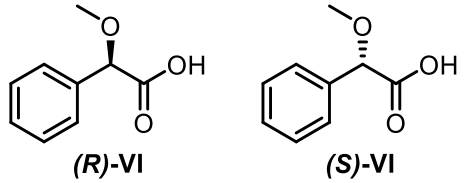

Figure 3 Methoxyphenylacetic acid (MPA)

The conformation equilibria of MPA is significantly simpler compared to MTPA: only two major conformers were described therefore MPA is preferred to MTPA for analysis of chiral alcohols.[29]

Further modification of the structure of MPA were performed At first, a change of methoxy group to other alkyls or acyls was attempted.[30] This modification however did not provide significant improvement and in most cases, the $\Delta\delta^{RS}$ differences were smaller compared to MPA. The further modification was exchanging the phenyl ring for different aryls .[29,31] The structures of some of the arylmethoxyacetic acids are shown in Figure 4

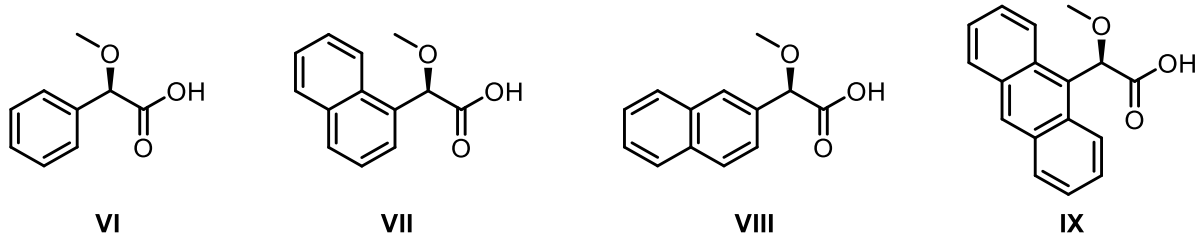

Figure 4 (*R*)-MPA **VI**, (*R*)-1-NMA **VII**, (*R*)-2-NMA **VIII** and 9-AMAA **IX**

The most promising is 9-AMAA **61** which showed the most significant $\Delta\delta^{RS}$ differences as can be seen in Figure 5 on a model substrate: 3,3-dimethylbutan-2-ol **X,** 1-phenylethanol **XI**, or menthol **XII**.

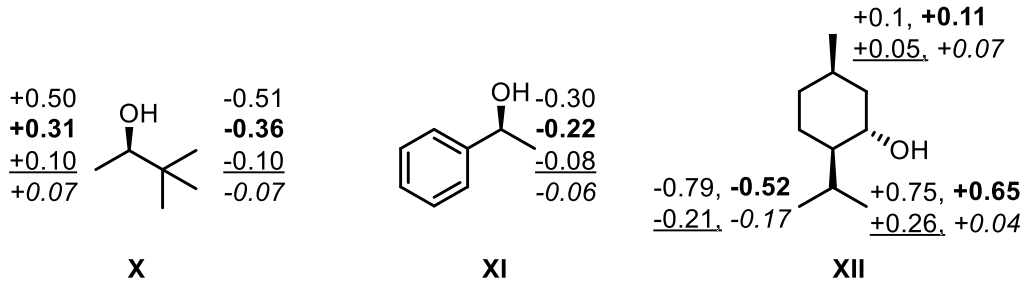

Figure 5 Comparison of $\Delta\delta^{RS}$ differences between 9-AMAA, **1-NMA,** MPA, and *MTPA*

There is a difference between MTPA and MPA in the magnitude of the $\Delta\delta^{RS}$ parameter as can be seen in **X-XII**, however, the substitution of the phenyl ring for larger rings such as naphthyl in 1-NMA or anthryl in 9-AMAA shows significant improvement in the differentiation of signals of interest. This effect can be seen in **X**, **XI**, **XII**. The substitution of the aromatic moiety plays dual role: first, the larger aromatic ring is able to project the shielding effect towards larger area and second, the larger aromatic rings shift the conformational equilibrium towards more desirable conformer.[29]

Analysis of β-chiral primary alcohols

The size of the aryl ring is especially significant in analysis of chiral primary alcohols as exemplified by alcohols **XIII-XV** (Figure 6). In this case, only 9-AMAA provided enough differentiation which allows reliable structural assignment of the absolute configuration.[9,11] The difference between 9-AMAA, MPA and MTPA is depicted in Figure 6.

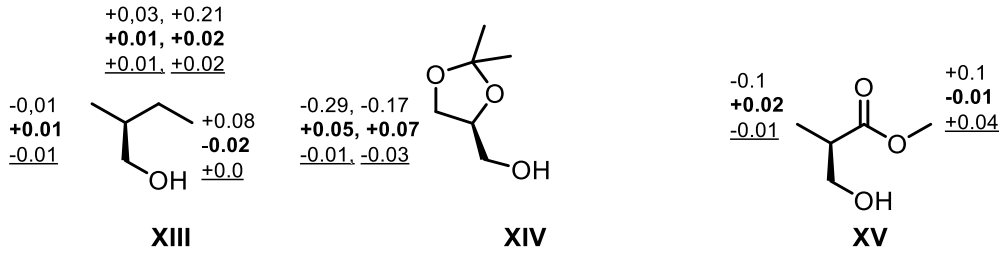

Figure 6 Comparison of $\Delta\delta^{RS}$ differences between 9-AMAA, **MPA,** MTPA esters

The analysis of chiral primary alcohols and similar substrates is significantly more complex compared to analysis of chiral secondary alcohols:

a) The additional bond increases flexibility of the whole system and increase the ammount of possible conformers.
b) The chiral atom is located further apart from the functional group where the CDA is tethered.
c) The substituents L^1 and L^2 are also located further apart from the anisotropic group which causes the differences in the chemical shift

Those effects combined together cause the observed $\Delta\delta^{RS}$ values being significantly smaller compared to α-chiral secondary alcohols.

Organocatalytic $HSiCl_3$ reduction of ketimines

The reduction of prochiral ketones or ketimines leading to chiral amines or alcohols is one the most important chemical transformations. Those reaction often require use of metal catalysts which, although used in low loadings, are not environmentally friendly.[35,36] The organocatalytic reductions provide interesting alternative because they do not require the use of transition metals. There are several approaches available: transfer hydrogenation using Hantzsch ester or other hydrogen sources and chiral acids, frustrated lewis pairs and hydrogen gas, borane reduction with CBS catalyst or trichlorosilane reduction using chiral catalysts.[37,38] Allylation raction using allyl-trichlorosilanes were reviewed by Denmark.[39] Due to the focus of the last project of this thesis on trichlorosilane reductions, only this area was reviewed. Structurally different oxazoline-pyridine ligands were reported by Kočovský[40] (Figure 7)

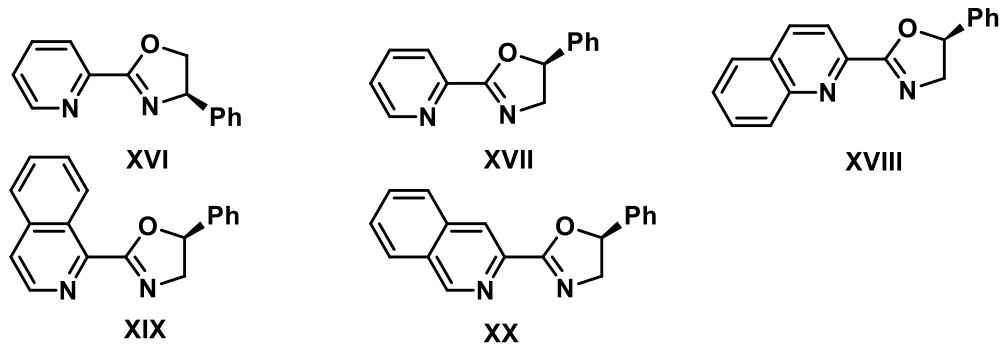

Figure 7 Oxazoline-based catalysts

At first acetophenone was used as model ketone. Ligand **XVI** derived from phenylglycinol yielded products in low 29% yield and 66 %ee. The isomeric ligand **XVII** derived from mandelic acid on the other hand provided enantioenriched alcohol in 85% yield and 78 %ee which is more comparable to previously reported ligands. Lower reactivity of ligand **XVI** is caused by close presence of the phenyl ring which is hindering the approach of the substrate as can be seen in intermediate **XXI**. This effect is not noticeable in assumed intermediate **XXII** derived

from ligand **XVII** as can be seen in Figure 8. For this reason, further ligand optimization was conducted using the mandelate based structures **XVIII-XX.**[40]

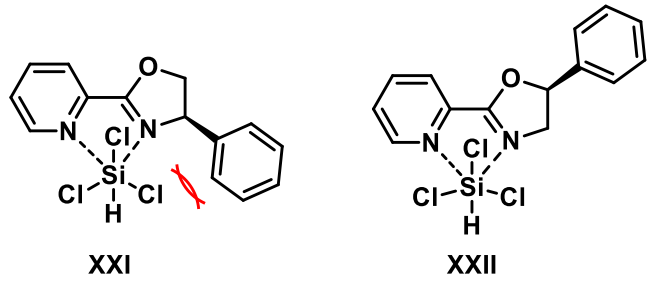

Figure 8 Proposed differences in transition states in reduction of imines with ligands **XVI** and **XXVII**.

The best ligand showed to be **XVIII** which provided reduced ketones in high yields 50-85% and enantioselectivities 70-95 %ee. Interestingly, in the case of ligand **XVII**, no products were obtained at all. Reduction of aliphatic ketone, cyclohexylmethylketone, provided product in 70% yield but as a racemate which suggests π – π interactions might play a key role. The proposed transition state is shown in Figure 9.[40]

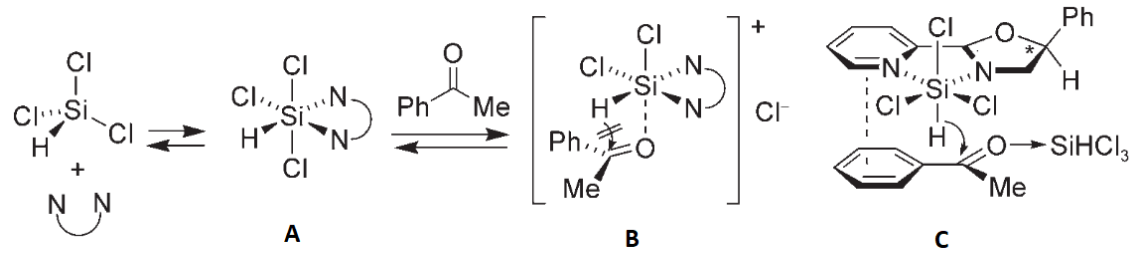

Figure 9 Proposed transition state for the $HSiCl_3$ reduction with ligand **107.** Taken from ref.[40]

Discussion and results: Project NMR

Introduction

The structure of 2-(2-(trifluoromethyl)-1*H*-benzo[*d*]imidazol-1-yl)benzoic acid (TBBA) **1** is shown in Figure 10. The main features include the CF_3 group which should allow easy configuration assignment based on ^{19}F NMR. The carboxylic group functions as a tether to connect the analyte *via* an ester or amide bond. Last, the shielding effect is produced by the benzimidazole ring towards one of the substituents of the analyte. The main advantage over other CDAs was thought to be lower flexibility of the mostly aromatic system which possesses less flexible bonds compared to arylmethoxyacetic acids.

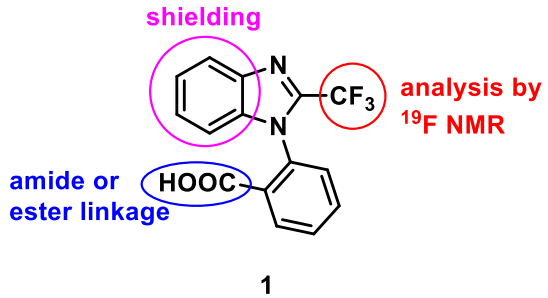

Figure 10 Structure of 2-(2-(trifluoromethyl)-1*H*-benzo[*d*]imidazol-1-yl)benzoic acid (TBBA) **1**

The synthesis (Scheme 1) started with copper catalyzed Ullman arylation which after recrystallization from acetic acid yielded nitroacid **2** in 70%. The reaction worked on multiple scales ranging from 0.7 g to 33 g and was reproduced multiple times on the large scale with yields between 70-80%. Reduction with 1 mol% of Pd/C catalyst and hydrogen was used followed by imple filtration through a short pad of silica or celite and evaporation provided **3** in quantitative yields.

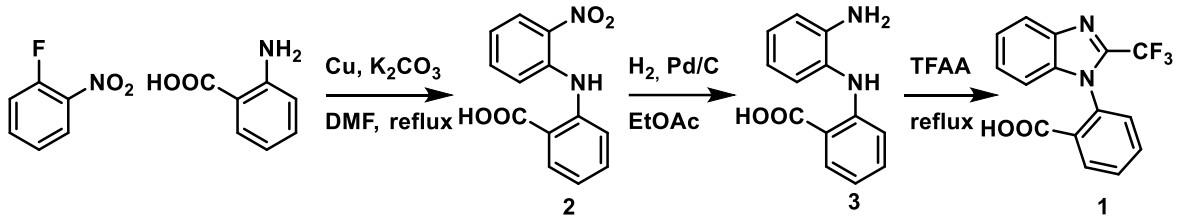

Scheme 1 Proposed synthesis of TBBA

The cyclization in the boiling neat TFAA provided complete conversion to the product which was isolated in 95% yield after simple precipitation in cold water on 15 g scale multiple times with high reproducibility. Resolution of the enantiomers by crystallization of their diastereomeric salts did not provide any enantioenriched material, neither did conversion to various diastereomeric amides.

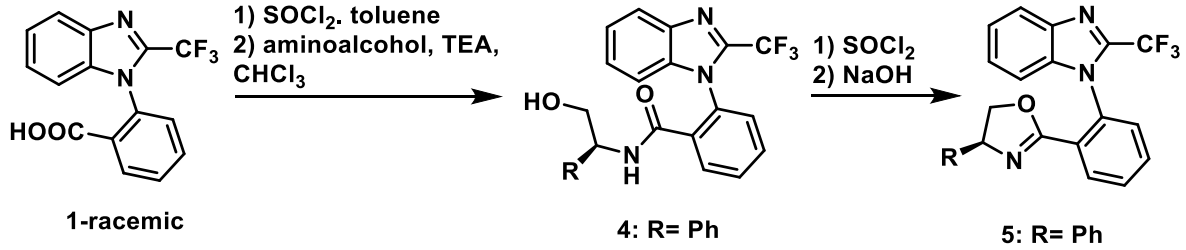

Scheme 2 Two step synthesis of oxazoline **15**

The resolution was then performed by conversion to less flexible oxazoline derivative **5** (Scheme 2). Two step cyclization of hydroxyamide **4** using $SOCl_2$ followed by base promoted cyclization provided full conversion to diasteremeric oxazoline **5** which were then separated using common column chromatography with 60 and 80% yields for each diastereomer.

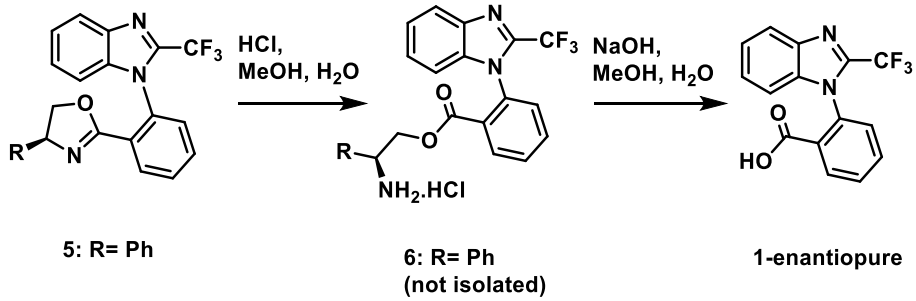

Scheme 5 Hydrolysis of oxazolines **15**

The oxazoline **5** was then hydrolyzed using HCl promoted ring opening followed by NaOH hydrolysis of the resulting ester **6** (Scheme 5) and enantiopure acid **1** was isolated by precipitation from water in 60-70% yield. The enantiomeric purity was confirmed by chiral SFC analysis. Conformational stability was tested as well: TBBA is stable up to 65 °C. At 65°C slow racemization was observed (2% racemization after 16 hours) which was further sped up with the increase of temperature (full racemization after 3 hours at 140°C)

The absolute configuration of the chiral axis was determined by single crystal X-Ray crystallography of the derivative **11** prepared from enantiopure TBBA (Figure 11).

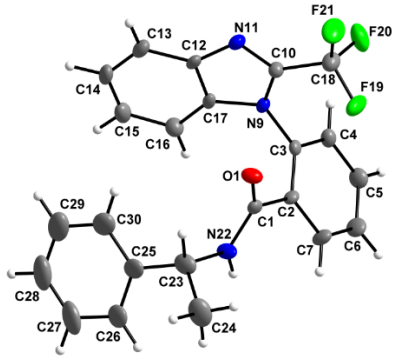

Figure 11 The molecular structure of **7** (CCDC 1871600) together with the atom labelling scheme. The thermal ellipsoids are drawn at the 50% probability level. Only one of the seven crystallographically independent molecules is depicted for clarity.

Analysis of α-chiral amines and alcohols

^{1}H-NMR analysis

Compounds **7-18** (Figure 12) were prepared by EDC/HOBt coupling and isolated in 50-98% yields with after column chromatography. The shielding effects are displayed as $\Delta\delta^{PM}$. $\Delta\delta^{PM}$ is calculated by subtraction of the chemical shift of the given signal in *M*-diastereomer from the chemical shift of the same signal in *P*-diastereomer:

$$\Delta\delta^{PM} = \delta L1(P) - \delta L1(M)$$

If the $\Delta\delta^{PM} < 0$, the given proton is shielded in the *P*-diasteromer and analogously, if $\Delta\delta^{PM} > 0$ is deshielded in the *P*-diasteromer. This information then allows to locate the given substituents in space to deduce the correct configuration with the aid of conformational model (vide infra).

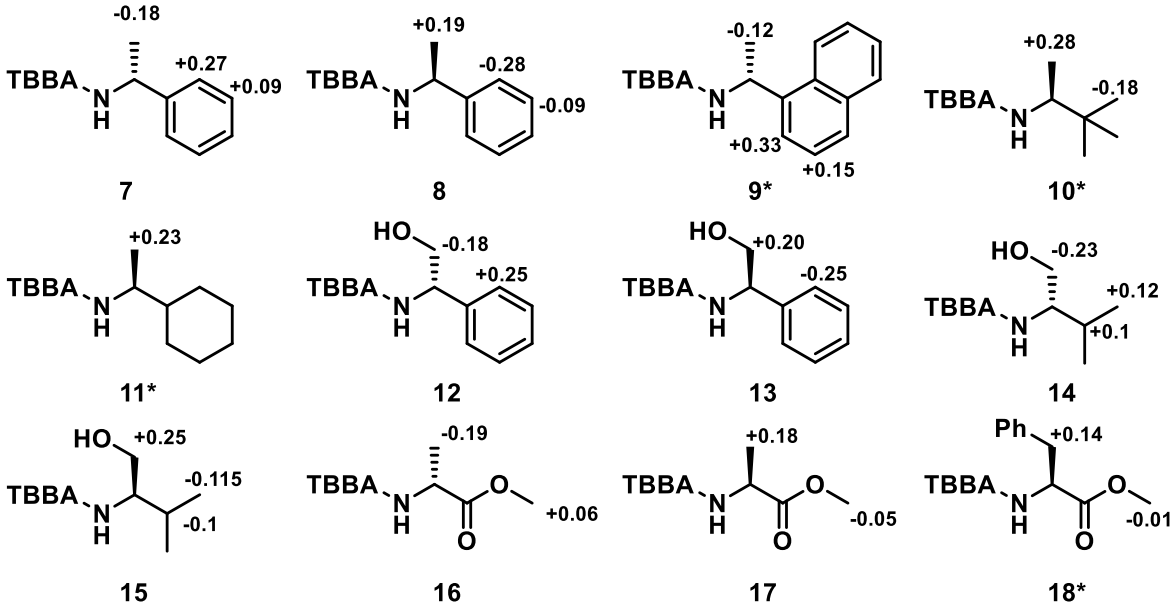

Figure 12 Observed $\Delta\delta^{PM}$ for compounds **7-18** *Compounds **9-11** and **18** were prepared by David Profous.

Furthermore, esters **19-27** (Figure 13) were prepared in 50-86% yields. Different acylation conditions were used for synthesis of esters: dicyclohexylcarbodiimide (DCC) and dimethylaminopyridine (DMAP) in DCM.

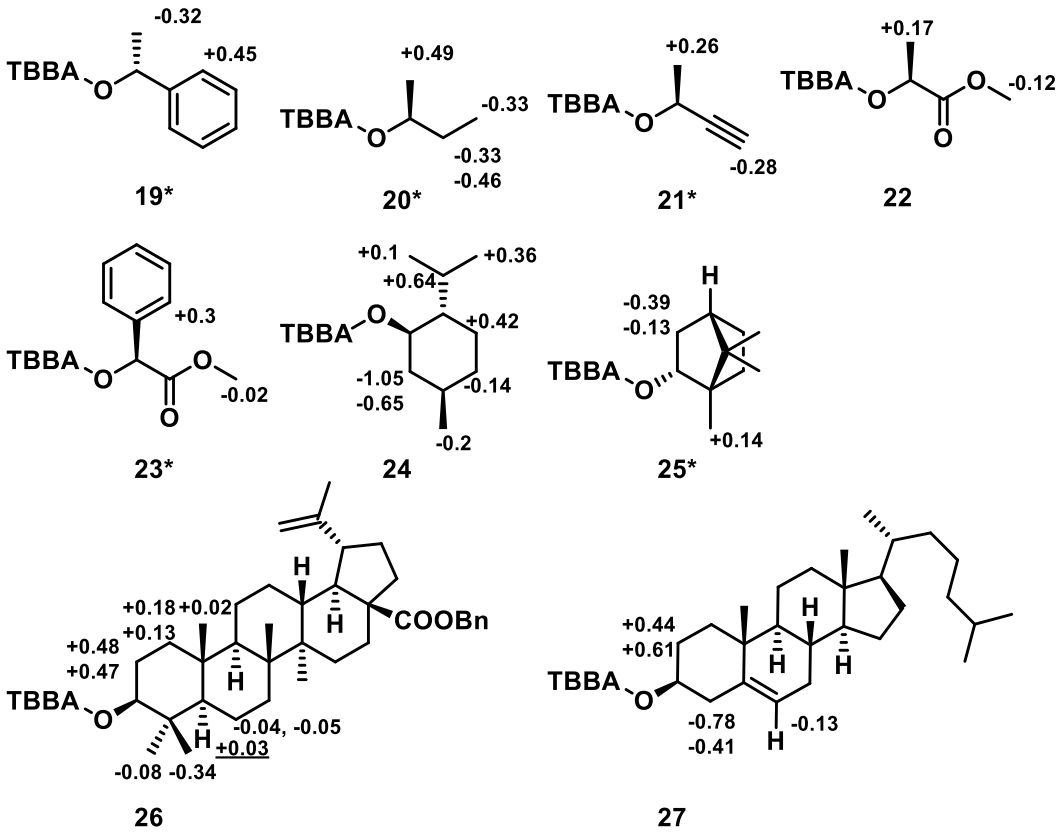

Figure 13 observed $\Delta\delta^{PM}$ for esters **19-27,** *compound was prepared by David Profous

^{13}C NMR analysis

In addition, ^{13}C NMR spectra were analyzed as well. Compared to ^{1}H, the use of ^{13}C for the configuration assignment is limited. This limitation comes from the two major factors: a) larger amounts of sample and time are required to obtain high quality ^{13}C NMR spectra and b) the $\Delta\delta^{RS}$ values observed in ^{13}C spectra are in most cases small when the whole scale (0-200 ppm) of ^{13}C NMR spectra is considered.[27] Nevertheless, modern NMR techniques allow to obtain high quality NMR spectra even from tiny amounts of sample.

To our delight, analyzed $^{13}C\Delta\delta^{PM}$ data followed the general trend observed in ^{1}H spectra. The easily distinguishable methyl groups in compounds **7-11**, **16-17** showed $^{13}C\Delta\delta^{PM}$ absolute values between 0.14 and 0.4 ppm. The methylene signals in **12-15** displayed differences 0.3 and 0.33 ppm. On the other hand, the methylene carbons in **16** were shifted by 0.08 ppm. Most importantly, the alkynyl carbon in **21** without protons demonstrated a difference of 0.45 ppm. Furthermore, in accordance with the general trend, the more remote methylester signals in **16-18, 22- 23** displayed low $^{13}C\Delta\delta^{PM}$ values ranging from 0.04 (compounds **16**, **18**) to 0.06 (compounds **22**, **23**) ppm. Despite the fact that observed values are small when the entire ^{13}C NMR chemical shift range is considered, in most cases, the $\Delta\delta^{PM}$ value was high enough to assign the absolute configuration, especially, when results were coupled with ^{1}H chemical shifts data.

Conformational model for assignment of absolute configuration by ^{1}H or ^{13}C NMR

Based on the data, conformational model was devised, which allows for assignment of the absolute configuration of tested compounds (Figure 14).

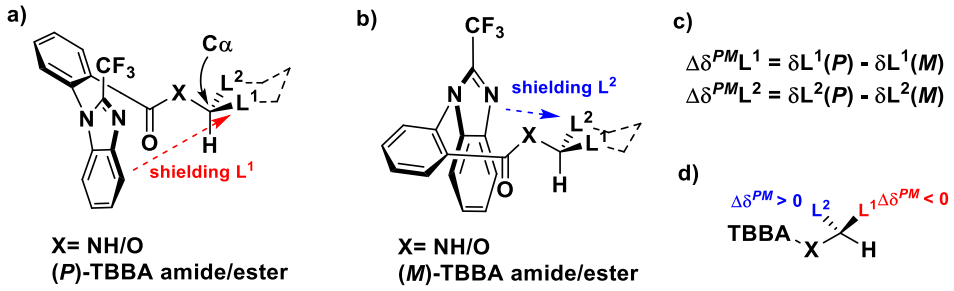

Figure 14 Model for assignment of the absolute configuration if chiral secondary alcohols and primary amines a) (*P*)-TBBA amide/ester b) (*M*)-TBBA amide/ester c) calculation of $\Delta\delta^{PM}$ d) simplified model

In this proposed model, the benzimidazole and phenyl rings are perpendicular to each other. The carbonyl group is oriented opposite compared to the trifluoromethyl group. The proton at Cα is in *syn*-periplanar position to the carbonyl group which orients one of the the substituents L^1 and L^2 in front of the benzimidazole ring, which projects the shielding effect on this substituent (figure 14a/14b). This projected shielding effect causes the chemical shift of the substituent to be shifted upfield. In the example on Figure 14, assuming the displayed configuration, substituent L^1 in the (*P*)-derivative (Figure 14a) is going to have lower chemical shift compared to the L^1 in the (*M*)-derivative (Figure 14b). Analogously, the chemical shift of the L^2 substituent in the (*P*)-derivative is going to be higher compared to the same substituent in the (*M*)-derivative.

These changes on chemical shifts can be expressed as the $\Delta\delta^{PM}$ parameter, which was calculated according to equation shown in Figure 10c. Based on the observed $\Delta\delta^{PM}$ values, the substituents L^1 and L^2 can then be located in space and absolute configuration can be deduced. If the substituent has a negative $\Delta\delta^{PM}$ value (as does L^1 in Figure 14), it is located above the plane of coplanar amide/ester function and Cα. If the substituent posess a positive $\Delta\delta^{PM}$ value (as does L^2 in Figure 10), it is located bellow the plane. The simplified model is shown in Figure 14d.

^{19}F-NMR analysis

Attempts to correlate the ^{19}F spectra with the absolute configuration were conducted as well. The ΔCF_3 was calculated analogously to the $\Delta\delta^{PM}$ parameter using following equations:

$$\Delta CF_3 = \delta L1^{19F}(P) - \delta L1^{19F}(M)$$

by substracting the chemical shift of the ^{19}F spectrum of the (*M*)-diastereomer from the ^{19}F spectrum of the (*P*)-diastereomer. The results are summarized in Figure 15 and 16.

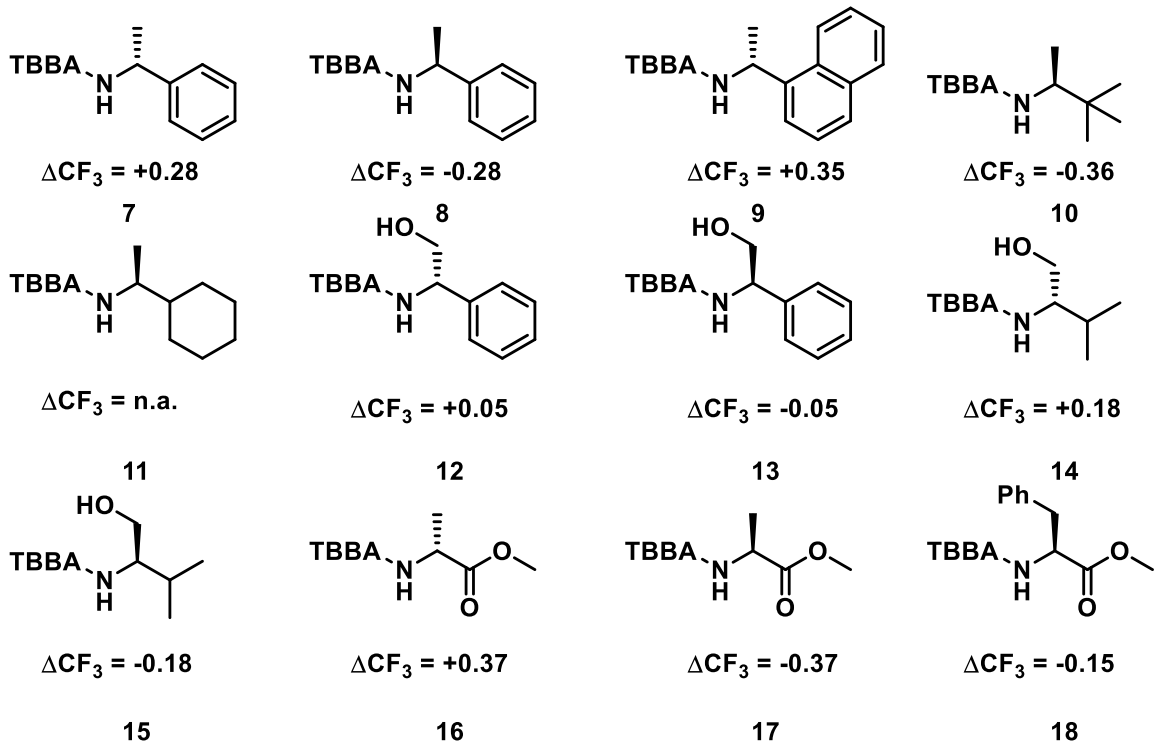

Figure 15 Observed ΔCF_3 for amides **7-18,** na: not available

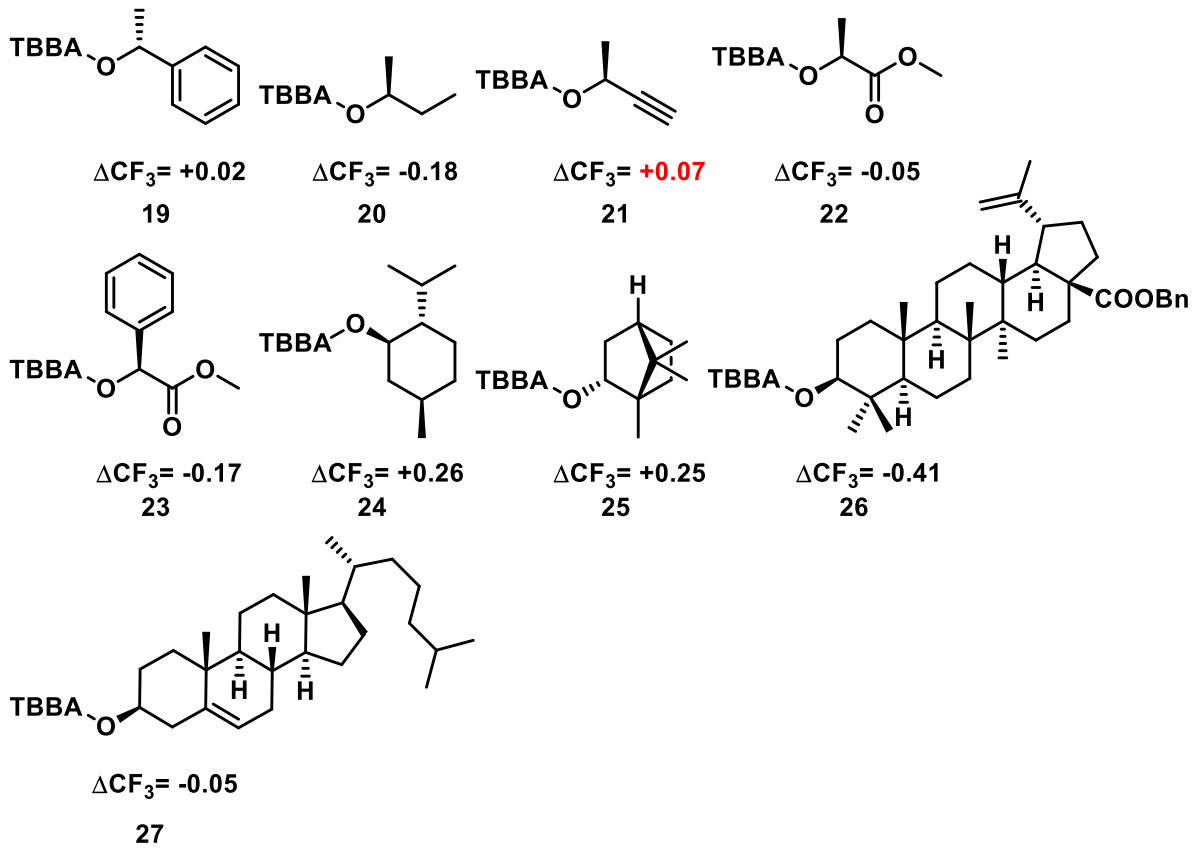

Figure 16 observed ΔCF_3 for esters **19-27**

The difference in the ^{19}F spectra are likely caused by shielding or deshielding of the trifluoromethyl group by the substituents L^1 and L^2 of the analyte. The shielding cones are displayed in Figure 17.[49,50]

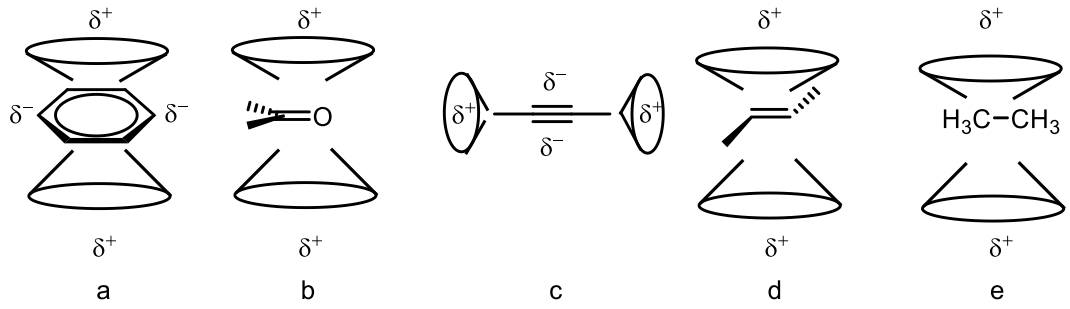

Figure 17: shielding cones a) aryl b) carbonyl group c) alkyne d) alkene e) alkane

δ^+: shielding δ^-: deshielding

Those shielding effects projected by substituents shield or deshield the CF_3 group (Figure 18) and, then, it is observed as a difference of the ^{19}F chemical shifts (Figure 15 and 16).

This model explains the observed differences of ^{19}F spectra and, furthermore, reveals the origin of the anomalous value for alkyne **21**, where the anisotropic effect of the alkyne is different. This difference is displayed in Figure 18, where the shielding effects of amide (***P***)**-8** and ester (***P***)**-21** are compared.

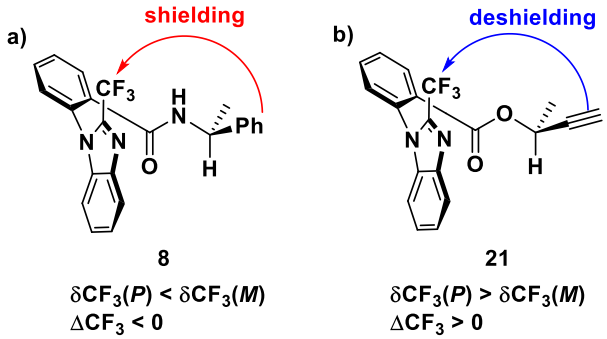

Figure 18 Possible explanation for observed ΔCF_3 values of compounds **8** and **21**

As can be seen in Figure 18, the same arrangement of the substituents in space causes the different chemical shifts of ^{19}F spectra. The phenyl ring causes shielding of the CF_3 group in the (***P***)**-8** and, therefore, it resonates upfield. For this reason, a lower chemical shift was observed compared to the (***M***)**-8** and, as a result, the negative ΔCF_3 was obtained after subtraction. The alkyne moiety in (***P***)**-21**, although located at the same position in space as the phenyl ring in (***P***)**-8**, causes deshielding of the CF_3 group. Then the higher chemical shift is observed, therefore a positive ΔCF_3 is obtained.

Since the simple alkyl group cause the shielding effect as well,[50,51] the observed ΔCF_3 in aliphatic derivatives **10, 14, 15, 20, 24-27** can be also explained. Our explanation is based on the hypothesis that the branched or longer aliphatic chains project stronger shielding effect compared to unbranched or shorter chains. The lack of branching or multiple bonds on the A-ring of the cholesterol derivative is the likely cause of the low observed ΔCF_3 (-0.05).

Analysis of β-chiral alcohols and amines

After the analysis of α-chiral compounds was finished, we turned our attention towards more complex β-chiral compounds. The analysis of this type of compounds is more complicated due to following reasons:[9,11,52,53]

a) Additional carbon in the structure highly increases the conformational flexibility; therefore, the NMR relevant conformer is less prevalent compared to α-chiral compounds.
b) The chiral center is located further away from the group projecting the anisotropic shielding effect.

For those reasons, the observed $\Delta\delta^{RS}$ values are smaller compared to the α-chiral derivatives and the only CDA that is able to produce sufficient and reliable differentiation is 9-AMAA.While MPA or MTPA work in some cases, the differentiation is significantly smaller compared to 9-AMAA and in some cases no differences in chemical shifts are observed.[9,11]

^{1}H NMR analysis

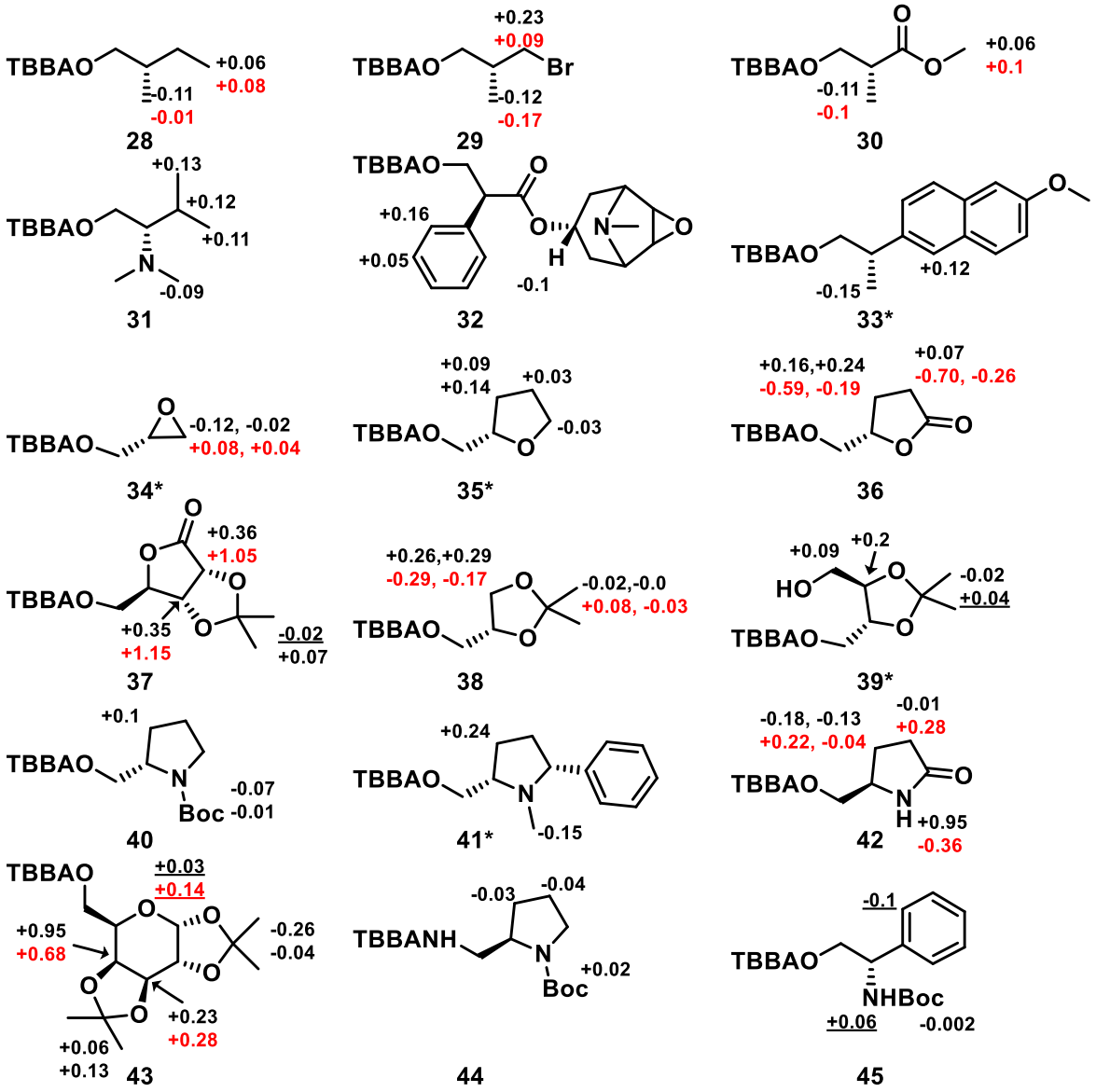

Figure 19 Observed $\Delta\delta^{PM}$ for compounds **28-45,** black: TBBA, red: 9-AMAA, anomalous values are underlined*Compound was prepared by undergraduate student David Profous.

** 9-AMAA esters **34**, **38**, **42** were prepared from the starting materials with opposite absolute configuration compared to TBBA esters. Therefore, the sign of the $\Delta\delta^{RS}$ is opposite compared to TBBA

Interestingly, (*S*)-Boc-Phenylglycinol **77** was not in accordance with the proposed model, and the opposite configuration was observed. This limitation of the method was likely caused by the sterically demanding Boc group, which impacts the conformational equilibrium. This seemed to be in the agreement with the fairly low $\Delta\delta^{PM}$ values for Boc-substituted derivatives **40** and **44**.

Conformational model for assignment of absolute configuration by 1H or 13C NMR

Based on the experimental data, conformational model (Figure 20) for assignment of the absolute configuration was proposed. At first, the proton at the chiral center (Cα) is in *anti*-periplanar conformation to the carbonyl group.

This allows the benzimidazole to project the shielding effect towards the L^2 substituent (Figure 20a). Naturally, in the (*M*)-diastereomer (Figure 20b), the shielding effect is produced towards the substituent L^1. Analogously to the α-chiral compounds, the $\Delta\delta^{PM}$ parameter is calculated following the equation in Figure 20c. The simplified model is shown in Figure 20d: if the substituent has $\Delta\delta^{PM}$ less than zero, it is located above of the carbonyl-Cα plane while if the $\Delta\delta^{PM}$ is higher than zero, the substituent is located under the plane.

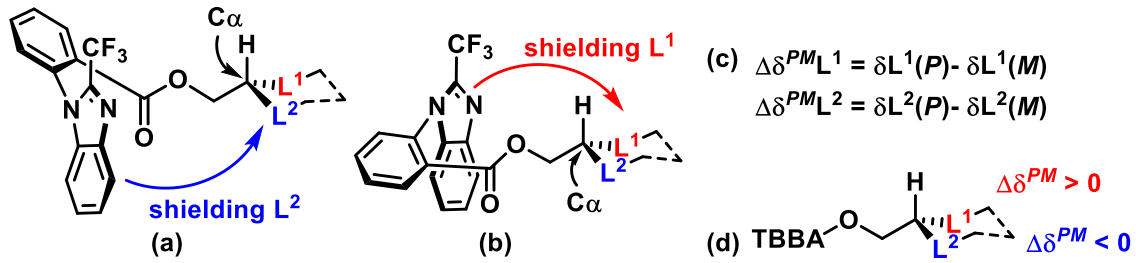

Figure 20 Conformational model for assignment of absolute configuration of chiral primary alcohols a) (*P*)-TBBA ester b) (*M*)-TBBA ester c) calculation of $\Delta\delta^{PM}$ d) simplified model.

To further strenghten the proposed model, DFT calculations were performed using Spartan 16 software using ester **60** as the model compound. The populations of theoretical conformers were calculated with the molecular mechanics model MMFF. Depending on the total number of theoretical conformers, this was followed by sorting of the conformation candidates with relative energies lower than 10−20 kJ/mol. The energies of sorted candidates at the ground state in the nonpolar solvent were calculated using density functional theory (B3LYP, 6-31G*) to find the lowest energy conformer.

Investigation of the Boc-protected aminoalcohols

Because boc protected aminoalcohol **45** displayed anomalous $\Delta\delta^{PM}$ values leading to incorrect configuration, we decided to further investigate this class of compounds. At first, small library of Boc-protected aminoalcohols was synthesized to confirm, if the unexpected conformations of compound **45** are only anomaly or if there is an ongoing trend (Figure 21)

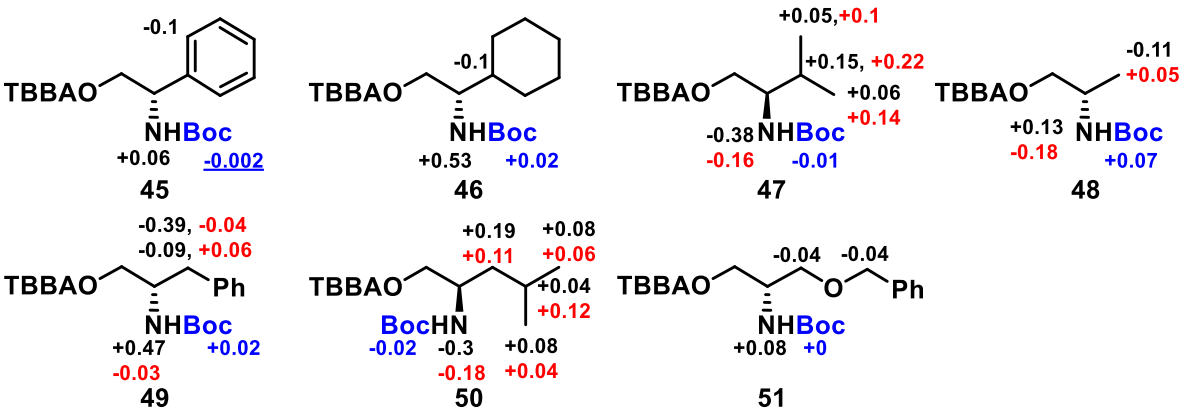

Figure 21 Analyzed Boc-aminoalcohols and their $\Delta\delta^{PM}$ values. Underlined values follow the previously proposed model. 9-AMAA values[11] shown in red. 9-AMMA esters **47** and **50** were prepared from alcohol with opposite configuration compared to TBBA ester. $\Delta\delta^{PM}$ of the Boc group is displayed in blue for higher clarity

Analysis of phenylglycinol derivatives

Because the Boc-protected aminoaclohols clearly displayed preference for different conformation states compared to the previously developed model for β-chiral alcohols, the library was further expanded with various *N*-substitued phenylglycinols (Figure 22) to further investigate the conformational model.

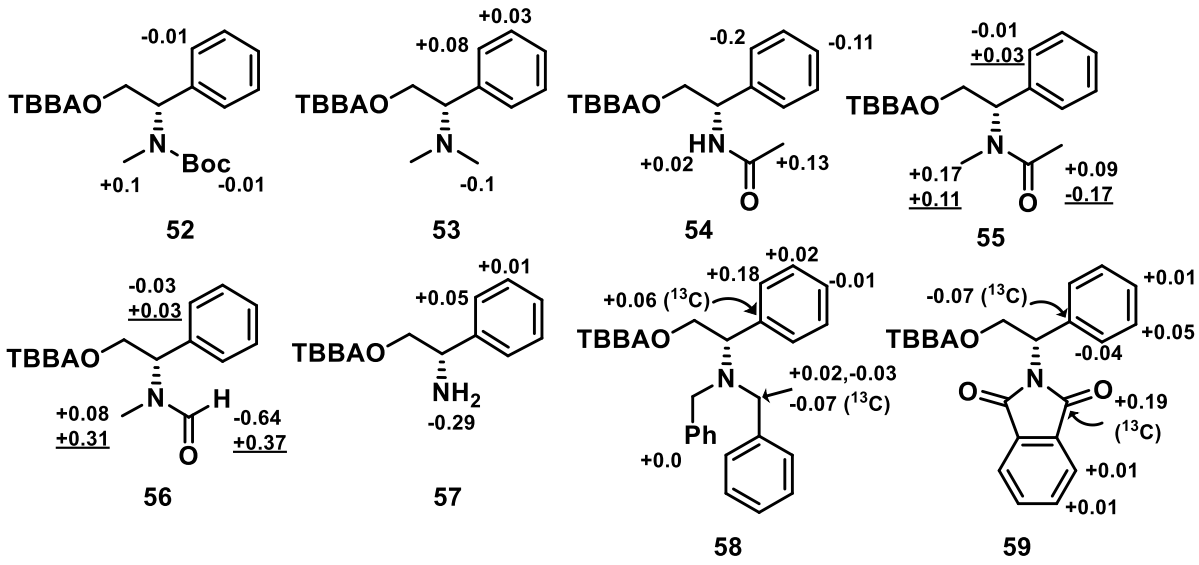

Figure 22 Observed $\Delta\delta^{PM}$ in derivatives **52-59**, minor rotamers are underlined

Investigation of the possible bonding interactions

Based on those experiments we suspected hydrogen bond between boc hydrogen and fluorine which would favor opposite conformation. Furthermore, interaction between fluorine and boc carbonyl [66,67] could not be ruled out as well as repulsion between partially negatively charged carbonyl oxygen and trifluoromethyl group .Further NMR measurements were conducted with compounds **45-52** as model substrates in acetone-D_6 which was considered as a competing hydrogen bond acceptor and further in $CDCl_3$ with methyl trifluoroacetate (TFAOMe) as a source of external trifluoromethyl group which could interact with the Boc carbonyl group of the substrates. Observed $\Delta\delta^{PM}$ values are depicted in Figure 23.

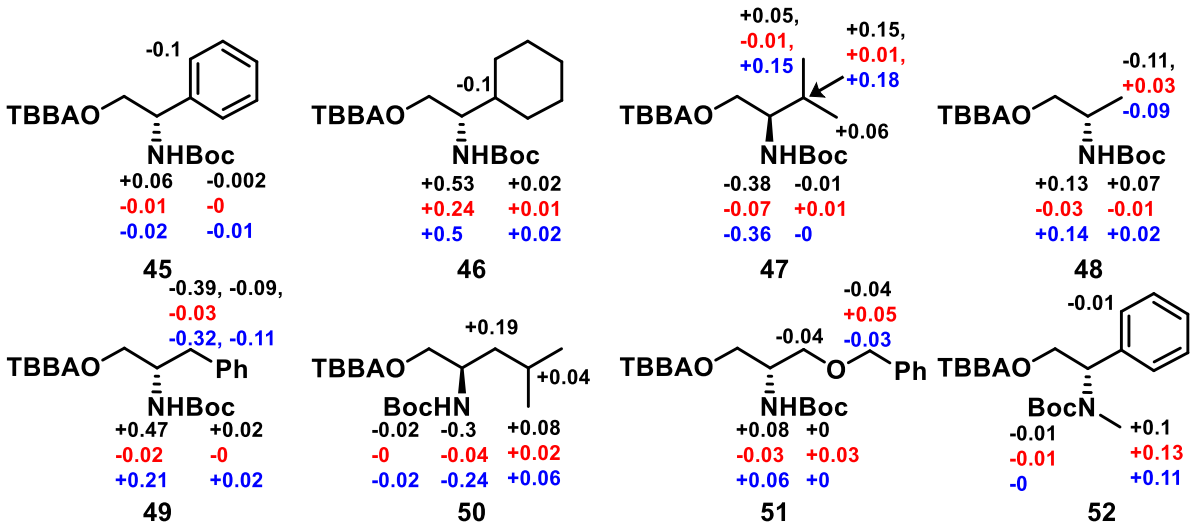

Figure 23 Observed $\Delta\delta^{PM}$ for compounds **45-52** in various solvents, black: $CDCl_3$, red: acetone-D_6, blue: $CDCl_3$+ TFAOMe

Those results suggest the hydrogen bond might be present in the compounds although its likely not the only cause of the obtained opposite configuration in the Boc-protected aminoalcohols. This can be seen in the examples on Figure 23. Conducting the NMR measurement in acetone-D_6 had significant effect on the observed $\Delta\delta^{PM}$, although not all of the derivatives displayed fully inverted $\Delta\delta^{PM}$. This suggests the presence of other interactions. The previously mentioned F…CO interaction is less likely because the addition of TFAOMe (as an external CF_3 source) had only marginal effect on the chemical shifts., Steric effects could play an important role as well although sterically dibenzyl derivative **58** (Figure 22) followed the proposed model eventhough it displayed an anomalous

value at one of the benzylic protons while ^{13}C spectra showed the expected sign. Pthalimide **59** (Figure 25) displayed mix of positive and negative $\Delta\delta^{PM}$ values which would make the assignment of absolute configuration impossible or at least very speculative eventhough it does not contain acidic NH within its structure. The sterically less demanding derivatives **53** and **57** (Figure 22) fully follow the proposed model. The N-methyl derivatives **52**, **55** and **56** display mix of positive and negative $\Delta\delta^{PM}$ values due to the complex conformational equilibrium with various amide rotamers. Very likely all those effects are combined and play a role in the conformational equilibrium. In the case of Boc-protected or acetylated aminoalcohols, the hydrogen bond is the reason for preference of different conformers. However, based on the structure of the specific substrate, the electronic repulsion could predominate.

Computational investigation of the conformation of N-boc aminoalcohols

Last, more complex, in-silico modeling was performed using Spartan software. Conformer distribution was calculated with density functional theory (ωB97X-V/6-311+G(2df,2p)[6-311G*]) using ωB97X-D/6-31G* geometry.[68] Boc-derivative **77** was used as a model substrate. In general, lower number of conformers was observed. This is likely due to the method which included three subsequent re-calculations and subsequent removal of high energy conformers. Based on the experimental results and the in-silico modeling we propose alternative conformation model for N-Boc aminoalcohols (Figure 24).

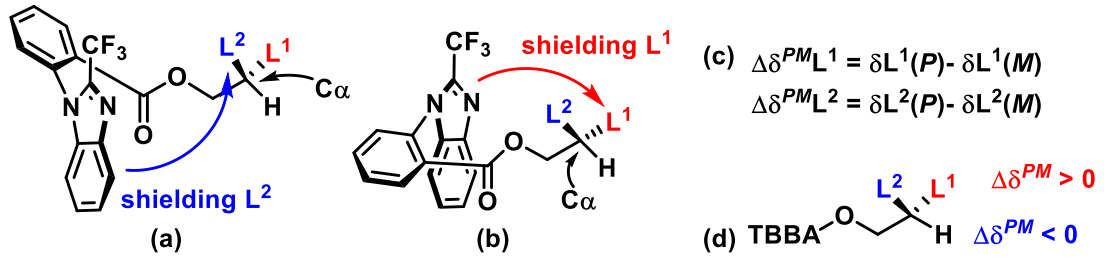

Figure 24 Conformational model for analysis of the Boc-substituted derivatives

In this model, the proton at Cα and the ester carbonyl group are in *syn*-periplanar conformation which moves one of the substituents into the shielding zone of the benzimidazole (Figure 24a/b). Compared to the previously devised model for β-chiral esters, the rotation around Cα-CH_2O bond causes the shielding effect to be projected towards the opposite substituents. The shielding/deshielding $\Delta\delta^{PM}$ is calculated in a same way as in the other models (Figure 24c) and the simplified model is shown on Figure 24d). Importantly, the model is suitable for compounds containing NHCOR (ie. Amide, carbamate) as one of the substituents. The presence of the more acidic hydrogen causes the likely formation of hydrogen bonds which change the preferred conformer which has effect on the observed $\Delta\delta^{PM}$ values.

Conclusion

In conclusion, novel CDA for configuration assignment by NMR was developed. The conformational model was validated on a set of seventeen α-chiral esters and amides which allows the configuration assignment by means of ^{1}H, ^{13}C, and ^{19}F NMR spectroscopy. Similar model was developed for β-chiral compounds and was validated on a set of eighteen compounds. Seventeen of them fully followed the model while in one case, an opposite configuration was obtained. Further investigation of 15 derivatives revealed different conformation preference for *N*-Boc aminoalcohols and *N*-acyl aminoalcohols. This conformational preference is likely caused by the hydrogen bond between NH and CF_3 or benzimidazole nitrogen as suggested by in silico modelling. This was confirmed by ^{1}H NMR spectra measured in acetone-D_6 as an external hydrogen bond acceptor which caused significant changes in observed $\Delta\delta^{PM}$ compared to $CDCl_3$. Use of TFAOMe as an external CF_3 group did not provide any improvement compared to acetone-D_6. Based on experimental data and in silico modelling, alternative conformational model was proposed for N-acyl aminoalcohols. Unfortunately, compunds of the R-N-COR or RCO-N-OCR type of functional groups did not follow any proposed models and provided highly anomalous $\Delta\delta^{PM}$. The removal of the protecting group changed the conformation equilibrium again. The unprotected compound followed the unmodified model for β-chiral compounds which allows for two subsequent analyses one of the protected compounds using the modified model and another one using deprotected aminoalcohol ester and the unmodified model. Unfortunately, the ^{19}F NMR yields inconclusive results and therefore cannot be recommended for this type of compounds.

Results and discussion: Project catalysis

Design of the ligand

Two structures of the ligand (Figure 25) were envisioned at first. The benzimidazol-2-one/thione **53** which was reported multiple times as a ligand for Pd-catalyzed or organocatalytic reactions.[69–72] The benzimidazole-pyridine ligand **54** is based on pyridine-oxazoline catalyst developed by Kočovský.[40]

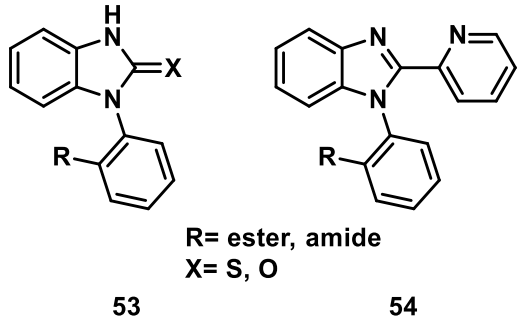

Figure 25 Proposed structures of the ligands

The cyclization-based synthesis was developed (Scheme 6) for the synthesis of ligands **53**/**54**.

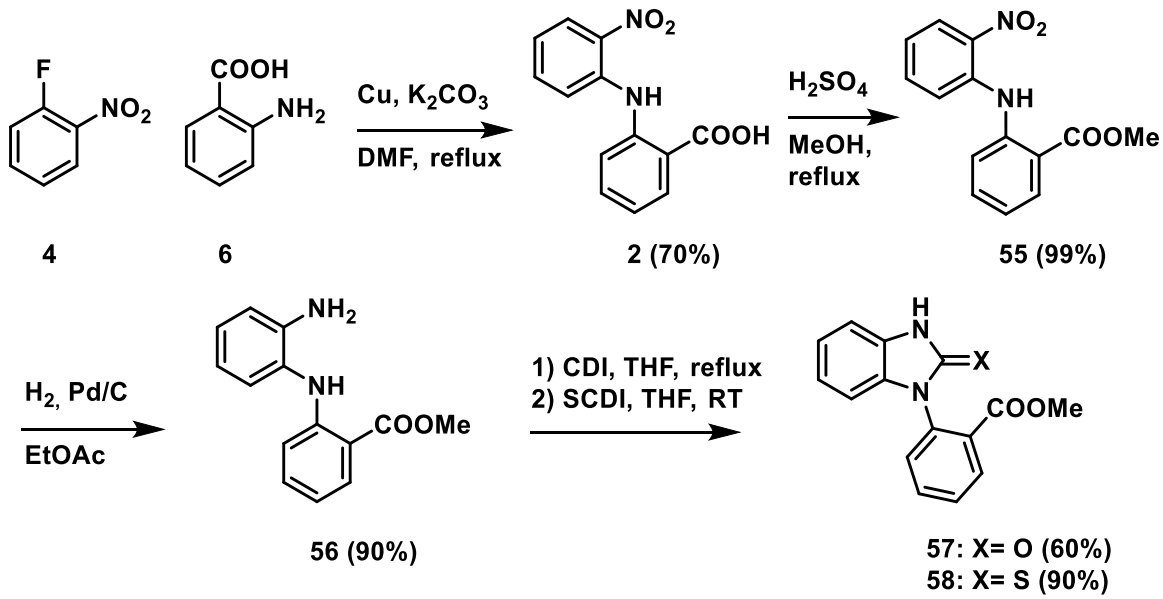

Scheme 6 Synthesis of **57** and **58**

Synthesis of pyridine-based ligand

Because the preliminary results (vide infra) did not show any catalytic activity of the compounds **57** and **58**, alternative structure **59** was developed. Synthesis (Scheme 7) starts with the intermediate **56** which was acylated with 2-picolinic acid to yield intermediate **60** which was cyclized with BF_3 to yield racemic **59**. Nitrile derivative **60** was also prepared analogously. The nitrile group would allow synthesis of various other derivatives. Most importantly, diastereomeric oxazoline **61** (Figure 27) could be prepared in one step from the nitrile, which would allow for separation of the atropoisomers by the same method as was used for separation of TBBA.

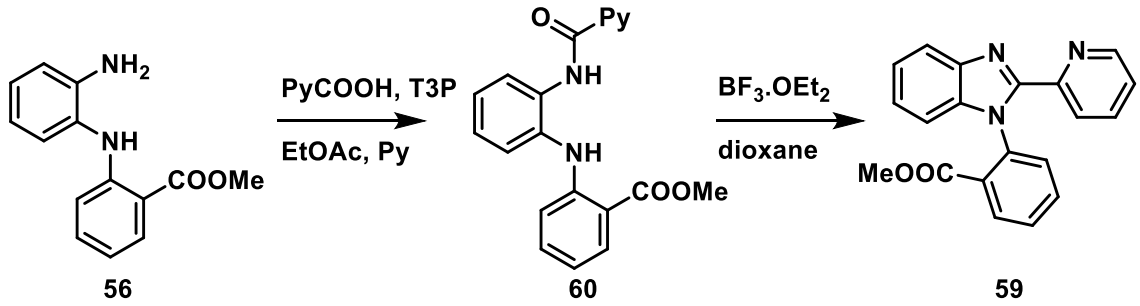

Scheme 7 Synthesis of **59**

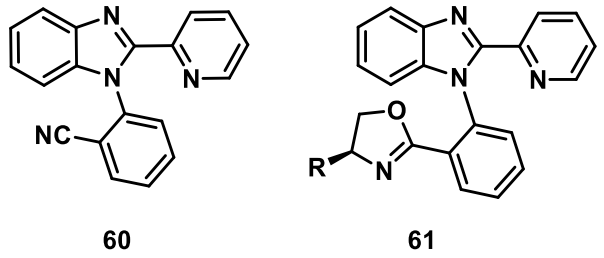

Figure 26 Structure of nitrile **60** and oxazoline **61**

The resolution via formation of oxazolines was possible, but only small amounts. Therefore, further structural diversification was not possible, howeer the ester was resolved by crystallization with dibenzoyltartaric acid in acetonitrile.

Modifications of the structure of the ligand 128

For further modifications, ester **59** was hydrolyzed to acid **62** using LiOH (Scheme 8). Unfortunately, the acid was found to be racemic after further derivatization to amide **63** and **64** (scheme 9).

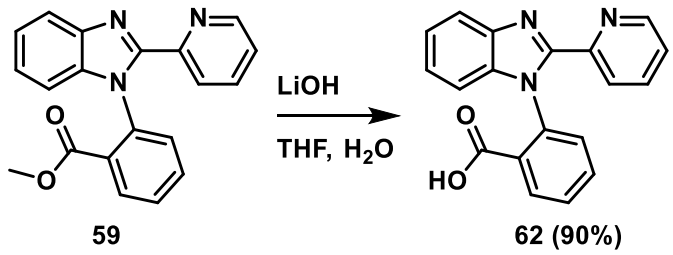

Scheme 8 Hydrolysis of ester **128**

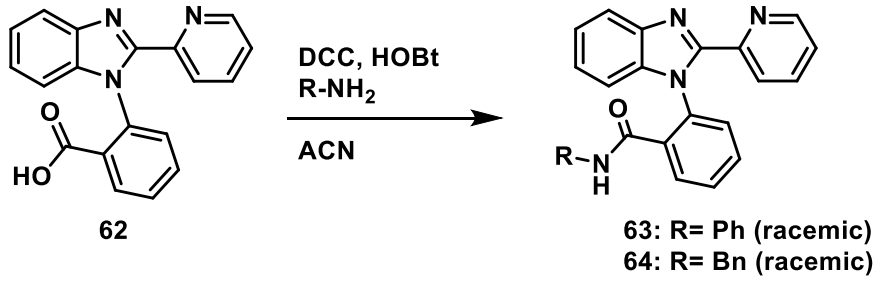

Scheme 9 Amidation of **62**

Multiple other amides were prepared (Figure 27) as racemates and some were separated on preparative HPLC with chiral stationary phase by Ondřej Kurka, Ph.D. from Department of Analytical chemistry at our university. This separation yielded enough material for reduction experiments (vide infra). However, due to a lack of time and COVID-19 only ligands **63** and **64** were separated. Ligands **63-67** were prepared by simple amidation using

DCC/HOBt. Ligand **68** was prepared by two step synthesis. First, *ortho*-phenylene diamine was acylated with acid **62** using DCC/HOBt and then the amide was cyclized into benzimidazole using $BF_3.OEt_2$ mediated cyclization.[74]

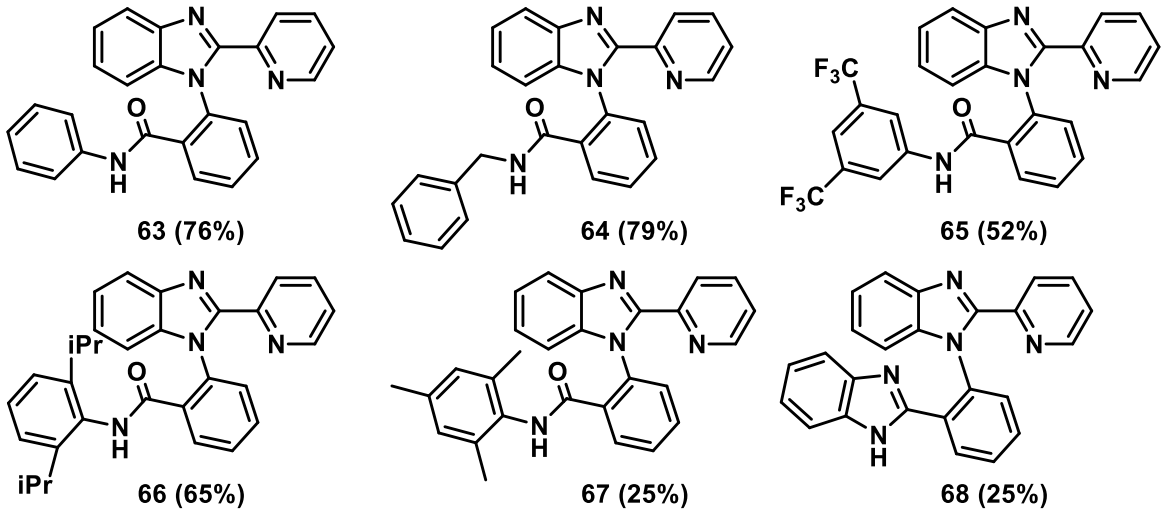

Figure 27 Prepared amide ligands

Further modifications of the structure were attempted (Scheme 10). Addition of phenyllithium yielded triarylmethanol derivative **69** in high yield and purity with no racemization. Reduction of methylester **59** with $LiAlH_4$ in diethylether provided hydroxymethyl ligand **70** with no loss of enantiomeric purity. Transesterification using NaH and isopropylalcohol yilded ligand **71** again with no loss of enantiomeric purity. The oxidation towards N-oxide **72** provided only racemic product.

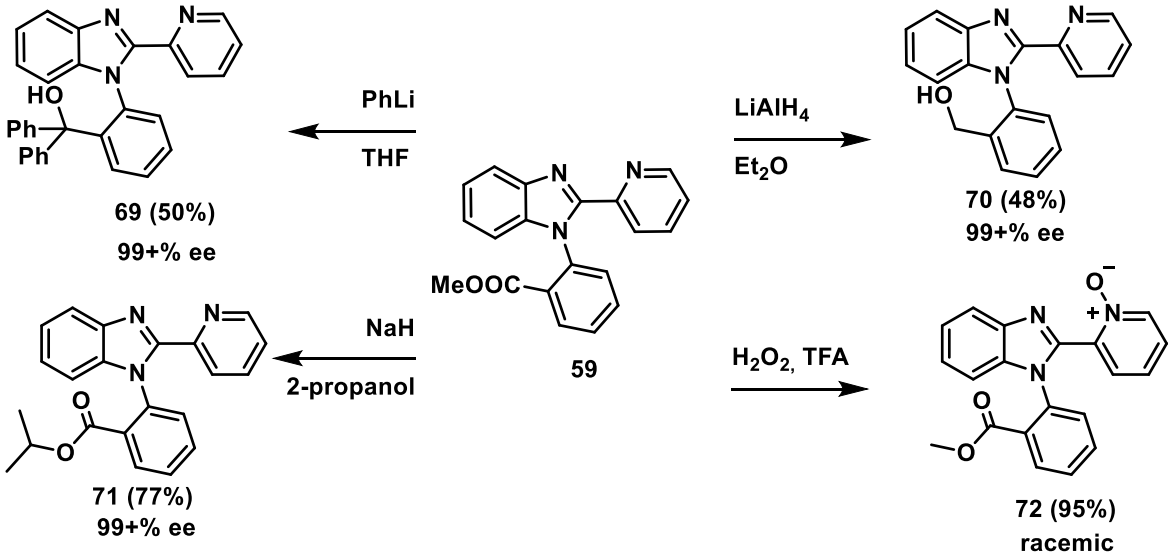

Scheme 10 Structural modifications of ligand **59**

Reduction experiments

At first, reduction attempts to reduce acetophenone into 1-phenylethan-1-ol failed and no conversion was observed. Afterwards, we turned our attention towards reduction of imines. Imine **73** was used as a model substrate for reduction (Scheme 11). Multiple ligands were tested and the results are summarized in Table 1.

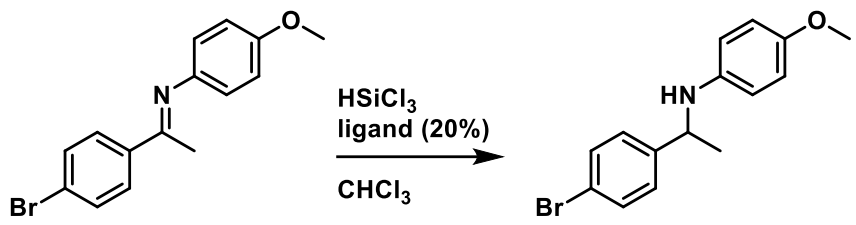

73 74

Scheme 11 Model reaction of imine reduction for ligand screening

Table 1 Ligand screening

entry	ligand	Loading (mol%)	solvent	Er.	yield
1	57	20	$CHCl_3$	--	--
2	70	20	$CHCl_3$	--	--
3	71	20	$CHCl_3$	--	--
4	59	20	$CHCl_3$	67/33	70%
5	61	20	$CHCl_3$	65/35	65%
6	63	20	$CHCl_3$	81/19	70%
7	64	20	$CHCl_3$	80/20	70%
8	69	20	$CHCl_3$	82/18	65%
9	59	20, TES used instead of $HSiCl_3$	$CHCl_3$	--	--

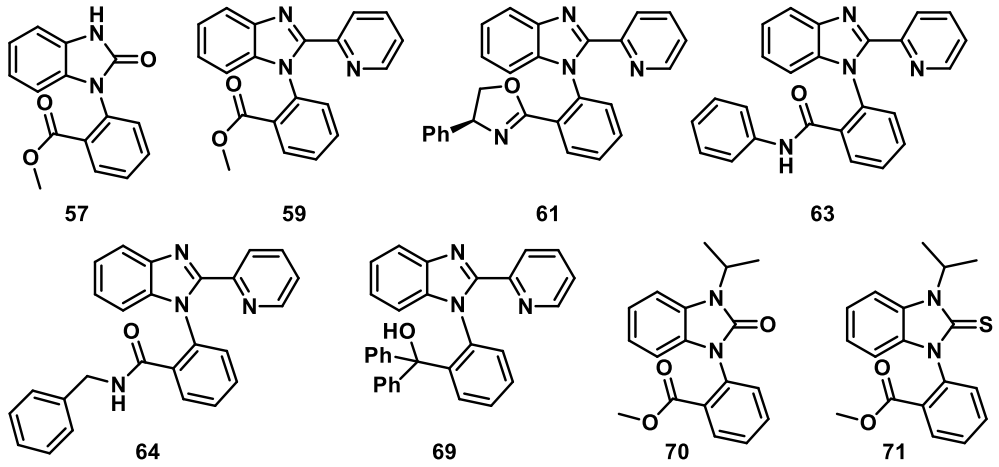

Further experiments were highly complicated by the available amounts of the ligands. For this reason, we used methylester **59** as a model ligand for optimization of the procedure and then the optimized conditions were used with other ligands.

Reducing the ligand loading to 10% (Table 2, entry 2), 5% (entry 3), or 1% (entry 4) did not have a significant impact on the enantioselectivity contrary to the expectations. Furthermore, it seemed that the reduction of the ligand loading proved to be beneficial (compare entry 1 and 4).

Table 2 Effect of ligand loading on the reduction

entry	ligand	Loading (mol%)	solvent	Er.
1	59	20	$CHCl_3$	69/31
2	59	10	$CHCl_3$	72/28
3	59	5	$CHCl_3$	73/27
4	59	1	$CHCl_3$	74/26
5	59	1	$CHCl_3$	75/25
6	64	1	$CHCl_3$	75/25
7	69	1	$CHCl_3$	Slow reaction

Next, the solvent effect was tested (Table 3). At first, reaction was conducted in dichloromethane (entry 2). Slight improvement in enantioselectivity was observed compared to chloroform (entry 1). Changing solvent to toluene unexpectedly improved the enantioselectivity of the reduction to 60% enantiomeric excess (85:15 enantiomeric ratio) (entry 3). Similar results were obtained after reproducing the experiment (entry 4). The expected role of π-π interactions to stabilize the transition state[75] was not proven although it has positive effect in combination with ligand **59**.

Table 3 Solvent effect on the reduction

Entry	**ligand**	**Loading (mol%)**	**solvent**	**Er.**
1	59	1	$CHCl_3$	74/26
2	59	1	DCM	77/23
3	59	1	toluene	85/15
4	59	1	toluene	83/17
5	63	1	toluene	80/20
6	64	1	toluene	76/25
7	69	1	toluene	85/15
8	71	1	toluene	72/28
9	59	5	toluene	63/37

Last, other imines **75-80** (Figure 28) were tested with using the optimized conditions (1 mol% of ligand, toluene, RT). The results are summarized in Table 34. The reduction of dimethoxyimine **75** yielded the resulting amine in 60% yield and moderate enantioselectivity (er 73/27) (entry 1). The reduction of the nitro-methoxy derivative **76** proceed in similar manner with moderate enantioselectivity (e.r. 78/22) and yield 65% (entry 2). Unfortunately, only decomposition to the acetophenone and aniline was observed in the case of compounds **77** and **78**. The exact cause is unknown since the reaction was also attempted in dry solvents with molecular sieves. Possibly, the higher steric hinderance on the aniline part plays a role. Last, the cyclic imines **79** and **80** were reduced. The imine **79** was reduced with low enantioselectivity (er. 65/35) (entry 5). The reduction of imine **80** did not proceed, possibly due to the low solubility of the imine in toluene. Further addition of chloroform to dissolve the starting material did not have significant effect and no conversion was observed (entry 6).

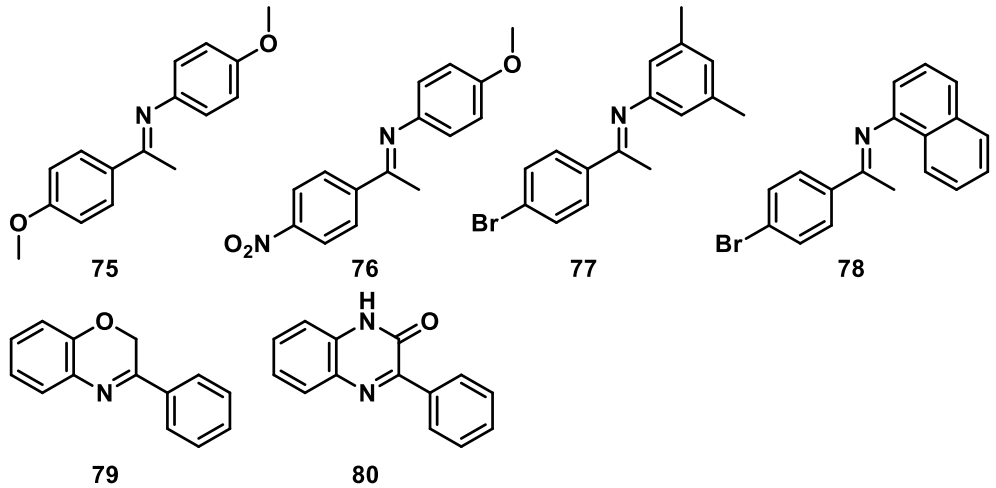

Figure 28 Structures of prepared imines

Table 4: Reduction of imines under optimazed conditions

entry	**imine**	**er**	**yield**
1	75	73/27	60 %
2	76	78/22	65 %
3	77	Decomposition	
4	78	Decomposition	
5	79	65/35	70 %
6	80	No reaction	

Conclusion

In conclusion, this thesis deals with two projects. At first, novel CDA, 2-(2-(trifluoromethyl)-1*H*-benzo[*d*]imidazol-1-yl)benzoic acid (TBBA) was developed for assignment of absolute configuration of chiral alcohols and amines. The synthesis of racemic TBBA and chiral resolution *via* conversion of diastereomeric pair of oxazolines was developed. Atroposelective approaches to the synthesis of TBBA were attempted as well but only with partial success.

Eighteen chiral secondary alcohols and α-chiral primary amines with known absolute configuration were used to evaluate TBBA.All model compounds followed the proposed conformational model for assignment of absolute configuration.

Furthermore, eighteen β-chiral primary alcohols and amines with known absolute configuration were tested as well. Seventeen of them fully followed the devised conformational model while one, (*S*)-N-Boc-Phenylglycinol, offered the opposite absolute configuration after using the previously devised conformational model.

Further investigation of this irregularity involved synthesis of six more Boc-protected aminoalcohols derivatives and eight (*S*)-phenylglycinol derivatives to probe limitations of TBBA. Syntheiss of multiple N-substituted derivatives revealsed strong influence of the N-carbonyl functionality. Hydrogen bond was revelaed by B3LYP-G-31* and ωB97X-D/6-31G* in silico modelling. This hydrogen bond was further confirmed by 1H experiments in acetone-D_6 which acts as a H-bond acceptor. Significant differences in the $\Delta\delta^{PM}$ were observed in acetone-D_6 compared to $CDCl_3$. The influence of the hydrogen bond is further increased by the presence of N-carbonyl functionality. While for compounds of the NH-COR type, alternative conformational model was devised, compounds with the R-N-COR or ROC-N-COR does not follow any of the models and therefore, alternative procedures shall be considered.

The aim of the second project was to develop new axially chiral ligands for asymmetric reduction of imines using $HSiCl_3$ as a cheap hydride source. 2-(2-Pyridyl)benzimidazole-based ligand was prepared and resolved into enantiomers on a multigram scale. Other structural modifications were attempted; however, racemization was observed in most cases and, therefore, the new ligands were prepared as racemates and some of them were resolved by chiral semipreparative HPLC. Unfortunately, external reasons did not allow for resolution of all prepared racemates.

Several reduction experiments were performed and revealed methyl 2-(2-(pyridin-2-yl)-1*H*-benzo[*d*]imidazol-1-yl)benzoate as the best ligand when used in toluene at low catalytic loadings. Multiple imines were reduced in moderate enantioselectivity and negative nonlinear effect was observed in those reductions. Some of the prepared imines were not reduced due to their poor solubility in toluene. This project remained unfinished due to time reasons.

List of used literature sources

(1) Stephens, P. J.; Devlin, F. J.; Pan, J.-J. The Determination of the Absolute Configurations of Chiral Molecules Using Vibrational Circular Dichroism (VCD) Spectroscopy. *Chirality* **2008**, *20*, 643–663.

(2) Brummel, B. R.; Lee, K. G.; McMillen, C. D.; Kolis, J. W.; Whitehead, D. C. One-Pot Absolute Stereochemical Identification of Alcohols via Guanidinium Sulfate Crystallization. *Org. Lett.* **2019**, *21* (23), 9622–9627. https://doi.org/10.1021/acs.orglett.9b03792.

(3) Rychkov, D. A.; Arkhipov, S. G.; Boldyreva, E. V. Simple and Efficient Modifications of Well Known Techniques for Reliable Growth of High-Quality Crystals of Small Bioorganic Molecules. *J. Appl. Crystallogr.* **2014**, *47* (4), 1435–1442. https://doi.org/10.1107/S1600576714011273.

(4) Spingler, B.; Schnidrig, S.; Todorova, T.; Wild, F. Some Thoughts about the Single Crystal Growth of Small Molecules. *CrystEngComm* **2012**, *14* (3), 751–757. https://doi.org/10.1039/c1ce05624g.

(5) Hoshino, M.; Khutia, A.; Xing, H.; Inokuma, Y.; Fujita, M. The Crystalline Sponge Method Updated. *IUCrJ* **2016**, *3*, 139–151. https://doi.org/10.1107/S2052252515024379.

(6) Seco, M.; Quin, E.; Riguera, R. The Assignment of Absolute Configuration by NMR †. **2004**.

(7) Latypov, S. K.; Seco, J. M.; Quinoa, E.; Riguera, R. Are Both the (R)- and the (S)-MPA Esters Really Needed for the Assignment of the Absolute Configuration of Secondary Alcohols by NMR? The Use of a Single Derivative. *J. Am. Chem. Soc.* **1998**, *120* (5), 877–882. https://doi.org/10.1021/ja9700055.

(8) Latypov, S. K.; Seco, J. M.; Quiñoá, E.; Riguera, R. MTPA vs MPA in the Determination of the Absolute Configuration of Chiral Alcohols by 1H NMR. *J. Org. Chem.* **1996**, *61* (24), 8569–8577. https://doi.org/10.1021/jo960719i.

(9) Ferreiro, M. J.; Latypov, S. K.; Quiñoá, E.; Riguera, R. Determination of the Absolute Configuration and Enantiomeric Purity of Chiral Primary Alcohols by 1H NMR of 9-Anthrylmethoxyaceates. *Tetrahedron Asymmetry* **1996**, *7* (8), 2195–2198. https://doi.org/10.1063/1.1654326.

(10) Seco, J. M.; Quiñoá, E.; Riguera, R. Boc-Phenylglycine : The Reagent of Choice for the Assignment of the Absolute Configuration of α -Chiral Primary Amines by 1 H NMR Spectroscopy. *J. Org. Chem.* **1999**, *64* (13), 4669–4675.

(11) Latypov, S. K.; Ferreiro, M. J.; Quiñoá, E.; Riguera, R. Assignment of the Absolute Configuration of β-Chiral Primary Alcohols by NMR: Scope and Limitations. *J. Am. Chem. Soc.* **1998**, *120* (19), 4741–4751. https://doi.org/10.1021/ja972550b.

(12) Hoye, T. R.; Renner, M. K. MTPA (Mosher) Amides of Cyclic Secondary Amines : Conformational Aspects and a Useful Method for Assignment of Amine Configuration. *J. Org. Chem.* **1996**, *61* (7), 2056–2064. https://doi.org/10.1021/jo952043h.

(13) Hoye, T. R.; Renner, M. K. Applications of MTPA (Mosher) Amides of Secondary Amines : Assignment of Absolute Configuration in Chiral Cyclic Amines. *J. Org. Chem.* **1996**, *61* (7), 8489–8495. https://doi.org/10.1021/jo960373b.

(14) Izumi, S.; Moriyoshi, H.; Hirata, T. Identification of Absolute Configuration of Tertiary Alcohols by Comination of Mosher´s Method and Conformational Analysis. *Bull. Chem. Soc. Jpn.* **1994**, *67* (9), 2600–2602.

(15) Takahashi, H.; Kato, N.; Iwashima, M.; Ihuchi, K. Determination of Absolute Configurations of Tertiary Alcohols by NMR Spectroscopy. *Chem. Lett.* **1999**, *28* (11), 1181–1182.

(16) Porto, S.; Seco, J. M.; Ortiz, A.; Quiñoá, E.; Riguera, R. Chiral Thiols: The Assignment of Their Absolute Configuration by 1H NMR. *Org. Lett.* **2007**, *9* (24), 5015–5018. https://doi.org/10.1021/ol7022196.

(17) Louzao, I.; Seco, J. M.; Quiñoá, E.; Riguera, R. The Assignment of Absolute Configuration of Cyanohydrins by NMR. *Chem. Commun.* **2006**, No. 13, 1422–1424. https://doi.org/10.1039/b517917c.

(18) Louzao, I.; García, R.; Seco, J. M.; Quiñoá, E.; Riguera, R. Absolute Configuration of Ketone Cyanohydrins by 1H Nmr: The Special Case of Polar Substituted Tertiary Alcohols. *Org. Lett.* **2009**, *11* (1), 53–56. https://doi.org/10.1021/ol8023314.

(19) Louzao, I.; Seco, J. M.; Quiñoá, E.; Riguera, R. The Use of a Single Derivative in the Configurational Assignment of Ketone Cyanohydrins. *European J. Org. Chem.* **2010**, No. 34, 6520–6524. https://doi.org/10.1002/ejoc.201001107.

(20) Leiro, V.; Freire, F.; Quiñoá, E.; Riguera, R. Absolute Configuration of Amino Alcohols by 1H-NMR. *Chem. Commun.* **2005**, *1* (44), 5554–5556. https://doi.org/10.1039/b510806c.

(21) Leiro, V.; Seco, J. M.; Quiñoá, E.; Riguera, R. Cross Interaction between Auxiliaries: The Chirality of Amino Alcohols by NMR. *Org. Lett.* **2008**, *10* (13), 2729–2732. https://doi.org/10.1021/ol8008528.

(22) Dale, J. A.; Dull, D. L.; Mosher, H. S. α-Methoxy-α-Trifluoromethylphenylacetic Acid, a Versatile Reagent for the Determination of Enantiomeric Composition of Alcohols and Amines'. *J. Org. Chem.* **1969**, *34* (9), 2543–2549.

(23) Sullivan, G. R.; Dale, J. A.; Mosher, H. S. Correlation of Configuration and F Chemical Shifts of α -Methoxy-α -Trifluoromethylphenylacetate Derivatives. *J. Org. Chem.* **1973**, *38* (12), 2143–2147. https://doi.org/10.1021/jo00952a006.

(24) Dale, J. A.; Mosher, H. S. Nuclear Magnetic Resonance Enantiomer Reagents. Configurational Correlations via Nuclear Magnetic Resonance Chemical Shifts of Diastereomeric Mandelate, O-Methylmandelate and α-Methoxy-α-Trifluormethylphenylacetate (MTPA) Esters. *J. Am. Chem. Soc.* **1973**, *95* (2), 512–519.

(25) Ohtani, I.; Kusumi, T.; Kashman, Y.; Kakisawa, H. High-Field FT NMR Application of Mosher's Method. The Absolute Configurations of Marine Terpenoids. *J. Am. Chem. Soc.* **1991**, *113* (11), 4092–4096. https://doi.org/10.1021/ja00011a006.

(26) Seco, J. M.; Quiñoá, E.; Riguera, R. The Assignment of Absolute Configuration by NMR. *Chem. Rev.* **2004**, *104* (1), 17–117. https://doi.org/10.1021/cr000665j.

(27) Seco, M.; Quin, E.; Riguera, R.; Louzao, I. 13C NMR as a General Tool for the Assignment of Absolute Configuration. *Chem. Commun.* **2010**, *46*, 7903–7905. https://doi.org/10.1039/c0cc02774j.

(28) Trost, B. M.; Bunt, R. C.; Pulley, S. R. On the Use of O-Methylmandelic Acid for the Establishment of Absolute Configuration of α-Chiral Primary Amines. *J. Org. Chem.* **1994**, *59* (10), 4202–4205.

(29) Latypov, S. K.; Seco, J. M.; Quiñoá, E.; Riguera, R. Conformational Structure and Dynamics of Arylmethoxyacetates: DNMR Spectroscopy and Aromatic Shielding Effect. *J. Org. Chem.* **1995**, *60* (3), 504–515. https://doi.org/10.1021/jo00108a008.

(30) Chataigner, I.; Lebreton, J.; Durand, D.; Guingant, A.; Villiéras, J. A New Approach for the Determination of the Absolute Configuration of Secondary Alcohols by 1H NMR with O-Substituted Mandelate Derivatives. *Tetrahedron Lett.* **1998**, *39* (13), 1759–1762. https://doi.org/10.1016/S0040-4039(98)00059-8.

(31) Seco, J. M.; Latypov, S. K.; Quiñoá, E.; Riguera, R. Determining Factors in the Assignment of the Absolute Configuration of Alcohols by NMR . The Use of Anisotropic Effects on Remote Positions. *Tetrahedron* **1997**, *53* (25), 8541–8564.

(32) Latypov, S. K.; Seco, J. M.; Quiñoá, E.; Riguera, R. Determination of the Absolute Stereochemistry of Chiral Amines by 1H NMR of Arylmethoxyacetic Acid Amides: The Conformational Model. *J. Org. Chem.* **1995**, *60* (6), 1538–1545. https://doi.org/10.1021/jo00111a011.

(33) Hawkins, J. M.; Watson, T. J. N. Asymmetric Catalysis in the Pharmaceutical Industry. *Angew. Chemie Int. Ed.* **2004**, *43* (25), 3224–3228. https://doi.org/10.1002/anie.200330072.

(34) Farina, V.; Reeves, J. T.; Senanayake, C. H.; Song, J. J. Asymmetric Synthesis of Active Pharmaceutical Ingredients. *Chem. Rev.* **2006**, *106* (7), 2734–2793. https://doi.org/10.1021/cr040700c.

(35) Noyori, R.; Hashiguchi, S. Asymmetric Transfer Hydrogenation Catalyzed by Chiral Ruthenium Complexes. *Acc. Chem. Res.* **1997**, *30* (2), 97–102. https://doi.org/10.1021/ar9502341.
(36) Ikariya, T.; Blacker, A. J. Asymmetric Transfer Hydrogenation of Ketones with Bifunctional Transition Metal-Based Molecular Catalysts. *Acc. Chem. Res.* **2007**, *40* (12), 1300–1308. https://doi.org/10.1021/ar700134q.
(37) Rossi, S.; Benaglia, M.; Massolo, E.; Raimondi, L. Organocatalytic Strategies for Enantioselective Metal-Free Reductions. *Catal. Sci. Technol.* **2014**, *4* (9), 2708–2723. https://doi.org/10.1039/c4cy00033a.
(38) Herrera, R. P. Organocatalytic Transfer Hydrogenation and Hydrosilylation Reactions. *Top. Curr. Chem.* **2016**, *374* (3), 1–40. https://doi.org/10.1007/s41061-016-0032-4.
(39) Denmark, S. E.; Fu, J. Catalytic Enantioselective Addition of Allylic Organometallic Reagents to Aldehydes and Ketones. *Chem. Rev.* **2003**, *103* (8), 2763–2793. https://doi.org/10.1021/cr020050h.
(40) Malkov, A. V.; Stewart Liddon, A. J. P.; Ramírez-López, P.; Bendová, L.; Haigh, D.; Kočovský, P. Remote Chiral Induction in the Organocatalytic Hydrosilylation of Aromatic Ketones and Ketimines. *Angew. Chemie - Int. Ed.* **2006**, *45* (9), 1432–1435. https://doi.org/10.1002/anie.200503941.
(41) Greene, T. W.; Wuts, P. G. M.; Protective, O. F. a; Groups, P.; Edition, T.; Greene, T. W.; Wuts, P. G. M. *Protective Groups in Organic Synthesis*, 2nd ed.; Willey, 2007. https://doi.org/10.1002/9780470053485.ch2.
(42) Ohtani, I.; Hotta, K.; Ichikawa, Y.; Isobe, M. Application of Modified Mosher´s Method to α-Aromatic Secondary Alcohols. Exception of the Rule and Conformational Analyses. *Chem. Lett.* **1995**, *24* (6), 513–514.
(43) Omata, K.; Fujiwara, T.; Kabuto, K. Use of a Diamagnetic Lanthanide Complex for Extending the Scope of NMR Determination of Absolute Configuration by the Modified Mosher's Method. *Tetrahedron Asymmetry* **2002**, *13* (15), 1655–1662. https://doi.org/10.1016/S0957-4166(02)00414-7.
(44) García, R.; Seco, J. M.; Vázquez, S. A.; Quiñoá, E.; Riguera, R. Role of Barium(II) in the Determination of the Absolute Configuration of Chiral Amines by 1H NMR Spectroscopy. *J. Org. Chem.* **2006**, *71* (3), 1119–1130. https://doi.org/10.1021/jo0522207.
(45) Orlov, N. V; Ananikov, V. P. NMR Analysis of Chiral Alcohols and Amines: Development of an Enviromentaly Benign "in Tube" Procedure with High Efficiency and Improved Detection Limit. *Green Chem.* **2011**, *13* (7), 1735–1744.
(46) Yukibaru, F.; Yaima, C.; Mizutani, J. A New Method for Establishment of Absolute Configurations of Secondary Alcohols by NMR Spectroscopy. *Tetrahedron Lett.* **1994**, *35* (4), 599–602.
(47) Bautista-Hernández, C. I.; Trejo-Carbajal, N.; Zúñiga-Estrada, E. A.; Aristeo-Dominguez, A.; Meléndez-Rodríguez, M.; Suárez-Castillo, O. R.; Sánchez-Zavala, M.; Cruz-Borbolla, J.; Morales-Ríos, M. S.; Joseph-Nathan, P. 2-Cyano-2-Indolylpropanoic Acid as a Chiral Derivatizing Agent for the Absolute Configuration Assignment of Secondary Alcohols and Primary Amines by 1H NMR and VCD. *Tetrahedron Asymmetry* **2017**, *28* (6), 762–782. https://doi.org/10.1016/j.tetasy.2017.04.011.
(48) Hoye, T. R.; Jeffrey, C. S.; Shao, F. Mosher Ester Analysis for the Determination of Absolute Configuration of Stereogenic (Chiral) Carbinol Carbons. *Nat. Protoc.* **2007**, *2* (10), 2451–2458. https://doi.org/10.1038/nprot.2007.354.
(49) Alkorta, I.; Elguero, J. Ab Initio Hybrid DFT-GIAO Calculations of the Shielding Produced by Carbon-Carbon Bonds and Aromatic Rings in 1H NMR Spectroscopy. *New J. Chem.* **1998**, *22* (4), 381–385. https://doi.org/10.1039/a708743h.
(50) Baranac-Stojanović, M. New Insight into the Anisotropic Effects in Solution-State NMR Spectroscopy. *RSC Adv.* **2014**, *4* (1), 308–321. https://doi.org/10.1039/c3ra45512b.
(51) Alkorta, I.; Elguero, J. Ab Initio Hybrid DFT-GIAO Calculations of the Shielding Produced by Carbon-Carbon Bonds and Aromatic Rings in 1H NMR Spectroscopy. *New J. Chem.* **1998**, *22* (4), 381–385. https://doi.org/10.1039/a708743h.
(52) Freire, F.; Seco, J. M.; Quiñoá, E.; Riguera, R. Challenging the Absence of Observable Hydrogens in the Assignment of Absolute Configurations by NMR: Application to Chiral Primary Alcohols. *Chem. Commun.* **2007**, *1* (14), 1456–1458. https://doi.org/10.1039/b617184b.
(53) Seco, J. M.; Qui??o??, E.; Riguera, R. The Assignment of Absolute Configuration by NMR. *Chem. Rev.* **2004**, *104* (1), 17–117. https://doi.org/10.1021/cr000665j.
(54) Matsui, T.; Kondo, T.; Nishita, Y.; Itadani, S.; Tsuruta, H.; Fujita, S.; Omawari, N.; Sakai, M.; Nakazawa, S.; Ogata, A.; Mori, H.; Kamoshima, W.; Terai, K.; Ohno, H.; Obata, T.; Nakai, H.; Toda, M. Highly Potent Inhibitors of TNF-α Production. Part II: Metabolic Stabilization of a Newly Found Chemical Lead and Conformational Analysis of an Active Diastereoisomer. *Bioorganic Med. Chem.* **2002**, *10* (12), 3787–3805. https://doi.org/10.1016/S0968-0896(02)00380-2.
(55) Ren, Y.; Su, Y.; Sun, L.; He, S.; Meng, L.; Liao, D.; Liu, X.; Ma, Y.; Liu, C.; Li, S.; Ruan, H.; Lei, X.; Wang, X.; Zhang, Z. Discovery of a Highly Potent, Selective, and Metabolically Stable Inhibitor of Receptor-Interacting Protein 1 (RIP1) for the Treatment of Systemic Inflammatory Response Syndrome. *J. Med. Chem.* **2017**, *60* (3), 972–986. https://doi.org/10.1021/acs.jmedchem.6b01196.
(56) Karim, A.; Mortreux, A.; Petit, F.; Buono, G.; Peiffer, G.; Siv, C. Synthese d'aminophosphinephosphinites Chiraux. Utilisation En Reduction Asymetrique Catalytique. *J. Organomet. Chem.* **1986**, *317* (1), 93–104. https://doi.org/10.1016/S0022-328X(00)99348-3.
(57) Boyle, G. A.; Govender, T.; Kruger, H. G.; Maguire, G. E. M. Synthesis of Chiral Pentacyclo-Undecane Ligands and Their Use in the Enantioselective Alkylation of Benzaldehyde with Diethylzinc. *Tetrahedron Asymmetry* **2004**, *15* (17), 2661–2666. https://doi.org/10.1016/j.tetasy.2004.07.038.
(58) Agami, C.; Couty, F.; Hamon, L.; Venier, O. Chiral Oxazolidinones from N-Boc Derivatives of β-Amino Alcohols. Effect of a N-Methyl Substituent on Reactivity and Stereoselectivity. *Tetrahedron Lett.* **1993**, *34* (28), 4509–4512. https://doi.org/10.1016/0040-4039(93)88071-P.
(59) Micouin, L.; Jullian, V.; Quirion, J. C.; Husson, H. P. Origins of Diastereoselectivity in the Alkylation of N-Substituted Lactams and Amides Derived from Optically Active Aminoalcohols. *Tetrahedron Asymmetry* **1996**, *7* (10), 2839–2846. https://doi.org/10.1016/0957-4166(96)00374-6.
(60) Waki, M.; Meienhofer, J. Efficient Preparation of N-Formylamino Acid Tert-Butyl Esters. *J. Org. Chem.* **1977**, *42* (11), 2019–2020. https://doi.org/https://doi.org/10.1021/jo00431a046.
(61) Profous, D. Využití TBBA pro Určení Absolutní Konfigurace Chirálních Aminů a Alkoholů, 2020.
(62) Andrés, J. M.; Barrio, R.; Martínez, M. A.; Pedrosa, R.; Pérez-Encabo, A. Synthesis of Enantiopure Syn-β-Amino Alcohols. A Simple Case of Chelation-Controlled Additions of Diethylzinc to α-(Dibenzylamino) Aldehydes. *J. Org. Chem.* **1996**, *61* (13), 4210–4213. https://doi.org/10.1021/jo960017t.
(63) Zheng, M.; Xue, W.; Xue, T.; Gong, H. Ester Formation via Nickel-Catalyzed Reductive Coupling of Alkyl Halides with Chloroformates. *Org. Lett.* **2016**, *18* (23), 6152–6155. https://doi.org/10.1021/acs.orglett.6b03158.
(64) Erhardt, P. W. Benzylamine and Dibenzylamine Revisited. Syntheses of N-Substituted Aryloxypropanol Amines Exemplifying a General Route to Secondary Aliphatic Amines. *Synth. Commun.* **1983**, *13* (2), 103–114. https://doi.org/10.1080/00397918308061967.
(65) Le, Z. G.; Chen, Z. C.; Hu, Y.; Zheng, Q. G. Organic Reactions in Ionic Liquids: N-Alkylation of Phthalimide and Several

Nitrogen Heterocycles. *Synthesis (Stuttg).* **2004**, No. 2, 208–212. https://doi.org/10.1055/s-2003-44383.
(66) Holl, M. G.; Struble, M. D.; Siegler, M. A.; Lectka, T. The Close Interaction of a C-F Bond with a Carbonyl π–System: Attractive, Repulsive, or Both? *J. Fluor. Chem.* **2016**, *188*, 126–130. https://doi.org/10.1016/j.jfluchem.2016.06.016.
(67) Holl, M. G.; Pitts, C. R.; Lectka, T. Fluorine in a C−F Bond as the Key to Cage Formation. *Angew. Chemie - Int. Ed.* **2018**, *57* (11), 2758–2766. https://doi.org/10.1002/anie.201710423.
(68) Hehre, W.; Klunzinger, P.; Deppmeier, B.; Driessen, A.; Uchida, N.; Hashimoto, M.; Fukushi, E.; Takata, Y. Efficient Protocol for Accurately Calculating 13C Chemical Shifts of Conformationally Flexible Natural Products: Scope, Assessment, and Limitations. *J. Nat. Prod.* **2019**, *82* (8), 2299–2306. https://doi.org/10.1021/acs.jnatprod.9b00603.
(69) Gao, Y. X.; Chang, L.; Shi, H.; Liang, B.; Wongkhan, K.; Chaiyaveij, D.; Batsanov, A. S.; Marder, T. B.; Li, C. C.; Yang, Z.; Huanga, Y. A Thiourea-Oxazoline Library with Axial Chirality: Ligand Synthesis and Studies of the Palladium-Catalyzed Enantioselective Bis(Methoxycarbonylation) of Terminal Olefins. *Adv. Synth. Catal.* **2010**, *352* (11–12), 1955–1966. https://doi.org/10.1002/adsc.201000070.
(70) Liang, B.; Liu, J.; Gao, Y. X.; Wongkhan, K.; Shu, D. X.; Lan, Y.; Li, A.; Batsanov, A. S.; Howard, J. A. H.; Marder, T. B.; Chen, J. H.; Yang, Z. Synthesis of Thiourea-Oxazolines, a New Class of Chiral S,N-Heterobidentate Ligands: Application in Pd-Catalyzed Asymmetric Bis(Methoxycarbonylation) of Terminal Olefins. *Organometallics* **2007**, *26* (19), 4756–4762. https://doi.org/10.1021/om700311x.
(71) Dai, M.; Liang, B.; Wang, C.; Chen, J.; Yang, Z. Synthesis of a Novel C2-Symmetric Thiourea and Its Application in the Pd-Catalyzed Cross-Coupling Reactions with Arenediazonium Salts under Aerobic Conditions. *Org. Lett.* **2004**, *6* (2), 221–224. https://doi.org/10.1021/ol036182u.
(72) Pesch, J.; Harms, K.; Bach, T. Preparation of Axially Chiral N,N???-Diarylimidazolium and N-Arylthiazolium Salts and Evaluation of Their Catalytic Potential in the Benzoin and in the Intramolecular Stetter Reactions. *European J. Org. Chem.* **2004**, No. 9, 2025–2035. https://doi.org/10.1002/ejoc.200300762.
(73) Janíková, K.; Jedinák, L.; Volná, T.; Cankař, P. Chan-Lam Cross-Coupling Reaction Based on the Cu2S/TMEDA System. *Tetrahedron* **2018**, *74* (5), 606–617. https://doi.org/10.1016/j.tet.2017.12.042.
(74) Tandon, V. K.; Kumar, M. BF3.Et2O Promoted One-Pot Expeditious and Convenient Synthesis of 2-Substituted Benzimidazoles and 3,1,5-Benzoxadiazepines. *Tetrahedron Lett.* **2004**, *45* (21), 4185–4187. https://doi.org/10.1016/j.tetlet.2004.03.117.
(75) Malkov, A. V.; Mariani, A.; MacDougall, K. N.; Kočovský, P. Role of Noncovalent Interactions in the Enantioselective Reduction of Aromatic Ketimines with Trichlorosilane. *Org. Lett.* **2004**, *6* (13), 2253–2256. https://doi.org/10.1021/ol049213+.